The Engineering Characterization of Melanges and Similar Block-in-Matrix Rocks (Bimrocks)

by

Edmund William Medley

B.A.Sc (University of British Columbia, Canada) 1978
M.S. (University of California, Berkeley) 1991

a dissertation submitted in partial satisfaction of the requirements for the degree of

DOCTOR OF PHILOSOPHY

in

Engineering-Civil Engineering

in the

GRADUATE DIVISION

of the

UNIVERSITY of CALIFORNIA at BERKELEY

Commitee in charge:

Professor Richard E. Goodman, Chair
Professor Tor L. Brekke
Professor David L. Jones

1994

Abstract

The Engineering Characterization of Melanges and Similar Block-in-Matrix Rocks (Bimrocks)

by

Edmund William Medley

Doctor of Philosophy in Civil Engineering

University of California at Berkeley

Professor Richard E. Goodman, Chair

Melanges are composed of competent blocks of rock embedded in generally sheared, argillaceous or serpentinite matrices. Blocks were characterized by d_{mod}, their maximum observed dimension. Log-histograms of the block size distributions of some melanges of the Franciscan Complex of California were determined to be scale-independent, by normalizing them over 7 orders of magnitude by $\sqrt{A}$ (where A was the area containing the blocks). The size of the most frequent blocks was about 5 percent of the size of $\sqrt{A}$, and the fractal dimensions averaged 1.2. The apparent scale-independence allowed image analysis work on *graphic models* of real and model melanges. Stereology principals were used to relate linear and areal measurements to volume properties. Melanges, and some similar heterogeneous rock masses, were classified as *bimrocks*, (block-in-matrix rocks), or: *mixtures of rocks, composed of geotechnically significant blocks within a bonded matrix of finer texture*. The largest block, d_{max}, is the engineer's choice of : a) the largest expected block in any population of blocks, b) equivalent to $\sqrt{A}$, or c) the characteristic engineering dimension, which is a length (such as a tunnel diameter or footing width) that represents the rock mass at the engineering scale. To be geotechnically significant, blocks must be mechanically superior to the matrix; have sizes ranging between 5 percent

and 75 percent of d_{max} ; and have volumetric proportions between 25 percent and 75 percent. The overall strength of bimrocks depends on the block volumetric proportion (Lindquist, 1994b), hence the volumetric proportion and other bimrock characteristics must be characterized. Estimates can be made by *scanlines*, such as exploration drill core. A total scanline length of greater than 10 times d_{max} generates sufficient to estimate the block volumetric proportion and approximate the three-dimensional block size distribution. Case histories of a dam, landslide and tunnel afforded opportunities to validate the techniques developed by the research.

Richard E. Goodman

Professor Richard E. Goodman, Chair

The dissertation of Edmund William Medley is approved:

Richard E Goodman July 17, 1994
Chair **Date**

W L Briggs 7/14, 1994
Date

David Aldous 7/2/94
Date

University of California at Berkeley

1994

The Engineering Characterization of Melanges and Similar Block-in-Matrix Rocks (Bimrocks)

by

Edmund William Medley

TWO KINDS OF CHAOS

CHAOS 1: *Mélange*

When a drifting arc of island docks
Acting something like a dredge,
It brings along all kinds of rocks
And piles them in the cont'nents edge

Far up the modern mountain face
Are pillow lavas, welded tuff,
Sheeted dikes of diabase
Geywackes, andesite- (enough

To keep one baffled and alert);
Quartz veins of the Mother Lode,
Bits of radiolarian chert,
Blocks of Limestone à la mode,

Peridotite and serpentine,
Breccia with its matrix clay,
granite, mudflows submarine-
The Gods of Chaos had their day!

The puzzle was as dark as night
Until we saw the ophiolite!

(from Robert L. Bates' "The Geologic Column", in the January, 1993 edition of *Geotimes*)

CHAOS 2: *A First Draft*

To Ed Med
BSD & CLD & BIMHAHAWHOWHO
(To the tune "I've been working on the gravel")

Tell
Tell them
Tell them what
Tell them what & how
Tell them what & how & why
Tell them what & how & why & then
Tell them all of this and then again
And tell them this again
and then still again
and then again
and again
and

Poetic reaction from Professor Richard E. Goodman, upon ploughing through the chaos of the first draft of this dissertation. Thanks Dick...

Keywords

Bimrocks, Block-in-Matrix rocks, California, Case Histories, Characterization, Fractals, Franciscan Complex, Geological Engineering, Geotechnical Engineering, Hetereogeneity, Image Analysis, Landslides, Melange, Olistostromes, Ophiolites, Rock Mechanics, San Francisco, Scale-Independence, Self-Similarity, Serpentinites, Stereology, Tunnels

Acknowledgments

First and foremost, this work could not have been completed without the love and help of my best friend, number one field assistant, and beautiful wife, Julie Grau, who all along insisted on quality recreation, and encouraged me when the course seemed interminable.

In the beginning there were Dr. Roger Foott and Prof. Bill Dietrich, who in their own ways, challenged me sufficiently that I had to return to school: I couldn't beat them, so I have joined them. Along the way, I was fortunate to share a research project with Eric Lindquist, and benefit from his cheerful companionship and thoughtful analyses. I was ably guided by Prof. Richard Goodman, who enthusiastically supported me in my struggle to characterize melange; by Prof. David Jones, who patiently repeated the fundamentals of the geology of the California Coast Ranges; and Prof. Tor Brekke, who encouraged me during many chats on his office balcony. My research was financially supported by Pacific Gas & Electric Corp.(San Francisco): thanks to PG&E's Mr. Charles Ahlgren. I am also grateful for the generous help and advice of Dr. Steve Ellen (USGS, Menlo Park) and Joan Van Velsor (CALTRANS, Oakland).

The search for geo-mechanical information on melanges and other bimrocks rewarded me with correspondents scattered between Antarctica and Norway; California and Kazakhstan. Many people have given time to me either in person, on the phone, in letters; or they published requests for information on melanges and bimrocks. Others provided me with work facilities and equipment. I gratefully acknowledge the help of: Prof. Ken Aalto, Dr. Andy Afrouz, Prof. J. Anderson, The BC Professional Engineer Magazine, Don Bain, Dr. Rex Baum, Prof. Z. Bieniawski, Ed Blackey, Prof. Vladimir Bochkarov, Dr. Earl Brabb, Dr. Anders Bro, Prof. Paulo Canuti, Prof. Mark Cloos, Prof. Darrell Cowan, Prof. David Cruden, Jim Cunningham, Prof. Bill Dietrich, Dr. John Dohrenwend, Margaret Ennis, Dr. Rolfe Erikson, Prof. Aziz Ertunc, John France (USCOLD), Prof. Okay Gürpinar, John Gadsby (Geotechnical News), Dr. Jim Gamble, Earl Hart, Wayne Haydon, Craig Herzog, Michael Hobbs, Prof. Anna Hyánková, Dr. T.Yalcin Irfan, Prof. K. Ercin Kasapoglu, Prof. John Kemeny, Dr. Vadim Khazin, Dave Kidd, Fred Kintzer, Steve Klein, Stephen Korbay, Dr. Greg Korbin, Dr. Padma Lai Shrestha, Prof. Peter Laznicka, Steve Maiolini, Prof. Paul Marinos, Prof. Chris Marone, Prof. Matt Mauldon, Verne McGuffey, Dr. Eric McHuron, Doug Milne, Dr. Roger Moore, Dr. Rolando Mora Chinchilla, Prof. Edward Nowatzki, Mark Olsen, Dr. Akin Onalp, Prof. Stanislaw Ostaficzuk, Dr. Carlos Pérez Pérez, George Petrides, Pierre Pothral, Prof. Loren Raymond, Salem Rice, Ken Rodda, Dr. Dave Rogers, Damon Runyan, Prof. Paul Ryan, Dr. Julius Schlocker, Tony Silveira, Ernie Solomon, Tom Spittler, Prof. Yusuf Tatar, Prof. Kazimierz Thiel, D. Thompson, Dr. Michael Thomson, Dr. Morten Thoresen, Dr. Resat Ulusay, Dr. Rex Upp, Jim Vantine, Prof. Barry Voight, Dr. von Poschinger, Prof. Skipp Watts, Dr. Chow Weng Sum, Dr. Jared West, Rob White, W. M. Williams, Dr. Bob Wright, Perry Wood, Dr. Ronald Yeung, Dr. Ilyas Yilmazer, and Dr. Hiroyuki Yosimatsu.

TABLE OF CONTENTS

List of Figures

CHAPTER 4

CHAPTER 5

Lone Tree Slide: Figures

Scott Dam: Figures

Storage Tunnel Portion of Richmond Transport Project: Figures

FIGURES IN APPENDIX A

FIGURES IN APPENDIX B

FIGURES IN APPENDIX C

FIGURES IN APPENDIX D

FIGURES IN APPENDIX E

List of Tables

LIST of ABBREVIATIONS and SYMBOLS

$\sqrt{A}$	square root of the area of measurement; used to normalize d_{mod} (endclass) to prepare dimensionless log histograms
γ_s	unit weight if soil
γ_w	unit weight of water (1.0 gms/cm^3)
ϕ	angle of internal friction
2DBSD	two-dimensional block-size distribution, numerical frequency basis, for blocks embedded in a matrix
3DBSD	three-dimensional block size distribution, numerical basis; for blocks embedded in a matrix
A_A	Areal proportion of blocks or particles in a matrix
BSD	block bize distribution: analagous to the the weight-based PSD (see below) used in of soil mechanics, not practical except for small blocks. See also WBSD.
CLD	one-dimensional, chord length distribution, numerical basis; suitable for both particles and blocks.
D	Fractal dimension; the slope of a best fit line through a scatter of data plotted using logarithmic axes
D_S	Diameter of a sphere
d	generic symbol representing dimension or "diameter" of a block in two- or three-dimensions.
d_m	average soil particle size, mean of two adjacent sieve sizes
d_{max}	the size of the largest block in a population of blocks
d_{mod}	maximum observed dimension of an **individual** block: the maximum measureable distance between the two furthest points on the perimeter or surface of a block. In one dimension this is the the maximum chord measured through a block. At the limit, this measurement is the "diameter", or characteristic dimension of the block.
d_{peak}	d_{mod} (endclass) at the peak of a log histogram of a block size distribution
E_{block}	stiffness of block, expressed in terms of Young's Modulus (psi or kPa)
E_{matrix}	stiffness of matrix, expressed in terms of Young's Modulus (psi or kPa)
G_s	Specific Gravity of a soil particle
L_L	Linear proportion of blocks or particles in a matrix
N	Number of soil particles; and Standard Penetration Test values
P_P	Proportion of Points (point density) occupying particles or blocks in a matrix
PSD	Particle Size Distribution curve; as conventional soil mechanics representation of cumulative percent frequency, on weight basis (arithmetic ordinate) vs. grain size dimensions as represented the by

	the opening size of mechanical sieves (logarithmic abscissa). See also WPSD.
q_u	Unconfined Compressive Strength
RF_{peak}	peak numerical relative frequency of a log histogram plot
V_p	Volume of a single soil particle
V_s	Volume of a soil mass
V_V	Volumetric proportion of blocks or particles in a matrix
WBSD	weight-based block size distribution, for populations of blocks embedded in a matrix.
WPSD	weight-based particle size distribution, for populations of particles (sand, gravels) suspended in air or water.
W_s	weight of soil

CHAPTER 1: INTRODUCTION

1.1 SUMMARY DESCRIPTION OF THE RESEARCH SCOPE

This dissertation summarizes research into the *engineering characterization of melanges and similar block-in-matrix rocks (bimrocks)*. Melanges are chaotic, heterogeneous rock masses composed of competent rock blocks of varying size, embedded in a weaker argillaceous matrix; other terms are discussed in more detail in the remainder of this chapter. Figure 1.1 illustrates a typical melange. The research summarized in this dissertation developed methods useful for estimating the in-situ volumetric proportion and size distribution of blocks in some melanges of the Franciscan Complex (the Franciscan) in California. This research complements work performed by Lindquist (1994b), who related the strength and deformation properties of melanges to their volumetric proportions of blocks. The research was prompted by an engineering problem related to Franciscan melange which constitutes the foundation of Scott Dam, Lake County, California (Volpe and others, 1991).

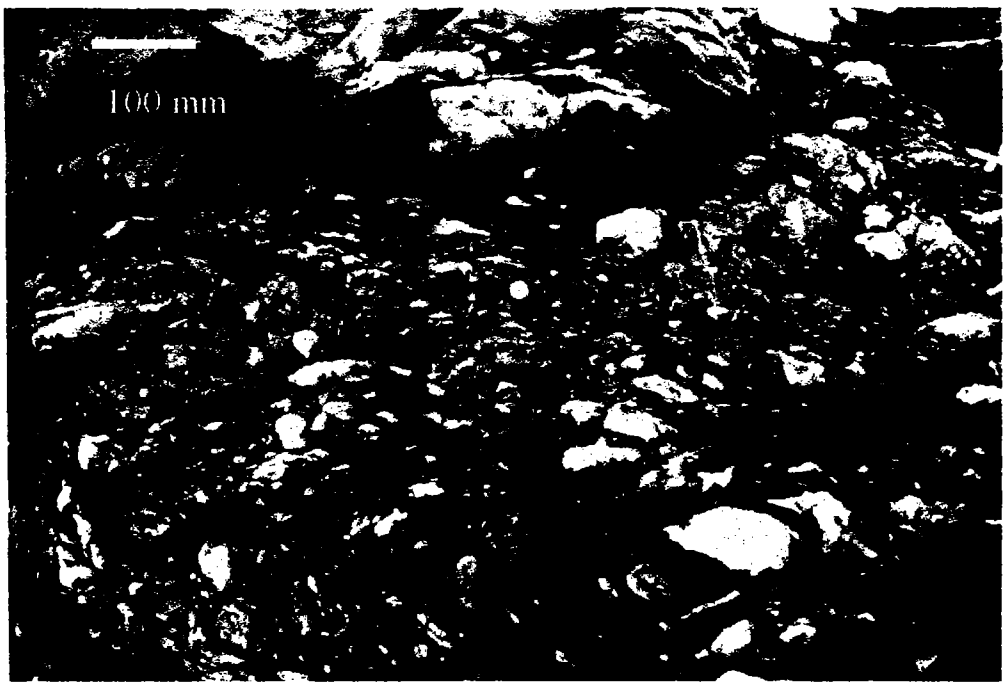

Figure 1.1 Melange of the Franciscan at Point Delagada, California. The exposure is 1 m wide.

Some basic concepts fundamental to the research are introduced in the remainder of this Chapter. Amplifications of these concepts and descriptions of several techniques developed for the research are presented in Chapter 2. Aspects of melanges of geological interest are described in Chapter 3. Chapter 4 includes summaries of the engineering properties of melanges, illustrates the relevance of block volumetric proportion and block size distributions; and describes some of the engineering problems related to melanges and sheared serpentinites. In Chapter 5 the findings of the research are applied to three Case Histories. Chapter 6 contains a summary of findings, conclusions and recommendations for further research. Appendices A through E include data and procedures considered too distracting to include in the main text.

1.2 BLOCK-IN-MATRIX ROCKS and BIMROCKS

The research was directed at *block-in-matrix rocks*. Many geologic processes produce block-in-matrix rocks, and a partial list could include: sedimentary rocks (boulder conglomerates, lithified colluvium and talus, and tillites); igneous volcanic rocks (agglomerates, pyroclastics, lahars, xenolithic inclusions in volcanic extrusions); plutonic rocks (xenolithic inclusions in igneous intrusions); structural brittle cataclastics (fault breccias); rocks formed by structural ductile deformation on the interference zones of folds (mylonites); rocks formed by diapirism (some sheared serpentinites; and rocks formed by chemical and mechanical weathering (saprolites, decomposed granites, cemented colluvium). Over 50 branches of Geology focus attention on fragmented rocks, and Laznicka (1988, chapter 1) estimated that there are in excess of 200,000 references. A significant proportion of fragmented rocks are block-in-matrix rocks, but during the research, a search of the rich geological literature yielded less than a dozen references that address their engineering behavior..

Laznicka (1988) defined the generic term *rudrocks* to encompass the wide spectrum of fragmented and mixed rocks ranging between the barely cracked, with none or little matrix (*blocky rock*, in Rock Mechanics parlance), to thoroughly crushed fault gouge. Block-in-matrix rocks are described by Raymond and others (1989) as "blocks of one lithology enclosed in materials of another lithology ". This definition is not entirely satisfying, since it excludes monolithologic systems of blocks enclosed by matrix, such as sheared serpentinites. The geology of block-in-matrix rocks is further confused by more than 1000 words or terms to describe the fabric of breccias, coarse fragmented rocks and block-in-matrix rocks (Laznicka,1988, p. 809-819). The typical geologically naïve civil engineer, may learn some of the names for block-in-matrix rocks, but confusing one for another is easy and misleading. Hence, the term "block-in-matrix rock" is preferable to using an incorrect geological name, but it is cumbersome, and was shortened to *bimrock* (block-in-matrix rock). Initially used for the writer's convenience, the word was later defined to be more useful to an engineer.

A bimrock is defined here as:

a mixture of rocks, composed of geotechnically significant blocks within a bonded matrix of finer texture.

Components of the definition are introduced below and discussed further in Chapter 2.

Blocks includes all geotechnically significant fragments within a matrix. Block sizes are characterized by their *maximum observable dimension*, or $\mathbf{d_{mod}}$. In two or three dimensions, d_{mod} is the distance between the two furthest points on the exposed perimeter of a block, and is not necessarily the block "diameter" or maximum possible dimension. In one dimension, d_{mod} is a chord through the block, and may not be the longest one possible. A bonded matrix of finer texture requires an arrangement of finer grains or fragments which are cemented into a rock fabric binding the blocks. The blocks and matrix may show common or separate deformation fabrics.

Blocks are *geotechnically significant* if they satisfy all the criteria below, for which justifications are provided in Chapter 2:

1. *There is a mechanical difference between the blocks and the matrix.* Criteria are suggested in Chapter 2 for distinguishing blocks from matrix on the basis of their mechanical contrasts, such as $(\tan \phi'_{block} / \tan \phi'_{matrix}) \geq 2.0$.

2. *There are significant ratios between the largest and smallest blocks, and a characteristic engineering dimension of the rock mass.* Characteristic engineering dimensions range between tens to hundreds of meters (slopes heights, tunnel diameters, zones of plastic flow around openings, footing widths, pressure bulb depths and so on); and centimeters (the dimensions of laboratory test specimens and diameters of in-situ down-hole tests). This range of scale is referred to here as *engineering scales.* Tentatively, a minimum ratio of 0.05 is suggested for the smallest blocks, and a maximum ratio of 0.75, for the largest blocks. Criteria are suggested in Chapter 2 for distinguishing blocks from matrix on the basis of the relative size of the smallest block to the largest block (or to a characteristic engineering dimension); and for discriminating large blocks from blocky rock.

3. *The volumetric proportion of the blocks is greater than 25 percent and less than approximately 75 percent.* The lower limit of this criteria was discovered by Lindquist (1994b) and Lindquist and Goodman (1994): with volumetric proportions below 25 percent, the overall mechanical behavior of a bimrock was found to be similar to that of the matrix. But, the overall strength of the "matrix" will be enhanced at the characteristic engineering dimensions of geotechnical laboratory tests, if the proportion of small blocks in the "matrix" exceeds 25 percent. The upper limit of 75 percent is based on the general observation that blocks tend to touch when the volumetric proportion exceeds approximately 70 percent. A block-in-matrix rock with block content beyond 75 percent is considered here to be *blocky rock.*

1.4 MELANGES and SIMILAR BLOCK-IN-MATRIX ROCKS

Bimrocks are exemplified by *melanges*, which were the primary focus of the research. Melanges (French, mélange, or mixture; Figure 1.1) are located in over 70 countries of the world, as described in Chapter 3 and Appendix A. The word *mélange* was first used by Greenly (1919, p. 193, as Autoclastic Mélange) and thought to have been reintroduced by Hsü (1968), but was apparently used in 1941 by Edgar Bailey (Blake & Jones, 1974, p. 1), and by Bailey and McCallien (1950). There is no consistency in the literature about the use of the acute accent "é" in *mélange*: it is recommended here that the accent not be used unless one is writing in French. In other languages *melange* is known as mélange (French); melange (German) argille scagliose (Italian); mezcla (Spanish); меланж (Russian) (Dennis & Murawski, 1979).

A recognized definition of a melange is:
A body of rock mappable at a scale of 1:24 000 or smaller and characterized both by the lack of internal continuity of contacts or strata and by the inclusion of fragments and blocks of all sizes, both exotic and native, embedded in a fragmented matrix of finer-grained material - Glossary of Geology (Bates and Jackson, 1987) and Raymond (1984).

The definition is unsatisfactory to a geological engineer. The condition that a melange be mappable at 1:24 000 or smaller, excludes melange bodies of less than 24 m, since geological maps rarely show features less than 1 mm wide. But many engineering works are smaller than 24 m and geotechnical engineers must solve the problems associated with relatively small exposures of melange; and the chaotic fabric of melange described in the definition is evident even at hand-specimen scale. So, for the purpose of this dissertation, a melange is defined as:
At the scale of engineering interest, a chaotic rock mass composed of competent blocks of various size and lithology, embedded within a weaker, usually argillaceous, matrix.

The concept of scale is critically important in an engineering study of melanges, and the topic is considered more deeply in Chapter 2. It is also important to understand that, from an engineering viewpoint, there is no one melange, at a particular location, albeit that one body may have been mapped geologically. Lindquist (1994b), showed that the mechanical behavior of a melange depends on the volumetric proportion, and that there is some dependence on the overall block orientation fabric. Variations in these characteristics from place to place within a melange, may be grounds to discriminate melanges (plural).

About 2000 references to melanges were encountered during the research. Some of the older references use terms and descriptors for melanges and melange fabrics which differ from those in current use, such as: *argille scagliose* or *scaley clay* (D'Elia and others, 1986); *sedimentary chaos, block clay; crush breccia and crush conglomerate* (Wood,

1974); *mega-breccia, chaotic structure* (Manfredini and others, 1985); *complex formations; lenticular fabric, tectonic mixtures, tectonic breccias, stratal disruption* (Cowan, 1985); *friction carpet* (Brown, 1964); *Varicolored Clays;* and *wildflysch* (also used by European geologists to describe reworked chaotic breccias and mega-blocks within turbidite sequences: Laznicka, 1988; p. 388). The variety of aliases for melange reflects the range of geological opinions regarding melange. The genesis of melanges is controversial and there is little consensus amongst geologists regarding the definition and classification of melange (Raymond, 1984), but some ideas on the formation of melanges are presented in Chapter 3.

Part of the scope of the dissertation was to investigate other heterogeneous mixtures of stronger blocks within weaker matrices, formed by sedimentary, tectonic or cataclastic processes, that are geotechnically similar to melanges. Such *similar block-in-matrix rocks* or *similar bimrocks,* tentatively include olistostromes, sheared serpentinites and serpentinite melanges. *Olistostromes* are melanges of sedimentary origin, generally with blocks of *native* sandstones, cherts and intact siltstone within shale or argillite matrices, but also containing exotic rocks of enigmatic provenance. They form by submarine landslides (Flores, 1955). *Melanges* are often considered to be of tectonic origin, and the mix of native rocks is further garnished by exotic metamorphic blocks such as eclogites, marble, limestone, greenstone and blueschists. Blocks are exotic when their origin is obviously remote from the site of matrix deposition, such as high-grade metamorphic blocks within unmetamorphosed shale. (Although there is little difference between melanges and olistostromes from an engineering perspective, the distinctions are most controversial amongst geologists: the topic is explored further in Chapter 3). *Sheared serpentinites* are masses of serpentinite blocks within sheared serpentinite matrices. *Serpentinite melanges* are the same as melanges, with matrices of serpentinite instead of shale.

The results of the research presented in this dissertation are based on a study of melanges. Hence, further work must be performed to justify the term, *similar bimrocks* for other rock mixtures, and verify that the results presented in this dissertation can be applied to them. However, it is probable that mechanically, many heterogeneous and block-in-matrix rocks, although of varying lithologies and genesis, may behave like melanges and may conform to the definition of *bimrocks* (lahars, fault breccias, tillites and saprolites, for example), they are excluded from this dissertation, since little time was spent researching them. If the family of bimrocks broadens to include these rocks, the results of the research summarized in this dissertation and that of Lindquist (1994b) will be useful to geotechnical engineers

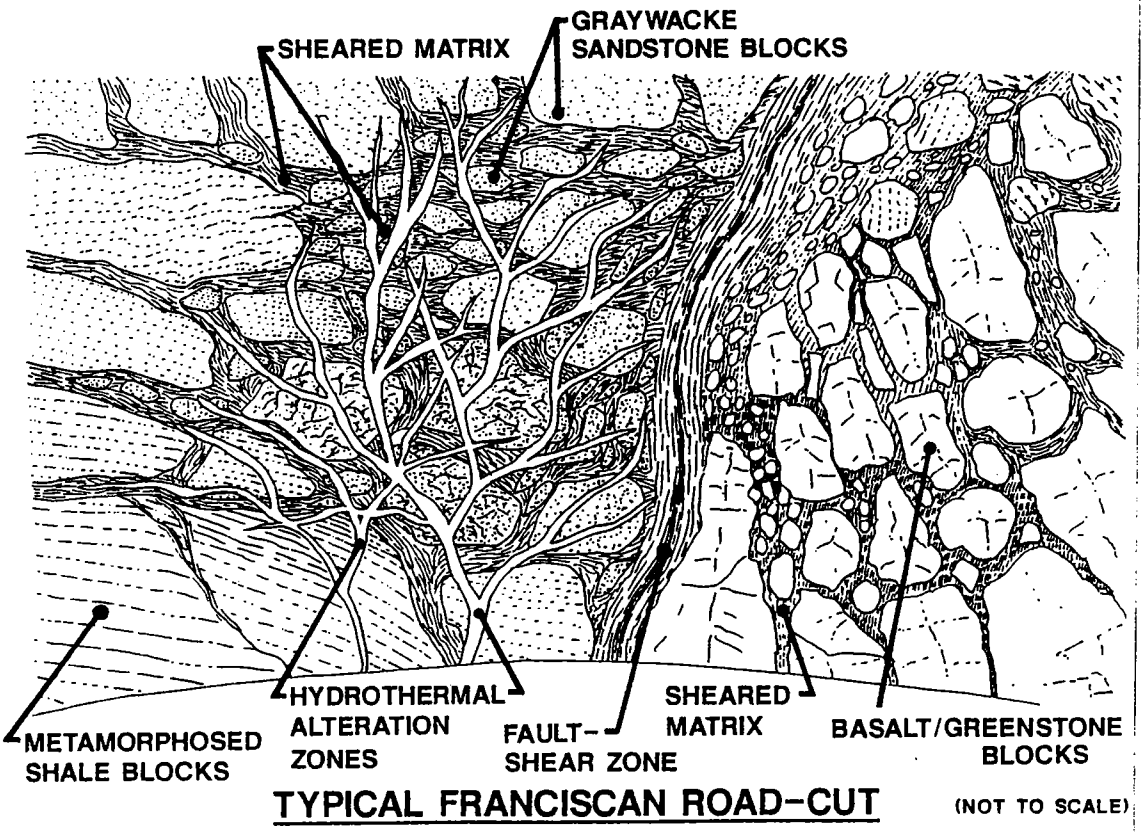

Figure 1.2 The chaos of a Franciscan melange exposed at a road cut. (Artist: Chris Alger, CEG; sketch reproduced with the permission of Dr. David Rogers, GE, CEG, Rogers/Pacific Inc., Pleasant Hill, CA)

1.4 THE ENGINEERING CHARACTERIZATION OF CHAOS

From an engineering viewpoint, the outstanding aspect of a melange is its heterogeneity and complexity, resulting from the spatial, lithologic and structural variations between the blocks and the matrix. The inherent heterogeneity is further complicated by the separate discontinuity characteristics of the blocks and the matrix. As illustrated by Figure 1.1 and Figure 1.2, the complexity can comfortably called *chaos.* Melanges may be chaotic at many scales, but it is the range of characteristic engineering dimensions, or engineering scales (from laboratory test specimen to engineering site) that are of interest here.

The geological engineer can simplify the complexity and heterogeneity of most rock and soil masses by using the established and reputable methods (ISRM, 1981; Hunt, 1984) of *engineering characterization,* a term which encompasses many endeavors related to exploring, describing and testing the mechanical and geometric properties of rock and soil masses. Such approaches work, particularly for soil, because the small-scale chaos is

homogenized once the scale of interest is enlarged. Key geological and geotechnical features may then be chosen to further represent the engineering properties of the rock mass or soil mass by the use of classification schemes (Goodman, 1990; Wittke,1990, p. 7-41; Bieniawski, 1989; Barton et al., 1974; Afrouz, 1992). In rock engineering, the key variables for characterizing blocky rock include discontinuity spacing and orientation, discontinuity roughness and type of infilling and water pressure. These variables are determined by geological mapping, drilling and trenching, geophysics and in-situ geotechnical testing. For this research on melanges, the principal properties considered important for engineering characterization were: the *block volumetric proportion* and *block size distribution, block lithology, matrix lithology, block sizes, block shapes, block orientations, block discontinuities, matrix fabric, and block matrix contacts.* The primary focus of the research was on the first two attributes, since these appear to have the greatest influence on the mechanical behavior. These and the other characteristics are reviewed in Chapter 3, where data and discussion on the characterization of bimrocks is related to some melanges of the Franciscan of California.

1.5 INTRODUCTION TO THE APPARENT SCALE-INDEPENDENCE OF SOME FRANCISCAN MELANGES

The techniques of engineering characterization described in the previous section mask the difficulties of actual rock masses. Furthermore, melanges do not lend themselves easily to the approaches of standard engineering characterization, since they are similarly chaotic throughout the range of engineering scales, which is a property called *scale independence*. The apparent scale-independence of some Franciscan melanges is of fundamental importance to this dissertation and allowed much work to be performed using conveniently sized photographs of melanges, such as that shown in Figure 1.1.

Many geological block-in-matrix fabrics are scale-independent: fault breccias and fault gouge (Laznicka, 1988, p. 41; Sammis et al., 1987; Biegel & Sammis, 1989); anastamosing shear zones (Tchalenko, 1970; Archambault et al., 1990; Bosworth, 1984); fragmented rock masses (Turcotte ,1986); Nagahama, 1993; Nagahama and Yoshii, 1993; Xie and Pariseau; 1993); fragmented tectonic crust (Korvin,1989); tuff breccias and tuff (Laznicka, 1988; p. 41); and ophiolitic chaotic debris deposits (Phipps, 1984). Several of these workers used the techniques associated with *fractals* to distinguish order in chaotic block-in-matrix fabrics. Fractal techniques were used by Lindquist (1991)[1] in a pioneer study of the block size distribution of an outcrop of melange in northern California, and his work was extended during the research. The discussion of the fundamental principals of fractals and a demonstration of the scale-independence of some Franciscan melanges is presented in Section 2.5.

---

[1]Eric S. Lindquist; "Fractals- Fracture and Franciscan", Spring 1991, term paper for CE 280, Rock Mechanics, Dept. Civil Engineering; Univ. California, Berkeley; Prof. Richard E. Goodman, Instructor

1.6 THE USE OF IMAGE ANALYSIS and STEREOLOGY FOR THE RESEARCH

The spatial properties of blocks were measured in order to demonstrate the scale-independence of melanges; to establish geometric criteria for the determination of the geotechnical significance of blocks; and to develop methods for estimating the volumetric proportion of blocks and block size distributions from measurements made from two-dimensions (outcrops, maps and photographs) and one-dimension (drill hole core and outcrop measurement traverses, or *scanlines*). Measurement was facilitated by *Image Analysis*, techniques which extract information from photographs by the use of computer programs, as summarized in Chapter 2, and elaborated upon in Appendix B. The principles of *Stereology* allowed the estimation of two-dimension and three-dimension geometrical parameters from one-dimensional measurements. The essential principals of stereology, as used in the research, are presented in Chapter 2. Although many stereological exercises were performed, only the results relevant to the estimation of volumetric proportion and block size distributions of melanges are discussed in this dissertation.

Many of the techniques used in the research were developed by using *graphic models*, which were photographs of melanges and model block-in-matrix materials. *Gravel Tests* were image analysis and stereological exercises performed on photographs of arrays of gravel and sand contained within a 50 cm square white board. The *Gravel Tests* procedures are described in Chapter 2, the relevant results are summarized in Chapter 4; and the data are summarized in Appendix C. Also, photographs of the unrolled tracings of the surfaces of 14 *Triaxial Test Specimens* of model melanges, fabricated by Lindquist (1994b), were used to make stereological measurements of block arrangements of known block volumetric proportions and block size distributions. The procedures are described in Chapter 2, the relevant results are presented in Chapter 4, and the data are summarized in Appendix D.

1.7 PRACTICAL APPLICATIONS OF THE RESEARCH FINDINGS

The techniques developed from the research were tested at three *Case History* sites, the results being summarized in Chapter 5. Excavation and geotechnical remediation of the Lone Tree Slide, on Highway 1, near Stinson Beach, Marin County, California provided an opportunity to compare predictions based on measurements of drill core of Franciscan melange against the results obtained from mapping and the construction experience of the earthwork contractor. Photographs of drill core of a Franciscan melange allowed estimates to be made of the volumetric proportion of blocks in the foundation rock of Scott Dam, which impounds Lake Pillsbury, Lake County, California. Measurements were made of drill core recovered during the geological exploration in Franciscan melange for the Richmond Transport Project Storage Tunnel, San Francisco, California,

which permitted estimates to be made of the volumetric proportion of blocks and block size distribution.

In a separate office study using large-scale geological maps, an attempt was made to relate the hillside slope angles at several locations in Franciscan melanges to the apparent proportion of blocks in the hillsides. The results of these *Franciscan Area Studies* are discussed in Chapter 4, the procedures outlined in Chapter 2, and the data summarized in Appendix E.

An example application of some research results is presented in Section 4.9.

CHAPTER 2 BACKGROUND CONCEPTS and RESEARCH PROCEDURES

2.0 INTRODUCTION

This chapter summarizes fundamental concepts and data-collecting techniques used during the research, the results of which are presented in other chapters. Lengthy or distracting procedures and data are presented as Appendices.

2.1 MELANGE LITERATURE DATABASE AND WORLD-DISTRIBUTION MAPS

Melange bodies have been mapped in several parts of the world. As a part of the literature search for this dissertation, academic and government agencies were contacted in many of the approximately 70 countries that host melanges. The search yielded some useful information, and generated considerable interest in the engineering characterization of melanges among engineers and geologists world-wide. Prior to contacting correspondents, a relatively comprehensive database of melange references was developed, and summary maps of the regional distribution of melanges were prepared. The maps, and associated references, are shown in Appendix A.

The database was created in several steps:

1. The GeoRef™ computer-based geoscience database (published by the American Geological Institute) was searched for all references (to summer 1993) showing the keyword "melange". Some 1960 references identified by the search were downloaded onto 1.2 MB floppy disks in ASCII format. There were virtually no references that addressed the engineering aspects of melanges.

2. Using Papyrus™ (version 7.0)[1], a bibliographic computer program, the reference data were imported into a database by modifying the software import protocols to retain several useful data fields for each reference, including map co-ordinates of study areas. Almost 7000 keywords were preserved, including hundreds of geographic place names.

3. The Papyrus™ database was sorted by country. References for the United States and Canada were subdivided by state, and those for California further subdivided by county.

---

[1]Research Software Design; 2718 SW Kelly St., Suite 181; Portland, Oregon 97201; phone: (503) 796-1368; FAX: (503) 241-4260; e-mail: RSWD@applelink.apple.com

4. Many references were plotted onto maps printed from the geographic computer programs World Atlas (v. 3.0)[2] and US. Atlas (v.3.0)[2], using the map coordinates of reference study-areas, the geographic place names and a comprehensive atlas with a gazetteer. Some imagination was necessary in interpreting foreign place names (particularly Chinese and Russian); consequently some melange locations may be shown incorrectly. A sample of the locations were plotted on the world and regional maps of Appendix A. Papyrus™ was used to cite references and prepare the List of References shown in Appendix A.

5. After the countries and the general areas of the melange bodies had been identified, requests were made of foreign scholars and agencies to provide information on the geo-mechanical properties and behavior of melanges in their countries. Most of the names and addresses of the correspondents were obtained on a floppy disk from the National Landslide Information Center in Denver[3]. During the course of the research, nearly 180 letters and E-mail messages were sent, and over 70 people replied. Some of the literature received was of considerable interest, particularly to Lindquist (1994b) in his study on the mechanical behavior of melanges

2.2 SUMMARY OF IMAGE ANALYSIS PROCEDURES

Since a major goal of the research was to characterize blocks, it was necessary to measure block sizes, areas and orientations. Initially, such work was done manually, but the work was tedious and inaccurate. Subsequently, measurements were made using *image analysis* procedures, which extract quantitative information from images by using computer programs. Some geotechnical and geological practitioners of image analysis use some very sophisticated methods (Fabbri, 1984; Bhatia and others, 1987; Farmer and others, 1991; Frost and Wright, 1993; Kemeny, 1993; Kemeny and others, 1993). However, the procedures used in the research were relatively straightforward and used readily available computer software. A brief summary of the procedures is presented below and Appendix B contains technical details, illustrations and computer program codes.

Snapshot-sized color photographs were digitally scanned at resolutions of less than 100 dpi (*dots per inch*), and the images converted to computer data files as arrays of *pixels* (*pic*ture *el*ements), each pixel having a gray scale value, ranging from 0 (pure black) to 256 (pure white). Scanning was performed using a hand scanner controlled through the graphics programs Micrografx™ Picture Publisher (v.3.0)[4] or Adobe Photoshop. These programs were also used to change image dimensions and gray shade contrast; enhance

---

[2]The Software Toolworks, Inc.; 60 Leveroni Court; Novato, California 94949; phone (415) 883-5157
[3]National Landslide Information Center; US Geological Survey; Box 25046-MS 966; Denver Federal Center; Denver, Colorado 89225-0046; phone (800) 654-4966; FAX (303) 273-8600
[4]Micrografx; 1303 Arapaho, Richardson, TX 75081; phone 214-234-1769; 800-733-3729; approx. $250

the edges of blocks; convert gray scale images to binary images (just black and white); add text and symbols, and delete or change the orientation of parts of the images.

Most image analysis programs are intended for biological research, astronomy or military surveillance. Initially, image analysis work was performed with NIH Image[5], a powerful, user-friendly program originally developed by the National Institute of Health for the measurement of images of body particles and tissue. The program, which required a Macintosh computer, recognized clearly distinguished particles surrounded by matrix and automatically measured each particle's area, maximum and minimum dimensions, orientation, and the user's choice of many other features. To be used, the image had to be converted to a *binary image* composed of only black and white pixels ("0"s and "1"s).

Access to Macintosh computers was limited, and the NIH Image program could not easily discriminate blocks from matrix on images of melange. So, most subsequent work was performed using SigmaScan/Image™ (v.1.0)[6], a Windows-based program which did not perform automatic measurement of particles, and manipulated gray scale, rather than binary, images. The outlines of blocks were traced onto virtual "overlays", and the program measured the areas and maximum dimensions (the most important parameters) as well as perimeter lengths and orientations of each block. Using SigmaScan/Image™, one-pixel wide traverses (*scanlines*) across images were made, in which the gray scale pixel values along the traverse were recovered, and then converted into block chord lengths by short computer programs written for the research.

More detailed explanations of procedures, example illustrations and program codes are presented in Appendix B. Records of the image analysis work are presented in Appendix C and D.

2.3 STEREOLOGIC METHODS USED IN THE RESEARCH

2.3.1 Introduction

Most of the quantitative work of the research involved the estimate of areal and volumetric proportion of blocks from the linear proportion of blocks as measured from scanlines (linear measurement traverses). True three-dimensional block size distributions (3DBSDs) and two dimensional block size distributions (2DBSDs) were estimated from chord length distributions (CLDs) developed by measuring the length of the intercepts (chords) of scanlines and blocks. 2DBSDs were constructed using

---

[5] NIH Image available via FTP from alw.nih.gov or (128.231.128.251). I obtained my version from Mr. Don Bain, Manager of the Geography Computing Center, McCone Hall, Univ. California, Berkeley

[6] SigmaScan/Image available from Jandel Scientific, 2591 Kerner Boulevard, San Rafael, CA 94901; phone 415 453-6700; FAX: 415-453-7769; released at $500, currently approx. $250, lower for education discount.

measurements of the *maximum observed dimensions* ($\mathbf{d_{mod}}$) of blocks measured from plan views or vertical sections through model and real bimrocks.

The use of linear measurements to estimate areal and volumetric parameters is one of the most common techniques of *Stereology*. Stereologic methods were originally developed to use zero-, one- and two-dimensional measurements to predict the geometry, spatial arrangement and other properties of three-dimensional systems. Much of the literature of stereology describes the application of stereological techniques to the biosciences, metallurgy, and petrology ((Holmes, 1921; Underwood, 1970; Weibel, 1980; Russ, 1986)), and there are only a few references in the geotechnical engineering or engineering geology literature ((Warburton, 1980; Tang and Quek, 1986; Maurenbrecher and Kronieger, 1991; Mauldon, 1993)). The principal research interest in stereology was to investigate the feasibility of making measurements from measurement lines (*scanlines*) through two-dimensional projections of block-in-matrix volumes in order to estimate the volumetric proportion and size distribution of blocks. The two-dimensional projections modeled outcrops and maps, and the scanlines modeled boreholes. Since there were few opportunities to measure the three-dimensional properties of blocks in real bimrocks, a stereological study of models was the best available approach.

2.3.2 The Equivalence of Point, Linear, Areal and Volumetric Proportion

Delesse (1848) showed that the areal proportion of some phase within a matrix (as expressed on a planer section) was equal to the volumetric proportion of the phase. Rosiwal (1898) then showed that the linear proportion of the phase, measured by many random lines across the plane, was equal to the areal proportion. Thomson (1930) showed that the proportion of points that intersected a phase, out of some larger array of points, was also equal to the areal proportion. So, compressing almost 100 years of discovery; extrapolating from microscopic particles to macroscopic blocks; and using the standard symbology of stereology:

$$\mathbf{P_P = L_L = A_A = V_V},$$

or, point density, block linear proportion, block areal proportion and block volumetric proportion are equivalent.

These relationships were independently discovered and rediscovered by workers in many fields (Underwood, 1970; p 27.) The derivations and proofs are not provided here, since they are comprehensively reviewed by Underwood (1970). Of most relevance to the research problem was the equivalence of L_L to V_V, since block volumetric proportion is the independent variable in the work of Lindquist (1994b); and linear proportions, obtained by measuring block intercepts in core from bore holes, are the most accessible data. For the research, the term *scanlines*, was used for any linear measurement line, or traverse. Scanlines were drill core, measurement lines drawn across photographic images of outcrops, model bimrocks, and are thus similar to the real measurement traverses of

Rock Mechanics tradition. The linear proportion was the sum the lengths of intersections between scanlines and blocks, divided by the total length of the scanlines. The sum of the areas of individual blocks, divided by the area of the image, yielded the areal proportion. Comparisons between linear and areal proportions were made to check the validity of the stereological equivalence.

There are many conditions to the applicability of stereological methods (Weibel, 1980 p55-61; Underwood, 1970; Weibel, 1979; Aherne and Dunnill, 1982; Russ, 1986). The more important of these are: the length of the scanlines be kept approximately the same (Underwood, 1970; p 29); scanlines should be traced either extremely close together (so that blocks are intersected by many scanlines) or else far enough apart (so scanlines intersect blocks only once) (Weibel, 1979; p172). To estimate $\mathbf{V_V}$, it is not necessary that the scanlines be parallel nor do they need to occupy the same plane. Of interest was the extent to which the requirement that scanlines be approximately equal could be relaxed. Real scanlines, such as boreholes, are rarely of equal length.

It was difficult to find consistent statistical guidelines for the total length of scanlines, although guidance is given for *point-counting* by Aherne and Dunnill (1982; p. 33-45). Based on his experience, Holmes (1921) recommended that the total length of lines be 100 times the average diameter of the grains being measured. But Krumbein and Pettijohn (1938) quoted others when writing: "it is generally said....that a total traverse length equal to 1000 times the largest particle gives a fair degree of accuracy....". In measuring air bubbles in concrete with diameters of the order of microns, Brown and Pierson (1950), recommended that a 100 inch "Rosiwal Traverse" was sufficient to estimate the air content and mean bubble spacing with a standard error of 0.0005 inches in bubble spacing and 0.4 percent in the air content. Lord and Willis (1951) used a total traverse length of 284 inches to estimate the size distribution of air bubbles (average diameter of 0.008 inches) in concrete, from the distribution of intercept lengths (a traverse to diameter ratio of 35,000). And, the current standard practice for air-content determinations requires that measurement traverses total between 160 inches and 55 inches, depending on the diameter of aggregate in the concrete (ASTM, 1992; Test Designation C-457-90, Table 2).

Because of the considerable range in these recommended lengths of traverses to estimate particle volumetric proportion and size distributions, the problem was investigated empirically with the *Gravel Tests* and exercises with tracings of the surfaces of *Triaxial Test* specimens, as described later in this chapter.

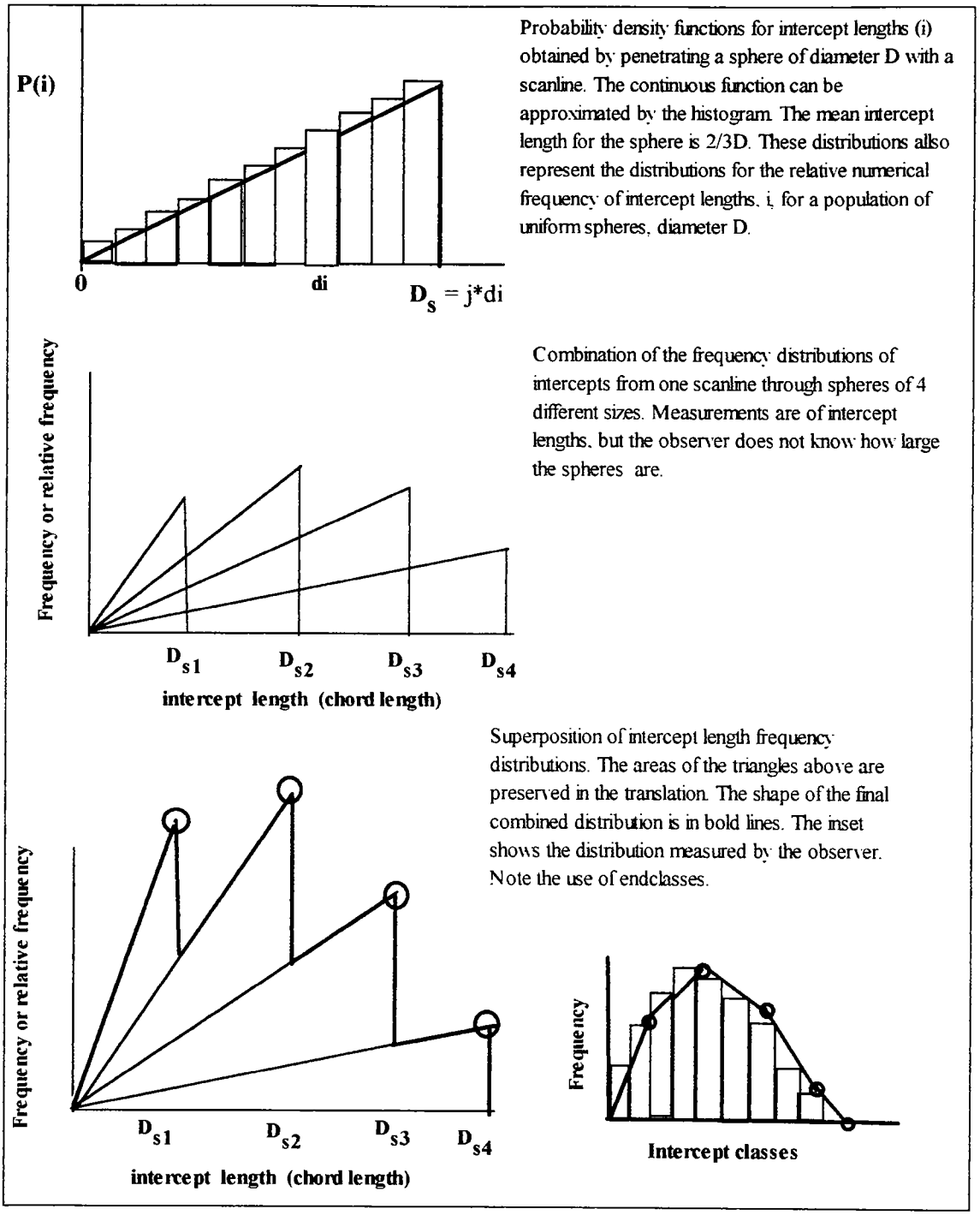

Figure 2.1 Development of the fundamental principles supporting the stereological method of decomposing a distribution of intercept lengths into a distribution of spherical particle diameters. Adapted from (Underwood, 1970; Weibel, 1980; Russ, 1986). Refer to Figure 2.2 for the empirical and classical technique of Lord and Willis (1951).

2.3.3 Background to Stereological and other Methods for Converting Chord Length Distributions (CLDs), and Two-Dimensional Block Size Distributions (2DBSDs), to 3-Dimensional Block Size Distributions (3DBSDs)

The blocks of bimrocks are generally seen only as one-dimensional chord lengths from the intersection of the blocks as drilled core or in two dimensions (on geological maps, or in outcrops). The true block dimensions must be inferred from these projections. This section outlines some (generally) stereological methods for discerning a particle size distribution from a sample population of chord lengths (block intercepts) or cross-sections (block "diameters, or other characteristic dimension) through spherical particles. It should be noted that stereological methods are not the only approach to solving the problems: geotechnical workers have developed statistical and empirical methods to estimate the true 3DBSDs from one-dimensional chord measurements (CLDs) (Tang and Quek, 1986; Savely, 1990).

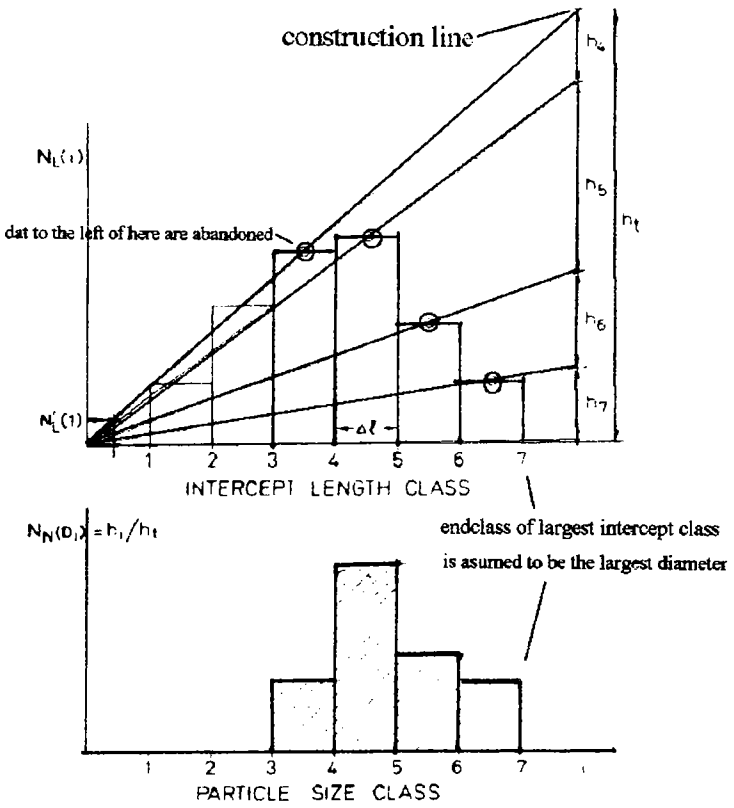

Figure 2.2 The method of Lord and Willis (1951), after Weibel (1979; p.201)

The problem of constructing size distributions from distributions of chords is a classic problem in geometrical probability (Kendall and Moran, 1963; p. 86-91) and stereology

(Underwood, 1970; Weibel, 1979, 1980; Russ, 1986). The mathematical justification for the several methods available, and outlines to the procedures used, are reviewed by the authorities cited. The fundamental problem is: *what is the probability of measuring a certain length of intercept,* **i,** *through a sphere of given diameter,* $\mathbf{D_S}$? From the solution of this problem flows the development of solutions to the extended problems of discovering the probability distribution functions for the numerical frequency of intercepts from one linear traverse through :

1. many uniform-sized spheres
2. many spheres of different sizes
3. arrangements of irregular shapes.

The derivation of the fundamental solution will not be repeated here. (For guidance to the solution of the fundamental problem, the treatments by Weibel (1980; chapter 7) and Underwood (1970; chapter 5) are the most lucid.) The basic principal is that the probability distribution function for intercept lengths, obtained by penetrating a line through a sphere, is a straight line which varies between a probability of 0 for an intercept length of 0, to a maximum probability at the intercept length equal to the diameter D_S. The same triangular probability function can be derived for intercept lengths measured from a line through many spheres of diameter D_S (see Figure 2.1). Because the distribution is triangular in shape, the mean intercept length is $2/3D_S$.

But populations of single-sized spheres are rarely encountered. For a population of many spheres of different sizes, one can superimpose the individual probability distributions as shown in Figure 2.1. Then, for any given intercept length, the frequency is a sum of all the individual frequencies of the separate spheres. The peaks of the distorted triangles are points on a discontinuous curve of a histogram of intercept lengths, as shown in the small inset at the bottom of Figure 2.1.

Note that the distribution of chord lengths from scanline measurements resembles the inset of Figure 2.1, and that it is the inverse of the diameter distribution sought. The problem has been tackled in many ways as shown by Underwood (1970; chapter 5). The approach of Lord and Willis (1951), shown in Figure 2.2, classifies the intercept (chord) data into equal-sized bins in a histogram. The centers of the tops of each class bar are joined by a vector to the origin of the plot, and extrapolated to a vertical construction line to the right of the histogram, the altitude (h_t) of which is defined by the highest such vector. The endclass of the largest intercept length class is taken as the largest diameter. The proportionate length of the segment of construction line between adjacent intersections (e.g.: h_6, for intercept class 5 to 6) is a measure of the relative number of spheres of the same size as that intercept class. The proportion is used in the simple formula, $\mathbf{N_N = h_i / h_t}$, that provides the relative number of spheres for each associated intercept interval. Observe that data classes, smaller than that which defines the altitude of the construction line, are abandoned. Figure 2.2 also shows that, for the example given, for some maximum intercept length, there is an equivalent maximum diameter. In

other words, the maximum diameter is predicted by the maximum chord, although the numerical frequencies will be different. The equivalence is not certain; in some situations the maximum diameter will not be predicted by the maximum chord because of insufficient sampling (either insufficient scanlines or low block proportion).

The problem of converting two-dimensional block size distributions (2DBSDs) into 3DBSDs is similar to the problem of converting two-dimensional microscope measurements of the longest axes of sediment grains, measured from two-dimensional microscope images, into the true diameters of the grains (Herdan and Smith, 1953, p. 237-238; Krumbein and Pettijohn, 1938, p.128-134). In general, the stereological and petrographic literature indicate that the mean "diameter" in two-dimensions is less than the true diameter. For spheres, Krumbein and Pettijohn (1938; p.132) estimate the ratio to be $\pi/4$, or 0.763. Sammis and others (1987, appendix) show a stereological approach to converting a distribution of circular areas into a distribution of spheres.

2.4 SELF-SIMILAR BLOCK SIZE DISTRIBUTIONS

2.4.1 Introduction and Definitions

Work was performed to confirm the scale-independence of the blocks size distributions (**BSDs**) of some Franciscan melanges at several scales. The characteristic dimension of all blocks was defined as the *maximum observed dimension*, symbolized as $\mathbf{d_{mod}}$, and was rarely the same as the maximum dimension ("diameter") through the blocks. Particle size distributions based on the weight of the various size fractions of particles, as encountered in Soil Mechanics, are referred to as "weight-based particle size distributions" (**WPSDs**). BSDs are distinguished from PSDs because they are based on the numerical frequency of the various size fractions of blocks rather than the weight of the fractions. Using BSDs is necessary for melanges since the size of blocks and the difficulty of isolating blocks from the bonded matrix, means that weight-based block size distributions are generally not practical except for small, easily-removed blocks. BSDs constructed using measurements of d_{mod} in two-dimensions and three-dimensions are referred to as **2DBSD**s and **3DBSD**s respectively; one constructed from a distribution of chord lengths is referred to as a **CLD**.

2.4.2 The Concepts of Self Similarity and Fractal Dimension

The chaos of melanges, illustrated in Figure 1.1 and 1.2, can be analyzed in an orderly fashion using the concept of *self-similarity*, which is one aspect of the large field of study devoted to *fractals*. Although the self-similarity of melanges had been pointed out before (Cowan, 1985, his figure 9), no quantitative work was done on the self-similar

aspects of melanges prior to the work of Lindquist (1991)[7] (Professors Darryl Cowan, Kenneth Aalto, Mark Cloos and Loren Raymond; personal communications).

A self similar system is one composed of elements that are replicas of a parent whole. The self-similarity of chaotic physical systems has been demonstrated formally (Mandelbrot, 1983; Peitgen and others, 1992; Turcotte, 1992; Barnsley, 1988), and several review papers on fractals are helpful for earth scientists (Genske and others, 1992; Barton, in press; Middleton, 1991; Turcotte, 1986). Specific papers have been published by workers in Rock Mechanics (Brosch et others., 1992; Carr, 1987; Sen, 1992).

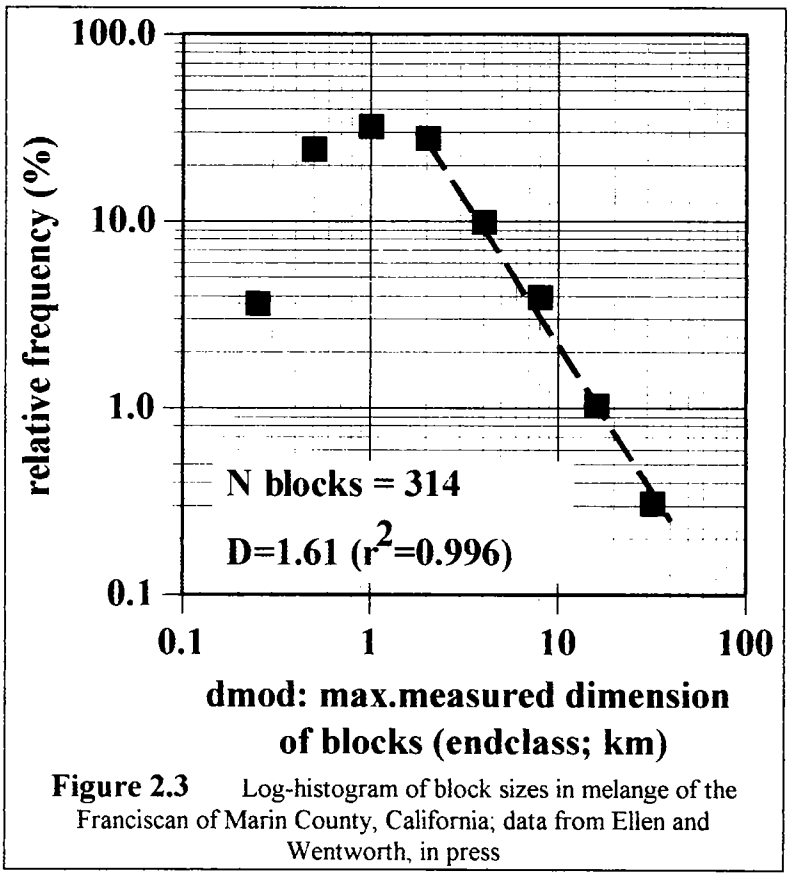

Figure 2.3 Log-histogram of block sizes in melange of the Franciscan of Marin County, California; data from Ellen and Wentworth, in press

Relative to melange, self-similarity means that a sub-area of an outcrop or image of melange, will contain an arrangement of blocks that appears similar to that in the larger area. If the blocks are replaced by vectors representing the d_{mod}s, or maximum dimensions of the blocks, the arrays of vectors in sub-areas will also be similar to those in the larger area. Furthermore, there will be a relative similarity between frequency histograms and cumulative block size distributions constructed from the d_{mod}s of sub-

[7]Eric S. Lindquist; "Fractals- Fracture and Franciscan", Spring 1991, term paper for CE 280, Rock Mechanics, Dept. Civil Engineering; Univ. California, Berkeley; Prof. Richard E. Goodman, Instructor

areas and parent area, although the magnitude of the class intervals of d_{mod} lengths will differ. To discern self-similarity, frequency histograms are plotted using logarithmic axes, and are referred to here as *log-histograms*, adopting a term from Bagnold and Barndorff-Nielsen (1980), who studied grain size distributions, but not self-similarity.

The basic requirement of a self-similar system is that the *fractal dimension*, **D**, be measurable (Mandelbrot, 1983). A fractal dimension is a "broken dimension" (*fractal* is from the Latin *frangere,* "to break") or a dimension that is a fraction. There are over 10 related varieties of fractal dimensions (Peitgen and others, 1992 p.202).The formal definition for the most common fractal dimension is:

$$\mathbf{D} = \log N(r)/ \mathrm{Log}(r)$$

Or, **D** is the ratio of N(r), the numerical frequency of variable r, to the variable r, where r is a frequency class interval. **D** is the absolute magnitude of the slope of the function. Conventionally, data are plotted using logarithmic axes, and the fractal dimension is thus the absolute exponent of a Power Law relation. For the research, it was assumed that the fractal dimensions of a log-histogram of chords through blocks (one-dimensional chord length distributions or CLD); or distributions of d_{mod}s, the maximum observed dimensions of blocks measured in two dimensions (two-dimensional block size distributions, 2DBSDs) were numbers generally between about 1.0 and 2.0. The assumption seemed reasonable since the CLDs and 2DBSDs represented the distributions of a one-dimensional line in one (line) or two dimensions (area). And, intuitively, the fractal dimension for a d_{mod} representing three-dimensional volumes should be between 2.0 and 3.0. (However, Sheridan and others, 1992) discovered that D for large volcanic ejecta varied between 3.3 and 8.0, and Turcotte (1986, his Table 1) listed D between 1.44 and 3.54 for 21 fragmented materials, with 15 of these between 2.0 and 3.05.)

Few other log-histogram representations for grain size distributions were found in the geological literature, except for those of Ghilardi and others (1993); and Bagnold and Barndorff-Nielsen (1980). A linear arrangement of data on a log-histogram is here termed *log-log linear.* Block size distributions which are log-log linear could also be referred to as having *fractal distributions*, although the term in not much used here. As an example of such a distribution, Figure 2.3 shows a log-histogram of block sizes measured from a geological map of Marin County, California (see Figure 3.4), with a fractal dimension, **D**, of 1.61. The right side of the parabola is referred to here as the *descent limb*, which is log-log linear. The left side, the *ascent limb*, is characteristic of log-histograms, and represents data that are *censored*, or undercounted. The apparent undercounting is partly a result of the leftward narrowing of endclass intervals: as the classes shrink, the number of blocks which can be assigned to the classes also diminishes. But the undercounting is also due to the difficulty of identifying and accurately measuring small blocks.

Block size distributions, plotted as log-histograms with well-defined descent limbs and measurable fractal dimensions, established the self-similarity of the bimrock at *the scale of measurement only.* Most self-similar block size distributions were for d_{mod}s ranging over between two and three orders of magnitude. Self-similarity was considered to be a necessary but insufficient indicator of scale-independence. *Scale-independence* required the comparison of several log-histograms covering many scales of measurement and is discussed further in Section 2.5

2.4.3 Selection of d_{mod} Endclasses for Log-Histograms

Relative to the definition of **D** in the previous Section, $N(d_{mod})$ was the number of blocks within some size class containing a range of d_{mod}s (the maximum observed dimension of blocks). It was often convenient to calculate the *relative numerical frequency* of each data set for comparison purposes between different sample populations of d_{mod}. The relative frequency for a class interval was the number of blocks with the range of d_{mod}s in the class, divided by the total number of d_{mod} measurements. The d_{mod} classes were serially "doubled" rightward (i.e.: $x_n = 2x_{n-1}$; ...0.5, 1, 2, 4, ...32, 64, 128....), and the right limit (*endclass*) of an interval was used for x_n. (For example: the numbers above would be endclass values).

The use of endclasses was a departure from conventional statistics where mid-class values are often used, but the *largest* class intervals of block sizes were generally of most interest. (Mechanical sieve analyses also use class limits, in this case "beginclasses"). However, the endclass magnitude for larger classes did not always accurately reflect the d_{mod} data contained in them. For instance, relative to the example series of endclasses in parentheses above, suppose that a d_{mod} of 66 m was the largest block measured in a sample population. The 66 m value would be included in the 128 m endclass, and plotted as such on a log-histogram, giving an incorrect impression of $\mathbf{d_{max}}$, the size of the largest block in the population (an apparent 128 m, rather than the true 66 m). This implies that it was not necessary to precisely measure large block dimensions, since they would later be assigned to wide endclasses. However, care was taken to accurately measure d_{mod}s wherever possible in order to calculate the descriptive statistical parameters of the data.

To develop a series of endclasses, a "node" endclass was selected, and the remaining classes "doubled-up" and "halved-down" from the node. The doubling of classes is originally based on the "box-counting" technique commonly used to automatically determine fractal dimensions using computers (Peitgen and others, 1992). (Box-counting requires that the system to be measured be overlain by a series of measurement grids, each of which has a mesh double that of its predecessor). A major problem was deciding on a node. Possibilities included starting with the very largest d_{mod} (this is $\mathbf{d_{max}}$) and defining the other classes by halving-down from this size (e.g.: 12.6 m, 6.3 m, 3.15

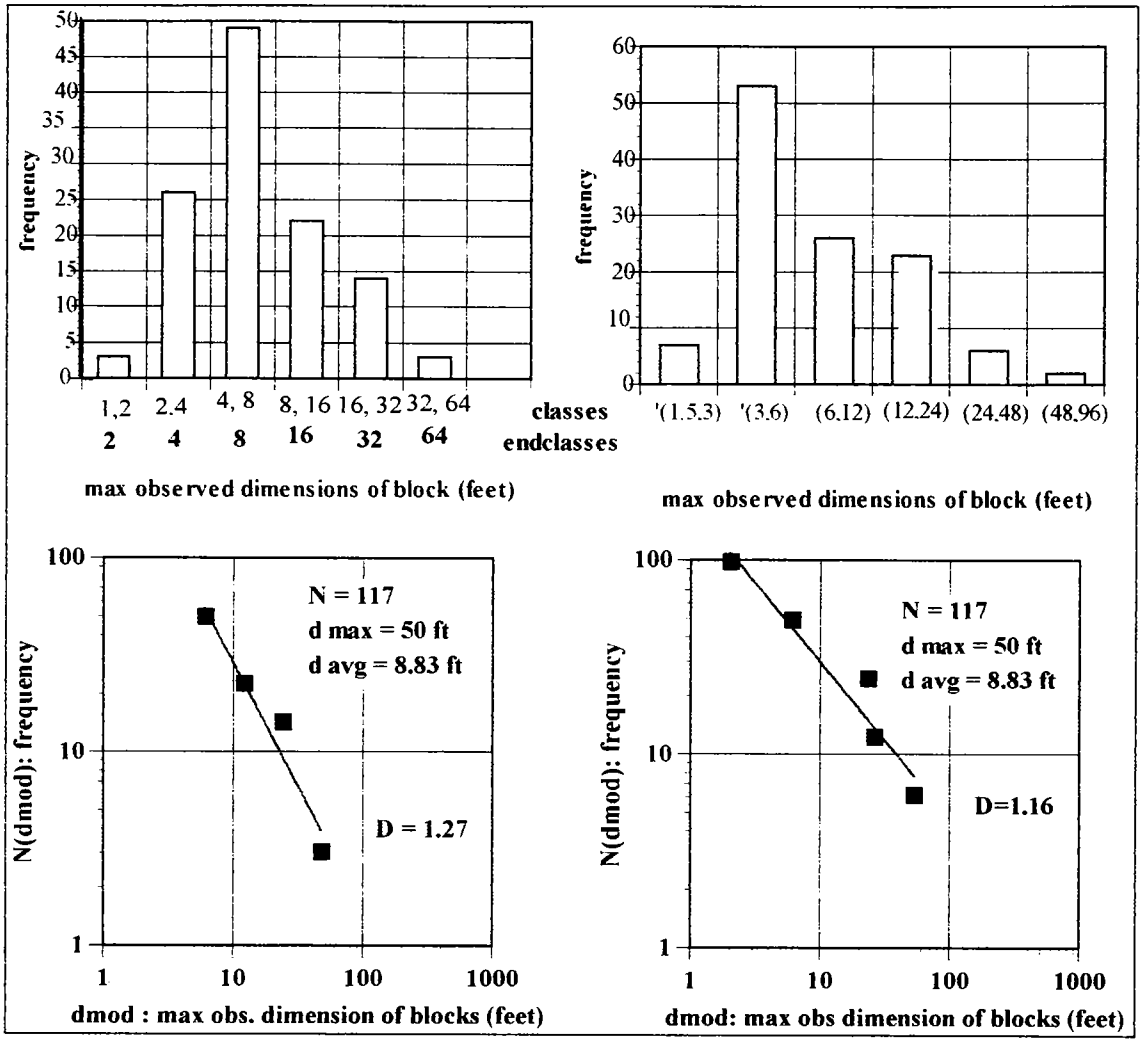

Figure 2.4 The effect of changing histogram classes on the fractal dimension, **D.** Data are d_{mod}s measured for blocks exposed at Lone Tree Slide on Hwy. 1, Marin County, California

m,.....1.975 m, 0.098m) Or, to avoid awkward numbers one could round-off d_{max} and halve-down (e.g.: 15 m, 7.5m, 3.75 m .....).

But making minor adjustments to the magnitude of the endclasses, sometimes resulted in dramatic changes to the fractal dimension of the log-histogram. Figure 2.4 shows the conventional histograms and the log-histograms (descent limb data only) for the same set of measurements of d_{mod} of blocks exposed at Lone Tree Slide (one of the Case Histories: see Chapter 6). The apparent fractal dimensions are different in the two plots.

Based on the demonstration of the scale-independence of Franciscan melanges (section 2.5), a standardized approach to the selection of endclasses was developed. For blocks measured in two dimensions, such as from maps, the total area containing blocks and matrix was measured. The individual areas of blocks partially within the measured area

were subtracted from the total area to yield a block measurement area, **A.** , with a square root, $\sqrt{\mathbf{A}}$. The value of $\mathbf{0.04\sqrt{A}}$ was calculated and used as a node around which the endclasses were expanded (halved-down leftwards for increasingly narrower endclasses, and doubled-up rightwards for increasingly wider endclasses). For example, with a $0.04\sqrt{A}$ value of 52 m, the progression would be ...., 13, 26, 52, 104, 208..... .

For chord length data such as the length of blocks as measured in drill core, the procedure was not standardized. The *characteristic engineering dimension* (see Chapter 1) was used or the size of the largest block (as observed by field work) was selected, and the node selected as 5 percent of that dimension. (Suggestions for the selection of the characteristic engineering dimension for various situations are given in Section 2.6.3). For example, for the Lone Tree Slide core data, the node was 5 percent of the average thickness of the landslide.

2.5. DEMONSTRATION OF THE SCALE-INDEPENDENCE OF SOME FRANCISCAN MELANGES

For the purpose of this dissertation, *self-similarity* refers to the fractal block size distribution at one particular scale. A self-similar, or fractal, block size distribution shows a well-defined, generally linear, descent limb when plotted as a log-histogram, as shown by Figure 2.3 and Figure 2.4, despite the sizes of the maximum blocks differing by 4 orders of magnitude. If the self-similarity can be shown to extend over several scales, then the block size distributions are termed *scale-independent.* At the beginning of the research, the qualitative scale-independence of melange was apparent in outcrops (for example Fig 1.1 at Point Delgada, California) which looked much like the geological map of an area of melange (Figure 3.4) or the microphotograph of a thin section of melange (for example: Aalto, 1989, his figure 24). One of the results of the research was to formally demonstrate the scale-independence of <u>some</u> Franciscan melanges. The word "some" is important because, although measurements were made of many areas of melange in the Franciscan, more are required to conclusively demonstrate that <u>all</u> Franciscan melanges are invariably scale-independent.

This section provides a demonstration of the scale-independence of a Franciscan melange at Caspar Headlands, near Mendocino, California, where Lindquist (1991) had determined the fractal dimension, **D** to be 1.18. for a 6 m^2 melange outcrop. Lindquist (1991) measured blocks manually, but for the work summarized here, image analysis was used to measure blocks from a series of six photographs taken at another outcrop of melange at Caspar Headlands. The series was generated by incrementally "zooming-in" on one portion of the outcrop. Except for the smallest scale photograph (largest area), each photograph contained small blocks that appeared larger in the next larger-scale photograph. The photographs were scanned at a resolution of about 100 dpi. A 1.52 m (5 ft) measuring tape in each image allowed spatial calibration for image analysis. SigmaScan/Image™ was used to measure between 75 and 300 blocks for each image, for

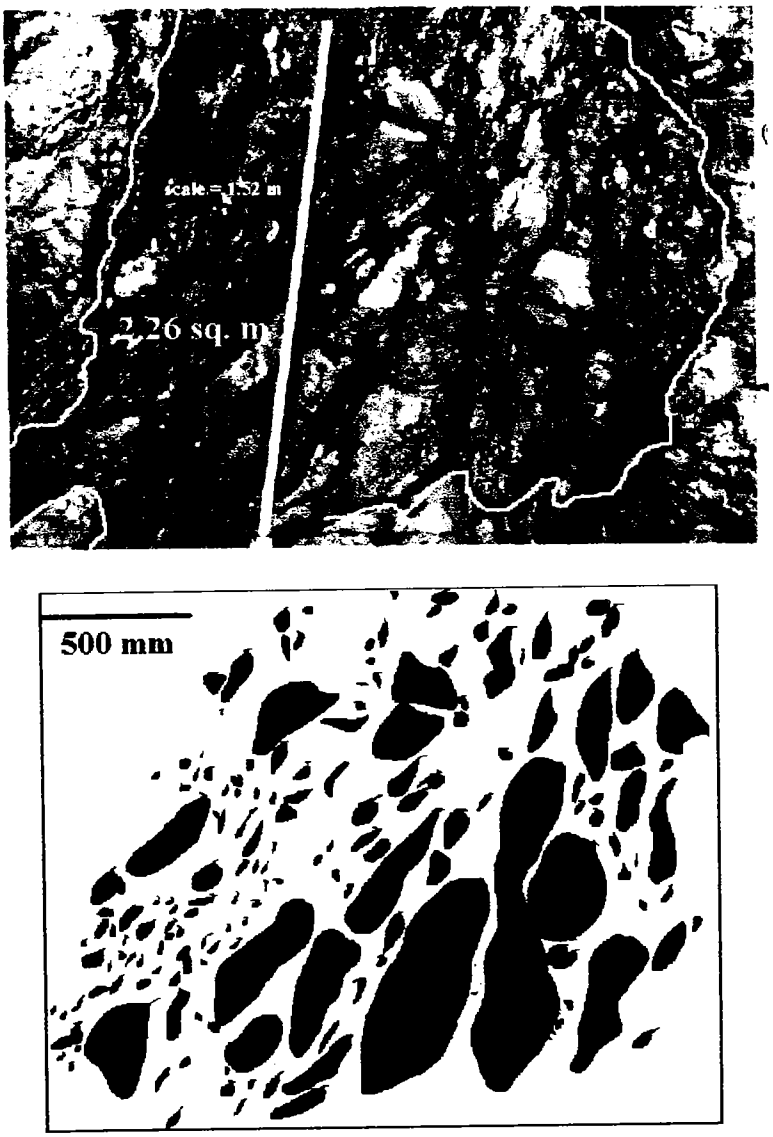

Figure 2.5 The top picture is one of a series of 6 photographs of the same outcrop at Caspar Headlands. The white bar is 1.52 m, and the area measured (within the white line) is 2.26 m^2. The bottom picture shows the 173 blocks measured by SigmaScan/Image™

a total of 1080 blocks. Blocks that were not completely contained within the photographs were excluded from the measurements.

The top picture of Figure 2. 5 shows a typical image, with a measured area of 2.26 m^2 within the white boundary. The lower picture of Figure 2. 5 shows the tracings of the 173 blocks measured. For the six images, measurement areas ranged between 0.04 m^2 and 18.92 m^2. Not all blocks were measured or were measurable, due to the low resolution of

scanning. But blocks under-counted at one scale were measured in the next, larger scale (smaller area). The maximum block in Figure 2.5 is 95 cm, the minimum 2 cm, the average 9 cm and the standard deviation, 11.5 cm. The wide interval between the mean block size and the maximum block size is typical of a self-similar block size distribution.

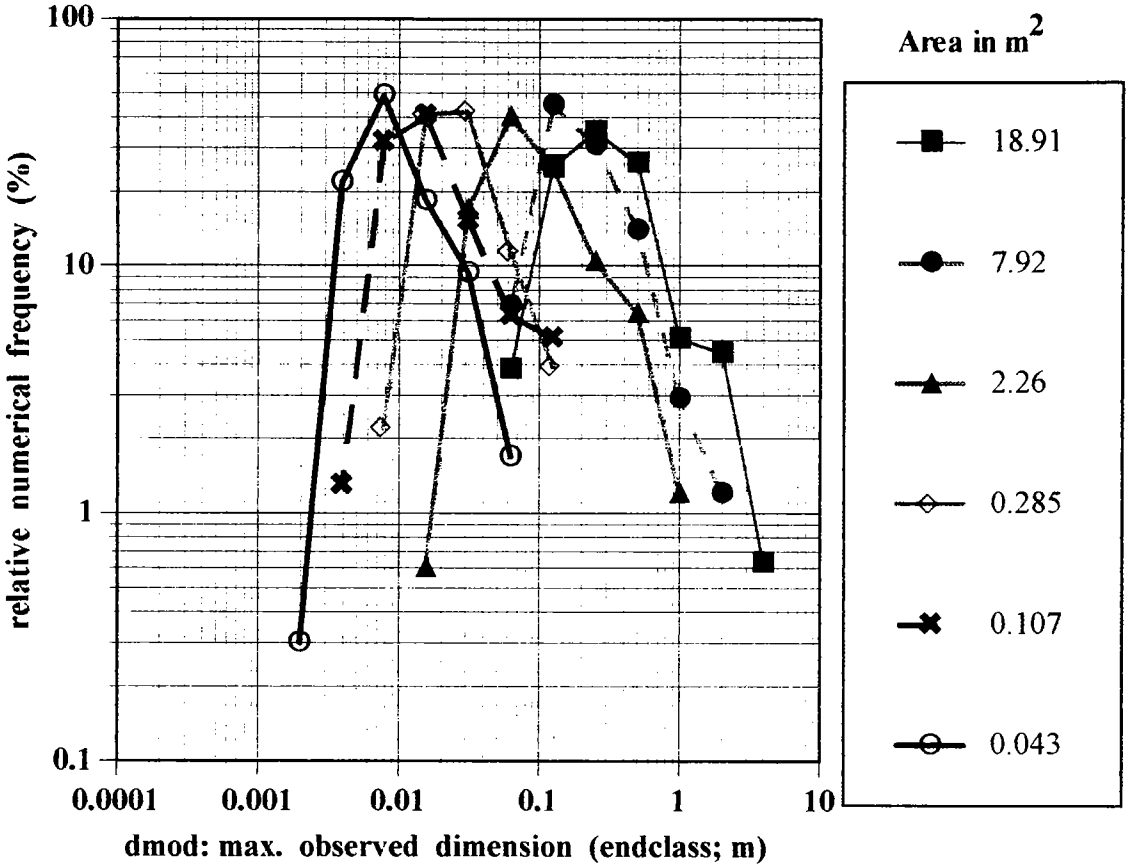

Figure 2.6 Log-histograms of the 2DBSDs at several scales from one outcrop of Franciscan melange at Caspar Headlands, Mendocino, California. Approximately 1080 blocks were measured using SigmaScan/Image™.

Log-histogram plots were prepared for each of the six sets of d_{mod} results, and are compiled as Figure 2.6. The plots are remarkably similar. Also, d_{mod} data on the ascent limb of a particular plot (representing under-counted or censored data) are well represented on the descent limb of the plots for the larger scales of measurement (toward the left). In this sense, there is *overlap* between the log-histograms since censored d_{mod} values at one scale are not censored at larger sales.

In order to compare the plots, and verify the scale-independence of the melange at this outcrop, the plots of Figure 2.6 were normalized by the square root of the measurement areas containing the measured blocks, ($\sqrt{\mathbf{A}}$), which is an easily determined parameter that is independent of the block size distribution. Figure 2.7 shows the individual data points

of the six plots collapsed to a well-defined constellation, which resembles any one of the individual log-histograms. The plot in Figure 2.7 is convincing evidence for the scale-independence of the melange at this one outcrop, over 3 orders of magnitude. Regarding the envelope of data, other observations are made:

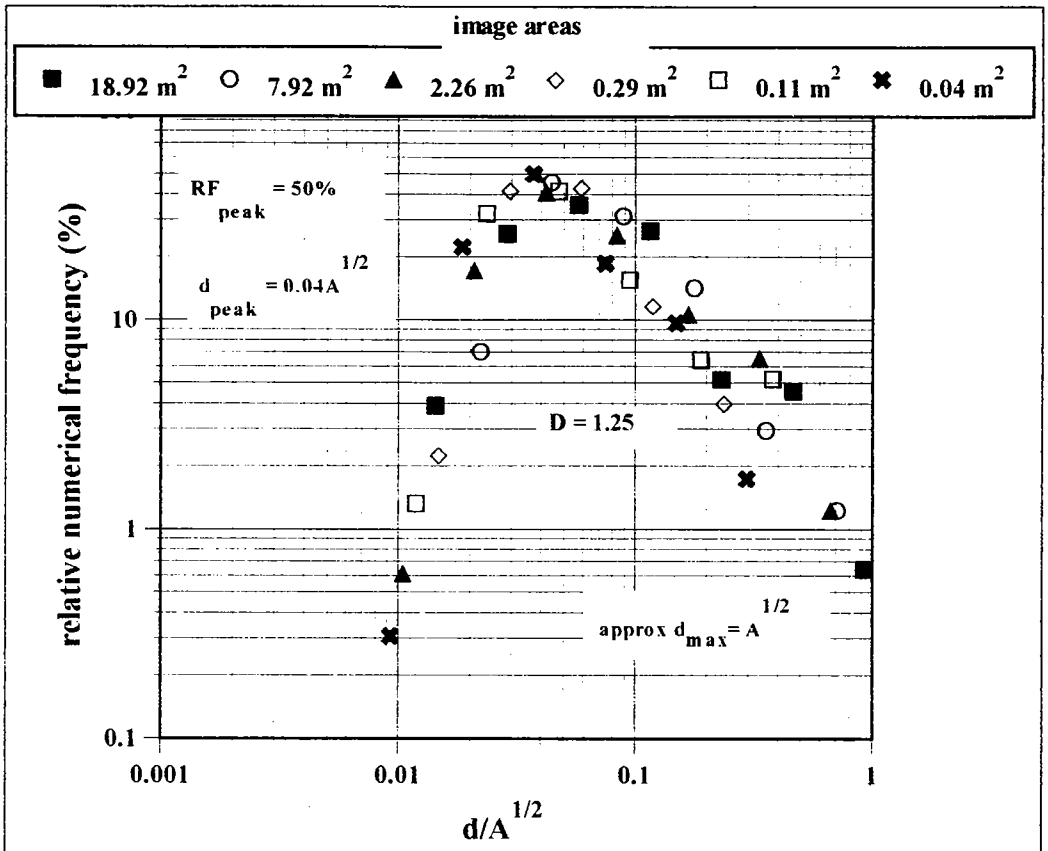

Figure 2.7 Log histograms of block sizes (2DBSDs) at a melange outcrop, Caspar Headlands; collapsed by normalizing the d_{mod} data by the square root of the area containing each set of blocks. The plot summarizes measurements of 1080 blocks.

1. the peak relative frequency, $\mathbf{RF_{peak}}$ is 50 percent.
2. the largest block size, d_{max} , is approximately equal to the square root of the measurement area ($\sqrt{A}$), or : $\mathbf{d_{max} = \sqrt{A}}$, at a Relative Frequency of 0.6 percent.
3. the d_{mod} (endclass) at the peak, or $\mathbf{d_{peak}}$ is 4 percent of the square root of the measurement area ($\sqrt{A}$), i.e.: $\mathbf{d_{peak} = 0.04\sqrt{A}}$, or from expression 2.: $\mathbf{d_{peak}=0.04d_{max}}$
4. **D**, the fractal dimension, is approximately 1.25.
5. 99 percent of the blocks are less than $\mathbf{d_{mod}/\sqrt{A} = 0.7}$
   or since $d_{max} = \sqrt{A}$, $\mathbf{d_{mod}/d_{max} = 0.7}$

The results of this exercise, performed for one outcrop of Franciscan melange at Caspar Headlands, were an encouraging and satisfying extension to the work of Lindquist

(1991), in which he measured a fractal dimension of 1.18 for a 6 m^2 outcrop of melange located several hundred feet away.

However, the overall scale-independence of Franciscan melanges at engineering scales could not be demonstrated on the basis of the study of one outcrop, so the work was expanded to incorporate measurements of blocks of Franciscan melanges with areas ranging between 1 km^2 and 40 km^2. The data were measured from the geological maps of Peterson (1979), Reid (1978), Savina (1982), Seiders (1982), and Erikson (1994): the descriptive details and the data from these *Franciscan Area Studies* are presented in Appendix E. Additional measurements were added of blocks from a geology map of Marin County (1000 km^2), prepared from originals by Ellen and Wentworth (in press), and shown in simpler form as Figure 3.4. Data from field mapping at the Lone Tree Slide (Chapter 5) were also included. All d_{mod} data were normalized by the square root ($\sqrt{A}$) of the various measurement areas, which thus ranged between 0.04 m^2 and 1000 km^2. The compilation of data are presented in Figure 2.8

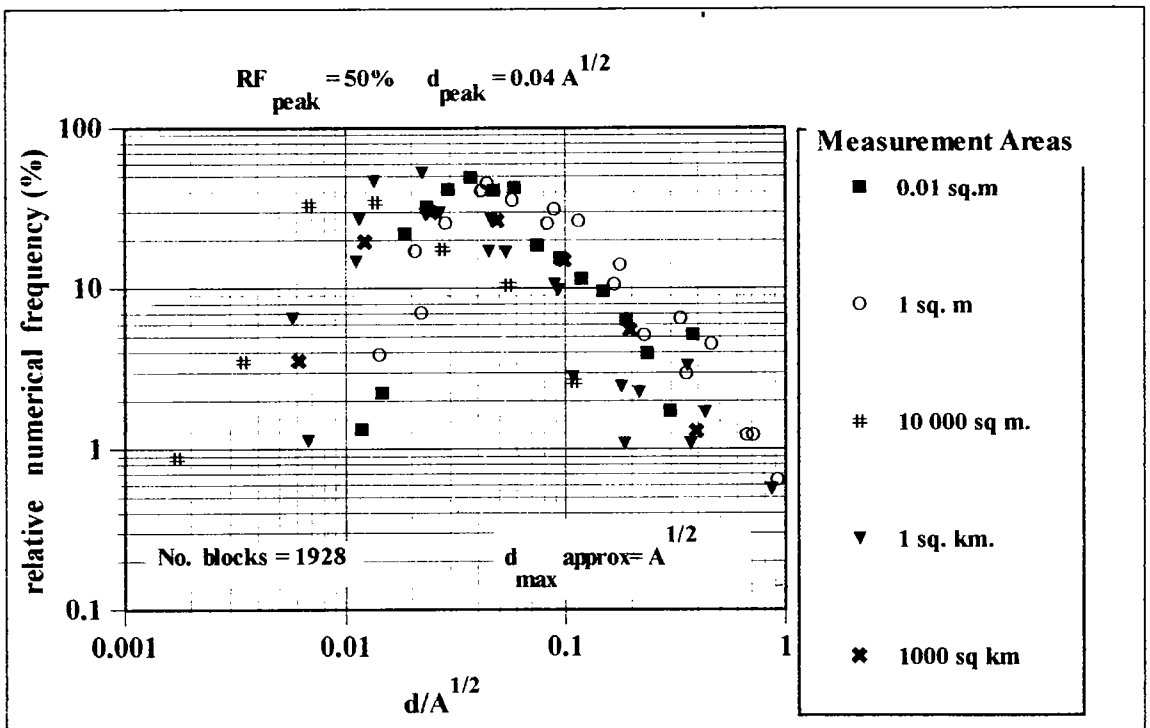

Figure 2.8 Compilation of all Franciscan block size distributions (2DBSDs); measurement areas range over seven orders of magnitude. $A^{1/2}$ is $\sqrt{A}$, the square root of measurement area; d is d_{mod}, the maximum observed dimension.

Despite the range of seven orders of magnitude in the scales of measurement, the data array resembles the individual log-histograms. Further, the observations made for Figure 2.7 are generally valid for Figure 2.8 as well: $\mathbf{d_{peak}}$ is approximately $\mathbf{0.04\sqrt{A}}$; $\mathbf{RF_{peak}}$ is

approximately 50 percent; $\mathbf{d_{max}}$ approximately ($\sqrt{A}$) and **D**, approximately **1.2** (with r^2 = 0.8 for the curve fit; the fractal dimensions of the individual Franciscan melanges measured from several areas, varied between approximately 1.0 and 1.6). Also, 99 percent of the blocks are less than $\mathbf{0.7\ d_{mod}/d_{max}}$; in other words, nearly all the blocks have measured dimensions (d_{mod}) less than 70 percent of the size of the largest block.

Based on the data of Figure 2.8, the two-dimensional block size distributions (2DBSD) of some Franciscan melanges appear to be scale-independent. Accordingly, studies of melanges or models of melanges at tractable scales were useful in understanding the properties of a melange at engineering scales. The $\mathbf{0.04\sqrt{A}}$ result was used to define "nodes for the selection of endclasses for subsequent log-histograms, as discussed in Section 2.4. The $\mathbf{0.7\ d_{mod}/d_{max}}$ result supports the 0.75 d_{max} criteria used to determine the upper size of geotechnically significant blocks in a bimrock (Chapter 1, and next Section).

2.6 DETERMINATION OF THE GEOTECHNICAL SIGNIFICANCE OF BLOCKS IN A BIMROCK

2.6.1 Introduction

In Chapter 1, part of the definition of a bimrock required that the blocks be *geotechnically significant*, meaning that all the criteria below be satisfied:
1. There must be a mechanical contrast between the strength of the blocks and the matrix.
2. The smallest and largest blocks must influence the rockmass properties at the scale of the characteristic engineering dimension.
3. The block volumetric proportion must be between 25 percent and 75 percent.

These tentative criteria mean that some block-in-matrix rocks are <u>not bimrocks at all scales</u>, because they lack mechanical contrast between blocks and matrices and/or do not have geotechnically significant block sizes. For example, a pebbly mudstone being penetrated by a Tunnel Boring Machine, may be a bimrock at the scale of laboratory testing, but is not a bimrock at the scale of the tunnel diameter.

2.6.2 Determination of the Mechanical Contrast Between Blocks and Matrix

The determination of the mechanical contrast between blocks and matrix is relatively straightforward, since the separate mechanical properties of the matrix and blocks are usually measurable. Research is necessary to establish appropriate criteria for the contrast between blocks and matrix using various mechanical properties. However, it is tentatively suggested that any one or a combination of the following be used:
1. Stiffness (E)
2. Friction angle (ϕ)

3. Unconfined Compressive Strength (q_u)
4. Cohesion (c; or S_i , the shear strength intercept).

As examples, the use of stiffness and friction angle for establishing the contrast between blocks and matrix are presented. But, the formal definition of these and other criteria would be useful research.

Stiffness Contrast: In his work with model melanges fabricated using different lean concretes for the matrix and blocks, Lindquist (1994) found that a stiffness contrast (E_{block}/E_{matrix}) of about 2 was sufficient to mechanically discriminate the components, such that failures invariably passed around the blocks.

Friction Angle Contrast: The average friction angles for melange below the foundation of Scott Dam, near Ukiah, California, with ϕ'_{block} of 54 degrees, and ϕ'_{matrix} of 29 degrees (Volpe and others, 1991) provides a ratio ($\tan \phi'_{block} / \tan \phi'_{matrix}$) of 2.48. This result can be compared with the friction angle contrast of 1.6 between the blocks and matrix for the model melanges prepared by Lindquist (1994) (ϕ_{block} of 37 degrees and ϕ_{matrix} of 25 degrees). Since the latter relatively low block/matrix contrast was sufficient for Lindquist's work, it is possible that a minimum block/matrix contrast (ϕ-basis) of between 1.5 and 2.0 may suffice for real bimrocks.

2.6.3 Selection of a Characteristic Engineering Dimension

Criteria for determining the geotechnical significance of blocks, as described in the following sections, require that a decision be made on the length of the characteristic engineering dimension. Tentatively, it is suggested that the choice is a matter of geotechnical engineering judgment, at least until more research is conducted. In general, the dimension should be the minimum necessary to describe the site, engineering facility, laboratory specimen, in-situ test set-up, and so on. Suggestions are presented here for some engineering situations:

1. **Plan view,** reconnaissance estimate: $\sqrt{\mathbf{A}}$, where A is the area of the site, and excludes partial blocks.
2. **Cross-section view**, reconnaissance estimate: the lesser of the average depth of the cross-section, or $\sqrt{\mathbf{A}}$ of the cross-section area.
3. **Cross-section, landslide:** average depth of landslide, or the average depth of exploratory borings, if the landslide geometry is poorly defined.
4. **Footings**: the more critical of; minimum footing dimension, or depth to substantial pressure bulb diminishment (a function of footing width, and bimrock fabric orientation; see Goodman (1989, Chapter 9).

5. **Tunnels**: the more critical of; excavated diameter, or the width of the zone of influence of rock mass stress (usually a factor of diameter; see for example Brady and Brown (1985, Chapter 7).
6. **Excavations:** the more critical of; cut height, or depth to design failure surface.
7. **Dam foundations**: the more critical of; dam width, dam height, or minimum design depth (shear failure surface; pressure bulb diminishment; thickness of grouted region; and so on).
8. **Laboratory specimens:** diameter, if cylindrical; minimum dimension if some other shape.

2.6.4 Determination of the Limiting Sizes of Blocks at the Scale of the Characteristic Engineering Dimension.

The limiting sizes (*smallest* and *largest*) of geotechnically significant blocks depend on the scale of engineering interest. At the scale of some characteristic engineering dimension, blocks smaller than the smallest geotechnically significant block can be considered to be part of the matrix, so a threshold size between blocks and matrix must be discriminated. On the other hand, at the same scale there is an upper limit to the size of blocks, beyond which the rock mass may be considered to be *blocky rock*, or a rock mass composed of prisms of rock separated by weaker discontinuity infillings. Blocky rock is well addressed in Rock Mechanics, and is little considered in this dissertation.

The problem of finding the limiting sizes of blocks is separate from that of the determination of the block size distribution (BSD), which is concerned with the measurement of the sizes of individual blocks in the bimrock between the limiting sizes. But there is a relationship between the determination of BSD and block volumetric proportion. For example: higher block proportions mean that for a given length of scanlines, there will be more chord length data, and the BSD will be better estimated. Geometrical probability considerations such as this were not deeply considered during the research. The relationship between BSD and block volumetric proportion relative to bimrock strength is considered in Section 4.4.2.

2.6.4.1 Determination of the Smallest Block (Block/Matrix Threshold) Using the 0.05 d_{max} Criterion

An empirical approach was devised to select the threshold size between matrix particles and blocks. Figure 2.9 shows the dimensionless plots of the cumulative contribution of blocks to the total length of block "diameters", circumferences, cross-sectional areas, block surface areas, and volumes. With melanges, a dimensionless approach is necessary since blocks are found at all scales. The distribution shown is for a self-similar block size with **D** of 1.2, based on data measured for the Lone Tree Slide Case History, presented in Chapter 5.

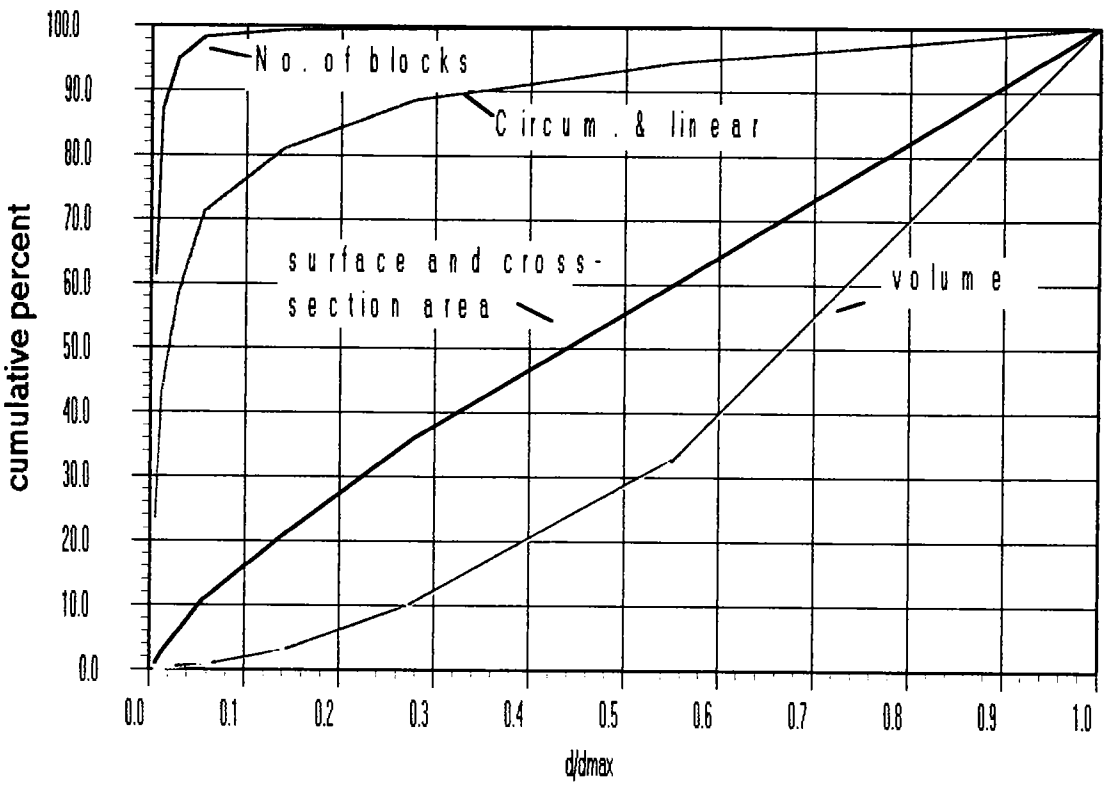

Figure 2.9 Plot of dimensionless BSD (Block Size Distribution) for a typical population of blocks in Franciscan melange, with "diameters" ranging between 0.3m and 55m. Blocks smaller than 5 percent of the largest block (d_{max}) represent 95 percent of the total number of blocks but less than 1 percent of the total volume of blocks. The threshold dimension between blocks and matrix was selected as $0.05d_{max}$

In Figure 2.9, d_{mod} is the maximum observed dimension, (here assumed to be the diameter of spherical blocks) and ranges from 0.3 m to 55 m. The largest size is $\mathbf{d_{max}}$, which is generally the size of the largest likely block. But in some situations the length of d_{max} may be approximated by $\sqrt{\mathbf{A}}$, where A is the area of interest; and in other situations the characteristic engineering dimension, (see suggestions presented in Section 2.6.3) of the site may be substituted for d_{max}, in order to determine the limiting sizes of blocks as described in Chapter 1, and amplified in Section 2.6. The plot shows that small blocks (low d_{mod}/d_{max}) constitute the greatest numerical proportion of the block population, but make only small contributions to the total surface area, cross-sectional area and volume of the blocks. For instance, blocks with a diameter of 5 percent of d_{max} ($d/ d_{max} = 0.05$), constitute 95 percent of the total number of blocks, but contribute less than 1 percent of the total volume of blocks. Since Lindquist (1994a,b) showed that there is a direct relationship between the volumetric proportion of blocks and the overall strength of a bimrock, it is justified to assume that the blocks smaller than $0.05\ d_{max}$ contribute little to the strength of the bimrock. In other words, the smaller

blocks are not *geotechnically significant.* (However, the smaller blocks do contribute a considerable proportion of the circumferential length of the blocks, which would be an important consideration for a two-dimensional analysis of potential failure surfaces around the blocks (i.e.: the "roughness", or asperity considerations).

The reasoning behind the 0.05 d_{max} criterion described above, is supported by the $0.04\sqrt{A}$ or $0.04d_{max}$ rule deduced in Section 2.5, where it was shown that some Franciscan melanges appeared to be scale-independent. Figure 2.8 of Section 2.5 illustrated that $\mathbf{d_{peak} = 0.04\sqrt{A}}$, where $\sqrt{A}$, is the square root of the area of measurement, and d_{peak} is the block size below which the blocks are under-represented, or too small to be completely counted. In other words, d_{peak} represents a matrix/block threshold, and can be taken as the size of the smallest block. But d_{max}, the largest block at the scale of measurement, is approximated by $\sqrt{A}$, in which case $\mathbf{d_{peak} = 0.04d_{max}}$. Hence, the block/threshold matrix criteria can be taken as 5 percent of $\sqrt{A}$, (or d_{max}), recognizing that there will be some small error in substituting 5 percent for the 4 percent in $0.04\sqrt{A}$. But more error is inherent in the fact that the apparent d_{max} on a log histogram may appear to be the d_{mod} of the actual largest block, because of the wider intervals for large classes (as discussed in Section 2.4.3). It is preferable to use the actual d_{max} rather than the apparent d_{max}, assuming that this is smaller than the characteristic engineering dimension.

Hence, a conservative threshold size between blocks and matrix; or the size of the smallest geotechnically significant block, is: ***5 percent of d_{max},*** *which is the engineers's choice of: a) the size of the largest block likely to be encountered at the scale of engineering interest; b) the characteristic engineering dimension, or c)* ***$\sqrt{A}$.***

As an example of the use of the criteria, assume that the largest block in a melange is 55 m, based on $d_{max} = \sqrt{A}$, where A is the area of interest. Hence, the $0.05d_{max}$ threshold size is 2.75 m and the blocks below 2.75 m can be considered as part of the matrix, at that scale of interest. Now, for a 10 m high road cut in the same melange, the characteristic engineering dimension may be taken as the height of the excavation, and the threshold block size would be 0.5 m. If the scale of interest is further reduced to that of a 150 mm diameter laboratory test specimen collected from the road cut "matrix" (material with blocks less than 0.5 m diameter) then the characteristic engineering dimension is assumed to be the diameter of the specimen, and the matrix/block threshold would be 7.5 mm. It is clear that "matrix" at one scale is "bimrock" at another. As discussed in the section on the volumetric proportion criteria, it is advantageous to test the "matrix" in the laboratory since the blocks in it will contribute strength. The matrix strength must be used if the recommendations of Lindquist (1994b) and Lindquist and Goodman (1994) are to be followed.

Another example is offered. In fabricating model melanges with self-similar block size distributions, Lindquist (1994b) used blocks ranging in size from a minimum of approximately 9 mm to a maximum of about 125 mm to 135 mm. Thus, the smallest particle was approximately 7 percent of the largest ($d/d_{max} = 0.07$), or slightly above the 5 percent criterion suggested by Figure 2.9, and the related discussion above. As a check, using the $d_{peak} = 0.05d_{max}$, criterion where d_{max} is approximated by the characteristic engineering dimension of the test cylinder diameter (150 mm), yields a threshold d_{peak} of 7.5 mm, which again is almost the same as the actual smallest size of block Lindquist used. Thus, smaller blocks were unnecessary since they would have been geometrically (and possibly, mechanically) part of the matrix. Anyway, blocks smaller than 9 mm would not have been manageable, since specimens with high block proportion mixes incorporated at least 900 of the smallest blocks into the mix for one mold (Dr. Eric Lindquist; personal communication).

The two-dimensional block size distributions (2DBSDs) and chord length distributions (CLDs) generated from measuring the blocks of the Triaxial Specimen Tracings showed that d_{mod} s below d_{peak} did not contribute much to the distributions, and from stereological considerations, as shown in Figure 2.2, the data could be neglected. .In the Triaxial Specimen images, some particles were smaller than 9 mm because the cut surfaces had intercepted particles elsewhere than through their diameters. BSDs show these "small" particles to be numerically less than the number of particles at d_{peak}. (Consult the plots in Appendix D, pages D-2 through D-21, which show the inflexions of the semi-log CLDs and 2DBSDs at about 10 mm. Also refer to the compilation plots of pages D-22 to D-28, particularly the log-histogram at the bottom of each of these pages.)

The practical significance for these findings is that it is not generally necessary to measure d_{mod}s less than $0.05d_{max}$ (or $0.05\sqrt{A}$). But in some situations, where it is important to measure as many blocks as possible, the threshold can be lowered to 1 percent. Prior to the development of the 5 percent criterion ($0.05d_{max}$), a 1 percent criterion ($0.01d_{max}$) was used for much of the field mapping work and core measurement conducted for the research. For the Scott Dam Case History (Chapter 5), the lower criterion was used in order to generate as much data as possible from photographs. For the drill core from the Lone Tree Slide, the block chord lengths were generally less than 5 percent of characteristic engineering dimension, but the resulting CLD was self-similar and was useful in generating a synthetic 2DBSD scaled to the site dimensions (Section 4.9 and Section 5.1).

The criterion suggested here is based on geometry. It is likely that from a mechanical point of view, the distinction between blocks and matrix is different. Given a sufficient stress distribution, failure may occur through smaller blocks as well as matrix. The threshold size could then be that minimum size of block that resists failure under that particular stress condition. The problem would be suitable for further research

2.6.4.2 Determination of the Smallest Block (Block/Matrix Threshold) Using the PSD Method

Soils engineers develop particle size distributions (PSDs) to characterize well-graded soils. PSDs allow the grain size at certain cumulative percentages to be determined: D_{90} for instance, is the grain size at 90 percent cumulative frequency, and represents the size below which are 90 percent of all the grains. Other measures such as D_{25}, D_{50} may be identified, and these have significance to soils engineers, particularly for the design of granular filters. Conventional PSD curves are generated using the weight proportion of the size fractions. But for the purpose being discussed, the numerical frequency proportion of the blocks within each fraction would have to be determined, in order to develop a three dimensional block size distribution (3DBSD)

Using the PSD approach, a comparison of, say, D90 (matrix) against D10 (block) could be made by computing the ratio of these measures and comparing against a standard criterion such as:

D_{90} (matrix) < 5D_{10} (block)

A major problem with this method is the requirement that samples of the matrix would have to be disaggregated sufficiently to be able to determine the PSD. Also, counting the number of small blocks could be onerous, although empirical conversions between the weight fractions and numerical frequency could be developed. An example of the conversion of a WPSD to a 3DBSD for a glacial till is given in Section 3.5.2.

2.6.4.3 Determination of the Largest Allowable Block in a Bimrock, Using the 0.75d_{max} Criterion

It is tentatively recommended that the conservative upper size limit of blocks in a bimrock be: ***75 percent of d_{max}***, *which is the engineers's choice of: a) the size of the largest block likely to be encountered at the scale of engineering interest; b) the characteristic engineering dimension, or c)* ***vA.***
Blocks larger than 0.75 d_{max} are considered to be *blocky rock.*

The recommendation is based on the work of Lindquist (1994b), who limited the largest blocks to approximately 115 to 135 mm, or some 75 to 85 percent of the 150 mm diameter of triaxial specimens. Also, the analysis of section 2.5 (Figure 2.8) showed that for a wide range of scales, 99 percent of the blocks in some Franciscan melanges were less than 0.7d_{mod} / d_{max} . In other words nearly all the blocks were less than 70 percent of the size of the largest block.

The size of the largest blocks in bimrocks such as Franciscan melanges may exceed the characteristic engineering dimensions at all scales, due to scale-independence. For instance, if a tunnel of 10 m diameter penetrates several kilometers of melange it will intercept blocks considerably greater than 10 m in size. Assuming that the mining method

is appropriate, excavation of such blocks will not be a problem. (However, encountering blocks that are a significant fraction of the tunnel diameter may lead to tunneling difficulties, some of which are discussed in Section 4.7). In other engineering situations, such as conducting laboratory tests, or performing cost take-offs for excavations, predicting or limiting the size of the largest block may be important.

2.6.5 Determination of The Upper and Lower Bounds of the Volumetric Proportion of Blocks

The lower bound of volumetric block proportion is tentatively set at 25 percent, based on the work of Lindquist (1994b) and Lindquist and Goodman (1994). At first glance this is restrictive. But the scale-independence of bimrocks means that, at the smaller characteristic engineering dimensions of geotechnical laboratory tests or in-situ down-hole tests, the "matrix" (at the smaller scale) is "bimrock" at the larger scale, and if there is a sufficient proportion of blocks at the larger scale, the overall strength of the "matrix" will be enhanced, thus benefiting geotechnical design at the smaller scale.

The upper bound of 75 percent was selected on the basis of the experience of Lindquist (1994b) who, in fabricating model melanges, found that volumetric proportions greater than 75 percent to 80 percent resulted in block-supported mixes. (Figure 2.21 shows a cross-section through a triaxial specimen with 74% volumetric proportion: the blocks almost touch.) Also, literature on the theoretical limits for the packing of various systems of matrix-supported particles indicates that blocks start to touch at about 75 percent block proportion, although there is dependence on block shapes and block size distributions (Section 3.11).

Procedures for the determination of the volumetric proportion of blocks are similar to those for finding the block size distribution. The emphasis of the research was on the use of stereological methods, principally those that provided a means of estimating the block volumetric proportion from scanlines. The underlying stereological relationship is that the block linear proportion is equivalent to both the block areal proportion and block volumetric proportion: $\mathbf{L_L = A_A = V_V}$, as discussed in Section 2.3. The stereological methods used in the research to measure the volumetric proportion of models are summarized in Sections 2.7 and 2.8. At smaller engineering scales, the volumetric proportions were estimated from blocks measured in core from drill holes, in photographs of core and outcrops, those intercepting field scanlines, and from field maps. The procedures are described in sections 2. 11 through 2.12, and Appendix E.

For laboratory test specimens two methods were used by Lindquist (1994b):
1. Use of a chart relating specimen unit weight to block volumetric proportion. The densities of the matrix and blocks were assumed to be constant.

2. Disaggregation of the specimens, and weighing of the blocks. The volumetric proportion was found via the known densities of the rock lithologies composing the blocks.

2.7 GRAVEL TESTS

2.7.1 Background to the Gravel Tests

Initial attempts to measure blocks in photographs of melanges by using image analysis were frustrating since there was insufficient contrast between the blocks and the matrix for the NIH Image image analysis program to automatically measure blocks. Consequently *Gravel Tests* were performed, initially to develop image analysis techniques using well-defined particles contrasted against a plain matrix, and later to verify that stereological methods were valid for the research.

Before performing the Gravel Tests, the accuracy of the NIH Image program was checked by using photocopied blow-ups of the Comparison Charts for Estimating Percentage Composition, published by the American Geological Institute (Dietrich and others, 1982, sheets 15.1,15.2). The charts contained arrays of black particles with areal proportions between 5 percent and 50 percent. NIH Image measured the areas of the particles (see Appendix B for procedures), and the areal proportions were calculated as the sum of the areas of the particles divided by the areas of the charts. The results differed by only a few tenths of a percentage point from the percentage labels shown for the charts.

Much work was performed using photographs of arrays of gravel and sand distributed in various areal proportions within a white cardboard square of 50 cm side dimension, which were individually known as Gravel Tests *setups*. The areal proportions of the particles ranged between about 5 percent and 50 percent. The areal extents of the setups were considerably greater than the average height of the particles, and were assumed to be two-dimensional arrays, more suitable for measuring block areal proportions rather than volumetric proportions.

The principle goal of the Gravel Tests was to verify that linear measurements across arrangements of particles in two-dimensional images, with known areal proportions, do in fact estimate the "true" areal proportions as predicted by stereology. Additionally, it was of interest to determine the effect of varying scanline intervals and lengths on the estimates of areal proportions. Additional work was performed to estimate the two-dimensional block size distributions from measurements made of d_{mod} in two dimensions; and the one-dimensional chord length distribution (CLD) constructed from measurements of the lengths of intercepts (chords) and the scanlines. Methods were sought to convert CLDs to 2DBSDs.

Because there were between 250 and 600 particles in each image, it was important to accurately determine individual particle areas, d_{mod}s, and areal proportions. The measurements were done using image analysis. The Gravel Tests demonstrated that sufficient scanline measurements estimated areal proportions, and that there was consistent patterns between the CLDs and the 2DBSDs. Following work on Case History sites (Chapter 5) with melanges of low block volumetric proportions (5 percent and 35 percent) further studies were performed using Gravel Tests results, since these had been generated for images with relatively low areal proportions of between 5 percent and 50 percent; whereas the Triaxial Specimen tracings (Section 2.8), had volumetric proportions ranging between 30 percent and 70 percent.

The Gravel Tests relevant to this dissertation included:

1. The calculation of the areal proportion of the gravel.
2. The comparison of the "true" areal proportion of the gravel particles to the "apparent" areal proportion evident from linear traverses (*scanlines*) across the images.
3 The investigation of the effects of varying scanline length and interval on the estimates of block areal proportions, CLDs and 2DBSDs.
4. The identification of the optimum number of scanlines required to satisfactorily estimate both the block areal proportions and approximate the 2DBSDs from the CLDs.

Results from the Gravel Tests are presented in Section 4.3, and the data are summarized in Appendix C.

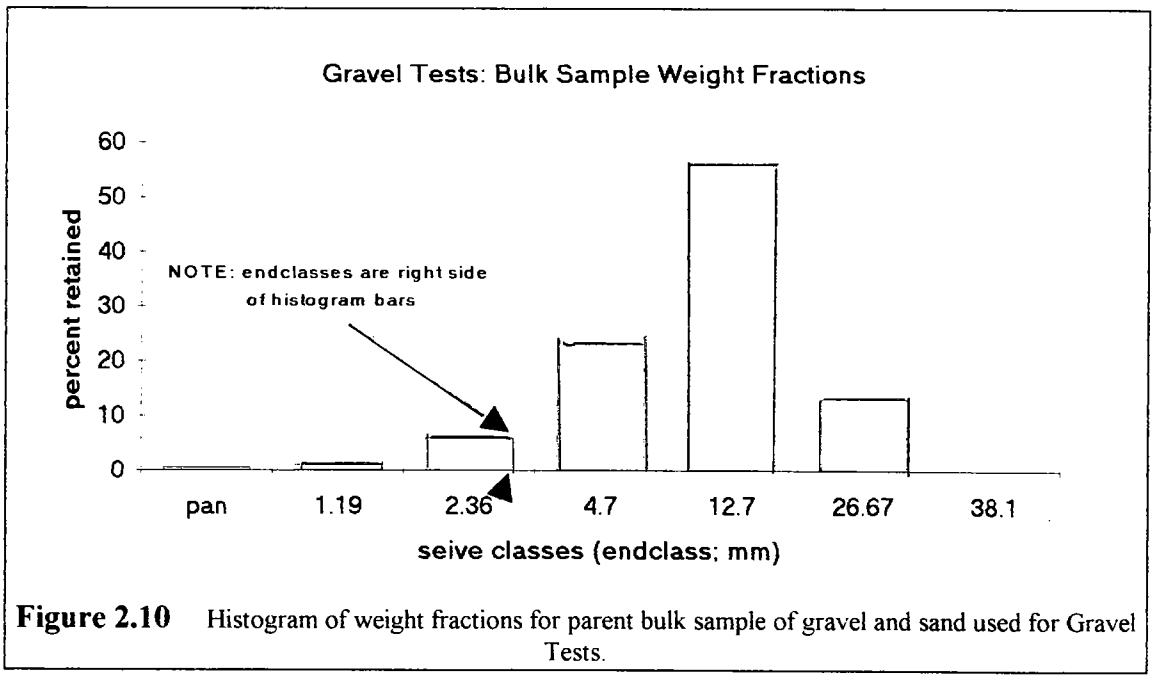

Figure 2.10 Histogram of weight fractions for parent bulk sample of gravel and sand used for Gravel Tests.

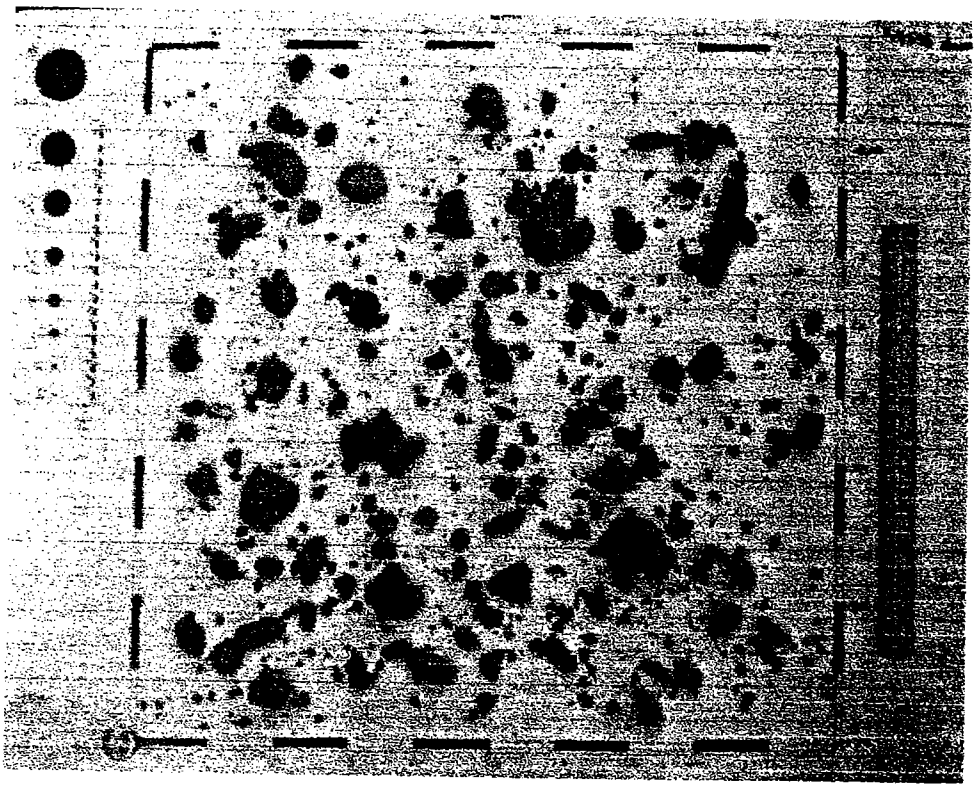

Figure 2.11 Scanned image of a typical Gravel Tests setup with a 24% areal proportion of gravel.

2.7.2 Preparation of Gravel Tests Images and Outline of Measurement Procedures

Areal proportions for the six setups were 5.1%, 5.3%, 12.2%, 24%, 37% and approximately 50%. There was some bias to the distribution of gravel since all grains were constrained within the bounds of the 50 cm square; consequently, regions of the board close to the boundary were sometimes relatively sparsely or densely populated because groups of maverick particles that had strayed over the boundary were relocated. The overall weight-based size gradation of the parent blend of gravel and sand is shown as Figure 2.10. For each image setup the particles were graded sufficiently to provide at least two orders of magnitude between the diameter of the smallest particle (approximately 1 mm maximum in two dimensions) and the largest (approximately 100 mm maximum in two dimensions). The WPSDs (weight-based particle size distribution) for each of the Gravel Test setups were determined by sieving, and are shown in Appendix C. Although not intentional, and not discovered until the end of the research, the block size distributions (2DBSDs) of the individual setups were roughly self-similar, as shown by the example log-histogram of page C-22 in Appendix C.

Each setup was photographed in color and in daylight with sufficient contrast that each particle could be discriminated when the photograph was scanned. Figure 2.11 shows a typical Gravel Tests setup and image. The scanned images were enhanced by image processing in NIH Image or Adobe Photoshop (for the work performed on a Macintosh computer), or Picture Publisher (when using a PC computer). NIH Image was used to find the individual areas of about 200 to 600 gravel particles in each image, using the procedures outlined in Appendix B. NIH Image wrote the areas and maximum dimensions of individual particles to internal spread sheets which were later exported into Microsoft® Excel. The areal proportion of the setups were calculated by summing the individual areas of the particles, and dividing the total by the area of the setup.

Scanline data were initially measured manually, but most were generated using SigmaScan/Image™, as described in Appendix B. Scanline data were used for both the estimate of block areal proportions (results in Section 4.3) and for estimating 2DBSDs and CLDs (results in Section 4.4).

The effect of varying scanline intervals and lengths on estimates of areal proportions and CLDs, was investigated. Random numbers between 0.0 and 1.0 were generated by a pocket calculator, and these multiplied by the width or the height of the setup board (50 cm square). The resultant dimension was used to either spot the location of a scanline relative to an origin at the left side of the board, or else a define a scanline length. The investigation provided an opportunity to compare data from "random scanlines" with those from scanlines of regular spacing and constant length .

In addition, a series of tests were performed in which incremental scanlines were added to an image, additional data generated, and the revised estimates of block areal proportion and revised CLDs compared with predecessor estimates, in order to establish some guidelines for efficient total scanline lengths. Series of 5, 10, 20, and 40 scanlines were measured on three images (5.3 percent, 12 percent and 24 percent): the data are presented in Appendix C.

2.8 TRIAXIAL SPECIMEN TRACINGS

2.8.1 Background to Work With The Triaxial Specimen Tracings

Lindquist (1994b) fabricated over 60 triaxial test specimens of model melanges composed of concrete blocks within weak concrete matrices. Each of the 150 mm diameter cylinders had one of four possible block orientation configurations (0, 30, 60 and 90 degrees relative to the vertical axis), and one of three block volumetric proportions ("Low", "Medium" and "High"; equivalent to approximately 30, 50 and 70 percent block proportions). Hence, the combination of these variables resulted in many

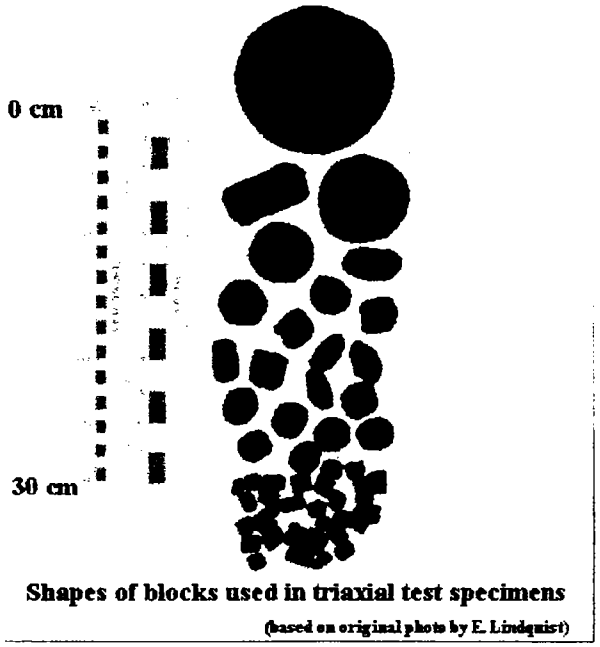

Figure 2.12 Variety of block sizes used by Lindquist (1994) in triaxial specimens. (Scanned from a photo by Eric Lindquist)

different model melanges. Block shapes and sizes ranged between 9 mm rectangular prisms and 115 mm-135 mm disks, as illustrated by Figure 2.12

The mixes modeled melanges with the same self-similar block size distribution, and had model fractal dimensions of 2.0 (in three dimensions: 3DBSD) and 1.0 (in two-dimensions: 2DBSD). The mathematical basis for the simple relationship between a self-similar 2DBSDs and 3DBSDs is presented by Mandelbrot (1983); Biegel and Sammis (1989); Sammis and others (1987) and Marone and Scholz (1989): The fractal dimension for the 3DBSD is the fractal dimension for the 2DBSD plus 1.0; that is:

$$\mathbf{D_{3dim} = D_{2dim} + 1.0}$$

(Using this relationship it is relatively simple to convert self-similar two-dimensional block size distributions (2DBSDs) into 3DBSDs (three dimensional block size distributions) once the descent limb of a log-histogram has been defined. As shown in Chapter 4, in some cases a CLD may approximate a 2DBSD, in which case the procedure outlined here can be used to convert a CLD into a 3DBSD).

Hence, the model **D** for the 2DBSD was approximately the same as the best-fit **D** = 1.2 for typical Franciscan melange 2DBSDs (Figure 2.8). Figure 2.13 shows the log-histograms (3DBSDs) of the Low and High block proportion mixes, which are parallel. The separate log-histograms collapsed to a composite log-histogram when plotted against

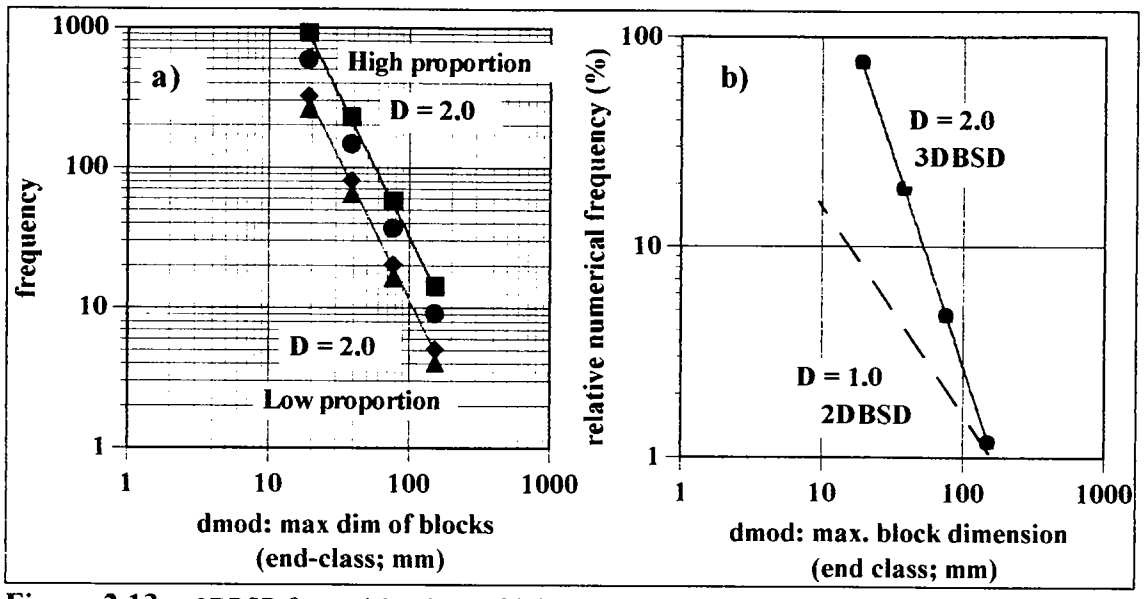

Figure 2.13 3DBSD for model melange, fabricated by Lindquist (1994b), and used for triaxial specimens. **a)** shows log histograms for "High" and "Low" mixes ("Medium" is between them); **b)** shows the individual log-histograms collapsed by plotting the relative numerical frequency of the distributions; and then normalized by the numerical frequencies of the total number of blocks in each mix. **D=1.0** for melange model mix 2DBSDs, and **D=2.0** for the 3DBSDs.

the relative numerical frequency of the blocks in each of the mixes. As shown in Section 2.10, although the composite 3DBSD has a fractal dimension of 2.0, an equivalent 2DBSD could be constructed with a fractal dimension of 1.0, "hinged" at d_{max} (150 mm endclass) since d_{max} was assumed to be the same in both two and three dimensions. It was necessary to know the model 2DBSD in order to later compare the 2DBSDs and CLDs generated from image analysis measurements of the blocks. Use of the 2DBSD in Figure 2.13b to predict the number of blocks with two-dimensional d_{mod}s requires that the ordinate of the plot be re-scaled so that the highest relative frequency percent, for the smallest block size, about 19 mm, be about 40 percent (this observation is based on the research); and not the approximate 10 percent as shown. More work is required to develop the procedure, but it was the basis for an example of the practical application of the results of the research, given later in Section 4.9.

Fourteen of the specimens, of various block orientations and block proportions were selected for image analysis. The specimens provided an opportunity to compare data from two-dimension and one-dimension measurements with known three-dimensional configurations. Image analysis methods permitted the relatively efficient collection of several thousand data values.

Exercises with **triaxial specimen images** relevant to this dissertation included:

1. The estimate of areal proportions and comparison with known volumetric proportions.

2. The estimate of linear proportions and comparison with measured areal and known volumetric proportions.
3. The comparison of CLDs (chord length distributions) to 2DBSDs (two-dimension block size distributions) and known 3DBSDs (three-dimension block size distributions).
4. The study of the effects of varying block proportions and block orientations on CLDs and 2DBSDs.

The principal focus here is on:

a) The estimation of block volumetric proportion by scanlines
b) The estimation of three-dimensional block size distributions (3DBSDs) from chord length distributions (CLDs)

Summaries of the results and the data are presented in Chapter 4, and Appendix D, respectively.

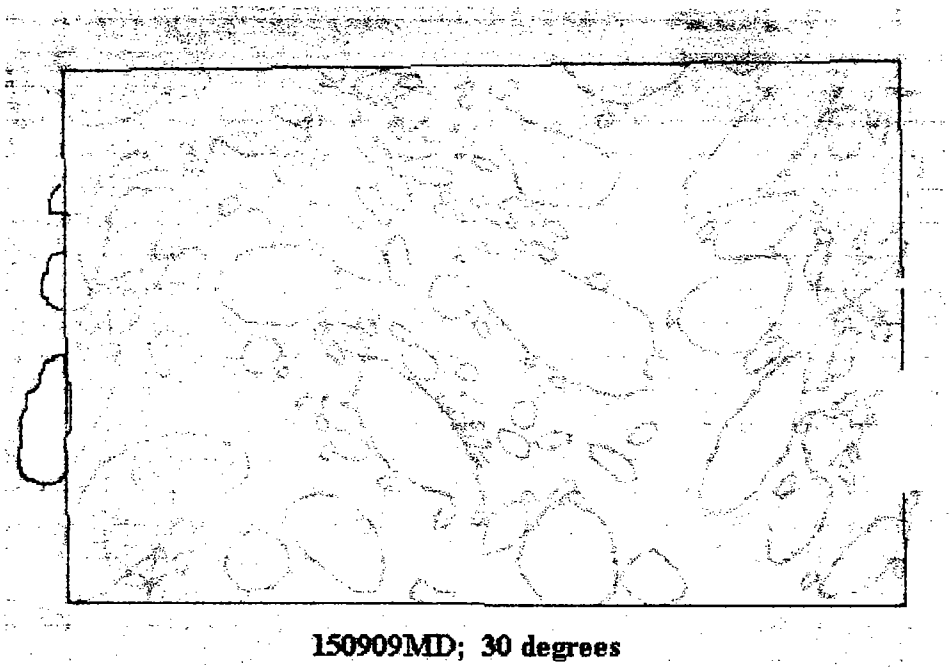

Figure 2.14 Scanned image of the unrolled tracing of the surface of a triaxial specimen, showing outlines of blocks. The portions of bisected blocks were re-joined.

2.8.2 Preparation of Triaxial Specimen Images, Measurement Procedures and Corrections to Data

Tracings of the surfaces of 14 triaxial specimens were prepared by wrapping transparent plastic kitchen wrap (SaranWrap) around the cylinders, and drawing the outlines of the

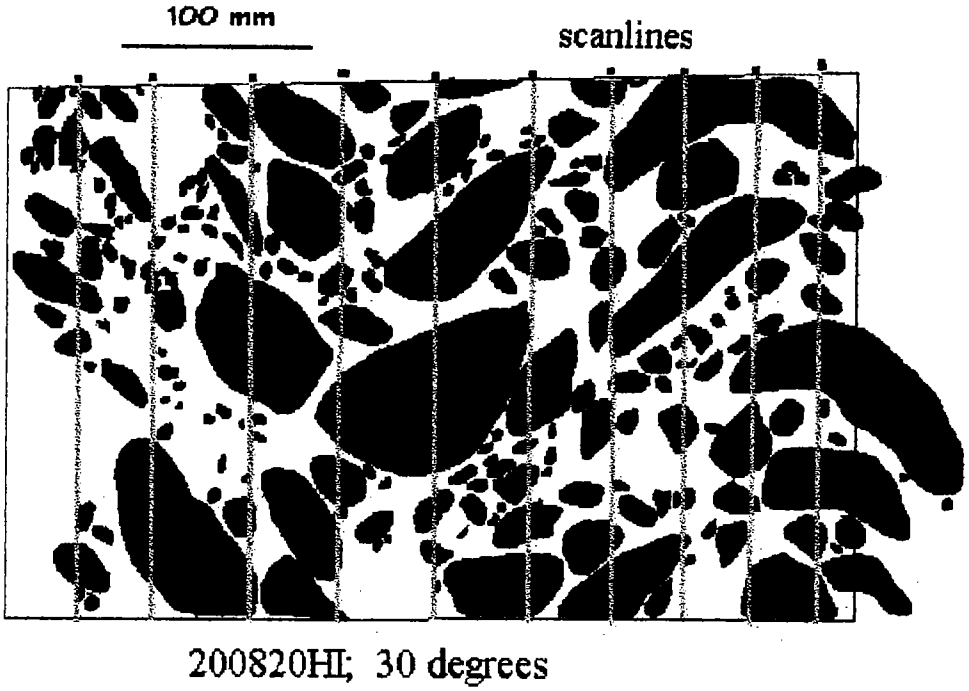

Figure 2.15 Example of unrolled surface of a triaxial specimen, after scanning and tracing blocks using SigmaScan/Image™. Scanlines were added later.

blocks with a felt pen. Lindquist (1994b) completed tracings of the remainder of the failed specimens. The SaranWrap tracings were laid flat on a white board and photographed in dim daylight since bright light reflected from wrinkles in the wrap, and tended to spoil film exposures. The photographs were scanned using resolutions of less than 100 dpi and 256 gray scales.

Many images were manipulated graphically since the blocks at the vertical boundary of several pictures were bisected by the join of the SaranWrap tracings. The blocks were actually whole and the determination of the true area and maximum dimension of these blocks required that they be rejoined. The graphics software Picture Publisher was used for the operation, which is illustrated by Figure 2.14

Approximately 3000 blocks were manually traced using SigmaScan/Image™ and the individual block areas and d_{mod} were determined by the program. Figure 2.15 is a record of a block tracing; others are presented in Appendix D. The data were exported into Microsoft® Excel, and the areal proportion of the blocks was calculated by adding the individual block areas and dividing the sum by the total area of the image.

Scanline spacing was constant for all images, and all scanlines were parallel and "vertical" (oriented along the axial direction). Nearly all image had 10 scanlines, a couple had 9 or 11 scanlines. The scanline spacing of about 30 mm was chosen to exceed the range of average d_{mod} of the blocks (21 mm to 29 mm). Scanlines (for example: Figure 2.15) were drawn across the image of the traced blocks using SigmaScan/Image™, and the pixel value data converted into linear proportions and chord lengths using specially written programs described in Appendix B.

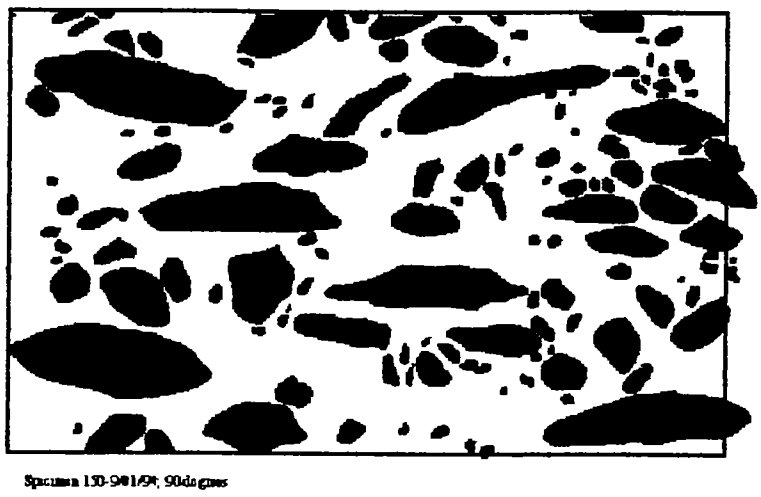

Figure 2.16 "Stretching" effect on blocks oriented parallel to direction of unrolling of triaxial specimen tracing

The scanline data had to be corrected. Since the tracings were of unrolled cylindrical surfaces, the blocks appeared stretched, with the effect being most noticeable for large blocks oriented parallel to the direction of unrolling (block orientation at 90 degrees to the axial direction). Stretching was as much as +11 percent for a 125 mm "true" block dimension. The effect is shown in Figure 2.16. Stretching did not affect the areal proportion of the blocks, since both matrix and blocks stretched by the same proportion. A correction factor was applied to the apparent maximum dimension of the blocks measured by SigmaScan/Image™:

$$\mathbf{d_{mod} = (D/\sin\alpha) \sin \{(\sin\alpha L) / D\}};$$ where

α is the angle (degrees) between direction of d_{mod} (major axis) and the vertical axis
D is the diameter of the specimen
L is the apparent maximum dimension measured by SigmaScan/Image™ ,
and the second {argument} is in radians

Due to an oversight, the orientation of the major axis,(α), was not recorded when the blocks were measured, so it was assumed that α for the particles was the same as the nominal angle that Lindquist (1994b) had declared for the block orientation of the specimens (0, 30, 60 or 90 degrees). This was approximately true for the larger particles, but the orientation of the major axis (α) for smaller blocks often did not coincide with that of the major blocks. (This suggests that one should not depend on the orientation of small blocks to reflect the orientation of the large blocks in a real melange). However, the correction for small blocks was minor due to the shorter observed major axis length, L. The corrections were judged to be sufficient, since the corrected d_{mod}s were invariably less than 135 mm, the size of the largest blocks that Lindquist (1994b) had used in his mixes.

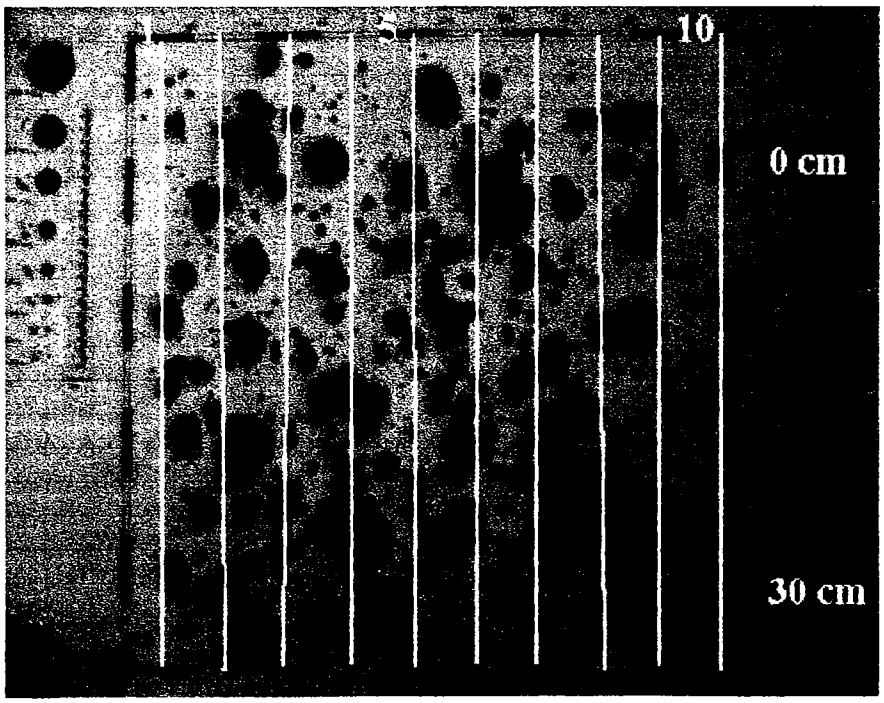

Figure 2.17 10 scanlines across a gravel test of 24% block areal proportion

2.8.3 Method Used to Determine the Block Proportions of Gravel Test Images and Triaxial Specimens Using Scanlines

Initial estimates of the areal proportion of particles of the Gravel Tests setups were determined by tracing scanlines on photocopies of the setups, and manually measuring the chord lengths defined by the intersection of the scanlines and the particles. The data

were entered manually into computer spreadsheets. Later in the research, scanline were data generated from the setup images using SigmaScan/Image™. As described in Section 2.8.2, scanlines were drawn at regular intervals across the Gravel Test setup images and Triaxial Specimen images. A series of very closely-spaced scanlines were drawn across some of the Gravel Tests images to investigate the effect of increasing the density of data on the estimates of areal proportion and block size distribution. Data were generated using SigmaScan/Image™.

Figure 2.17 shows a typical configuration for a Gravel Tests setup, the data for which are shown as Figure 2.18. The procedure described here was essentially the same for both the Gravel Tests images and the Triaxial Specimens tracings. Observe in Figure 2.18 that for each numbered scanline row, there is a "cumulative scanline percent" column: this is the proportion of current total scanline length up to an including the particular scanline considered. Also, for each numbered scanline row, there is a "percent chords" column, which shows the sum of all chord intercepts measured for that scanline, divided by the length of the scanline (shown in column 2). Each scanline row ends in a "cumulative percent chords" column, which represents the running average percent of chords.

The data shown in the table of Figure 2.18 are plotted as "series 1" in Figure 2.21. "Series 2" has exactly the same individual scanline data, but accumulated in a different order. The summation order for Series 1 was 1, 2, 3.....9, 10; and for Series 2, was arbitrarily 5,2,9,....6,4. The benefit in plotting two series was to observe if the data *effectively* converged before the last data point. In Figure 2.19 the two series converge to the same block linear proportion (cumulative chord percent) of about 22 percent. The actual areal proportion was 24 percent. The effective convergence, to 23 percent block linear proportion, occurred at approximately 55 percent of the total scanline length.

scanline	scanline length (mm)	cumul. scanline (mm)	cum. scanline	chords length (mm)	cumul. chords (mm)	% chords	cum. chords series 1
1	498.60	498.60	10.01	42.10	42.10	8.44	8.44
2	498.60	997.20	20.01	139.00	181.10	27.88	18.16
3	495.80	1493.00	29.96	99.70	280.80	20.11	18.81
4	501.40	1994.40	40.02	119.30	400.10	23.79	20.06
5	498.60	2493.00	50.03	108.00	508.10	21.66	20.38
6	501.40	2994.40	60.09	161.30	669.40	32.17	22.36
7	495.80	3490.20	70.04	108.00	777.40	21.78	22.27
8	501.40	3991.60	80.10	98.20	875.60	19.59	21.94
9	495.80	4487.40	90.05	113.80	989.40	22.95	22.05
10	495.80	4983.20	100.00	61.70	1051.10	12.44	21.09

Figure 2.18 Scanline data for Figure 2.19 showing method of accumulating chord lengths, and linear proportion for increasing proportion of total scanline length. Data plotted as Figure 2.19

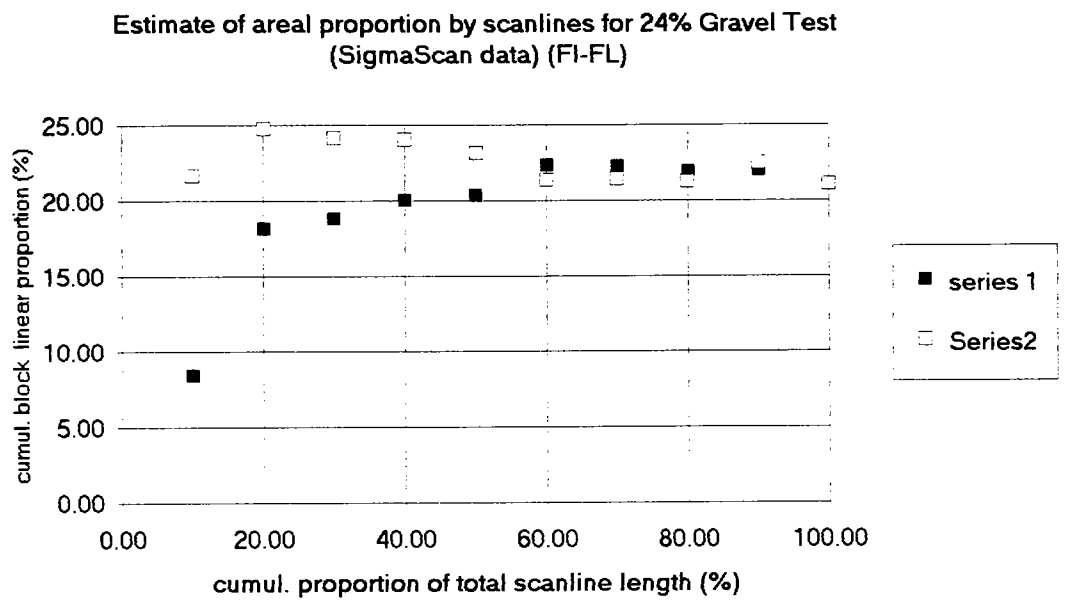

Figure 2.19 Plot of data shown in Figure 2.18, generated from the scanlines shown in Figure 2.17, shows effective convergence to 23 percent block linear proportion, within about 55 percent total scanline length. Actual block areal proportion is 24 percent

Results of the studies performed to estimate block areal proportion and block volumetric proportion by scanlines are presented in Chapter 4. Data for the Gravel Tests images are summarized in Appendix C, and for the Triaxial Specimen tracings in Appendix D.

2.8.4 Explanation for A Discrepancy Between A_A and V_V for Triaxial Specimen Tracings

The block areal proportions (A_A) estimated from SigmaScan/Image™ measurements were significantly less than the block volumetric proportions (V_V) declared by Lindquist (1994b) for each of the 14 specimens. The discrepancy between the areal and volumetric proportions was an apparent contradiction to the stereological principle of $A_A = V_V$. The difference is illustrated in Figure 2.20, in which the data (open squares) suggest that:

$$(V_V)_{actual} = 12 + (A_A)_{image\ analysis}$$

The dashed line represents the stereological ideal: $A_A = V_V$.

To resolve the problem, 6 of the 14 triaxial specimens were cut, and the sliced interiors photographed and scanned. SigmaScan/image™ was used to determine the areal proportions of the blocks exposed on the surface of one half of the sliced specimens. As shown in Figure 2.20 there is good agreement between the actual block volumetric proportion and the block areal proportions measured from the cross-sections (filled circles).

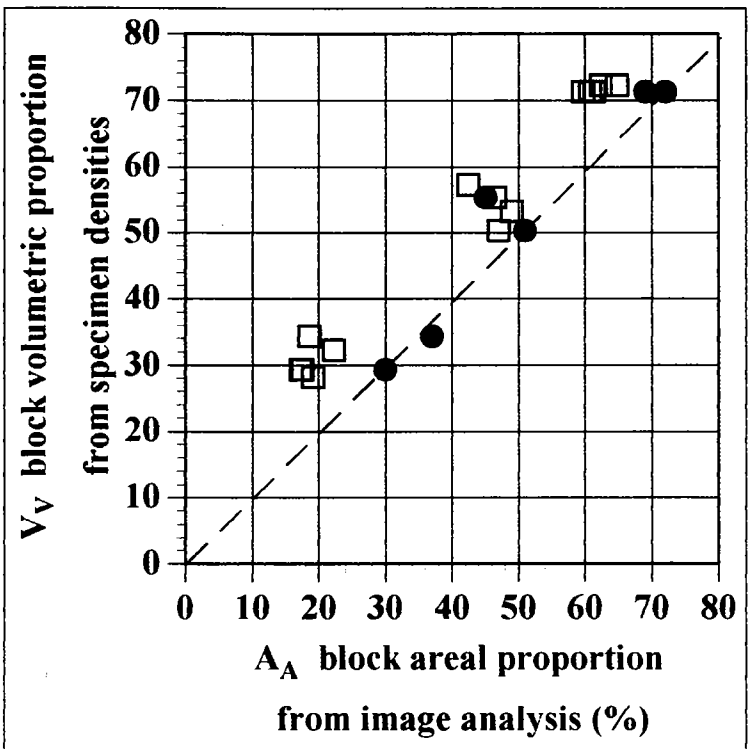

Figure 2. 20 Scatter plot of block areal proportions, A_A (open squares) of 14 triaxial specimens based on the measurements of blocks traced from the surface of the cylinders; compared to actual volumetric proportion V_V determined by Lindquist (1994b) from specimen densities. Filled circles represent areal proportions measured from cross-sections through 6 specimens. The dashed line is the ideal, $A_A = V_V$

Figure 2.21, an illustration through one of the sliced specimens, shows that the bulk of the blocks are concentrated in the center of the specimen. Their expression at the circumference is a matter of geometric probability. The specimen 72 percent block areal proportion as measured from the cross-section, but only 54 percent measured from the circumferential area. The actual volumetric proportion was 74 percent. (Observe that the fabric approaches that considered to be blocky rock). The 150 mm diameter cylinders were cut from rectangular moulds that had 180 mm square sections. With little room to pack blocks as large as 135 mm, it is apparent that a large proportion of the larger blocks would be concealed from the circumference of the cylinder.

Because the block linear proportions from scanlines were approximately the same as the areal proportions measured on the specimens surfaces ($L_L = A_A$); and because $A_A = V_V$, when measured on the cross-sections, it was assumed that the linear proportions would have estimated the volumetric proportions if there had been better distributions of blocks.

Useful research could be performed by fabricating models of virtual (on a computer) or real bimrocks, cutting random slices through them, and performing stereological studies, in order to better understand the geometric probability considerations.

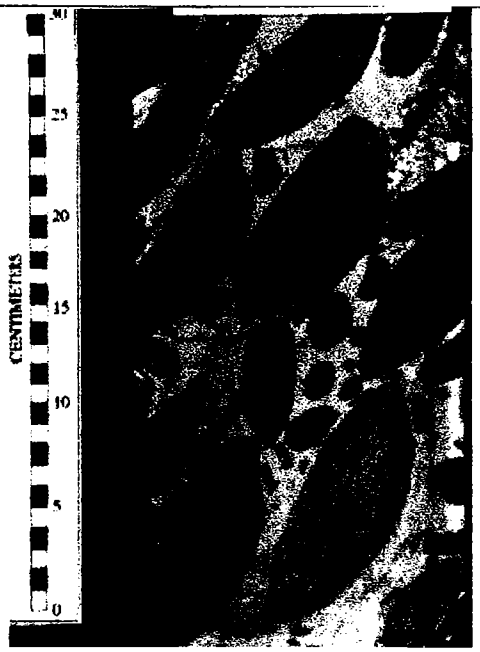

Figure 2.21 Cross-section through triaxial specimen shows why areal proportion measured at the circumference (54%) is lower than that measured from the cross-section (72%) The volumetric proportion was 74%, almost "blocky rock".

2.9 THE USE OF SCANLINES TO ESTIMATE THE BLOCK SIZE DISTRIBUTIONS OF GRAVEL TESTS AND TRIAXIAL SPECIMENS

Scanlines were drawn across the Gravel Tests images and the Triaxial Specimen tracings, and SigmaScan/Image™ used to generate pixel data, which were then converted into chord lengths by the specially-written programs described in Appendix B. For the gravel tests, the resulting chord length distributions (CLDs) were compared with the two-dimensional block size distributions (2DBSDs). For the Triaxial Specimen tracings, the CLDs were compared to both the 2DBSDs and the three-dimensional block size distributions (3DBSDs) provided by Lindquist (1994b). As indicated above, Lindquist (1994b) varied the volumetric proportion of his mixes (30 percent, 50 percent and 70 percent), but the relative numerical frequency of the different classes of blocks remained the same. The blocks size distributions were designed to be self-similar, with a fractal dimension for the 2DBSDs of 1.0 and for the 3DBSDs, 2.0. (The relationship between fractal dimensions for 2DBSDs and 3DBSDs is discussed in Section 2. 10)

For the Triaxial Specimen tracings, the log-histogram approach of plotting data allowed a check on the self-similarity of the data. If the data points of the descent limb of the plots were approximately linear, self-similarity was demonstrated. The log-histograms also permitted comparisons between the scanline CLDs, the 2DBSDs, (determined from the d_{mod} (major axes) measurements obtained when particle areas were measured); and the 3DBSDs, obtained from Lindquist (1994b), and previously shown as Figure 2.13. Some comparisons are presented in Appendix D (pages D-22 to D-28). Different styles of plotting block size distributions were used, as shown in Appendix D. Data were grouped into plots with either a common volumetric proportion or a common block orientation. For example, all plots with a volumetric proportion of 30 percent were grouped, and the variations of the block size distributions with changing block orientations studied. A principal goal was to devise some empirical guidelines for converting CLDs into 3DBSDs for self-similar blocks size distributions. The results and analyses are presented in Chapter 4, and the data in Appendix D.

For the gravel tests the CLDs and 2DBSD plots were conventional semi-log plots in the particle size distribution (PSD) style used in Soil Mechanics. Although effort was expended to discover ways of converting CLDs into 2DBSDs, the primary concern was to investigate the effect on CLDs of increasing the density of scanlines across images. The results are discussed in Chapter 4, and typical data are presented in Appendix C.

2.10 FIELD METHODS

Field procedures were elementary. A combination of a 25-foot carpenter's measuring tape, and home-made stadia rods were used to measure blocks in outcrops and the axes of free blocks. At outcrops, the furthest two points of a block (d_{mod}) were measured. For free blocks the approximate length of the major, intermediate and minor axes were measured to be used in block shape analyses.

Conventional measuring lines (scanlines) were set up at Lone Tree Slide. These were approximately 15m to 30 m long. Block d_{mod}s were measured as chord intercepts. At the same time the two-dimensional d_{mod} of the intercepted blocks was measured. Most of these scanlines were time consuming, since a $0.01d_{max}$ criterion (1 percent of the size of the largest block expected locally) was used to establish the matrix/block threshold. This length was generally about 0.1m. Smaller blocks were measured but were later found to be censored data. Later in the research, a less restrictive $0.05d_{max}$ criterion (5 percent of the largest local block) was used.

A method was devised to estimate the d_{mod} of blocks at the Lone Tree Slide excavation, greater than about 1 m, without having to work on the dangerous slopes of the excavation. The method, illustrated in Figure 2.22, is based on the geometry of similar triangles and was inspired by the *subtense bar* once used by surveyors (Brinker and Wolf, 1977; p53). Two pieces of equipment were used: a 6-inch Engineer's scale,

graduated in tenths of an inch; and a range-finder, capable of measuring to about 100 m with an accuracy of 95 percent. The scale was held at arm's length and the largest dimension of a distant block "measured" with the scale (variable 'I" in Figure 2.22). The distance to the block was determined with the range-finder, or scaled from a map if the approximate location of the block was known (variable 'L' in Figure 2.22). Slope distances were not corrected to horizontal distances. To find d_{mod} , the chart in Figure 2.22 was entered with the values of 'I' and 'L'. (Before use, the chart was checked by measuring 1.52 m stadia rods over a range of known distances).

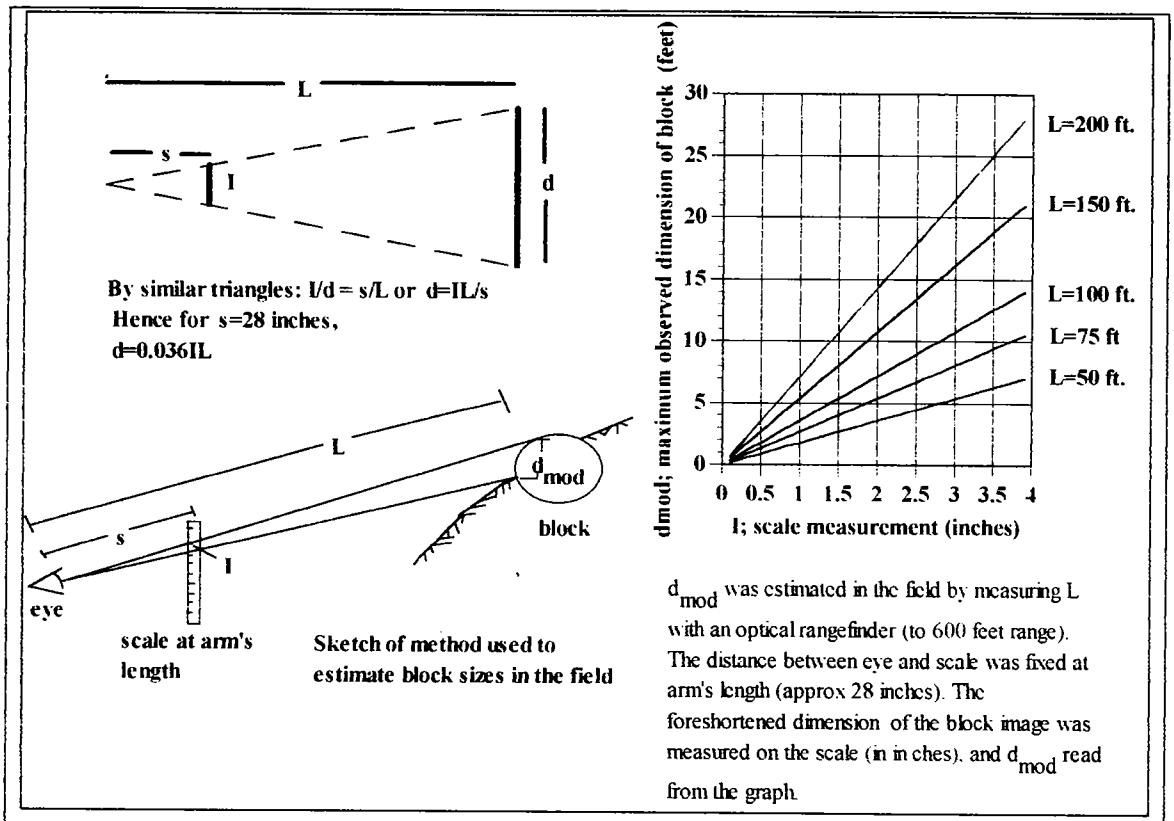

Figure 2.22 Method of estimating d_{mod} in the field.

2.11 MEASUREMENT OF BLOCK INTERCEPT LENGTHS IN DRILL CORE

The block intercept lengths in approximately 1080 m of core were measured during the project. The California Dept. of Transportation (CALTRANS) provided 345 m of HQ core recovered from geotechnical exploration of the Lone Tree Slide. The core was reviewed and the block intercepts (chord lengths) measured at Davis Hall, University of California. Segments of core were selected for geophysical and geomechanical testing,

the results of which are not presented here. The results of the core examination are presented in the Lone Tree Slide Case History, Chapter 5.

Some 740 m of HQ core, recovered during geotechnical exploration for the Richmond Transport Project Storage Tunnel (RTP), was examined at a temporary storage facility at the North Beach Pump Station in San Francisco. Results from the measurement of the Richmond Transport Project core are presented in Chapter 5.

No detailed geological logging of the core was performed but the lithology of each block was recorded. Block intercepts greater than 5 cm were measured along a centerline scanline. For the Lone Tree Slide core, there was no difficulty discriminating blocks from matrix, since the matrix was very sheared. There was more difficulty with the RTP core, since some of the core contained turbidite sequences with intermittent deranged zones, which had the chaotic appearance of melange. Photographs of core were reviewed in order to estimate the block linear proportion of the melange in the foundation rock below Scott Dam, on the Eel River, near Ukiah. Approximately 100 m of core was represented by the photographs, which were examined using a magnifying glass and a measuring scale. The Scott Dam Case History is discussed further in Chapter 5

2.12 DESCRIPTION OF FRANCISCAN AREA STUDIES

Five separate studies were made of geology maps from Marin County (Reid, 1978; Peterson, 1979; Savina, 1982), Sonoma County (Erikson, 1994) and San Luis Obispo County (Seiders, 1982). The maps were studied for two reasons:

1. To measure the block size distributions of Franciscan melange at housing sub-division scales (1 to 2 km^2) and bridge the difference in scales between the self-similar BSD studies of Caspar Headlands (to 20 m^2) and that of Marin County, as shown in Figure 3.4 (1000 km^2). Most of the results were incorporated into Figure 2.8. The d_{mod} of blocks were measured using a magnifying lens and a measuring scale, and the lithology of the blocks were recorded. The details of the work are presented in Appendix E.

2. To measure block proportions and hillslope to verify a postulated relationship between these two variables. The procedure is outlined below, but presented in more detail in Appendix E.

There were significant problems in estimating volumetric block proportions and determining hillslopes from maps. Several sets of air photos were examined; there was a lack of large-scale imagery, although 1964 BATS (Bay Area Transportation Study; scale 1:4800) images on 3 foot square diapositives were useful, but required a light table. (The BATS images are located at the Map Library, UC Berkeley). The maps of Trautmann (1976) Savina (982), Reid (1978) and Peterson (1979) were the most useful sources, being geology and engineering geology theses used to ground-truth air photo

interpretations of the Franciscan (Ellen and others, 1977; Ellen and Wentworth, in press). Maps from these references were also used to measure block sizes at the same time, as indicated in the previous paragraph.

120 measurements of block linear proportion and block area proportion, together with hillslope angles were made of from the maps and air photos (43 of failed melange, and 77 of stable ground). It was assumed that the linear and area proportions were equivalent to the volumetric proportion. Actually, the volumetric proportion is probably not as important as area or linear proportion, since the depth of the majority of failed earth masses was of the order of a few meters at most; whereas the areal extents of most earthflows were at least two orders larger. Savina (1982, p. 246-264) observed that the failure mode of the earthflows seemed generally translational rather than rotational.

The problem with calculating the areal proportion was: *how to define the area?* This was not difficult for failed masses, but was for unfailed ground. Having defined a group of blocks on a map, what was the representative area: that within a line tightly bounding the blocks, or one in which there was a more generous freeboard between blocks and boundary?. For that reason, it is suggested that the best measure is the linear proportion, measured on the same line as the slope gradient. Fortunately, the maps used showed field-measured slopes which were superior to slopes that were measured from the topographic base maps (magnified USGS quads). Better methods would be to use stereo-pairs of large-scale air photos and a parallax bar or photogrammetric surveying; or perform field studies and use GIS (Geographic Information Systems) with a computer database of topography and imagery which could be ground-truthed (calibrated) with the field results.

The individual plots based on the measurements of the study maps of Savina (1982); Peterson (1979) and Reid (1978) and the detailed procedures, results and summaries of the data are presented in Appendix E. The summary plot is presented as Figure 4. 17 in Section 4.6

CHAPTER 3: GEOLOGICAL ASPECTS OF MELANGES AND SIMILAR BIMROCKS

3.1 INTRODUCTION

This Chapter summarizes several geological aspects of melanges and the *similar bimrocks* of sheared serpentinites and olistostromes. Although the behavior of melanges is of the most importance to engineers, the geological aspects of the rock are relevant to the characterization of melange. Accordingly, effort was expended to understand the controversial theories associated with melanges, and these are summarized. Because reference is made to the melanges of the Franciscan Complex of California (*the Franciscan*), a general description of Franciscan geology is presented. Information from literature searches is combined with results and data obtained during the research. Melanges are widely distributed throughout the world, and advances in understanding the engineering aspects of Franciscan melanges is of international interest, although the knowledge may not apply to all melanges everywhere.

The complexity of melanges can be lessened if an orderly approach is adopted to the geological engineering description of their *architecture*, a word adapted from Laznicka (1988; p. 37). From an engineering point of view the most important mechanical and architectural aspects of a bimrock, such as a melange, are: *block volumetric proportion, block size distribution, overall block orientation, matrix and block discontinuity fabrics, matrix strength* and *matrix block contact strength.* Of lesser importance are: *block lithology, matrix lithology and individual block shapes.* The architecture of melanges is discussed in this chapter; and the engineering aspects are considered in Chapter 4.

3.2 WORLD-WIDE DISTRIBUTION OF MELANGES AND SERPENTINITES

Laznicka (1988, p.28) considered breccia masses between tens of meters and tens of kilometers, to be *Bodies*; and larger than that he described them as or *Terrains* or *Belts*. (The word *terrain* has a geomorpological flavor, distinct from that of *terrane* which describes fault-bounded lithotectonic slivers of crust (Jones and others, 1983; Howell, 1989). All melange rock masses are referred to as *bodies* in this dissertation but they are generally organized as belts, reflecting their association with convergent crustal margins. Figure 3.1 shows the location of representative melange bodies, based on the maps presented in Appendix A, and also shows the approximate location of some ophiolites, which are associated with serpentinite bodies.

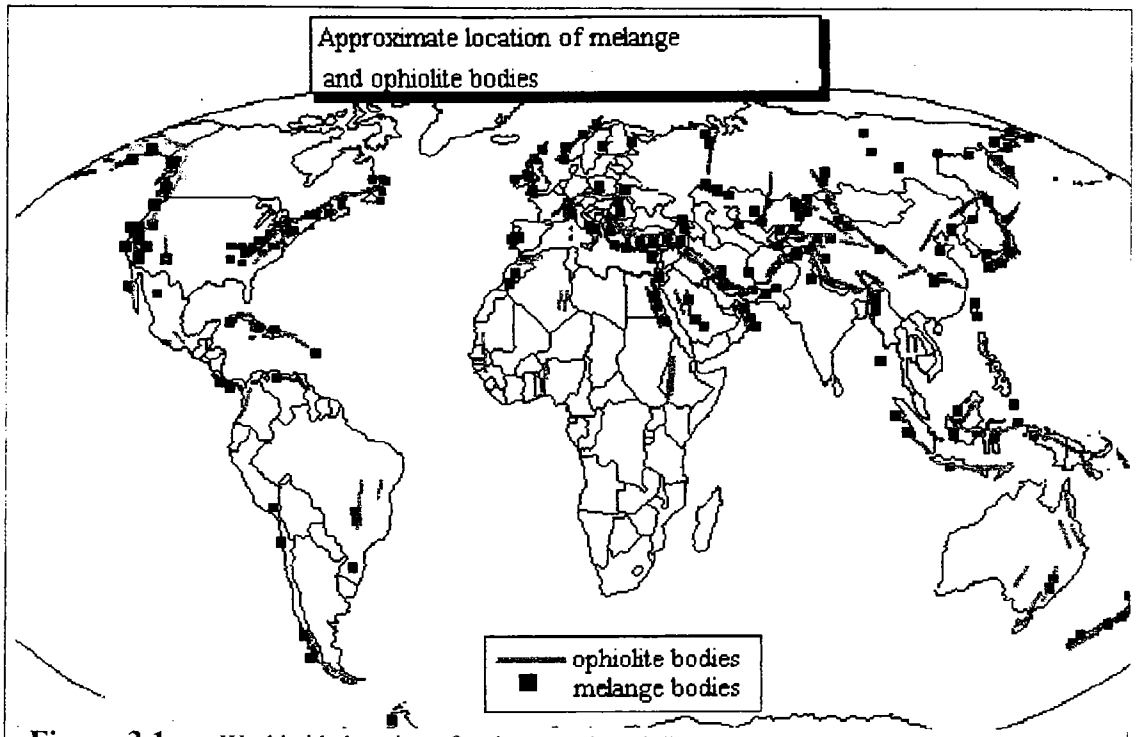

Figure 3.1 Worldwide location of melange and ophiolite bodies. Serpentinite bodies are closely associated with ophiolites. Location of ophiolites after Gass (1990)

3.3 THE FRANCISCAN OF CALIFORNIA

Understanding of the Franciscan of California has evolved over nearly 150 years (Cloos, 1990), as it has been variously known as the Franciscan Series, Franciscan Formation, Franciscan Assemblage, and Franciscan Complex (Berkland and others, 1972). It is now commonly referred to simply as *the Franciscan.* Although "Complex" is geologically objectionable (Fox, 1983), the word is semantically appealing: the rocks, the structures, the history and the geological arguments are complicated, as evident in over 450 references to the melanges of the Franciscan (for example, these useful technical and lay resources: Bailey and others, 1964; Blake, 1984; Blake and Jones, 1974, 1981; Blake and Harwood, 1989, p. 3-18; Cowan, 1974, 1978; Hsü, 1985; Takeshi and Mizutani, 1979, p. 82-95; Bilodeau and Davis, 1990 p. xix-xxii; Alt and Hyndman, 1975, p.13-80; Norris and Webb, 1990, p. 359-411).

The Franciscan covers about a third of northern California, and chunks of it have been identified in Baja California, the Catalina Islands, central California north of the Coast Ranges, and continuously from San Francisco north into Oregon. In northern California it is composed of three roughly parallel belts: the Coastal Belt, the Central (Melange) Belt and the Eastern (Metamorphic or Yolla Bolly) Belt (Figure 3.2). The Franciscan Belts were defined on the basis of their lithology and tectonic separation and show increasing

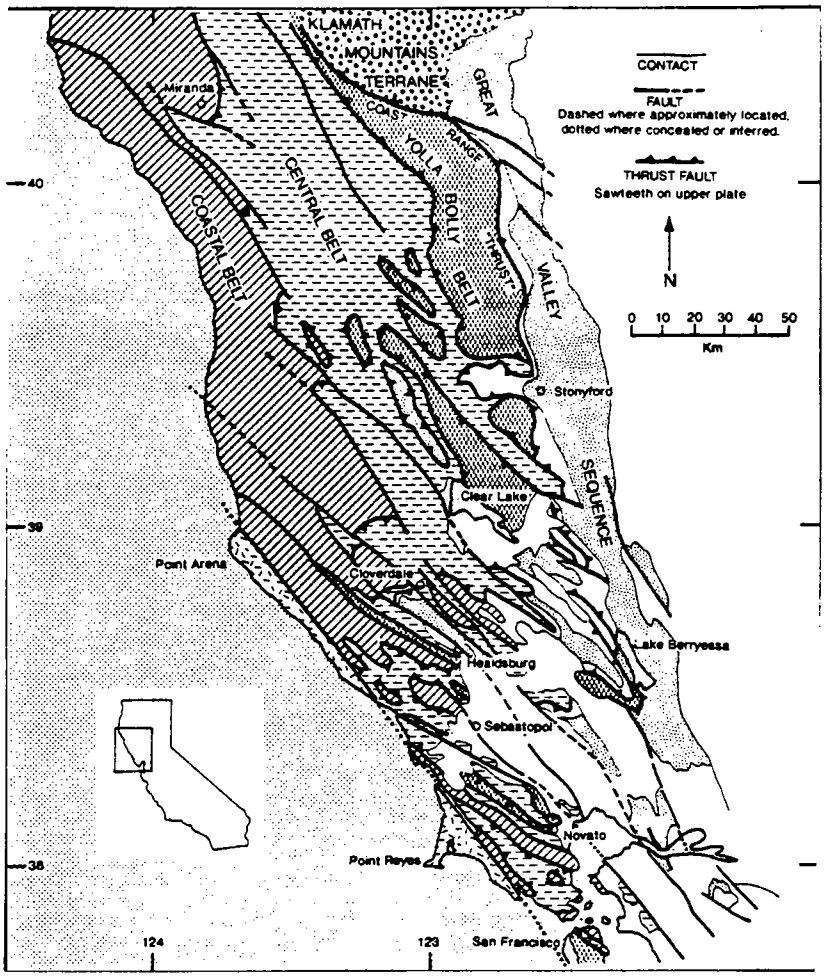

Figure 3.2 Part of the Franciscan of northern California, which is divided into three lithotectonic Belts (from Bilodeau and Davis, 1990; after Blake and Jones, 1981)

age and degree of metamorphism from west to east, which indicates deepening immersion in a subduction zone (Blake and Jones, 1981).

The Coastal Belt is composed mostly of clastic sediments (sandstone and shale) and minor tuff layers that are tectonically disrupted but relatively coherent, known as *broken formation.*

The Central Belt is a regional melange with a matrix of sheared mudstone with blocks mostly of greywacke, metagreywacke and tuff, and lesser blocks of volcanics, chert, serpentinite, limestone, high-grade blueschist, amphibolite and eclogite. The matrix and greywacke blocks have been slightly metamorphosed, as indicated by lawsonite mineralization. The presence of the high grade metamorphic blocks is enigmatic because they have a provenances of tens of kilometers deep in subduction zones, which is much deeper than the minor degree of burial suggested by the lawsonite in the greywackes.

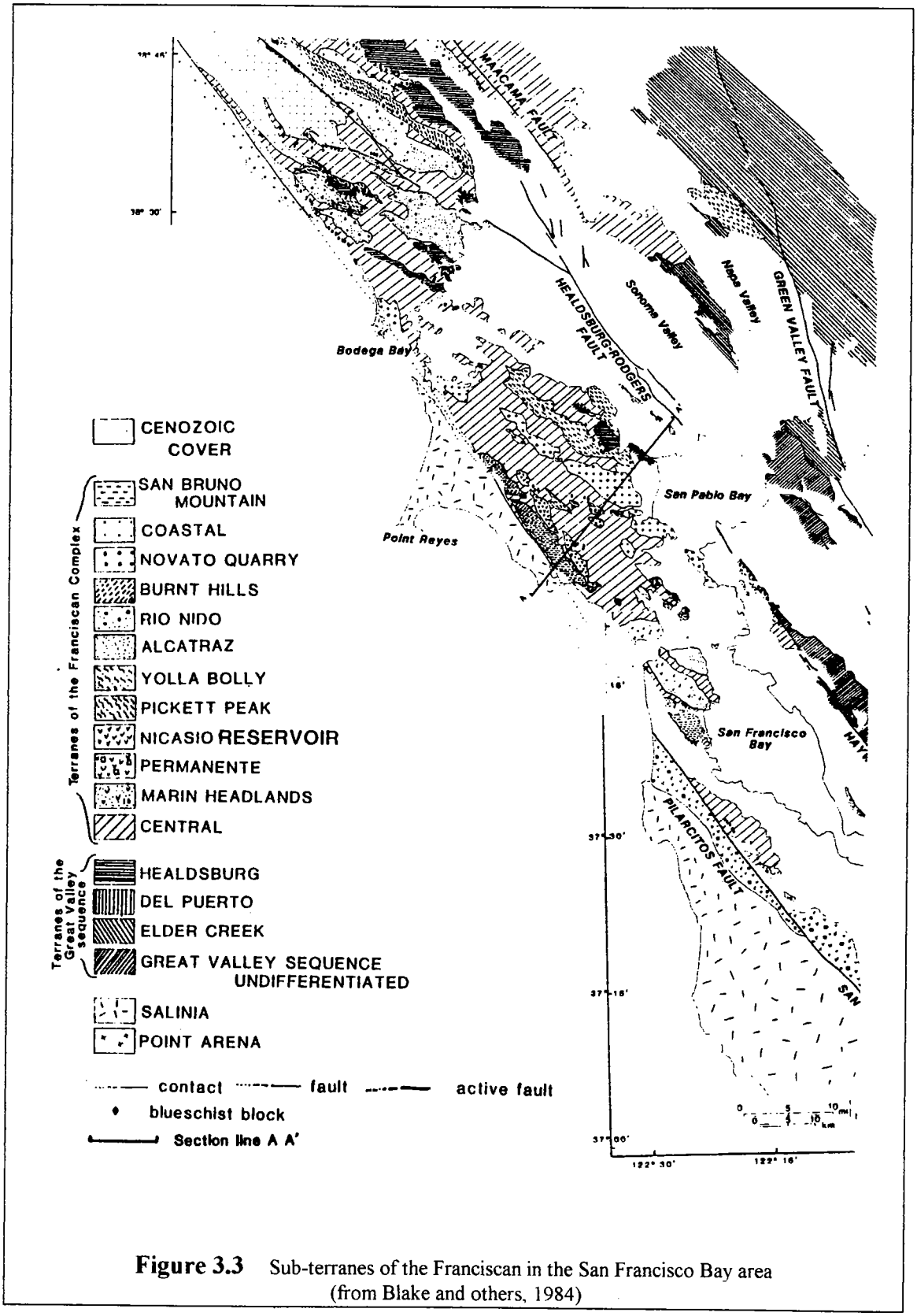

Figure 3.3 Sub-terranes of the Franciscan in the San Francisco Bay area (from Blake and others, 1984)

The Eastern Belt is generally composed of semi-schistose graywacke, lawsonite-bearing mica schist, and glaucophane-bearing meta-volcanics, that differ from the high grade blocks in the Central Belt. The Belt is discontinuous on the east, with blobs of it within the Central Belt melange. It is everywhere structurally overlain by the Coast Range Fault, which has been called both the Coast Range Thrust and the Coast Range Detachment. Since the style of tectonism between thrusts (compression) and detachment (extension) are so different, the name Coast Range Fault seems a safe compromise. Above the Coast Range Fault is a package of ultramafic, mafic and pelagic rocks, often distinguished by the presence of serpentinites (altered oceanic plate), known as the Coast Range Ophiolite (CRO). The CRO is the basement of the Great Valley Sequence, which is a thick, relatively well-behaved series of sediments, with local melanges and olistostromes. One theory, suggests that the CRO is the remnant of an oceanic plate stranded on the forearc side of a subduction zone (Bailey and others, 1970) as shown in Figure 3.5.

Although many geologists agree that the Franciscan developed at a convergent plate margin, there is considerable controversy over the duration, and style of the convergence. One group believes that there was head-on subduction of oceanic plate under the North American continental plate for over 150 plus million years, until the mid-Tertiary, when plate interaction became oblique, and the oceanic Pacific Plate started to slide northwest (relative to the North American Plate) along transform faults, "ancestors" to the San Andreas Fault. This model is called the "two-stage model" (Cloos, 1990) and is the standard text-book model of a continental/oceanic plate convergence for which geologists make pilgrimages to California.

Others disagree with the classic two-stage model, and do not consider long-term subduction to have been the cause of the heterogeneity of the Franciscan Central Belt melanges. Instead, they envisage the entire western margin of the continental North America to be a jigsaw puzzle of *terranes*, discrete, fault-bounded lithological and stratigraphical packages of crust that were transported by the converging Pacific Plate and its ancestors, docked against Central and North America, and then distributed along the western margin of the continent by the northward directed component of a long-lived oblique convergence. Pieces of ocean crust, proximal sediments and seamounts were shredded and amalgamated as alien slivers in a trail between Central America and Alaska (Blake and others, 1982; Jones and others, 1983; Silberling and others, 1987; Howell, 1989).

Many terranes have been identified in California, and smaller sub-terranes in the San Francisco Bay area (Blake and others, 1982, 1982) as shown in Figure 3.3. The terranes are large blocks within the "matrix" of the Central Belt, or Central Terrane (Blake and others, 1984). According to the Terrane School, some of the sub-terranes were further shredded and incorporated into the matrix. The general northwest regional trend of these trains of blocks is apparent in Figure 3.4. The best example is the Marin Headlands Terrane: blocks of oceanic crust basalts and chert, with overlying sandstones are

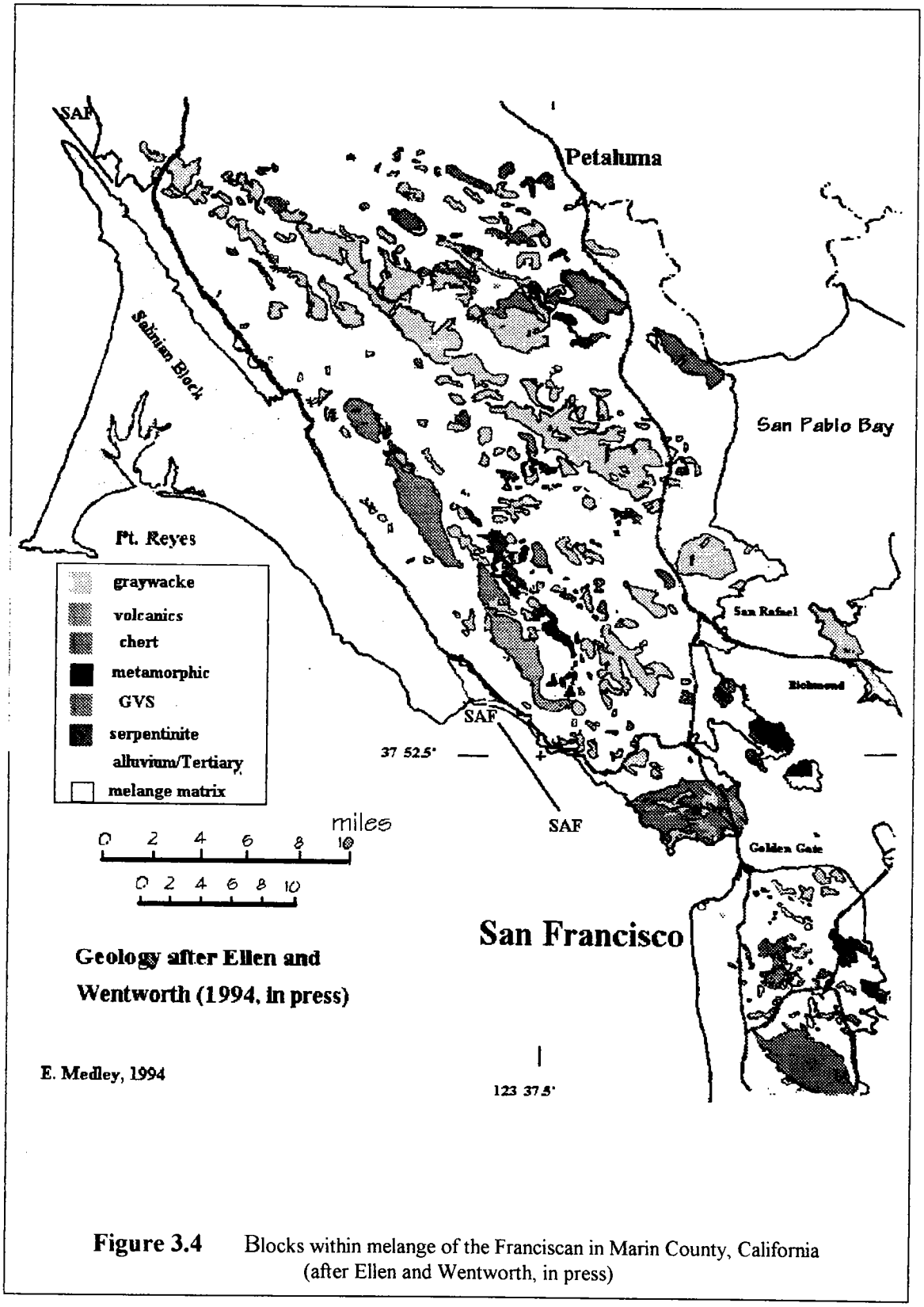

Figure 3.4 Blocks within melange of the Franciscan in Marin County, California (after Ellen and Wentworth, in press)

scattered widely in the Central Terrane melange (Murchey and Jones, 1984). Similarly, the San Bruno Mountain Terrane, is expressed as fragments of turbiditic sandstones and shales between the Coyote Hills on the east shore of San Francisco Bay, northwest through San Bruno Mountain and Point Lobos in San Francisco, through Bolinas Ridge, in Marin County (Blake and others, 1984). Also, fragments of the Nicasio Reservoir Terrane, composed of serpentinite, ultramafics, pillow lava basalts, greenstone and chert overlain by arenaceous sediments, have been identified as having once belonged to the same portion of volcanic arc upon oceanic crust (Blake and others, 1984; Wright, 1984).

3.4 SOME THEORIES ON THE GENESIS OF MELANGES

The genesis of melanges is controversial, as summarized in many reviews ((Silver and Beutner, 1980; McCall, 1983, p.1-11; Raymond, 1984; Raymond and Terranova, 1984; Horton and Rast, 1989; Rast and Horton, 1989); Cowan, 1991), although there is popular, but not universal, agreement that melanges formed at convergent plate margins. But all ideas related to the genesis of melanges are controversial since no melanges have been found in any modern accretionary prism (Prof. David L. Jones; personal communication). Although, from an engineering viewpoint, most of the debate over how melanges *formed* are secondary to how they *behave*, some of the current ideas on the genesis of melanges are of interest to the curious geological engineer.

Greenly (1919), who first used the word *melange*, attributed the chaos of melanges to "shearing down" of the rocks. Ironically the melanges of Greenly's type locality (Anglesey, North Wales) are considered by some have formed mixing due to submarine landslides, sedimentary processes which resulted in *olistostromes* (Woods, 1974). Attempts have been made to distinguish olistostromes from *tectonic melanges* on the basis that tectonic melanges contain exotic blocks such as high-grade metamorphics and olistostromes do not (Hsü, 1974). (Exotic blocks formed somewhere else from where they are now found, or are *allocthonous*). To complicate the situation, melanges that do not contain any exotic blocks are also known as *broken formation*. Similarities between olistostromes and melanges (in California, Italy and Taiwan) have been pointed out (Page, 1978), while others highlight the differences between olistostromes, orogenic landslides (gravity slides), and tectonic melanges (Abbate and Sagri, 1981).

There have been attempts to short-circuit the genetic implications of geological labels, by insisting that "melange" be a descriptive term only, and the qualifiers such as "tectonic" or "olistostromal" be added to suggest genesis. The problem is that olistostromal melanges can be become tectonized, and tectonic melanges further mixed as olistostromes (Aalto, 1981); and the mixing of both types is exaggerated by gravity sliding and earthflow when the melanges are exposed at the Earth's surface. The result is that often the genetic process is not at all clear. Bosworth (1989) suggested that melanges be defined on the basis of their fabric and Cowan (1985) also suggested fabric-based criteria for a classification of melanges, since he considered that most melanges formed

1984; Orange et al., 1993; Brown & Orange, 1993). Based on evidence obtained by drilling into contemporary accretion prisms, diapirism is considered by some to have been a major cause for melanges (Barber and others 1986; Barber and Brown, 1988). Cloos (1984) suggested that the churning of fluidized sediments caused plucking of xenoliths from near-surface deposits and deeper metamorphosed rocks, such as blueschists, from the flow channel walls. Cloos (1984) and Ernst (1984) have suggested that blueschists and other high-pressure, low-temperature metamorphic rocks were injected from their sources at 10-35 km depths by upward flow. Blocks of high-pressure metamorphics have been found incorporated into serpentinite diapirs and volcanoes (Fryer, 1992; Moore and others, 1991). The fluidized flow deposits, freighted with exotic blocks, may have spilt onto the surface of the accretion prism and became incorporated into the sediments.

As a result of the active seismicity of the accretion prism and subduction zone, submarine debris flows and liquefaction of the accretion prism sediments mixed and re-mixed the surface sediments. The downslope movement of debris flows initially *extended* the bedded sediments, and the disrupted sediments may then have further deformed if compressed at the lobe when the slide slowed. Blocks within olistostromes and broken formations tend to show boudinage and be phacoidal (lens-shaped), a result of extension. Crustal thinning during periods of plate separation, or shallowing of subduction, could have resulted in transform faults with high submarine cliffs of exotic rock that shed rock-slides and talus that became incorporated into olistostromes (Johnson and others, 1991; Krueger and Jones, 1989). Also, enormous submarine debris flows of hundreds if kilometers in size are known to spall from the flanks of seamounts (Schwab and others, 1988), and in the vicinity of modern accretionary prisms (Jacobi, 1984). Such slides which would have provided debris of basalt, chert and coralline limestone to be off-scraped and accreted at the continental margin, as well as create untectonized debris deposits (olistostromes), often indistinguishable from melanges (Jacobi, 1984).

Approximately 25 percent of the blocks within the Franciscan appear to have a seamount provenance (see Figure 3.8), and some 90 percent of the ophiolite in North America is thought to have originated from seamounts and plateaus (Prof. David L. Jones; personal communication). Several of the sub-terranes in the Franciscan (Figures 3.3 and Figure 3.4) are considered to be portions of seamounts, including the Nicasio Reservoir Terrane (Wright, 1984). The origin of the ophiolitic seamount material is also controversial, but it is thought that as oceanic plate was subducted, volcanic seamounts and plateaus were consumed. (There are thousands of seamounts in the western Pacific (Cloos, 1990, and it can assumed that they were as common in the "Eastern Pacific" during the 150 million years of Mesozoic subduction). Cloos (1990) suggests that the relatively narrow tops of tall mounts, (greater than 1 km) may have been decapitated intact, while the roots descended into the subduction zone, to be fragmented and incorporated into the accretionary prism, as shown in Figure 3.6. The size and presumed mechanical resistance of some of these mountains suggests that they would not easily be pulverized

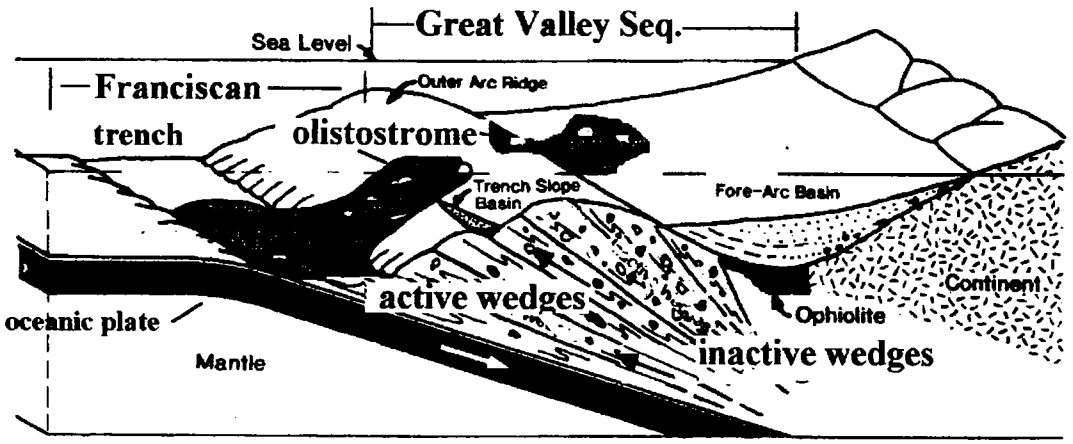

Figure 3.5 Several possible modes of melange formation at a convergent plate margin (after Bilodeau and Davis, 1990; Page, 1981)

by a combination of olistostromal, tectonic and/or diapiric processes, and it was difficult to distinguish a single genetic process.

As indicate above, convergence, with possible sporadic events of crustal separation, may have occurred for over 150 million years, in western North America. The subduction zones may have migrated fitfully several hundred kilometers westward, and oblique convergence is possibly still occurring as evident by ongoing crustal compression which continues to uplift California Coast Ranges. An early subduction zone, with proto-melanges, was interpreted in the Sierra Nevada foothills (Durrell, 1987, p97; Duffield and Sharp, 1973; Girty and Pardini, 1987), but other workers have proposed a terrane model (Edelman and others, 1989; Graymer and Jones, 1994).

Some of the supposed processes of melange formation are summarized in Figure 3.5, which illustrates a popular theory of melange formation. As an oceanic plate subducts, the surface sediments are scraped off and piled into an *accretionary prism.* The accretionary prism deforms, with the newest sediments ruptured by compressive thrusts and secondary extensional faults, in a manner akin to the response of a windrow of soil being pushed by a bulldozer. The mechanics of the accretion process can be analyzed as Coulomb failure prism, or *accretion wedges* (Davis and others, 1983; Suppe, 1985, p304-307; Platt, 1986). As the active accretion wedge migrates and gradually thickens oceanward, older wedges are abandoned.

It has been suggested that the compressive stress regime and saturated sediments in the active wedges result in high fluid pressures, and that fluidized sediments may migrate toward the surface of the accretion prism as diapirs and within flow channels (Cloos,

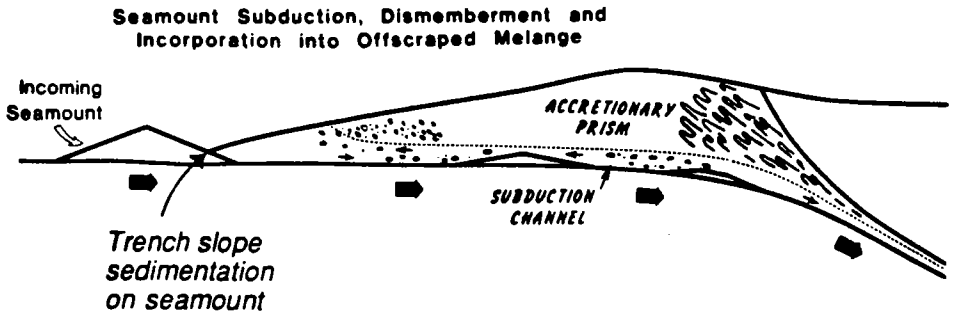

Figure 3.6 Conceptual sketch showing the partial incorporation of a seamount into an accretionary prism (from Bilodeau and Davis, 1990, p. 15; originally in Cloos and Shreve, 1988)

and that there may have been a lower limit to the amount of fragmentation, which would be evident from the block size distributions of seamount blocks (considered in Section 3.12(.

3.5 The FORMATION of BASAL TILLS and the KNEADING OF DOUGH AS POSSIBLE ANALOGIES FOR THE GENESIS OF MELANGE

3.5.1 Introduction

The apparent scale-independence of melanges was demonstrated in Section 2.6. If the fabric of melanges are self-similar then there must be fundamental relationships between the fabric and the geological processes responsible. Some insight is provided by consideration of glacial basal tills and the mathematical model of *mixing*, which is illustrated by the kneading of dough. Additional insight into the process of fragmentation and "nearest-neighbor" communition processes is provided by studies of the formation of fault gouge, which produces self-similar particle size distributions (Marone and Scholz, 1989; Sammis and others, 1987; Biegel and Sammis, 1989). Clearly, though, there are many geological fragmentation processes, and probably many produce self-similar block size distributions. So, such distributions should not be considered the signature of a particular genetic processes. Hence, although the ideas presented here require more work to verify their applicability to melanges, they may have broader application to the larger family of fragmented and mixed rocks.

3.5.2 Basal Tills as Possible Analogies for Melanges

The geological processes responsible for the wide range of block sizes in melanges are unknown. However, glacial lodgment tills have some similarities to melange (Raymond, 1984), since they contain well-graded, fragmented and mixed geological materials with block dimensions ranging over several orders of magnitude as shown by the weight-based particle size distribution (WPSD) in the upper graph of Figure 3.7, and other PSDs prepared by McGown and Derbyshire (1977), McKinlay and others (1974), and Boulton (1976). At the beginning of the research it was thought that a study of tills would be useful, since the genesis of glacial tills is better understood than the genesis of melange; and comparisons with melange may have provided insight into the geological processes responsible for melange, if the self-similarity of a glacial till could be demonstrated. Accordingly, a WPSD for Glasgow Lodgement till (basal till) was converted to a three-dimensional block size distribution (3DBSD) as shown in the lower graph of Figure 3.7.

WPSDs have previously been compared to numerically-based size distributions using a characteristic particle dimension measured from thin sections (Adams, 1977), but the conversion here used some principles of Soil Mechanics. Twenty kg of till, a Specific Gravity (G_s) of 2.7, and spherical particles, were assumed (although sphericity is unlikely for silt and clay particles). Other assumptions were:

1. the average particle size between two adjacent sieve sizes was d_m
2. the volume of one particle, V_p, was $(0.166)\pi d_m^3$, or $0.5236 d_m^3$
3. $\gamma_s = W_s/V_s$, the unit weight of soil = dry weight of soil/volume of soil (gm/cm^3)
4. $V_s = NV_p$, where N = number of particles
5. $G_s = \gamma_s/\gamma_w$, where γ_w is the unit weight of water

Using expression (5) as a starting point, substituting and re-arranging the other variables; leads to:

6. $\mathbf{N = 0.7W_s/(d_m^3)}$.

To construct the 3DBSD of Figure 3.7(b), individual data points of Figure 3.7(a) were read, the equivalent weight proportion calculated for an assumed 20 kg sample; the mean d_m calculated for each pair of adjacent values, and N, the number of particles of size d_m, calculated using expression 6. Plotted logarithmically, the linear fit of the data and the relatively large number of small particles show that the till has a self-similar 3DBSD, like melange, although the fractal dimension, D, is much lower than the melange fractal dimensions measured for melanges. This demonstration of the apparent self-similarity of till clasts suggests that further work could be performed to compare till and melange, if only because there may be similarities in the mechanical and characterization aspects of the two materials.

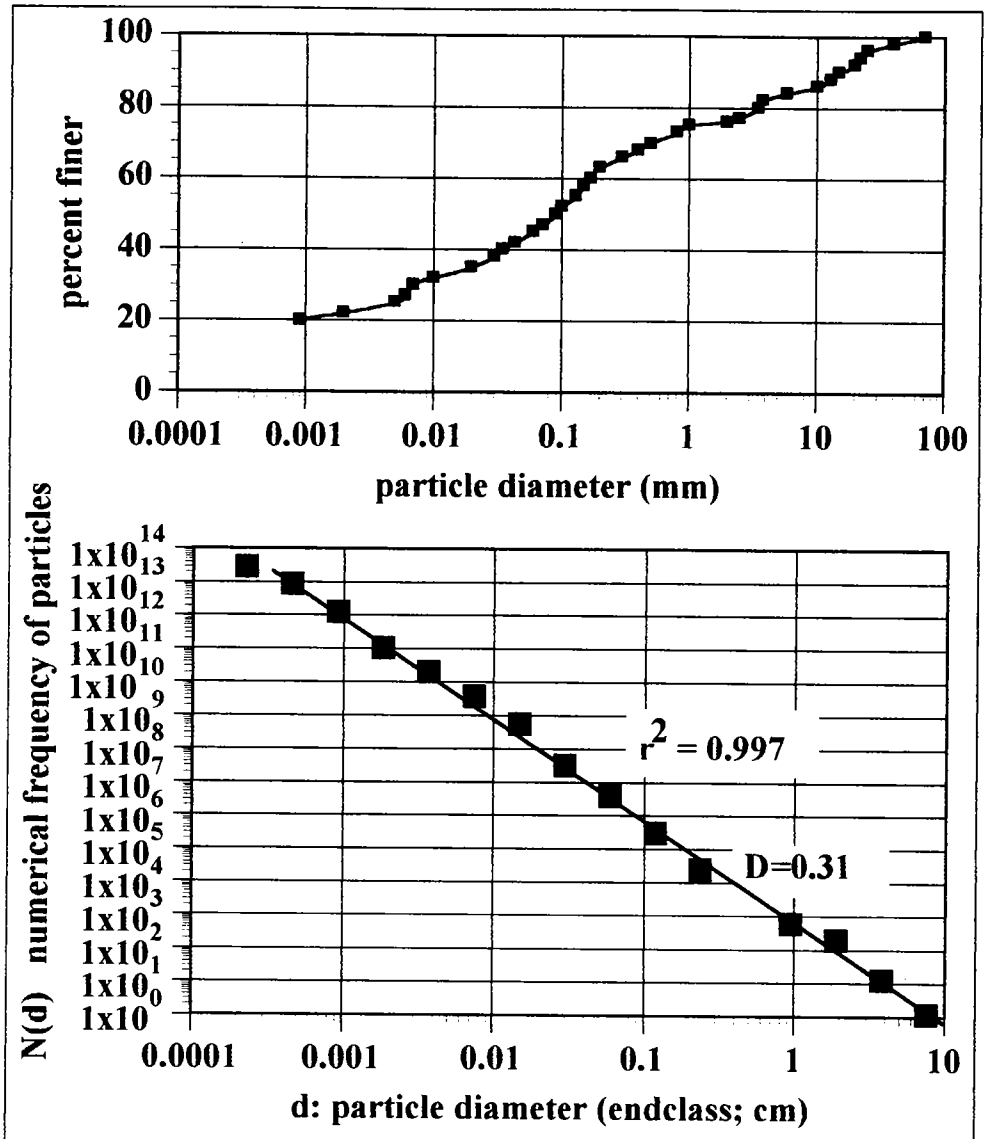

Figure 3.7 Equivalence of a WPSD to a 3DBSD for a glacial till; PSD data from McKinlay and others (1974).

3.5.3 The Kneading of Dough

In a mathematical treatment of the theories of *mixing*, Peitgen and others (1992, p. 508-583) gave an analogy which described mixing in terms of the kneading of dough. Imagine that a piece of dough is rolled flat. If patches of spice are placed at the center of the dough sheet, and the sheet rolled, folded, re-rolled, folded, re-rolled and so on, the spice will be mixed throughout the dough. An enhancement to the analogy is to cut the rolled dough, and juxtapose one half on top of the other half without rotation, "pasting"

the halves together, re-rolling and repeating the cut-and-paste many times (Peitgen and others, 1992, p.536-540). The result is that the distribution of patches of spice is self-similar.

It is speculated here that "geological kneading" is equivalent to repeated cycles of olistostromal extension (stretching and thinning) followed by compression (severe folding) and cutting (faulting). The kneading analogy may be applicable for the block size distribution of originally bedded shale and sandstone sediments into a mixture of graywacke blocks within a shale matrix. There is presumably a correlation between the final chaotic state of the block size distribution and: the number of cycles of kneading; the energy available to fragment the protoliths of the blocks; the time available for fragmentation and mixing; the strength and other physical properties of the protoliths and the fragments once broken (density, viscosity, stiffness, and so on); and the energy available to mix the blocks with the matrix. But if the block size distributions of exotic blocks (blueschist, volcanics/chert/limestone packages (shredded seamounts) and serpentinite) have poorer self-similar distributions, it suggests that they were introduced later, suffered fewer cycles, or were more resistant to fragmentation. The range of size of blocks, the lithology of the blocks and their relative numbers should reflect the geologic process that has created the fragmentation and mixing. The block size distribution of various lithologies are considered further in Section 3.12.

There are many questions that can be asked about the dough kneading model:

1. Are there kneading cycles in an accretionary prism? The understanding of the tectonics of even contemporary accretion prisms is primitive; and that of ancient convergent margins is contentious (a useful review is provided by Park, 1988; p.112-165).
2. If melanges form purely as olistostromes, with no tectonism involved, do they also exhibit self-similar and scale-independent fabrics? To answer this question, work should be performed to discern the block-size distributions of Great Valley Sequence olistostromes, which are clearly not the result of tectonic processes, since they are bounded by coherent and unfaulted sediments (for example, Bailey and others, 1964, Photo 75, p. 134). If olistostromes do show self-similarity, then self-similarity may not be a useful tool for discovering the processes responsible for tectonic melanges. (On the other hand, many of the procedures presented here can be used).
3. Is there a scale limit for kneading? A Significant problem, yet to be resolved, is that at the microscopic scale, the matrices of melange may not be as mixed as they appear to be megascopically (Prof. David L. Jones; personal communication), which suggests that there is a lower limit to the scale-independence of melanges. Presumably there is an upper limit, too.

3.6 GENESIS OF SHEARED SERPENTINITE BODIES

Sheared serpentinites are similar in appearance to sheared shale melanges, with rounded, lenticular, slickensided and often mirror-smooth blocks of hard, serpentinized ultra-mafic rocks enclosed within matrices of scaley, sheared serpentinite. Not considered in this dissertation are *serpentinite melanges*, which are similar to sheared shale melanges, containing blocks of diverse lithologies, with matrices of sheared serpentinite rather than sheared shale. Little is known about their origins, although they are well represented in the Franciscan, neither have they been well described (Prof. David L. Jones; personal communication).

The protoliths of serpentinites are the ultramafic rocks which compose the basement of *ophiolites*. Ophiolites were once known as Steinmann's Trinity. The word "ophiolite" is descriptive and non-genetic. An ophiolite series consists of (from the base upward): cumulate-textured ultramafic plutonic rocks (such as harzbergite and peridotite), gabbro, overlain by a complex of sheeted mafic dikes or sills, then a mass of mafic pillow lavas, associated with radiolarian cherts. The series is often capped with pelagic shales, with an association of sandstones and limestones (McCall, 1983, p. 1). The ultrabasic rocks below the gabbro are generally altered to serpentinite. Ophiolites have been identified all over the world (Lockwood, 1971; and Figure 3.1), and include belts such as The Kurosegawa Zone, a 600 km string of individual serpentinite melange bodies in southwest Japan (Maruyama and others, 1984). Ophiolites are recognized as *obducted* slabs of oceanic plate, resulting from the over-plating of oceanic crust *over* the continental plate at a convergent tectonic boundary, as opposed to *subduction* or under-plating. Oceanic plate may also have been exhumed by crustal thinning resulting from protracted crustal extension (subduction results in compression and crustal thickening).

A major regional ophiolite in California, generally incomplete in any one place, is the Coast Range Ophiolite (CRO) that forms the basal boundary between the Great Valley Sequence and the Franciscan. Serpentinite bodies are also found throughout the Franciscan, trending northwesterly and generally linear, tabular, plug-like, or lenticular in shape, many being of the order of kilometers. Phipps (1984) and Lockwood (1971) described sedimentary deposits of serpentinite in northern California, one of which is described as a chaotic ophiolitic of about 1 km thick, above the basal serpentinite of the Great Valley Sequence (Phipps, 1984).

Serpentinization is a chemical reaction between the olivene in peridotite, the main constituent of the base of an oceanic plate; and water. (Olivene is the Mg-rich end member in the forsterite-fayalite series; Bailey and Everhart, 1964, p. 55). Serpentinization occurs in the high-pressure but relatively low-temperature regime of over 15 km depths in a subduction zone, where it is thought that the presence of the "cold" descending oceanic plate lowers the normal geothermal temperatures; and the sediments carried down by the plate dehydrate, thus providing the water necessary for

serpentinization (Fryer, 1992). The hydration of peridotite produces serpentine and brucite (O'Hanley, 1992; Bailey and Everhart, 1964, p. 55), and the altered peridotite expands, which decreases its specific gravity from about 3.3 to 2.65, and its density by about 20 percent to 45 percent (O'Hanley, 1992). There has been considerable debate for over 80 years as to whether the hydration results in a positive, negative or no volume change: evidence has been produced to show positive volume change is accommodated by fracturing within the serpentinite, and it is these cracks that later host the asbestos minerals exploited in serpentinite bodies (O'Hanley, 1992). Serpentinites are often intensely faulted and sheared at all scales of observation (Gates, 1992). Subsequent hydrothermal alteration of serpentine produced distinctive white silica-carbonate rocks host cinnabar, the ore mineralization for mercury, amongst others. Nephrite jade is a rare but sought-after accessory to serpentine (Crippen, 1951; Yoder and Chesterman, 1951; Chesterman, 1951).

Smaller bodies (100's of meters?) are generally intensely sheared throughout and there is little evidence of their igneous ancestry. Larger bodies are sheared at their peripheries, and grade to a melange of sheared matrix surrounding blocks that range from rounded cobbles to blocky chunks ranging to meters or tens of meters, with most being less than a meter (Bailey and Everhart, 1964, p. 49). Closer to the center of a larger body, the ultramafic protolitholgy may be recognized. Geological maps, (for example figure 2 of Page, 1968) may show the apparent self-similar arrangement of serpentinite blocks, within shear zones or melange in which other Franciscan rocks may be mixed. Such zones have been interpreted as faults (for example, Page, 1968) composed of a myriad of faults, which may not show displacements. Sheared Franciscan, sheared serpentinite and mixtures of both were once classified under the more generic term "sheared rock" (Schlocker, 1974, p. 55-66)..

It was once though that serpentinite bodies were "cold" igneous intrusions, because they lack thermally metamorphosed aureoles at the margins of the serpentinized masses, and "xenoliths" within the larger sheared serpentinites often cannot be associated with any surrounding rocks (Bailey and Everhart, 1964). The impression of an igneous intrusion is reinforced by the geomorphology of serpentinite bodies, which are often stark and sparsely vegetated with a reddish, whitish or greenish-black appearance distinguishable from great distances (Blake, 1984, p77-89). Manzanita and targrass have an affinity for the fat clays that develop on serpentinites, and in the early summer, the relative greenness of the vegetation are clues to the presence of underlying serpentinite (Bailey and Everhart, 1964, p. 49). (As inhospitable as sepentinite masses appear, serpentinite hosts fauna and flora found in no other environments, and serpentine and the associated minerals of talc, steatite, soapstone and jade, were treasured raw materials for weapons and bowls used by Early Man in North America : Dann, 1988; Crippen, 1951).

Sheared serpentinite is mobile, and may rise as " serpentinite mud" diapirs, or flow via faults penetrated through the accretionary prism, carrying slabs of partially serpentinized

ultramafic rock, blueschist and greenschist rocks from deep in the subduction zone (Fryer 1992). Cowan (1985) recognized a similarity between mobile sheared serpentinite in diapirs, and mobile, sheared diapiric sedimentary mud, which could inject melange into relatively recent faults. Phipps (1984, p. 112) proposed that sedimentary serpentinite masses formed as serpentinite debris flows from oceanic crust exposed either subaerially, or in shallow waters, due to exhumation of the crust by uplift of the forearc basin.

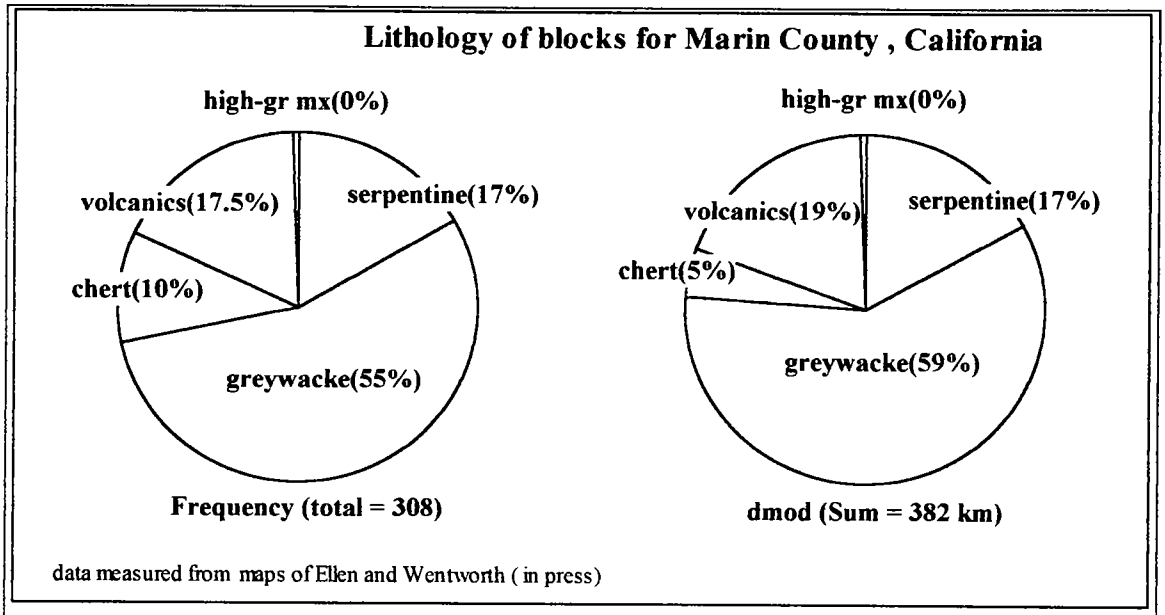

Figure 3.8 The relative proportion of blocks of various lithologies in some Franciscan melanges of Marin County, California, calculated on the basis of numerical frequency (left chart) and proportion of total d_{mod} (right chart).

3.7 BLOCK LITHOLOGIES

From an engineering point of view, the lithology of the geotechnically significant blocks in a bimrock does not matter if the overall strength of bimrock is the only consideration. The blocks may be of varying lithologies but due to weathering or alteration look the same, and from a geomechanical point of view, may behave the same. However, excavation and tunneling in the Franciscan is made more difficult is when blocks of tough greenstone, or high grade blueschists are encountered. Greywacke blocks are well fractured and often contain ground water under pressure, and chert blocks shatter. Thus, it would be useful to have some guidelines as to the relative frequency of the blocks relative to their lithology. The size distribution of blocks of various lithologies is considered in Section 3.12.

Not considered here are siltstone blocks. Lithologically these are "matrix" that have escaped shearing. Nevertheless, mechanically they behave as other blocks, perhaps

because the mechanical contrast between blocks and matrix need not be high, as speculated in Section 2.6.2. Significant proportions of siltstone blocks, were observed in drill core and in the field at the Lone Tree Slide in the core for the Richmond Transport Project, and in the graphical boring logs for Scott Dam; and specific data are presented in the appropriate Sections of Chapter 5.

In the Franciscan melanges studied, the relative proportions of blocks, classified by lithology, is generally consistent, as shown by Figure 3.8 for blocks measured from a geological map of Marin County, California (Ellen and Wentworth, in press). The proportions calculated on a numerical basis are similar to the proportions calculated on the basis of block size. That is to say, if 65 of 100 blocks are graywacke, then the ratio of the sum of the d_{mod} lengths for the all graywacke blocks to the sum of the lengths of the d_{mod} for all the blocks is about the same as the numerical proportion of graywacke blocks. This implies that the average size of the blocks within each lithological group is similar. (Eric Lindquist; personal communication). For the Marin County blocks, the average block size for each lithology is about 1.1 to 1.3 km (except for chert, 0.5 km). (The maximum block is graywacke, of about 18 km size). However, the idea of average size in a self-similar block-size distributions is misleading, since the distribution is skewed significantly toward the numerous smaller blocks.

3.8 MATRIX LITHOLOGY

Matrix is the arrangement of finer particles that binds the blocks in a bimrock. Laznicka (1988; table 2-3, p64,65) distinguished several varieties of matrix for block-in-matrix rocks, amongst which he included *ductile and viscous matrix* (sheared or flaky serpentinite in serpentinite melanges); and *rock matrix* such as the invariably sheared argillaceous or serpentinite matrices of Franciscan melanges. But, matrices of relatively competent sandstone enclosing blocks of shale are found in olistostromes, where there was soft-sediment deformation during submarine debris flows or earthquake-induced liquefaction, when saturated sand layers fluidized and engulfed relatively coherent chunks of mud. As indicated above, matrix rock that escapes shearing may be considered blocks.

Shale, argillite and mudstone matrices commonly have a significant smectite clay content (Schlocker, 1974, p.19; Blake, 1984, p. 38). Sheared serpentinite and sheared shale can closely resemble each other (Schlocker, 1974, p.55) because the shale is often black or gray, due to organic carbon, and the serpentinite may be bentonitic (smectite, or montmorillonite). Sheared serpentinite is commonly greenish-gray, streaked blue, but may be white or dark gray when altered (Schlocker, 1974, p. 57).

3.9 INDIVIDUAL BLOCK SIZES and BLOCK SHAPES

There are many geological synonyms for "block" which have a size and/or genetic connotation, including: *autoclasts, blocks, bombs, boulders, chips, clasts, fragments, friction balls, horses, inclusions, knobs, lenticles, lumps, knockers, lapideous fraction, lonestones, megalumps, olistoliths, phacoids, pillows, slabs, tectoliths, xenoclasts, and xenoliths*. Hsü (1969; p.11) described inclusions in the Franciscan melanges near Morro Bay, California, based on the maximum dimension of blocks: large slabs (5000 feet); through small slabs, large blocks; small blocks (5 - 50 feet); and fragments and chips (5 feet). Block sizes in Franciscan melanges range to the size of the sub-terranes of the San Francisco Bay Area (Blake and others, 1984: and see Figure 3.3 above). Because of the many descriptors, it is recommended here that the word ***block*** be used exclusively. As defined in Chapter 1, blocks are the geotechnically significant fragments within a matrix , and are characterized by $\mathbf{d_{mod}}$, the maximum observed dimension.

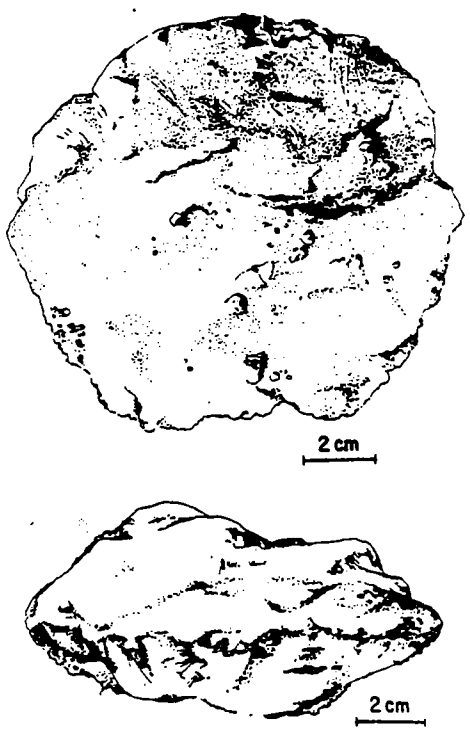

Figure 3.9 Typical deformed block (Phacoid) from Franciscan melange near San Simeon, California from Cowan (1978

Block shapes influence block size distribution, block volumetric proportion, and frictional resistance at the block/matrix contact. For instance: considerably more platy blocks can be accommodated by imbrication than by spherical packing; and streamlined

blocks have smoother failure surfaces, whereas the asperities of jagged profiles contribute more resistance.

Block shapes can be compared qualitatively against standard images on charts (e.g.: Dietrich et al., 1982, sheets 15, 16, 18, 19), and are sometimes described by likeness, such as: *carburetor-shaped*, *bossom-shaped*, *balloon*, *amoebid*, and *almond* (Laznicka, 1988, p. 49). More utilitarian descriptors are: *boudin* (cylindrical, European-style sausage), *irregular* (such as wisps and contortions, common in olistostromes where there has been soft-sediment deformation); and *phacoid* (oblate disk), common in Franciscan melanges, as shown in Figure 3.9. Phacoids conform to the surrounding sheared argillite with smooth and polished surfaces. Blocks of schist in Franciscan melanges tend to be rounded, even when very large (Prof. David L. Jones; personal communication).

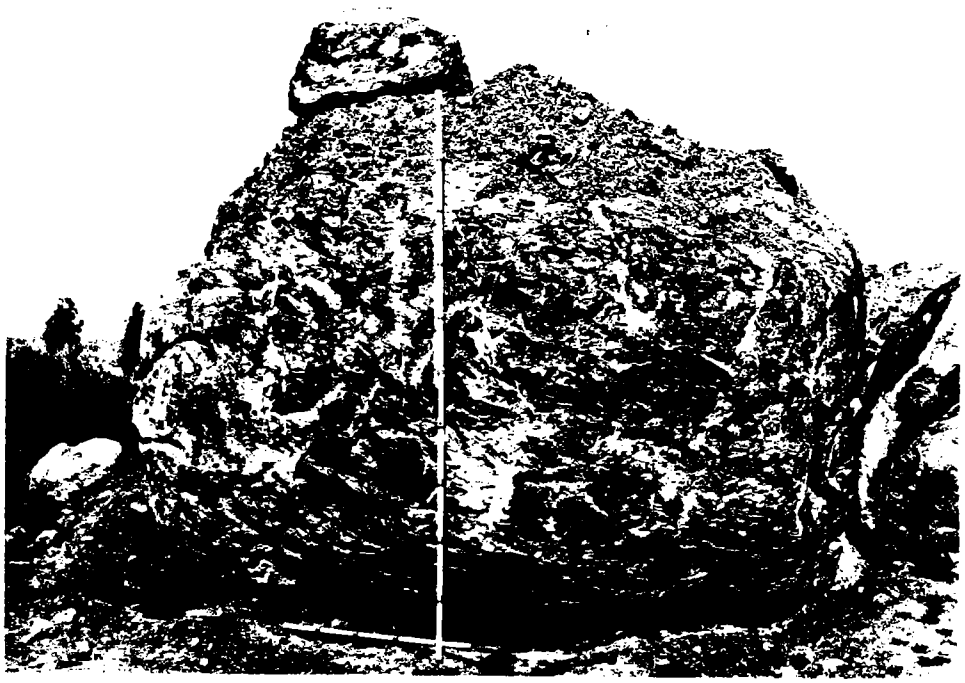

Figure 3.10 Free graywacke block of up to 3m size, released from an excavation at Redwood Landfill, near Petaluma, Sonoma County, California. At least 50 percent of the block surface was smooth and slickensided.

The shapes of particle shapes are researched extensively in industries that depend on fine powders (Allen, 1990, p.217-247; 124-191), with specialized stereological attention to *morphometry* (Aherne & Dunnill, 1982; Underwood, 1970 p.195-254; Weibel, 1979, p.162-203; 1980, p. 140-1740. But, little work has been done to quantify shapes for fragmental rocks, despite the large literature devoted to clast shapes in sedimentary rocks (Laznicka 1988; p44-49; Blatt et al., 1972, p62-71; Selley, 1988, p. 38-40). For the

research, simple geological methods were used. Ratios of the characteristic dimensions of blocks (such as the minor, intermediate and major axes) allow the use of standard graphs to characterize shapes (Blatt and others, 1972, p. 66-67; or Flinn diagrams: Hobbs and others, 1976, p. 36). Clarke and Hansen (1993) adapted such graphs to classify the shapes of fluvially transported boulders with major axes of up to 2.7 m.

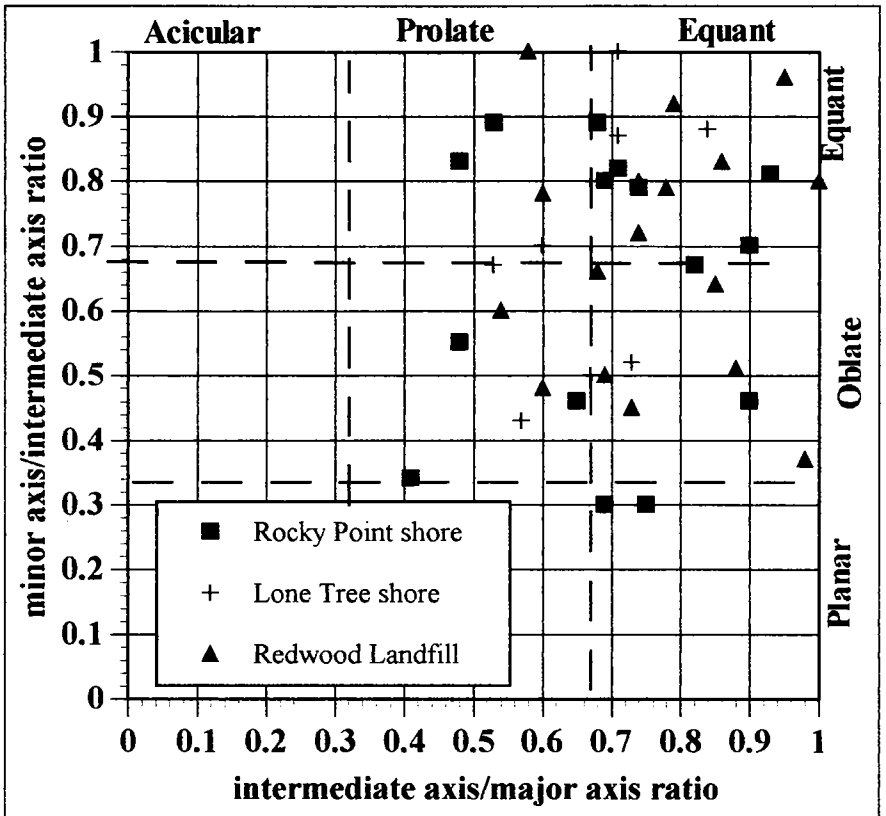

Figure 3.11 Axial plots of 41 blocks from Franciscan melanges

The shapes of 41 *free blocks (*not in-place) at seashores, along river beds and at construction excavations were measured from three characteristic dimensions (approximately major, minor and intermediate axes). Caution was exercised since the free blocks were rarely their original shape, due to buffeting suffered from ocean waves and bulldozers, which had tended to fragment them. Measurements were made only where more than 50 percent of the blocks' surfaces showed original smoothness and slickensides. Figure 3.10 is a photograph of such a block. Other blocks were measured at the seashores near Rocky Point and Lone Tree Creek, Marin County, California. The blocks ranged up to 5 m in maximum dimension, and were measured with a carpenters' tape and home-made stadia rods. Nearly all the blocks were graywacke and serpentinite.

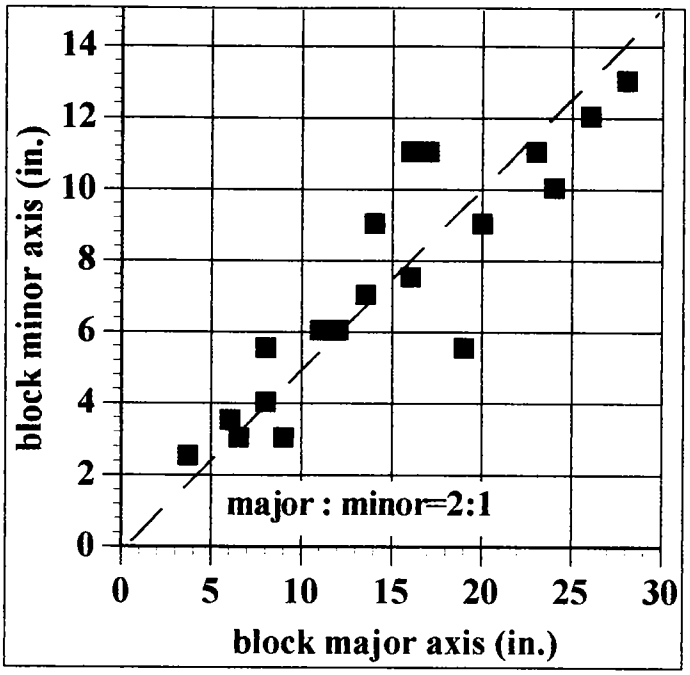

Figure 3.12 Major and minor ratio axes lengths for serpentinite blocks near Rocky Point, Marin County. Average axial ratio is about 2:1

The axial ratios of the blocks are plotted in Figure 3.11: the blocks tended toward equant-shaped (spherical). The aspect ratios (minor axes/major axes) ranged between 1:1 and 1:3, which supported Lindquist's (1994b) decision to use aspect ratios of 2:1 to 3:1 when he fabricated blocks for incorporation into physical model melanges.

Measurements were also made of serpentinite blocks in an outcrop of sheared serpentinite at the intersection of the access road to Rocky Point Environmental Camp and Highway 1, Marin County, California. The graph in Figure 3.12 indicates a distinct 2:1 trend to the minor:major ratio. The measurements do not represent the absolute maximum and minimum lengths of the block axes, since they were made in two dimensions.

3.10 BLOCK ORIENTATIONS

The geological engineering implications of block fabrics are important, since the mechanical behavior of a bimrock is partially dependent on the overall structure of the blocks, in as much as failures in the matrix will be forced around them. In researching the mechanical properties of physical model melanges Lindquist (1994a, 1994b) and Lindquist and Goodman (1994) discovered that blocks oriented parallel to axial loading (vertical) stiffened the model melanges significantly more than blocks oriented normal to the loading. To display preferred orientations blocks must be other then spherical. If they

tend toward ellipsoid or phacoid, the mean planar attitudes or the linear trends can be measured, and analyzed vectorially and statistically. Small blocks tend to reflect the fabric of the sheared shale which flows around the larger blocks. In general, larger blocks trend toward the northwest in Franciscan melanges (see Figure 2.8), and appear to be steeply dipping (have low block orientation angles relative to the vertical).

3.11 BLOCK VOLUMETRIC PROPORTION OF FRANCISCAN MELANGES

For a block/matrix proportion of between 5 percent and 10 percent, Laznicka, (1988; chapter 2) considers "knockers" in melanges, "exotic" blocks in wildflysch olistostromes, and "horses" in fault zones/gouge to be *lonestones.* In the case of melanges, such lonestones are relative giants within a matrix of numerous, smaller blocks. When the block/matrix ratio is less than approximately 3:7 (43 percent), fragments in block-in-matrix rocks tend to be is matrix-supported, or have a *diamictite texture* (Laznicka, 1988; p. 72). Once the block/matrix proportion is greater than about 1:1 (50 percent) to 2:3 (67 percent) blocks tend to touch and the bimrock then becomes block-supported, or as defined by Laznicka (1988, p. 72) to show a *block-to-block fabric.*

But the threshold at which blocks touch depends on the block shapes and block size distribution. Rodine (1975 p. 137-159) and Rodine and Johnson (1976) showed that mono-size distributions of glass of 45 percent to 55 percent volumetric proportion spheres interlocked, compared to 64 percent for bimodal distributions of spheres. For well-graded distributions of debris flow slurries from 89 percent to 95 percent volumetric proportion was necessary before interlocking of the particles was accomplished. The block/matrix proportion of a bimrock theoretically will vary from 0 percent (pure matrix) to 100 percent (pure blocks), but a more realistic range is of the order of 10 percent to 90 percent, and the geotechnically significant block volumetric proportion has been defined previously as the range between 25 percent and 75 percent (Chapter 1).

The block volumetric proportion of Franciscan melanges varies considerably. Blake and others (1974) indicated that the block proportion in a mapped area of Napa. Sonoma and Marin Counties, varied between 1 and 50 percent. At her study site near Nicasio Reservoir, Marin County, Savina (1982,p. 144-146) estimated that the block/matrix ratio ranged between 1:1 (50 percent) and 1:10 (9 percent) with 1:4 (20 percent) being an average. Block volumetric proportions measured during the research varied between 5 percent for failed rock at the Lone Tree Slide (measured from field work and from drill core) and 50 percent at the Richmond Transport Project (measured from drill core).

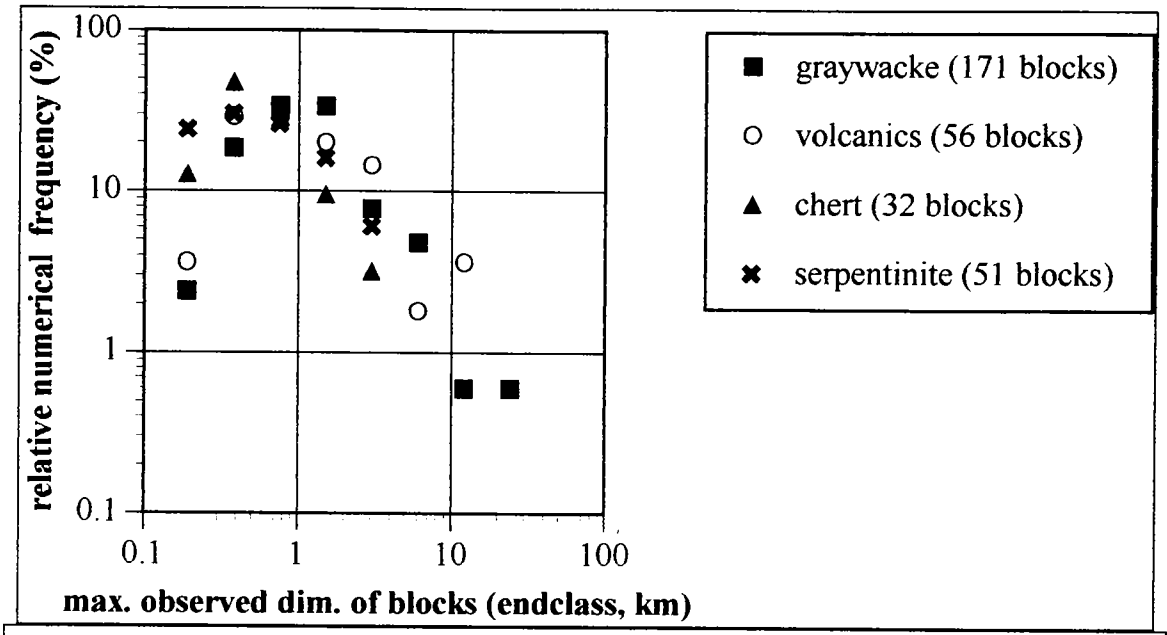

Figure 3.13 **Block size distribution of blocks in Marin County, sorted by gross lithology. Blocks have reasonable log-log linear trends, except for volcanics. Data measured from the maps of Ellen and Wentworth (in pres**

3.12 BLOCK SIZE DISTRIBUTIONS IN FRANCISCAN MELANGES

The block size distributions of some Franciscan melanges have been shown here to be self-similar in Section 2.4 and Section 2.5, but the lithology of the separate blocks was not considered . However, the blocks within some Franciscan melanges exhibit self-similar block size distributions when the d_{mod} data are plotted as log-histograms on a lithological basis. This has been done for the blocks of the Franciscan in Marin County measured from the maps of Ellen and Wentworth (in press), and are shown in Figure 3.13. The relative numerical frequency of the blocks allow for easier comparison between different sized groups. The descent limbs of the plots, generally trend log-log linear suggesting that the block size distributions are self-similar. However, there is more scatter for the data of the volcanic blocks, which suggests that the volcanic blocks may not have suffered the same degree of fragmentation and mixing as the graywacke blocks. The few serpentinite data suggest self-similarity. The block sizes of volcanic\chert blocks (measured as chords) in drill core at Lone Tree Slide show poor self-similarity.

It was thought that the enigmatic high-grade metamorphic blocks would not show self-similarity, so a study was made of he block size distribution for several hundred metamorphic blocks in the Cazadero-Ward Creek area of Sonoma County, where a dense population of unusual and exotic metamorphic blocks draws geologists from around the world (Erikson, 1992?; 1994). Data are from a 41 km^2 area mapped by Erikson (1994, p.11-39; and 1:12000 map). No attempt was made to sort the blocks by proto-lithology.

One 5 km block (Big Oat Creek metabasalt) was excluded from the block measurements, which were assumed to be d_{mod}.(maximum observed dimensions).

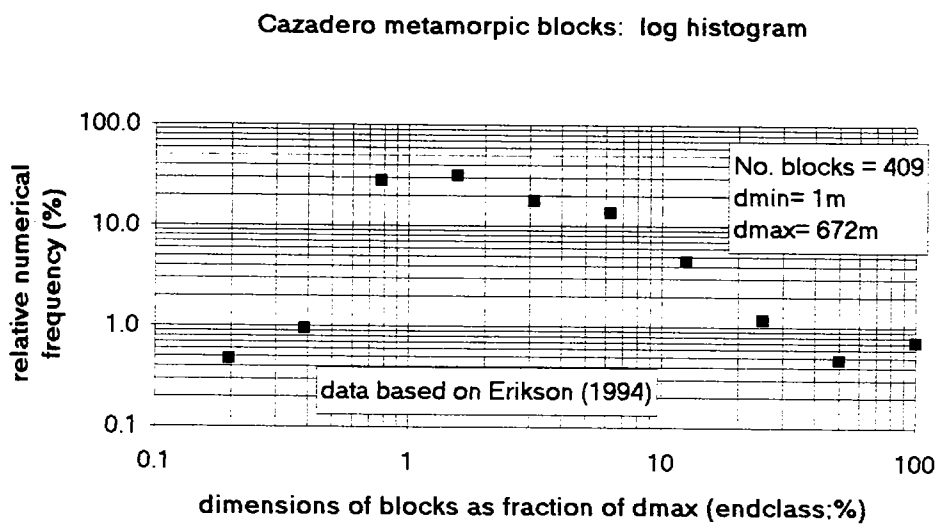

Figure 3.14 Log-histogram of metamorphic blocks in the Cazadero-Ward Creek area, Sonoma County, California. Data are generally organized log-log linear, possibly with two segments.

The data are plotted in Figure 3.14, which shows the well-defined descent limb of the log-histogram of to be kinked, but linear. (Kinked descent limbs for the particle in simulated fault gouge imply different fragmentation processes: Sammis and others, 1987). The implication of the general linearity is that, at least in this area, the size distribution of the metamorphic blocks is organized fractally, and presumably the blocks were originally mixed in the same fashion as graywacke blocks. Erikson (1992?, p3-5) considers the matrices of the melanges in the area to have originally been olistostromes, which incorporated blocks of various lithologies that "...rolled or slid...." into the trench. The entire packages were then metamorphosed, some slightly (Kings Road Ridge Melange unit) and others more severely (Cazadero phyllite melange unit). But this process may not be same one that introduces the solitary exotic blocks found in the Franciscan. Appendix E contains additional details and a geological sketch map of the area.

3.13 BLOCK DISCONTINUITIES

The internal defects of blocks are as diverse as those of the original protoliths, overlaid with the disruption resulting from the formation of the blocks. For olistostromes, the parent materials for the blocks were incompetent and deformation was relatively plastic; the block defects were inherited from subsequent deformation, diagenesis, and

exhumation (stress relief). Small blocks of greywacke, and blocks of chert tend to be shattered, whereas blueschist, greenstone and serpentinite blocks tend to be competent. However, large graywacke blocks may be massive, showing few defects over several meter intervals (see for example, figure 7 of Bailey and others, 1964). An important engineering consideration is whether a discontinuity is confined to the blocks or if it continues into the matrix, since thoroughgoing defects provide a potential failure route through the block.

3.14 MATRIX FABRIC

The matrix fabric in Franciscan melanges ranges between thoroughly sheared and relatively continuous, but the sheared matrices are more common. As indicated previously, volumes of unsheared matrix can be considered to be blocks it they satisfy the criteria for geotechnical significance (Section 2.6). Peterson (1979, p.21) observed a relationship between the fabric of the matrix and the proportion of blocks: the higher the proportion the blocks, and the greater the variation in lithologic composition, the greater the disturbance to the matrix. Blake and others (1974) also reported that the degree of shearing in shale was "abundant in areas where knockers were abundant" for Franciscan melanges of Napa, Sonoma and Marin Counties, California. Savina (1982, p. 142) measured up to 800 shears per meter in the field, and shears were spaced as close as 5 microns when viewed under a scanning electron microscope (SEM). Peterson (1979, p.22) characterized matrix shearing as "semischistose", and some have referred to the sheared melange as "phyllite", which is petrographically incorrect for Coastal Belt and Central Belt melanges, but does convey an impression of penetrative deformation.

The pervasive shearing of the shale matrices results in a fabric of anastamosing discontinuities analagous to the complex, but organized, distribution of Reidel and thrust shears in a fault zone, what Skempton (1966) referred to as *mille feuille* (French for a thousand sheets). The matrix may be so shattered that little consistent matrix fabric can be observed, but must be deduced by the organization of blocks. The sheared shale is hard, overconsolidated, and breaks easily into the shiny chips and lenses, that has prompted the names *lustrous clay, block clay, scaley clay* and *argille scagliose*, and is often confused for serpentinite. Some believe that the scaley clay fabric is diagnostic of tectonic shearing, whereas the less sheared matrices are thought to be diagnostic of olistostromes. The scaley (asymmetric) fabric and lenticular blocks are attributed to non-co-planar deformation (simple-shearing) within accretion wedges by Kano and others (1991) and Needham (1987), and is thought to be the result of overconsolidation resulting from "tectonic loading" (Enriquez-Reyes and Jones, 1991), as reflected in the high unit weights of both the matrix and blocks compared to "coherent" or non-sheared parts of the melange of the Shimanto Belt of Japan (Hada, 1988).

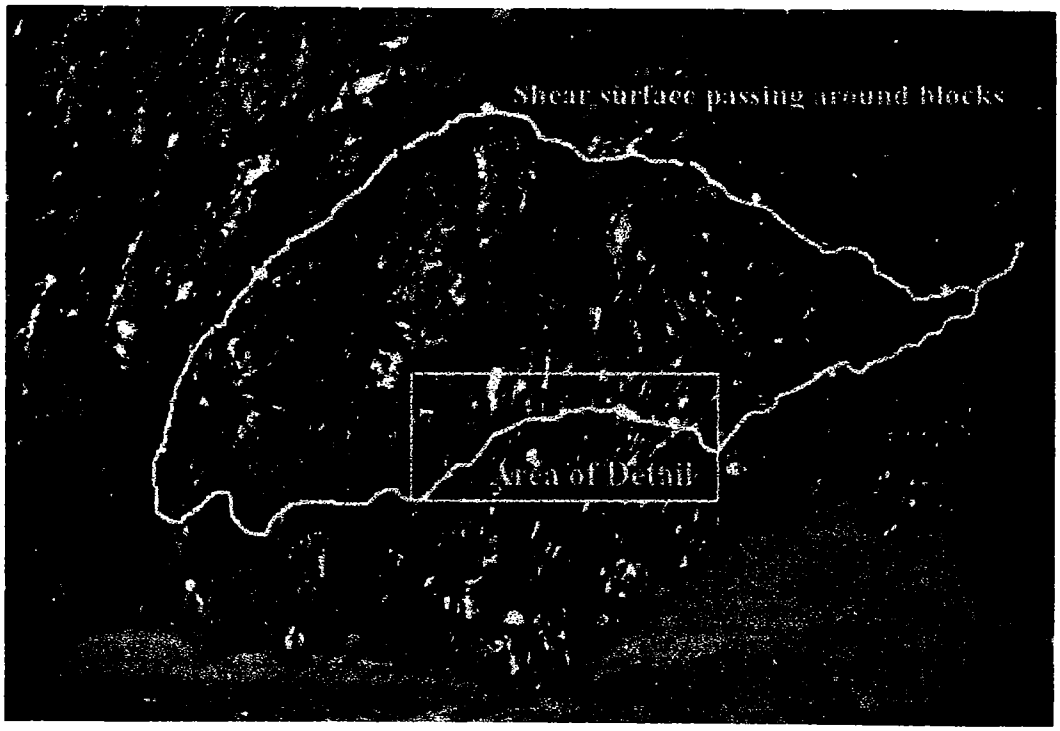

Figure 3.15 Shear passing around blocks in a Franciscan melange, at beach near Fort Bragg, near Mendocino, California. Detail is shown in next figure.

Shears invariably pass around blocks, no matter how tortuous the route taken, as shown in Figure 3.15, which illustrates a shear in a Franciscan melange; and Figure 3.16 which is a detailed view (the image is inverted to improve an overly-dark photograph). Since melanges have a history in which shears negotiated blocks, it is not unreasonable that new deformations may occur on tortuous surfaces that pass around blocks (Lindquist, 1994; Lindquist and Goodman, 1994).

Sandstone matrices are found in the Franciscan. In places the sandstone envelopes weaker blocks of shale; examples are found in the Crescent City area of California and elsewhere in the Coastal Belt where olistostromal deposits and broken formation are common. (Savina, 1982, p.142-144) described sheared sandstone matrix at her study site near Nicasio Reservoir, Marin County. The sheared sandstone broke into thin plates and deformation appeared to have been constrained to narrow shear zones in the greywacke, unlike the ubiquitous and pervasive shearing in the shale matrix.

Figure 3.16 Detail of shear shown in Figure 3.15. Image is a negative.

3.15 BLOCK/MATRIX CONTACTS

The surface conditions of blocks influence the shear strength of failure surfaces that may develop around the blocks. The relief of the surfaces of blocks may vary from ultra-smooth, like the "tectonic mirrors", found in fault zones and certain shear surfaces, through polished, striated, pitted, and jagged. (see location 12; Wahrhaftig , 1984, p.15, for a spectacular, smooth wall)..Figure 3.16 illustrates the lustrous surface of a small block plucked from a Franciscan melange.

The sheared matrix and competent blocks, can be distinctly contrasted. In fresh exposures, the contacts may be occupied by a wafer-thin film that can be pulled away with tweezers,. And in weathered outcrops, the safe wafers are decomposed to a greenish tissue of clay, slick enough that small blocks may be rotated and removed relatively easily. The *moulds*, or cavities that remain when a block is removed also reveal a clay skin. Such observations suggest that the condition and strength of the block/matrix contact is of critical importance relative to the characterization of bimrocks. (The word "mould", is an adaptation of a term used to describe the half space remaining when a Joint Pyramid is removed: Hatzor and Goodman, 1992; Hatzor, 1992 But Schlocker, 1974, referred to the blocks and molds as *knobs* and *sockets*, which are perhaps more descriptive terms).

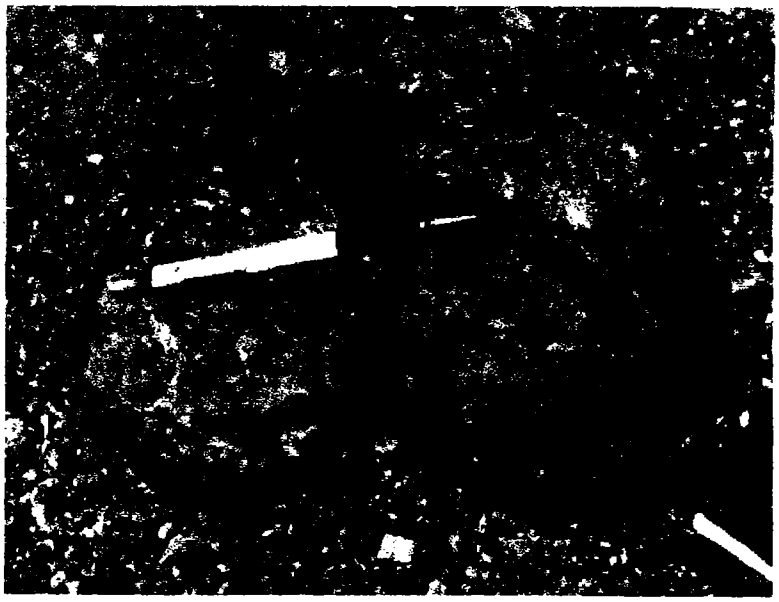

Figure 3.17 Greenstone block with a lustrous, smooth surface; from a Franciscan melange at San Simeon, California.

CHAPTER 4 ENGINEERING ASPECTS OF REAL AND MODEL BIMROCKS

4.1 INTRODUCTION

This chapter summarizes the engineering aspects of work performed for the research on Franciscan melanges, and model bimrocks. The models included physical model melanges (fabricated by Lindquist, 1994b), and *graphic models*, or images of melanges, the Gravel Tests setups, and Triaxial Test Tracings. The estimation of block volumetric proportions and block size distributions is emphasized, and problems encountered by engineers when working with melanges and similar bimrocks are summarized.

4.2 SUMMARY OF GEOTECHNICAL LITERATURE PERTAINING TO BLOCKY ROCK AND BIMROCKS

4.2.1 Geotechnical Experience with Characterizing Blocky Rock

Much of Rock Mechanics is concerned with predicting the engineering behavior of blocky rock masses, which are volumes of rock disrupted by at least three sets of discontinuity surfaces (faults, bedding, shears, and joints), that influence the mechanical behaviour of the mass once it is invaded for an engineering purpose (Hoek and Bray, 1977; Hoek and Brown, 1982; Goodman, 1989). Priest (1993, p. 2; citing Piteau , 1973), listed six properties of discontinuities that have the greatest influence on the mechanical behavior of blocky rock masses: *orientation, size, frequency, surface geometry, genetic type* and *infill material*. Generally, *blocky rock*, is not *bimrock*: for the purposes of this dissertation, a blocky rock mass is a block-in-matrix mass that has a block volumetric proportion of more than 75 percent. Blocks larger than 75 percent of the characteristic engineering dimension are also considered to be blocky rock. Bimrocks can be partly distinguished from blocky rocks on the basis of a finer textured, weaker matrix; and the generally smoother-shaped blocks

But blocky rocks, given wide enough regions of weaker infilling between the blocks, may approach the condition of bimrocks; i.e.: a matrix-supported array of blocks. (Figure 2.21 shows a model bimrock, with a block areal proportion of 72 percent, which approaches the condition of blocky rock). So, some blocky rocks may be candidates for analysis as bimrocks, and alternatively, existing methods in the Rock Mechanics literature may be relevant to the characterization of bimrocks and prediction of rock mass behaviors. For instance, the standard approach to characterizing blocky rock is by the use of measuring lines on rock exposures (scanlines) and borehole core, which provide measurable lengths between discontinuities. For the research, scanlines were any measurement lines used to characterize the blocks of real or model bimrocks.

Much has been written in Rock Mechanics on the statistical characterization of blocky rock from scanlines and borehole data (Priest and Hudson, 1976, 1981; Call and others, 1977; Hudson and Priest, 1979, 1983; Warburton, 1980; Pahl, 1981), and procedures have been described to estimate the size distribution of prisms of blocky rock (Sadagah and Sen, 1992; R.D. Call's numerical method, described by Savely, 1987, p. 46-50). On the other hand, the determination of block size distributions (**BSDs**) for block-in-matrix rocks other than sedimentary rocks have only rarely been performed, as pointed out by Laznicka (1988; p.68), although the weight-based size distribution of several metric tonnes of fragmented mine muck was compared to the size distribution predicted by computer-assisted image analysis (Farmer and others, 1991; Kemeny and others, 1993). So, the conventional Rock Mechanics approaches of rock mass characterization may be applicable to the characterization of bimrocks with high volumetric block proportions.

4.2.2 The Geotechnical Literature on Rock Mass Classification and Behavior

There are very few written treatments on the engineering aspects of block-in-matrix rocks (Prof. Peter Laznicka; personal communication), although several of the major mines in the world exploit ore deposits hosted within breccias and melanges (Laznicka, 1988, Chapter 1; for example, the McLaughlin gold mine, in California), and presumably mining engineers must design for heterogeneous rock for both underground and open pit operations. Further, it is common practice to backfill mine stopes with a mixture of lean concrete and waste rock (gangue), a mix that could be viewed as an artificial block-in-matrix rock. No satisfying mining engineering literature on real or artificial block-in-matrix rocks was found (and there probably is none: Prof. Z. Bieniawski, and Dr. Andy Afrouz; personal communications), so considerable effort was expended to find Rock Mechanics literature dealing with the behavior of block-in-matrix and blocky rock masses.

The likely response of rock masses to engineering works cannot easily be predicted by sampling and testing and assuming that the results of such tests "model" the in-situ prototype (Goodman, 1990). Consequently, several approaches have been devised to predict the deformation and failure modes of blocky rock masses (Goodman and Shi, 1985; Bieniawski, 1989; Wittke, 1990; Afrouz, 1992; Priest, 1993; Shi, 1993). Many of these methods depend on *rock mass classifications* which describe a blocky rock mass in terms of several variables deemed by some to be the most important. The schemes are calibrated empirically, often for a particular engineering application, by rock mass lithology, or locale. Unfortunately, such schemes tend to be extrapolated to situations not originally intended, nor supported, by their creators.

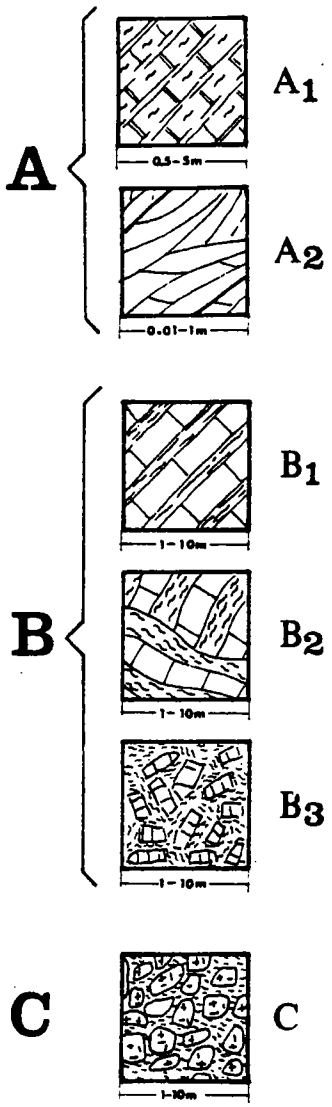

TYPES OF STRUCTURAL COMPLEXITY

Layered clay shales and shales (with or withour fissility), more or less fissured and /or jointed; geotechical complexity depending upon mineralogy and stress history (mainly vertical loading).
Scale: 0.5 m to 5 m

Sheared clay shales and shales; geotechncial complexity depending on mineralogy and stress history (mainly shearing)
Example: Capo di China mudstones (D'Elia and others; 1985, 1986).
Scale: 0.01 m to 1 m

Ordered sequences of more or less fissured and jointed layers of rock and clay or shale; geotechnical complexity depending on heterogeneity, mineralogy, and stress history (mainly vertical loading). Example: Keuper Marls.
Scale: 1 m to 10 m

Disarranged layers of rock; and highly fissured and jointed, to sheared clay or clay shale; geotechnical complexity depending upon heterogeneity, mineralogy, and stress history (flexural, torsional and shearing loads). Example: Panagopoula Slide.
Scale: 1 m to 10 m

As B_2, but with chaotic structure; geotechnical complexity depending on heterogeneity, mineralogy and stress history (repeated cycles of flexural, torsional and shearing loads with large displacements). Example: Irpinia variegated clay shales (Evangelista and others, 1977)
Scale: 1 m to 10 m

Blocks or fragments of more or less weathered rocks in a clayey matrix of various origin; geotechnical complexity depending upon heterogeneity and mineralogy. Examples: residual and colluvial soils.
Scale: 1m to 10 m

Figure 4.1 Italian geological classification scheme showing types of Structural Complexity; after Manfredini and others (1985); D'Elia and others (1986).

At the start of the research, a tentative Bimrock Classification Scheme was outlined which would have related block volumetric proportion to a measure of matrix discontinuity fabric, such as volumetric joint count (Sadagh and de Freitas, 1993). It was intended to correlate the scheme with the slope stability and mechanical properties of

blocky rock, as predicted by other rock mass classification schemes such as the *Q-system* (Barton and others, 1974) and *Rock Mass Rating* (RMR) scheme (Bieniawski, 1989). However, a Geotechnical Flysch Rock Mass Classification (KF) (Popiolek and others, 1993) and a Geophysical Flysch Rock Mass Classification (KFG) (Bestynski, 1993) have already been correlated to the RMR scheme, for use with the coherent and brecciated rock of the Carpathian Flysch in underground excavations. No further time was spent on the proposed Bimrock Classification Scheme, because research was focused on the more fundamental problem of estimating the in-situ block volumetric proportions).

Prior attempts have been made to classify rock masses that cannot easily be classified by other schemes. Laznicka (1988; p. 6; 1989) devised the Universal Rudrock Code, a geological classification scheme for fragmented rocks and block-in-matrix rocks, but this has no geotechnical aspects. Italian engineers have classified *structurally complex rocks* into three geological categories, with geotechnical connotations: A) layered shales, with and without shearing; B) inter-layered hard and weak rock, with structures ranging between mild disarrangement and chaotic; and C) chaotic mixtures of weathered blocks in a clayey matrix (Manfredini and others, 1985; D'Elia and others, 1986). The Italian Geotechnical Society stated that "... a given geological formation is complex from a geotechnical point of view if the properties that control its engineering behaviour vary erratically within a wide range of values..." (D'Elia and others, 1986). The classification is illustrated in Figure 4.1. Italian "structurally complex formations" (commonly olistostromes) have a weak argillaceous component and a strong rock component, and the in-situ strength is considered to be influenced by the structural fabric (Esu and others, 1985; Manfredini and others, 1985).

4.2.3 Geotechnical Experience With The Mechanical Properties of Model and Real Block-in-Matrix Materials

4.2.3.1 The Mechanical Behavior of Model Bimrocks Lindquist (1994b) found that there was a direct and simple relationship between the volumetric proportion of blocks in a physical model melange and the overall strength and deformation properties of the material. He found that cohesion decreased, that the friction angle (ϕ) increased and the modulus of deformation increased as the block proportion increased beyond a lower threshold proportion of 25 percent. Summaries of Lindquist's (1994a, b) findings are presented in Figure 4.2. However, given that there is a relationship between the volumetric proportion of blocks in a bimrock and the mechanical properties, the volumetric proportion must be estimated: a requirement that prompted the research summarized in this dissertation. Lindquist (1994b) also determined that the overall orientations of blocks in model melanges influenced the mechanical properties. Blocks oriented parallel to the axial loading direction in triaxial specimens stiffened a model bimrock.

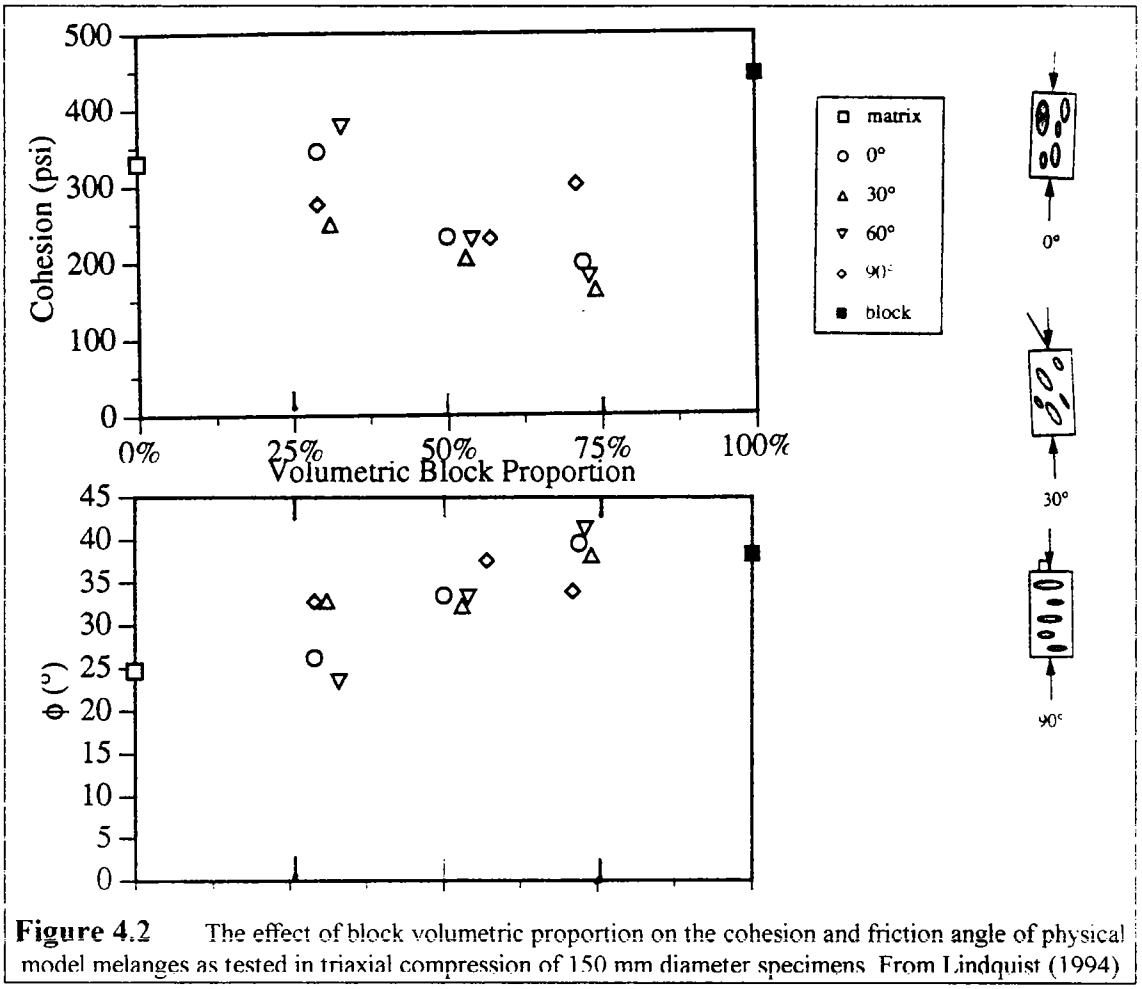

Figure 4.2 The effect of block volumetric proportion on the cohesion and friction angle of physical model melanges as tested in triaxial compression of 150 mm diameter specimens. From Lindquist (1994)

4.2.3.2 The Mechanical Behavior of Block-in-Matrix Soils The principal problems with determining the mechanical properties of block-in-matrix soils are: sample recovery and sample testing. In some bimsoils, boreholes drilled for geotechnical exploration may deflect around blocks because they are relatively impenetrable, and only the matrix materials will be sampled. For example, in glacial tills, small diameter (2.5 inches, 64 mm) borings may "snake" around boulders. One such boring resulted in considerable construction expense, when four 120 foot (37 m) borings indicated one boulder only in a glacial till with a 20 percent boulder content (Verne McGuffey, PE, New York Dept. of Transportation-retired; personal communication).

Soils engineers restrict the size of coarse material to about 15 percent of the diameter of a test specimen, but where necessary, an equivalent weight of smaller fragments of rock is substituted for the coarse fraction, a procedure called *scalping* (Donaghe and Torrey, 1985). It has been concluded that the coarse fraction adds little to the strength of a soil (Fragaszy and others, 1990, 1992), a conclusion similar to that of Baum and Reid (1992, p. 22), who reasoned that an average of 35 to 65 percent gravel to boulder content in a Honolulu earthflow did not contribute any strength; and once a shear surface did form,

the coarse fraction would comminute as originally described by Fleming and others (1988). But, Baum and Reid (1992) based their opinion on the work of Rodine and Johnson (1976), who had showed that debris flow slurry could accommodate considerable coarse material before there was any increase in strength, which was achieved by particle interlocking (since the fluid matrix imparts no shear strength). This is a different situation from colluvium, a block in-matrix soil, where both the block and the matrix contribute strength, as shown by Irfan and Tang, 1993, and West, 1992. Donaghe and Torrey (1985) also concluded that the coarse fraction of earth-rock mixtures added strength. (On the other hand, Shakoor and Cook (1990) found that the unconfined compressive strength of a compacted silty clay decreased with increasing weight proportion of angular and rounded stones.)

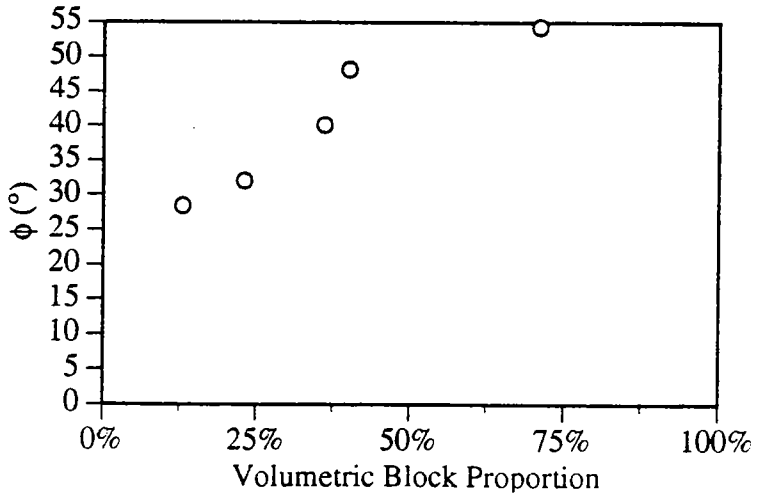

Figure 4.3 Direct relationship between block volumetric proportion and friction angle (ϕ) for Franciscan melange forming the foundation of Scott Dam, northern California; from Lindquist (1994b).

4.2.3.3 The Mechanical Behavior of Franciscan Melanges Lindquist (1994a,b) studied triaxial test data obtained from early geotechnical investigations of the Franciscan melange in the foundation of Scott Dam, in northern California. These data

show a systematic increase in ϕ with increased block volumetric proportion, as shown in Figure 4.3

The contribution of blocks in melange to the stability of hillslopes has been commented upon by several observers (D'Elia et al., 1986; Savina, 1982; Peterson, 1979; Reid, 1978; Bedrossian, 1980). Savina (1982,p. 144-146) surmised that low block/matrix ratios at her study site near Nicasio Reservoir, Marin County, influenced hillslope processes differently than high block/matrix ratios. Bedrossian (1980, p.24, citing Neilson, 1976) reported that the proportion of blocks in sheared serpentinite at the Geysers Geothermal Area, Lake County, California, "largely determines the stability and engineering properties of serpentinite", although Blake and others, 1974 observed that a greater proportion of blocks resulted in more shearing (see also Section 3.14), which presumably tends to decrease the stability, by decreasing rock mass cohesion and increasing the deleterious contribution of water, leaking from blocks. For low block proportion *argille scagliose* ("scaley clay": less than 25 percent block proportion) at several sites, Esu and others (1985) reported that the "lapideous fragments" (blocks), which range from a centimeter to a few meters, are "either scarce or absent and never affect the overall mechanical behaviour." But the same authors also reported that steep slopes occur where the "....lapideous component is dominant, forming a continuous frame of the clay mass....." (Esu and others, 1985, p. 215-225).

4.2.3.4 The Mechanical Behavior of Argille Scagliose Italian geotechnical engineers have researched the mechanical properties of the low block-content melange *(argille scagliose)* which shapes the landscape of the Apennines (Abbate and Sagri, 1981; Manfredini and others, 1985; Canuti and others, 1988; Beneventi and others, 1989; Canuti, 1993a). Italian melanges are younger than the Franciscan (Eocene and Pliocene), and apparently of low block proportions (less than 25 percent?). The engineering properties of Italian melanges have been described by AGI (1977, 1979), Braga (1977); Cotecchia and others (1977,1984); D'Elia (1977); Esu (1977); Evangelista and others (1977); and D'Elia and others (1984, 1986, 1988), and some of their findings are summarized here.

Esu and others (1985; p. 195-225) and D'Elia and others (1986, p. 432) considered that the overall mechanical behaviour of *structurally complex formations,* which includes melange, was due to the *pelitic* (argillaceous) component only when the scaley clay matrix could be tested in a laboratory. Where the scaley clay scales were larger than one millimeter, in-situ tests were performed. Where the matrix scales were small, the samples could be obtained by using pressure samplers, and laboratory testing was feasible but the results varied. Because of dilation of the scaley matrix during sampling and trimming, the porosity and degree of saturation were greater than in the in-situ melange, and consequently deformability in the laboratory was greater than in the field. In-situ tests were performed to understand the influence of sampling disturbance.

Standard geotechnical laboratory tests (Index Properties, compressibility, swelling, shear strength, softening effects and residual strength) were performed on scaley clays. Swelling potential was high, and consequently, there was a decrease in the lab-tested shear strength. Under high confining stress, contractile and ductile behaviour was observed, but under low confining stress (σ'= 0.3 MPa) brittle and dilatant behaviour occurred. CD (Consolidated-Drained) shear tests, and DS (Direct Shear) tests gave results consistent for a low porosity soil for low confining stress (σ'= 0.05 MPa to 1.5 MPa), with strength gradually dropping from peak to residual. The peak and residual strength envelopes were curvilinear (Esu and others, 1985; p. 195-225; D'Elia and others, 1986, p. 432)

In-situ strength properties tended to be higher than laboratory-tested properties, since scale anisotropy influenced the laboratory properties; an effect mitigated by in-situ testing. Typically, there could be significant differences between strengths measured by laboratory tests and in-situ testing; ratios between the two were 0.6 and 0.3 for two sites (Cotecchia and others, 1977; p. 76). Moreover, D'Elia and others (1986, p. 432) stated that "...The in-situ properties of *argille scagliose* because of the presence of lapideous components, can reasonably be kept somewhat higher than those measured in the laboratory..", and that the upper limit of the strength envelopes could be taken in order to model the *argille scagliose* in-situ strength. But at the field scale, the larger scale shears had to be taken into account.

It was determined from geophysics that the longitudinal elastic velocity of argille scagliose was about 2.0 km/sec, or essentially that of hard clays or weak argillaceous rocks (Esu and others, 1985; p. 195-225; D'Elia and others, 1986, p. 432)

4.2.3.5 The Mechanical Behavior of Serpentinite A summary of the geological aspects of serpentinites were presented in Section 3.6, but there is remarkably little information on the engineering characteristics, but there is remarkably little engineering literature considering the problems that engineers suffer because of serpentinites. However the poor reputation of serpentinites is due to the troublesome sheared matrix rather than the blocks. For instance, the south pier and abutment of the Golden Gate Bridge in San Francisco are founded on massive serpentinite; and massive serpentinite of the Mammonia Fm. melange forms the foundation for the Mavrokolymbus Dam in southwest Cyprus (Morgenstern and Cruden, 1977). Nevertheless, serpentinite was implicated in the failure of the 47m high Zerbino gravity-arch dam, which failed in 1935, allowing the drowning of 100 residents of nearby Ovada, Italy (Goodman, 1990).

Sepentinites are associated with asbestos fibres (mainly acicular chrysotile and antigorite), which have environmental and worker health ramifications, if encountered in excavations. State of California regulations classify rock with greater than 1 percent of asbestos to be a hazardous material, but the proportions measured depend on the test method used (WCC, 1994b, p. 3-10).

Sheared serpentinites may weather to highly plastic, hydrophilic clays such as montmorillonite (Schlocker, 1974, Table 8. p. 58 and p. 61); with accessory chlorite, talc and vermiculite. Expansive and plastic clino-chrysotile and pyroaurite have been found in strongly sheared and friable serpentinite at several locations in San Francisco (Shlocker, 1974, p. 61). The easy erosion of the serpentinite soil may undermine the rounded, and slickensided blocks which roll elsewhere, leaving a remolded soft, weak clay soil (Goodman, 1992, p. 228). Cowan and Mansfield (1970) reported that the shear strength of sheared serpentinite was of the order of 1 bar (14.5 psi; 100 kPa), and that it could spread like a glacier or a debris flow. Consequently, landslides are common in serpentinite landscapes. In San Francisco, close to the solid serpentinite foundation of the Golden Gate Bridge, deep-seated and persistent slides of sheared sepentinite have been moving for many decades (Goodman, 1992, p. 28; Schlocker, 1974, p. 87-88).

As part of an innovative program of testing weak rocks Dr. Anders Bro[1] tested 13 specimens of sheared serpentinite, with confining stresses ranging between 0 and 470 psi (0 and 3.2 MPa), and the average stress ratio, $\sigma_1 / \sigma_3 = 4.5$. Assuming that q_u, the Unconfined Compressive Strength, was zero (not unreasonable for the weak material), the friction angle, φ, was 39.5 degrees (calculated using Goodman, 1989, Eqn. 3.8).

In a 1963 study of serpentinite, Damon Runyan[2] searched geotechnical consulting reports and compiled a summary of geotechnical test results, based on about 200 samples, for Index Properties, density, strength (UCS and triaxial), consolidation, and compaction characteristics. Runyan plotted UCS (unconfined compressive strength) against the Standard Penetration Test results (N: blows per foot) obtained by pounding a sampler into the serpentinite during the drilling exploration. The sample soils were classified as completely decomposed and clay-rich; decomposed with little clay content; weathered serpentinite; and sound serpentinite. The UCS/N data points were sorted into 30 fields bounded by N= 25, 50, and 100 blows per foot, and UCS = 500 psf, 1000, 2000, 4000, and 8000 psf. The maximum UCS was about 10,000 psf (70 psi; 490 kPa). UCS and N were correlated as UCS = 100N and there was some correlation with dry density. Little swell was observed in the few samples tested for consolidation behavior. Triaxial testing (Undrained, Unconsolidated: U-U) indicated that there was no cohesion, and the friction angle, ϕ, was 41 degrees. C-U (Consolidated-Undrained) triaxial tests resulted in ϕ=32 degrees to 38 degrees; and ϕ'=34 degrees to 41 degrees, again with no cohesion. Axial pressures were limited to about 13 kPa (185 psi; 26,600 psf)

---

[1]Anders Bro.; Novel techniques for testing serpentinite and fractured sandstone in triaxial and unconfined compression; Draft report by GeoTest Unlimited, 800 Peralta Avenue, San Leandro, CA 94577

[2]Damon R. Runyan; "Progress Report on Serpentines" and "Engineering Properties of Serpentinites Determined by Soil Tests"; for course GE 299, Spring Term, 1963; Geological Engineering (now Geotechnical Enginering Group, Dept. Civil Engineering), University of California, Berkeley, CA 94720

Further research into sheared serpentinites is long overdue, particularly given the recent work of Lindquist (1994b), and the development of techniques to protect and handle weak rock specimens developed by Dr. Anders Bro (see previous footnote 2) and Jason Choi of the Rock Mechanics Laboratory at UC Berkeley. Choi's procedure was developed to protect 150 mm diameter core specimens of melange by immediately wrapping 12 inch to 24 inch lengths core with plastic, embracing the core with halves of rigid PVC pipe compressed by strap clamps, and placing the protected core in wooden cradles.

4.3 THE ENGINEERING ASPECTS OF BLOCK VOLUMETRIC PROPORTION

4.3.1 Introduction

In this Section, the engineering aspects of the block volumetric proportion in bimrocks is discussed: the geological aspects were discussed in Section 3.11. Much of the emphasis of the research was on the estimation of block areal proportions and block volumetric proportions measured from scanlines traced across two-dimensional images called *graphic models:* the Gravel Tests setups and the unrolled cicumferential surfaces of the Triaxial Specimens Tracings; both were model bimrocks.

The stereologic principles behind the work was: $\mathbf{L_L = A_A = V_V}$; or the block linear, areal and volumetric proportions are equal, as discussed in Section 2.3. Ideally, $\mathbf{V_V}$ would have been estimated directly from $\mathbf{L_L}$ but since all scanlines were measured from two-dimensional planes, the block areal proportions of the planes first had to be determined in order to check that the validity of the stereological results. In the case of the Gravel Tests, the estimation of areal proportion was sufficient, because the setups were essentially two-dimensional. For the Triaxial Specimen tracings, the areal proportions were compared to the actual volumetric proportion as given by Lindquist (1994b), and then the linear proportions compared to the areal proportions.

The stereological basis for the work is presented in Section 2.3; and the image analysis procedures used are described in Section 2.7 and Section 2.8.3, with more detail in Appendix B. The Gravel Tests data are summarized in Appendix C, and that from the Triaxial Specimen tracings in Appendix D.

4.3.2 Block Volumetric Proportions Estimated from Block Areal Proportions Measured in Two Dimensions

The volumetric proportions of the Gravel Tests setups were not measurable. As discussed in Section 2.8.4, measurement of the blocks on the tracings of Triaxial Test Specimens showed that $A_A \neq V_V$ since the blocks were not uniformly distributed throughout the volume. But the discrepancy between the areal proportion and volumetric proportion was consistent (see Figure 2.20) and could be explained. Six specimens were

sliced in half, and there was generally excellent agreement between the measured block areal proportions of the cross-sections and the actual block volumetric proportions (Figure 2.20). Thus, it was assumed that the areal proportions measured for the triaxial specimens were the volumetric proportions, in order to investigate the correlation with linear proportions, discussed in the next Section.

4.3.3 Areal and Volumetric Proportions Estimated from One Dimensional Scanlines

4.3.3.1 Results from the Gravel Tests Because the six Gravel Tests setups had considerably more area than height, they were essentially two-dimensional, and so no attempts were made to estimate the volumetric proportions. The areal proportions ranged between 5.1 percent and approximately 50 percent. As outlined in Section 2.7. The images provided opportunities to :

1. Estimate areal proportions from scanlines

2. Investigate the effect of varying scanline intervals and lengths, to model a geotechnical exploration drilling program where borehole locations and depths would probably be chosen for reasons other than the estimation of volumetric proportion, and would thus vary in spacing and depth.

3. Determine the most efficient total length of scanlines to estimate both block areal proportion, and the 2DBSDs (via CLDs).

In general, the cumulative block linear proportions measured from scanlines were within 1 percent and 5 percent of the block areal proportions; the larger the areal proportion, the greater the error. The ratio of error to areal proportion was less than 0.1. For the usual setup image using 10 scanlines of 50 cm true length (not the length on photographs), block areal proportions were generally estimated within 45 percent to 65 percent (average 55 percent) of the total scanline lengths (see Section 2.8.3 for procedure), or between about 225 cm and 325 cm, (average 275 cm). The ratio of effective scanline lengths to average particle d_{mod}s (maximum observed dimensions, here effectively "diameters"), was between 290 and 440, with an average of 350. The ratios of effective scanline lengths to d_{max} (the d_{mod}s of the largest particles), were not specifically computed but were of the order of 40 to 60.

The block areal proportions measured from the "random scanlines" were generally little different from those of regularly-spaced scanlines, or from the arrays of scanlines of equal length. Page C-4 of Appendix C shows an example of one of the images with scanlines of regular spacing but randomly-determined lengths. Other configurations, including those with scanlines of fixed length but randomly located, were tested but not included in Appendix C.

The investigation of the effect of increasing the total length of scanlines was conducted by incrementally measuring 5, 10, 20, 30 and 40 scanlines on each images of three

setups. (This configuration is most unrealistic: field drilling investigations would not likely be so densely spaced). The results indicated that for most images, between 5 and 10 scanlines, or 35 to 65 times d_{max}, were sufficient to estimate the block areal proportions. The data for this investigation are summarized in Appendix C (pages C-8, C-9; C-12, C-13; and C-16, C-17).

4.3.3.2 Results from the Triaxial Specimen Tracings As indicated in Section 2.8.4, although the block areal proportions measured from the Triaxial Specimen tracings were significantly different from the actual volumetric proportions, it was assumed that the measured areal proportions were the block volumetric proportions. In general, there was good agreement between the estimates of the block areal proportions and the block linear proportions determined from scanlines (see Appendix D, p. D-2 through D-21, individual data summaries). The linear proportions did not seem to be influenced by the block orientations, and were generally within 3 percent and 11 percent of the block areal proportions, and there was no consistent increase in error with increased areal proportion. The ratio of error to areal proportion was generally less than 0.1 For the typical image, using 10 scanlines of 30 cm true length (not the length on photographs), block areal proportions were generally estimated within 45 percent to 75 percent (average 55 percent) of the total scanline lengths (see Section 2.8.3 for procedure), or between about 135 cm and 225 cm, (average 165 cm). The ratio of effective scanline lengths to "average" block d_{mod}s was between 54 and 90 with an average of 66. The ratios of effective scanline lengths to the d_{max} s were approximately 10 to 17.

Some of the results above have been related to "average" block sizes, and by extension, "average" chord lengths representing some mean particle). But, the notion of "average" is misleading when considering self-similar distributions. There are so many small particles that the average becomes skewed leftward. Since the power-law function (which is the arithmetic equivalent of the log-log linear function), behaves much like the negative exponential that is commonly encountered in Rock Mechanics, it may be useful to analyze the data from self similar block size distributions using the tools of Rock Mechanics.

4.4 THE ENGINEERING ASPECTS OF BLOCK SIZE DISTRIBUTIONS

4.4.1 Introduction

Although the block size distributions in block-in-matrix materials may have an important influence on their mechanical properties, little prior geotechnical information was found during the literature search for this dissertation. The geological aspects of block size distibutions were discussed in Section 3.12.

In order to investigate the contribution of block volumetric proportions to the behavior of model melanges, Lindquist (1994b) maintained a relatively constant self-similar block

size distribution when fabricating the models. The known and constant three dimensional block size distribution (3DBSD) was useful for the research. As described in Section 2.8, two-dimensional block size distributions (2DBSDs) were constructed from measurements from the d_{mod} s (maximum observed dimensions) of blocks as expressed on the surface of 14 triaxial specimens. Chord length distributions (CLDs) were developed from measurements of the lengths of scanline intercepts through the blocks (as expressed on the specimen surfaces). The 2DBSDs and CLDs were then compared to the parent 3DBSD in order discern any systematic relationships between them. Empirical guidelines were developed to convert CLDs and 2DBSDs to 3DBSDs. Block proportion and block size distribution data (from scanlines only) are presented in Appendix E (pages D-2 through D-21) for each of 14 Triaxial Specimen tracings and an additional 6 cross-sections. Additional summaries of block size distributions (CLDs) are organized in two ways:

1. Plots sorted by nominal Block Proportions (LOW=30%; MEDIUM=50% and HIGH=70%), with a separate sheet for each block orientation ((0, 30, 60 and 90 degrees: Appendix D, pages D-22 to D-25)

2. Plots sorted by Block Orientation (0, 30, 60 and 90 degrees), and a separate sheet for each block proportion (HIGH, MEDIUM and LOW: Appendix D, pages D-26 to D-28)

Additional investigations were performed using the Gravel Tests setups, which were essentially two-dimensional arrays of gravel and sand. The procedures are described in Section 2.7, and have been referred to in Section 4.3, above. CLDs were developed from the Gravel Tests setups and compared to the 2DBSDs. The relatively low block areal proportions of the setups (5 percent to 50 percent) allowed conclusions to be made regarding the optimum length of scanlines necessary to define a useful CLD; and the relationships between CLDs and 2DBSDs for low-block proportion mixtures. A selection of the Gravel Tests data are summarized in Appendix C.

4.4.2 The Relationship Between Block Size Distribution and Bimrock Strength

Lindquist (1994b) showed that failure surfaces passed around blocks in a physical model melange, and that the increase in the friction angle component of the strength (ϕ) was due to the *tortuosity* of the failure surfaces negotiating the blocks. The concept was a confirmation of the work of Savely (1990), who used a D9 bulldozer to show that boulders contributed strength to the Gila Conglomerate in Arizona, by forcing tortuous failure surfaces to negotiate them.

Lindquist's (1994b) test specimens had approximately the same block size distributions, but different block volumetric proportions and block orientations. However, the volumetric proportion of blocks in a bimrock is probably partially dependent on both block shapes and block size distribution. The sketches of Figure 4.4 show the influence of varying the block size distribution on the apparent roughness of the failure surface for two block configurations with roughly the same block volumetric proportion. The graded

distribution forces a more tortuous failure path, despite the unrealistically smooth, rounded blocks.

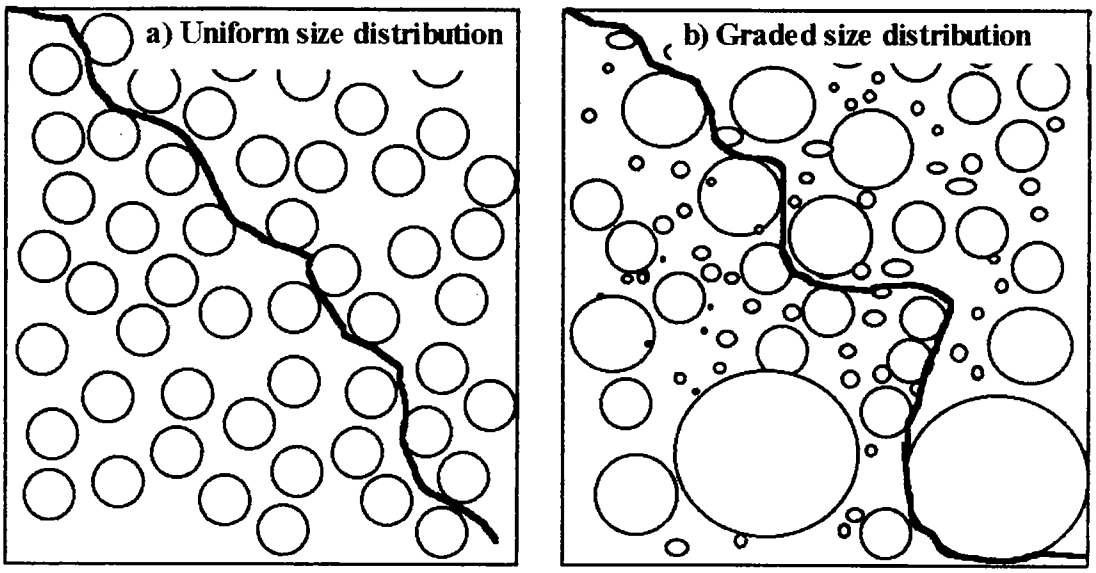

Figure 4.4 The influence of block size distribution on failure surface "roughness" for two different distributions with the same block volumetric proportion.

4.4.3 Comparison of 2DBSDs and CLDs for the Gravel Tests

It is instructional to review Figure 4.5, a typical plot which compares a chord length distribution (CLD) with the parent two-dimensional block size distribution (2DBSD) and weight-based particle size distribution (WPSD) for a Gravel Tests setup. The plots are relatively simple to interpret since the blocks of the setups had no preferred orientation or shape, as did the blocks of the Triaxial Specimen tracings. Plots for other Gravel Tests setups, included in Appendix C, are similar. The 2DBSD was constructed from the 296 d_{mod}s (maximum observable dimensions) of all the particles, as determined by image analysis. The CLD was constructed from 45 d_{mod}s, or the lengths intercepts (chords) between some blocks and scanlines. The WPSD is identical to a conventional Particle Size Distribution as used in Soil Mechanics, except that the WPSD weight fractions were assigned to the next coarsest sieve (*endclass)* rather than the sieve on which the particles were retained (*beginclass*).

There is little similarity between the WPSD and the other two size distributions. The maximum dimension of the WPSD is smaller than the maxima of either the CLD or the 2DBSD, because the WPSD is based on the weight fraction of particles with minimum to intermediate dimensions, rather than their maximum dimensions. CLDs and 2DBSDs

generally shared the maximum dimension endclass, although the absolute maximum length of chord was rarely the same length as the maximum d_{mod}. The long chords constitute a relatively small proportion of the total number of chords, because there are few large particles. But, there are many smaller particles, and intersections with these constitute a relatively high proportion of the 45 chords, compared to the smaller proportion (but absolutely greater number) of d_{mod}s measured for the 2DBSD. The result is that the CLD appears to be "coarser" than the 2DBSD, and this appearance was typical of the block size distribution plots for both the Gravel Tests and the Triaxial Specimens. Generally, the slopes of the CLDs and 2DBSDs were similar between approximately 25 percent and 85 percent cumulative percent finer.

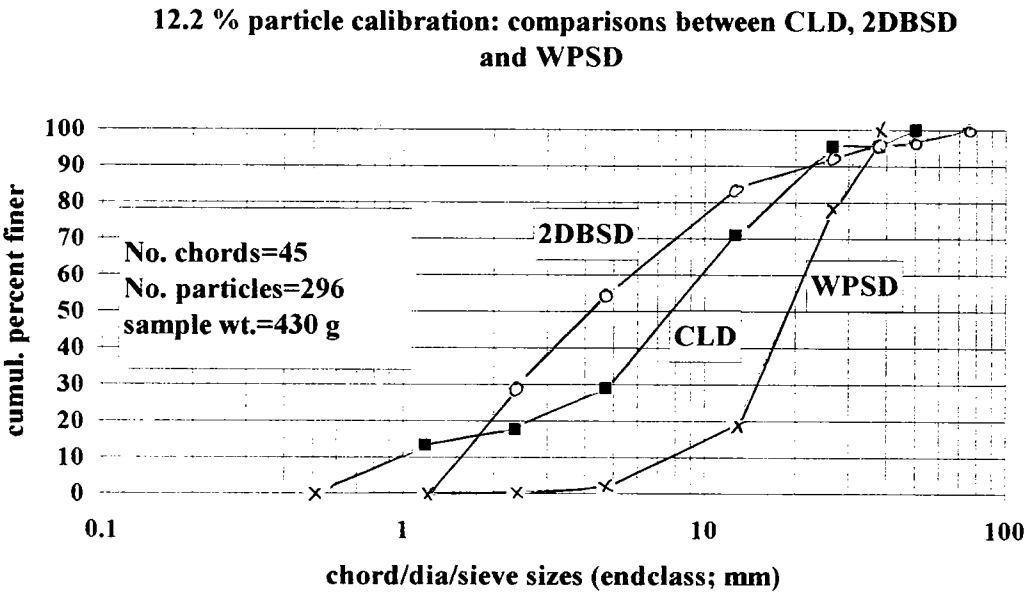

Figure 4.5: Comparisons between CLD, 2DBSD and WPSD for Gravel Tests setup of 12.2 percent block areal proportion

The apparent "coarseness" of the CLDs was an unexpected result. Intuitively, a distribution of chords should be "finer" than a distribution of block "diameters" (d_{mod}s) because chords would rarely be as long as block "diameters". The minimum dimensions of the 2DBSDs were generally the same as that for the WPSDs. And, there was an inevitable "fines tail" (*coda*) to the CLD due to the numerous chords shorter than the smallest d_{mod}. The coda was composed of chords shorter than about 1 percent to 5 percent of the length of the longest chord. Because they were so small, the coda could be neglected, just as small classes are abandoned in the stereological method of Lord and Willis (1951), illustrated in Figure 2.2. The endclass size of the smallest particle was assumed to be about 2 percent of the of the magnitude of the largest endclass.

In summary, plots such as Figure 4.5 showed :
1. The largest CLD endclass was generally was the same as the largest 2DBSD d_{mod} class
2. The CLDs and 2DBSDs had similar appearances, but the CLD was generally "coarser"
3. The CLD coda was for very small sizes could be abandoned, and an endclass size for the smallest particle could be approximated.

The results of the Gravel Tests suggested that the CLDs for some arrays of particles could serve as approximate 2DBSDs, particularly if the CLDs were translated leftward ("finer"). A procedure was devised to effect such translations but is not presented here since it was not tested on self-similar CLDs.

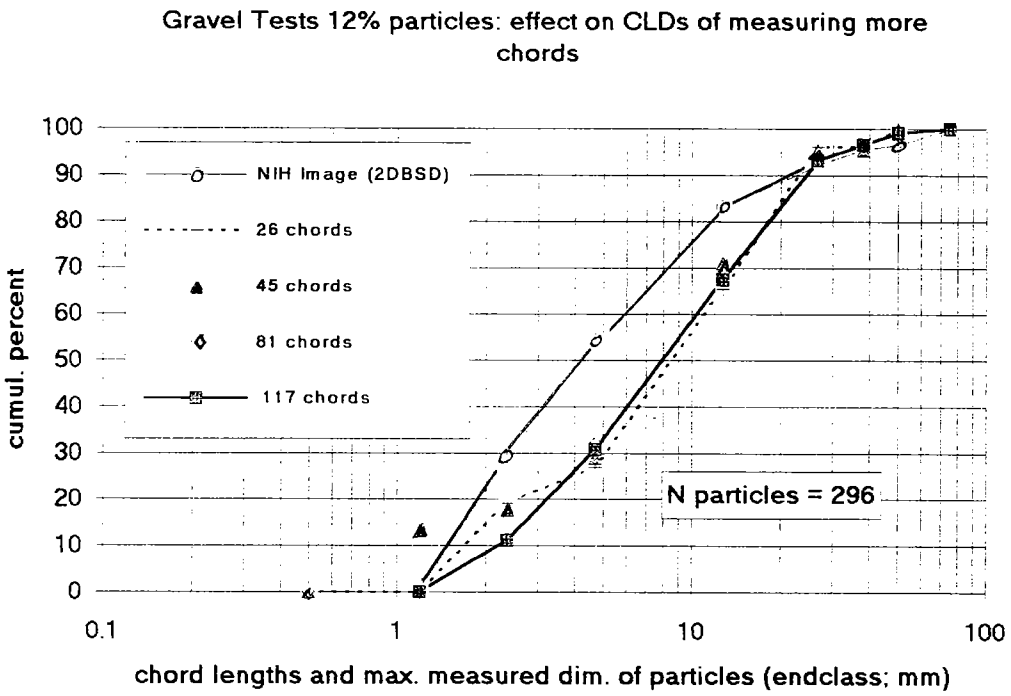

Figure 4.6 Showing that there was relatively little effect on CLDs when the total length of scanlines was increased and more chords were measured for the 12% areal proportion Gravel Tests setup. Even when the number of chords was half the number of blocks, the CLDs maintained their relative appearance and distance from the 2DBSD. The 26, 45, 81 and 117 chords were measured from 10, 20, 30 and 40 scanlines (respectively) on the same image.

4.4.4 Determination of the Optimum Total Length of Scanlines to Estimate 2DBSDs

One of the Gravel Tests was an exercise to identify the optimum number of scanlines such that both the block volumetric proportions and CLDs could be efficiently determined. The results of the exercise relevant to block areal proportion are described in Section 4.3.3.1. The results of the exercise are shown as CLDs in Figure 4.6 for the same setup featured in Figure 4.5. The image was traversed by sets of 10, 20 30 and 40 scanlines (see Appendix C, page C-12), which generated 26, 45, 81 and 117 chords, respectively. The resulting CLDs are presented in Figure 4.6, with the parent 2DBSD. All CLDs resemble each other, and the CLD shown in Figure 4.5. Since there was relatively little difference in the CLDs, 10 scanlines was considered sufficient for this setup. In general, since 10 scanlines appeared to be sufficient to estimate both the block areal proportion construction of CLDs for Gravel Tests images, it was assumed that 10 scanlines would also suffice for the Triaxial Specimen Tracings.

4.4.5 The Influence of Volumetric Proportion and Block Orientation on the CLDs and 2DBSDs of the Triaxial Specimen Tracings

In a real melange, the main block variables are: block shape, block size distribution , block orientation and block volumetric proportion. In investigating the mechanical behavior of a physical model melange, Lindquist (1994b) held block size distribution and block shape constant, and varied block volumetric proportion and block orientation. The variation of these two variables influenced the geometric probabilities of the scanline/block intersections, and the lengths of the resulting chords. Consequently, the interpretation of

CLDs from the work with the Triaxial Specimen Tracings was more difficult than for the Gravel Tests images (see Section 4.4.3). Scanline spacing and length were held constant for all scanline measurements of the Triaxial Specimen tracings. The approximate spacing of the (generally) 10 scanlines per tracing was chosen to exceed the average d_{mod} of the blocks (between 20 mm and 30 mm, at true scale) and minimize those events where the same block was intersected by more than one scanline, although adverse block orientations tended to increase the frequency of such events, as discussed later in this Section.

The number of chords intersected was directly related to the block areal proportions, because higher block proportions increased the probability that a scanline would intersect blocks. (As indicated previously, the block areal proportions were more relevant than the block volumetric proportions because the scanlines were drawn on tracings of the circumferential areas of the Triaxial Specimens). Intersection with the larger blocks was more probable than with smaller blocks because of their larger areas, even for tracings with low block areal proportion. Figure 4.7a and Figure 4.7b show two tracings with the

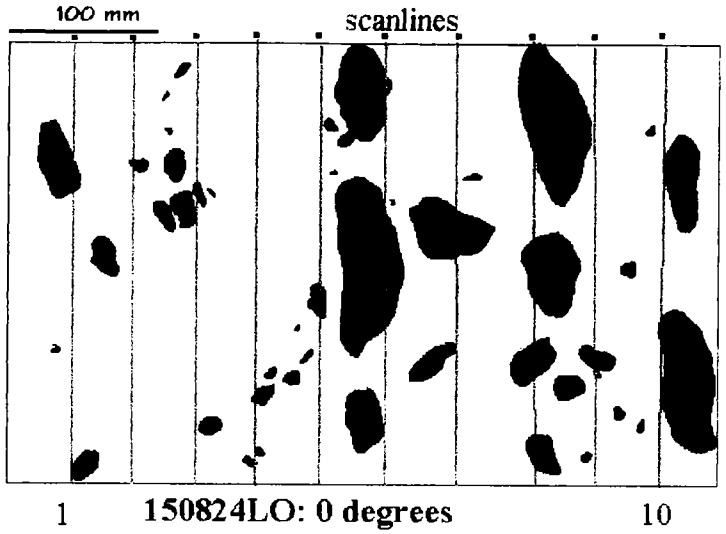

a) LOW proportion
$V_V = 34\%$
$A_A = 18.6\%$
$L_L = 15.6\%$

block orientations = 0°

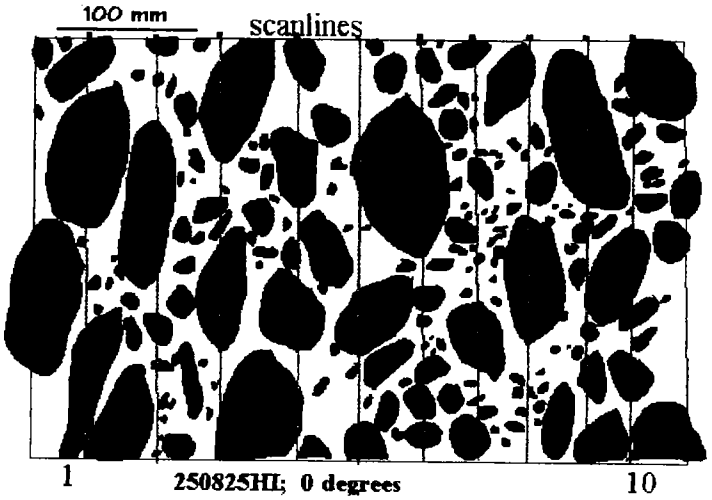

b) HIGH proportion
$V_V = 72\%$
$A_A = 64.8\%$
$L_L = 61.1\%$

block orientations = 0°

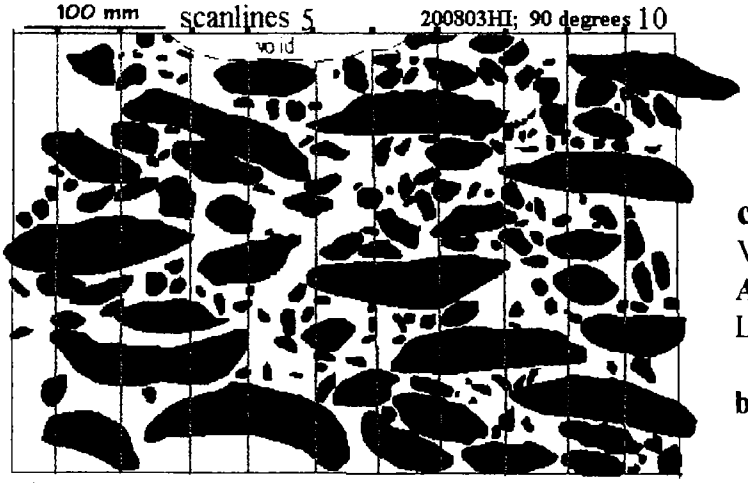

c) HIGH proportion
$V_V = 71\%$
$A_A = 60.7\%$
$L_L = 57.6\%$

block orientations = 90°

Figure 4.7 Triaxial Specimen Tracings of different block proportions and orientations

same block orientations but different block areal proportions ("Low", about 30 percent; and "High", about 70 percent). The tracings show that the number of intersections between blocks and scanlines increases with areal proportion and block sizes. The effect of varying block areal proportion is shown on summary plots in Appendix D (pages D-22 through D-25; one plot for each block orientation: 30, 60 and 90 degrees).
It is instructive to review the summary plots for the configurations shown in Figure 4.7a and Figure 4.7b, with the addition of the data for the "Medium" block proportion (about 50 percent). Figure 4.8 shows the effect of varying block proportion on CLDs plotted in the semi-logarithmic fashion used in Section 4.4.3.

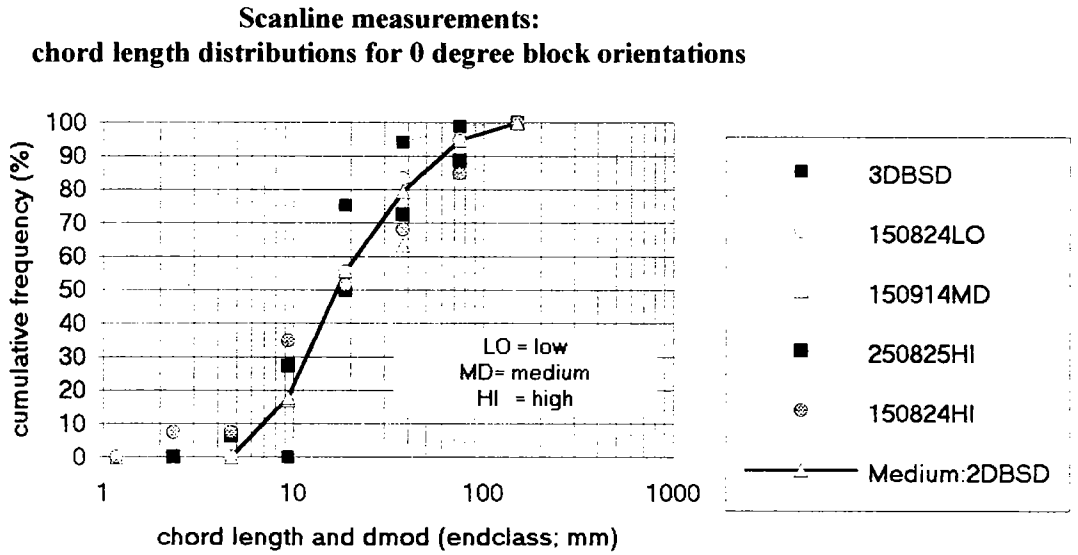

Figure 4.8 CLDs for Low, Medium and High block proportions and 0 degrees block orientation; compared to parent 3DBSD and typical 2DBSD (for the Medium specimen).

The CLDs are shown by unconnected data points. The parent 3DBSD is shown together with an example 2DBSD generated from measuring the block d_{mod}s for the specimen with the "Medium" block proportion (Specimen 150914MD). A number of observations are made:

1. The CLDs are more "graded", or cover a much wider range of size classes, than both the 3DBSD and the 2DBSD.

2. The inflexions of the CLD and the sample 2DBSD occur at a size class close to the smallest class of the 3DBSD (approximately 10 mm in Figure 4.8).

3. As the block proportion increases, the CLDs become more graded: that for the lowest proportion is closest in appearance to both the sample 2DBSD and the 3DBSD.

The parent 3DBSD of the model melange was designed to be a self-similar. Hence, it was appropriate for the 2DBSD and CLD data measured from the images of the Triaxial

Specimens to be plotted as log-histograms. Consequently, the data shown in Figure 4.8 is repeated in Figure 4.9 in log-histogram form. The data points have not been connected, in order to preserve clarity. The summary plots in Appendix D also show log-histograms.

As shown in Section 2.8, a self-similar 3DBSD can be generated from a self-similar 2DBSD, simply by adding 1.0 to the absolute magnitude of the slope of the descent limb of the log-histogram of the 2DBSD, and hinging it at d_{max}. The guideline shown in Figure 4.9 should be considered as an ideal parent 2DBSD for the model melange, and is useful for judging the appearance of the CLDs.

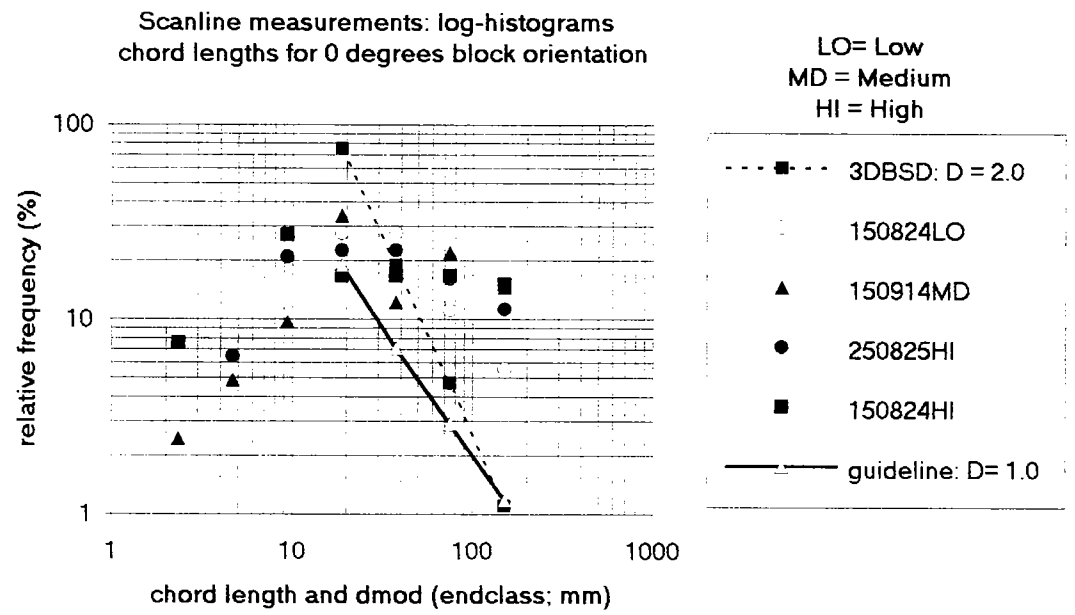

Figure 4.9 Log-histograms of CLDs for Low, Medium and High block proportions, and 0 degrees block orientations; compared to parent 3DBSD and a guideline with slope D =1.0

Some interesting and useful observations are made regarding the plots in Figure 4.9:

1. All CLDs have a log histogram appearance; with relatively well-defined ascent and descent limbs.

2. All CLDs are represented in the largest endclass of the 3DBSD, (the d_{max} endclass), which contains the size of the largest block used in the fabrication of the model melange. In this regard, the CLDs "predict" the d_{max} class, although the longest chords will rarely be the same as the dimensions of the largest blocks.

3. The d_{peak} of all CLDs, or the endclass containing the highest proportion of chords, is the same as the endclass containing the size of the smallest block used in the fabrication of the model melange. The d_{peak}s also correspond to the chord length endclasses at the inflexions of the semi-log plots of the CLDs, shown in Figure 4.8. Data to the left of

d_{peak} (on the ascent limbs) correspond to the coda, or "fines tail" of the semi-log plots in Figure 4.8, and represent data that can be abandoned (as discussed in Section 4.4.3).
4. The slopes of the descent limbs decrease as the block proportions increase. The descent limb of the lowest block proportion specimen (150824LO) has a slope approaching that of the 3DBSD (D=2.0), whereas the descent limb of the specimen with the highest block proportion (150824HI) has a slope flatter than that of the guideline (D=1.0).

Taken together, the information shown in Figure 4.8 and Figure 4.9 suggest that at low block proportions (assuming constant block orientation), the CLDs approach the appearance of the 3DBSD; whereas at high proportions, the CLDs approach the appearance of the 2DBSD. The apparent tendency for the CLDs for low proportions to approach a parent block size distribution was observed when performing the Gravel Tests, (discussed in Section 4.4.3). Since estimation of 3DBSDs is ultimately what is of interest, the behavior is fortunate.

Not considered so far has been the influence of block orientations (and to a lesser extent, block shapes) on the frequency of multiple intersections between blocks and scanlines. For instance, an equant block (spherical) presents the same the probability of penetration independently of its orientation. But Lindquist's (1994b) ellipsoidal blocks, with an aspect ratio of between 2 and 3, presented different probabilities of penetration depending on their orientation relative to the scanlines, as shown in Figure 4.7c. Large blocks that were at 90 degrees orientation relative to the scanlines were intersected often; whereas, for the same shapes and block volumetric proportion, blocks oriented at 0 degrees were generally intersected only once (Figure 4.7a and Figure 4.7b). The longest dimension of blocks oriented at 90 degrees cannot be predicted, although the standard deviation of chord lengths is decreased. For a real melange, the largest dimensions of large blocks could be estimated if field mapping provides information on both the local block orientation, and the aspect ratios of blocks.

The influence of block orientation on CLDs was studied by plotting log-histograms. An example for specimens with High block proportions is shown in Figure 4.10. The data of Figure 4.10 include those for the specimens shown in Figure 4.7b and Figure 4.7c, and show that as the block orientations increase, the descent limbs of the CLDs tend to approach the slope of the parent 3DBSD, but the CLDs of specimens with low block orientation angles tend to be decrease, and at 0 degrees (blocks oriented parallel to scanlines), are flatter than the 2DBSD guideline. The effect of varying block orientations is further shown on summary plots in Appendix D (pages D-26 through D-28; one plot for each block volumetric proportion: (Low, Medium and High; or nominally 30 percent, 50 percent and 60 percent).

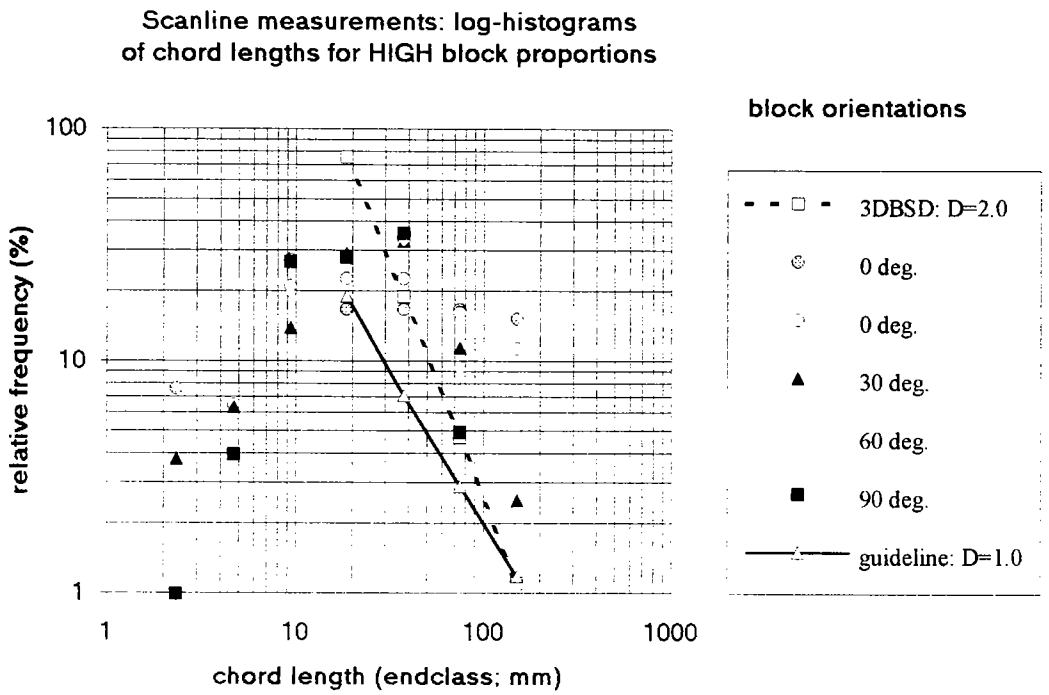

Figure 4.10 Log-histograms of CLDs for the range of block orientations (0°, 30°, 60°, and 90°), plotted for specimens with High block proportions; compared to parent 3DBSD and a guideline with slope D=1.0

An important, and often distinct component of a log-histogram is the descent limb (the ascent limb data can be abandoned), the slope (**D**, the fractal dimension) of which is characteristic. D was measured for all 2DBSDs and CLDs (although in some cases there were only 2 points on the descent limbs of the CLDs). Plots of fractal dimensions against block linear proportions for 2DBSDs and CLDs are presented as Figure 4.11. The block volumetric proportion was chosen as the independent variable since in a real melange this could be more easily determined from scanlines than the overall block orientation fabric. The data are organized for the four block orientations, which makes the plots useful for discerning the combined influence of block proportion and block orientations on the 2DBSDs and the CLDs. The nominal block volumetric proportions (Low, Medium and High; or 30 percent, 50 percent and 70 percent) are highlighted. Several features of the plots are of interest:

1. The block areal proportions in Figure 4.11a are not grouped around the nominal block volumetric proportions. The discrepancy between areal and volumetric proportions was discussed in Section 2.8.4. The linear proportions in Figure 4.11b are even more

dispersed, and are only approximately correlated to the areal proportions, shown in Figure 4.11a, and the nominal volumetric proportions.

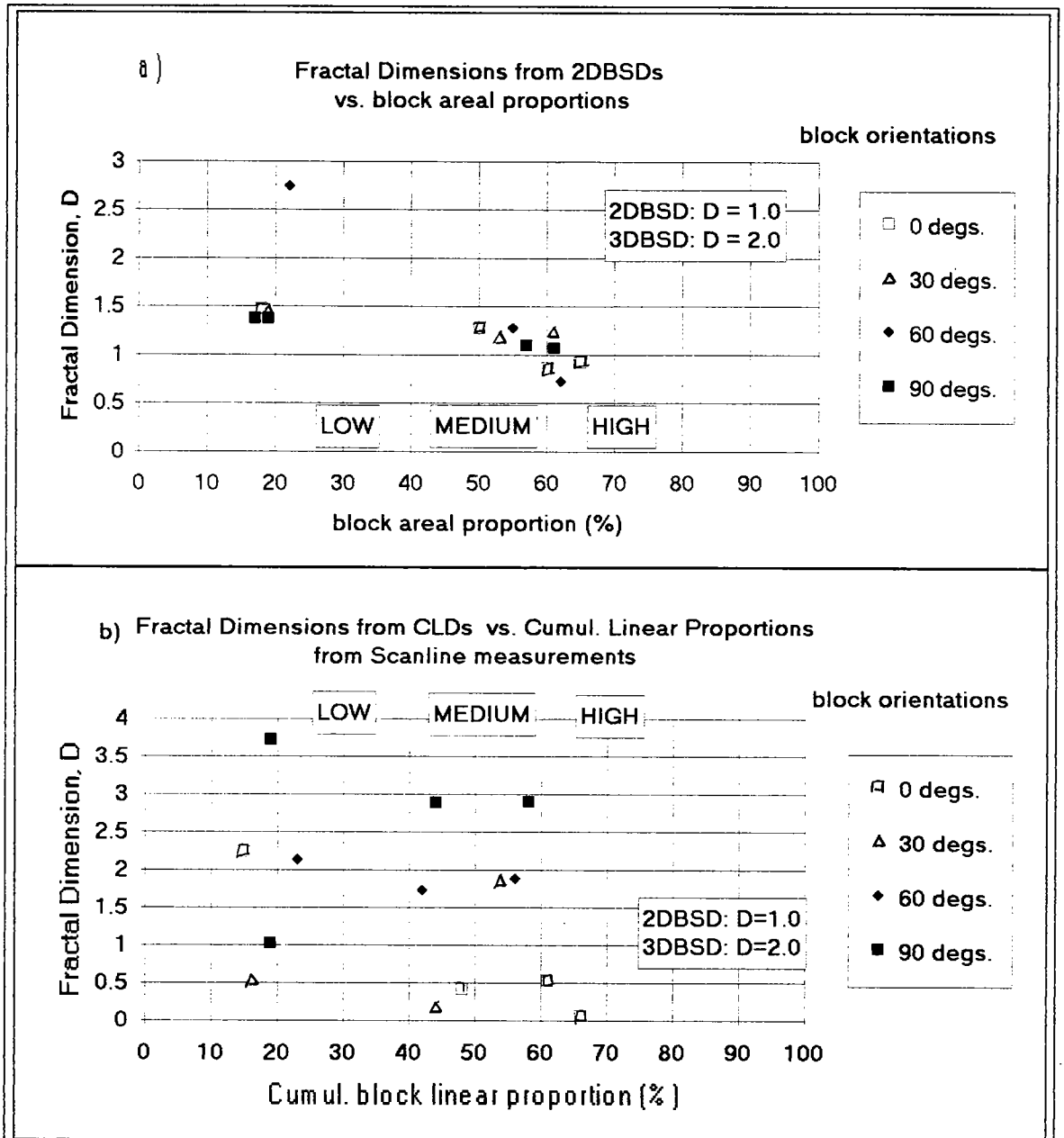

Figure 4.11 Relationships between Fractal Dimensions, block orientations and block linear proportions or 14 Triaxial Specimen tracings: a) 2DBSDs from d_{mod} measurements; and b) CLDs from scanline data

2. The block areal proportions in Figure 4.11a are clustered into two groups, except for the maverick point at (21%, 2.7). In general, the fractal dimensions of the 2DBSDs range between 0.7 and 1.5, with an average of about 1.0. This is the theoretically expected fractal dimension for the self-similar 2DBSD, since the 3DBSD for the model melange

was designed for a fractal dimension of 2.0. This result suggests that the fractal dimensions of the 2DBSDs are relatively insensitive to both block areal proportion and to block orientation. A practical implication is, that in a real melange, measurements of block d_{mod}s from maps and photographs may yield relatively invariable fractal dimensions, regardless of block volumetric proportion and orientation.

3. The fractal dimensions of the CLDs plotted in Figure 4.11b are dispersed, but there are some trends, if the possibly spurious points at (18%, 1.0) and (55%, 1.9) are ignored. In general, as the block linear proportion increases, the fractal dimension decreases. Also, the higher the block orientation angle (relative to the scanline), the higher the fractal dimension. The optimum block orientation angle for estimating the fractal dimension of the parent 3DBSD (D=2.0) appears to be 60 degrees, or a dip of 30 degrees, relative to the configurations shown in Figure 4.10. Franciscan melanges tend to be steeply dipping, or have low block orientations relative to the vertical.

As indicated in the discussion above, the general trend of the data suggest that, the combination of relatively low block proportion and relatively high block orientation results in fractal dimensions that approach the fractal dimension of the 3DBSD, which is the ultimate goal of the work. If these apparent relationships are true, and artifacts of the experiments, then they are worthy of more research.

4.5 CHARACTERIZING BIMROCK ARCHITECTURE FROM SCANLINE OBSERVATIONS

4.5.1 Problems with Developing Cross-Sections in Melange Using Borehole Observations

One of the major difficulties in characterizing bimrocks is the problem of knowing what to draw on cross-sections. Given that geological simplifications are the basis for engineering designs, the lack of an adequate geometrical representation of the sub-surface conditions of a bimrock is a handicap. The problem is made more difficult because the recovery of drill core in melanges is selectively poor in the weak matrix, and relatively good in blocks. This is misleading since the matrix strength is fundamental for geotechnical design, granted that adjustments may be made reflect the presence of blocks. So, the geological engineer often has to make do with an imperfect set of data.

The point is illustrated by the following drawings. Let Figure 4.12, a sketch through a Franciscan melange, represent an ideal, typical sub-surface representation. Figure 4.12 is based on a photograph of a specific scale, but the scale-independence of Franciscan melanges allows the photograph to represent a melange of any scale. Thus, the sketch is a *graphic model* of a vertical cross-section through the melange, although the picture could as easily represent a plan view, in which case the lines represent field scanlines. However, for illustration purposes, assume that the graphic model shows four boreholes

intersecting different proportions of white blocks within the gray matrix, much as would be expected in a real situation.

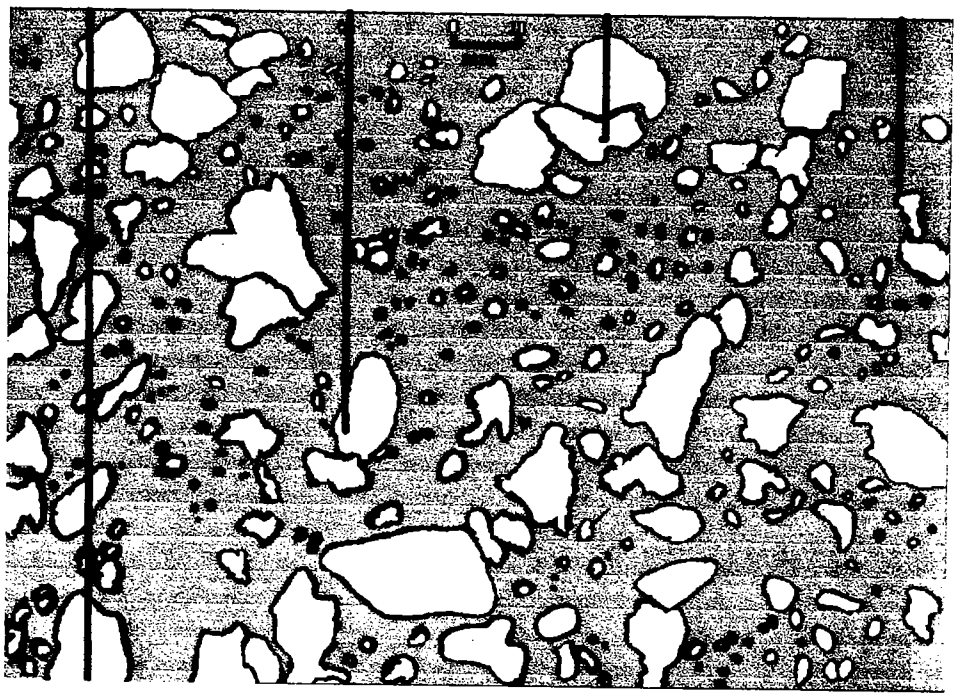

Figure 4.12 Graphic model of melange, representing a vertical cross-section, with boreholes.

But the geological engineer very rarely sees such a perfect cross-section as Figure 4.12, at least not until the site is excavated. More typical is the situation pictured in Figure 4.13 which shows the geological engineer's misinterpretation of the geology, based on the borehole observations, as thick shale and sandstone beds, with the awkward "turbidite sequence" (apparent finely "interbedded shales and sandstones") explained by a "fault". Although this is a hypothetical example, it is based on geotechnical experience with Franciscan melange. Some difficulties could be avoided if apparent shale/sandstone sequences in were not invariably labeled as "interbedded" on borehole logs, because in melanges only some of these sequences are coherent turbidites. But the chaos of a melange is often reflected in small-scale chaos, evident in drill core by micro-blocks swirled in sheared matrix. The blocks need not be measured, perhaps, but the fabric is a valuable clue, nevertheless. It is thus imperative to have both good core and good geological logging.

Yet, assuming that the geological engineer made the correct geological interpretation that the boreholes intersected melange, it is still impossible to accurately reconstruct the sub-surface conditions, or to easily characterize the *block volumetric proportion*, *block size distribution*, *block shapes* and *block orientation*. These properties must be estimated

from geological mapping and analyses of measurements of the lengths of blocks intercepted in drill core.

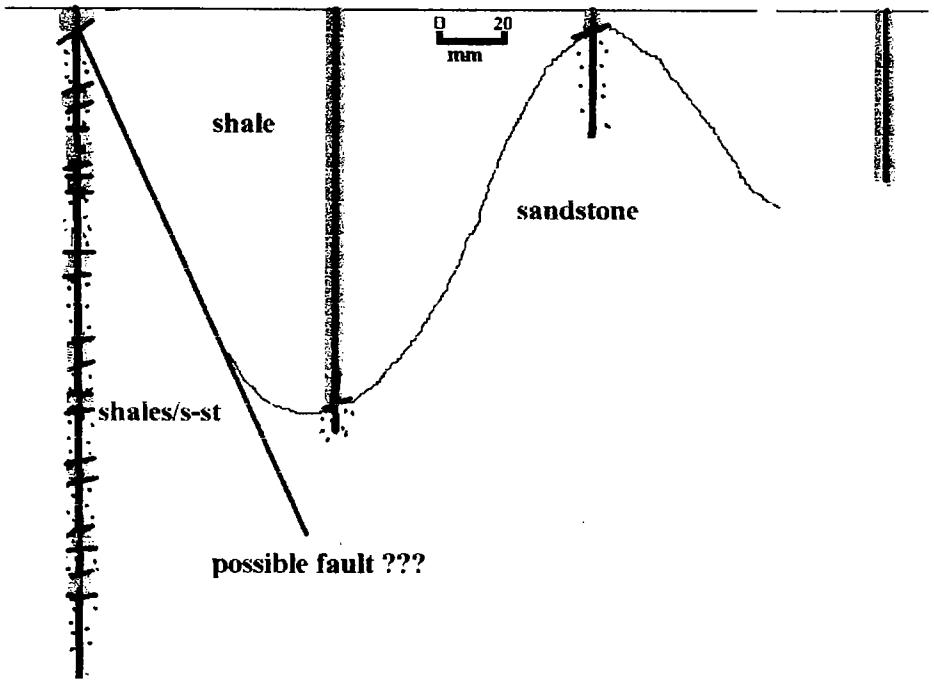

Figure 4.13 The subsurface conditions shown in Figure 4.1, but represented by scant borehole observations.

These and other aspects of *block architecture* were reviewed in Chapter 3. The *block volumetric proportion* can be estimated by applying the principles of stereology and the methods outlined in Chapter 2. Estimation of *block size distribution* is a more difficult problem, and a methodology is presented in Chapter 2, amplified by the results of presented in the Sections above. *Block shape* can be inferred by looking at outcrops and studying the smaller blocks in the core: spherical (more common in serpentinites) to ellipsoidal shapes are the most common shapes in melanges, as discussed in Chapter 3. The characterization of *block orientations* is more difficult. In drill core, certain orientations of micro-blocks in the matrix may be prevalent, but these should not be depended on as indicators of the orientation of large blocks. Small blocks, entrained in the shear fabric of the matrix, swarm around larger blocks and will change orientation depending on the attitude of the shears around the larger blocks (for example: see Figure 1.1). However, as indicated previously, large blocks in Franciscan melanges (100s of meters) tend to be steeply dipping and generally strike north-westerly

4.5.2 Characterizing Melange Using Field Scanlines and Trial Pits

Many guides have been published on characterizing engineering sites (Goodman, 1976; Dowding, 1978; ISRM, 1981; Hunt, 1984), but these authorities offer little advice specific to the characterization of melanges and similar bimrocks. However, a set of procedures was developed by the Geotechnical Control Office of the Government of Hong Kong (GCO, 1988; Irfan and Tang, 1992, 1993) who estimated the volumetric proportion of boulders in colluvium by the use of scanlines in the form of narrow bands chipped through the shotcrete cover of slopes or stripped through vegetation; test pits and borings. The observations included: boulder identifier; weathering state; dimensions; angularity; roughness of the surface; nature of the surface and lithology. The volumetric proportion was assessed to the closest 5 percent to 10 percent; by linear proportion in borings, or by areal proportion from the strips. It was found that cobble and boulder content were visually overestimated by about 50 percent, (which is consistent the writer's experience in estimating the coverage of particles on Gravel Tests setups described in Chapter 2). Core photographs permitted better estimates than boring logs. The strength of boulders was estimated by using a Schmidt Hammer, and that of matrix by using a hammer driven probe (like a compaction test hammer). Interpretation of the results was complicated by the layering of the colluvium, with each layer having its own geological and geotechnical character. In general the data on boulder and matrix characteristics allowed semi-quantitative adjustments to be made to the strength of the matrix (Irfan and Tang, 1993), in a manner similar to that of Lindquist (1994b).

The Hong Kong work showed the benefit of excavating trial pits, although these were generally limited to 3 m depth. In California, the depths of trial pits are limited by OSHA regulations on shorings, but valuable information can be obtained by logging hand-dug or bucket-auger shafts (Scullin, 1994), which are better than boreholes for characterizing melange, assuming large blocks are not encountered. For example: a shaft to 13 m depth in Sausalito, Marin County, California, allowed the recognition of block-rich melange in what had previously been considered weak and potentially unstable colluvium (Dr. David Rogers, Rogers/Pacific Engineering Consultants; personal communications).

4.6 LANDSLIDES AND SLOPE STABILITY PROBLEMS IN MELANGES

4.6.1 Introduction

Because of the relation of melanges to landslides, there is some emphasis on landslides in this dissertation, and this Section summarizes some of the available literature; discusses hillslope instability in melange landscapes, and presents some tentative ideas for further research.

As shown in Chapter 3 (Figure 3.1) and Appendix A, melanges and sheared serpentinites are located in the mountains of over 70 countries. The younger of these deposits are Mesozoic and Tertiary, but Taconic and Caledonian events left their signatures in the melanges of the Appalachians and mountains of northwest Europe. There are close associations between mountains, landslides and melanges but the geotechnical literature on landslides in melange is sparse.

In Cyprus, entire villages have been relocated because of landslides in melange (Northmore and others, 1986, 1988; Gostelow and Loucaides, 1988), but the problems of geotechnical characterization has not been easy (G. Petrides, Geological Survey of Cyprus; personal communication). Turkey is rich in melanges, landslides and geological studies, but has little geotechnical literature (Yilmazer, 1993)., a situation similar to that in Greece (Dounias and Marinos, 1993). Landslides in melange have been reported in Taiwan (Page, 1978; Page and Suppe, 1981); Indonesia (Audley Charles, 1965; Moore and Karig, 1980); Barbados (Cleary and others, 1984; Enriquez-Reyes and Jones, 1991); New Zealand (Kear and Waterhouses, 1976); and Japan (Hada, 1988; Watari, 1988).

4.6.2 Hillslope Instability of Franciscan Melanges

The primary association of Californian engineers working with the melanges, sheared serpentinites and serpentinite melanges is that of remediating and mitigating earthflows, which are ubiquitous in the Central melange terrane of California, and well-represented along the coast, the Eel River basin, the Van Duzen River basin, and other rivers; and the hillsides of Marin, Sonoma, Mendocino, Lake and Humboldt Counties (Kelsey, 1978); CDWR, 1973; Bedrossian, 1978; Ellen and others, 1977; Radbruch-Hall, 1976). Melange terrain in California is commonly referred to as "melted ice-cream topography" (Savina, 1982, p. 134) due to the hummocky, earthflows with their flotsam of protruding, resistant blocks, as illustrated in Figure 4.14. Debris flows from terrain underlain by graywacke blocks in Franciscan melanges are also common. (Earthflows manifest relatively slow gravitational pervasive deformation, or mass rock creep, whereas debris flows are relatively rapid, fluidized avalanches of rock and soil: Varnes, 1978, p. 17-18). In general, hill-sized blocks are the source of debris flows, and the melange "matrix" hosts earthflows.

Much quantitative work has been done on the physical processes of debris flows in the Franciscan, and their relationship to geomorphology (Ellen and others, 1977; Keefer and Johnson, 1983; Pascucci, 1983; Ellen and Fleming, 1987; Johnson and Sitar, 1987; Reneau and Dietrich, 1987; Ellen and Wieczorek, 1988; Dengler and Montgomery, 1989). But the morphology, geology and mechanics of earthflows in Franciscan melanges has been little researched, except for the surveys of Savina (1982), Peterson (1979), Reid (1978), Trautmann (1976), and Keefer and Johnson (1983). Neither has there has been any prior effort to quantitatively investigate the effect of blocks on the in-situ strength of

Franciscan melanges. Later in this section, the relationship between block proportion and hillside slopes for three areas within Marin County is shown.

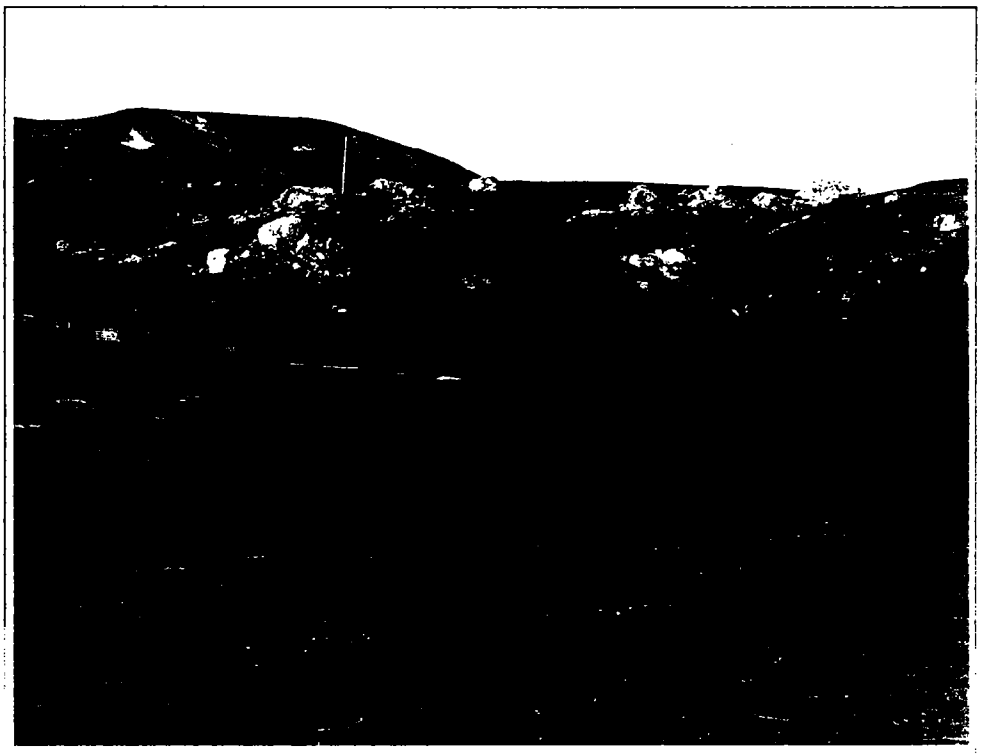

Figure 4.14 "Melted ice-cream" topography in a Franciscan melange: low hummocky relief with resistant blocks; near Bodega bay, Sonoma Co., California

4.6.3 Glaciers as Physical Analogies for Earthflows

The tectonic strains suffered by melanges and sheared serpentinite bodies during formation result in fractured blocks and plastic flow once the rock is exhumed and the confining stress is lessened. In this regard, melange could be thought of as highly overconsolidated clay. Compounding the problem of weak matrices and pre-existing shears is the relatively steady supply of water from graywacke blocks. Deformation in melanges can be slow but impressive: St. Francis Drake Blvd, west of San Anselmo, Marin County, has deformed due to melange earthflows, and at one location, over 30 vertical feet of asphalt road cover has been placed in the last several decades to maintain the highway grade (Craig Herzog, Herzog-Huntingdon Consultants, Petaluma; personal communication).

There is a strong resemblance between a melange earthflow creeping into the ocean or a river bed, and the convex snout of a glacier, littered with rock debris at its toe. Mechanically, an ice glacier may be an apt analogy for an earthflow (Savage and Smith, 1986; Ter-Stepanian, 1963; Savage and Chleborad, 1982; Iverson, 1983; Baum and Fleming, 1993); and a rock glacier may be an even more appropriate analogy (Wahrhaftig and Cox, 1959). Sheared serpentinites are sufficiently mobile that they have been analyzed using lava, glacier and debris flows as mathematical analogies (Cowan and Mansfield, 1970; Johnson, 1970; p. 433-534). However, Savina (1982, p. 245-246) points out fundamental differences between glaciers and earthflows:
1. Glaciers accumulate winter snows, but earthflows do not accumulate clay soils.
2. Glacial ice melts and re-freezes around obstacles, whereas earthflow clays do not.
3. Glacier ice does not resist movement, whereas the rock and soil of earthflows resist by deforming internally

Like a glacier, which changes its behavior in response to changes in the roughness of the basal contact, the rougher the failure surfaces in an earthflow, the more resistant to shear they may become; a concept which is as suggested by the idea of tortuosity around blocks, previously shown in Figure 4.4. Savina (1982, p. 222) observed that shallow earthflows carrying much blocky debris, were "bumpy" and the blocks moved slower than the smoother earthflows. Failure surface irregularities, internal water levels, earthflow driving force and earthflow velocity are interconnected and balanced (Baum and Johnson, 1993), and more research could be performed to investigate how block size distribution, and the related roughness of failure surfaces, may influence the behavior of earthflows (Dr. Rex Baum; personal communication).

4.6.4 The Contribution of Blocks to the Stability of Franciscan Melanges

Blocks are prominent in Franciscan melange, as freight in earthflows, or as debris at the toe, and blocks often act as buttresses to earthflows. Alternating recessive melange earthflows between resistant headland blocks support ridges of weak "matrix", and are characteristic of "melange coastlines" in northern California, as shown in Figure 4.15. Savina (1982, p. 222) also noted that blocks, greater than 1m to 3m, "anchored" earthflows. On the Eel River in northern California, blocks were observed which appeared to buttress landslides. Huge blocks, relicts of earlier earthflow advances, stand isolated along shorelines (Figure 4.15) and in river beds. The sculpting of several columnar blocks in northern California (Skunk Rock, Eel Rock, Squaw Rock) may be the result of residual horizontal stresses within the blocks exaggerating the natural tendency for unsupported blocks to split, forming cliffs; but narrow, towering blocks in Franciscan melanges may also reflect their tendency to be steeply dipping . Figure 4.15 shows the relative competence of the blocks (cliffs), and the instability of relatively weak and erodible "matrix", which at the location pictured, protected by seawalls.

Figure 4.15 View of coastline near Coleman Beach, Sonoma County: active erosion and slope instability of melange "matrix" contrasted with the relative stability of graywacke block cliffs, which support ridges of "matrix". Seawalls protect toes of the slopes.

Since melange "matrix" is relatively unstable, grass is commonly the only vegetation that can thrive, but trees may develop on large and relatively immobile blocks. In the Spring, the sandy soil above blocks dries, while the grass on the moister clayey "matrix" remains verdant. Hence, melange is distinguished as mottling on monochrome air photos exposed early in the Summer. (Savina, 1982, p. 137-140; and Dr. Steve Ellen, personal communication).

Blocks are the main source of water in rural areas of northern California. Relatively permeable graywacke blocks can be likened to water tanks: attempts to stabilize melange landslides with hydraugers to relieve "excess pore pressure", may result in dramatic but short-term success as long until the water is drained from the blocks. Water leaking from blocks also tends to diminish the strength of the sheared matrix. Presumably, an increase in the block volumetric proportion leads to a decrease in rock mass cohesion (due to increased shearing and water) at the same time that frictional resistance is increased (because of greater tortuosity). Lindquist (1994b) came to similar conclusions following research with dry model melanges.

4.6.5 Slope Stability Problems in the Argille Scagliose of Italy

Italian geotechnical engineers reported a number of important geotechnical features of melange masses on slopes, which may be applicable to Franciscan melanges. Italian melanges tend to be have low block volumetric proportions (generally less than 25 percent), and are called *argille scagliose* (scaley clay), and occasionally, *varicolored clays.*

In the opinion of D'Elia and others (1986), the behavior of natural slopes and cuts in argille scagliose cannot be predicted by site and laboratory investigations only; full-scale investigations and the monitoring of field performance is required. When weathered, argille scagliose becomes relatively homogeneous and isotropic soil, in which the strength of the matrix is considered to control the stability of the slopes. Esu and others (1985, p. 195-225) and D'Elia and others (1986, p.432) reported that geotechnical testing showed that the back-calculated shear strength parameters along slope failure surfaces were close to but *lower* than the average peak values given by lab testing triaxial tests, and the mobilized cohesion was smaller than that given by the laboratory tests. (Compare this with other Italian findings that the in-situ strength tends to be higher than laboratory strengths: Section 4.2.3.3). For shallow slides, where the average effective stress was low, <50 kPa[?], ϕ' required for equilibrium at the failure surface was close to that given by a curved failure curve. Back analyses are performed for *translational* failures due to the low thickness/length ratio of most flows. However, some flows deform by "viscous flow" rather than failing along the boundaries in a discrete mass (Esu and others, 1985, p195-225; D'Elia and others, 1986, p.432).

The Italian experience with slopes in argille scagliose is illustrated by the following examples:

1. Degradation of argille scagliose and surficial slope instability: The in-situ behaviour of argille scagliose is controlled mainly by the sheared fabric of the matrix, which influences the mass behavior by permitting progressive failure (Esu and others, 1985, p. 215). Due to recent tectonic uplift, stress levels are high, even for low slopes. Low confining stresses, overconsolidation and low strength results in the progressive weathering of the rock to relatively homogeneous, weak and permeable clay soils, in which fully drained conditions prevail within a short time. The degradation is accomplished by dilatancy, loosening of the scaley fabric, separation of scales, infiltration of water and consequent softening. Low applied stresses tend to produce surface failures in excavations or, in natural ground, slumps or mud slides. The mass strength resulting from back-analysis of failures is, "...always intermediate between the peak and residual strength parameters, and is very often close to the strength of the reconstituted normally consolidated material, or critical state strength ...." (Prof. P. Canuti; personal communication; citing work by Bertocci and others (1993). The

experience summarized here is useful in understanding how relatively fresh Franciscan melanges can accommodate steep slopes but will, over time, degrade.

For example, at Risalaimi, in Sicily, a slide in lustrous, slickensided argille scagliose (Numidian Flysch) occurred at a 11.5 m high road cut some 6 months after excavation. The slide occurred in essentially drained conditions due to the high secondary permeability afforded by the scales. Back-analyses showed that the average mobilized shear strength was in good agreement with the CD (Consolidated Drained) lab shear strength tests (Esu,. and others, 1985, p. 215). Similarly, at Capo di China, in central Italy, a large failure occurred by bulging and cracking of a 20 m high, steep (36°) road cut some four years after excavation. Pore pressure had been relieved fast due to drainage along several shear surfaces within the formation. Laboratory tests showed $\phi' = 28$ degrees and c'=35 kPa for samples that were tested confined sufficiently to restrain the matrix scales. But 8 months after sampling, when the samples were tested in a loosened condition, ϕ' =18 degrees and c'=18 kPa. The residual strength for the soil was ϕ'=13, c'=0, which was lower than the back-calculated in-situ shear strength for the fully softened material, indicating that the slope failure had occurred when the material was only partially loosened after excavation unloading.(Esu,. and others, 1985) (p. 215).

The implication here is that carefully preserved test specimens should be immediately tested, and others reserved for testing at a later date.

2. Deep-seated slope instability due to high in-situ stress states: In argille scagliose, high stresses at shallow depths result in landslides; and high stresses at great depths result in internal deformations ("creep") (Esu and others, 1985, p. 215). For example: Argille scagliose formed the lower bound to lacustrine sands and clays at the Santa Barbara open pit coal mine at Arezzo, in Tuscany. The pit slopes were up to 200 m high. The argille scagliose had a block/matrix proportion of 15 percent, and the matrix clays were scaley, slickensided and striated. The blocks were siliceous limestones ranging in size from centimeters to a few meters, unevenly distributed in the clay shales. Inclinometers were installed to monitor deformations. The mine was excavated in two phases, with the first phase excavated to 50 m, after which there were gradually decreasing settlements. During the second phase, after some 90 m of excavation, the horizontal and vertical deformations (on the order of meters) suddenly accelerated as the mine deepened. The locus of deformation was below both the excavation and the inclinometers and rotated the inclinometers. However, only shallow, surficial slides occurred in the argille scagliose, and the considerable deformation was attributed deep-seated plastic flow (creep) of "a statistically homogeneous and isotropic viscous-plastic medium" (Esu,. and others, 1985; D'Elia and others, 1986, p. 435-436; D'Elia and others, 1989).

The experience quoted here may be relevant to large highway cuts, or hillslopes in Franciscan melanges at coastal and river environments where active erosion of hillslope toes may promote spasmodic surges in earthflow deformations.

3. Lateral spreading of argille scagliose beneath rigid capstone: Conglomerate and other brittle rocks commonly cap Italian melanges, and these may fracture and settle as much as centimeters and decimeters, because of ductile, lateral spreading of the underlying melange due to stress relief (Esu,. and others, 1985; p. 215). For example: shaking by the 1965 Irpinia earthquake caused portions of the conglomerate caprock below the town of Bisaccia to deform and impinge on the underlying melange (*varicolored clays)*, which caused stress concentrations leading to viscous deformation ("creep") and further movement of the brittle caprock (Esu,. and others, 1985). A similar process was identified at the monastery of La Verna as shown in Figure 4.16, and is described further in Casagli (1992), Canuti and others (1993), and Canuti, (1993b). The problem of lateral spreading may be relevant in California, where relatively rigid masses of Tertiary volcanics overlie the Franciscan melange in Sonoma, Napa and Lake Counties, and earthquakes are relatively common. Similar behavior may occur below large blocks. The problem of the likely site response of Franciscan melanges to seismicity has not been researched.

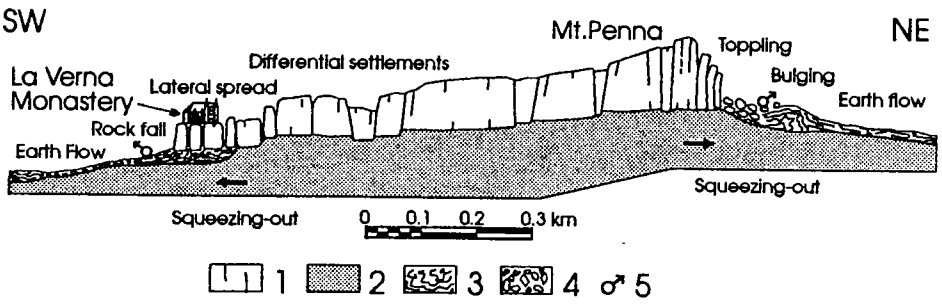

Figure 4.16 Lateral spreading of melange below a rigid conglomerate caprock at the monastery of La Verna, Italy ; from (Canuti, 1993a, p.23). Symbols: 1: calcarenites and calcrudites; 2: Sillano Fm. argillite; 3: deformed, mobile material; 5: debris; 6: *sorgenti* (tiltmeter?)

4.6.6 Relationship Between Hillslope Angles and Block Proportions of some Franciscan Melanges in Marin County, California

The relationship discovered by Lindquist (1994b) between volumetric block proportion and overall bimrock strength should be reflected in the natural slopes of melange landscapes. Accordingly, an attempt was made to discern any relationship between hillslopes and block proportions; and also to identify any threshold between failed and stable melange for some Franciscan melanges in Marin County, California. The geological maps of Savina (1982), Reid (1978) and Peterson (1979) were used to

measure the data, following the procedures outlined in Section 2.12. More detailed explanations, individual plots, maps and other details are presented in Appendix E.

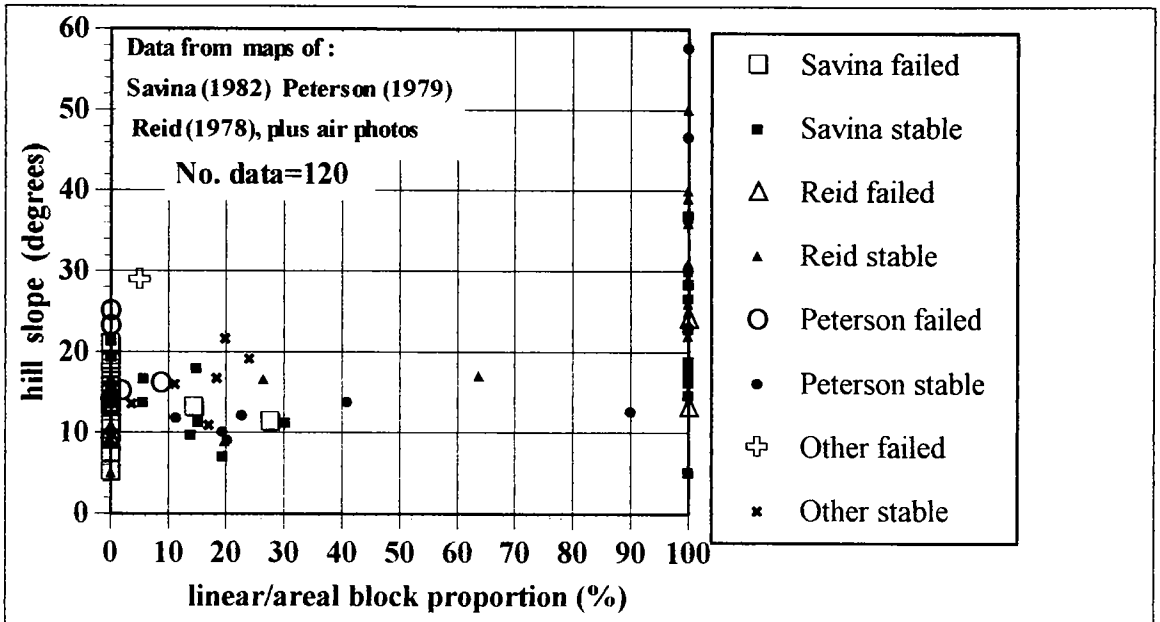

Figure 4.17 Scatter plot of block linear and area proportions for hill slope angles at three areas of Franciscan in Marin County, California

Figure 4.17 is a summary plot of the data measured from each of the sources cited, and relates block proportions and hillslope angles. In general, the blocks (100% block proportion) are graywacke: the average hillslope is about 35 degrees, with a range of almost 55 degrees. The "matrix" ("melange", in the source studies), is shown with 0 percent blocks, has an average slope angle of 15 degrees and a range of 20 degrees. The "matrix " also had blocks, as typical of Franciscan melanges elsewhere., but the smallest block mapped was about 3 m in size due to the limitations of the map scales,
The plot shows:

1. A threshold between "failed" and "stable" is not well-defined. Even for the pure block or pure matrix the failed and stable data are jumbled together. In the open portion of the plot, there are insufficient failed data points to define a threshold, but a threshold would have to be at least 25 degrees since there are many stable points at lower slopes. The solitary failed point at 5 percent block content and 29 degrees slope (representing the Lone Tree Slide: see Chapter 5) is anomalously steep, but may be typical of coastal landslides where the toes are constantly being eroded and the slopes accordingly intermittently adjusting.

2. The scant data beyond about 30 percent block proportion suggest that, at the scale of the areas mapped by Savina, Reid and Peterson, (approximately 1 km^2) the melanges do

not contain much more than 30 percent blocks. Thus, for these areas, there is little opportunity to use the strength relationship that Lindquist (1994b) developed, in which he recommended that below 25 percent the strength of the melange be taken as the strength of the matrix.

This was an incomplete study and should be extended, because Figure 4.17 shows that considerably more data must be collected in order to validate the hypothesis that higher block proportions should result in steeper, stable slopes.

4.7 TUNNELING PROBLEMS IN MELANGES

Tunneling through melange may be problematic, Residual stresses in the matrix may result in squeezing ground where the overburden stresses exceed the unconfined compressive strength. Sheared pelitic and serpentinite matrix, often contains montmorillonite and other expansive clays which swell in wet conditions, particularly from leaking blocks. Blocks, often highly fractured, may ravel. The mechanical contrast between the blocks and matrix in mixed face conditions (blocks and matrix exposed in the face) may result in differential cutting that tend to bind or divert a TBM (Tunnel Boring Machines) since the cutting heads of TBMs are usually selected to excavate limited range of design rock types. But rocks in melange range in lithology (and strength) between sheared shale, relatively weak siltstone and tuff, through limestone, graywacke, greenstone and amphibolite schist and eclogite. The weak matrix, especially in wet conditions, may yield differentially under reaction pads pressed against the walls of the tunnel (although TBMs can also thrust against tunnel linings). Highly pressured water may instantaneously release when blocks are breached, The extensive shear zones around large blocks present similar problems as faults but are less predictable. Since blocks are often smooth, rounded and coated with a slick rind, they may hazardously drop from walls and roofs, and the sockets, or moulds, of the blocks may constitute "overbreak" (excavation beyond the contract limits of mining). Small blocks may pass intact through the "muck windows" of TBM cutter heads, collect behind the cutting head, and interfere with the passage of muck onto the conveyors (Mr. Michael Kobler, Resident Engineer, City of Scan Francisco; personal communication).

Many tunnels have been excavated through melange and some of them have fared reasonably well, including the Pacheco tunnel near San Jose, California (Prof. Richard Goodman, personal communication), but the excavation of other tunnels in Franciscan melange have been extremely difficult. For example, the original design of the Stockton Street Tunnel in San Francisco (constructed about 1915) was based on the "...belief that the ground was dependable...", but instead, construction was hampered by squeezing ground (Engineering & Contracting News, 1915; p. 93-96). Difficulties were also experienced about the same time during construction of the Twin Peaks Tunnel in San Francisco, where "extremely variable" conditions and a deluge of water had to be accommodated (Engineering News Record, 1914). (The Twin Peaks area is underlain by

blocks of chert, volcanics, sandstone and shale within melange, and is assigned to the Marin Headlands Terrane within the Franciscan: Figure 3.3 and Figure 3.4).

The Storage Tunnel of the Richmond Transport Project tunnel, currently under construction (July, 1994) is discussed in Chapter 5.

4.8 PROBLEMS WITH FOUNDING DAMS ON MELANGES

Except for Scott Dam (Volpe and others, 1991; and also discussed in Chapter 5), there is little information related to dams founded on melange, despite the certainty that others exist. In general, dams within melanges are built on large blocks, rather than on the matrix. An example is the Crystal Springs Dam, south of San Francisco, founded on a graywacke block surrounded by sheared shale and serpentinite. But the foundation rock conditions are secondary to the fact that the dam is located only a few hundred feet from the 1906 rupture of the San Andreas Fault (Wahler Associates, 1977; Solomon and Bahr, 1982). Other dams built within the Franciscan are the Calaveras Dam (Kintzer, 1980) near San Jose, California; and Warm Springs Dam, near Healdsburg, Sonoma County, California. In the Former Republic of Czechoslovakia, the earthen Terlicko Dam is founded in "....Carpathian flysch, with sandstones and shales with lens-shaped teschanites (theralite, a mafic plutonic rock) ...." (Czechoslovak Dam Committee, 1967; p28), wording that suggests an ophiolitic melange. In Cyprus the Mavrokolymbus Dam is founded on a block of serpentinite within the Mammonia Melange, with pillow basalts and highly deformed shales nearby (Morgenstern and Cruden, 1977).

4.9 A PRACTICAL EXAMPLE USING SOME OF THE RESULTS OF THE RESEARCH

A practical application of some the results summarized in the previous sections is illustrated, but the procedure is tentative and so is presented here rather than in Chapter 2. The procedure may be useful for making rough predictions about the size and the numbers of blocks at an engineering site, particularly for earthwork construction in melange. Such estimates are useful, since blocks of about 0.6 m (2 feet) interfere with scraper blades; blocks greater than 2 m (6 feet) require D9 bulldozers to remove them; and blocks greater than 3 m (10 feet) must be blasted (Michael Hobbs, Earthwork Superintendent, Ford Construction, Lodi, CA; personal communication). The data for the example here were 190 chord lengths measured from blocks in 1300 feet (395 m) of drill core obtained from a Franciscan melange at the Lone Tree Slide, near Stinson Beach, Marin County, California. The Case History is discussed further in Chapter 5.

For the purposes of the example, assume that an earthflow-type landslide of about 100 feet thickness (30 m) is known to underlay a site, and the approximate areal extent is known as 8 acres (38,000 m^2). Surface mapping suggests the block proportion of a Franciscan melange is much less than 25 percent, and drill core from geotechnical

exploration is available for review. These data are all that are available. Assume that a rough prediction of the 3DBSD is required, perhaps for estimating the costs of excavating and blasting oversize rock. The following procedure could be used:

1. **Determine the characteristic engineering dimension.** For a landslide this is assumed to be the thickness; in this case, 30m (Section 2.6.3).
2. **Estimate the block/matrix threshold.** Calculate 5 percent of the characteristic engineering dimension, or 1.5 m (Section 2.6.4.1).
3. **Measure the chord lengths of blocks in the core.** Measure chords to as small as 5 cm (Section 2.12), although the block/matrix threshold is larger.
4. **Construct the log-histogram of chords.** Using the block/matrix threshold of 1.5 m as a node, construct the range of endclasses by "doubling" to the right, and "halving" to the left (Section 2.4.3). This procedure resulted in Figure 4.18.

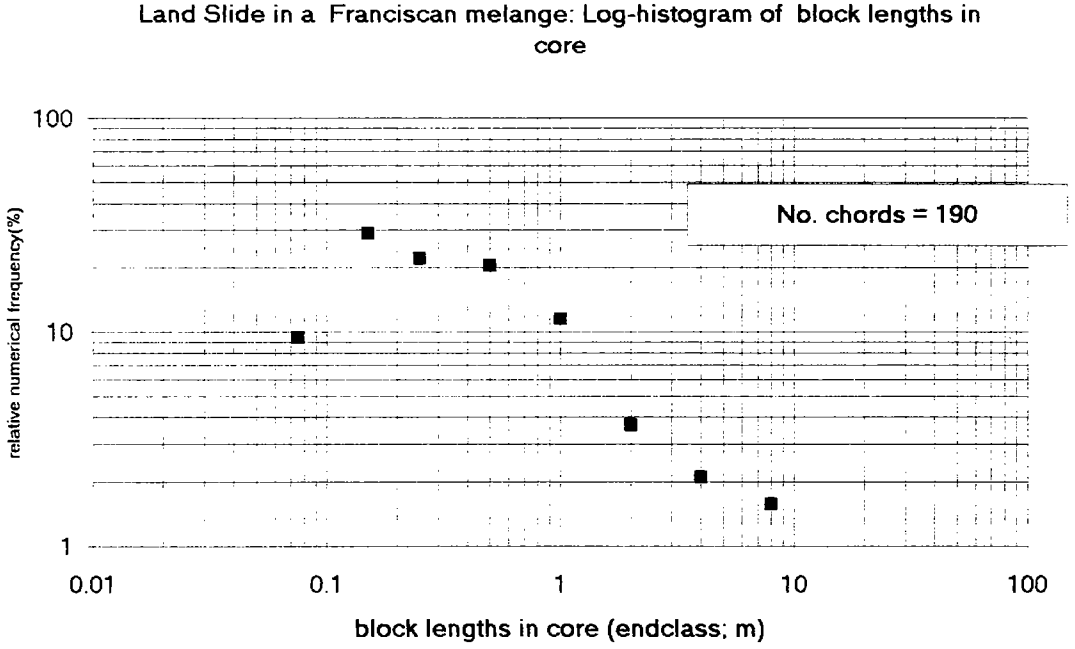

Figure 4.18 Log-histogram CLD of chords measured in blocks from 395 m of drill core.

Inspection of the log-histogram suggests that the CLD severely underestimates the possible CLD for the site, because the d_{peak} is about 0.4 m, whereas the block/matrix threshold (the theoretical d_{peak} : Section 2.6.4.1) was computed to be about 1.5 m. The approximately linear descent limb has a slope, **D**, of about 0.9, and is consistent with the range of fractal dimensions for the Franciscan (Section 2.5, Figure 2.8). The maximum block size, d_{max} is approximately 15 m (extrapolation of descent limb to 1 percent relative frequency). The low block proportions of the melange probably resulted in an

insufficient number of chords through the larger blocks. The low block proportion, coupled with the assumption that the blocks are oriented steeply, as is typical for the Franciscan (Section 3.10), means that the CLD can be assumed to have the same relative shape as a 2DBSD, with the same descent limb slope (Section 4.4.5, Figure 4.11).

5. Calculate possible maximum block for the site. In two-dimensions, d_{max} can be assumed to be approximately equivalent to $\sqrt{A}$, where A is the area of interest. Here A is 8 acres, hence $\sqrt{A}$ is about 590 feet (180 m). This is the possible largest block: it may not exist at the site.

6. Scale the CLD to d_{max} for the site. This is done by a rightward translation of the whole CLD, to anchor it such that the $\mathbf{d_{max}}$ of the core CLD (15m) is located at the theoretical d_{max} of the site (180 m). The scaled CLD, now assumed to be a 2DBSD, is shown in Figure 4.19. The re-scaled CLD/2DBSD is here defined a *synthetic* 2DBSD.

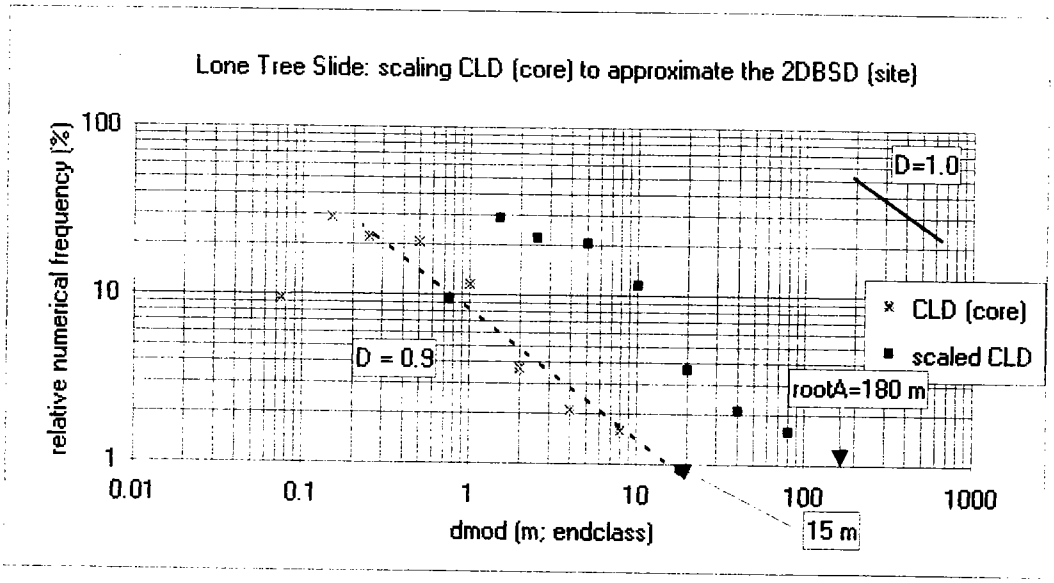

Figure 4.19 CLD from drill core, scaled to a 2DBSD at site dimensions by rightward translation.

7. Construct the 3DBSD. Since the translated CLD is now assumed to represent a 2DBSD, the conversion to a 3DBSD could be followed using the procedure outlined in Section 2.8.1 (Figure 2.13): that is, adding 1.0 to the magnitude of D. In this case the three-dimensional fractal dimension would be 0.9 + 1.0 = 1.9, as shown in Figure 4.20. (However, if the block orientation is known to be about 60 degrees, Figure 4.11 suggests that the CLD can be taken to represent the 3DBSD directly).

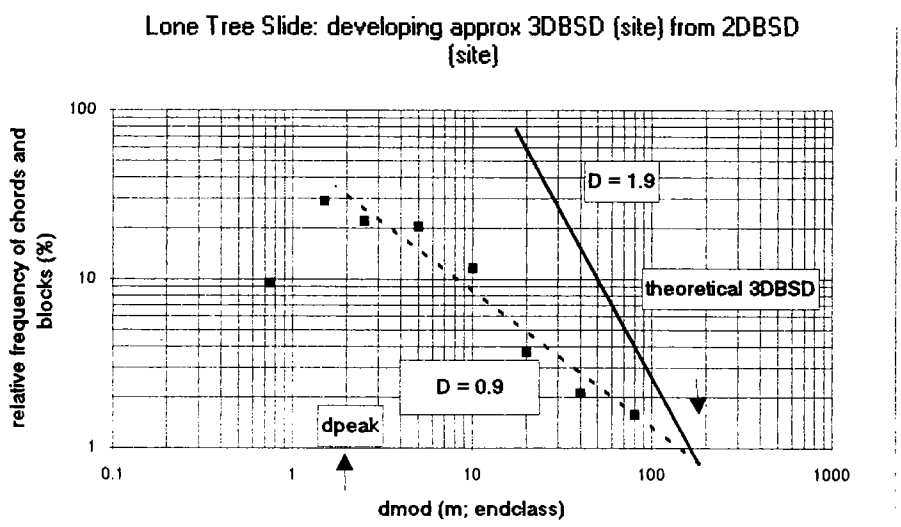

Figure 4.20 Developing the site 3DBSD by adding 1.0 to **D** of the site 2DBSD (0.9 + 1.0 = 1.9), and hinging the 3DBSD at d_{max} of the 2DBSD.

8. Re-scale the Relative Frequency axis for the 3DBSD: The relative frequencies of the 3DBSD extends off-scale in Figure 4.20; and the Relative Frequency scale used for the 2DBSD is not correct for the 3DBSD. As a guide to re-scaling, use the results of Section 2.5, particularly Figure 2.8, which shows that, in two-dimensions for a some Franciscan melanges over 7 orders of magnitude in scale, $\mathbf{d_{peak}}$ occurs at a Relative Frequency of 50 percent. Assume that this is true in three-dimensions. Hence, re-scale the relative frequency axis of Figure 4.20 so that the 3DBSD d_{peak} is approximately 50 percent, and show the descent limb only. The approximate 3DBSD is shown as Figure 4.21.

9. Possible Approaches to Estimating the Numbers and Size of Blocks: Figure 4.21 could be used to estimate the frequency of blocks if the number of very large blocks is estimated. For example, if it is known that there is one block of 80 m, then according to Figure 4.21, the relative frequency is 0.08, which would allow the absolute numerical frequency of the smaller blocks to be calculated. An assumption of spherical geometries would allow volumes to be calculated, and the sum of these should constitute a volumetric proportion similar to that assumed at the beginning of the procedure. The estimate should be checked against the cumulative block linear proportion developed form measuring core. Re-iterations of the procedure to estimate the numerical frequency of blocks may be necessary so that the resultant estimated volumetric proportion and the measured linear proportions match.

Alternatively, the knowledge of the approximate fractal dimension would allow construction of a graph similar to Figure 2.9, in which the cumulative volumetric proportions are related to dimensionless $\mathbf{d_{mod}/d_{max}}$. And, since it is assumed that the block areal proportion is the same as the block volumetric proportion, the relative frequencies of ranges of blocks could be read from the synthetic 2DBSD, and the resulting proportions applied to the estimated volumetric proportion of blocks.

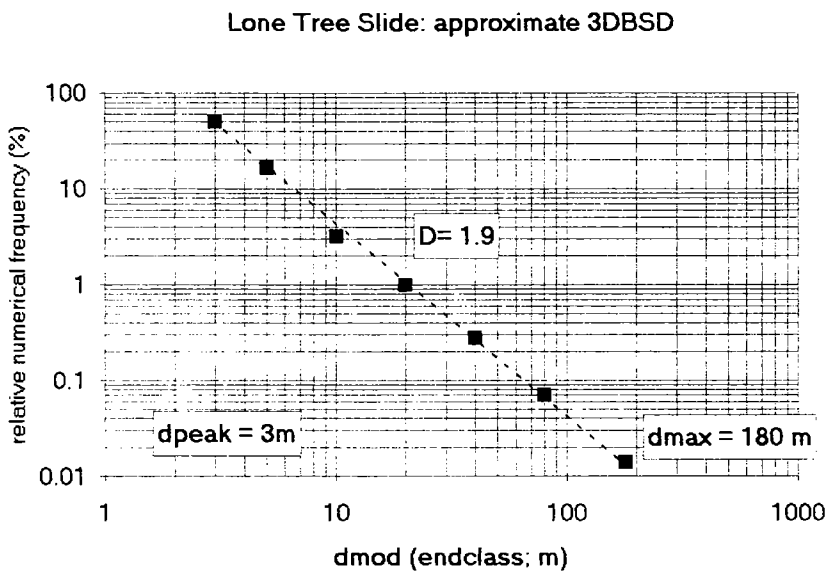

Figure 4.21 Approximate 3DBSD which can be used to estimate frequency and sizes of large blocks for the example site.

Part of the procedure illustrated here was used to develop a the 2DBSD for Lone Tree Slide, and estimate the volumetric proportion of blocks The comparison with field data and contractor records is reserved for the discussion of that Case History in Chapter 5. More research must be conducted to verify the value of this method for other Franciscan melanges.

CHAPTER 5 CASE HISTORIES

5.0 INTRODUCTION

The three case histories presented here demonstrate the applicability of the methods developed to estimate the block volumetric proportion and block size distributions of some Franciscan melanges from measurements of drill core. At the Lone Tree Slide, the estimates were checked against field work, and from a contractor's records. The locations of the Case Histories are shown on Figure 5.1.

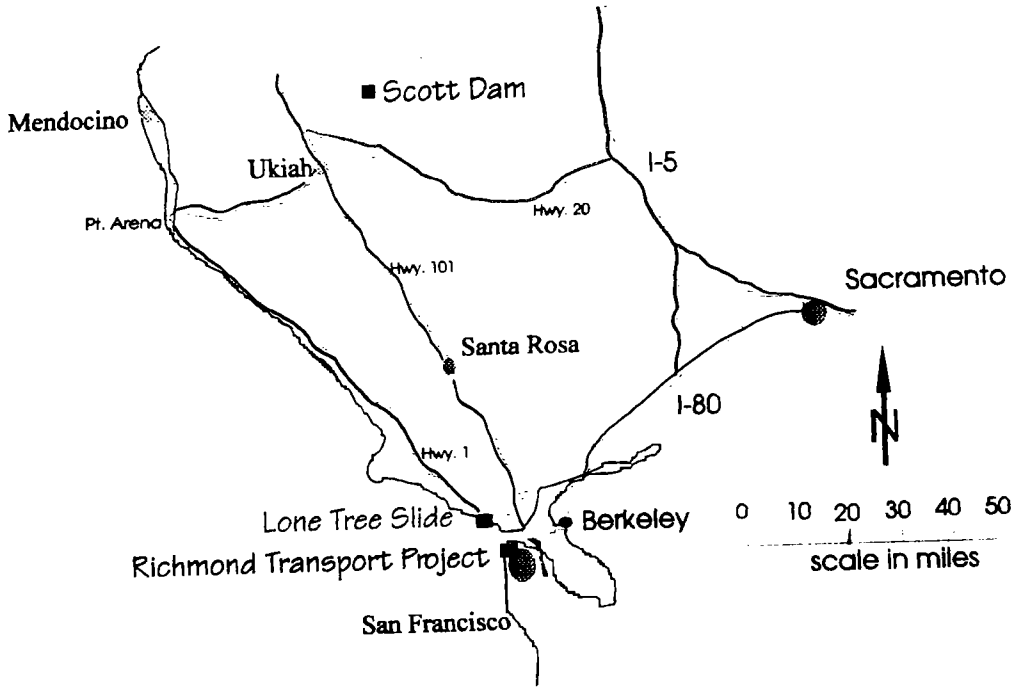

Figure 5.1 Locations of the Scott Dam, Lone Tree Slide and Richmond Transport Project Case Histories

5.1 LONE TREE SLIDE, HIGHWAY 1, MARIN COUNTY, CALIFORNIA

5.1.1 Introduction

Shortly after the Loma Prieta earthquake in October, 1989, California Highway 1, south of Stinson Beach, Marin County, was closed by the Lone Tree Landslide (Figure 5.2). The California Department of Transportation (CALTRANS) restored access by excavating 956,000 m^3 (1.25 million yd^3) of failed and intact Franciscan melange to an average depth of 37m (Van Velsor and Walkinshaw, 1993) to provide stable cut slopes (Figure 5.3). The volume and sizes of blocks far exceeded what been anticipated from the geotechnical exploration: blocks of up to 30m in exposed largest dimension were blasted during the excavation work (Michael Hobbs, Ford Construction, Inc.; personal communication). Fill from the excavation was placed on the downhill side of the cut to buttress remnants of the landslide, and large blocks were used as protective rip-rap at the shoreline toe of the fill. CALTRANS anticipates that the fill will be removed by coastal erosion over several decades, mimicking natural attrition.

Prior to construction, nine exploratory borings, shown at the locations in Figure 5.2 and Figure 5.3, were drilled to between 37m and 82m deep to investigate the stability of the melange that would be exposed in the cut slopes. Coring started some distance below the ground surface and 375m of HQ size core (61 mm diameter) was recovered, of which 82m was from those sections of the boreholes located above the future excavated surface. The core from these segments was assumed to represent the melange excavated, and are referred to here as the *excavation segments*. The landslide was determined by CALTRANS to be approximately 100 feet. Besides, failed melange in the landslide, much relatively intact melange was removed from below and behind the assumed failure surface, in order to accommodate the re-aligned highway and a new grade.

The analysis of data from the measurement of core and field work evolved throughout the research, and resulted in a number of preliminary conclusions (Medley and Goodman, 1994; Medley, 1994) that are re-evaluated here.

5.1.2 Measurement of Core and Field Work

CALTRANS eventually gave the core recovered from exploration drilling of the landslide to the Department of Civil Engineering, University of California, Berkeley for research purposes, once it considered the remediation project to have been successfully concluded. The method of reviewing the core was as described in Section 2.11. Initially, the block/matrix threshold size was estimated to be about 1 foot (0.3 m), or 1 percent of the size of the largest block observed immediately adjacent the site; approximately 100 feet (30m). But blocks were measured to as small as 5 cm. The

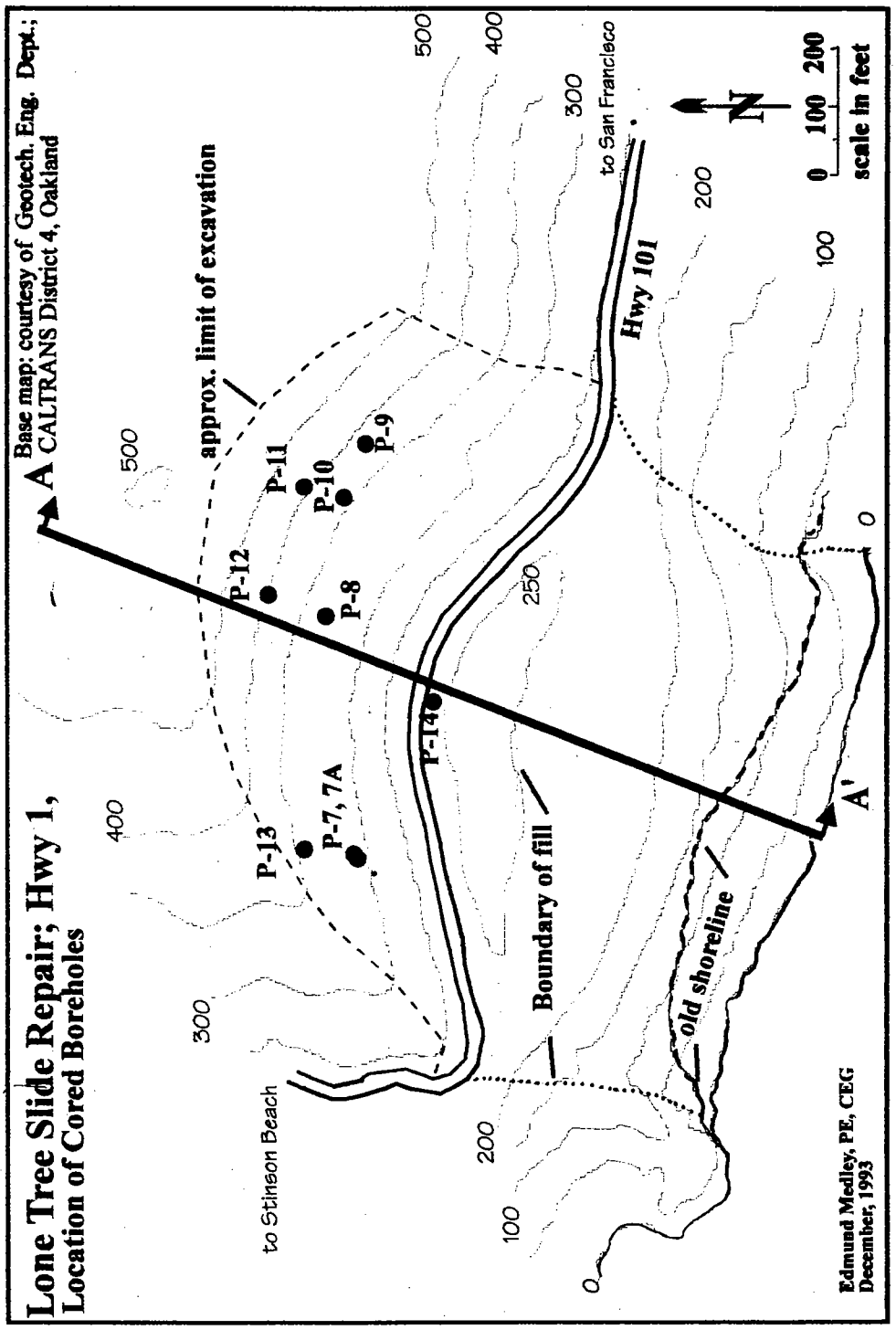

Figure 5.2 Plan of Lone Tree Slide, Highway 1, Marin Co., California

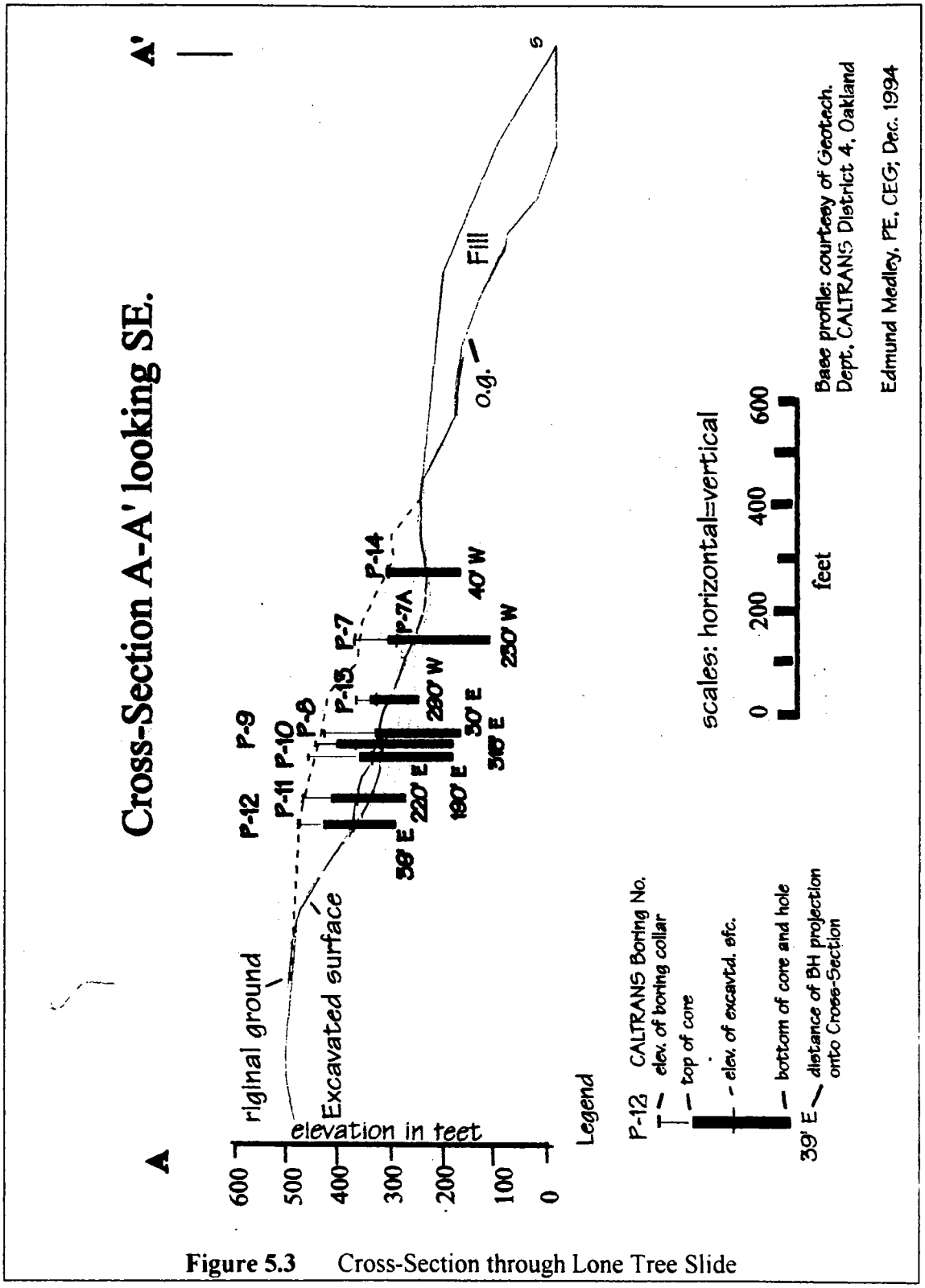

Figure 5.3 Cross-Section through Lone Tree Slide

lithology of the blocks was recorded. Sections of core were selected for later laboratory testing, but the results are not reported here.

To verify the block volumetric proportion estimated from the drill core, the block areal proportion of blocks larger than about 1.0 m was also estimated by mapping the excavation. The block areal proportion was assumed to be the same as the block volumetric proportion. The blocks are relicts of larger blocks blasted or ripped during excavation, and were prominently exposed on the largely unvegetated slopes of the excavation. The 8 acre site (38,000 m^2) was divided into 21 sub-areas and the maximum observed dimension (d_{mod}) of blocks greater than 1 m in each sub-area was visually estimated, using the method described in Section 2.11. The areas of individual blocks were calculated by assuming that the maximum observed dimensions were circular diameters, and these summed for each sub-area and then for the entire site. The block areal proportion was calculated by dividing the sum of block areas by the site area. The estimates of block volumetric proportion and size distribution were checked against the statistics of size ranges and volumes of oversize material excavated from the landslide provided by the earthwork contractor later in the research program.

5.1.4 Summary of Data

The data obtained by measuring the core and field mapping are shown in Table 5.1 below.

Table 5.1: Data obtained from measurements of Lone Tree Slide core and from field mapping

Measurement	All core	Excavation Segments Core	Field Mapping
number of boreholes	9	8	-
length of core measured	375 m	82 m	-
avg. length core/borehole	42 m	10 m	-
number of blocks	190	44	117
average block size	0.43 m	0.03 m	2.7 m
min. block measured	0.05 m	0.05 m	0.3 m
max. block measured	7.9 m	0.6 m	15 m
max. predicted block size	15 m	1 m	> 30 m
block proportion (>1m)	**10%**	**0%**	**4 %**

The lithology of the blocks was recorded when the core was reviewed, and Figure 5.4 summarizes the observations. The plot is similar to that of Figure 3.8, and shows block

lithologies sorted by the relative numerical proportion of the blocks as well as by the proportion based on blocks sizes, as characterized by the d_{mod}s of the blocks. The proportions are similar, as they were for Figure 3.8. The similarity is because the average size of the blocks, of any lithology, are alike. At Lone Tree Slide, siltstone blocks were significant, and composed about 10 percent of the total number of blocks.

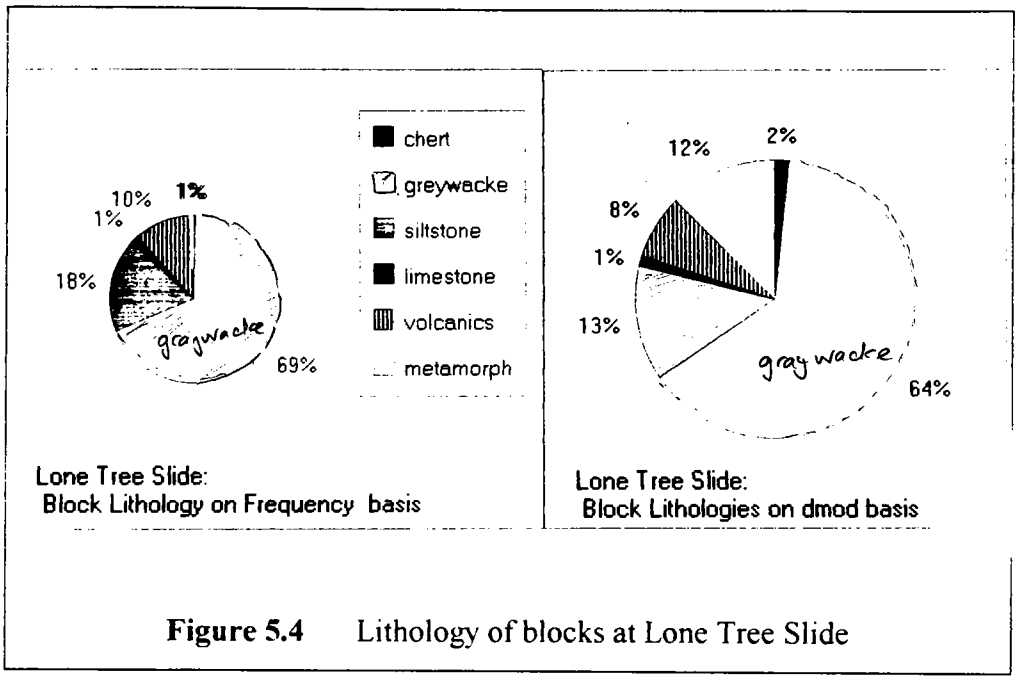

Figure 5.4 Lithology of blocks at Lone Tree Slide

5.1.5 Estimation and Verification of Block Volumetric Proportion

Medley and Goodman (1994) and Medley (1994) estimated that the block volumetric proportion of the landslide material was 4.5 percent, as measured in the portions of the core previously defined as "excavation segments". The block volumetric proportion of the intact melange below the excavated surface was estimated as 28 percent. These estimates were based on the proportion of all blocks in the core, including those as small as 5 cm. The plot in Figure 2.9 shows that the fractional contribution of small blocks to the total of d_{mod}s is considerable, and inclusion of small blocks in this case gave too high a block volumetric proportion for both intact and failed melange. The revised estimates here are based on the concept of the geotechnical significance of blocks introduced in Section 1.2 and amplified in Section 2.6. As indicated in Section 6.1, the geotechnically significant blocks at the Lone Tree Slide were blocks larger than 1.5 m, the block/matrix threshold size at the scale of the landslide thickness. Because most of the blocks mapped had been greater than about 1 m, the threshold was relaxed to 1.0 m.

Figure 5.5 shows the proportion of all blocks in each borehole with chords greater than 1.0 m. Using the procedure outlined in Section 2.8.3, and summarized in Figure 5.6, the

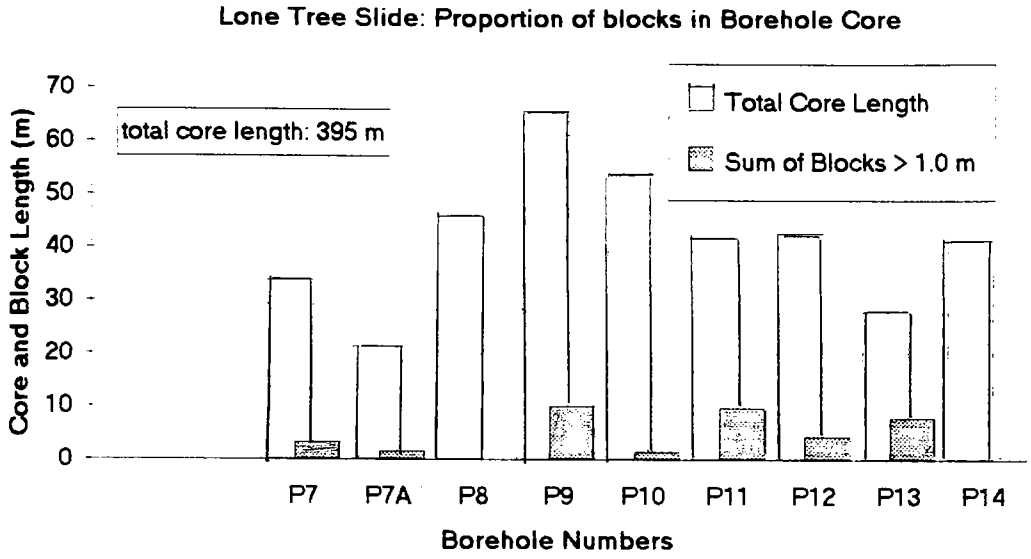

Figure 5.5 Proportions of blocks in Lone Tree Slide core

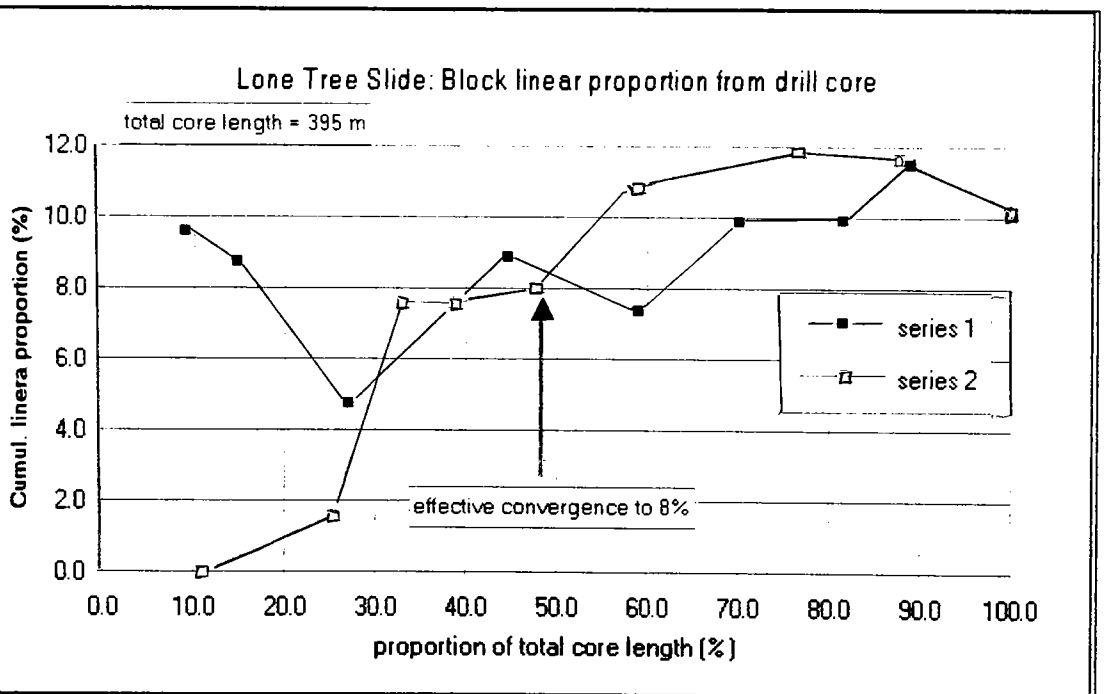

Figure 5.6 Estimation of block linear proportion at Lone Tree Slide, based on drill core.

cumulative block linear proportion was estimated as 10 percent, with an effective convergence to 8 percent at approximately 50 percent of the total length of the core, or about 190 m, (620 feet). Since the largest local block was estimated to be about 30 m, the

ratio of effective convergence length to maximum block was about 6. (This ratio was about half that of the lowest ratio determined from the exercises performed to estimate block volumetric proportion from scanlines traced across the Triaxial Specimens: Section 4.3.3.2). The core of the excavation segments contained no block chords greater than about 0.6 m; hence the volumetric proportion of the landslide material is now estimated to be none. (Medley, 1994; and Medley and Goodman, 1994 estimated were that there was about 5 percent block proportion at the site, based on the core from the excavation segments.)

The contractor estimated that there were approximately 80, 000 yd^3 (60, 000 m^3) of blocks greater than 2 feet to 4 feet (0.6 m to 1.2 m); and an additional 60, 000 yd^3 (46, 000 m^3) of blocks greater than 4 feet (1.2 m) Michael Hobbs, Ford Construction, Lodi, CA; personal communication). Thus, as a proportion of the total excavation of 1, 250, 000 yd^3 (956, 000 m^3), blocks greater than about 0.6 m constituted some 11 percent of the excavation, and blocks greater than 1.2 m, were 6 percent. This range of proportions independently confirmed the block volumetric proportion of about 10 percent estimated here.

5.1.6 Estimation and Verification of Block Size Distribution

Table 1 indicates that there were great differences between the maximum sizes of blocks in all the core, the excavation segments core, and blocks mapped in the field. Since it was of interest to relate the block size distributions, a log-histogram of the lengths of block intercepts in the drill core (chords) was constructed, as shown in Figure 5.7. this is the same data used for the example problem of Section 4.9 (Figure 4.18).

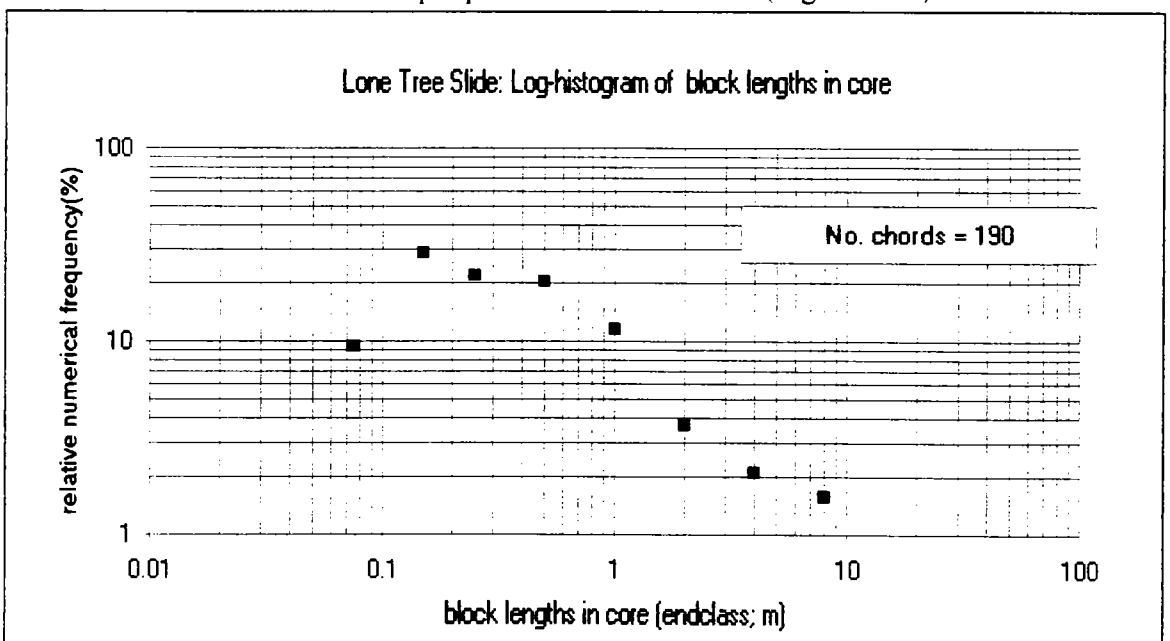

Figure 5.7 Log-histogram of block lengths in Lone Tree Slide core

The log-histogram is a is self-similar chord length distribution (CLD), with an approximately linear descent limb, and a slope (fractal dimension, **D**) of about 0.9. The predicted maximum block, at 1 percent relative frequency, is about 15 m. Because of the low block volumetric proportion, the log-histogram, based on the core, severely under-estimated the actual block size distribution at the site, particularly since casual observations in the locale of the site revealed that there are several nearby blocks with d_{mod}s in excess of 100 m, although the maximum size measured at the excavation was

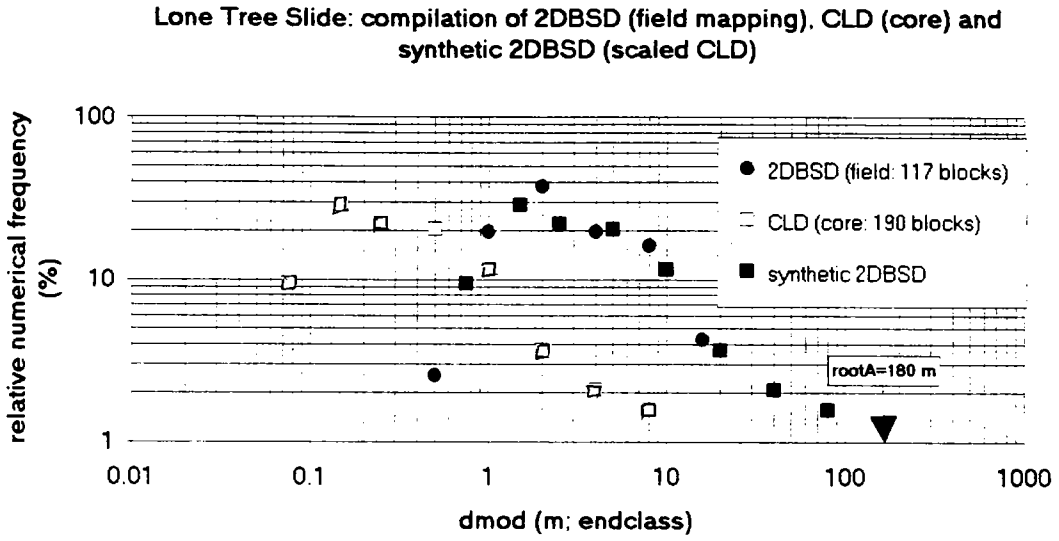

Figure 5.8 Compilation of CLD from drill core, log-histogram of block sizes from field mapping, and synthetic 2DBSD constructed from CLD; using the procedure of Section 4.9.

approximately 15 m. The procedure of Section 4.9 was used to scale the CLD by translating the entire log-histogram rightward, in order to estimate a more likely two-dimensional block size distribution (2DBSD). The synthetic 2DBSD was then compared to the actual 2DBSD block d_{mod}s measured during the field work.

The synthetic 2DBSD was scaled to the maximum d_{mod} (d_{max}) that could be expected for an 8 acre (or A=38, 000 m^2) area of Franciscan melange; with a $\sqrt{A}$ of 180 m, using the empirical guide of Section 2.5. The re-scaled CLD was assumed to be a 2DBSD because the volumetric proportion of blocks was low (10 percent) and the blocks were assumed be oriented relatively steeply, as is typical for Franciscan melanges (see Section 4.9). It is apparent from Figure 5.8 that the original CLD and the field 2DBSD are separate, scale-independent log-histograms; and that the synthetic 2DBSD, which is identical in form to the source CLD, matches the actual 2DBSD quite well for d_{mod}s less than about 20 m. The fractal dimension of the field 2DBSD is approximately 0.9.

In Section 4.9, the data from the Lone Tree Slide study were used to develop a procedure for estimating the three-dimensional block-size distribution (3DBSD), which could be used to predict the numbers and sizes of blocks. However, the relative proportion of ranges of block sizes was also estimated from the synthetic 2DBSD, by assuming that the relative frequencies in two dimensions were approximately the same as those in three dimensions. Table 5.2 summarized the relative proportions for blocks within three size ranges provided by the contractor. The largest block encountered by the contractor was greater than 30 m in size.

Table 5.2 Comparison Between Estimated and Actual* Proportions of Blocks in Three Size Ranges

	From synthetic 2DBSD	From Contractor records*	
Size Range (m)	**Proportion of Blocks (%)**	**Volume (m^3)**	**Proportion of all Blocks (%)**
0.6 - 1.2	50	60,000	57
2.4 -10	35	30,000	28
10 - 40	15	15,000	14

(* **Note:** from Michael Hobbs, Superintendent, Ford Construction, Lodi, CA; personal communication)

5.1.7 Summary and Conclusions

The core of the "excavation segments" contained no geotechnically significant blocks, or blocks greater than 1.0 m, the selected block/matrix threshold size. But the proportion and size of blocks encountered during excavation were much greater than anticipated from the exploration drilling. Removal of these blocks or reducing them to grade, required more effort than had originally been anticipated. (But in this case, the extra blocks were welcome since they were used as protective rip-rap at the shoreline toe of the fill). In many cases, the discovery and removal of blocks has potentially expensive "changed conditions" contractual ramifications. The procedure developed during the research reasonably estimated the block volumetric proportion of the melange, the two-dimensional block-size distribution (2DBSD), and the relative proportions of blocks of certain size ranges. Field work and independent statistics from the contractor generally confirmed the estimates, and thus the utility of the methods used.

Since the volumetric proportion of the excavated melange was significantly less than 25 percent, it was geotechnically prudent and justified to assume the rockmass strength to be equal to that of the weak, sheared matrix, at the scale of the landslide. Siltstone appeared to constitute a significant proportion of the blocks in the core and in the field: it should not be assumed by geotechnical engineers that intact siltstone and shale are invariably "weak matrix".

5.3 SCOTT DAM, EEL RIVER AT LAKE PILLSBURY, LAKE COUNTY, CALIFORNIA

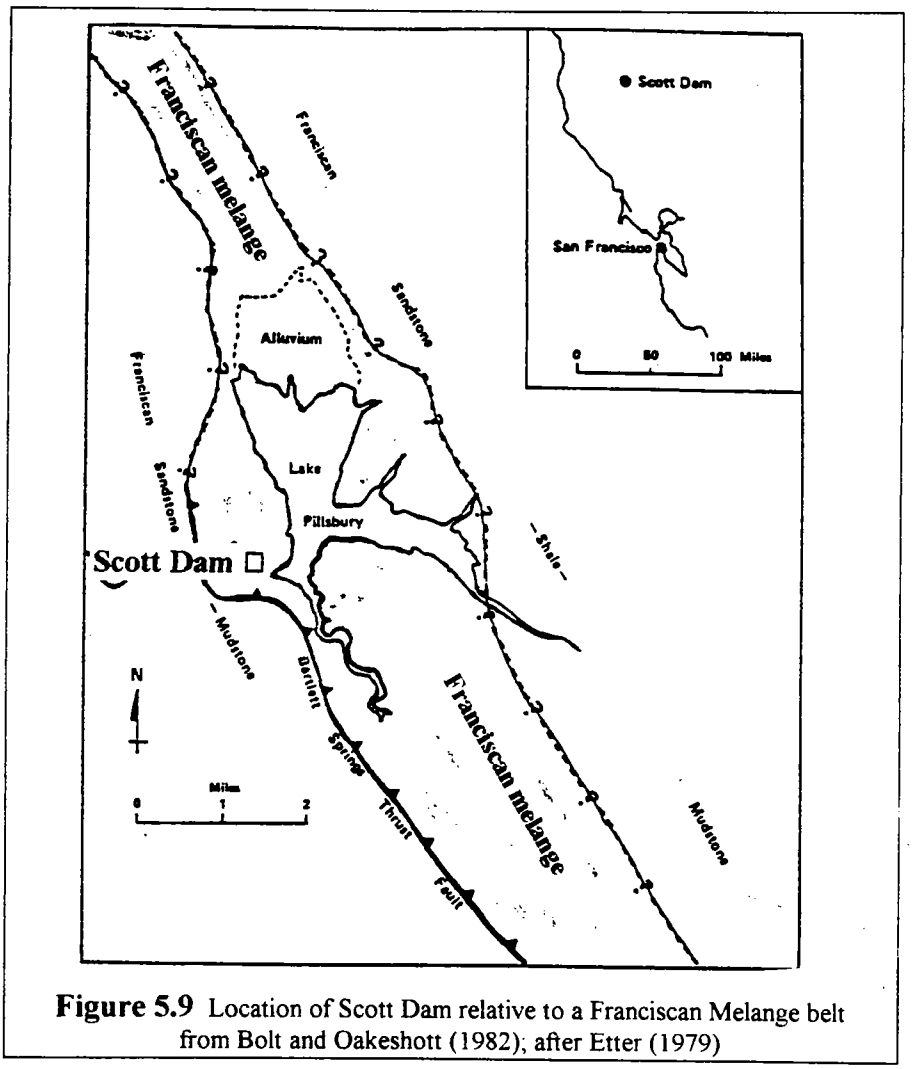

Figure 5.9 Location of Scott Dam relative to a Franciscan Melange belt from Bolt and Oakeshott (1982); after Etter (1979)

5.3.1 Introduction

The initial impetus for the research was given by a geotechnical engineering problem related to Scott Dam, Lake County, California. Scott Dam is a concrete gravity dam on the Eel River, impounding Lake Pillsbury, about 25 miles northeast of Ukiah and approximately 100 miles north of San Francisco (Figure 5.1 and Figure 5.9). The dam, built in the 1920's The dam is about 130 feet high, and up to 150 feet wide, with a footprint as shown in Figure 5.10. Figure 5.11 contains a profile of the dam, and Figure 5.12 shows a typical cross-section (E-E'). The dam was built after many years of

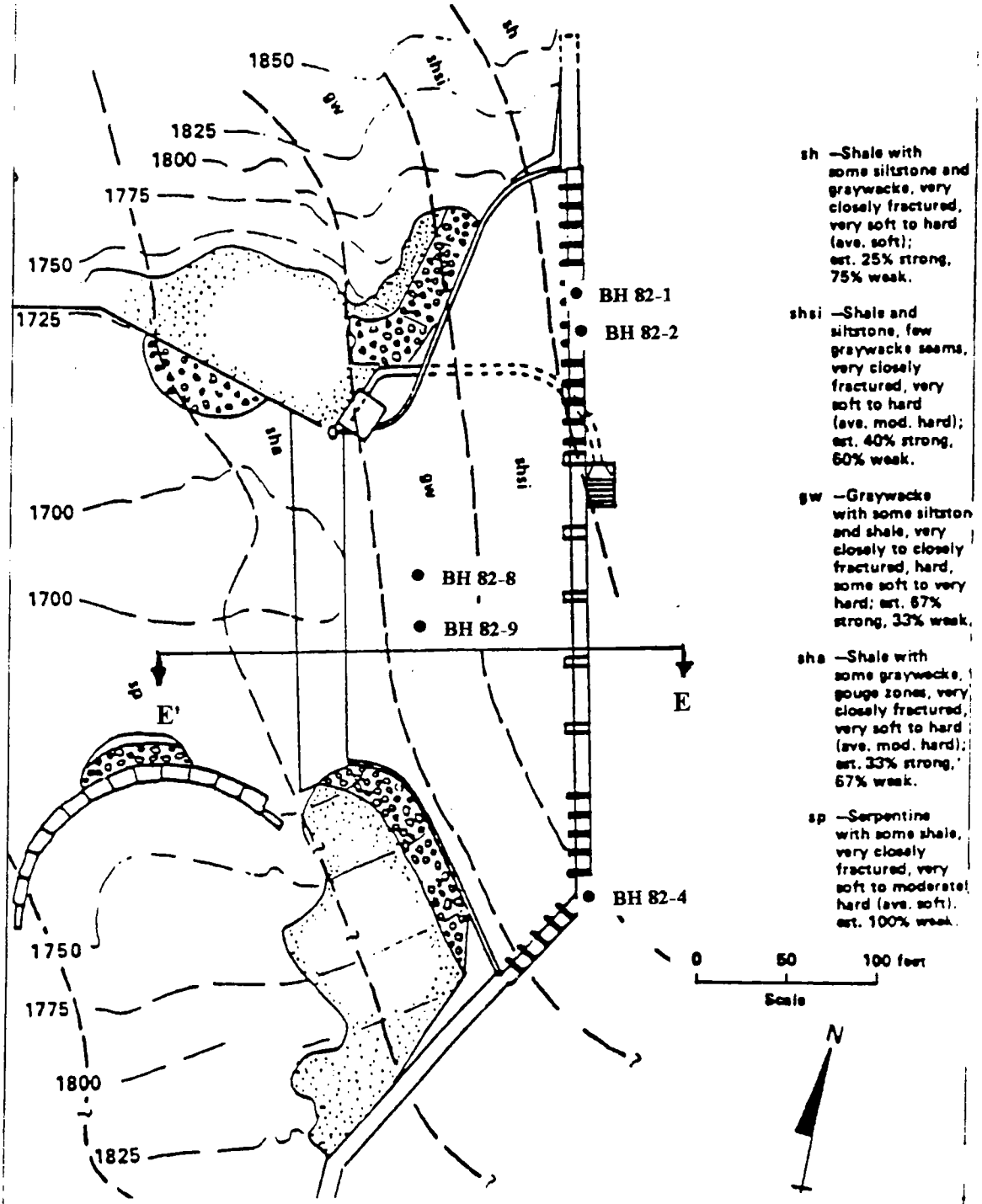

Figure 5.10 Footprint of Scott Dam showing interpreted bands of melange; after Volpe and others, 1991)

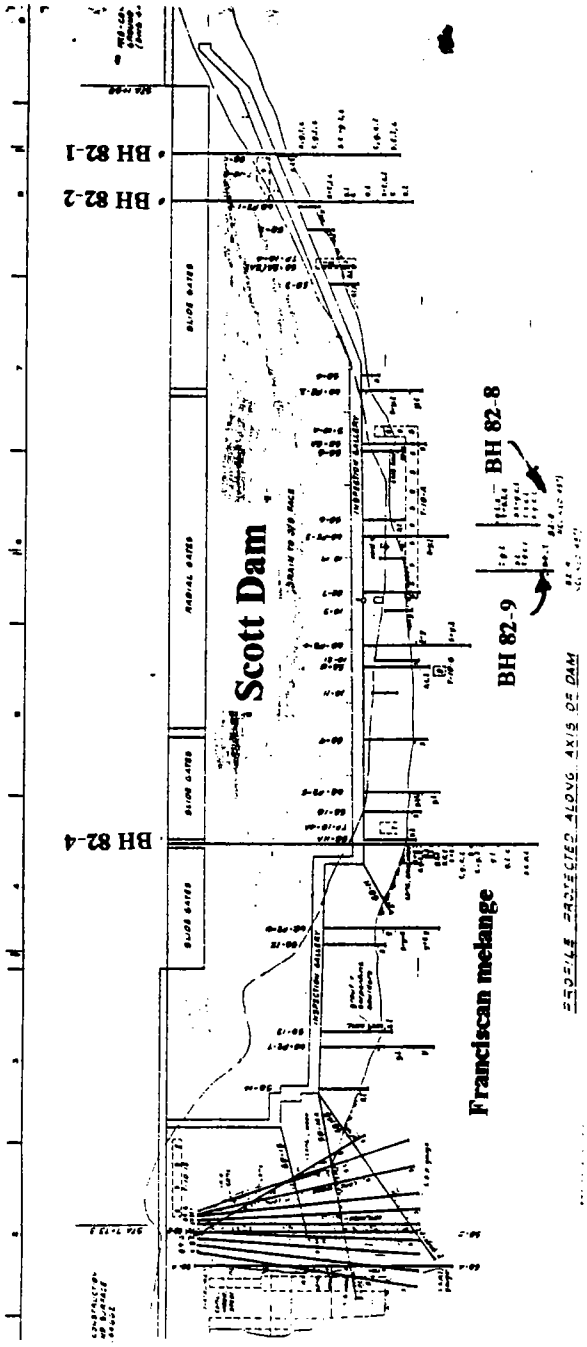

Figure 5.11 Profile Section of Scott Dam looking downstream (west), showing boring locations; from PG&E Drawing No. 521172

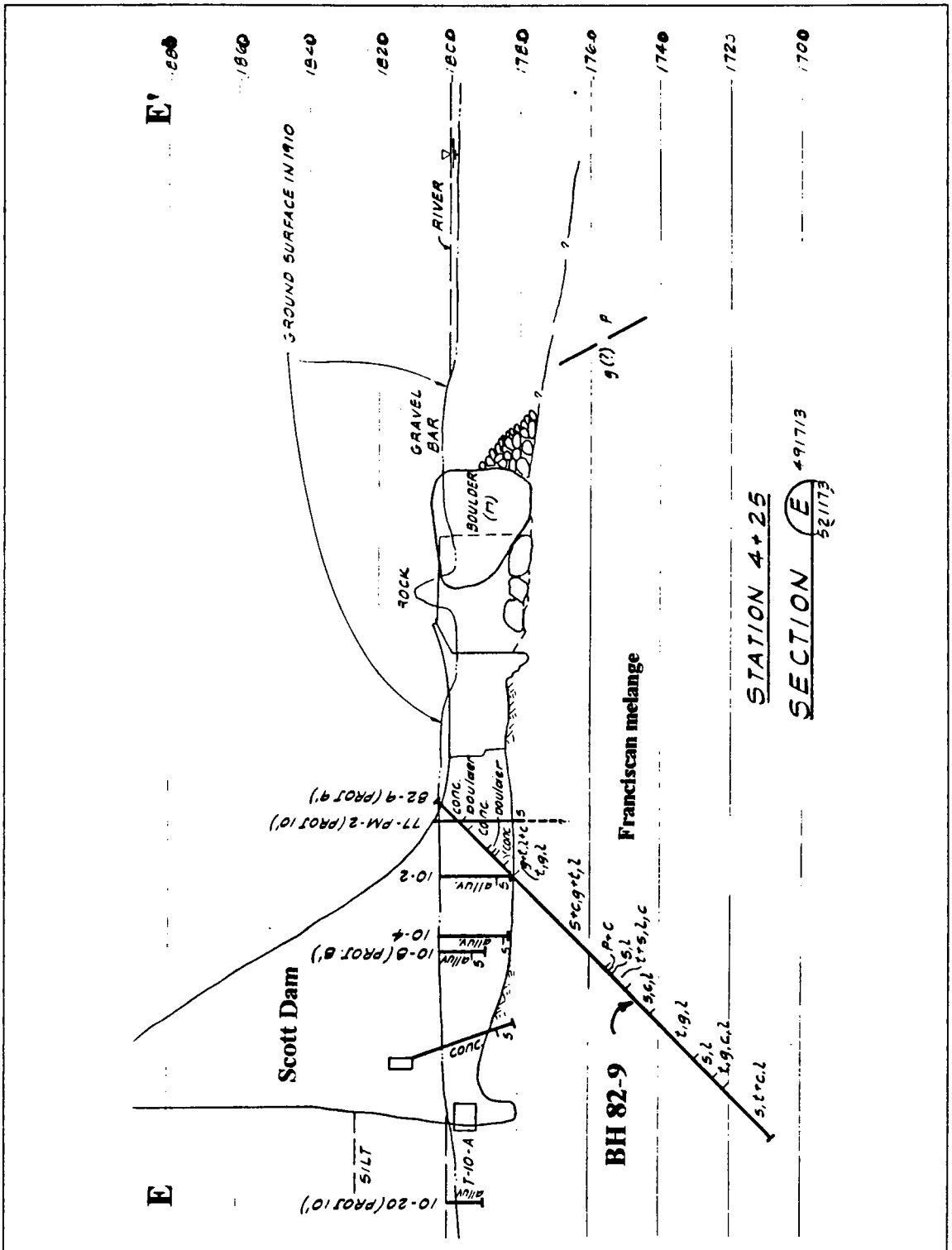

Figure 5.12 Cross-Section EE' through Scott Dam, showing typical lithological symbols on graphical boring logs; (from PG&E Drawing No. 521173)

exploratory tunneling and drilling in what was thought to be a relatively strong shale unit, but what is now known to be a Franciscan melange (Figure 5.9). The current understanding of the geology is summarized in Figure 5.10. It shows what are believed to be bands of steeply dipping melange, striking northwesterly. The bands of melange have been defined on the basis of different proportions of blocks ("strong" rock) within a "weak" matrix.

Considerable work has been performed over the last 25 years to characterize the foundation rock of the dam, which Authorities consider to be in some danger of failing in sliding mode through the presumed weak "shale". But analysis of the sliding stability of the dam performed by the Owner, yielded a Factor of Safety of about 0.7 if the shear strength of the melange matrix was used (the conventional engineering approach). In other words, the dam should have failed, yet the dam has been standing almost 70 years. A constitutive model was devised that accounts for both the strength of the matrix and the blocks, since it was believed that the blocks add strength to the melange matrix, and any failures in the foundation rock would be forced to negotiate the blocks (Volpe and others, 1991). A modification of the constitutive model by Lindquist and Goodman (1994) and Lindquist, (1994b), showed that the overall melange strength is independent of the strength of the blocks, but required that a preliminary assessment be made of the volumetric proportion of blocks under the dam. This Case History describes the work performed to roughly estimate the block volumetric proportion.

5.3.2 Measurement of Photographs of Core

Prior to 1982 , there had been much drilling at the site but no consistent description of the geology ("shale" and "phyllite" being the most common rock described). Some 240 feet (74 m) of core was recovered in 1982, the last time there was any exploration drilling, from 5 boreholes that extended relatively deeply below the dam, to an average depth of 85 m. The borehole locations are shown in Figure 5-10 (prefixed by "BH 82-"). Since the core was inaccessible, the measurements were performed on photographs of the 1982 drill core. Figure 5.13 is a copy of a photograph of the core which shows that some blocks could be discerned easily.

A magnifying glass and a measuring scale were used to measure blocks greater than 1 cm to 2 cm (true dimensions) from the photographs. The rationale for measuring such small blocks was that the top 3 m of melange below the dam was assumed to be most critical relative to the shearing resistance of the foundation, and was thus a characteristic engineering dimension. Alternative characteristic engineering dimensions could have been the dam width (50 m) or the dam height (40 m). A conservative 1 percent d_{max} criterion was used to establish a block/matrix threshold size; although elsewhere in this dissertation, 5 percent is considered adequate. The 3 m characteristic engineering dimension was substituted for d_{max} (see Section 2.6), to yield a block/matrix threshold size of 3 cm..

Figure 5.13 Photograph of drill core from a Franciscan melange below Scott Dam. The white blocks are probably graywacke, which contrast markedly with the dark shale matrix.

5.3.3 Estimation of Block Volumetric Proportion

Based on the photographs, the measurements indicated that there was an average of 41 percent cumulative lineal proportion for the average borehole depth of 85 feet, but this dropped to 36 percent for the top 20 feet of bedrock, and 33 percent for the top 10 feet. These estimates are on the basis of the 1982 borings only, and are for all blocks greater than about 3 cm. If a longer characteristic engineering dimension is chosen, such as the width of the dam (50m), and the more usual 0.05 d_{max} criterion used, the block/matrix threshold size becomes 1.5 m. In that case, using only the 1982 core measurement data, the cumulative block linear proportions for various depths drops to zero for depths up to about 50 feet below the dam, and then increases to about 15 percent at greater than 70 feet (21 m) feet below the dam.

The graphical logs on several cross-sections of the dam, indicated that there are probably some significantly sized blocks in the melange. For instance, a greenstone block of greater than 140 feet (40 m) in size has been much explored, as shown by the congregation of boreholes at the left abutment in Figure 5.11. Nearly all the pre-1982 borings show lithological symbols, such as "S" (for "shale"): any additional data regarding the block content of these shales, will result in some advantage, since even the "pure" shale has small blocks. Consequently, an attempt was made to include the pre-1982 data, in order to estimate a more representative block volumetric proportion for the

melange below the dam. This was done by correlating the detailed geological logs of the 1982 core, with their lithological symbols, to the block measurements from the photographs. A compilation was prepared of the various descriptors for several rock types within the melange, as shown in Table 5.3.

Table 5.3 Compilation of lithological descriptors and associated linear block proportions*

lithology group	symbol	Avg. block linear prone. (%)	Assigned Block Propn. (%)
graywacke (g,..)	g+t,l+c; g,l; g,l,c	**88**	**100**
siltstone (t..);	t; t,l,c; g,s,l; g+s;	**100**	**100**
siltstone/graywacke and graywacke-rich	t+c,g+l,c; t,g,c; ..	**68**	**66**
siltstone/shale	t+s; t,s,l,c; t,s; ...	**46**	**33**
shale/graywacke/siltsone	s,t: s,g; s+t; s+g; s,t,g; y+g; ...	**28**	**25**
shale (includes "phyllite")	s..; s+y; y; s,l; s,l,s; s,c,t; ...	**8**	**10**
clay	c	**0**	**0**
serpentinite	p; p+c	**0**	**0**

* **Note**: compilation is based on measurements of photographs of core from boreholes 82-1, 82-4, 82-8 and 82-9 at Scott Dam

Since the graphical logs of pre-1982 borings show a wide variety of lithological symbols, the chart appeared useful in assigning block proportions to sections of pre-1982 boring logs with the symbols or combinations of symbols. Accordingly, the graphical logs of approximately 960 feet (290 m) pre -1982 borings were measured from several cross-sections, similar to the portion shown in Figure 5.12. The data were entered into a spreadsheet, and section of graphical logs with different lithological symbols were assigned the presumed block proportions shown in the last column of Table 5.3. The cumulative linear proportion for all data was about 33 percent. This result did not include any contribution from the massive greenstone block below the left abutment.

Different block proportions could be assigned to the lithological symbols so that fast "what-if?" analyses were possible with the spreadsheet. It is recognized that this is a preliminary approach only: firm, confident assessment of the block volumetric proportion of the melange below the dam will require careful scrutiny of the original boring logs and core, if still available.

5.3.4 Conclusions

The determination of the block linear proportion depended on the choice of the block/matrix threshold. In this case, the characteristic engineering dimension was not known, and the threshold was chosen to be 1 percent of an assumed critical 3 m thickness of rock below the dam. The block linear proportion was estimated on the basis of limited data, although the measurement of the blocks from photographs of core was considerably easier than handling real core. Good geological boring logs made this procedure an acceptable alternative to measuring real core. The refinement of the preliminary estimates of block proportions given here would require scrutiny of previous drilling records, and re-interpretation of the geological logs into terms of the blocks and matrix of Franciscan melange. Additional information would also allow some estimate to be made of the block size distribution.

5.4 STORAGE TUNNEL PORTION OF THE RICHMOND TRANSPORT PROJECT, SAN FRANCISCO, CALIFORNIA

5.4.1 Introduction

Currently under construction (July, 1994), the Richmond Transport Project (RTP) will be a system of underground storm water storage tunnels and conduits designed to accommodate storm water flows. The location of the system is shown in Figure 5.1 and Figure 5.14. This case history is a demonstration of the use of the techniques developed during the research to estimate the block volumetric proportion and block size distribution of a Franciscan melange. The results developed by measuring blocks in, the RTP drill core cannot be verified until construction is completed.

The following project description is summarized from WCC (1993a,b). The principal component of the project is a 10, 233 foot (3120 m) long Storage Tunnel which will be excavated between Lobos Creek (East Portal) and near the Cliff House (West Portal), as shown in Figure 5.15. The tunnel will be excavated by a Tunnel Boring machine (TBM) to approximately 19 feet diameter (5.8 m), and will have a concrete-lined finished diameter of about 14 feet (4.3 m). Some 9000 feet (2740 m) at the western end of the tunnel will be excavated in rock of the Franciscan, with the remainder being excavated in soil/rock (mixed-face) and soil. Cover above the tunnel roof ranges between about 30 feet (9.2 m) and 330 feet (100 m). The Storage Tunnel will be connected by some 500 feet (150 m) of separate Overflow Tunnels and an Overflow Chamber to the existing, but abandoned, Mile Rock Tunnel, the seaward portion of which will be rehabilitated as an outfall (Figure 5.15).

5.4.2 Summary of Geology in the Area of the Storage Tunnel

As shown in Figure 5.15, it is anticipated that the RTP Storage tunnel will traverse three zones of Franciscan bedrock types, which have been discriminated in various ways by various workers (WCC, 1993a,b; Dames & Moore, 1979b; Schlocker, 1974; and Blake and others, 1984). The zones are referred to here as the western, central and eastern zones. The approximate boundaries of the three zones, which are roughly based on the references cited, are shown on Figure 5.15. Pertinent features of the zones are :

1. The **western zone** will be traversed by Segment I of the Storage Tunnel (Sta. 0+00 to Sta. 14+00, 425 m: WCC, 1993a; p. 6-2) The zone has large coastal exposures of interbedded sandstone/shale turbidites, that have been correlated with the turbidite series of San Bruno Mountain to the southeast and Bolinas Ridge (Marin County) to the north, and identified as part of the San Bruno Mountain Terrane (Blake and others, 1984; see also Figure 2.7 and text of Section 2.1.3.2 in Chapter 2). During the geotechnical

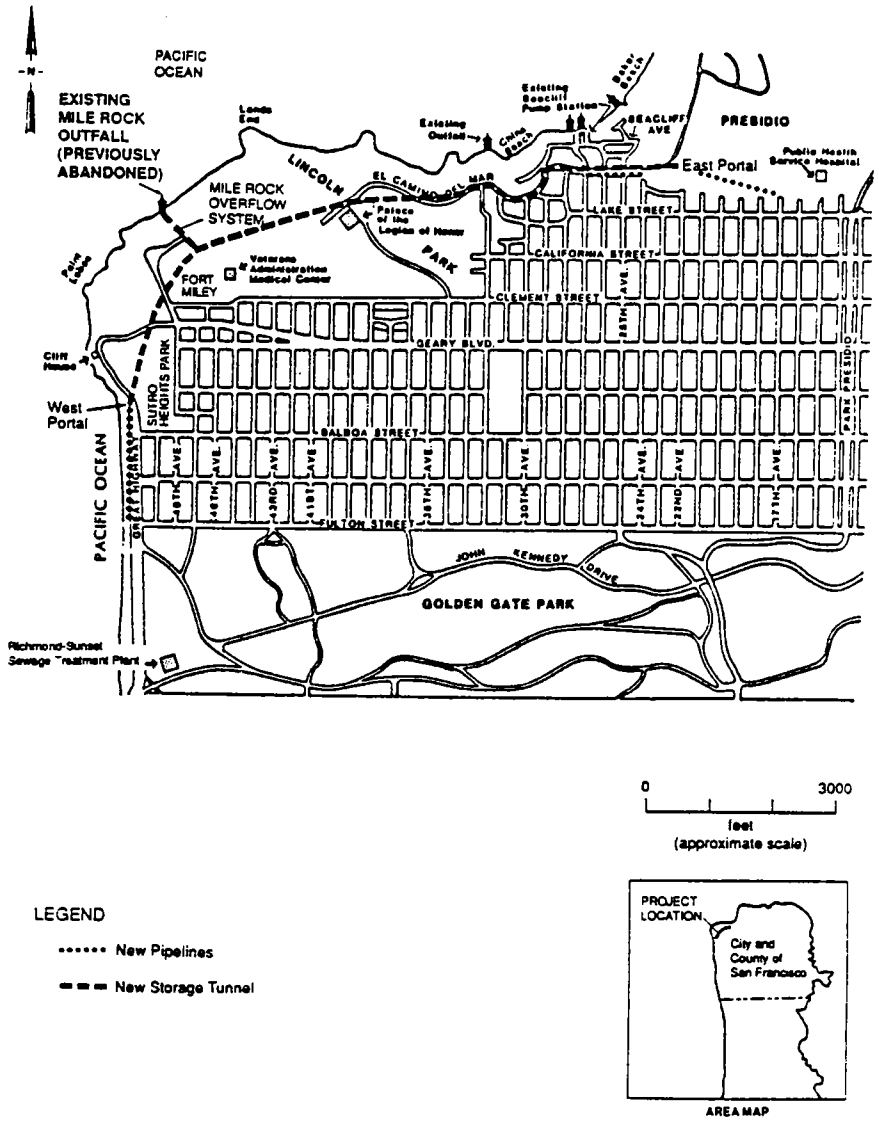

Figure 5.14: Location of Richmond Transport Project, San Francisco, California; from WCC, 1993a, figure 1)

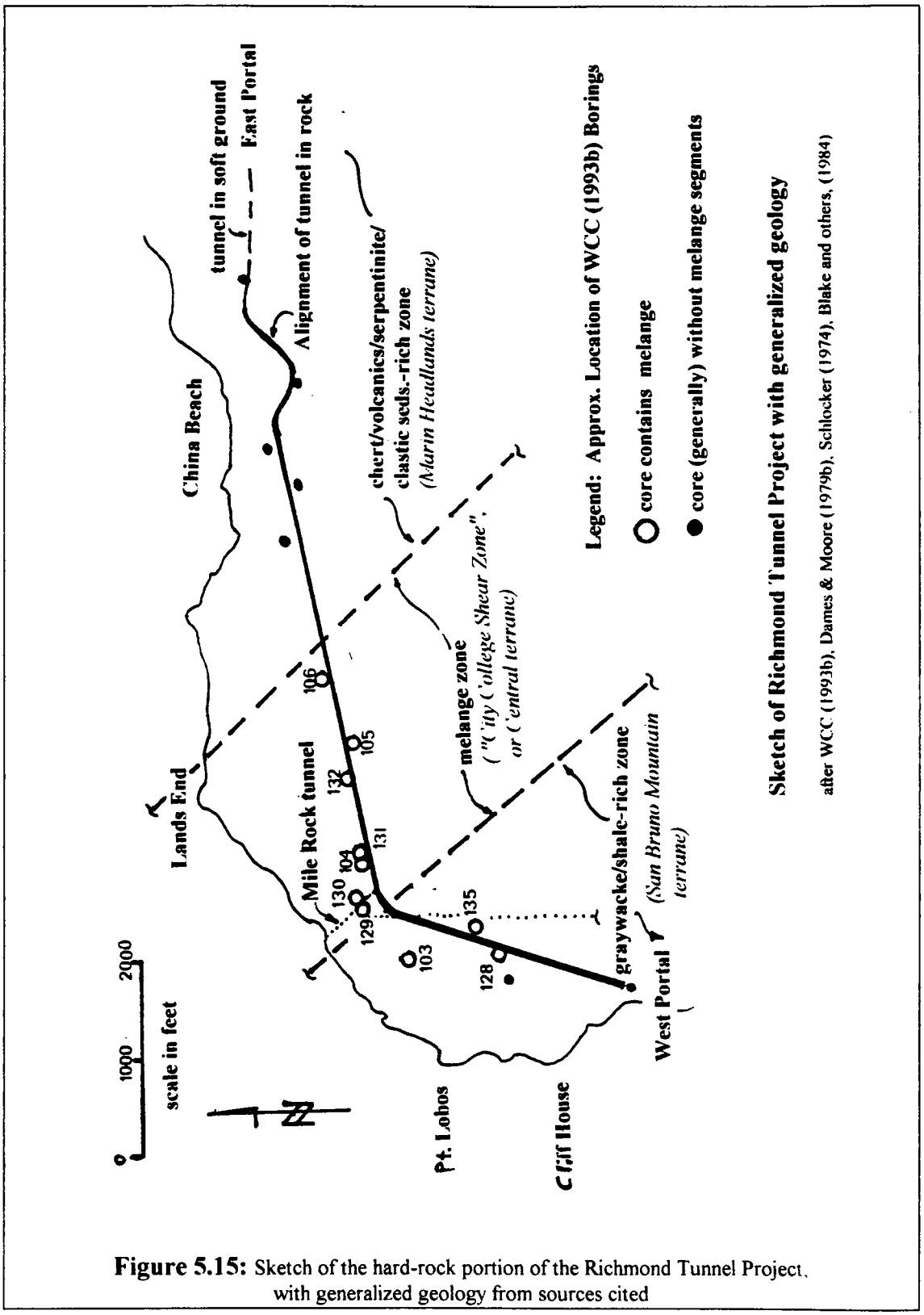

Figure 5.15: Sketch of the hard-rock portion of the Richmond Tunnel Project, with generalized geology from sources cited

exploration program for the RTP, three boreholes within the western zone penetrated melange (Borings 103, 128 and 135: see Figure 5.15)

2. The **central zone** will be traversed by Segment II of the Storage Tunnel (Sta. 14+00 to Sta. 53+00: 1190 m; WCC, 1993a, p. 6-3) The zone is a belt of Franciscan melange, estimated to be approximately 3900 feet wide (1190 m), but 1070 m wide at tunnel grade (WCC, 1993b, p. 3-15). Several boreholes intercepted melange within this zone as shown in Figure 5.15. The melange is composed of pervasively sheared shale studded with blocks of various sizes and lithology. The zone as shown in Figure 5.15 approximates what has previously been identified as the City College Fault (Bonilla, 1961), the City College Shear Zone (Schlocker, 1974), the City College Fault (?) - Melange Zone (Dames & Moore, 1979b), and the Central Terrane (Blake and others, 1984). The City College shear zone was geotechnically explored for the once-proposed Crosstown Transport Facility tunnel (Gonzales and Dunne, 1983), and found to be difficult to characterize, because of the considerable variation in subsurface geology.

3. The **eastern zone** will be traversed by Segment III of the Storage Tunnel (Sta. 53+00 to 89+50: 1110 m; WCC, 1993b, p. 6-4). The zone has extensive sandstone and shale sequences exposed along the coast, which are interrupted by serpentinite, chert, and greenstone blocks. Inland, outcrops of these diverse lithologies have been found within the zone (WCC, 1994b, figure 3: Geology Map). . Dames and Moore (1979), identified melange in their Boring 13, which was located close to the alignment of the RTP in the eastern zone. Blake and others (1994) considered the area of the eastern zone to be part of the Marin Headlands Terrane, composed of chunks of a volcanic arc ophiolite that is widely dispersed within the Central terrane melange (Blake and others, 1994; Murchie and Jones, 1984; Wahrhaftig, 1984b; and see Section 2.1.3.2 and Figure 2.8).

5.4.3 Measurement of Drill Core

During the geotechnical exploration for the bedrock portion of the RTP some 2945 feet (900 m) of rock was drilled, and 740 m of core was recovered. The core was measured for research purposes, in order to estimate the volumetric proportion of blocks in the Franciscan melange and determine the chord length distribution of the blocks intercepted by the drill core. Access to the core was arranged by the San Francisco Dept. of Public Works, and Woodward Clyde Consultants, the geotechnical consultants.

Initially, no determination of the block/matrix threshold size was made, and all blocks greater than about 5 cm were measured. The intercept lengths of blocks were measured and the lithology of the blocks recorded in the manner described in Section 2.11. Although all the available core was reviewed and measured, particular attention was paid to the 645 m of core from 10 boreholes (shown as open circles on Figure 5.15) which showed a chaotic fabric in the shale matrix, and which had penetrated what was described in the boring logs as "melange", "shale/siltstone breccias" and "shale breccias".

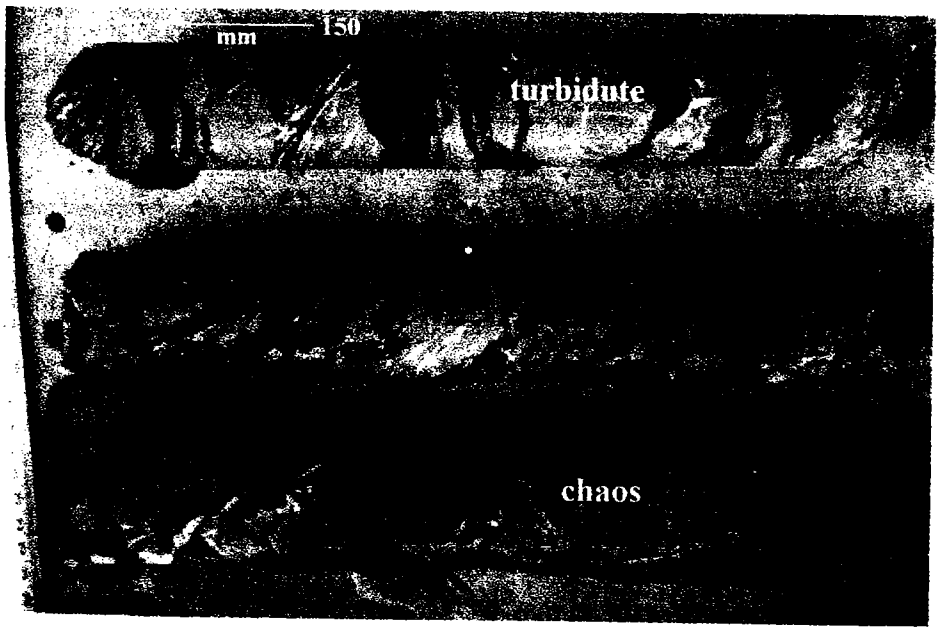

Figure 5.16 Sections of core from geotechnical exploration performed for Richmond Transport Project; Boring B-130 at 147 feet. Top segment of core is coherent turbidite sequence, but core shows rock fabric becoming chaotic within a few feet (bottom segment).

Not all segments of graywacke were "blocks", nor all shale "matrix". Some sections of alternating (interbedded) sandstone and shale sequences may have been chunks of relatively coherent turbidites within the melange. The melange matrix shales were discriminated from the turbidite shales by the presence of a chaotic fabric surrounding "mini-blocks" which were often less than a centimeter long. Figure 5.16 shows three pieces of core grading from relatively coherent (top) to chaotic (bottom) over the space of a few feet.

The 10 "melange" borings, averaged 65 m in depth. A total of 508 blocks were measured, with chord lengths ranging in size between 42 m and 3 cm. Of these, 139 were longer than 0.25 m (approximately 0.3 m, the threshold size), ranged to 28.0 m long, with a mean chord length of 1.8 m, and a standard deviation of 4.0 m. Figure 5.17 shows the relative proportions of blocks with chords greater than 0.25 m for each borehole. The block proportions in the individual boreholes varied between 13 percent and 70 percent.

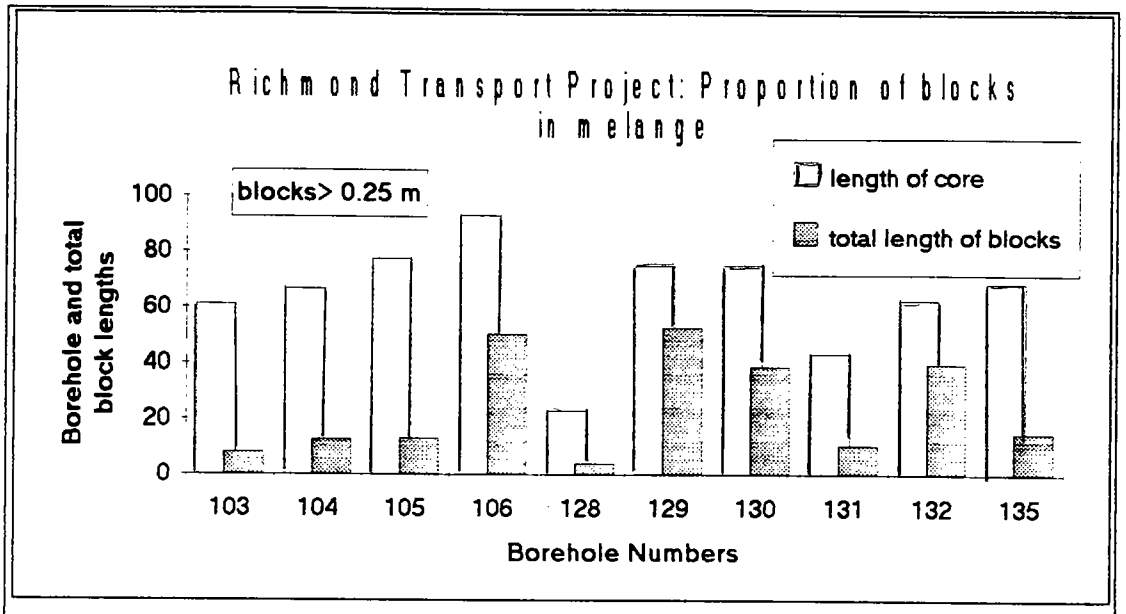

Figure 5.17: Proportion of blocks in boreholes penetrating melange

The proportions of blocks classified by lithology generally matched the relative proportions shown previously (Section 3.7, Section 5.1). Figure 5.18 shows the proportions computed on the basis of the proportion of total chord lengths for each lithology relative to the total length of all chords through blocks.

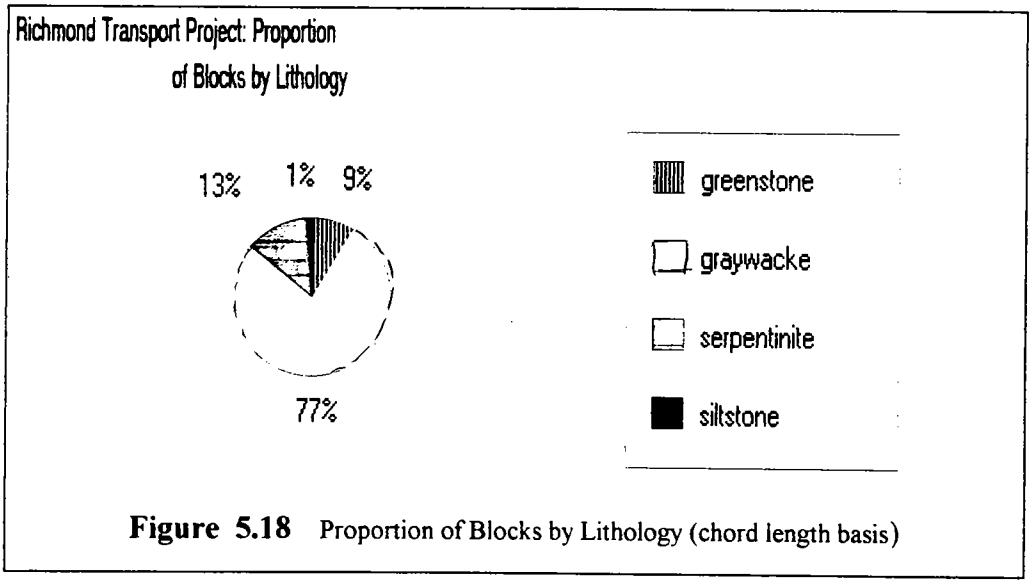

Figure 5.18 Proportion of Blocks by Lithology (chord length basis)

5.4.4 Estimation of Block Linear Proportion

For a tunnel, with a length considerably greater than its diameter, the block linear proportion is probably more appropriate than the block volumetric proportion, although they have been assumed to be equivalent for the research. The block linear proportion was estimated in the same way as previously shown (Section 2.8.3 and Section 5.1).

Accumulating the individual proportion data for each borehole yielded a cumulative block linear proportion of 38 percent as shown in Figure 5.19. The accumulation used two series of summations, in the manner described in Section 2.8.3. The effective block linear proportion is about 40 percent, achieved in approximately 60 percent of the total core length of 645 m, or about 390 m. Since the largest chord in the "melange core" was 28 m, the ratio of the effective proportion of total cord length, to the length of the maximum chord, was about 14. This ratio is within the range determined from scanline work with the Triaxial Test Tracings (Section 4.3.3.2). Dames & Moore (1979b, p. 18) estimated that 60 percent of one broad part of the central zone melange was composed of "tectonic inclusions" or blocks, and surmised that the proportion may be as high as 75 percent to 80 percent.

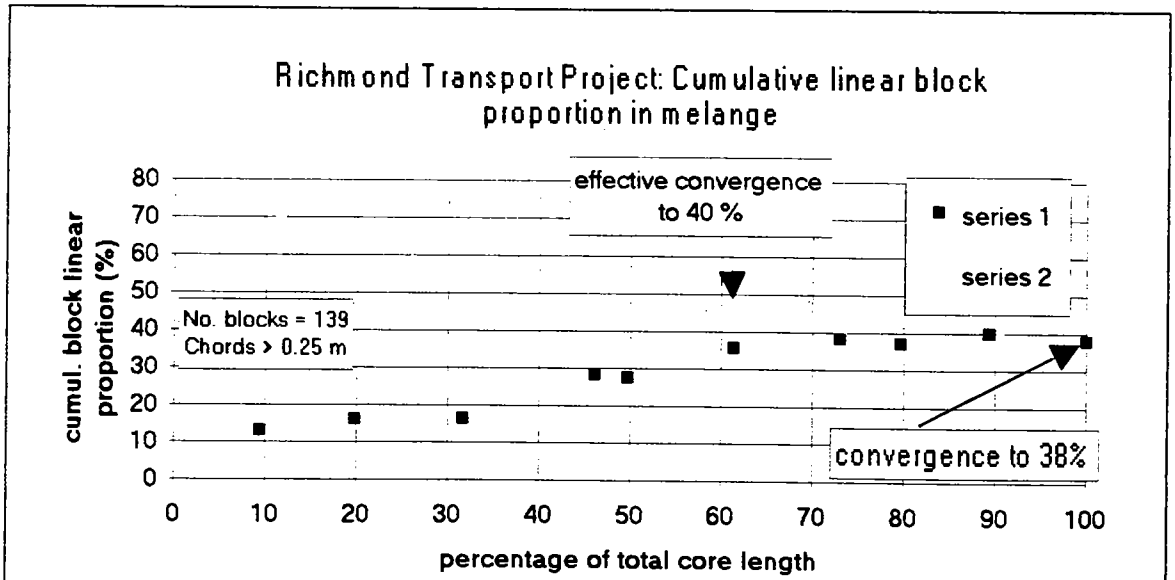

Figure 5.19 Estimate of cumulative block linear proportion for core from boreholes in melange

5.4.5 Estimation of Theoretical Maximum Block Sizes and Block Size Distribution

An attempt was made to estimate d_{max} , the size of the largest block that may be present in the neighborhood of the RTP tunnel. The dimension of the largest block within an area underlain by Franciscan melange is approximately $\mathbf{d_{max}} = \sqrt{\mathbf{A}}$, where A is the area

measured (see Section 2.5). For the RTP study, the measurement area was determined to be the region between the coastline and approximately Segment II, the portion of the Storage Tunnel alignment within the melange of the central zone. The coastline was chosen as a boundary since the geology had been mapped along the shore (WCC, 1993b, figure 3), and the majority of the exploration boreholes had been drilled close to the RTP alignment or the Overflow Tunnels. Using the $\sqrt{A}$ criterion, the d_{max} for the selected area is 1935 feet (590 m). This is a theoretical size and there is no certainty that blocks this large exist along the tunnel alignment, or even within the mapped area.

It has been empirically demonstrated (Figure 2.8), that the most abundant size of blocks (d_{peak}) in an area of Franciscan melange is $0.04\sqrt{A}$. For the selected area of Franciscan bedrock in the locale of the RTP tunnel, d_{peak} is approximately 80 feet (24 m). The estimate is useful as a guide to the approximate size of the most frequent larger blocks that may be encountered, at the scale of the mapped area north of the StorageTunnel alignment. Again, there is no certainty that this size will be frequently encountered during excavation. But, the scale independence of Franciscan melanges (Section 2.5) suggests that at the scale of the excavated diameter of the tunnel (19 feet; 5.8 m), the most abundant size of blocks will be considerably smaller.

Because of the difference in scales between the whole RTP area, and the area of a tunnel face, it was not possible to use d_{peak} , as estimated from the site area, as a "node" around which block size frequency classes could be expanded (Section 2.4.3). Instead, a log-histogram was generated from the block lengths as measured from the 10 boreholes which penetrated melange (Section 2.4.3). The node class, around which the remaining end-classes were expanded, was defined as 5 percent of the 6 m diameter of the tunnel, which was chosen as a characteristic engineering dimension (Section 2.6.3) Hence 0.3 m, was the block/matrix threshold size at the scale of the tunnel diameter. Each successive class was twice the value of the previous class, in the fashion described in Section 2.4.3. The resulting log-histogram (Figure 5.20) is a block chord length distribution (CLD) of the melange relative to the scale of the tunnel. All block chords were counted including those smaller than 0.5 m.

As shown in Figure 5.20, the CLD has descent limb slope, **D**, of approximately 1.0. If it is assumed that the melange has steeply dipping blocks typical of Franciscan melanges, then the work performed on the Triaxial Specimens suggests, for a melange with approximately 40 percent block proportion, that the parent two-dimensional block size distribution (2DBSD) is approximately the same as the CLD (Section 4.5; Figure 4.11). For the two-dimensional face of the RTP tunnel, it is thus appropriate to use the CLD/2DBSD of Figure 5.20.

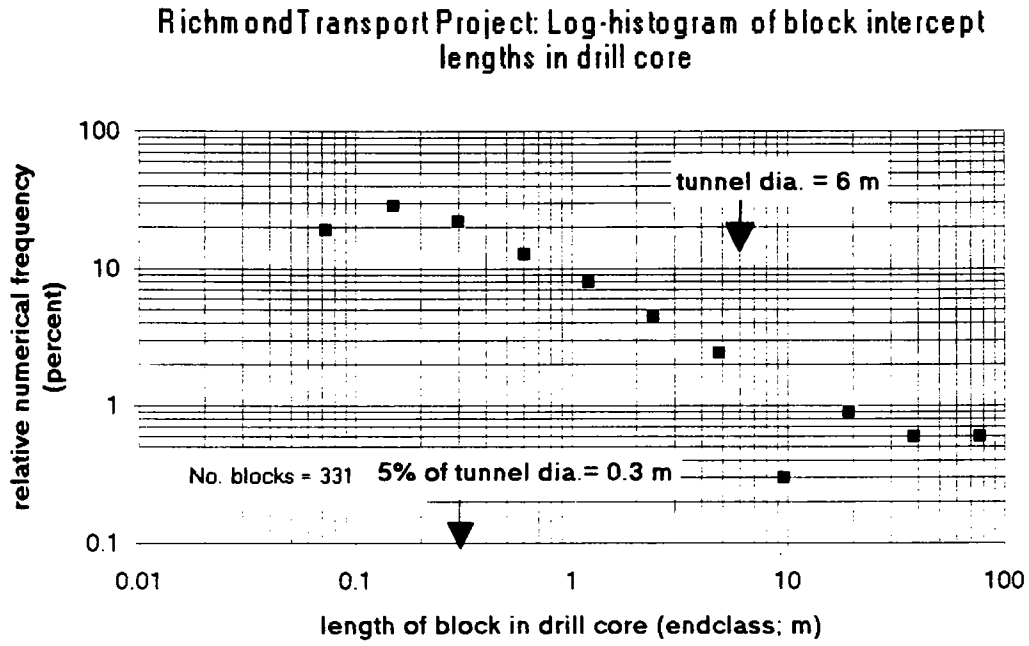

Figure 5.20 Log-histogram form of a chord length distribution (CLD) of block lengths in core from boreholes that penetrated melange. The CLD approximates a two-dimensional block size distribution (2DBSD) and is scaled to the RTP tunnel diameter. The slope of the descent limb is approximately **D**=1.0.

The log-histogram in Figure 5.20 has a d_{peak} of approximately 0.15 m (6 inches) with a peak relative frequency of 30 percent. The next two largest classes, 0.3 m (1 foot) and 0.6 m (2 feet) together comprise 33 percent relative frequency. The maximum block size, at the scale of the tunnel, is approximately 40 m to 80 m long. However, as indicated above, at the scale of the map, or length of Segment II of the Storage Tunnel, much longer blocks could be encountered.

5.4.6 Summary and Conclusions

Based on the measurements of the lengths of blocks measured in the core several estimates have been made. Based on the empirical relation $d_{max} = \sqrt{A}$, where A is the area of measurement, the longest block may be approximately 600 m at the scale of the length the Storage Tunnel. At the same scale, the most prevalent sizes of block may be between 33 m and 24 m. And, at the scale of the diameter of the excavated Storage Tunnel, approximately one-third of the blocks encountered in a tunnel face in the melange could be in the size range of 0.3 m to 0.6 m. The cumulative block linear proportion of blocks (greater than about 0.3 m) within the melange penetrated by the exploration borings is approximately 38 percent. Some 80 percent of the blocks may be

graywacke sandstone; an additional 13 percent may be serpentinite blocks, and the remainder chert, volcanic and exotic metamorphic blocks. The lithologies of the blocks have mechanical implications which have not been considered in this case history, but are addressed by WCC (1993a,b, c) and Dames & Moore (1979b).

CHAPTER 6: SUMMARY, CONCLUSIONS and SUGGESTIONS FOR FURTHER RESEARCH

6.1 SUMMARY OF WORK PERFORMED

The work performed for this dissertation included:

1. Development of a relatively comprehensive database of the geological literature of melanges, preparation of maps showing the worldwide distribution of melanges, and over 180 requests sent to US and international engineers and geologists for their experience and literature pertaining to melanges. There were over 70 responses.

2. Adaptation of image analysis techniques, commonly used in the biological sciences, to measure the areas and characteristic dimensions of blocks from photographs of melanges, arrays of gravel strewn on white boards, and tracings of blocks expressed on the the cicumferential surfaces of triaxial specimens of model melange fabricated by Lindquist (1994b).

3. Measurement of block properties in two-dimensions and in one-dimension, and use of the principals of *stereology* to prove that such measurements can reasonably estimate the volumetric proportion of blocks in a block-in-matrix mass, and approximate the block size distribution.

4. Demonstration of the scale-independence of some Franciscan melanges over 7 orders of magnitude of area, and identification of several simple parameters useful for describing the block size distributions.

5. Field observations of block and matrix properties of some Franciscan melanges.

6. An attempt to relate the block proportion of several Franciscan melanges to hillslope angles.

7. Development of procedures to estimate the block volumetric proportion of melanges by measuring block chord lengths in drill core; estimation of block size distributions; and approximate methods to estimate the number and volumes of large blocks for construction purposes.

8. Demonstration of the applicability of techniques developed by the research to case histories of a landslide, a dam foundation and a tunnel.

6.2 SUMMARY OF FINDINGS and CONCLUSIONS

The following are summaries of the principal findings of the research:

1. There is very little geotechnical literature related to melanges or other block-in-matrix rocks, despite a rich geological literature and the engineering problems related to melanges world-wide; except for the contributions of Italian geotechnical engineers working with *argille scagliose.* The melanges studied in California were part of the Franciscan Complex, commonly referred to as *the Franciscan.*

2. Melanges are part of a family of geological materials defined as *bimrocks* (block-in-matrix rocks) a non-genetic term that can be used for many rocks, and defined as:

a mixture of rocks, composed of geotechnically significant blocks, within a bonded matrix of finer texture.

The geotechnically significant blocks in a bimrock satisfy the following criteria:

a) There is a significant mechanical contrast between the blocks and the matrix, measured as a ratio between friction angles, stiffness, or other properties .

b) There is a significant ratio between the limiting sizes of the blocks and the *characteristic engineering dimension.* The characteristic engineering dimension is some length that describes the engineering rock mass, such as footing width, tunnel diameter, or laboratory specimen diameter; and its selection is a matter of geotechnical engineering judgment. The upper limit for blocks is 75 percent of the characteristic engineering dimension: above that the block is *blocky rock.* The lower limit is 5 percent of the characteristic engineering dimension. The size of the largest likely block to be encountered in the rock mass may be substituted for the characteristic engineering dimension.

c) The volumetric proportion of the blocks is between 25 percent and 75 percent; above 75 percent the rock mass is *blocky rock.*

Rock mass that is matrix at the scale of one characteristic engineering dimension, may be bimrock at a larger scale.

3. The block size distributions of some Franciscan melanges at a particular scale can be plotted as *log-histograms*, which are block size frequency histograms plotted against logarithmic axes. Melange block size distributions invariably plotted as hyperbolas on log-histograms. The right limb, or *descent limb*, was generally linear with a slope (termed the fractal dimension, **D**), of between 1.0 and 1.6. Several log-histograms were collapsed into one by normalizing all block size data by $\sqrt{\mathbf{A}}$, the square root of the areas bounding the blocks, which varied between 0.04 m^2 and 1000 km^2. The resulting well-defined constellation, was similar the contributory log-histograms. The exercise sucessfully demonstrated the *scale-independence* of some Franciscan melanges. In other words, no matter at what scale one looks at a melange, it will always appear similar, at least within the range of engineering scales (10s to 100s of meters). The scale-

independence of melanges allowed much useful work to be performed using photographs of melange at outcrop scales, or *graphic models*.

4. The scale-independence plot referred to in **3)**, above, showed that the descent limb of the block size distribution of a melange could be characterized by:

- **a)** $\mathbf{d_{max}}$ which is the maximum block expected at some scale of measurement, and is approximately equal to $\sqrt{\mathbf{A}}$.
- **b) D,** the fractal dimension, is generally between 1.0 and 1.6 for blocks measured from plans and other two-dimensional representations.
- **c)** $\mathbf{d_{peak}}$, the block size at the block/matrix threshold, equal to $\mathbf{0.04\sqrt{A}}$, or substituting $d_{max} = \sqrt{A}$ from **a)** above, $\mathbf{d_{peak} = 0.04\sqrt{A}}$
- **d)** 99 percent of all blocks are less than 70 percent of the size of the largest block, d_{max}

5. *Scanlines*, or measurement traverses, were used to estimate block volumetric proportions and the block size distribution. Scanlines modeled drilled core obtained from geotechnical exploration boreholes. Graphic models were created by constructing *Gravel Tests* setups, arrays of gravel and sand of different areal coverage. And, tracings were made of the surfaces of 150 mm diameter *Triaxial Specimens* of model melanges, fabricated by Lindquist (1994b), with known volumetric proportions, block shapes, block orientations and blocks size distributions. Scanlines were used to measure block characteristics from these graphic models. The successful use of the scanlines depended on *image analysis* and *stereology*. Using image analysis techniques, computer software measured information from photographs. Stereology principals were used, in which one- and two-dimensional measurements predicted three-dimensional properties. It was discovered that a total length of scanlines greater than 10 times the length of the largest block provided a sufficient number of chord lengths through blocks so as to both estimate the volumetric proportion well and to roughly approximate the block size distributions.

6. Relatively simple techniques were devised to tranform distributions of chord lengths through blocks (measured from scanlines) into approximate two-dimensional and three-dimensional distributions. For self-similar three-dimensional size distributions, the fractal dimension is equal to the fractal dimension of the two-dimensional distribution plus 1.0. The descent limb of the former was assumed to hinge at the dimension of the mutually largest block. A tentative procedure was devised to predict the volume of the desired ranges of blocks sizes, starting with relatively little information. The procedure may have practical application for predicting block sizes in excavations where some forewarning may save time and money.

7. Studies with the graphical models showed that the fractal dimension of two-dimensional blocks size distributions were relatively insensitive to the block volumetric

proportion and block size distributions, and tended to cluster about one value, equivalent to the three dimensional fractal dimension, less 1.0. But the fractal dimension of chord length distributions were much more variable, tending toward the three-dimension fractal dimension when blocks were oriented at large angles relative to the scanlines or if block volumetric proportion was low. In other words, the worse the situation from a geometric probability standpoint, the closer the data approached the required three dimensional block size distribution. This was a surprising, fortuitous, and useful result.

8. Field measurements showed that melange blocks are generally ellipsoidal. Shears pass around blocks tortuously, and it is not unreasonable to believe that future deformations will be accommodated by these defects. Since the volumetric proportion and block size distribution influenced the original failures, it is important to estimate them in order to assess future stability. Much attention should be paid to the nature of the block/matrix contact which in Franciscan melanges may be thin but weak. Since it is likely that any the future deformation will occur along the existing boundaries of blocks, an understanding of the integrity of the contacts is of critical importance to geotechnical design.

9. The lithology of melange blocks is relatively consistent. Graywacke constitutes between generally 65 percent and 75 percent of the blocks, the remainder of the blocks vary between volvanics, chert and high-grade metamorphics.Although the strength of blocks is not particularly important when considering the overall strength of a bimrock (Lindquist, 1994b), the mechanical properties are of paramount importance to earthwork contractors and tunnelers. Siltstone matrix masses may be considered blocks if they are not sheared and pass the tests for geotechnical significance, as outlined in 2), above.

10. There was some emphasis on landslides since these are ubiquitous in California melanges. Little research has been done on the mechanisms responsible for the earthflows in Franciscan melanges, but much could be learned by a study of the work of Italian geotechnical engineers, who appear to be the farthest ahead in understanding the geotechnics of block-in-matrix rocks. An attempt was made to relate the block proportion of melanges, measured from detailed geological maps of Franciscan melanges, to the average hillslope of the area containing the blocks. The resulting plot was inconclusive, and did not show any clear trend between the two variables, nor a threshold between failed and stable melange terrain. But the plot did suggest that many Franciscan melanges have block proportions of the order of 30 percent and lower.

10. Little was added to the state of knowledge regarding the origin of melanges, but two models were considered which may shed light on the processes of fragmentation and mixing.. It was shown that a glacial basal till had a self-similar distribution of clasts; and reference was made to a mathematical model of mixing which is analagous to the kneading of dough. It was recognized that self-similarity is a result of many fragmentation and mixing processes, and cannot be considered the unique signature of

any one. Nevertheless, that means that many rock mixtures, if they exhibit self-similarity, may lend themselves to the sort of analysis conducted for this research, and investigators may benefit from the findings here.

6.3 RECOMMENDATIONS FOR FURTHER RESEARCH

A number of possibly fruitful directions for further research are suggested:

1. **Research Blocky Rock:** Research the similarities and lessons to be learned from blocky rock, particularly for high volumetric proportion bimrocks. The statistics of scanlines, negative exponential block size distributions and blocky rock mass characterizations and classifications, are all possibly applicable to some bimrocks.

2. **Measure the Block Size Distributions of Olistostromes, Lahars, Sheared Serpentinites and Decomposed granites:** These rocks are common in California, and are all potentially bimrocks. Self-similar block size distributions for these rocks would show that melanges are not unique in that regard, and that the various geological processes causing fragmentation result in fractal distributions. The enquiry then becomes one into the extent of scale-independence, identification of useful characterization parameters, and so on. And, in that case, the results of work here and that performed by Lindquist (1994b), which have been based on a study of melanges, will have broader application.

3. **Refine the Criteria for Geotechnical Significance, Characteristic Engineering Dimension and Block/matrix Thresholds**: The criteria offered here are sketchy and based on empirical observation, and geotechnical experience. They should be refined by more formal study. Research should also be performed to determine if the geometric threshold size is the same one as that size of block which resists failure under a certain stress distribution.

4. **Explore the Geometric Probability Aspects of Stereology:** The results learned during the research were not analyzed from a geometric probability point of view. The relationships between block size distributions; block volumetric proportion; scanline orientations, lengths and intervals; and block orientations and shapes have statistical ramifications. An understanding of these would be useful, particularly for stochastic studies into block size distributions relative to geohydrology, and seismic site response. Of great interest would be the probability aspects of certain critical failure surfaces and their relation to block size distribution, and so on. More empirical studies could be performed by modeling bimrocks on computers, and penetrating these virtual volumes with scanlines and surfaces. This work would have most pragmatic benefits.

5. **Perform Field Verifications:** Field verifications of some of the procedures developed are required. This work would be suitable for people with a construction interest.

6. **Extend the Block Proportion-Hillslope Research:** This work would be suitable for geotechnical engineers or engineering geologists interested in field work. Ideally, the data could be generated using GIS (Geographic Information Systems), coupled with field work to correlate the results.

7. **Research the Earthflow Processes in Franciscan Melanges:** Earthflows have not been much researched, possibly because they do not have the catastrophic nature of debris flows. But earthflows create considerable damage in California, particularly along highways. Geotechnical guidelines to exploration, analysis and remediation would be welcome. Particular attention needs to be paid to the analytical methods used for assessing slope stability: conventional rigid-block failure approaches, such as the Method of Slices, are possibly inappropriate for masses that deform with widely distributed shear zones, in the nature of glaciers.

REFERENCES

Aalto, K.R., 1981, Multistage melange formation in the Franciscan Complex, northernmost California: Geology, v. 9, p. 602-607.

---, 1989, Franciscan Complex geology of the Cresecent City area, northern California, in Aalto, K.R., and Harper, G.D., eds., Geologic Evolution of the northernmost Coast ranges and western Klamath Mts; Field Trip Guidebook T308, Field trip for 28th International Geological Congress; Galice Oregon to Eureka, California, July, 1989; Washington, DC, American Geophysical Union, p. 21-46;

Abbate, E., and Sagri, M., 1981, Excursion No. 5: Olistostromes in the Oligocene Macigno Formation (Florence area), in Lucchi, R., ed., Excursion Guidebook, with contributions on sedimentology of some Italian basins: Rome, International Association of Sedimentologists and Consiglio Nazionale delle Richerce, p. 165-203; Excusion Guidebook for 2nd European Regional Meeting, Bologna, Italy.

Adams, J., 1977, Sieve size statistics from grain measurement: Journal of Geology, v. 85, p. 209-227.

Afrouz, A., 1992, Practical handbook of rock mass classification systems and modes of ground failure: Boca Raton, Florida, CRC Press, 195 p.

AGI, 1977, Proceedings of the International Symposium on the Geotechnics of Structurally Complex Formations; Capri, Italy: Milano (Milan), Associazone Geotecnica Italiana (Italian Geotechnical Association), vol 1: 470; v 2: 418 p.

---, 1979, Some Italian experience on the mechanical characterization of structurally complex formations, in Proceedings of the 4th Intrnational Congress on Rock Mechanics; Montreux, Switzerland: International Society for Rock Mechanics, v. 1, p. unknown.

Aherne, W.A., and Dunnill, M.S., 1982, Morphometry: London, Edward Arnold (Publishers) Ltd., 201 p.

Alt, D.D., and Hyndman, D.W., 1975a, Roadside Geology of Northern California: Missoula, Montana, Mountain Press, 243 p.

---, 1975, Roadside Geology of Northern California: Missoula, Montana, Mountain Press, 243 p.

Archambault, G., Daigneault, R., Rouleau, A., and Tavchandjian, O., 1990, Mechanics of shear zones and fault belts development by anastomosing patterns of fractures at all scales, in Rossmanith, ed, ed., Mechanics of Jointed Rock: Rotterdam, AA Balkema, p. 197-204.

ASTM, 1992, Standard Test Method for Microscopical Determination of Parameters of the Air-Void System in Hardened Concrete: ASTM Test Designation C 457-90, vol 4.02 Concrete and Aggregates, ASTM, Philadelphia, p. 232-244

Audley Charles, M.G., 1965, A Miocene gravity slide deposit from E. Timor: Geological Magazine, v. 102, p. 267-332.

Bagnold, R.A., and Barndorff-Nielsen, O., 1980, The pattern of natural size distribution: Sedimentology, v. 27, p. 199-207.

Bailey, E.B., and McCallien, W.J., 1950, The Ankara Melange and the Anatolian thrust: Nature, v. 4231, p. 938-940.

Bailey, E.H., and Everhart, D.L., 1964a, Geology and quicksilver deposits of the New Almaden District Santa Clara County, California, 360 of US Geological Survey Professional Paper:

Bailey, E.H., Blake, M.C., and Jones, D.L., 1970, On-land Mesozoic oceanic crust in California Coast ranges, in US Geol. Survey Prof-Paper 700-C; p. C70-C81.

Barber, A.J., and Brown, K., 1988, Mud diapirism: the origin of melanges in accretionary prisms?: Geology Today, v. 4, p. 89-94.

Barber, A.J., Tjokrosapoetro, S., and Charlton, T.R., 1986, Mud volcanoes, shale diapirs, wrench faults and melanges: Bulletin of the American Association of Petroleim Geologists, v. 70, p. 1729-1741.

Barnsley, M., 1988, Fractals everywhere: New York, Academic Press, Inc, 396 p.

Barton, C.C., in press, Fractal analysis of the scaling and spatial clustering of fractures, in Barton, C.C., and LaPointe, P.R., eds., Fractals and their use in the Earth Sciences, Memoirs of the Geological Society of America: Boulder, CO, Geological Society of America; *preprint* dated Fall, 1992.

Barton, N.R., Lien, R., and Lunde, J., 1974, Engineering classification of rock masses for the design of tunnel supports: Rock Mechanics, v. 6, p. 189-236.

Bates, R.L. and Jackson, J.A., eds., Glossary of Geology, 3 rd Edition; American Geological Institute, Alexandria, VA, 788 p.

Baum, R.L., and Fleming, R.W., 1993, Patterns of movement in clay-rich landslides, Abstract with Programs; Presentation H42E-3; Annual Meeting of the American Geophysical Union; 1993 Fall Meeeting; San Francisco; p 300.

Baum, R.L., and Johnson, A.M., 1993, Steady movement of landslides in fine-grained soils- a model for sliding over an irregular slip surface, in ch. D of US Geological Survey Bulletin 1842-D, 1842-D of USGS Bulletin 1842: Landslide processes in Utah-observation and theory; p. D1-D28

Baum, R.L., and Reid, M.E., 1992, Geology, hydrology and mechanics of the Alani-Paty Landslide, Manoa Valley, Oahu, Hawaii, 92-501 of Open-File Report; United States Geological Survey, 87 p.

Bedrossian, T.L., 1978, Geology and slope stability in the Geysers Geothermal Resources area: California Geology, v. 31, p. 151-159.

---, 1980, Geology and Slope Stability in Selected Parts of the Geysers Geothermal resources Area, No. 142 of Special Reports: Sacramento, California, California Division of Mines and Geology, 66 p.

Beneventi, S., Cecere, V., Fioresi, G., Ricciardi, C., and Sciotti, M., 1989, Stability conditions in the Larderello area (Italy), in Proc. XII Int. Conf. Soil Mechanics and Foundation Engineering; Rio de Janeiro: Rotterdam, AA Balkema, v. 1, p. 1603-1606.

Berkland, J.O., Raymond, L.A., Kramer, J.C., Moores, E.M., and O'Day, M., 1972, What is Franciscan?: Bulletin of the American Association of Petroleim Geologists, v. 56, p. 2295-2302; reprinted in McCall, 1983 (Ophiolites and Related Melanges; Benchmark Papers, v. 66).

Bertocci, R., Canuti, P., Casagli, N., Garzonio, C.A., and Vannocci, P., 1993 (in press), Landslides on clay and shale hillslpes in Tuscany (Italy), in Reviews in Engineering Geology, vol ?: Boulder, Colorado, Geological Society of America, p. in press.

Bestynski, Z., 1993, Geophysical Flysch Rock Mass Classification (KFG), in Thiel, K., and Zabuski, L., eds., Proc. Seminar on Underground structures in complex geoogical conditions; Swinna Poreba, Poland: Warsaw, Poland, Institute of Meteorology and Water Management, p. 17-26.

Bhatia, S.E., Nye, E., and Soliman, A., 1987, An Image analysis application for soil fabric study, in Symposium on computer aided design and monitoring in geotechnical engineering: Rotterdam, AA Balkema; Preprint: no page details.

Biegel, R.L., and Sammis, C.G., 1989, The frictional propeties of a simulated gouge having a fractal particle distribution: Journal of Structural Geology, v. 11, p. 827-846; N.

Bieniawski, Z.T., 1989, Engineering rock mass classifications: New York, John Wiley and Sons, 251 p.

Bilodeau, B.J., and Davis, S.O., 1990, Geologic Guidebook to the Point Reyes Are, Northern California, 66 of AAPG Pacific Section Guidebook: Bakersfield, Am. Assn. Petroleum Geologists, 49 p.

Blake, M.C., 1984, Franciscan Geology of northern California: Los Angeles, CA, The Pacific Section of the Soc. Econ. Paleontologists and Mineralogists, 254 p.

Blake, M.C., and Harwood, D.S., 1989, Tectonic Evolution of northern California, T108 of Field Trip Guidebook:; American Geophysical Union, Washington, D.C.

Blake, M.C., and Jones, D.L., 1974, Origin of Franciscan melanges on northern California, in Dott, R.H., and Shaver, R.H., eds., Modern and ancient geosynclinal sedimention: Tulsa, Oklahoma, Society of Economic Paleontologists and Mineralogists, p. 345-357.

---, 1981, The Franciscan Assemblage and related rocks in northern California: a reinterpretation, in ch. 12 of Ernst, W.G., ed., Geotectonic development of California: Rubey vol. 1: Englewood CLiffs, New Jersey, Prentice-Hall, Inc, p. 308-328.

Blake, M.C., Bartow, J.A., Frizzell, V.C.A., Jr., Schlocker, J, Sorg, D., Wentworth, C.M., and Wright, R., 1974, Preliminary geologic map of Marin and San Francisco Counties and part of Alameda, Contra Costs, and Sonoma Counties, California: USGS Misc. Field Inv.?, scale unknown.

Blake, M.C., Howell, D.G., and Jones, D.L., 1982, Preliminary tectonostratigraphic terrane map of California: USGS Open File Reports Map 82-593, scale approx 1:750,000.

Blake, M.C., Howell, D.G., and Jayko, A.S., 1984, Tectonostratigraphic terranes of the San Francisco Bay region, in Blake, M.C., ed., Franciscan geology of northern California: Los Angeles, CA, Pacific Section, Soc. Econ. Paleo. and Min., p. 5-22.

Blatt, H., Middleton, G., and Murray, R, 1972, Origin of sedimentary rocks [1st ed.]: Englewood Cliffs, New Jersey, Prentice-Hall, Inc, 634 p.

Bonilla, M.G., 1961, City College Fault, San Francisco, California: USGS Professional Paper 424-C, p. 190-192.

Bosworth, W., 1984, The relative role of boudinage and "structural slicing" in the disruption of layered rock sequences: Journal of Geology, v. 92, p. 447-456.

---, 1989, Mélange fabrics in the unmetamorphosed extermnal terranes of the northern Appalachians, in Horton Jr., J.W., and Rast, N., eds., Mélanges and Olistostromes of the U.S. Appalachians: Boulder, CO, Geological Society of America, Special Paper 228, p. 65-91.

Boulton, G.S., 1976, The development of geotechnical properties in glacial tills, in Legget, R.F., ed., Glacial Till: an Inter-disciplinary Study, 12 of Special Publications: Ottawa, Canada, Royal Society of Canada, p. 292-303.

Brady, B.H.G. and Brown, E.T., 1985, Rock Mechanics for Underground Mining, George Allen & Unwin, London; 527 p.

Braga, G., 1977, Panel Discussion: Operational methods in geological investigations: informations acquirable from them, in Proceedings of the International Symposium on the Geotecnics of Structurally Complex Formations; Capri, Italy: Milano, Associazione Geotecnica Italiana, p. 305-311.

Brinker, R.C., and Wolf, P.R., 1977, Elemtary Surveying: New York, Harper & Row, Publishers, 568 p.

Brosch, F.J., Pölsler, P., and Riedmüller, G., 1992, The use of fractal dimension in Engineering Geology: Bulletin of the International Association of Engineering Geologists, v. 45, p. 83-88.

Brown, K.M., and Orange, D.L., 1993, Structural aspects of diapiric mélange emplacement: the Duck Creek Diapir: Journal of Structural Geology, v. 15, p. 831-847.

Brown, L.S., and Pierson, C.U., 1950, Linear traverse technicque for measurement of air in hardened concrete: Journal of the American Concrete Institute, v. 22, p. 117-123; Article 47-7.

Brown, R.D., 1964, Geological map of the Stoneyford Quadrangle, Glenn, Colusa, and Lake Counties, California: USGS Min Inv. Field Studies Map MF-279, scale 1:48,000.

Busch, D.D., 1993, The hand scanner handbook: PC Edition: Homewood, IL, Business One Irwin.

Call, R.D., Savely, J.P., and Nicholas, D.E., 1977, Estimation of joint set characteristics from surface mapping data, in ch. 9 of Brown, W.S., Green, S.H., and Australid, W.A., eds., Monograph on Rock Mechanics Applications in Mining: New york, Am Inst Mining Engineering (AIME), p. 2 B2-1 to 2 B2-9.

Canuti, P., 1993, Deformazione gravitative profonde in Toscana" aspetti geologici, geomorfologici e geotecnici di alcune are rappresentative (Trans:"Deep-seated slope movements: geologic, geomorphologic and geotechnical aspects of a representative area"); Florence, Italy, Dept Earth Sciences, University of Florence, Proceeding of IV Symposium , 24-28 May, 1993; 73 p.

Canuti, P., Cascini, L., Dramis, F., Pellegrino, A., and Picarelli, L., 1988, Landslides in Italy: occurence, analysis and control, in Siccardi, F., and Bras, R.L., eds., Workshop on Natural Disasters in European Mediterranean Countries: University of Salerno, Institute of Civil Engineering, p. 165-184;

Canuti, P., Casagli, N., and Garzonio, C.A., 1993, Lateral spreads and landslide hazards in the northern Apennine: the examples of Mt. Fumaiolo (Emilia-Romagna) and Chiusi della Verna (Tuscany), in Proc. 6th Int. Cogress of the IAEG; Amsterdam.

Carr, J.R., 1987, Rock mass classification using fractal dimension, in Farmer, I.W. et al., eds., Proc. 28th Symposium on rock Mechanics: Rotterdam, AA Balkema, p. 73-80.

Casagli, N., 1992, Slope instability in rock masses overlying a soft substratum: some analyses in the northern Apennines: Rock Mechanics Group, Royal School of Mines, Imperial College, London, MSc Thesis.

CDWR, 1973, Geology and sediment production for ten Eel River landslides, Memorandum report prepared by Northern District of the California Dept. of Water Resources; in Reference Section of DWR Central Records, Sacramento; N.

Chesterman, C.W., 1951, Nephrite in Marin County, California, 10-B of Special Publication: San Francisco, California Division of Mines (and Geology), 11 p.

Clarke, A.O., and Hansen, C.L., 1993, Arroyo boulders: California Geology, v. 46, p. 100-109.

Cleary, W.J., Curran, H.A., and Thayer, P.A., 1984, Barbados Ridge Inner Trench slope sedimentation: Jornal of Sedimentary Petrology, v. 54, p. 527-541.

Cloos, M., 1984, Flow melanges and the structural evolution of accretionary wedges, in Raymond, L.A., ed., Melanges: Their nature, origin and significance, 198 of Special Papers: Boulder, CO, Geological Society of America, p. 71-79.

---, 1990a, Evolution of the geological interpretation of the Franciscan Complex in the San Francisco Bay region: a comparison of cross-sections, in Bilodeau, B.J., and Davis, S.O., eds., Geologic Guidebook to the Point Reyes area, northern California: Bakersfield, CA, Pacific Section, Amer. Assn. Petroleum Geols., p. xxiii-xxxi.

---, 1990b, Nicasio Dam pillow basalts, in Bilodeau, B.J., and Davis, S.O., eds., Geologic Guidebook to the Point Reyes area, northern California: Bakersfield, California, Pacific Section, Am. Assn. Petroleum Geologists, p. 9-18.

Cloos, M., and Shreve, R.L., 1988, Subduction channel model of prism accretion, mélange formation, sediment subduction, and subduction erosion at convergent plate margins: 2. Implications and discussion: Pure and Applied Geophysics, v. 128, p. 501-545.

Cotecchia, V., Monterisi, A., Salvemini, A., Spilotro, G., and Trisorio-Liuzzi, G., 1977, Geolithological, structural and geotechnical aspects of some arenaceous-marly formations cropping out in central-southern Apennines, in Proceedings of the International Symposium on the Geotecnics of Structurally Complex Formations; Capri, Italy: Milano, Associazione Geotecnica Italiana, v. 2, p. 71-78.

Cotecchia, V., Del Prete, M., Federico, A., Fenelli, G.B., Pellegrino, A., and Picarelli, L., 1984, Some observations on a typical mudslide in a highly tectonized formation in sothrn Apennines, in Proc. IV Int. Symposium on Landslides; Toronto, Canada: p. 39-44.

Cowan, D.S., 1974, Deformation and metamorphism of the Franciscan Subduction Zone Complex Northwest of Pacheco Pass, California: Bulletin of the Geological Society of America, v. 85, p. 1623-1634.

---, 1978, Origen of blueschist-bearing chaotic rocks in the Franciscan Complex, San Simeon, Californa: Bulletin of the Geological Society of America, v. 89, p. 1415-1423.

---, 1985, Structural styles in Mesozoic and Cenozoic melanges in the western Cordillera of North America: Geological Society of America, v. 96, p. 451-462.

---, 1991, Melanges, Abstract from Symposium; in: Controversies in Modern Geology: Evolution of geological theories in Sedimentology, Earth History and Tectonics; ed. D.W.Müller, J.A. McKenzie, and J.H. Weissert; p. 482; Academic Press, New York.

Cowan, D.S., and Mansfield, C.F., 1970, Serpentinite flows on Joaquin Ridge, southern Coast Ranges, California: Bulletin of the Geological Society of America, v. 81, p. 2615-2628.

Cowan, D.S., and Page, B.M., 1975, Recycled Franciscan material in Franciscan mélange west of Paso Robles, California: Bulletin of the Geological Society of America, v. 86, p. 1089-1095.

Crippen, R.A., Jr., 1951, Nephrite jade and associated rocks of the Cape San Martin region, Monterey County, California, 10-A of Special Report: San Francisco, California Division of Mines (and Geology), 13 p.

Czechoslovak Dam Committee, 1967, Dams in Czechoslovakia, published by Czechoslovak Dam Committe, Suvorovova, 4A, Bratislava

da Cunha, P., 1990, Scale effects in rock mechanics, in Scale efects in Rock Masses: Proc. 1st Int. Workshop; Loen, Norway: Rotterdam, AA Balkema, p. 3-27.

Dames & Moore, 1979a, Interpretive Report, Engineering Recommendations; Contract N1; North Shore Outfalls Consolidation Project; for the City and County of San Francisco, Dames & Moore Job No. 185-135-03.

----------, 1979b, Final Report, Geotechnical Investigation, Route Selection Study, Richmond Transport Sewer, San Francisco; for the City and County of San Francisco, Dames & Moore Job No. 185-131-03.

Dann, K.T., 1988, Traces on the Appalachians A natural history of Serpentine in eastern North America: New Brunswick, Rutgers University Press, 159 p.

Davis, D., Suppe, J., and Dahlen, F.A., 1983, Mechanics of fold-and-thrust belts and accretionary wedges: Journal of Geophysical Research, v. 88, p. 1153-1172.

Delesse, A., 1848, Pour determiner la composition des roches: Ann. des Mines, fourth series, v. 13, p. 379.

D'Elia, B., 1977, Geotechnical complexity of some Italian variegated clay shales, in Proceedings of the Int. Symposium on the Geotechnics of Structurally Complex Formations; Capri, Italy: Milano, Associazione Geotecnica Italiana, p. 215-221.

D'Elia, B., Distefano, D., Federico, G., and Oliva, S., 1984, Full-scale study of a high cut in a structurally complex formation, in Proc. IV International Symposium on Landslides; Toronto, Canada: p. 57-62.

D'Elia, B., Distefano, D., Esu, F., and Federico, G., 1986, Slope Movements in Structurally Complex Formations, in Tan Tjong Kie (Chairman), Li Chengxiang, and Yang Ling, eds., Engineering in Complex Rock Formations; Proceedings of the International Symposium; 3-7 Novenber, 1986, Beijing, China: Beijing, China, Science Press, p. 430-436; Also published by Pergamon Press, New York.

---, 1988, Deformations and stability of high cuts in a structurally complex formation: Analysis and prediction, in Proceedings of the 5th International Symposium on Landslides; Lausanne, Switzerland: p. 599-604.

---, 1989, Instrumental analysis of deformations in a high cut, in Proceedings of the XII Int. Conference of Soil Mechanics and Foundation Engineering; Rio de Janeiro: p. 1555-1560.

Dengler, L., and Montgomery, D.R., 1989, Estimating the thickness of colluvial fill in unchanneled valleys from surface topography: Bulletin of the Association of Engineering Geologists, v. XXVI, p. 333-342.

Dennis, J.G., and Murawski, H., 1979, International Tectonic Lexicon: Stuttgart, E. Schweizerbart'sche Verlagsbichhandlung.

Dietrich, R.V., Dutro, J.T., and Foose, R.M., 1982, AGI Data Sheets: for geology in the field, laboratory and office [2nd ed.]: Falls Church, VA, American Geological Institute; loose leaf data sheets.

Donaghe, R.T., and Torrey, V.H., III, 1985, Strength and deformation properties of earth-rock mixtures, GL-85-9 of Technical Report: Washington, DC, Department of the Army, US Corps of Engineers, 100+ p.

Dounias, G.T., and Marinos, P.G., 1993, Soil-like and rock-like bahaviour of a flysch in slope stability, in Proceedings of Int. Symp on Hard Soils-Soft Rocks; Athens, Greece; Sept. 1993: Rotterdam, AA Balkema, preprint.

Dowding, C.H., 1978, Site characterization and exploration: New York, American Society of Civil Engineers, 395 p.; Proceedings of Specialty Workshop, Northwestern University, Illinois.

Duffield, W.A., and Sharp, R.V., 1973, Geology of the Sierra Foothills Melange and adjacent areas, Amador County, California, 827 of USGS Profesional Paper; 1-30 p.

Durrell, C., 1987, Geologic history of the Feather River country: Berkeley, Univ. of California Press, 357 p.

Edelman, S.H., Day, H.W., Moores, E.M., Zigan, S.M., Murphy, T.P., and Hacker, B.R., 1989, Structure across a Mesozoic ocean-continent suture zone in the northern Sierra Nevada, California, 224 of Special Paper: Bouldr, Colorado, Geological Society of America, 56 p.

Ellen, S.D., and Fleming, R.W., 1987, Mobilization of debris flow from soil slips, San Francisco Bay region, California, in Costa, J.E., and Wieczorek, G.F., eds., Debris flows/avalanches: process, recognition and mitigation, VII of Review in Engineering Geology: Boulder, Colorado, Geological Society of America, p. 31-49.

Ellen, S.D., and Wentworth, C.M., in press, Hillside Bedrock Materials of the San Francisco Bay Area, California: USGS; sheets 1,2 and 3, scale 1:125,000.

Ellen, S.D., and Wieczorek, G.F., 1988, Landslides, floods and marine effects of the storm of January 3-5, 1982, in the San Francisco Bay Region, California, 1434 of U.S. Geological Survey Professional Paper, 310 p.

Ellen, S., Peterson, D.M., Reid, G.O., and Savina, M.E., 1977, Hillslope forms and landslide processes in erosional terrain on Franciscan rocks of the Marin Peninsula, California, Abstract; GSA Abstracts with programs, v 11, p77.

Engineering& Contracting News, 1915, Stockton Street tunnel, portion of article from vol XLIII, no. 5; Jan 3, 1915.

Engineering News Record, 1914, Highway and Street Railway Tunnels in San Francisco, vol 73; February 12, 1914; p 315-?

Enriquez-Reyes, M.D.P., and Jones, M.E., 1991, On the nature of the scaley texture developed in melange deposits, in Roegiers, ed., Rock Mechanics as a multi-disciplinary science: Rotterdam, AA Balkema, p. 713-722.

Erikson, R., 1992?, Geology of northern Marin and Sonoma Counties, California: Three Trips: Rohnert Park, California, Dept. Geology, Sonoma State University, 169 p.

Erikson, R.C., 1994, The geology of the Franciscan Complex in the Ward Creek-Cazadero area, Sonoma County, California, in press: Report and 1:12,000 map, submitted to California Dept of Mines and Geology, Sacramento,.

Ernst, W.G., 1984, Californian blueschists, subduction, and the significance of tectonostratigraphic terannes: Geology, v. 12, p. 436-440.

Esu, B., 1977, General Report: Behaviour of slopes in structurally complex formations, in Proceedings of the International Symposium on the Geotecnics of Structurally Complex Formations: Milano, Associazione Geotecnica Italiana, v. 2, p. 292-304.

Esu, F., Pescatore, T., Pellegrino, A., Billota, E., D'Elia, B., Federico, G., and Tancredi, G., 1985, Geotechnical Properties and slope stability in structurally complex clay soils, in Capuzzo, md, Jappelli, R., Martinetti, S., Nova, R., Troiano, V., and Viggiani, C., eds., Geotechnical Engineering in Italy: an overview, 1985: Rome, AGI- Associazione Geotecnica Italiana, p. 415.

Evangelista, A., Paparo Filomarino, M., and Pellegrino, A., 1977, On the mechnaical behavior of variegated clay shales of Irpinia, in Proceddings of the Int. Symposium on the Geotechnics of Structurally Complex Formations; Capri, Italy: Milano, Associazione Geotecnica Italiana, v. 2, p. 229-237.

Fabbri, A.G., 1984, Image Processing of geological data, 3 of Computer methods in the Geosciences: New york, Van Nostrand Reinhold Co.

Farmer, I.W., Kemeny, J.M., and McDoniel, C., 1991, Analysis of rock fragmentaion in bench blasting using digital image processing, in Wittke, W., ed., 7th International Congess on Rock Mechanics: Aachen, International Society for Rock Mechanics, p. 1037-1042.

Fleming, R.W., Schuster, R.L., and Johnson, R.B., 1988, Physical properties and mode of failure of the Manti Landslide, Utah, in The Manti, Utah, Landslide, 1311 of US Geological Survey Professional Paper, p. 27-41.

Flores, G., 1955, Discussion: Proceedings of the 4th World Petroleum Conference, Sec. I/A/2; p.121-122.

Fox, K.F., 1983, Melanges and their bearing on Late Mesozoic and Tertiary subduction and interplete translation at the west edge of the North American Plate, USGS Professional Paper 1198 , 40 p.

Fragaszy, R.J., Su, W., and Siddiqi, F.H., 1990, Effects of oversize particles on the density of claen granular soils: Journal of Geotechnical Testing, v. 13, p. 106-114.

Fragaszy, R.J., Su, J., Siddiqi, F.H., and Ho, C.L., 1992, Modeling strength of sandy gravel: Journal Of Geotechnical Engineering; ASCE, v. 118, p. 920-935.

Frost, J.D., and Wright, J.R., 1993, Digital Image Processing: Techniques and Applications in Civil Engineering: New York, ASCE, 301 p.

Fryer, P., 1992, Mud volcanoes of the Marianas: Scientific American, v. February, p. 46-52.

Gass, I.G., 1990, Ophiolites, in Moores, E.M., ed., Shaping the Earth: Tectonics of continents and oceans: San Francisco, WH Freeman, p. 111-124; Originally published in Scientific American, August, 1982.

Gates, A.E., 1992, Domainal failure of serpentinite in shear zones, State-Line complex, Pennsylvania, USA: Journal of Structural Geology, v. 14, p. 19-28.

GCO, 1988, Guide to Rock and Soil Descriptions, 3 of Geoguide: Hong Kong, Geotechnical Control Office, 191 p.; available through Gov. Publications Centre, Hong Kong.

Genske, D.D., Herda, W., and Ohnishi, Y., 1992, Fractures and Fractals, in Hudson, J.A., ed., Eurock '92: Rock characterization: London, Thomas Telford, p. 19-24; Proc: Eurock '92,

Ghilardi, P., Kai Kai, A., and Menduni, G., 1993, Self-similar heterogeneity in granular porous media at the representative elementary volume scale: Water Resources Research, v. 29, p. 1205-1214.

Girty, G.H., and Pardini, C.H., 1987, Provenance of sand inclusions in the Paleozoic Sierra City mélange, Sierra Nevada, California: Bulletin of the Geological Society of America, v. 98, p. 176-181.

Gonzales, J. M. and Dunne, T.N., 1983, Geotechnical exploration for the proposed Crosstown Transport Facility, San Francisco, California; Proc. Rapid Tunneling and Excavation Conference (RETC), ed. Sutcliffe, H. and Wilson, J. W., vol 1, p. 25-41.

Goodman, R.E., 1976, Methods of geological engineering in discontinuous rock: St. Paul, MN, West Publ.

---, 1989, introduction to Rock Mechanics [2nd ed.]: New York, John Wiley & Sons, 562 p.

---, 1990a, Rock foundations for dams: A summary of exploration targets and experience in different rock types, in Proc. 10th Annual USCOLD Lecture Series; New Orleans, Louisiana: preprint, p. 31.

---, 1990, Soils versus rocks as engineering materials, in ch. 6 of Duncan, J.M., ed., Proceedings: H. Bolton Seed Memorial Symposium: Vancouver, BC, Canada, BiTech Publishers, v. 2, p. 111-132.

---, 1992, Engineering Geology [1st ed.]: New York, John Wiley and Sons, 410 p.

Goodman, R.E., and Shi, G.-H., 1985, Block theory and its application to Rock Engineering: Englewood Cliffs, New Jersey, Prentice-Hall, Inc, 338 p.

Gostelow, T.P., and Loucaides, G., 1988, Slope instability in allochthonous sediments: An example from the Mono Mélange, Cyprus, in Proc. 5th International Symposium on Landslides; Lausanne, Switzerland: p. 161-166.

Graymer, RW and Jones, DL, 1994, Tectonic implications of radiolarian cherts from the Placerville Belt, Sierra Nevada Foothills, California: Nevadan-age continental growth by accretion of multiple terranes: Bull. Geol. Soc. of America, v. 106, p. 531-540.

Greenly, E., 1919, The geology of Anglesey: London, Geological Survey of Great Britain, 980 p.

Hada, S., 1988, Physical and mechanicalproperties of sedimentary rocks in the Cretaceous Shimanto Belt: Modern Geology, v. 12, p. 341-359.

Hatzor, Y., 1992, Validation of Block Theory using field case histories: Dept. Civil Engineering, University of California, Berkely, California, Ph.D. Dissertation, 213 p.

Hatzor, Y., and Goodman, R.E., 1992, Application of Block theory and the critical key block concept to tunneling: two case histories, in Fractured and jointed rock masses: Symposium preprints: Rotterdam, AA Balkema; preprint of paper presented at US Rock Mechanics Symposium, June 1992;Granlibakken, Lake Tahoe, California; sponsored by Int. Soc. Rock Mechanics.

Herdan, G., and Smith, M.L., 1953, Small particle statistics: New York, Elsevier Publishing Co., 520 p.

Hobbs, B.E., Means, W.D., and Williams, P.F., 1976, An outline of structural geology: New York, John Wiley and Sons, 571 p.

Hoek, E., and Bray, J.W., 1977, Rock slope engineering [2nd ed.]: London, Institution of Mining and Metallurgy, 402 p.

Hoek, E., and Brown, E.T., 1982, Underground excavations in rock [2nd ed.]: London, Institution of Mining and Metallurgy, 525 p.

Holmes, A., 1921, Petrographic Methods and Calculations: London, England, Thos. Murray and Co.

Horton, J.W., Jr., and Rast, N., 1989, Mélanges and olistostromes of the US Appalachians, 228 of Special Paper: Boulder, Colorado, Geological Socity of America.

Howell, D.G., 1989, Tectonics of suspect terranes: mountain building and continental growth, 3 of Topics in the Earth Sciences: New york, Chapman and Hall, 232 p.

Hsü, K.J., 1968, Principles of melanges and their bearing on the Franciscan-Knoxville Paradox: Geological Society of America, v. 79, p. 1063-1074.

---, 1974, Melanges and their distinction from olistostromes, in Dott, R.H., and Shaver, R.H., eds., Modern and ancient geosynclinal sedimentation: Tulsa, Oklahoma, Society of Economic Paleontologists and Mineralogists, Special publication No. 19, p. 321-333.

---, 1985, A basement of melanges: A personalaccount of the circumstances leading to the breakthrough in Franciscan research, in Drake, E.T., and Jordan, W.M., eds., Geologists and Ideas: a history of North American geology, 1 of Centennial Special Volumes: Boulder, Co, Geological Society of America, p. 47-64.

Hudson, J.A., and Priest, S.D., 1979, Discontinuities and rock mass geometry: International Journal of Rock Mechanics, Mineral Science and Geomechanics Abstracts, v. 16, p. 339-362.

---, 1983, Discontinuity frequency in rock masses: International Journal of Rock Mechanics, Mining Science and Geomechanics Abstracts, v. 20, p. 73-89.

Hunt, R.E., 1984, Geotechnical engineering investigation manual: New York, McGraw-Hill, 983 p.

Irfan, T.Y., and Tang, K.Y., 1992, An engineering geoogical characterization of colluvium in Hong Kong, TN 4/92 of Technical Note: Hong Kong, Geotechnical Engineering Office; Special Projects Division, 128 p.; (publication is not freely available).

---, 1993, Effect of the Coarse Fraction on the Shear Strength of Colluvium, 23 of GEO Report: Hong Kong, Hong Kong Geotechnical Engineering Office, Civil Engineering Department, 21 p.

ISRM, 1981, Part 1: Site Characterization, in Brown, E.T., ed., Rock Characterization, testing and Monitoring: New York, Pergamon Press, p. 3-70; Published for the Commission on Testing Methods, International Society for Rock Mechanics.

Iverson, R., 1983, Discussion and Reply: A model for creeping flow in landslides (Savage & Chleborad, 1982): Bulletin of the Association of Engineering Geologists, v. XX, p. 455-459.

Jacobi, R.D., 1984, Modern submarine sediment slides and their implications for melange and the Dunnage Formation in north-central Newfoundland: in Raymond, L.A., ed., Melanges: Their nature, origin and significance; Special Paper 198, Geological Society of America, Boulder, CO; p. 81-99.

Johnson, K.A., and Sitar, N., 1987, Debris flow initiation: an investigation of mechanisms, GT/87-02 of UCB Geotechnical Engineering Reports: Berkeley, Univ. of California, Dept. of Civil Eng., 179 p.

Johnson, L., Fryer, P., Taylor, B., Silk, M., Jones, D.L., Sliter, W.V., Tesumaru, I., and Teruaki, I., 1991, New evidence for crustal accretion in the outer Mariana forearc: Cretaceous radiolarian cherts and mid-ocean ridge basalt-like lavas: Geology, v. 19, p. 811-814.

Jones, D.L., Howell, D.G., Coney, P.J. and Monger, J.W.H., 1983, Recognition, character, and analysis of tectonostratigraphic terranes in western North America, in Hashimoto, M. and Uyeda, S,. eds., Accretion Tectonics; Proceedings of the Oji International Seminar on Accretion Tectonics, Tomokamai, Japan, 1981: Advances in Earth and Planetary Sciences, Tokyo, Terra Scientific Publishing Co., p. 21-35.

Kano, K., Nakaji, M., and Takeuchi, S., 1991, Asymmetrical melange fgabrics as possible indicators of the convergent direction of plates: a case study from the Shimanto Belt of the Akasihi Mountains, central Japan: Tectonophysics, v. 185, p. 375-388.

Kear, D, and Waterhouses, B.C., 1976, Onerahi Chaos breccia of Northland, New Zealand: Journal of Geology and Geophysics, v. 10, p. 629-646.

Keefer, D.K., and Johnson, A., 1983, Earth flows: morphology, mobilization and movement; US Geological Survey Professional Paper 1264, 56 p.

Kelsey, H.M., 1978, Earthflows in Franciscan melange, Van Duzen River basin, California: Geology, v. 6, p. 361-364.

Kemeny, J.M., 1993, A practical technique for determining the size distribution of blasted benches, waste dumps and heap-leach sites: Mining Engineering; Preprint dated August 1993.

Kemeny, J.M., Devgan, A., Hagaman, R.M., and Wu, X., 1993, Analysis of rock fragmentation using digital image processing: Journal of Geotechnical Engineering; ASCE, v. 119, p. 1144-1160.

Kendall, M.G., and Moran, P.A.P., 1963, Geometrical probability, 10 of Griffin's statistical monographs and courses: London, Charles Griffin & Company, 125 p.

Kintzer, F.C., 1980, Geology and landslides at Calaveras Reservoir, Alameda and Santa Clara counties, California: Hayward State University?, MS Thesis, 130 p.

Korvin, G., 1989, fractured but not fractal: Fragmentation of the Gulf of Suez basement: Pure and Applied Geophysics, v. 131, p. 289-305.

Krueger, S.W., and Jones, D.L., 1989, Extensional fault uplift of regional Franciscan blueschists due to subduction shallowing during the Laramide orogeny: Geology, v. 17, p. 1157-1159.

Krumbein, W.C., and Pettijohn, F.J., 1938, Manual of sedimentary petrography: New York, D. Appleton-Century Co., 549 p.

Laznicka, P., 1985, Emprical Metallogeny; vol 1: Phanerozoic Environments and Associated Ores: New York, Elsevier, v. 1.

---, 1988, Breccias and Coarse Fragmentites: Petrology, Environments, Associations, Ores, 25 of Developments in Economic Geology: New York, Elsevier, 832 p.

Lindquist, E.S., 1991, Fractals-Fracture and Franciscan Melange, Term Paper for CE 280, Rock Mechanics; instructor: Prof. R E Goodman; Dept Civil Engineering, University of California, Berkeley.

---, 1994a, The mechanical properties of a physical model melange, in Proc. 7th Congress of the Int. Assoc. Engineering Geologists: Rotterdam, Netherlands, AA Balkema; preprint, dated March 1994.

---, 1994b, The strength and deformation properties of melange: University of California, Berkeley, Ph.D. Dissertation; publ.: University Microfilms International; UMI Dissertations Service, Ann Arbor, MI.

Lindquist, E.S., and Goodman, R.E., 1994, The Strength and Deformation Properties of a Physical Model Melange, in Proceedings of First North American Rock Mechanics Symposium, Austin, Texas (June 1-3, 1994): Rotterdam, Netherlands, A.T.Balkema; N.

Lindquist, E.S., Medley, E., and Goodman, R.E., 1993, The engineering characterization of some Franciscan and physical model melanges, Abstract of presentation to 36th Annual Meeting of the Association of Engineering Geologists,"Aqua y Terra"; San Antonio, Texas: Program with Abstracts, p.60;.

Lockwood, J.P., 1971, Sedimentary and gravity-slide emplacement of serpentinite: Bulletin of the Geological Society of America, v. 82, p. 919-936.

Lord, G.W., and Willis, T.F., 1951, Calculation of Air Bubble Size Distribution from Results of a Rosiwal Traverse of Aerated Concrete: ASTM Bulletin, no. 177, p. 56-61 (TP220-TP225).

Maerz, N.H., and Franklin, J.A., 1990, roughness scale effects and fractal dimension, in da Cunha, P., ed., Scale efects in Rock Masses: Proc. 1st Int. Workshop; Loen, Norway: Rotterdam, AA Balkema, p. 121-126.

Mandelbrot, B.B., 1983, The fractal geometry of nature: New York, W.H. Freeman, 468 p.

Manfredini, M., Bertini, T., Cugusi, F., Grisolia, M., and Rossi-Doria, M., 1985, Geological outline of Italy: bearing of the geological features on the geotechnical characterization on the example (sic) of some typical formations, in Capuzzo, M.G., Jappelli, R., Martinetti, S., Nova, R., Troiano, V., and Viggiani, C., eds., Geotechnical Engineering in Italy: Rome, AGI-Associazione Geotecnia Italiana, p. 415.

Marone, C., and Scholz, C.H., 1989, Particle-size distribution and microstructures within simulated fault gouge: Journal of Structural Geology, v. 11, p. 799-814.

Maruyama, S., BAnno, S., Matsuda, T., and Nakajima, T., 1984, Kurosegawa Zone and its bearing on the development of the Japanese Islands: Tectonophysics, v. 110, p. 47-60.

Mauldon, M., 1993, Intersection probabilities of impersistent joints: Preprint:accepted for publication; (accepted for Int. Journal of Rock Mechanics; preprinted dated October, 1993).

Maurenbrecher, P.M., and Kronieger, R., 1991, Mass classification of Quaternary gravel deposits, in Forster, A., Culshaw, M.G., Cripps, J.C., Little, J.A., and Moon, C.F., eds., Quaternary Engineering Geology: p. unknown; Geological Society, Engineering Geology Special Publication No. 7.

McCall, G.J.H., 1983, Ophiolitic and related mélanges, 66 of Benchmark Papers: Shroudsberg, Penn, Hutchinson Ross Publishing Co., 447 p.

McGown, A., and Derbyshire, E., 1977, Genetic influences on the properties of tills: Quarterly Journal of Engineering Geology, v. 10, p. 389-410.

McKinlay, D.G., Tomlinson, M.J., and Anderson, W.F., 1974, Observations on the undrained strength of a glacail till: Géotechnique, v. 24, p. 503-516.

Medley, E., 1994, Using stereologic methods to estimate the volumetric proportion of blocks in melanges and similar block-in-matrix rocks (bimrocks), accepted for publication in : Proc. 7th Congress of the International Association of Engineering Geologists, Lisbon, Portugal

Medley, E. and Goodman, R.E., 1994, Estimating the block volumetric proportion of melanges and similar block-in-matrix rocks (bimrocks); Proc. 1st North American Rock Mechanics Conference (NARMS), Nelson, P.P and Laubach, S.E., eds.; A.A. Balkema, Rotterdam, p. 851-858.

Middleton, G.V., 1991, Nonlinear dynamics, chaos and fractals, Volume 9 of Short Course notes: Toronto, Ontario, Geological Association of Canada.

Moore, G.F., and Karig, D.E., 1980, Structural geology of Nias Island, Indonesia: Implications for Subduction Zone Tectonics: American Journal Science, v. 280, p. 193-227.

Moore, J.C., Taira, A., and Moore, G., 1991, Ocean drilling and accretionary proceses: GSA Today, v. 1, p. 265-270.

Morgenstern, N.R., and Cruden, D., 1977, Description and classification of geotechnical complexities, in Proc. of the Int. Symposium on The Geotechnics of Structurally Complex Formations; Capri, Italy: Milano, Associazione Geotecnica Italiana, v. 2, p. 195-204.

Murchey, B. L. and Jones, D. L., 1984, Age and significance of chert in the Franciscan Complex in the San Francisco Bay Region; in Franciscan Geology of Northern California, ed. Blake, M. C.: Los Angeles, CA; The Pacific Section of the Soc. Econ. Paleo. and Mineralogists; v. 43, p. 23-30

Nagahama, H., 1993, Technical Note: Fractal fragment size distribution for brittle rocks: International Journal of Rock Mechanics, Mining Science and Geomechanics Abstracts, v. 30, p. 469-471.

Nagahama, H., and Yoshii, K., 1993, fractal dimension and fracture of brittle rocks: International Journal of Rock Mechanics, Mining Science and Geomechanics Abstracts, v. 30, p. 173-175.

Needham, D.T., 1987, Asymmetric extensional structures and their implications for the generation of melanges: Geologists Magazine, v. 124, p. 311-318.

Neilson, J.A., 1976, A draft Environmental Impact Report for Shell Oil Company, US Geothermal Leasehold Drill Site E, Lake County, California, By Ecoview Environmental Consultants; 288 p; N.

Norris, R.M., and Webb, R.W., 1990, Geology of California [2nd ed.]: New York, John Wiley and Sons, 541 p.

Northmore, K.J., Charalambous, M., Hobbs, P.R.N., and Petrides, G., 1986, Engineering geology of the Kannaviou, "Melange" and Mamonia Complex Formations- Phiti/Statos area, SW Cyprus, G/EG/15 of GSD Reports: Nottingham, UK/Nicosia, Cyprus, British Geological Society/Geological Survey Department of the Ministry of Agriculture & Natural Resources, Cyprus.

Northmore, K.J., Hobbs, P.R.N., Charalanbous, M., and Petrides, G., 1988, Complex landslides in the Kannaviou Mélange and Mamonia Formations of south-west Cyprus, in Proc. 5th International Symposium on Landslides; Lausanne, Switzerland: p. 263-268.

O'Hanley, D.S., 1992, Solution to the volume problem in serpentinization: Geology, v. 20, p. 705-708.

Orange, D.L., Geddes, S., and Moore, J.C., 1993, Structural and fluid evolution of a young accretionary complex: the Hoh rock assemblage of the western Olympic Peninsula, Washington: Bulletin of the Geological Society of America, v. 105, p. 1053-1075.

Page, B.M., 1978, Franciscan melanges compared with olistostromes of Taiwan and Italy: Tectonophysics, v. 47, p. 223-246.

---, 1981, The southern Coast Ranges, in Ernst, W.G., ed., The geotectonic formation of California: Englewood Cliffs, New Jersey, Prentice-Hall, v. The Rubey Volume, Volume 1, p. 330-417.

Page, B.M., and Suppe, J., 1981, The Pliocene Lichi Mélange of Taiwan: its plate tectonic and olistostromal origin: American Journal Science, v. 281, p. 193-227.

Page, N.J., 1968, Sepentinization in a sheared serpentinite lens, Tiburon Peninsula, California, in US Geological Survey Professional Paper 600-B: p. B21-B28.

Pahl, P.J., 1981, Estimating the mean length of discontinuity traces: International Journal of Rock Mechanics, Mining Science and Geomechanics Abstracts, v. 18, p. 221-228.

Park, R.G., 1988, Geological structures and moving plates: New York, Blackie; 337 p.

Pascucci, V.N., 1983, Landslides in soils overlying Fraciscan Assemblage, in Yong, R.N., ed., Geological environment and soil properties: New York, American Society of Civil Engineers, p. 167-182;

Peitgen, H.-O., Jurgens, H., and Saupe, D., 1992, Chaos and Fractals: NY, Springer-Verlag, 984 p.

Herdan, G., and Smith, M.L., 1953, Small particle statistics: New York, Elsevier Publishing Co., 520 p.

Peterson, D.M., 1979, Hillslope erosional processes related to bedrock, soils, and topography of the the Three Peaks area, Marin County, California: San Jose State University, San Jose, California, MS Thesis, 94 p.

Phipps, S.P., 1984, Ophiolitic olistostromes in the basal Great Valley sequence, in Raymond, L.A., ed., Melanges: their nature, origin and significance, 198 of Special Paper: Boulder, Colorado, Geological Society of America, p. 103-125.

Piteau, D.R., 1973, Characterizing and extrapolating rock joint properties in engineering practice: Rock Mechanics Supplement, v. 2, p. 5-31.

Platt, J.P., 1986, Dynamics of orogenic wedges and the uplift of high-pressure metamorphic rocks: Bulletin of the Geological Society of America, v. 97, p. 1037-1053.

Popiolek, S., Sala, H., and Thiel, K., 1993, Geotechnical Flysch Rock Mass Classification (KF), in Thiel, K., and Zabuski, l, eds., Proc. of Seminar on Underground structures in complex geological conditions; Swinna Poreba, Poland: Warsaw, Poland, Institute of Meteorology and Water Management, p. 27-39.

Priest, S.D., 1993, Discontinuity analysis for rock engineering: London, Chapman & Hall, 473 p.

Priest, S.D., and Hudson, J.A., 1976, Discontinuity spacings in rock: International Journal of Rock Mechanics, Mining Science and Geomechanics Abstracts, v. 13, p. 135-148.

---, 1981, Estimation of discontinuity spacing and trace length using scanline surveys: International Journal of Rock Mechanics, Mining Science and Geomechanics Abstracts, v. 18, p. 183-197.

Radbruch-Hall, D.H., 1976, Maps showing areal slope stability in part of the northern Coast ranges, California: United States Geological Survey Misc. Investigations Map I-982, scale 1:62,500.

Rast, N., and Horton, J.W., Jr., 1989, Mélanges and olistostromes in the Appalachians of the United States and mainland Canada: An assessment, in : p. 1-14; Geological Society of America; Boulder, Colorado; Y; 276; Special Paper; 228.

Raymond, L.A., 1984a, Classification of Melanges, in Melanges: their nature, origin and significance, 228 of Special Paper: Boulder, Colorado, Geological Society of America, p. 7-20.

---, 1984b, Melanges: their nature origin and significance, 198 of Special Paper: Boulder, Colorado, Geological Society of America, 170 p.

Raymond, L.A., and Terranova, T., 1984, The melange problem - a review. (Prologue), in Raymond, L.A., ed., Melanges: Their nature, Origin and significance; Special Paper 198, Boulder, CO, Geological Society of America, p. 1-5.

Raymond, L.A., Yorkovich, S.P., and McKinney, M., 1989, Block-in-matrix structures in the North Carolina Blue Ridge belt and their significance for the tectonic history of the southern Appalachian orogen, in Horton Jr., J.W., and Rast, N., eds., Mélanges and Olistostromes of the U.S. Appalachians: Boulder, Colorado, Geological Society of America, v. Special Paper 228, p. 195-215.

Reid, G.O., 1978, The relationship between slope processes, soils, bedrock, and topography in an area of franciscan terrane in Marin County, California: San Jose State University, San Jose, California, MS Thesis, 90 p.

Reneau, S.L., and Dietrich, W.E., 1987, The importance of hollows in debris flow studies; Examples from Marin County, California, in Costa, J.E., and Wieczorek, G.F., eds., Debric flows/Avalanches: process, recognition and mitigation, VII of Reviews in Engineering Geology: Boulder, Colorado, Geological Society of America, p. 165-180.

Alt, D.D., and Hyndman, D.W., 1975, Roadside Geology of Northern California: Missoula, Montana, Mountain Press, 243 p.

Rodine, J.D., and Johnson, A.M., 1976, The ability of debris, heavily freighted with coarse clastic materials, to flow on gentle slopes: Sedimentology, v. 23, p. 213-234.

Rosiwal, A., 1898, Uber geometrische Gesteinsanalysen: Verhandl. der K-K geologische Reichanstalt, v. 5/6, p. 143.

Russ, J.C., 1986, Practical Stereology: New York, Plenum Press, 185 p.

Sadagah, B.H., and Sen, Z., 1992, block size distribution and quality classification in naturally fractured rocks: Bulletin of the Association of Enginering Geologists, v. XXIX, p. 405-414.

Sadagh, B.H., and de Freitas, M.H., 1993, Reconnaissance studies for assessing the stability of slopes in weak rock masses in the mountains of Western Saudi Arabia, in The enginering geology of weak rock: Rotterdam, AA Balkema, p. 347-352.

Sammis, C.G., King, G., and Biegel, R.L., 1987, The kinematics of gouge deformation: Pure and Applied Geophysics, v. 125, p. 777-812.

Savage, W.Z., and Chleborad, A.F., 1982, A model for creeping flow in landslides: Bulletin of the Association of Engineering Geologists, v. XIX, p. 333-338.

Savage, W.Z., and Smith, W.K., 1986, A model for the plastic flow of landslides, 1385 of US Geological Survey Professional Paper: Washington, DC, United States Geological Survey, 32 p.

Savely, J.P., 1990, Determination of shear strength of conglomerates using a Caterpillar D9 ripper and comparison with alternative methods: International Journal of Mining and Geological Engineering, v. 8, p. 203-225.

Savina, M.E., 1982, Studies in bedrock lithology and the nature of downslope movement: University of California, Berkeley, California, Ph.D. Dissertation, 298 p.

Schlocker, J., 1974, Geology of the San Francisco North Quadrangle [2nd printing, 1978 ed.] USGS Professional Paper 782; 105 p.

Schwab, W.C., Lee, H.J., Kayen, R.E., Quinterno, P.J., and Tate, G.B., 1988, Erosion and slope instability on Horizon Guyot, Mid-Pacific Mountains: Geo-Marine Letters, v. 8, p. 1-10.

Scullin, C.M., 1994, Subsurface explorations using bucket auger borings and down-hole geologic inspection: Bulletin of the Association of Engineering Geologists, v. XXXI, p. 91-105.

Seiders, V.M., 1982, Geologic map of an area near York Mountain, San Luis Opispo County, California: USGS Miscellaneous Investigations Map I-1369, scale 1:24,000.

Selley, R.C., 1988, Applied sedimentology: New York, Academic Press, 446 p.

Sen, Z., 1992, Fractal Dimension and Rock Quality Charts: Bulletin of the Association of Engineering Geologists, v. XXIX, p. 77-85.

Shakoor, A., and Cook, B.D., 1990, The effect of stone content, size and shape on the engineering proerties of a compacted silty clay: Bulletin of the Association of Engineering Geologists, v. XXVII, p. 245-253.

Sheridan, M.F., Zemtsov, A.N., and Macias, J.L., 1992, A detailed study of the size distribution of large volcanic blocks at Ksudach, Kamchatka: evidence for fractal fragmentation, Abstract SE22B-5, Program with Abstracts, Western Pacific Geophysics Meeting, American Geophysical Union; p 59.

Shi, G.-H., 1993, Block system modeling by Discontinous Deformation Analysis, 2 of Topics in Engineering: Boston, Computational Mechanics Publications.

Silberling, N.J., Jones, D.L., Blake, M.C., and Howell, dg, 1987, Lithotectonic terranes of the western United States: USGS Miscellaneous Field Studies, v. 1987, p. 20.

Silver, E.A., and Beutner, E.C., 1980, Melanges: Geology, v. 8, p. 32-34.

Skempton, A.W., 1966, Some observations on tectonic shear zones, in Proc. 1st Conference International Society of Rock Mechanics: p. 329-335.

Solomon, E., and Bahr, J., 1982, Seismic safety analysis of Lower Crystal Springs Dam: a case history: Bulletin of the Association of Engineering Geologists, v. XIX, p. 411-426.

Suppe, J., 1985, Principles of Structural Geology: Englewood Cliffs, New Jersey, Prentice-Hall, 537 p.

Taira, A., Byrne, T., and Ashi, J., 1992?, Photographic atlas of an accretionary prism: geologic structures of the Shimanto Belt, Japan: Tokyo, Univ. of Tokyo Press.

Takeshi, U., and Mizutani, S., 1979, Geological Structures: New York, John Wiley and Sons, 304 p.

Tang, W., and Quek, S.T., 1986, Statistical model of boulder size and fraction: Journal of Geotechnical Engineering; ASCE, v. 112, p. 79-90.

Tchalenko, J.S., 1970, Similarities between shear zones of different magnitudes: Bulletin of the Geological Society of America, v. 81, p. 1625-1640.

Ter-Stepanian, G., 1963, On the long-term stability of slopes, 52 of Norwegian Geotechnical Institute Publication: Oslo, Norway, Norwegian Geotechnical institute; p. 1-13.

Terzaghi, K., and Peck, R.B., 1967, Soil mechanics in engineering practice [2nd ed.]: New York, John Wiley and Sons, 730 p.

Thomson, E., 1930, Quantitative Microscopic Analysis: Journal of Geology, v. XXXVIII, p. 193-222.

Trautmann, C.H., 1976, Engineering Geology of Franciscan Melange terrane in the Red Hill area, Petalume, California: Stanford University, Stanford, Palo Alto, California, MS Thesis, 74 p.

Turcotte, D.L., 1986, Fractals and fragmentation: Journal of Geophysical Research, v. 91, p. 1921-1926.

---, 1992, Fractals and Chaos in Geology and Geophysics [1st ed.]: New York, NY, Cambridge University Press, 221 p.

Underwood, E.E., 1970, Quantitative Stereology: Reading, MA, Addison-Wesley Publ. Co. (Copyright 1981 by E. Underwood), 273 p.

Van Velsor, J.E., and Walkinshaw, JL, 1992, Accelerated movement of a large coastal landslide: Annual Meeting of the Transportation Research Board, Jan. 1992, Washington, DC

Varnes, D.J., 1978, Slope movement types and processes, in Schuster, R.L. and Krizek, R.J., eds.; Landslides: Analysis and Control, Special Report 176, Transportation Research Board, National Academy of Sciences, Washington, D.C., p. 11-33

Volpe, R.L., Ahlgren, C.S., and Goodman, R.E., 1991, Selection of engineering properties for geologically variable foundations, in Question 66:Proceeding of the 17th Int. Congress on Large Dams; Vienna: Paris, ICOLD, p. 1087-1101.

Wahler Associates, 1977, Final Report: Investigation of seismic stability, Lower Crystal Springs Dam; vol 1: text; prepared in association with Lindvall, Richter & Assoc and Group 10 Systems, for San Francisco Water Department.

Wahrhaftig, C., 1984a, Streetcar to Subduction [revised ed.]: Washington, DC, American Geophysical Union, 76 p.

---, 1984b, Structure of the Marin Headlands block, California: a progress report, in Blake, M.C., ed., Franciscan geology of northern California: Los Angeles, California, Pacific Section, Soc. Econ. Paleontologists and Mineralogists, p. 31-50.

Wahrhaftig, C. and Cox, A., Rock glaciers in the Alaska Range; Bull. Geol. Soc. America, v. 70, p. 383-436

Warburton, P.M., 1980, A stereological interpretation of joint trace data: International Journal of Rock Mechanics, Mining Science and Geomechanics Abstracts, v. 17, p. 181-190.

Watari, M., et al., 1988, Landslide in Japan: The Japan Society of Landslides/National Conference of Landslide Control, 54 p.

Weibel, E.R., 1979, Stereological Methods, vol. 1: Practical Methods for Biological Morphometry: New York, Academic Press, v. 1.

---, 1980, Stereological Methods, vol. 2: Theoretical Foundations: New york, NY, Academic Press, v. 2, 340 p.

West, L.J., 1992, The shear behaviour of heterogeneous soils: Department of Earth Sciences, University of Leeds, UK, Ph.D. Dissertation, 284 p.

West, L.J., Hencher, S.R., and Cousens, T.W., 1991, Assessing the stability of slopes in heterogeneous soils, in Bell, D.H., ed., Proc. of the 6th International Symposium on Landslides; Christchurch, NZ: Rotterdam, AA Balkema, p. 591-595.

Wittke, 1990, Rock Mechanics: Theory and applications with case histories (Translated from German by Richard Sykes, in cooperation with Stephen Semprich and Bertold Plischke): New York, Springer-Verlag, 1066+ p.

Wood, D.S., 1974, Ophiolites, melanges, blueschists and ignimbrites: early Cretaceous subduction in Wales?, in Dott, R.H., and Shaver, R.H., eds., Modern and Ancient geosynclinal sedimentation: Soc Econ Paleontologists and Mineralologists, p. 334-343.

WCC, 1993a, Richmond Transport Project, San Francisco, CA; Geotechnical Baseline Report; prepared for Dept. Public Works, City and County of San Francisco, California: Oakland, California, Woodward-Clyde Consultants.

-------, 1993b, Richmond Transport Project, San Francisco, CA; Geotechnical Data Report, vol 1- Report; prepared for Dept. Public Works, City and County of San Francisco, California: Oakland, California, Woodward-Clyde Consultants.

-------, 1993c, Richmond Transport Project, San Francisco, CA; Geotechnical Data Report, vol 2 - Appendices; prepared for Dept. Public Works, City and County of San Francisco, California: Oakland, California, Woodward-Clyde Consultants.

Wright, R.H., 1984, Geology of the Nicasio Reservoir Terrane, Marin County, California, in Blake, M.C., ed., Franciscan Geology of northern California: Los Angeles, California, Pacific Section, Soc. Ecom. Paleo and Min., p. 99-112.

Xie, H., and Pariseau, W.G., 1993, Fractal character and mechanism of rock bursts: International Journal of Rock Mechanics, Mining Science and Geomechanics Abstracts, v. 30, p. 343-350.

Yilmazer, I., 1993, Engineering characteristics of melanges in Turkey; Abstract sent to E. Medley; contact: Dr. I. Yilmazer, Earth Sciences Investigation and Consultant Co., Ankara, Turkey.

Yoder, H.S., and Chesterman, C.W., 1951, Jadeite of San Benito County, California, 10-C of Special Publication: San Francisco, California Division of Mines (and Geology), 8 p.

APPENDIX A

World-wide Distribution of Melanges

A1.0 INTRODUCTION

Melange bodies have been mapped in several parts of the world, as shown in abbreviated fashion by Raymond and Terranova (1984; their Figure 1). At the beginning of my work, I wished to better understand the world-wide distribution of melanges, so that I could locate engineering literature related to melanges by writing to academic and government agencies in the several dozen countries that host melanges. The search yielded some very useful information, and generated considerable interest amongst engineers and geologists in several parts of the world. Furthermore, I developed a relatively comprehensive database of melange references that allowed me to produce summary illustrations of the world-wide distribution melanges relative to countries and mountainous regions (Figures A1 and A2, also reproduced in the main body of the text).

More detailed regional maps of the distribution of melanges are also shown in this Appendix.

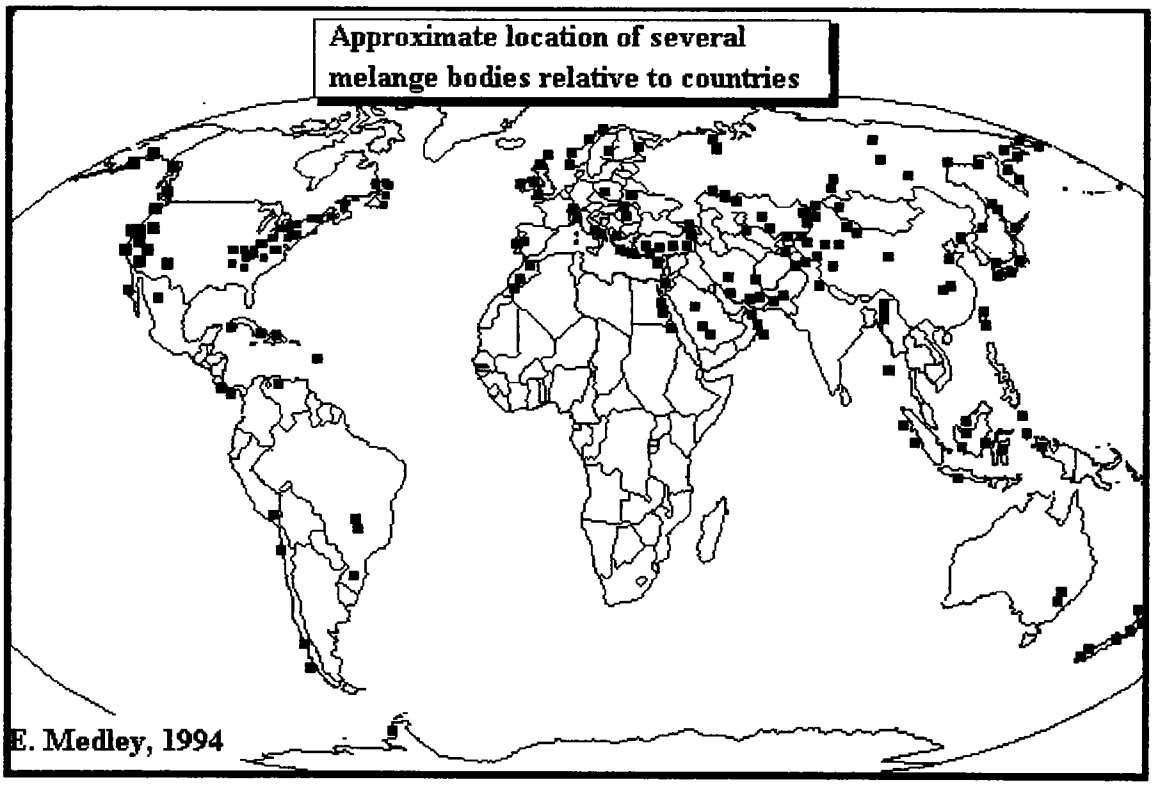

Figure A1. World-wide distribution of melanges, relative to countries.

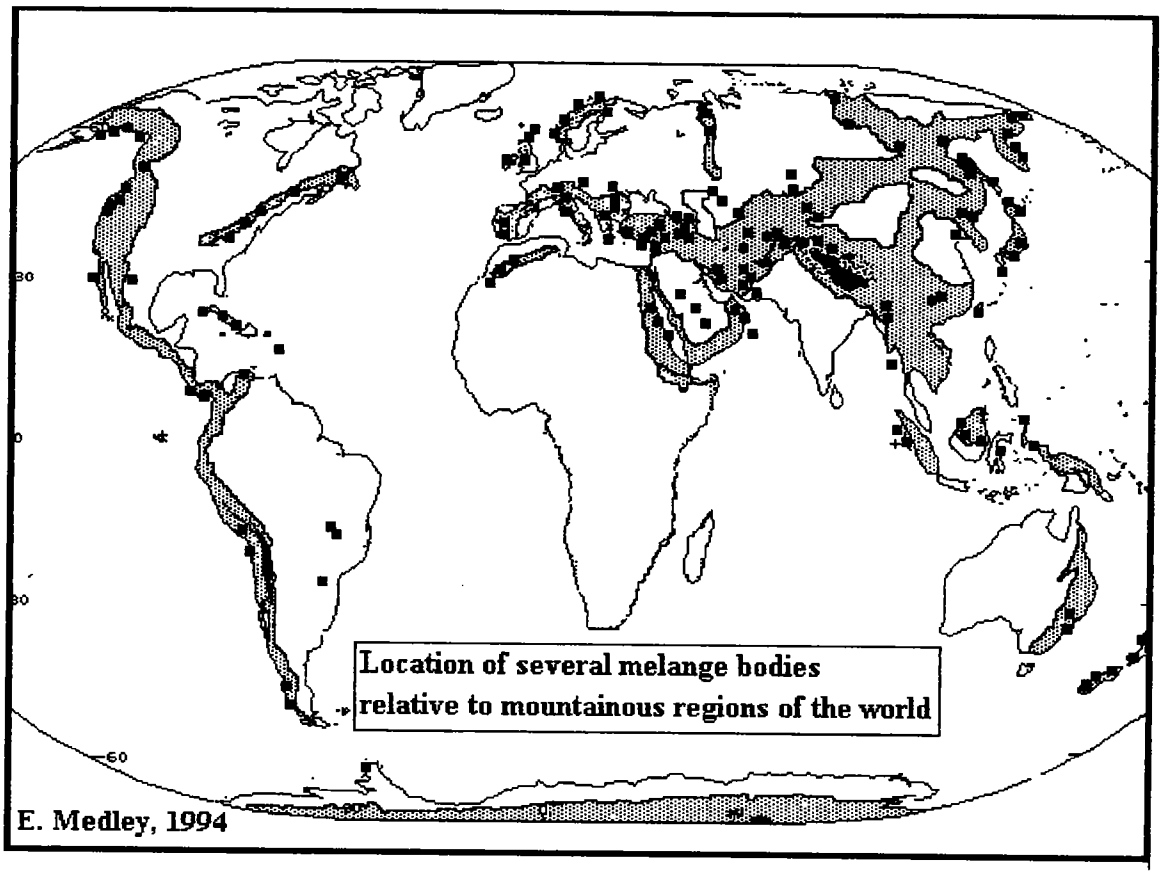

Figure A2. World wide distribution of melanges relative to mountainous areas of the world.

The database forming the basis for the figures in this Appendix was created in several steps:

1. The GeoRef ™ computer-based geosecience database (published by the American Geological Institute) was interrogated for all references (to summer 1993) showing the word "melange". Some 1960 references identified by the search were downloaded onto 1.2 MB floppy disks in ASCII format.

2. The source data were input into a computer-based bibliographic database. I used the Papyrus™ (version 7.0)[1] software to import the references. I modified the program's default import protocols in order to retain several useful data fields for each reference, including map co-ordinates of study areas. The import and subsequent automatic organization of the records took the better part of 12 to 16 hours for two computers (286 and 386 machines) running full-time. Almost 7000 thousand keywords were preserved, including over 70 country names.

---

[1]Research Software Design; 2718 SW Kelly St., Suite 181; Portland, Oregon 97201; phone: (503) 796-1368; FAX: (503) 241-4260; e-mail: RSWD@applelink.apple.com

3. The Papyrus™ database was interrogated to sort the literature references by country and group them accordingly. References for the United States and Canada were subdivided by state, and those for California further subdivided by county.

4. An attempt was made to plot the location of each country, state or county reference. Since the reference keywords often contained geographic names, a large, comprehensive atlas with a gazeteer were used. Many references in the database have map coordinates, which were useful. Using the geographic placenames and coordinates, the locations were plotted onto country maps produced from the geographic software World Atlas (v. 3.0)[2] . These maps are also the basis for the maps in this Appendix. Some imagination was neccessary in interpreting foreign place names (particularly Chinese and Russian), and it is readily confessed that some melanges may be shown incorrectly. (There is a big geographic difference between Redding, California and Reading, England, even if the phonetics of the names are the same....). My own extensive travel experience helped me in the enjoyable exercise of locating the reference study areas.

5. A selection of the locations were plotted on the world and regional maps, as shown in this Appendix (below). Having identified the countries and the general areas of the melange bodies, I was then able to write to foreign scholars and agencies requesting information related to the geo-mechanical properties and behavior of the melanges in their countries. Most of the names and addresses of the correspondents were provided on computer floppy disks (for a nominal charge) provided by the National Landslide Information Center of the USGS in Denver[3]. The request for literature was performed as a "mail-merge" blitz: some 180 letters were eventually mailed out, and several dozen people replied. Some of the literature received was of considerable interest, particularly to my colleague Eric Lindquist in his study on the mechanical behavior of model melanges (Lindquist, 1994).

6. Papyrus™ was used to print out the citations and the bibliography for the selected references shown in this Appendix; indeed, the exercise would not have been done without this invaluable software.

The remainder of this Appendix is considered a resource to others. It contains several regional maps showing the general location of melange bodies, and a selection of references in the geological literature. As will be seen, there are virtually no references that appear to address the engineering aspects of melanges.

---

[2]The Software Toolworks, Inc.; 60 Leveroni Court; Novato, California 94949; phone (415) 883-5157
[3]National Landslide Information Center; US Geological Survey; Box 25046-MS 966; Denver Federal Center; Denver, Colorado 89225-0046; phone (800) 654-4966; FAX (303) 273-8600

A2.0 APPROXIMATE LOCATION OF MELANGE BODIES WITHIN SEVERAL REGIONS OF THE WORLD

A2.1 NORTH AMERICA

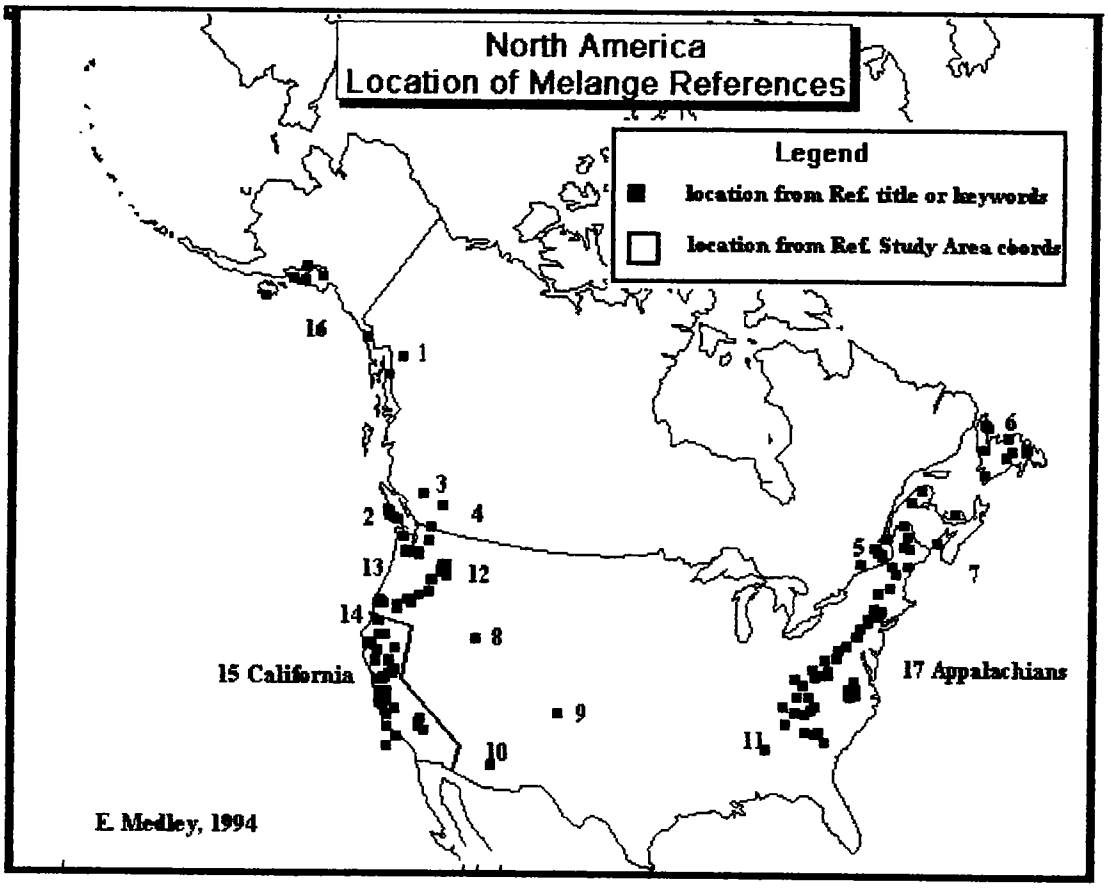

Figure A3. Approximate location of some melange bodies in North America.

Canada

British Columbia: **area 1**: Leaming, 1980
area 2: Page, 1974, 1975; Brandon, 1985, 1989a, b
area 3: Nagel, 1979
area 4: Orchard, 1984

Quebec: **area 5**: Doolan and others, 1981; de Broucker, G. and St Pierre, J., 1985; Boudette and others, 1989; Tremblay, 1990; Cousineau, 1991

Newfoundland: **area 6:** Kay, 1972, 1975, 1976; Williams, H. and Hibbard, 1976; Williams, H. and Talkington, 1978; Jacobi, 1980; Wasowski and Jacobi, 1982; Horne and McKibbin, 1983; Wasowski, 1983; Hibbard, 1987; Wojtal, 1987; Savci, 1988; Blewett, 1989

New Brunswick: **area 7:** Rast and Grant, 1974; Rast and Stringer, 1980

United States

Only a few references for the US are reported here, since there are over 450 references in the California list alone, and the intent is merely to hint at the locations of melanges. The samples of references are organized by state, as shown on the map.

Utah, **area 8:** Schurer, 1979
New Mexico, **area 9:** Shore and Duncan, 1983; Duncan and Shore, 1984
Arizona, **area 10:** Swift, 1987a, b
Alabama, **area 11**: Tull and Telle, 1989
Idaho, **area 12**: Mullen and Sarewitz, 1983
Washington, **area 13**: Frizzell and others, 1982; Tabor, 1987; Jett and Heller, 1988; Snavely and Kvenvolden, 1989; Orange, 1990
Oregon, **area 14:** Worley and Raymond, 1978; Schmidt, W.J., 1980; Ahmad, 1981; Gullixson, 1981; Mullen and Sarewitz, 1983; Brooks and Ferns, 1985; Carpenter and Walker, 1990

California, **area 15;** shown in approximate north to south order:
Hsu, 1969; Cowan, 1974; Gucwa, 1974, 1975; Kleist, 1974a, b; Crawford, K.E., 1975; Kelsey, 1976; Trautmann, 1976; Raymond and Aalto, 1978; Janda, 1979; Kelsey and others, 1979; Bedrossian, 1980a, b, 1982; Borchardt, 1980; Kintzer, 1980; Aalto, 1981, 1983, 1989a, b; Cloos, 1981, 1986, 1991; Barlow and Tracy, 1982; Petersen, 1982; Gonzalez and Dunne, 1983; Murphy and others, 1983; Wahrhaftig, 1984; Becker and Cloos, 1985; Herrington and Cloos, 1985; Kilbourne, 1986; Korbay and Russey, 1986; Larue and Hudleston, 1986; Barton and others, 1987; Blake and others, 1987; Lindsley and Fisher, 1989

Alaska, **area 16:** Plafker, 1973; Tysdal and Case, 1977; Byrne, 1981, 1985; Ditullio and Byrne, 1985; Shreve and Cloos, 1986

Appalachians, **area 17**: shown in approximate state order from north to south:
Maine: Pollock, 1982; Roy and Foster, 1990
Vermont: Bosworth and Kidd, 1985; Armstrong and Colpron, 1989
New Hampshire: Moench and others, 1984
Connecticut: Spinek, 1988
Maryland: Freeman and others, 1988
New York: Vollmer, 1981; Bosworth, 1983; Xia, 1983; Bosworth and Kidd, 1985
Pennsylvania: Lash, 1987
North Carolina: Higgins, J.B. and others, 1980; Horton and others, 1985; Raymond and others, 1989
South Carolina: Butler, 1987; Maybin and Mittwede, 1988; Mittwede, 1988; Mittwede and Maybin, 1989
Virginia: Brown, 1976, 1986; Schultz, 1979a

A2.2 CARIBBEAN REGION

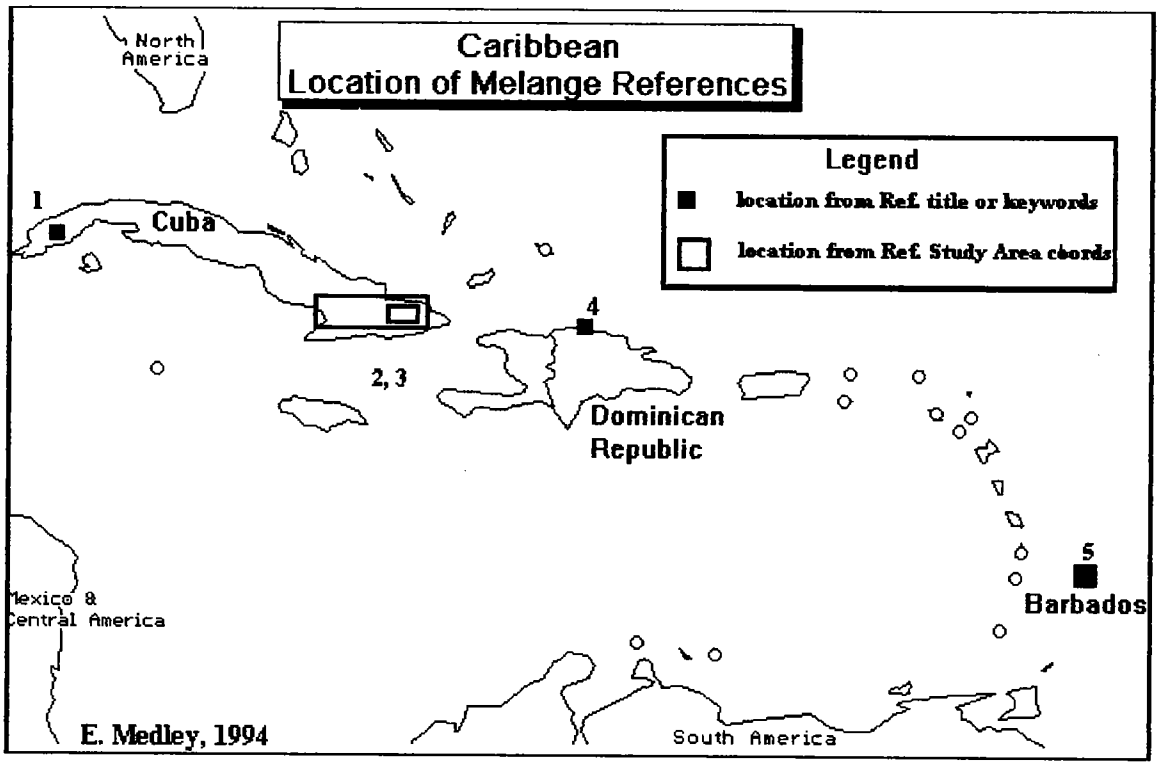

Figure A4. Approximate location of some melange bodies in the Caribbean Region.

Cuba area 1: Aniatov and others, 1982, 1983

area 2 and 3 : Cobiella, 1978; Quintas and Carralero, 1982

Dominican Republic area 4: Draper and others, 1984; Draper and Nagle, 1985

Barbados area 5: Larue, 1984; Larue and Speed, 1984; Larue and Suess, 1985; Torrini and others, 1985; Speed and others, 1991

A2.3 MEXICO and CENTRAL AMERICA

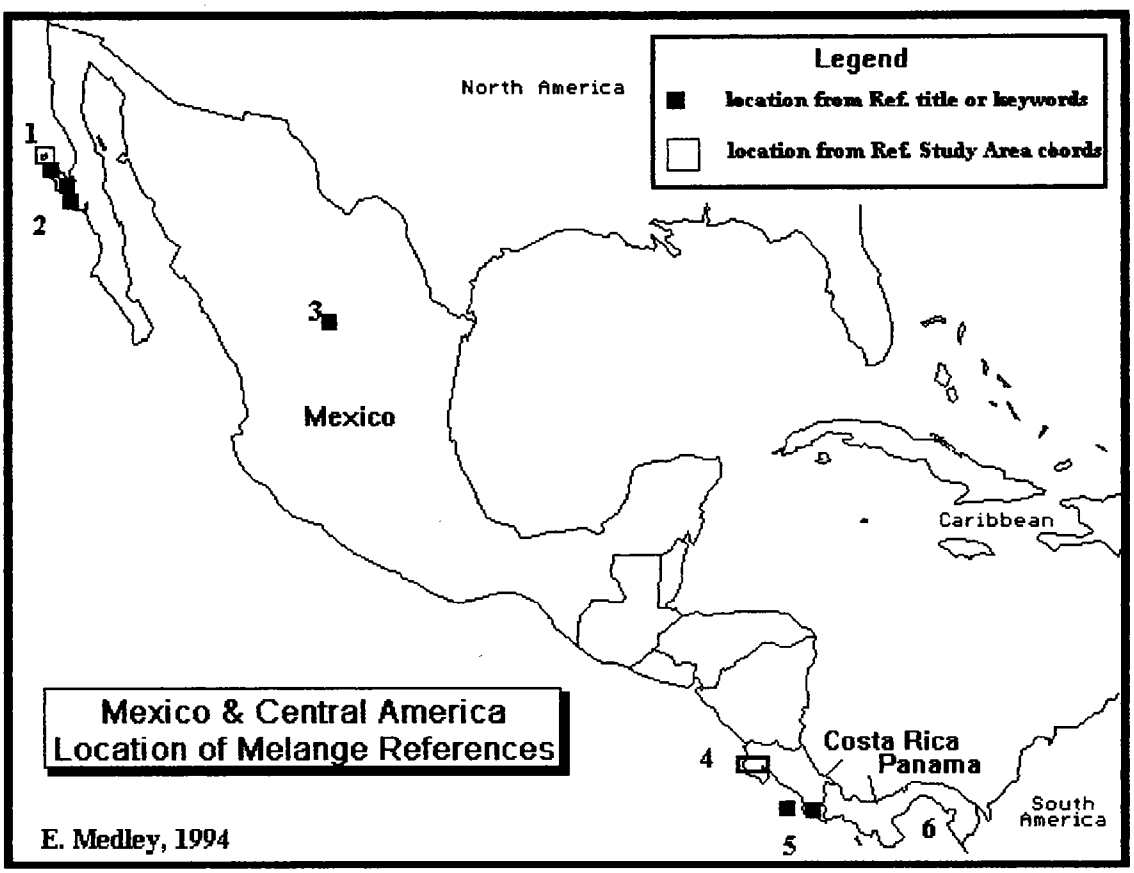

Figure A5. Approximate location of some melange bodies in Mexico and Central America.

Mexico area 1: Kimbrough, 1979, 1980, 1989; Rangin, 1979; Moore, T.E., 1980, 1984; Sedlock and Larue, 1984; Boles, 1986
area 2: Moore, T.E., 1976
area 3: Klein and others, 1990

Costa Rica area 4: Schmidt, E.R., 1979
area 5: Baumgartner, 1986

Panama area 6: Breen, 1987; Breen and others, 1988; McMillen and others, 1988

A2.4 SOUTH AMERICA

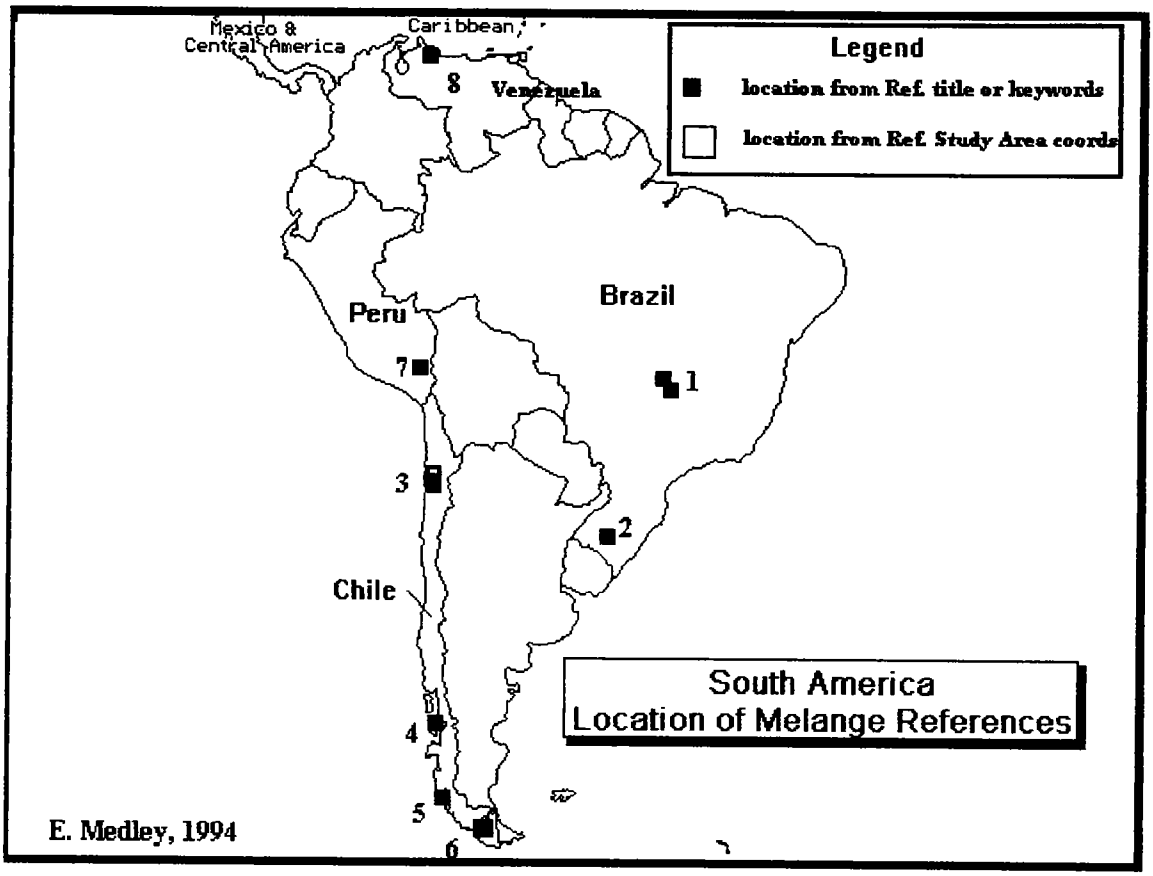

Figure A6. Approximate location of some melange bodies in South America.

Brazil area 1: Drake, 1980
area 2: Szubert, 1978

Chile area 3: Bell, 1982, 1987
area 4: Herve and others, 1981
area 5: Forsythe and Mpodozis, 1979, 1983
area 6: Wilson and others, 1987, 1989a, b

Peru area 7: DeJong, 1974

Venezuela area 8: Belizzia and others, 1972

A2.5 ANTARCTICA

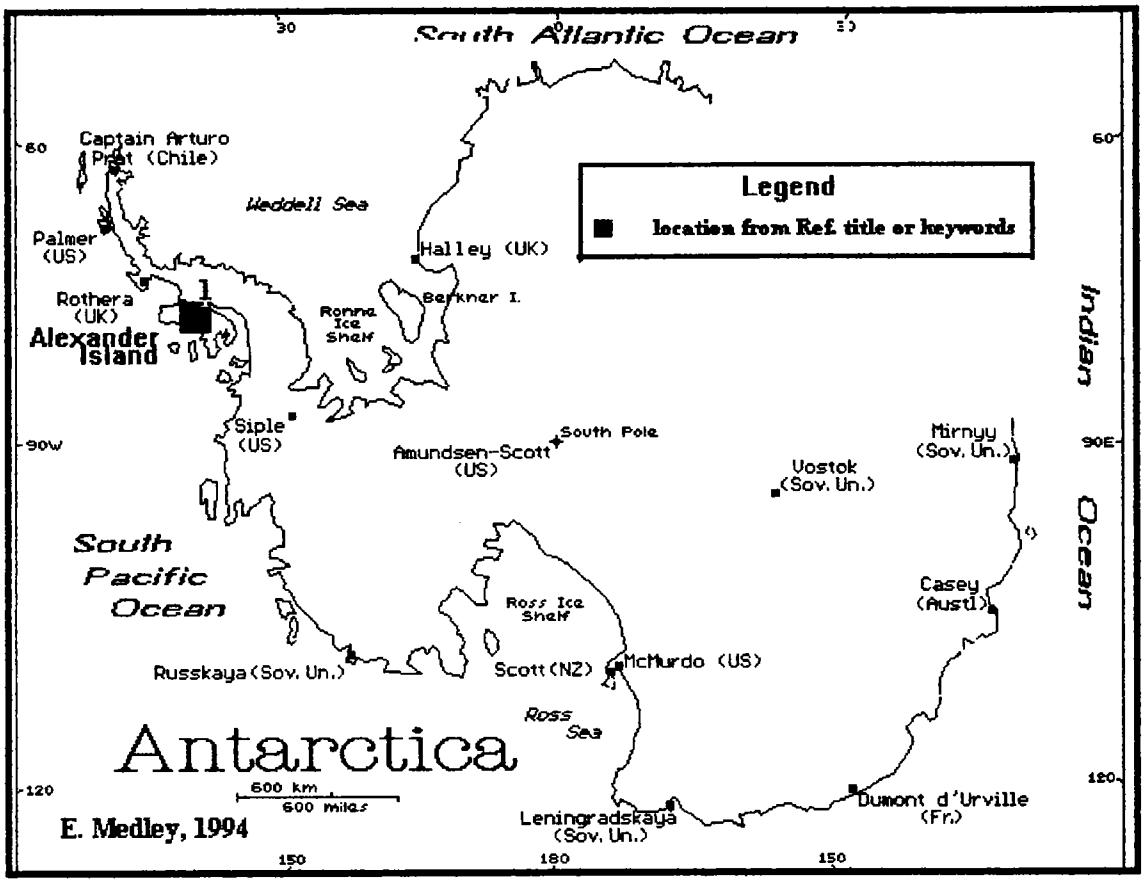

Figure A7. Approximate location of a melange body in Antartica.

Alexander Island: Tranter, 1986; Nell, 1990

A2.6 NORTH AFRICA

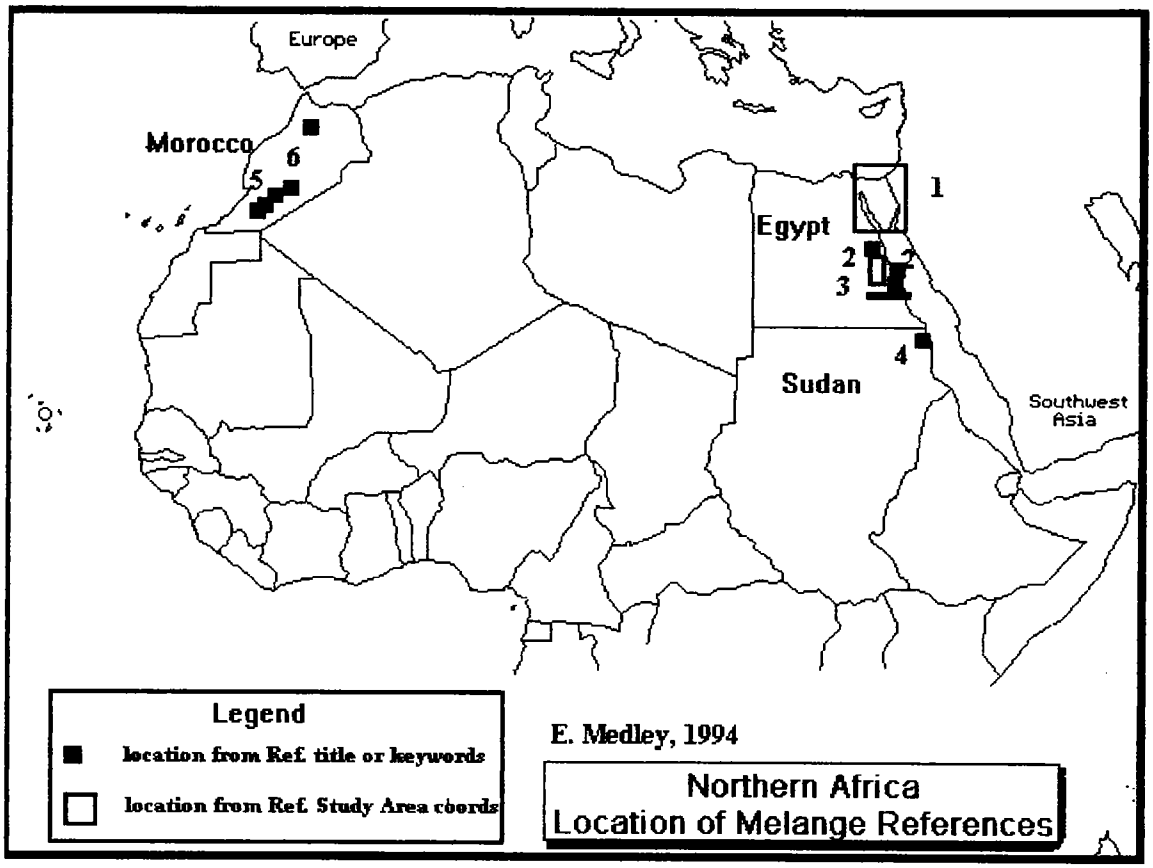

Figure A8. Approximate location of some melange bodies in North Africa.

Egypt area 1: Stern and others, 1985
area 2: Habib, 1987; Greiling and others, 1988; Abdel and others, 1990
area 3: El and El, 1979; Abdel and others, 1984; Rivard and others, 1988

Sudan area 4: Kroener, 1984; Abdelsalam and Dawoud, 1991

Morocco area 5: Saquaque and others, 1988, 1989; Naidoo and others, 1991
area 6: Pique, 1975; Saquaque and others, 1988, 1989; Naidoo and others, 1991

A2.7 EUROPE

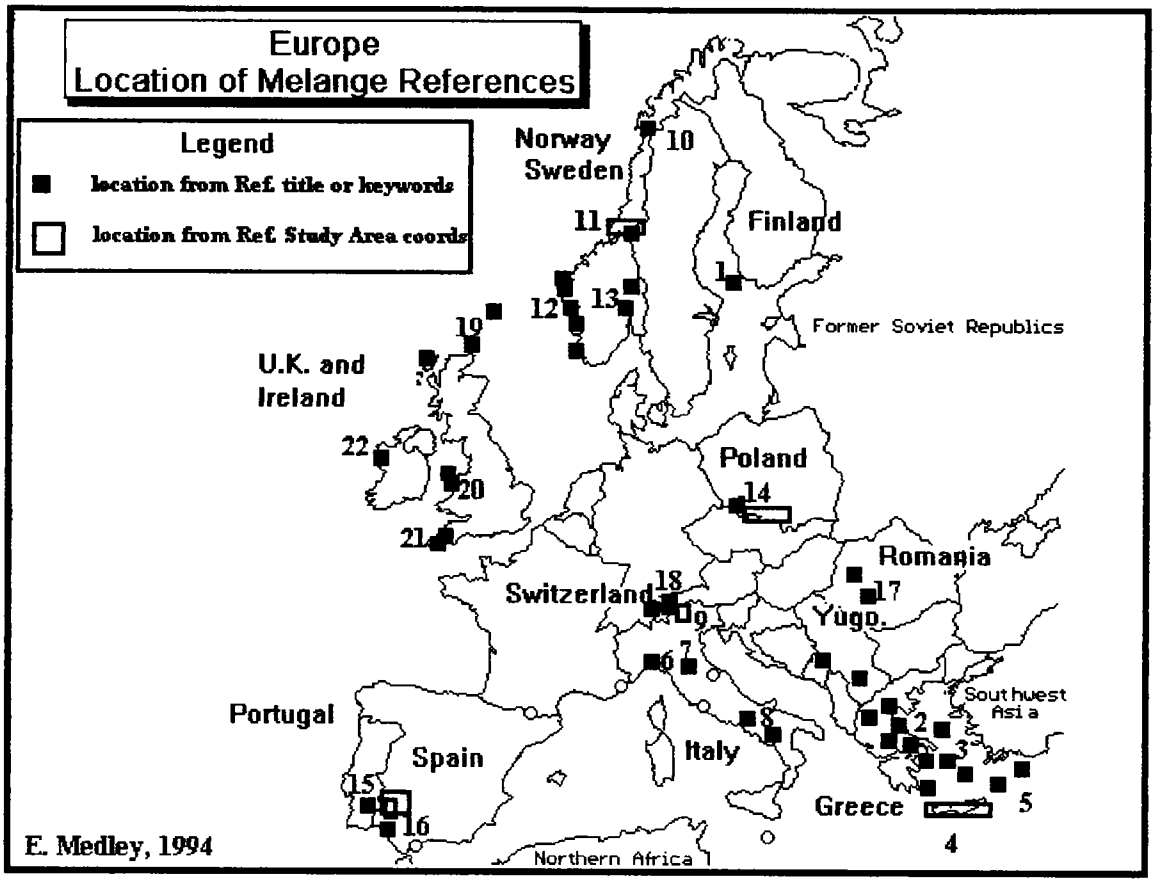

Figure A9. Approximate location of some melange bodies in Europe.

Finland area 1: Edelman and Jaanus, 1983

Greece area 2: Chiotis and Dimou, 1972; Jones and Robertson, 1991
area 3: Bonneau and others, 1980; Harder and others, 1983; Wallbrecher, 1983; Dietrich and others, 1987; Robertson, 1991
area 4: Seidel and others, 1977; Seidel, 1981; Hatzipanagiotou, 1983; Fortuin and Peters, 1984
area 5: Hatzipanagiotou, 1983, 1986

Italy area 6: Naylor, 1982; Hoogerduijn and Van, 1989
area 7: D'Elia and others, 1984
area 8: Spadea, 1982
area 9: Bosellini and others, 1982

Norway area 10: Crowley, 1985
area 11: Roberts and Horne, 1980; Nilsen, 1983
area 12: Thon, 1981; Bryhni and Lyse, 1985; Andersen and others, 1990
area 13: Horne, 1981; Nilsen, 1983

Poland area 14: Haydukiewicz, 1977; Wajsprych, 1978

Portugal area 15: Eden and Andrews, 1990a

Spain area 16: Chacon, 1982; Eden and Andrews, 1990b

Romania area 17: Maruntiu, 1983; Savu, 1984

Switzerland area 18: Dietrich, 1973; Weissert, 1975; Bayer, A.A., 1982

United Kingdom and The Republic of Ireland

area 19: Storey and Meneily, 1983; Flinn, 1985
area 20: Schuster, 1980; Grall and Bradbury, 1982; Bieler, 1983; Gibbons, 1989; Nicholson, 198?; Gibbons and Ball, 1991
area 21: Evans, 1981; Barnes, 1982, 1983, 1984; Eden and Andrews, 1990b
area 22: Kennedy, 1980

Yugoslavia area 23: Dimitrijevic and Dimitrijevic, 1976, 1979

A2.8 FORMER SOVIET REPUBLICS

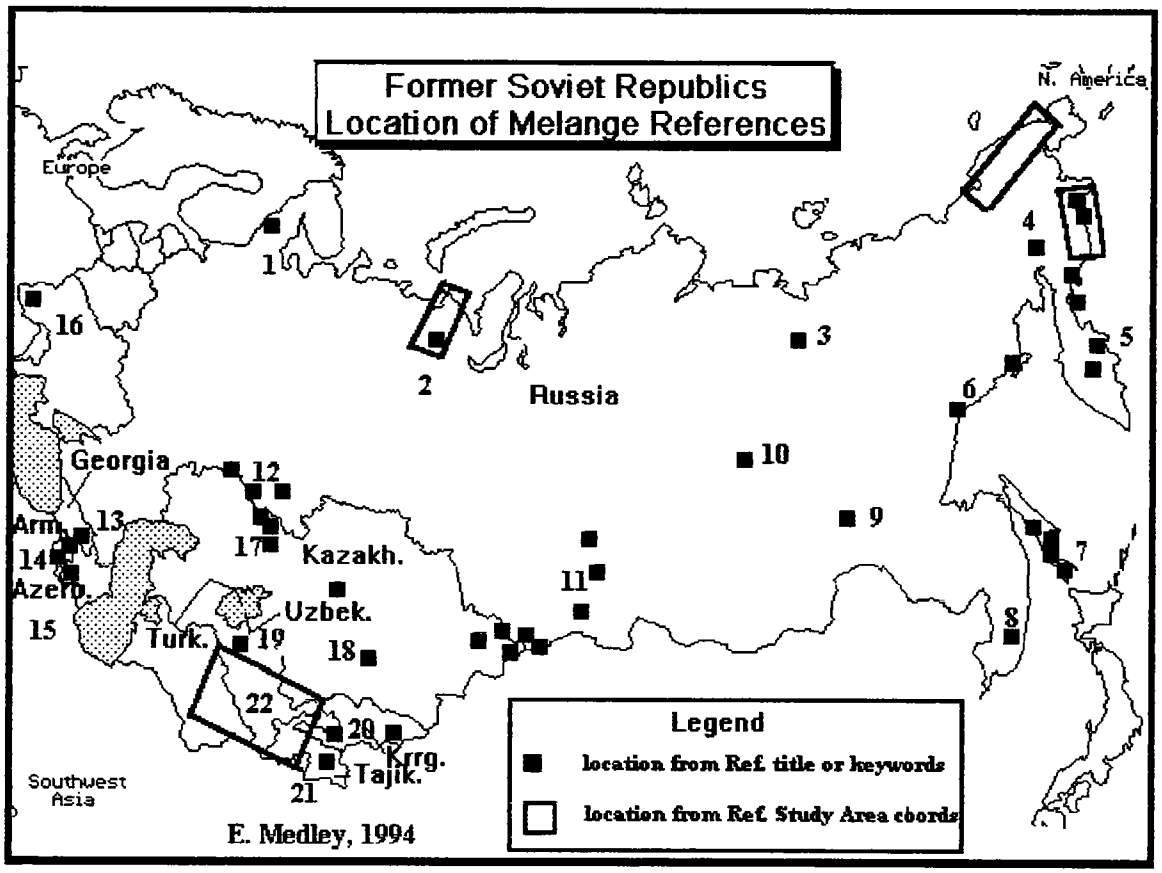

Figure A10. Approximate location of some melange bodies in the former USSR.

Russia area 1: Voytovich, 1983
area 2: Dergunov and others, 1975; Sobolev and Dobretsov, 1977
area 3: Parfenov, 1987
area 4: Aleksandrov, 1973; Ivanov and Baratov, 1974; Kolyasnikov, 1977; Nekrasov, 1978; Chekhov and others, 1980; Chekhov and Aleksandrov, 1982; Stavskii and others, 1988
area 5: Zhegalova, 1981; Simkin, 1982; Chekhovich and others, 1990
area 6: Itsikson, 1980; Bryan, 1990
area 7: Rozhdestvenskiy and Rechkin, 1975a, b; Raznitsin, 1978; Rikhter, 1981; Kimura and others, 1992
area 8: Mazarovich, 1978, 1979, 1982
area 9: Amarskii and Vetluzhskikh, 1990
area 10: Sizykh, 1984
area 11: Lyashenko, 1979; Golovko and Vishnevskaya, 1984; Akkermantsev and Yenikeyeva, 1986

Georgia area 13: Adamiya and others, 1989

Armenia area 14: Knipper, 1971a, b; Sokolov, 1974

Azerbaijan area 15: Satian, 1975; Dobrzhinetskaya and Ez, 1982

Ukraine area 16: Dolenko and Danilovich, 1975; Danilovich, 1981

Kazakhstan area 17: Abdulin and others, 1975; Kuzmin and Al'mukhamedov, 1983
area 18: Makarychev and others, 1983; Yermolov and Kotelnikov, 1991

Uzbekistan area 19: Sher and Vikhter, 1973; Ruzhentsev, 1975

Kyrgyzstan area 20: Kurenkov, 1978

Tajikistan area 21: Kukhtikov, 1974; Kurenkov, 1979

Turkmenistan area 22: Khristov and Khristova, 1979

A2.9 SOUTHWEST ASIA

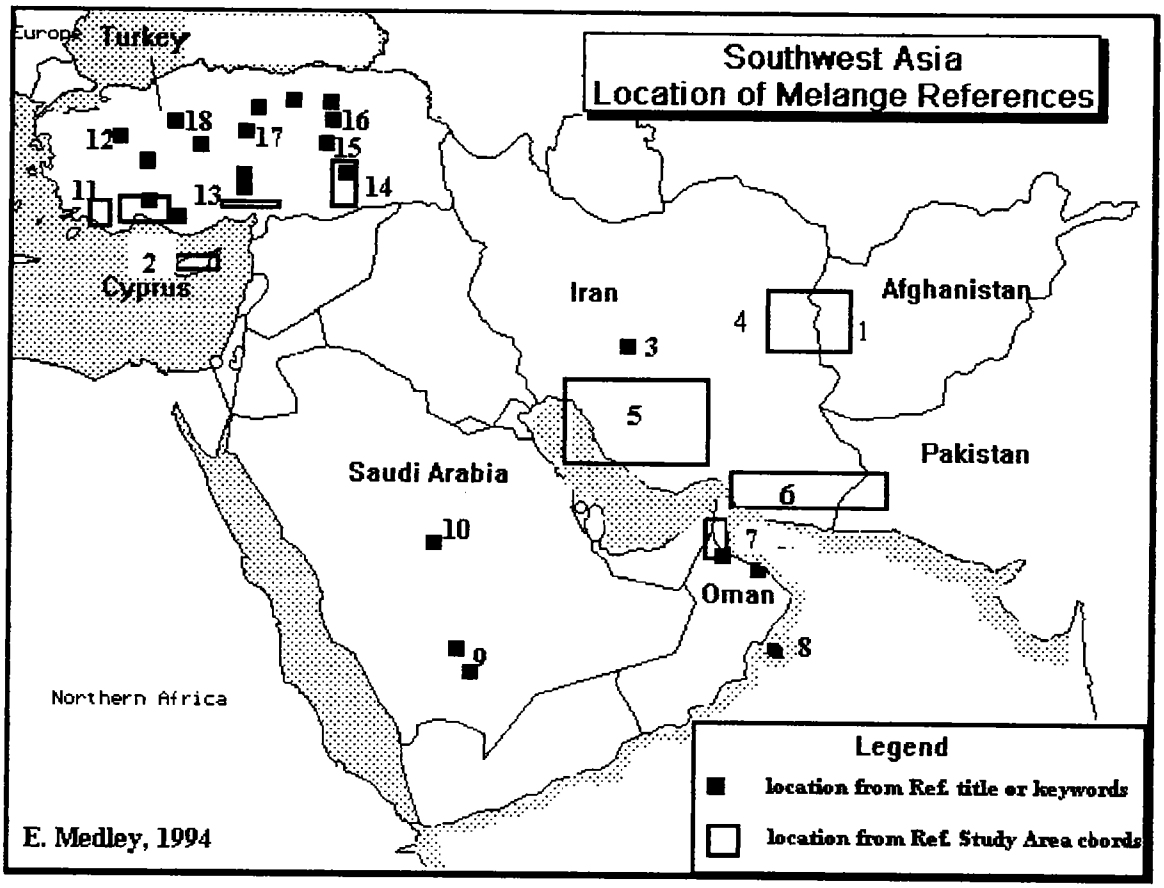

Figure 2.11. Approximate location of some melange bodies in Southwest Asia.

Afghanistan area 1: Sborshchikov, 1976; Sborshchikov and Sonin, 1977

Cyprus area 2: Auden and Robertson, 1978; Swarbrick and Naylor, 1980

Iran area 3: Davoudzadeh, 1969
area 4: Tirrul and others, 1983
area 5: Sestini and Pamic, 1980
area 6: McCall and Kidd, 1982

Oman area 7: Anonymous, 1981; Michard and others, 1981; Woodcock and Robertson, 1982
area 8: Abbotts, 1979; Moseley and Abbotts, 1979

Saudi Arabia area 9: Al and Warden, 1980; White, 1983
area 10: Camp and others, 1984

Turkey

area 11: Graciansky, 1973; Robertson and Woodcock, 1981; Hayward, 1984; Ozgul, 1984; Ozkaya, 1990
area 12: Okay, 1981; Kocyigit, 1984; Waldron, 1984
area 13: Floyd and others, 1992
area 14: Ozkaya, 1978; Hempton, 1982, 1985
area 15: Hempton, 1984
area 16: Tatar, 1975; Bektas, 1982; Oygur, 1990
area 17: Yilmaz, 1981, 1984a, b
area 18: Norman, 1975; Seymen, 1983

A2.10 SOUTH ASIA

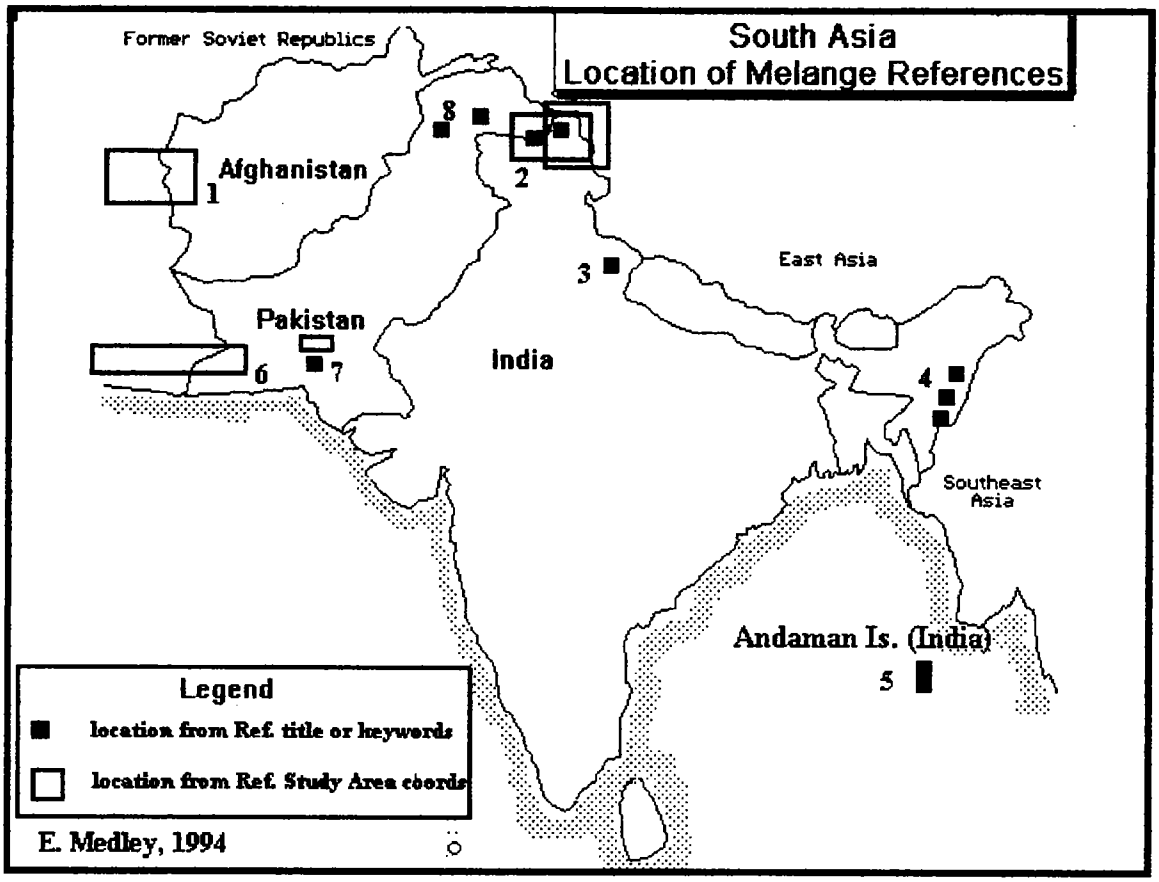

Figure A12. Approximate location of some melange bodies in South Asia.

Afghanistan area 1: see under Southwest Asia Region

India area 2: Shah and Gergan, 1980; Thakur, 1980; Tewari, 1981; Sharma, 1983; Rai, 1984, 1985
area 3: Chatterjee and Sen, 1984
area 4: Nandy, 1982; Roy and Kacker, 1984; Acharyya and others, 1990
area 5: Acharyya and others, 1990

Pakistan area 6: see Iran, area 6, Southwestern region
area 7: DeJong and Subhani, 1979; Sarwar, 1981, 1982
area 8: Kazmi and others, 1986; Chamberlain and others, 1991

A2.11 EAST ASIA

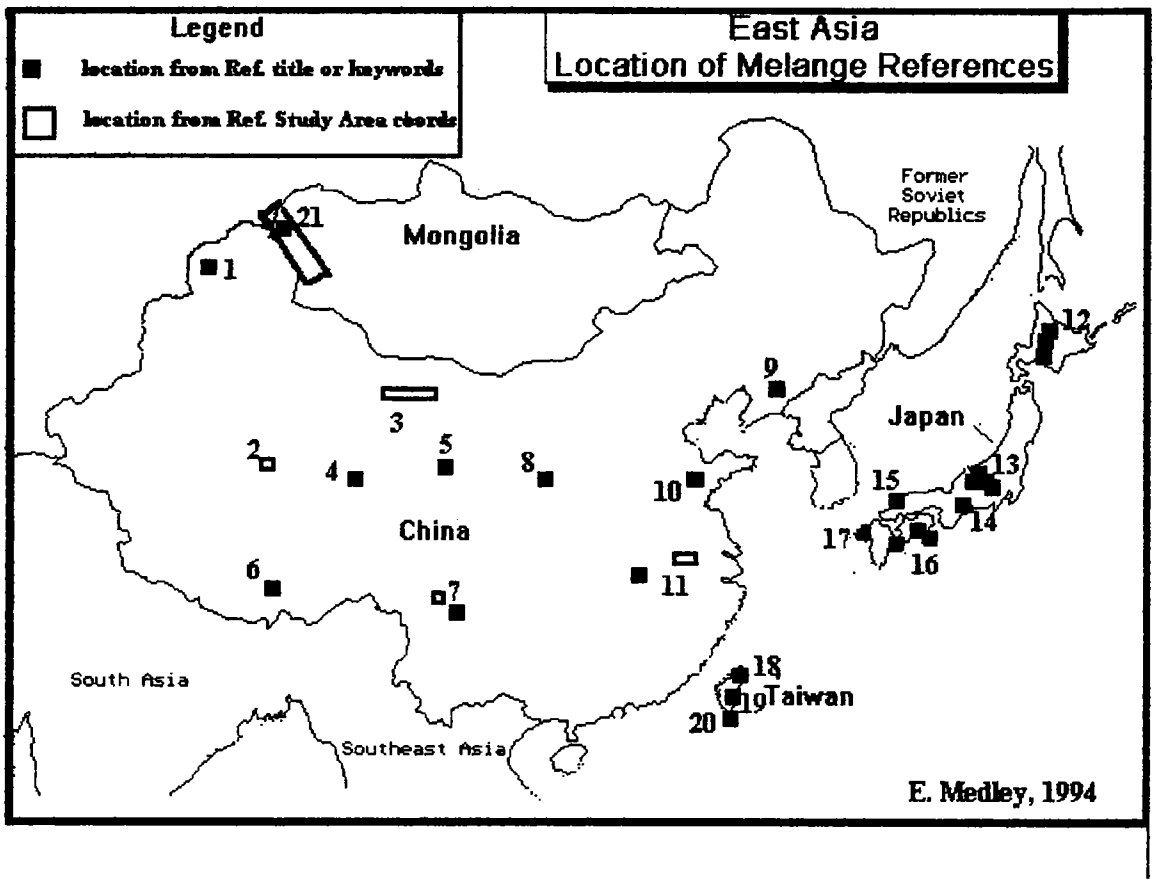

Figure A13. Approximate location of some melange bodies in East Asia.

China area 1: Feng and others, 1985; Xiao and others, 1985
area 2: Burchfiel and others, 1989
area 3: Huang, Q. and Liang, 1981; Zuo and others, 1987, 1990
area 4: Zhu and others, 1984
area 5: Pan and others, 1980
area 6: Wu and others, 1982
area 7: Zhang and Jin, 1979; Li and Zhang, 1985
area 8: Feng and Zhu, 1980
area 9: Cui, W., 1990
area 10: Liu and others, 1989
area 11: Zhang and Jin, 1979; Cui, K., 1987

Japan area 12: Maekawa, 1983, 1989; Nakagawa and Toda, 1987
area 13: Wakita, 1988; Nakamizu and others, 1989; Saito, 1989; Okamura, 1991
area 14: Saka and others, 1988
area 15: Watanabe and others, 1989
area 16: Sakai, 1981; Hada, 1988; Hibbard, 1988; DiTullio and Byrne, 1990
area 17: Nishiyama, 1989

Taiwan area 18: Lu and others, 1989
area 19: Page and Suppe, 1981; Suppe and others, 1981; Lee and Wang, 1987
area 20: Huang, C.Y. and others, 1985; Pelletier and others, 1985; Pelletier and Stephan, 1986

Mongolia area 21: Dergunov and Luvsandanzan, 1984, 1990

A2.12 SOUTHEAST ASIA

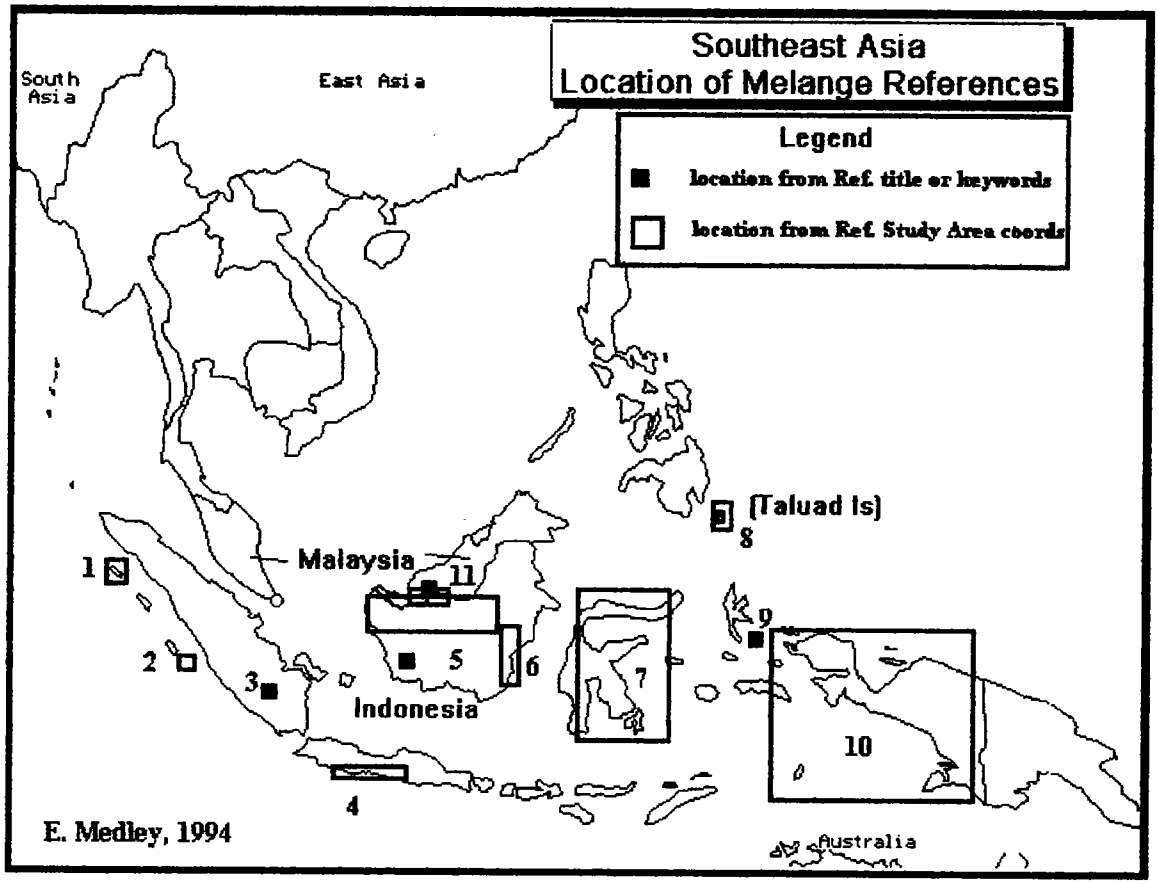

Figure A14. Approximate location of some melange bodies in Southeast Asia.

Indonesia area 1: Moore and others, 1976; Moore, 1978, 1979; Moore and Karig, 1980
area 2: Budhitrisna, 1989
area 3: Tasrif, 1985
area 4: Thayyib and others, 1977
area 5: Williams, P.R. and others, 1986
area 6: Supriatna, 1989
area 7: Silver, 1978, 1979
area 8: Moore and others, 1980; Sukamto, 1980; Evans and others, 1983
area 9: Sartono and Hadiwisastra, 1990
area 10: Williams, P.R. and others, 1984

Malaysia area 11: Kiat, 1975, 1979; Liaw, 1980; Tan, 1982

A 2.13 AUSTRALIA and OCEANIA

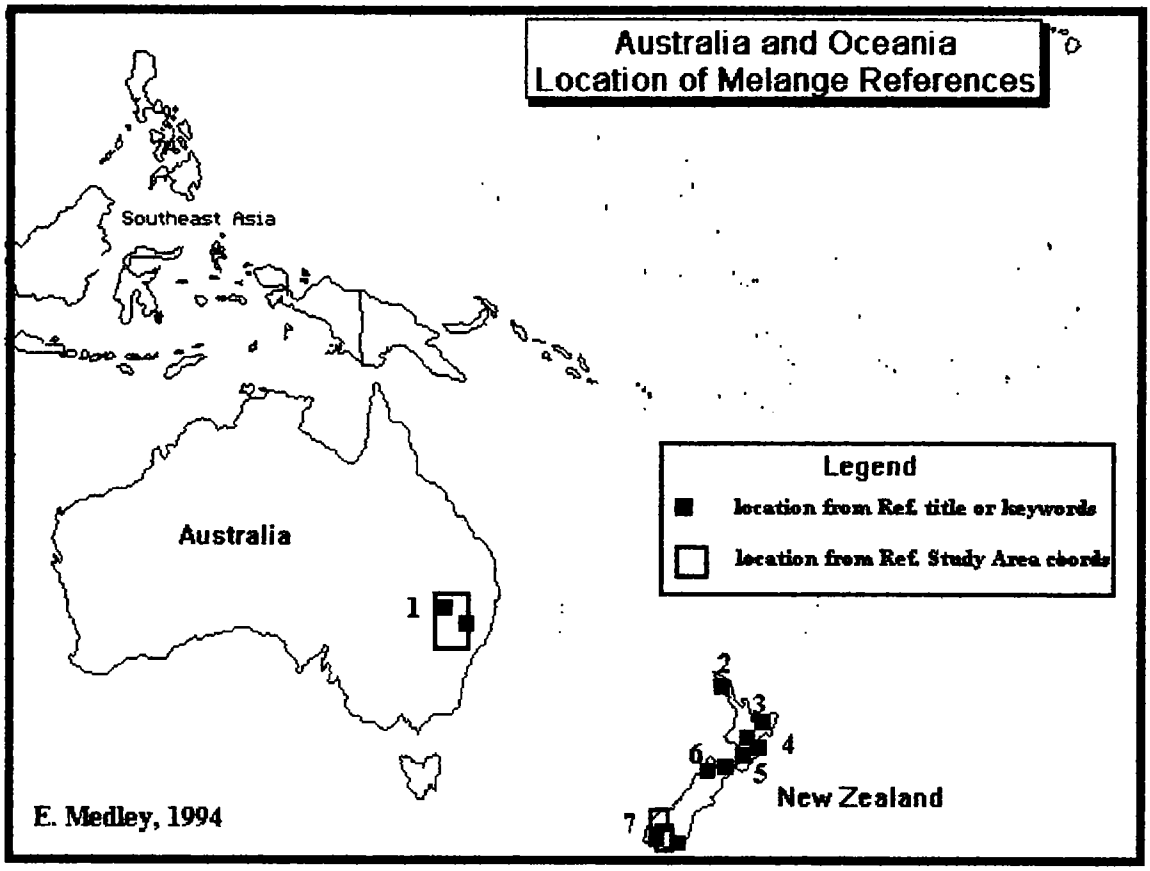

Figure A15. Approximate location of some melange bodies in Australia and New Zealand.

Australia area 1: Pooley, 1979; Williams, A.J., 1979; Fergusson, 1984

New Zealand area 2: Spoerli, 1987; Spoerli and Aita, 1988
area 3: Feary, 1979; Feary and Pessagno, 1980
area 4: Sporli and Bell, 1976; Kobe and Pettinga, 1984
area 5: Foley and Orr, 1984; Rattenbury, 1986
area 6: Dickens and others, 1985; Dickins and others, 1986
area 7: Bishop and others, 1976; Craw, 1979; Nelson, 1982; Kimbrough and others, 1992

A3.0 REFERENCES FOR APPENDIX A: World-wide distribution of melanges

Aalto, K.R., 1981, Multistage melange formation in the Franciscan Complex, northernmost California: Geology (Boulder), v. 9, p. 602-607.

---, 1983, Franciscan Complex geology of the Pilot Creek Quadrangle, Northern California: Anonymous. Abstracts with programs 1983; Geological Society of America; Rocky Mountain Section 36th annual meeting; Cordilleran Section 79th annual meeting. Abstracts-with-Programs-Geological-Society-of-America. 15. (5), p. 275; Salt Lake City, UT, May 2-4, 1983.

---, 1989a, Franciscan Complex geology of the Crescent City area, Northern California: Am. Geophys. Union, Washington, D.C.; United States, Dalziel, Ian W. D., Birkenmajer, Krzysztof, Mpodozis, Constantino, Ramos, Victor A., Thomson, Michael R. A.: Tectonics of the Scotia Arc, Antarctica; Punta Arenas, Chile to Ushuaia, Argentina.; Univ. Tex. at Austin, Inst. Geophys., Austin, TX, United-States, p. 21-46.

---, 1989b, Geology of Patrick's Point State Park, Humboldt County, California: California Geology, v. 42, p. 125-133.

Abbotts, I.L., 1979, Intrusive processes at ocean ridges; evidence from the sheeted dyke complex of Masirah, Oman: Tectonophysics, v. 60, p. 217-234.

Abdel, W.M., Abdel, K.M.L., and Hafez, A.M.A., 1984 [1988], Structural evolution of the gneisses and ophiolitic melange rocks, in the northern Migif-Hafafit area, south Eastern Desert, Egypt: Annals-of-the-Geological-Survey-of-Egypt. 14, p. 279-307.

Abdel, W.M., El, D.A.A., Awadallah, M.F., and Hamimi, Z., 1990, On the relation between the ophiolitic melange and the banded iron formation of Gabal El Hadid area, central Eastern Desert, Egypt: Annals of the Geological Survey of Egypt, v. 16, p. 57-67.

Abdelsalam, M.G., and Dawoud, A.S., 1991, The Kabus ophiolitic melange, Sudan, and its bearing on the western boundary of the Nubian Shield: Journal-of-the-Geological-Society-of-London. 148 (Part 1), p. 83-92.

Abdulin, A.A., Abdeyev, A., V, and Seitov, N., 1975, Ofiolity silura Sakmarskoy i Or'-Ilekskoy zon. Translated title: Silurian ophiolites of the Sakmar and Or'-Ilek zones: Akad. Nauk Kaz. SSR, Inst. Geol. Nauk, p. 39-74.

Adamiya, S.A., Gugunishvili, G.G., Kuparadze, D.M., Lordkipanidze, M.B., and Khutsishvili, O.D., 1989, Doverkhneyurskiy serpentinitovyy melanzh v Yuzhnoy Gruzii (Sadakhlo). Translated title: Pre-Upper Jurassic serpentinite melange in southern Georgia (Sadakhlo): (2), p. 357-60.; Soobshcheniya-Akademii-Nauk-Gruzinskoy-SSR. 134.

Ahmad, R., 1981, Stratigraphy, structure and petrology of the Lookingglass and Roseburg formations, Agness-Illahe area, southwestern Oregon, 150 p.

Akkermantsev, S.M., and Yenikeyeva, L.N., 1986, Diopsidovyy koshachiy glaz iz serpentinitov Kanskogo melanzha (Kirgiziya). Translated title: Diopside cat's eye from the serpentinites of the Kansk Melange, Kirghizia: Uzbekiston Geologiya Zhurnali = Uzbekskiy Geologicheskiy Zhurnal, v. 1986, p. 80-82.

Al, R.M.H., and Warden, A.J., 1980, Comparison of the Bir Umq and Hamdah ultrabasic complexes, Saudi Arabia: (4), p. 143-156.; Anonymous. Evolution and mineralization of the Arabian-Nubian Shield. I.A.G.-Bulletin. 3; Evolution and mineralization of the Arabian-Nubian Shield, Jeddah, 1980.

Aleksandrov, A.A., 1973, Sepentinite melange in the upper course of the Chirynay River, Koryak Highlands, Geotectonics. No. 4, p. 232-236, illus. (incl. geol. sketch maps), 1973.; English translation of Russian paper.

Alvarez, W., Kent, D., V, Premoli, S.I., Schweickert, R.A., and Larson, R.L., 1979, Franciscan limestone deposited at 17 degrees south paleolatitude: Geol. Soc. Am., Abstr. Programs, v. 11, p. 66; The Geological Society of America, Cordilleran Section, 75th annual meeting, San Jose, Calif., April 9-11, 1979.

Amarskii, V.G., and Vetluzhskikh, V.G., 1990, Packets of thrust sheets, melange, and formations of the Mesozoic at the juncture of the Stanovoi region and the Aldan Shield, Soviet-Geology-and-Geophysics. 31 (2), p. 6-10.

Andersen, T.B., Skjerlie, K.P., and Furnes, H., 1990, The Sunnfjord Melange, evidence of Silurian ophiolite accretion in the West Norwegian Caledonides: Journal of the Geological Society of London, v. 147, p. 59-68.

Anonymous, 1981, Oman-geological ophiolite project; Map 3, The Wadi Ahin-Yangul area; scale 1.100000, 9 Refs.; Open Univ., Milton Keynes; United-Kingdom.

Armstrong, T.R., and Colpron, M., 1989, Taconian tectonic melange in northern New England and southern Quebec; the Humber-Dunnage Suture: Anonymous. Geological Society of America, Northeastern Section, 24th annual meeting; abstracts with programs 1989; New Brunswick, NJ, Mar. 23-25, 1989.

Auden, J.B., and Robertson, A.H.F., 1978, Discussion on the Moni Melange, Cyprus, an olistostrome formed at a destructive plate marginwith reply: Geol. Soc. Lond., p. 349-351; For original article by Robertson, see Geol. Soc. London, J., Vol. 133, Part 5, 1976.

Barlow, S.G., and Tracy, W.C., 1982, Geology and slope stability of Point Delgada, California: Anonymous. AAPG-SEG-SEPM Pacific Section meeting. AAPG-Bulletin, v. 66, p. 1684; AAPG-SEG-SEPM Pacific Section meeting, Anaheim, CA, April 14-17, 1982.

Barnes, R.P., 1982, The stratigraphy of South Cornish melanges: Power, G. M. Proceedings; Conference of the Ussher Society. Proceedings-of-the-Ussher-Society, v. 5, p. 391.; Ussher Society; conference, Exeter, Jan. 1982.

---, 1983, The geology of South Cornish melanges, Univ. Southampton, United-Kingdom; Doctoral; Dissertation Abstracts, Vol. 45, No. 1.

---, 1984, Possible Lizard-derived material in the underlying Meneage Formation: Journal of the Geological Society of London, v. 141, p. 79-85.

Barton, M.D., Bebout, G.E., and Sorensen, S.S., 1987, Isotopic constraints on the geochemical evolution of an ultramafic subduction zone melange; Catalina schist terrane, California: Anonymous. AGU 1987 fall meeting. Eos,-Transactions,-American-Geophysical-Union. 68. (44), p. 1525; American Geophysical Union, 1987 fall meeting, San Francisco, CA, Dec. 6-12, 1987.

Baumgartner, P.O., 1986, Discovery of subduction-related melanges on Cano Island and Osa Peninsula (Pacific, Costa Rica, Central America): Kornprobst, Jacques. Onzieme reunion annuelle des sciences de la terre. 11th annual Earth sciences meeting. Reunion-Annuelle-des-Sciences-de-la-Terre, v. 11, p. 12; Onzieme reunion annuelle des sciences de la terre, Clermont-Ferrand, Mar. 25-27, 1986.

Bayer, A.A., 1982, Untersuchungen im Habkern-melange ("Wildflysch") zwichen Aare und Rhein. Translated title: Investigations of the Habkern Melange (Wildflysch) between Aare and Rhine, Mitteilungen-aus-dem-Geologischen-Institut-der-Eidgenoessischen-Technischen-Hochschule-und-der-Universitaet-Zuerich,-Neue-Folge. 240. 327 p. 250 Refs.

Bayer, R., and Matte, P., 1979, Is the mafic/ultramafic massif of Cabo-Ortegal (Northwest Spain) a nappe emplaced during a Variscan obduction? A new gravity interpretation: Tectonophysics, v. 57, p. T9-T18.26; Letter.

Becker, D.G., and Cloos, M., 1985, Melange diapirs into the Cambria Slab; a Franciscan trench slope basin near Cambria, California: Journal of Geology, v. 93, p. 101-110.

Bedrossian, T.L., 1980a, Description of rock units in The Geysers GRA underlain by Franciscan terrain: Bedrossian, T. L. Geology and slope stability in selected parts of The Geysers geothermal resources area: a guide to geologic features indicative of stable and unstable terrain in areas underlain by Franciscan and related rocks. Spec.-Rep.-Calif.-Div.-Mines-Geol, p. 36-43; Appendix B.

---, 1980b, Geology and slope stability in selected parts of The Geysers geothermal resources area: a guide to geologic features indicative of stable and unstable terrain in areas underlain by Franciscan and related rocks, Spec.-Rep.-Calif.-Div.-Mines-Geol. (142), 65 p.

---, 1982, Geology and slope stability, West Sebastopol area, Sonoma County: California Geology, v. 35, p. 71-79.

Belizzia, G.A., Rodriguez, D., and Graterol, M., 1972, Ofiolitas de Siquisique y Rio Tocuyo y sus relaciones con la falla de Oca. Translated title: Ophiolites of Siquisique and Tocuyo River and their relations with the Oca Fault, Venezuela], Caribb. Geol. Conf., Trans. No. 6, p. 182-183

Bell, C.M., 1982, The lower Paleozoic metasedimentary basement of the Coastal Ranges of Chile between 25 degrees 30' and 27 degrees S: Revista Geologica de Chile, v. 17, p. 21-29.

---, 1987, The origin of the upper Palaeozoic Chanaral melange of N Chile: Journal of the Geological Society of London, v. 144, p. 599-610.

Bieler, D.B., 1983, Melanges and glaucophanic schists of the Mona Complex (Precambrian), Southeast Anglesey, North Wales: University of Illinois, Urbana, United-States, Doctoral Thesis; 210 p.; Univ. Microfilms.

Blake, M.C., Jr., Jayko, A.S., Murchey, B.L., and Jones, D.L., 1987, Structure, age, and tectonic significance of the Coast Range ophiolite and related rocks near Paskenta, California: Dickinson, William R. Geological Society of America, 1987 annual meeting and exposition. Abstracts-with-Programs-Geological-Society-of-America. 19. (7), p. 590; Phoenix, AZ, Oct. 26-29, 1987.

Blewett, R.S., 1989, Melange development along the Luke's Arm-Sop's Head Fault (Red Indian Line); a major lineament controlling deformation in Notre Dame Bay, north-central Newfoundland, Canada: Stearn, Colin W., Geological Association of Canada, Mineralogical Association of Canada; annual meeting; program with abstracts, v. 14, p. 10, Montreal, PQ, May 15-17, 1989.

Boles, J.R., 1986, Mesozoic sedimentary rocks in the Vizcaino Peninsula-Isla de Cedros area, Baja California, Mexico: Abbott, Patrick L. Cretaceous stratigraphy, western North America. San Diego State Univ., Dep. Geol. Sci., San Diego, CA, United-States. Field-Trip-Guidebook-Pacific-Section,-Society-of-Economic-Paleontologists-and-Mineralogists, v. 46, p. 63-77.

Bonneau, M., Blake, M.C., Geyssant, J., Lepvrier, C., and Papanikolaou, D., 1980, Geology of Syros Island (Greece), type locality for glaucophane: Int. Geol. Congr. Abstr. Congr. Geol. Int., p. 21; 26th international geological congress, Paris, July 7-17, 1980.

Borchardt, G.A., 1980, Hydrothermal alteration and its effect on soil stability in The Geysers area: in Bedrossian, T. L. Geology and slope stability in selected parts of The Geysers geothermal resources area: a guide to geologic features indicative of stable and unstable terrain in areas underlain by Franciscan and related rocks. Spec.-Rep.-Calif.-Div.-Mines-Geol, p. 46-47.

Bosellini, A., Castellarin, A., Doglioni, C., Guy, F., Lucchini, F., Perri, M.C., Rossi, P.L., Simboli, G., and Sommavilla, E., 1982, Magmatismo e tettonica nel Trias delle Dolomiti. Translated title: Magmatism and tectonics of the Triassic of the Dolomites: Soc. Geol. Italiana, Bologna; Italy, p. 189-210. Centenariodella Societa; Castellarin, A., Vai, G. B. Guida alla geologia del Sudalpino Centro-Orientale.

Bosworth, W., 1983, Multiple generations of melange formation in the Taconic Orogen; structural and tectonic implications: Anonymous. Abstracts of the Geological Society of America, Northeastern Section, 18th annual meeting. Abstracts-with-Programs-Geological-Society-of-America, v. 15, p. 174; Kiamesha Lake, NY, Mar. 23-25, 1983.

Bosworth, W., and Kidd, W.S.F., 1985, Thrusts, melanges, folded thrusts and duplexes in the Taconic Foreland: Lindemann, R. H. New York State Geological Association, 57th annual meeting; field trip guidebook. Annual-Meeting-of-the-New-York-State-Geological-Association, v. 57, p. 117-147

Boudette, E.L., Boone, G.M., and Goldsmith, R., 1989, Day 4; The Precambrian Chain Lakes Massif and an adjacent Cambrian to Lower Ordovician ophiolite-melange-flysch succession: Am. Geophys. Union, Washington, D.C.; United States, Dalziel, Ian W. D., Birkenmajer, Krzysztof, Mpodozis, Constantino, Ramos, Victor A., Thomson, Michael R. A.: Tectonics of the Scotia Arc, Antarctica; Punta Arenas, Chile to Ushuaia, Argentina.; Univ. Tex. at Austin, Inst. Geophys., Austin, TX, United-States, p. 28-38.

Brandon, M.T., 1985, Pacific rim complex of western Vancouver Island; tectonic evolution of a late Mesozoic active margin: Anonymous. The Geological Society of America, Cordilleran Section, 81st annual meeting; Abstracts-with-Programs-Geological-Society-of-America, v. 17, p. 343, Vancouver, BC, May 8-10, 1985.

---, 1989a, Deformational styles in a sequence of olistostromal melanges, Pacific Rim Complex, western Vancouver Island, Canadawith Suppl. Data 89-16: Geological Society of America Bulletin, v. 101, p. 1520-1542.

---, 1989b, Origin of igneous rocks associated with melanges of the Pacific Rim Complex, western Vancouver Island, Canada: Tectonics, v. 8, p. 1115-1136.

Breen, N.A., 1987, Three investigations of accretionary wedge deformation: University of California, Santa Cruz, United-States, Doctoral Thesis; 132 p.; Univ. Microfilms, Ann Arbor, MI, United States.

Breen, N.A., Tagudin, J.E., Reed, D.L., and Silver, E.A., 1988, Mud-cored parallel folds and possible melange development in the North Panama thrust belt: Geology (Boulder), v. 16, p. 207-210.

Brooks, H.C., and Ferns, M.L., 1985, Melanges and associated rocks of Northeast Oregon; implications for timing of terrane assembly: Leviton, Alan E., Aldrich, Michele L., Chambers, Helena. Proceedings of the 66th annual meeting of the Pacific Division, American Association for the Advancement of Science. Proceedings-of-the-Pacific-Division, p. 23, Missoula, MT, June 9-14, 1985.

Brown, W.R., 1976, Tectonic melange (?) in the Arvonia Slate district of Virginia: Geol. Soc. Am., Abstr. Programs, v. 8, p. 142; The Geological Society of America Northeastern Section, 11th annual meeting, and Southeastern Section, 25th annual meeting, Arlington, Va., March 25-27, 1976.

---, 1986, Shores Complex and melange in the central Virginia Piedmont: Geol. Soc. Am., Boulder, CO; United States, v. 6, p. 209-214.

Bryan, W.B., 1990, Geology of the Mainits accretionary terrane, Chukotka District, Magadan Province, USSR: Anonymous. AGU 1990 fall meeting. Eos,-Transactions,-American-Geophysical-Union. 71. (43), p. 1592; San Francisco, CA, Dec. 3-7, 1990.

Bryhni, I., and Lyse, K., 1985, The Kalvag Melange, Norwegian Caledonides: John Wiley & Sons, Chichester; United Kingdom, v. 1, p. 417-427.

Butler, J.R., 1987, Nature and significance of ultramafic bodies in the Piedmont of North Carolina and South Carolina: Anonymous. The Geological Society of America, Southeastern Section, 36th annual meeting, Abstracts-with-Programs-Geological-Society-of-America, v. 19, p. 77, Norfolk, VA, Mar. 25-27, 1987.

Byrne, T., 1981, Structural geology of the Ghost Rocks Formation melange terranes, Kodiak Island, Alaska: Hestor, N. C., Noger, M. C. Geological Society of America, 94th annual meeting. Abstracts-with-Programs-Geological-Society-of-America, v. 13, p. 421; Cincinnati, OH, Nov. 2-5, 1981.

---, 1985, The Uyak Complex a brittle-ductile shear zone: Anonymous. The Geological Society of America, Cordilleran Section, 81st annual meeting; abstracts. Abstracts-with-Programs-Geological-Society-of-America, v. 17, p. 346; Vancouver, BC, May 8-10, 1985.

Camp, V.E., Jackson, N.J., Ramsay, C.R., Roobol, M.J., Stoeser, D.B., and White, D.L., 1984, Discussion on the upper Proterozoic ophiolite melange zones of the easternmost Arabian Shield: Brown, M. Metamorphic studies; research in progress. Kingston Polytech., Dep. Geol., Kingston upon Thames, United-Kingdom. Journal-of-the-Geological-Society-of-London, v. 141, p. 1083-1087; For original paper by Al-Shanti, A. M. S., and Gass, I. G., see J. Geol. Soc. London, Vol. 140, p. 867-876, 1983.

Carpenter, P.S., and Walker, N.W., 1990, Petrology, structure, and tectonic significance of the Aldrich Mountains serpentinite-matrix melange, NE Oregon: Zoback, Mary Lou, Rowland, Stephen M. Geological Society of America, Cordilleran Section, 86th annual meeting. Abstracts-with-Programs-Geological-Society-of-America, v. 22, p. 12-13; Tucson, AZ, Mar. 14-16, 1990.

Chacon, J., 1982, Las serias Precambricas de la Zona de Ossa Morena, Macizo Iberico Meridional. Translated title: The Precambrian of Ossa Morena Zone, southern Iberian Massif: R. Acad. Cienc. Exactas Fis. Nat., Madrid; Spain, p. 93-115; Curso Conferencias Programa International de Correlacion Geologica, Madrid, 1981.

Chekhov, A.D., and Aleksandrov, A.A., 1982, Ophiolite allochthons of the Penzhina Ridge: Geotectonics, v. 16, p. 162-165.

Chekhov, A.D., Aleksandrov, A.A., Palandzhyan, S.A., and Petrov, A.N., 1980, Verkhne-Khatyrskiy serpentinitovyy melanzh (tsentral'naya chast' Koryakskogo nagor'ya). Translated title: The Verkhne-Hatyr serpentinite melange in the central Koryak Range: (5), p. 51-59; .IGCPProject; Geologiya-i-Geofizika. 1980.

Chekhovich, V.D., Kravchenko, B.I.R., and Averina, G.Y., 1990, Geologicheskoye stroyeniye p-ova Govena i o-va Karaginskiy. Translated title: Geological structure of the Govena Peninsula and Karaginskiy Island: Izd. Nauka, Moscow; USSR, Til'man, S. M., Sobolev, S. F.: Geologiya zapadnoy chasti Beringovomor'ya. Translation: Geology of western Bering Sea region.; Akad. Nauk SSSR, Inst. Litosfery, Moscow, USSR, p. 4-110.

Chiotis, E., and Dimou, E., 1972, Peri ton eksoryssomenon serpentinton kai opitoasvestiton eis tin periokhin Drepanoy Mayrodendrioy Kozanis. Translated title: The serpentinites and ophicalcites of the Cape Drepanon-Mavrodendri region of Kozane, Greece: Geol. Soc. Greece, Bull, v. 9, No. 2, p. 536-566 (incl.Fr.sum.)

Cloos, M., 1981, Metamorphism of the pelitic matrix of melanges in the Franciscan Subduction Complex, California: Anonymous. The Geological Society of America, Cordilleran Section, 77th annual meeting, international meeting. Abstracts-with-Programs-Geological-Society-of-America, v. 13, p. 49; Hermosillo, Sonora, March 25-27, 1981.

---, 1986, Strain patterns and deformation mechanisms of deformed graywacke and greenstone blocks encased in mud-matrix melange near San Simeon, California: The Geological Society of America, Cordilleran Section, 82nd annual meeting. Abstracts-with-Programs-Geological-Society-of-America, v. 18, p. 95., Los Angeles, CA, Mar. 25-28, 1986.

---, 1991, Geologic maps of the seacliffs between San Simeon and Cambria, California; synsubduction interfingering of Franciscan mud-matrix melange and Late Cretaceous (?) slope deposits: Anonymous. Geological Society of America, Cordilleran Section, 87th annual meeting. Abstracts-with-Programs-Geological-Society-of-America, v. 23, p. 14, San Francisco, CA, March 25-27, 1991.

Cousineau, P.A., 1991, The Riviere des Plante ophiolitic melange; tectonic setting and melange formation in the Quebec Appalachians: Journal of Geology, v. 99, p. 81-96.

Cowan, D.S., 1974, Deformation and Metamorphism of the Franciscan Subduction Zone Complex Northwest of Pacheco Pass, California: Geol. Soc. Am., Bull, v. 85, No. 10, p. 1623-1634

Crawford, K.E., 1975, The geology of the Franciscan tectonic assemblage near Mount Hamilton, California: University of California, Los Angeles, United-States, Doctoral Thesis; 182 p. Diss. Abstr. Int., Vol. 36, No. 2, p. 617B, 1975.

Crawford, R.F., III, Higgins, M.W., and Crawford, T.J., 1985, The West Point Melange, remnants of a lower Paleozoic ophiolitic, eclogite-bearing melange in the Southern Appalachians, Alabama, Georgia, and North Carolina: The Geological Society of America, 98th annual meeting. Abstracts-with-Programs-Geological-Society-of-America, v. 17, p. 555; Orlando, FL, Oct. 28-31, 1985.

Crowley, P.D., 1985, The structural and metamorphic evolution of the Sitas area, Northern Norway and Sweden, 53 p. 115 Refs.

Danilovich, L.G., 1981, Fragmenty okeanicheskoy kory v strukture Karpat. Translated title: Oceanic crust fragments in the Carpathian structure: (4), p. 93-106.; Geologicheskiy-Zhurnal-(Kiev,-1968). 41.

Davoudzadeh, M., 1969, Geologie und Petrographie des Gebietes noerdlich von Nain, Zentral-Iran. Translated title: Geology and petrography of the region north of Nain, central Iran, Zuerich, Univ., Geol. Inst.-Eidgenoess. Tech. Hochsch., Geol. Inst., Mitt. No. 98, 90 p. (incl. Engl. sum.)

de Broucker, G., and St Pierre, J., 1985, Mictaw Group; Taconic flysch and melange of the Quebec Appalachians, evidences for a continental volcanic-arc and metamorphic terrane derivation: Anonymous. GAC, MAC, CGU 1985 joint annual meeting. Program-with-Abstracts-Geological-Association-of-Canada;.10, p. A13; Fredericton, NB, May 15-17, 1985.

DeJong, K.A., 1974, Melange (Olistostrome) near Lago Titicaca, Peru: Am. Assoc. Pet. Geol., Bull, v. 58, No. 4, p. 729-741

D'Elia, B., Di, S.D., Federico, G., and Oliva, S., 1984, Full-scale study of a high cut in a structurally complex formation: Univ. Toronto Press, Downsview, ON; Canada, p. 57-62.; IV international symposium on landslides -- Symposium International sur glissements de terrains, Toronto, ON, Sept. 16-21, 1984.

Dergunov, A.B., Kazak, A.P., and Moldavantsev, Y.Y., 1975, Serpentinite melange and structural position of the Ray-Iz ultrabasic massif (Polar Urals): Geotectonics, v. 9, p. 15-18.

Dickinson, W.R., Helmold, K.P., and Stein, J.A., 1979, Mesozoic lithic sandstones in central Oregon: J. Sediment. Petrol, v. 49, p. 501-516.

Dietrich, V., 1973, Development of oceanic crust in the Southeast Pennine Belt; the Arosa-Platta ophiolites: Eur. Geophys. Soc., Meet., Abstr, p. 27.

Dietrich, V.J., Oberhaensli, R., and Mercolli, I., 1987, A new occurrence of boninite from the ophiolitic melange in the Pindus-sub-Pelagonian zone S. L.; Aegina Island, Saronic Gulf, Greece: Anonymous. Geochemistry of ophiolites. Ofioliti, v. 12, p. 83-90; Geochemistry of ophiolites, Geneva, Dec. 1985.

Dimitrijevic, M.D., and Dimitrijevic, M.N., 1976, The polyphase melange of the Vardar Zone: (2), p. 205-208.; Soc.-Geol.-Fr.,-Bull. 18; V(e) colloque sur la geologie des regions egeennes, Orsay, Feb. 1-3, 1975.

---, 1979 [1980], Struktura i kinematika metamorfnog oboda Zlatiborskog ultramafitskog masiva. Translated title: Structure and kinematics of the metamorphic aureole, Zlatibor ultramafic massif: 37, p. 101-121.; Yugosl., Zavod Geol. Geofiz. Istrazivanja, Vesn., Geol.

Ditullio, L., and Byrne, T., 1985, Kinematic evidence for tectonic origin of a melange; Cretaceous/Paleocene Ghost Rocks FM., Kodiak Island, Alaska: The Geological Society of America, Cordilleran Section, 81st annual meeting. Abstracts-with-Programs-Geological-Society-of-America, v. 17, p. 351; Vancouver, BC, May 8-10, 1985.

Dobrzhinetskaya, L.F., and Ez, V., V, 1982 [1983], Metamorphic rocks in the melange of the ophiolite belt of the Lesser Caucasus (Adzharis Landmark): Geotectonics. 16. (3), p. 217-225.

Dolenko, G.N., and Danilovich, L.G., 1975, Novoye v uchenii o geosinklinalyakh i yego prilozheniye k Ukrainskim Karpatam. Translated title: New principles concerning geosynclines and their application to the Ukrainian Carpathians: (5), p. 3-10.; Geol.-Zh.-(Russ.-Ed.). 35.

Doolan, B.L., Smith, G.T., and Winner, P.S., 1981, Oblique collision and ophiolite dismemberment in the Vermont-Quebec serpentinite belt: Anonymous. Geological Society of America, Northeastern Section, 16th annual meeting , Abstracts-with-Programs-Geological-Society-of-America, v. 13, p. 129 Bangor, ME, Apr. 9-11, 1981.

Drake, A.A., Jr., 1980, The Serra de Caldas window, Goias: Anonymous. Tectonic studies in the Brazilian Shield. U.-S.-Geol.-Surv., p. A1-A11.12.

Duncan, I.J., and Shore, P.J., 1984, The Vadito Melange; a new perspective on the tectonic evolution of northern New Mexico: Anonymous. The Geological Society of America, Rocky Mountain Section, 37th annual meeting. Abstracts-with-Programs-Geological-Society-of-America, v. 16, p. 220; Durango, CO, May 11-12, 1984.

Edelman, N., and Jaanus, J.M., 1983, A plate tectonic interpretation of the Precambrian of the Archipelago of southwestern Finland, Bulletin-Geological-Survey-of-Finland. 325. 33 p. 38 Refs.

Eden, C.P., and Andrews, J.R., 1990a, Melanges beneath the Acebuches Amphibolite; Late Devonian extension or collision in Southwest Iberia?, Anonymous. Terranes in the Circum-Atlantic Paleozoic orogens; international conference on Paleozoic orogens in central Europe. 6 Refs. IGCP Project No. 233; Int. Geol. Correl. Prog.; Federal-Republic-of-Germany; International conference on Paleozoic orogens in central Europe, Gottingen-Giessen, Aug.-Sept. 1990.

---, 1990b, Middle to Upper Devonian melanges in SW Spain and their relationship to the Meneage Formation in South Cornwall: Nicholas, Clive. 29th annual meeting of the Ussher Society. Proceedings-of-the-Ussher-Society, v. 7, p. 217-222; 29th annual meeting of the Ussher Society, Exeter, Jan. 1990.

El, S.M.A., and El, B.R.M., 1979, The ophiolites of Wadi Ghadir area Eastern Desert, Egypt: Issawi, Bahay. Proceedings of the international meetings held on the occasion of the Fifth conference on African geology. Geol. Surv. Egypt and Min. Auth., Cairo, Egypt. Egypt,-Geol.-Surv.,-Ann, v. 9, p. 125-135; Fifth conference on African geology, Cairo, Oct. 6-10, 1979.

Evans, K.M., 1981, Lower Devonian brachiopod faunas from within the Meneage melange, South Cornwall: Edwards, R. A. Proceedings of the Ussher Society annual conference. Proceedings-of-the-Ussher-Society, v. 5, p. 243-244; Ussher Society; annual conference, Fowey, Cornwall, Jan. 1981.

Flinn, D., 1985, The Caledonides of Shetland: John Wiley & Sons, Chichester; United Kingdom, p. 1159-1172. 39Refs. IGCPProject.

Floyd, P.A., Kelling, G., Gokcen, S.L., and Gokcen, N., 1992, Arc-related origin of volcaniclastic sequences in the Misis Complex, southern Turkey: Journal of Geology, v. 100, p. 221-230.

Forsythe, R., and Mpodozis, C., 1979, El Archipielago Madre de Dios, Patagonia occidental, Magallanes; rasgos generales de la estratigrafia y estructura del "basamento" pre-Jurasico superior. Translated title: The Madre de Dios Archipelago, western Patagonia, Magallanes; general characteristics of the stratigraphy and structure of the pre-Upper Jurassic basement: (7), p. 13-29.; Rev. Geol. Chile.

---, 1983, Geologia del basamento Prejurasico superior en el Archipielago Madre de Dios, Magallanes, Chile. Translated title: Geology of the pre-upper-Jurassic basement in the Madre de Dios Archipelago, Magallanes, Chile, Boletin-Instituto-de-Investigaciones-Geologicas.-Chile. 39. 63 p. 100 Refs.

Fortuin, A.R., and Peters, J.M., 1984, The Prina Complex in eastern Crete and its relationship to possible Miocene strike-slip tectonics: Journal of Structural Geology, v. 6, p. 459-476.

Freeman, M.J., Palmer, D.F., and Heimlich, R.A., 1988, Magnetic survey of the western serpentinite belt, northern Harford County, Maryland: Southeastern Geology, v. 29, p. 103-128.

Friedman, G.M., 1979, Subaqueous gravity-displacement products: Am. Assoc. Pet. Geol., Bull, v. 63, p. 453; AAPG-SEPM annual meeting, Houston, Tex., April 1-4, 1979.

Frizzell, V.A., Jr., Tabor, R.W., Zartman, R.E., and Jones, D.L., 1982, Mesozoic melanges in the western Cascades of Washington: Anonymous. Geological Society of America, Cordilleran Section, 78th annual meeting. Abstracts-with-Programs-Geological-Society-of-America, v. 14, p. 164; Anaheim, CA, April 19-21, 1982.

Gibbons, W., 1989, Suspect terrane definition in Anglesey, North Wales: Dallmeyer, R. D. Terranes in the Circum-Atlantic Paleozoic orogens. Univ. Ga., Dep. Geol., Athens, GA, United-States. Special-Paper-Geological-Society-of-America, v. 230, p. 59-65.

Gibbons, W., and Ball, M.J., 1991, A discussion of Monian Supergroup stratigraphy in Northwest Wales: Journal-of-the-Geological-Society-of-London. 148 (Part 1), p. 5-8.

Golovko, A., V, and Vishnevskaya, S., 1984, Rubin iz kanskogo melanzha. Translated title: Ruby from the Kansk Melange: Zapiski Uzbekistanskogo Otdeleniya Vsesoyuznogo Mineralogicheskogo Obshchestva, v. 37, p. 6-8.

Gonzalez, J.M., and Dunne, T.N., 1983, Geotechnical exploration for the proposed Crosstown Transport Facility, San Francisco, California: Am. Inst. Min., Metall. and Pet. Eng., New York, NY; United States, p. 25-41.; 1983 Rapid Excavation and Tunneling Conference, Chicago, IL, June 12-16, 1983.

Graciansky, P.C., 1973, Le probleme des "coloured melanges" a propos de formations chaotiques associees aux ophiolites de Lycie (Turquie). Translated title: The problem of "colored melange" in relation to the chaotic formations associated with ophiolites in Lycia, Turkey]: Terre, [Programme Resumes], v. 1973, p. 210,illus.(incl.sketch; Reun. Annu. Sci.

Grall, H., and Bradbury, H.J., 1982, Melange deformation, Isle of Anglesey, U.K: The Geological Society of America, 95th annual meeting. Abstracts-with-Programs-Geological-Society-of-America, v. 14, p. 500; New Orleans, LA, Oct. 18-21, 1982.

Greiling, R.O., Kroener, A., El, R.M.F., and Rashwan, A.A., 1988, Structural relationships between the southern and central parts of the Eastern Desert of Egypt; details of a fold and thrust belt: Friedr. Vieweg & Sohn, Braunschweig; Federal Republic of Germany, El-Gaby, Samir, Greiling, Reinhard O.: The Pan-African Belt of Northeast Africa and adjacent areas; tectonic evolution and economic aspects of a late Proterozoic orogen.; Assiut Univ., Geol. Dep., Assiut, Egypt, p. 121-145.

Gucwa, P.R., 1974, Geology of the Covelo/Laytonville area, northern California: University of Texas, Austin, United-States, Doctoral Thesis; 101 p. Diss. Abstr. Int., Vol. 35, No. 8, p. 3986B, 1975.

---, 1975, Middle to Late Cretaceous sedimentary melange, Franciscan Complex, northern California: Geology (Boulder), v. 3, No. 3, p. 105-108

Gullixson, C.F., 1981, The structure, geologic evolution and regional significance of the Bethel Creek - North Fork area, Coos and Curry counties, Oregon, 86 p.

Habib, M.E., 1987, Microplate accretion model for the Pan-African basement between Qena-Safaga and Qift-Quseir roads, Egypt: (1), p. 199-239.; Bulletin-of-the-Faculty-of-Science,-Section-C:-Biology-and-Geology. 16.

Harder, H., Jacobshagen, V., Skala, W., Arafeh, M., Berndsen, J., Hofmann, A., Kusserow, H., Schelder, W., and Fluegel, E., 1983, Geologische Entwicklung und Struktur der Insel Skyros, Nord-Sporaden, Griechenland. Translated title: Geologic evolution and structure of Skyros Island, northern Sporades, Greece: 48, p. 7-39.; Jacobshagen, V. Untersuchungen zur Geologie der Nord-Sporaden (Aegaeisches Meer, Griechenland). Geologic studies on northern Sporades, Aegean Sea, Greece. Freie Univ. Berlin, Inst.

Geol., Berlin 33 1000, Federal-Republic-of-Germany. Berliner-Geowissenschaftliche-Abhandlungen,-Reihe-A:-Geologie-und-Palaeontologie.

Hatzipanagiotou, K., 1983, Die oberste Einheit des sued-aegaeischen Deckenstapels auf Rhodos und Karpathos (Dodekanes/Griechenland); relikte eines Ophiolith-Komplexes. Translated title: The upper South Aegean cover of Rhodes and Karpathos, Dodecanesus, Greece; relict of an ophiolite complex, 163 p. 149 Refs.; Bgr-1983 a 820.

Hatzipanagiotou, K.G., 1986, Plagiogranites in the ophiolitic melange of Rhodes, Dodecanese, Greece: Neues Jahrbuch fuer Mineralogie. Monatshefte, v. 1986, p. 400-406.

Haydukiewicz, A., 1977, Litostratygrafia i rozwoj strukturalny kompleksu Kaczawskiego w jednostce Rzeszowka i w zachodniej czesci jednostki Jakuszowej. Translated title: Lithostratigraphy and structural development of the Kaczawa Complex in the Rzeszowek Unit and western part of the Jakuszowa Unit: Geol. Sudetica, v. 12, p. 7-68.

Hayward, A.B., 1984, Sedimentation and basin formation related to ophiolite nappe emplacement; Miocene, SW Turkey: Jansa, L. F., Burollet, P. F., Grant, A. C. Basin analysis; principles and applications. Atlantic Geosci. Cent., Dartmouth, NS, Canada. Sedimentary-Geology, v. 4, p. 105-129; Eleventh international sedimentological congress, Hamilton, ON, Aug. 22-27, 1982.

Hempton, M.R., 1982, Structure of the northern margin of the Bitlis suture zone near Sivrice, southeastern Turkey: SUNY at Albany, United-States, Doctoral Thesis; 563 p.; Univ. Microfilms.

---, 1985, Structure and deformation history of the Bitlis suture near Lake Hazar, southeastern Turkey: Geological Society of America Bulletin, v. 96, p. 233-243.

Herrington, K.L., and Cloos, M., 1985, Metamorphism and metasomatic alteration of an eclogite block in the Franciscan Complex near Mt. Hamilton, Diablo Range, California: The Geological Society of America, 98th annual meeting. Abstracts-with-Programs-Geological-Society-of-America, v. 17, p. 609Orlando, FL, Oct. 28-31, 1985.

Herve, F., Mpodozis, C., Davidson, J., and Godoy, E., 1981, Observaciones estructurales y petrograficas en el basamento metamorfico del archipielago de los Chonos entre el canal King y el canal Ninualac, Aisen. Translated title: Structural and petrographic observations of the metamorphic basement of the Los Chonos Archipelago between King Canal and Ninualac Canal, Aisen: 13 14, p. 3-16.; Revista Geologica de Chile.

Hibbard, J., 1987, Ophiolitic melange along the Baie Verte Line, Coachman's Harbour, Newfoundalnd: Geol. Soc. Am., Boulder, CO; United States, v. 5, p. 457-462.

Hibbard, J., and Williams, H., 1979, Regional setting of the Dunnage Melange in the Newfoundland Appalachians: Am. J. Sci, v. 279, p. 993-1021.

Hietanen, A., 1979, Western Metamorphic Belt north of the North Yuba River, California: Geol. Soc. Am., Abstr. Programs, v. 11, p. 84; The Geological Society of America, Cordilleran Section, 75th annual meeting, San Jose, Calif., April 9-11, 1979.

Higgins, J.B., McSween, B.Y., Jr., and Keller, F.B., 1980, Petrology of a granulite-amphibolite-gneiss melange in the North Carolina Blue Ridge: Geol. Soc. Am., Abstr. Programs, v. 12, p. 179; The Geological Society of America, Southeastern Section, 29th annual meeting, Birmingham, Ala., March 27-28, 1980.

Higgins, M.W., Crawford, R.F., III, Cressler, C.W., and Crawford, T.J., 1987, Exotic marble slabs in the West Point Melange in the Murphy Syncline and revision of the "Murphy Sequence" in the Cartersville one-

degree quadrangle, Georgia; a progress report: Anonymous. Geological Society of America, Southeastern Section, 36th annual meeting. Abstracts-with-Programs-Geological-Society-of-America, v. 19, p. 89; Norfolk, VA, Mar. 25-27, 1987.

Higgins, M.W., Crawford, R.F., III, Atkins, R.L., and Crawford, T.J., 1989, The Macon Complex; an ancient accretionary complex in the Southern Appalachians: Horton, J. Wright, Jr., Rast, Nicholas. Melanges and olistostromes of the U.S. Appalachians. U. S. Geol. Surv., Reston, VA, United-States. Special-Paper-Geological-Society-of-America, v. 228, p. 229-246.

Hoogerduijn, S.E.H., and Van, W.W.A., 1989, The structure of the Bracco Ophiolite complex (Ligurian Apennines, Italy); a change from Alpine to Apennine polarity: Journal of the Geological Society of London, v. 146, p. 933-944.

Horne, G.S., 1981, The Selbusjoeen Melange; fabric of a tectonized melange in the Trondheim Nappe, Norwegian Caledonides: The Geological Society of America, 94th annual meeting. Abstracts-with-Programs-Geological-Society-of-America, v. 13, p. 476; Cincinnati, OH, Nov. 2-5, 1981.

Horne, G.S., and McKibbin, T.M., 1983, Ordovician melange on New World Island, Newfoundland; olistostrome or tectonite?: The Geological Society of America; Northeastern Section, 18th annual meeting. Abstracts-with-Programs-Geological-Society-of-America, v. 15, p. 189; Kiameska Lake, NY, Mar. 23-25, 1983.

Horton, J.W., Jr., Blake, D.E., Wylie, A.S., Jr., and Stoddard, E.F., 1985, The Falls Lake Melange, a polydeformed accretionary complex in the North Carolina Piedmont: The Geological Society of America, 98th annual meeting. Abstracts-with-Programs-Geological-Society-of-America, v. 17, p. 613; Orlando, FL, Oct. 28-31, 1985.

Hsu, K.J., 1969, Preliminary report and geologic guide to Franciscan melanges of the Morro Bay-San Simeon area, California, Calif.-Div.-Mines-Geol.,-Spec.-Publ. (35). 46 p.

Itsikson, G., V, 1980, Compressional structures, thrust blocks, and melange zones of the Okhotsk region: Geotectonics, v. 14, p. 222-233.

Ivanov, O.N., and Baratov, S.K., 1974, Serpentinitovyy melanzh basseyna reki Khatyrki; Koryakskoye nagor'ye. Translated title: Serpentinite melange of the Khatyrka River Basin, Koryak Mountains: Akad. Nauk SSSR, Dokl, v. 214, No. 2, p. 404-406

Jacobi, R.D., 1980, Geology of part of the terrane north of Lukes Arm Fault, North-central Newfoundland (Part I); Modern submarine sediment slides and their geological implications (Part II): Columbia University, United-States, Doctoral Thesis; 434 p.; Univ. Microfilms.

Janda, R.J., 1979, Summary of regional geology in relation to geomorphic form and process: Geol. Soc. Am., Cordilleran Sect., Boulder, Colo.; United States, Anonymous. A field trip to observe natural and management-related erosion in Franciscan terrane of northern California; a guidebook I.1-I.2, p. II.1-II.17.

Jett, G.A., and Heller, P.L., 1988, Tectonic significance of polymodal compositions in melange sandstones, western melange belt, North Cascade Range, Washington: Journal of Sedimentary Petrology, v. 58, p. 52-61.

Jones, G., and Robertson, A.H.F., 1991, Tectono-stratigraphy and evolution of the Mesozoic Pindos Ophiolite and related units, northwestern Greece: Journal of the Geological Society of London, v. 148, p. 267-288.

Kamaletdinov, M.A., and Kazantseva, T.T., 1975, Ob osobennostyakh stroyeniya i o proiskhozhdenii rifovykh vklyucheniy v ofiolitovykh kompleksakh. Translated title: Structure and provenance of reef inclusions in ophiolite complexes: Akad. Nauk SSSR, Dokl, v. 220, p. 167-170.

Kay, M., 1972, Dunnage Melange and Lower Paleozoic deformation in northeast Newfoundland: No, v. 24, p. 83,; Int. Geol. Congr. Abstr.--Congr. Geol. Int., Resumes.

---, 1975, Dunnage melange and subduction of the Protacadic Ocean, Newfoundland: Geol. Soc. Am., Abstr. Programs, v. 7, p. 1139-1140.

---, 1976, Dunnage melange and subduction of the Protacadic Ocean, Northeast Newfoundland, Geol.-Soc.-Am.,-Spec.-Pap. (175). 49 p. 99 Refs.

Kelsey, H.M., 1976, Landslide dams; prehistoric occurrences in the Franciscan Complex of northwestern California: Geol. Soc. Am., p. 387.

Kelsey, H.M., Weaver, W.E., and Madej, M.A., 1979, A field trip to observe natural and management-related erosion in Franciscan terrane of northern California; Road log for day 2; Geology, geomorphic processes, land use, and watershed rehabilitation in Redwood National Park, and vicinity, lower Redwood Creek Basin: Geol. Soc. Am., Cordilleran Sect., Boulder, Colo.; United States, p. XIII.1-XIII.18.

Kennedy, M.J., 1980, Serpentinite-bearing melange in the Dalradian of County Mayo and its significance in the development of the Dalradian Basin: J. Earth Sci., R. Dublin Soc, v. 3, p. 117-126.

Khristov, Y., V, and Khristova, M.P., 1979, The structural position and features of constitution of the ophiolites of the eastern part of the southern Tien Shan belt: Geotectonics, v. 12, p. 368-375.

Kilbourne, R.T., 1986, Geology and slope stability of the Fort Bragg area, Mendocino County, California: California Geology, v. 39, p. 56-68.

Kimbrough, D.L., 1979, Volcanic-plutonic sequences, Cedros Island: Geol. Soc. Am., Boulder, Colo.; United States, Brown, E. H., Ellis, R. C.: Geological excursions in the Pacific Northwest, p. 29-35.

---, 1980, Emplacement of an island arc ophiolite; Cedros Island, Baja California Sur: Int. Geol. Congr. Abstr. Congr. Geol. Int., p. 58; 26th international geological congress, Paris, July 7-17, 1980.

---, 1989, Franciscan Complex rocks on Cedros Island, Baja California Sur, Mexico; radiolarian biostratigraphic ages from a chert melange block and petrographic observations on metasandstone: Abbot, Patrick L. Geologic studies in Baja California. San Diego State Univ., Dep. Geol. Sci., San Diego, CA, United-States. Field-Trip-Guidebook-Pacific-Section,-Society-of-Economic-Paleontologists-and-Mineralogists, v. 63, p. 103-107.

Kimura, G., Rodzhestvenskiy, V.S., Okumura, K., Melinikov, O., and Okamura, M., 1992, Mode of mixture of oceanic fragments and terrigenous trench fill in an accretionary complex; example from southern Sakhalin: Tectonophysics, v. 202, p. 361-374.

Kintzer, F.C., 1980, Geology and landslides at Calaveras Reservoir, Alameda and Santa Clara counties, California, MSC thesis, Hayward State University, Hayward, California; 138 p. 108 Refs.

Klein, R.T., Hannula, S.R., Jones, N.W., McKee, J.W., Oshkosh, O., and Anderson, T.H., 1990, Cerro el Pedernal; block-in-melange features in northern Zacatecas, Mexico: Zoback, Mary Lou, Rowland, Stephen M. Geological Society of America, Cordilleran Section, 86th annual meeting. Abstracts-with-Programs-Geological-Society-of-America, v. 22, p. 35; Tucson, AZ, Mar. 14-16, 1990.

Kleist, J.R., 1974a, Deformation by Soft-Sediment Extension in the Coastal Belt, Franciscan Complex: Geology (Boulder), v. 2, p. 501-504

---, 1974b, Geology of the Coastal Belt, Franciscan Complex, near Ft. Bragg, California [abstr.]: University of Texas, Austin, United-States, Doctoral Thesis; Diss. Abstr. Int., Vol. 35, No. 5, p. 2263B-2264B, 1974.

Knipper, A.L., 1971a, Constitution and age of serpentinite melange in the Lesser Caucasus: Geotectonics., v. 5, p. 275-282

---, 1971b, Istoriya razvitiya serpentinitovogo melanzha Malogo Kavkaza. Translated title: Development of serpentinite melange in the Lesser Caucasus, Geotektonika. No. 6, p. 87-100

Kocyigit, A., 1984, Tectono-stratigraphic characteristics of Hoyran Lake region (Isparta Bend): Maden Tetkik ve Arama Enstituesue, Ankara; Turkey, p. 53-67; International symposium of the Geological Society of Turkey ; Geology of the Taurus Belt, Ankara, Sept. 26-29, 1983.

Kolyasnikov, Y.A., 1977 [1980], Genesis of serpentine melange of the Koryak Mountains: Acad.-Sci.-USSR,-Dokl.,-Earth-Sci.-Sect. 237. (1-6), p. 88-90.

Korbay, S.R., and Russey, G.W., 1986, Road, well pad, and power plant construction in landslide-prone terrain, The Geysers geothermal area, Northern California: Tryhorn, Alan D. Association of Engineering Geologists, 29th annual meeting; "Better living through engineering geology": Annual-Meeting-Association-of-Engineering-Geologists, v. 29, p. 54; San Francisco, CA, Oct. 5-10, 1986.

Kroener, A., 1984, Late Precambrian ophiolites and continental accretion in Northeast Africa and Arabia: Bogdanov, N. A. Special session of the International "Lithosphere" Programme. International-Geological-Congress. 27. (9, Part 1), p. 158; special session of the International "Lithosphere" Programme, Moscow, Aug. 4-14, 1984.

Kukhtikov, M.M., 1974, Melanzh osadochnogo proiskhozhdeniya na Yugo-Zapadnom Pamire. Translated title: Sedimentary origin of melange in the southwestern Pamirs: Akad. Nauk Tadzh. SSR, Dokl, v. 17, p. 52-54.

Kurenkov, S.A., 1978 [1981], Tectonic evolution of ophiolite complexes of the Turkestan-Alay region, southern Tien Shan: Doklady-of-the-Academy-of-Sciences-of-the-USSR,-Earth-Science-Sections. 243. (1-6), p. 50-52.

---, 1979, The serpentinite melange and olistostrome complexes of the Alai Range (Southern Tien Shan): Geotectonics, v. 12, p. 376-383.

Kuzmin, M.I., and Al'mukhamedov, A.I., 1983, The geochemistry of Paleozoic ophiolites and their primary nature: Bogdanov, N. A. Tezisy, 27-y mezhdunarodnyy geologicheskiy kongress--Abstracts, 27th International-Geological-Congress. 27. (3), p. 282-284; (Mezhdunarodnyy geologicheskiy kongress; 27), Moscow, Aug. 4-14, 1984.

Larue, D.K., and Hudleston, P.J., 1986, Foliated breccias in the active Portuguese Bend landslide complex, California; bearing on melange genesis: Anonymous. The Geological Society of America, 99th annual meeting. Abstracts-with-Programs-Geological-Society-of-America, v. 18, p. 667; San Antonio, TX, Nov. 10-13, 1986.

Lash, G.G., 1987, Diverse melanges of an ancient subduction complex: Geology (Boulder), v. 15, p. 652-655.

Leaming, S., 1980, Studies of ultramafic rocks in Dease Lake area, British Columbia: Current research, Part A. Pap.-Geol.-Surv.-Can, p. 349-350.

Lindsley, G.N., and Fisher, M., 1989, Significance of the tectonic contact between lower Paleozoic melange and shales of the Gazelle Formation, Yreka Terrane, Klamath Mountains, California: Anonymous. The Geological Society of America, Cordilleran Section, 85th annual meeting and Rocky Mountain Section, 42nd annual meeting. Abstracts-with-Programs-Geological-Society-of-America, v. 21, p. 107; Spokane, WA, May 8-11, 1989.

Lindquist, E.S., 1994, The strength and deformation properties of melange; PhD dissertation, University of California, Berkeley, (Dept.Civil Engineering); UMI Dissertations Service, Ann Arbor, Michigan

Lyashenko, O., V, 1979, New data on the structure of the Eastern Sayan ultramafic belt: Geotectonics, v. 13, p. 275-281.

Makarychev, G.I., Ges', M.D., and Pazilova, V.I., 1983, Precambrian ophiolites of Ulutau in the light of stage-by-stage development of the crust of the Earth: Geotectonics, v. 17, p. 306-316.

Maruntiu, M., 1983, Contributions to the petrology of ophiolitic peridotites and related rocks of the Mehedinti Mts (South Carpathians): Anonymous. Travaux du XIIeme congres de l'association geologique Carpatho-Balkanique; Metamorphisme-magmatisme-geologie isotopique (The 12th meeting of the Carpathian-Balkan Geological Association; Metamorphism, magmatism and isotope geology); Anuarul-Institutului-de-Geologie-si-Geofizica-=-Annuaire-de-l'Institut-de-Geologie-et-de-Geophysique, v. 61, p. 215-222; Association geologique Carpatho-Balkanique; Congres; 12, Bucharest, 1983.

Maybin, A.H., III, and Mittwede, S.K., 1988, The Enoree melange, Laurens County, South Carolina: Anonymous. Geological Society of America, Southeastern Section, 37th annual meeting, with the Southeastern Section of the Paleontological Society; abstracts with programs. Abstracts-with-Programs-Geological-Society-of-America, v. 20, p. 278; Columbia, SC, Apr. 6-8, 1988.

Mazarovich, A.O., 1978 [1980], Serpentinite melange of the southern Sikhote Alin: Doklady-of-the-Academy-of-Sciences-of-the-USSR,-Earth-Science-Sections. 241. (1-6), p. 32-34.

---, 1979 [1982], Ophiolite allochthons of the Maritime Region: Doklady-of-the-Academy-of-Sciences-of-the-USSR,-Earth-Science-Sections. 249. (1-6), p. 49-51.

---, 1982, Paleozoic-early Mesozoic tectonic evolution of the southern Maritime Territory: Geotectonics, v. 16, p. 61-73.

McCall, G.J.H., and Kidd, R.G.W., 1982, The Makran, southeastern Iran; the anatomy of a convergent plate margin active from Cretaceous to present: Leggett, J. K. Trench-Forearc geology; sedimentation and tectonics on modern and ancient active plate margins, conference. Imp. Coll. Sci. and Technol., Dep. Geol., London, United-Kingdom. Special-Publication-Geological-Society-of-London, v. 10, p. 387-397; London, June 23-25, 1980.

McMillen, K.J., Breen, N.A., Tagudin, J.E., Reed, D.L., and Silver, E.A., 1988, Mud-cored parallel folds and possible melange development in the North Panama thrust beltdiscussion and reply: Geology (Boulder), v. 16, p. 955-956; For reference to original see Breen, Nancy A., et al., Geology (Boulder), Vol. 16, p. 207, 1988.

Michard, A., Bouchez, J.L., and Misseri, M., 1981, Les Nappes metamorphiques de Mascate, nouvel element infra-ophiolitique en Oman. Translated title: The metamorphic nappes of Muscat, new elements of the infra-ophiolites in Oman: Anonymous. First meeting of the European Union of Geosciences. Terra-Cognita. issue, p. 19; Strasbourg, April 13-16, 1981.

Mittwede, S.K., 1988, Ultramafites, melanges, and stitching granites as suture markers in the central Piedmont of the Southern Appalachians: Journal of Geology, v. 96, p. 693-708.

Mittwede, S.K., and Maybin, A.H., III, 1989, Metamorphosed melange in the central Piedmont of South Carolina: Journal of Geology, v. 97, p. 632-639.

Moench, R.H., Hafner, K., and Jahrling, C.E., II, 1984, Metavolcanic stratigraphy of the Littleton-Moosilauke area, New Hampshire; revisions of a classic succession: The Geological Society of America, Northeastern Section, 19th annual meeting. Abstracts-with-Programs-Geological-Society-of-America, v. 16, p. 51; Providence, RI, Mar. 15-17, 1984.

Moore, D.E., and Liou, J.G., 1979, Mineral chemistry of some Franciscan blueschist facies metasedimentary rocks from the Diablo Range, California: Geol. Soc. Am., Bull, v. 90, p. I1089-I1091,II.

Moore, G.F., 1979, Petrography of subduction zone sandstones from Nias Island, Indonesia: J. Sediment. Petrol, v. 49, p. 71-84.

Moore, T.E., 1976, Structure and petrology of the Sierra de San Andres Ophiolite, Vizcaino Peninsula, Baja California Sur, Mexico: San Diego State University, United-States, Master's Thesis; unknown p.

---, 1980, The blueschist-bearing melange complex near Puerto Nuevo, Vizcaino Peninsula, Baja California Sur, Mexico: Anonymous. American Geophysical Union; 1980 fall meeting. Eos,-Transactions,-American-Geophysical-Union. 61. (46), p. 1155; San Francisco, CA, Dec. 8-12, 1980.

---, 1984, Geology, petrology, and tectonic significance of the Mesozoic paleooceanic terranes of the Vizcaino Peninsula, Baja California Sur, Mexico: Stanford University, United-States, Doctoral Thesis; 418 p.; Univ. Microfilms.

Moseley, F., and Abbotts, I.L., 1979, The ophiolite melange of Masirah, Oman: Geol. Soc. Lond., p. 713-724.

Mullen, E.D., and Sarewitz, D., 1983, Paleozoic and Triassic terranes of the Blue Mountains, Northeast Oregon; discussion and field trip guide; Part 1; a new consideration of old problems: Oregon Geology, v. 45, p. 65-68.

Murphy, J.M., Aalto, K.R., and Cloos, M., 1983, Flow melanges; numerical modeling and geologic constraints on their origin in the Franciscan subduction complex, California : discussion and reply: Geological Society of America Bulletin, v. 94, p. 1241-1244; For reference to paper by Mark Cloos, see Geol. Soc. Am., Bull., Vol. 93, p. 330, 1982.

Nagel, J.J., 1979, The geology of part of the Shulaps ultramafite; near Jim Creek, southwestern British Columbia: University of British Columbia, Canada, Master's Thesis; unknown p.

Naidoo, D.D., Bloomer, S.H., Saquaque, A., and Hefferan, K., 1991, Geochemistry and significance of metavolcanic rocks from the Bou Azzer-El Graara Ophiolite (Morocco): Stern, Robert J., Van Schmus, W. Randall. Special issue; Crustal evolution in the late Proterozoic. Univ. Tex. at Dallas, Richardson, TX, United-States. Precambrian-Research, v. 53, p. 79-97.

Naylor, M.A., 1982, The Casanova Complex of the Northern Apennines, a melange formed on a distal passive continental margin: Journal of Structural Geology, v. 4, p. 1-18.

Nekrasov, G.Y., 1978 [1980], New data on the structure of the Pekul'ney Range in the left-bank area of the Anadyr' River: Doklady-of-the-Academy-of-Sciences-of-the-USSR,-Earth-Science-Sections. 238. (1-6), p. 87-9.

Nell, P.A.R., 1990, Deformation in an accretionary melange, Alexander Island, Antarctica: Knipe, Robert J., Rutter, E. H. Deformation mechanisms, rheology and tectonics. Leeds Univ., Dep. Earth Sci., Leeds, United-Kingdom. Geological-Society-Special-Publications, v. 54, p. 405-416; International conference on Tectonics and microstructures, Leeds, Mar. 1989.

Nelson, K.D., Kidd, W.S.F., McKerrow, W.S., and Cocks, L.R.M., 1979, A lower Paleozoic trench-fill sequence, New World Island, Newfoundland discussion and reply: Geol. Soc. Am., Bull, v. 90, p. I985-I98I; For reference to paper by McKerrow, W. S., and Cocks, L. R. M., Geol. Soc. Am., Bull., Vol. 89, p. 1121, 1978.

Nicholson, R., 198?, The Mona Complex, Anglesy: interpretation and re-interpretation: Amateur Geologist, v. 9, p. 40-45.

Nilsen, O., 1983, The nature and tectonic setting of melange deposits in Soknedal, near Stoeren, central Norwegian Caledonides: Bulletin Norges Geologiske Undersoekelse, v. 378, p. 65-81.

Okay, A., 1981, Kuzeybati anadolu'daki ofiyolitlerin. Jeolojisi ve mavisist metamorfizmasi (Tavsanli-Kuetahya). Translated title: Geology and the blueschist metamorphism of the ophiolites of northwestern Turkey, Tavasanli-Katahya: (1), p. 85-95.1; Tuerkiye-Jeoloji-Kurumu-Buelteni-=-Bulletin-of-the-Geological-Society-of-Turkey. 24.

Orange, D.L., 1990, Criteria helpful in recognizing shear-zone and diapiric melanges; examples from the Hoh accretionary complex, Olympic Peninsula, Washington: Geological Society of America Bulletin, v. 102, p. 935-951.

Orchard, M.J., 1984, A tale of three terranes; contrasts in late Paleozoic stratigraphy across the western Cordillera: Geol. Assoc. Can., Paleontol. Div. Publ., Toronto, ON; Canada, p. 6; 1984 Canadian paleontology and biostratigraphy seminar, Ottawa, ON, Sept. 28-30, 1984.

Ozgul, N., 1984, Stratigraphy and tectonic evolution of the Central Taurides: Maden Tetkik ve Arama Enstituesue, Ankara; Turkey, p. 77-90; International symposium of the Geological Society of Turkey ; Geology of the Taurus Belt, Ankara, Sept. 26-29, 1983.

Ozkaya, I., 1978, Ergani-Maden yoresi stratigrafisi. Translated title: Stratigraphy of the Ergani-Maden region: (2), p. 129-139.; Tuerk.-Jeol.-Kurumu,-Buel. 21.

---, 1990, Origin of the allochthons in the Lycien Belt, Southwest Turkey: Tectonophysics, v. 177, p. 367-379.

Page, R.J., 1974, A tectonic melange on the west coast of Vancouver Island, British Columbia, a Franciscan equivalent: 6, No, v. 3, p. 233-234,; in Cordilleran Section, 70th Annual Meeting. Geol. Soc. Am., Abstr. Vol.

---, 1975, Sedimentology and tectonic history of the Esowista and Ucluth peninsulas, west coast, Vancouver Island, British Columbia: University of Washington, United-States, Doctoral Thesis; 97 p. Diss. Abstr. Int., Vol. 35, No. 8, p. 3990B-3991B, 1975.

Parfenov, L.M., 1987, Nadvigi i svyazannyy s nimi melanzh Kharaulakhskikh gor (Severnoye Verkhoyan'ye). Translated title: Thrust faults in relation to the Kharaulak Mountain melange; northern Verkhoyansk: Doklady Akademii Nauk SSSR, v. 296, p. 685-689.

Petersen, S.W., 1982, Geology and petrology around Titus Ridge, north-central Klamath Mountains, California, 73 p. 62 Refs.

Phipps, S.P., Kleinspehn, K.L., and Suppe, J.E., 1979, Ophiolitic olistostromes in the basal Great Valley Sequence, Napa County, California Coast Ranges: Geol. Soc. Am., Abstr. Programs, v. 11, p. 122; The Geological Society of America, Cordilleran Section, 75th annual meeting, San Jose, Calif., April 9-11, 1979.

Pique, 1975, Differentitaion of sedimentation regions in the northwestern Meseta, Morocco; the Devonian-Dinantian distribution: Comtes rendus de l'Academie des Sciences (Paris), D 281, v. v12, p. 767-770.

Plafker, G., 1973, Yakutat Group, an upper Mesozoic flysch and melange sequence in southern Alaska: 57, No, v. 4, p. 800,; Am. Assoc. Pet. Geol., Bull. Vol.

Pollock, S.G., 1982, Stratigraphy of the Caucomgomoc Lake area, northern Maine; example of an obducted ophiolite-melange complex: Wright, T. O., Medlin, J. H. Abstracts with programs; 1982 Northeastern and Southeastern combined section meetings. Abstracts-with-Programs-Geological-Society-of-America. 14. (1-2), p. 73; Washington, DC, Mar. 25-27, 1982.

Pospelov, I.I., and Ruzhentsev, S., V, 1973, The "ophiolitic complex" in the central part of the Sakmara Zone in the Southern Urals: Acad. Sci. USSR, Dokl., Earth Sci. Sect, v. 203, p. 24-26.

Rangin, C., 1979, Evidence for superimposed subduction and collision processes during Jurassic-Cretaceous time along Baja California continental borderland: Geol. Soc. Am., Boulder, Colo.; United States, Brown, E. H., Ellis, R. C.: Geological excursions in the Pacific Northwest, p. 37-51.

Rast, N., and Grant, R.H., 1974, An early Acadian melange in southern New Brunswick: Geol. Assoc. Can.--Mineral. Assoc. Can.; Canada, p. 71.

Rast, N., and Stringer, P., 1980, A geotraverse across a deformed Ordovician ophiolite and its Silurian cover, northern New Brunswick, Canada: Tectonophysics, v. 69, p. 221-245.

Rau, W.W., 1977, General geology of the southern Olympic Coast: Geol. Soc. Am., Boulder, Colo.; United States, p. 63-83.

Raymond, L.A., and Aalto, K.R., 1978, Sedimentology of a melange; Franciscan of Trinidad, California discussion and reply: J. Sediment. Petrol, v. 48, p. 674-679; For original article by Aalto, K. R., see this journal, Volume 46, p. 913-929, 1976.

Raymond, L.A., Ingersoll, R., V, Howell, D.G., and Smith, G.W., 1979, Late Cretaceous trench-slope basins of central California discussion and reply: Geology (Boulder), v. 7, p. 514-515; For reference to paper by Smith, G. W., et al., see Geology (Boulder), Vol. 7, p. 303, 1979.

Raymond, L.A., Yurkovich, S.P., and McKinney, M., 1989, Block-in-matrix structures in the North Carolina Blue Ridge Belt and their significance for the tectonic history of the Southern Appalachian Orogen: Horton, J. Wright, Jr., and Rast, Nicholas: Melanges and olistostromes of the U.S. Appalachians;Special-Paper-Geological-Society-of-America, v. 228, p. 195-215.

Raymond, L.A. and Terranova, T., 1984, Prologue: The melange problem-a review: Raymond, L.A.: Melanges: Their nature, origin and significance; Special Paper 198; Geological Society of America, v 198, p. 1-5.

Raznitsin, Y.N., 1978, Serpentinite melange and olistostromes in the southeastern part of the east Sakhalin Mountains, in Geotectonics. 12, ed., (2): p. 142;

Rikhter, A., V, 1981, Block structure of the Susunay Range (South Sakhalin): Geotectonics, v. 15, p. 162-167.

Rivard, B., Arvidson, R.E., Sultan, M., and El, K.B., 1988, Mapping of ophiolitic melanges of the Wadi Ghadir area, Nubian Shield of Egypt using a linear mixing model applied to Landsat thematic mapper data: Nineteenth lunar and planetary science conference, NASA, Lunar and Planetary Institute, 19 (Part 3), p. 986-97.; Houston, TX, Mar. 14-18, 1988.

Roberts, D., and Horne, G.S., 1980, Melange in Trondheim Nappe, central Norwegian Caledonides discussion and reply: Nature, v. 285, p. 593.; For reference to article by Horne, G. S., see Nature, Vol. 281, p. 267, 1979.

Robertson, A.H.F., 1991, Origin and emplacement of an inferred Late Jurassic subduction-accretion complex, Euboea, eastern Greece: Geological Magazine, v. 128, p. 27-41.

Robertson, A.H.F., and Woodcock, N.H., 1981, Goedene Zone, Antalya Complex; volcanism and sedimentation along a Mesozoic continental margin, S. W. Turkey: (3), p. 1177-1214.; Geologische-Rundschau. 70.

Roy, D.C., and Foster, J.E., 1990, Stratigraphic and structural relations of the St. Victor Synclinorium to the St. Daniel Melange; Quebec-Maine border near St. Pamphile, Quebec: Boone, Gary M. Geological Society of America, Northeastern Section, 25th annual meeting. Abstracts-with-Programs-Geological-Society-of-America, v. 22, p. 67; Syracuse, NY, March 4-7, 1990.

Rozhdestvenskiy, V.S., and Rechkin, A.N., 1975 [1976]-a, Serpentinite melange and some aspects of tectonic evolution of Sakhalin Island: Acad.-Sci.-USSR,-Dokl.,-Earth-Sci.-Sect. 221. (1-6), p. 121-123.

---, 1975b, Serpentinitovyy melanzh i nekotoryye osobennosti tektonicheskogo razvitiya ostrova Sakhalin. Translated title: Serpentinite melange and some characteristics of tectonic evolution of Sakhalin: Akad. Nauk SSSR, Dokl, v. 221, p. 1156-1159.

Ruzhentsev, S., V, 1975, Geologicheskoye stroyeniye Karatauskogo ofiolitovogo kompleksa v khrebte Sultan-Uizdag (Kyzylkumy). Translated title: Geological structure of the Karatau ophiolite complex of the Sultan-Uizdag Range, Kyzylkums: Akad. Nauk SSSR, Dokl, v. 223, p. 684-687.

Saquaque, A., Karson, J.A., Bloomer, S., Admou, H., Naidoo, D., Hefferan, K., and Reuber, I., 1988, Precambrian ophiolites and accretionary tectonics, Anti-Atlas, Morocco: Anonymous. AGU 1988 fall meeting; abstracts. Eos,-Transactions,-American-Geophysical-Union. 69. (44), p. 1453; San Francisco, CA, Dec. 6-11, 1988.

Saquaque, A., Admou, H., Karson, J.A., Hefferan, K., and Reuber, I., 1989, Precambrian accretionary tectonics in the Bou Azzer-El Graara region, Anti-Atlas, Morocco: Geology (Boulder), v. 17, p. 1107-1110.

Satian, M.A., 1975, Stroyeniye Yerevano-Ordubadskoy ofiolitovoy zony Malogo Kavkaza. Translated title: The structure of the Yerevan-Ordubad ophiolite zone in the Lesser Caucasus: Mosk. O vo Ispyt. Prir., Byull., Otd. Geol, v. 50, p. 46-57.

Savci, G., 1988, Structural and metamorphic geology of the subophiolitic dynamothermal metamorphic sole and peridotite tectonites, Blow Me Down Massif, Newfoundland- Canada; tectonic implications for subduction and obduction: University of Houston, United-States, Doctoral Thesis; 379 p.; Univ. Microfilms, Ann Arbor, MI, United States.

Savu, H., 1984, Melange-ul cu matrice piroclastica asociat arcului insular al zonei Mures. Translated title: The pyroclastic matrix melange associated with the southern island arc of the Mures Zone: 29, p. 36-43.1; Studii si Cercetari de Geologie, Geofizica, Geografie. Seria Geologie.

Sborshchikov, I.M., 1976, Tectonics of Afghanistan and structural evolution of the Alpine Belt (Pamirs-Eastern Iran Segment): Geotectonics, v. 10, p. 189-198.

Sborshchikov, I.M., and Sonin, I.I., 1977, Tektonicheskaya pozitsiya ofiolitov Afganistana. Translated title: The tectonic position of the ophiolites of Afghanistan: Vyssh. Uchebn. Zaved., Izv., Geol. Razved, v. 1977, p. 58-68.

Schmidt, E.R., 1979, Alter und Genese des Nicoya-Komplexes, einer ozeanischen Palaeokruste (Oberjura bis Eozaen) im suedlichen Zentralamerika. Translated title: Age and genesis of the Nicoya Complex, an oceanic paleocrust (Upper Jurassic to Eocene) in southern Central America: (2), p. 457-94.; Geol.-Rundsch. 68.

Schmidt, W.J., 1980, Structure of the Oxbow area, Oregon and Idaho, Thesis; 61 p.

Schultz, A.P., 1979a, Fault breccia, fault chaos, tectonic melange and deformed parautochthonous rocks in the Price Mountain and East Radford windows of the Pulaski Overthrust, Montgomery County, southwestern Virginia: Glover, L., III, Read, J. F.: Guides to field trips 1-3 for Southeastern Section meeting, Geological Society of America; Geology of the Pulaski overthrust near Blacksburg, Virginia, p. 112-132.

---, 1979b, Fault chaos and tectonic melange of the Pulaski Overthrust, Southwest Virginia: Geol. Soc. Am., Abstr. Programs, v. 11, p. 211; The Geological Society of America, Southeastern Section, 28th annual meeting, Blacksburg, Va., April 26-27, 1979.

Schurer, V.C., 1979, A Basin and Range chaos in the Oquirrh Mountains, sedimentary or tectonic?: Rocky Mountain Assoc. Geol., Denver, CO; United States, Newman, G. W., Goode, H. D.: Basin and Range symposium and Great Basin field conference, p. 267-271; Oct. 7-11, 1979.

Schuster, D.C., 1979, Gwna Melange, upper Precambrian olistostromal sequence, North Wales, United Kingdom: Am. Assoc. Pet. Geol., Bull, v. 63, p. 523; AAPG-SEPM annual meeting, Houston, Tex., April 1-4, 1979.

---, 1980, The nature and origin of the late Precambrian Gwna Melange, North Wales, United Kingdom: University of Illinois, Urbana, United-States, Doctoral Thesis; 389 p.; Univ. Microfilms.

Sedlock, R.L., and Larue, D.K., 1984, Structural features of Mesozoic Melange, Cedros Island, Baja California: American Geophysical Union, 1984 Fall Meeting. Eos,-Transactions,-American-Geophysical-Union. 65. (45), p. 1085; San Francisco, CA, Dec. 3-7 1984.

Seidel, E., 1981, On the petrology and geochronology of the Cretan ophiolite nappe: Anonymous. First meeting of the European Union of Geosciences. Terra-Cognita. issue, p. 23-24; First meeting of the European Union of Geosciences, Strasbourg, April 13-16, 1981.

Seidel, E., Schliestedt, M., Kreuzer, H., and Harre, W., 1977, Metamorphic rocks of Late Jurassic age as components of the ophiolitic melange on Gavdos and Crete (Greece): (28), p. 3-21.; Geol. Jahrb., Reihe B.

Sestini, G., and Pamic, J., 1980, Melanges and melanges of the Zagros coloured melange in SE Iran: Int. Geol. Congr. Abstr. Congr. Geol. Int., p. 88; 26th international geological congress, Paris, July 7-17, 1980.

Sharp, W.D., and Saleeby, J., 1979, The Calaveras Formation and syntectonic Mid-Jurassic plutons between the Stanislaus and Tuolumne rivers, California: Geol. Soc. Am., Abstr. Programs, v. 11, p. 127; The Geological Society of America, Cordilleran Section, 75th annual meeting, San Jose, Calif., April 9-11, 1979.

Sher, S.D., and Vikhter, B.Y., 1973, Ob odnoy vazhnoy osobennosti verkhnepaleozoyskikh otlozheniy Tsentral'nykh Kyzylkumov. Translated title: An important characteristic of upper Paleozoic rocks in central Kyzylkum, Sov. Geol. No. 6, p. 140-144,

Shore, P.J., and Duncan, I.J., 1983, New evidence for Precambrian plate tectonics; an differs from 1.7 Ga melange unit in the Vadito Group of the Picuris Mountains, New Mexico: Anonymous. AGU 1983 fall meeting. Eos,-Transactions,-American-Geophysical-Union. 64. (45), p. 844; San Francisco, CA, Dec. 5-9, 1983.

Shreve, R.L., and Cloos, M., 1986, Dynamics of sediment subduction, melange formation, and prism accretion: JGR. Journal of Geophysical Research. B, v. 91, p. 10,229-10,245.; Univ. Calif., Inst. Geophys. and Planet. Phys., Publ. No. 2642; Univ. Tex., Inst. Geophys., Contrib. No. 641.

Simkin, G.S., 1982, Tektonicheskiye pokrovy i serpentinitovyy melanzh ostrova Karaginskogo (Vostochnaya Kamchatka). Translated title: Nappes and melange with serpentinite in Karaginskii, eastern Kamchatka: Byulleten' Moskovskogo Obshchestva Ispytateley Prirody, Otdel Geologicheskiy, v. 57, p. 55-59.

Sizykh, V.I., 1984 [1985], The Tataurovo melange in the Selenga-Vitim subsurface shear zone: Soviet-Geology-and-Geophysics. 25. (11), p. 106-110.

Snavely, P.D., Jr., and Kvenvolden, K.A., 1989, Geology and hydrocarbon potential: Preliminary evaluation of the petroleum potential of the Tertiary accretionary terrane, west side of the Olympic Peninsula, Washington. U. S. Geological Survey, United-States. Geological-Survey-Bulletin-(Washington), p. 1-17; Chapter A.

Sobolev, V.S., and Dobretsov, N.L., 1977, Petrologiya i metamorfizm drevnikh ofiolitov (na primere Polyarnogo Urala i Zapadnogo Sayana). Translated title: Petrology and metamorphism of ancient ophiolites, e.g. the Polar Urals and western Sayan, Akad.-Nauk-SSSR,-Sib.-Otd.,-Inst.-Geol.-Geofiz.,-Tr. 368. International Geological Correlation Program, Project "Ophiol. 219 p.

Sokolov, S.D., 1974, Verkhnemelovaya olistostromovaya tolshcha yugo-vostochnoy chasti Sevano-Akerinskoy ofiolitovoy zony. Translated title: Upper Cretaceous olistostrome terrain in the southeastern part of the Sevan-Akerin ophiolite zone: Mosk. O vo Ispyt. Prir., Byull., Otd. Geol, v. 49, p. 141-142.

Spadea, P., 1982, Continental rocks associated with ophiolites in Lucanian Apennine, southern Italy: Bortolotti, V. Ophiolites and actualism; Proceedings of the meeting. Ofioliti, v. 7, p. 501-522; Ophiolites and actualism; meeting, Florence, Dec. 18-19, 1981.

Spinek, T.R., 1988, Polydeformed and polymetamorphosed melange within the Cameron's Line thrust sheet, southwestern Connecticut: Anonymous. Geological Society of America, Northeastern Section, 23rd annual meeting. Abstracts-with-Programs-Geological-Society-of-America, v. 20, p. 71; Portland, ME, Mar. 10-12, 1988.

St, J.P., 1973, Structural setting of the Thetford-Mines Ophiolitic Complex: in Northeastern Section, 8th Annual Meeting. Geol. Soc. Am., Abstr, v. 5, No. 2, p. 215

Stavskii, A.P., Berezner, O.S., Drachev, S.S., and Safonov, V.G., 1988, Structural peculiarities of melanges in the Mainit Zone of the Koryak Highland, Moscow-University-Geology-Bulletin. 43 (6), p. 40-46.

Stern, R.J., Gottfried, D., Hedge, C.E., and Shimron, A.E., 1985, Evolution of the Kid Group, Southeast Sinai Peninsula; thrusts, melanges, and implications for accretionary tectonics during the late Proterozoic of the Arabian-Nubian Shield; discussion and reply: Geology (Boulder), v. 13, p. 155-157; For reference to paper by Shimron, see Geology (Boulder), Vol. 12, p. 242, 1984.

Storey, B.C., and Meneily, A.W., 1983, Melange within subduction accretion complex rocks of Fredriksen Island, South Orkney Islands: Geological Magazine, v. 120, p. 555-566.

Swarbrick, R.E., and Naylor, M.A., 1980, The Kathikas Melange, SW Cyprus; Late Cretaceous submarine debris flows: Sedimentology, v. 27, p. 63-78.

Swift, P.N., 1987a, Early Proterozoic turbidite deposition and melange deformation, southeastern Arizona: University of Arizona, United-States, Doctoral Thesis; 161 p.; Univ. Microfilms, Ann Arbor, MI, United States.

---, 1987b, Subduction zone setting for early Proterozoic turbidite deposition and melange deformation, Southeast Arizona: Dickinson, William R. Geological Society of America, 1987 annual meeting and exposition. Abstracts-with-Programs-Geological-Society-of-America. 19. (7), p. 862; Phoenix, AZ, Oct. 26-29, 1987.

Szubert, E.C., 1978, Uma associacao ofiolitica completa, Palma, Sao Gabriel, RS; geologia e questoes estratigraficas. Translated title: A complete ophiolite complex, Palma, Sao Gabriel, Rio Grande do Sul; geology and stratigraphic questions: (1), p. 467-476.; Gomes Farias, Carlos Eugenio. Sociedade Brasileira de Geologia; anais do XXX congresso; Recife, Nov., 1978.

Tabor, R.W., 1987, The Helena-Haystack Melange, a fundamental western Washington structure, and its relation to the Straight Creek Fault: Anonymous. AGU; 34th annual Pacific Northwest regional meeting. Eos,-Transactions,-American-Geophysical-Union, v. 68, p. 1814; Olympia, WA, Sept. 2-4, 1987.

Thon, A., 1981, The Gullfjellet ophiolite complex and the structural evolution of the Major Bergen Arc, West Norwegian Caledonides: Anonymous. Uppsala Caledonide symposium (UCS); (with pre- and post-symposium excursions). Terra-Cognita, v. 1, p. 78-79; Uppsala, Aug. 24-28, 1981.

Tirrul, R., Bell, I.R., Griffis, R.J., and Camp, V.E., 1983, The Sistan suture zone of eastern Iran: Geological Society of America Bulletin, v. 94, p. 134-150.

Tranter, T.H., 1986, The LeMay Group of central Alexander Island: British Antarctic Survey Bulletin, v. 71, p. 57-67.

Trautmann, C.H., 1976, Engineering geology of Franciscan melange terrane in the Red Hill area, Petaluma, California: Stanford University, United-States, Master's Thesis; unknown p.

Tremblay, A., 1990, The oceanic domain from Eastern Townships, Appalachians, Quebec; Taconian versus Acadian tectonics: Colpron, Maurice, Doolan, Barry. Proceedings of the Quebec-Vermont Appalachian workshop. Univ. Vt., Dep. Geol., Burlington, VT, United-States. Vermont-Geology, v. 6, p. 12-14; Quebec-Vermont Appalachian workshop, Burlington, VT, Apr. 14-16, 1989.

Tselikov, N.N., 1977, Tectonic slabs and melange in the Medes region, Sakmarian Zone of the Urals: Geotectonics, v. 10, p. 256-260.

Tull, J.F., and Telle, W.R., 1989, Tectonic setting of olistostromal units and associated rocks in the Talladega slate belt, Alabama Appalachians: Horton, J. Wright, Jr., Rast, Nicholas. Melanges and olistostromes of the U.S. Appalachians; Special-Paper-Geological-Society-of-America, v. 228, p. 247-269.

Tysdal, R.G., and Case, J.E., 1977, The McHugh Complex in the Seward Quadrangle, south-central Alaska, in: Snavely, Parke D., Jr., Kvenvolden, Keith A., Rapp, John B., Hostettler, Frances D., Golan-Bac, Margaret, (eds): Preliminary evaluation of the petroleum potential of the Tertiary accretionary terrane, west side of the Olympic Peninsula, Washington.; p B48-9.6, Open-File-Report; U.-S.-Geological-Survey.

Virdi, N.S., 1978, The Mona Complex of Anglesey, North Wales and plate tectonic; reappraisal: Indian Geol. Assoc., Bull, v. 11, p. 11-23.

Vollmer, F.W., 1981, Structural studies of the Ordovician flysch and melange in Albany County, New York: SUNY at Albany, United-States, Master's Thesis; 151 p.

Voytovich, V.S., 1983, O dokembriyskom melanzhe i blokovykh strukturakh. Translated title: Precambrian melange and block structures: Doklady Akademii Nauk SSSR, v. 268, p. 939-942.

Wahrhaftig, C., 1984, Structure of the Marin Headlands Block, California; a progress report: Blake, M. C., Jr. Franciscan geology of Northern California.; Field-Trip-Guidebook-Pacific-Section,-Society-of-Economic-Paleontologists-and-Mineralogists, v. 43, p. 31-50.

Wajsprych, B., 1978, Allochtoniczne skaly paleozoiczne w osadach wizenskich Gor Bardzkich (Sudety). Translated title: Allochthonous Paleozoic rocks in the Visean of the Bardo Mountains; Sudeten Mountains: (1), p. 99-127.; Rocznik-Polskiego-Towarzystwa-Geologicznego-=-Annales-de-la-Societe-Geologique-de-Pologne. 48.

Waldron, J.W.F., 1984, Structural history of the Antalya Complex in the "Isparta Angle", Southwest Turkey: Dixon, J. E., Robertson, A. H. F. The geological evolution of the eastern Mediterranean. Univ. Edinburgh, Dep. Geol., Edinburgh, United-Kingdom. Geological-Society-Special-Publications, v. 17, p. 273-286; Edinburgh, Sept. 28-30, 1982.

Wallbrecher, E., 1983, Alpidischer Deckenbau und Metamorphose auf den Nord-Sporaden und auf der suedlichen Pelion-Halbinsel (Thessalien, Griechenland). Translated title: Alpine nappes and metamorphism of the northern Sporades and southern Pelion Peninsula; Thessaly, Greece: 48, p. 99-116.; Jacobshagen, V. Untersuchungen zur Geologie der Nord-Sporaden (Aegaeisches Meer, Griechenland). Geologic studies on northern Sporades, Aegean Sea, Greece. Freie Univ. Berlin, Inst. Geol., Berlin 33 1000, Federal-Republic-of-Germany. Berliner-Geowissenschaftliche-Abhandlungen,-Reihe-A:-Geologie-und-Palaeontologie.

Wasowski, J.J., 1983, Sedimentary and tectonic history of the northeastern portion of the Dunnage Melange and surrounding units, Newfoundland: SUNY at Buffalo, United-States, Master's Thesis; 86 p.

Wasowski, J.J., and Jacobi, R.D., 1982, Nature and significance of igneous-clast breccias and adjacent units in the Dunnage Melange, North-central Newfoundland: Northeastern and Southeastern combined section meetings. Abstracts-with-Programs-Geological-Society-of-America, v. 14, p. 94; Washington, DC, Mar. 25-27, 1982.

Weissert, H., 1975, Zur Geologie der Casanna bei Klosters. Translated title: The geology of Casanna, near Klosters, Eclogae-Geol.-Helv. 68. (1). p. 222-229

White, D.L., 1983, Geology and regional setting of Jabal Ashsha, Saudi Arabia: The Geological Society of America, 96th annual meeting. Abstracts-with-Programs-Geological-Society-of-America, v. 15, p. 717; Indianapolis, IN, Oct. 31-Nov. 3, 1983.

Williams, A.J., 1979, Foliation development in serpentinites, Glenrock, New South Wales: Bell, T. H., Vernon, R. H. Microstructural processes during deformation and metamorphism. Tectonophysics, v. 58, p. 81-95; Microstructural processes during deformation and metamorphism, South Mission Beach, Sept. 4-8, 1978.

Williams, H., and Hibbard, J.P., 1976, The Dunnage Melange, Newfoundland (2 E): Can. Geol. Surv., p. 183-185.

Williams, H., and Talkington, R.W., 1978, Distribution and tectonic setting of ophiolites and ophiolitic melanges in the Appalachian Orogen: Malpas, J., Talkington, R. W. Ophiolites of the Canadian Appalachians and Soviet Urals. Newfoundland,-Mem.-Univ.,-Geol.-Rep, p. 3-19.

Wilson, T.J., Hanson, R.E., and Grunow, A.M., 1987, Structural history of subduction complex rocks, Diego Ramirez Islands, southernmost Chile: Dickinson, William R. Geological Society of America, 1987 annual meeting and exposition. Abstracts-with-Programs-Geological-Society-of-America. 19. (7), p. 893; Phoenix, AZ, Oct. 26-29, 1987.

---, 1989a, Islas Diego Ramirez, in: Dalziel, Ian W. D., Birkenmajer, Krzysztof, Mpodozis, Constantino, Ramos, Victor A., Thomson, Michael R. A.: Tectonics of the Scotia Arc, Antarctica; Punta Arenas, Chile to Ushuaia, Argentina; p 76-81; Univ. Tex. at Austin, Inst. Geophys., Austin, TX, United-States.

---, 1989b, Multistage melange formation within an accretionary complex, Diego Ramirez Islands, southern Chile: Geology (Boulder), v. 17, p. 11-14.

Wojtal, S.F., 1987, Geometry and evolution of the thrust zone below Blow-Me-Down Massif, Bay of Islands Ophiolite, Newfoundland: Dickinson, William R. Geological Society of America, 1987 annual meeting and exposition. Abstracts-with-Programs-Geological-Society-of-America. 19. (7), p. 894-895; Phoenix, AZ, Oct. 26-29, 1987.

Woodcock, N.H., and Robertson, A.H.F., 1982, Stratigraphy of the Mesozoic rocks above the Semail Ophiolite, Oman: Geological Magazine, v. 119, p. 67-76.

Worley, P.L.H., and Raymond, L.A., 1978, Petrographic and structural reconnaissance of the Franciscan Complex (Dothan/Otter Point) in the Dillard Block, Southwest Oregon: Geol. Soc. Am., Abstr. Programs, v. 10, p. 155; The Geological Society of America, Cordilleran Section, 74th annual meeting, Tempe, Ariz., March 29-31, 1978.

Wright, J.E., 1979, Tectonic correlation between the South-central Klamath Mountains and Sierra Nevada foothill belt: Geol. Soc. Am., Abstr. Programs, v. 11, p. 136; The Geological Society of America, Cordilleran Section, 75th annual meeting, San Jose, Calif., April 9-11, 1979.

Xia, Z.G., 1983, Geology of the western boundary of the Taconic Allochthon near Troy and the anastomosing cleavage in the Taconic melange: SUNY at Albany, United-States, Master's Thesis; 189 p.

Yermolov, P., V, and Kotelnikov, P.Y., 1991, Composition and origin of jadeitites of Itmurundinsky Melange (northern Balkhash area), Soviet-Geology-and-Geophysics 32, (2), p. 44-51.

Zhegalova, G., V, 1981, Melange in the massifs of the gabbro-norite-cortlandite complex of the Sredinnyy [Middle] Range of central Kamchatka: Geotectonics, v. 15, p. 273-278.

APPENDIX B

Image Analysis Procedures and Program Codes

B1.0 INTRODUCTION

This Appendix contains a summary of image analysis procedures used during the research. Three short computer programs were written to convert data obtained from scanlines traced over images into chord lengths, the programs are described, examples given and the source code presented.

B2.0 SUMMARY OF DATA ACQUISITION METHODS: SCANNING AND IMAGE PROCESSING

Color photographs were scanned using either a flat-bed (rarely) or a handheld scanner, devices that translate the colors or gray shades of a photograph (or a drawing) into an array of *pixels* (*pict*ure *el*ements). During scanning, each pixel was assigned a gray scale or color value, ranging from 0 (pure black) to 256 (pure white). Color scanning was also possible, but was not performed in order to minimize the size of computer data files. The gray scale value was recorded as an 8-bit value. The size of the array of pixels is dependent on both the size of the source image and the *resolution* of the scanning. The resolution is measured in *dpi* (dots per inch): the higher the dpi, the more detailed the scanning. Although the degree of detail is improved by higher resolution, there is a cost in that both the size of the computer file increases, and the processing of the digitized data takes longer. For example, an image of 150 mm by 150 mm (six inches square), scanned at a resolution of 50 dpi will result in a file of the order of 720 kbytes. By doubling the resolution to 100 dpi, file size will expand to 2.9 MB. Having several files of this size adds quickly fills computer hard drives, and was the principal reason that resolutions of less than 100 dpi and photographs smaller than 6 inches were used.

Most scanning was performed with a Niscan GS 256 gray scale hand-held scanner, purchased for approximately $300. The hand scanner was adequate for the research, especially since scanning was performed using a template and scanning guide to prevent "wobble". Some useful tips to hand scanning were gleaned from Busch (1993). Since the scanning swathe was restricted to a 4 inch width, larger images had to be scanned in strips, and the strips "stitched" together using Micrografx™ Picture Publisher, v.3.0.[1]. Scanning was also performed from this program, which allowed the control of resolutions, image dimensions, gray shade contrasted image preview before saving it to a data file.

---

[1], Micrografx; 1303 Arapaho, Richardson, TX 75081; phone 214-234-1769; 800-733-3729: approx. $250

Using the Picture Publisher software, various manipulations to the images were possible, such as altering the contrast and brightness, enhancing the edges of features, converting the gray scale image to a binary image (just black and white), adding text and symbols, and deleting or changing the orientation of selected components of the image. Most images required several such enhancements.

The scanned images could have been saved in any of the many graphics files formats (.TIF, .BMP, .PCX, .GIF and so on). However, the image analysis software used required graphic files to be written as TIFF files (Tagged Image File Format; file extension .TIF). The management and conversion of graphics files was simplified by using Graphic Workshop for Windows[2], which can convert between a score of different graphics formats, enhance images and create *thumbnail* versions of the graphic files or miniatures of large graphics files. A gallery of thumbnails saved time since the full versions did not have to be loaded in order to see what they contained.

B3.0 IMAGE ANALYSIS SOFTWARE USED FOR THE RESEARCH

It took some time to find the computer software tools that were eventually selected. The principal requirements were for an accurate program to measure particle areas and characteristic dimensions. These requirements were met by many programs, but most are intended for biological research, astronomy or military surveillance; none of them were intended for the purposes for which they were used for this research. An initial reconnaissance revealed three types of software:

1. Software that will run on IBM PC-compatible platforms: usually expensive ($5k-$10k), or else cheap (<$500) and cumbersome to use.
2. Software that will run on Macintosh platforms: often free.
3. Software that will run on UNIX platforms: often free but huge system files (>100 MB)

Preliminary work was performed with NIH Image, a powerful, user-friendly program that required a Macintosh computer (at least System 7, with a minimum of 5 MB of RAM, and a 256 color monitor). The program was developed by the National Institute of Health for the measurement of images of body particles and tissue, and has evolved through more than 50 versions[3]. The program enhances a picture by image processing; performs automatic recognition of particles surrounded by matrix, and then measures each particle's area, axes, shape factor, orientation, and many other features. For automatic measurement of particles, the image must be converted to a *binary image* composed of only black and white pixels. The procedure is described in later in the Appendix.

---

[2]Graphic Workshop from Alchemy Mindworks; PO Box 500, Beeton, Ontario L0G 1A0, Canada; phone 416 729-3831; FAX: 416 729-4156; approx $45

[3] NIH Image available via FTP from alw.nih.gov or (128.231.128.251). I obtained my version from Mr. Don Bain, Manager of the Geography Computing Center, McCone Hall, Univ. California, Berkeley

Shortly after the image analysis work started, a newly-developed program, SigmaScan/Image™[4], was released. This Windows-based program satisfied the modest requirements of the research, and allowed work on a home-based 486/DX2-66 computer. Although the release version (v. 1.0) of the program did not allow the automatic measurement of particles, it did work with full 256 gray scale or color images, rather than binary images. (Actually, the program requires 8-bit, 256 color or gray scale TIFF images). Once the outline of a particle was traced onto a virtual "overlay", the program measured the characteristics of the traced particle, rather than the original. The benefit was that the particle shape could be defined by referring to the original photograph (preferably, color) to decide what was a block and what was matrix, shadow, vegetation or other superfluous detail. Tracings were saved as a separate image, although image processing by graphics software was required to massage the overlay image into a presentable graphic. Many tracings are presented in Appendix D.

Figure B1 Gray scale Image of melange at Caspar Headlands, near Mendocino,California. US 25 cent piece at top is 24 mm in diameter

In addition to the particle measurement capability of SigmaScan/Image™, the program also allowed traverses across the image to be made, in which the gray scale, or color, pixel values along the traverse were recovered as *intensity* measurements. By defining the traverse width to be one pixel wide, *scanlines* were traced across the images. The

[4]SigmaScan/Image available from Jandel Scientific, 2591 Kerner Boulevard, San Rafael, CA 94901; phone 415 453-6700; FAX: 415-453-7769; current v. 1.2 approx. $250, lower for education discount.

pixel gray scale data were converted into chord lengths by short computer programs written for the research. The program codes are presented in later sections of this Appendix.

Figure B2 Same image as Figure B1, but binarized. Pixels are either black or white In this case, the blocks are white, but they could as easily be changed to black.

B4.0 SUMMARY OF IMAGE ANALYSIS PROCEDURES

B4.1 Binarization

When using the automatic measurement capabilities of NIH Image, it was necessary to convert the image to a binary file of black and white pixels. Prior to binarization, two procedures were used to enhance the definition of particles so that they could be distinguished from the matrix: *erosion* removed pixels; *dilation* added them. Several program functions increased the brightness and relative contrast of particles and matrix, and *edge enhancement* sharpened the boundaries, by passing mathematical transforms (often 3x3, or 9x9 matrices) through the array of pixel values. Once the desired enhancements were achieved, the images were binarized by comparing each pixel gray scale value to a *threshold* pixel value: pixels of gray scale values below the threshold become white, and those above the threshold become black. The new pixel values were "0" and "1". But the image processing of poor to moderate quality photographs, with many shades and poorly distinguishable melange block boundaries, resulted in a loss of

definition of particle shapes when the images were translated from gray scale to binary format. The results of binarization are shown in Figures B1 and B2.

Figure B3 The effect of binarization of particles that touch: agglomeration.

One significant problem resulted from particles that touched or particles that, in three dimensions, were superimposed. Although such particles may have been distinguishable as separate when an image was composed of gray shades, binarization generally removed the boundary between the particles and they effectively became one graphic object. This effect could be mitigated by eroding the pixels along the common boundary, such that the particles remained separate, but the particles were then slightly smaller than they were

before the erosion. The agglomeration ("blobbing") effect of binarization on an image with contiguous particles is shown in Figure B3.

The frustrations of trying to obtain accurate measurements of poorly contrasted melange blocks with NIH Image prompted the suite of tests that are referred to here to as *particle calibration tests ("Gravel Tests")*. The Gravel Tests setups provided photographic images with clearly distinguishable particles against a plain monochromatic background (matrix). Binariazation was not necessary with SigmaScan/Image™.

B4.2 Particle Measurements

NIH Image and SigmaScan/Image™ measured particles in much the same way. For particle areas, all the pixels in the particle were summed, and the true area calculated using a spatial calibration factor that was entered before measuring. In the case of NIH Image, the program initially examined the entire image and automatically isolated discrete particles, which were distinguishable as colonies of white pixels in a black background. The program could label these (as shown in the bottom graphic of Figure B3) With SigmaScan/Image™, each particle was defined by tracing the outlines onto a virtual overlay using a mouse cursor. Once the outline was completed, the program performed the required measurements on the pixels contained within the area of the image below the traced boundary on the overlay. Each particle was processed individually. Processing time ranged from a fraction of a second to several seconds if the particle was large and several parameters were requested of the program. (It helps to have a fast, powerful computer if measuring scores of particles with SigmaScan/Image™; at least a 486/33 system). The tracing/measuring process was repeated a particle at a time until all desired particles were measured. The particles could be labeled, but labeling cluttered the screen and added to the calculation time.

Besides measuring particle areas, both programs computed the length and angular orientation of major and minor axes, the average gray scale value within the particle, the number of pixels, the length of the perimeter, the shape factor and other parameters. (The length of the major axis, was of most interest since this parameter is a characteristic dimension of bimrock blocks which can be readily measured in the field or from maps.) NIH Image computed the major axis by initially defining a best-fit ellipse to the particle, and then determining the length and orientation of the axes. This was not necessarily the same as the length of the longest line that could be drawn within an irregular shaped block. SigmaScan/Image™ determined the length of the longest line that could be drawn within the particle, which more closely matches the d_{mod} that can be measured for real bimrock blocks. With both programs, the length of the minor axis was determined as the longest line that could be drawn normal to the major axis. The orientation of the axes was the angle relative to a "horizontal" baseline ("x" axis). Both programs provided data in a selection of units: most work was performed using SI units.

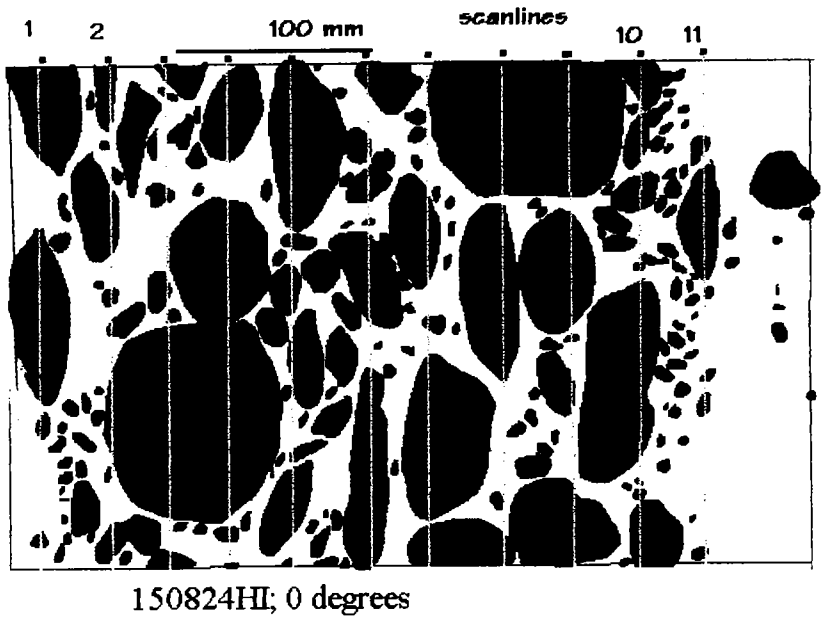

Figure B4 Example of a SigmasScan/Image™ overlay plane, enhanced by graphic processing

Both programs wrote data to internal spreadsheets concurrently while measuring. The spreadsheets were adequate for data manipulation. Statistical summaries were prepared and basic plots made of the data without leaving the programs. Data was exported in a limited number of formats, such as generic ASCII or Comma Delimited Text formats but it was easier to cut data to the Windows "clipboard" and then paste directly into other applications.

B4.3 Generation of Particle Overlay Planes

As indicated above, SigmaScan/Image required that particle outlines be traced onto virtual *overlay planes*. These were virtual in the sense that they acted as transparent sheets over the image onto which particle shape, labeling and other information was recorded. Theoretically, the actual TIFF (Tagged Image File Format) image should not change, the program did alter some details of the graphic file because it was no longer usable by other software, despite the standard .TIF file extension. The solution was to make two copies of the image and sacrifice one to SigmaScan/Image™. SigmaScan/Image™ permitted the overlays containing the traced particles to be saved with the image as separable recoverable images. But to be used as a graphic in its own right, the overlay first had to be saved as a part of the source image, then imported back into SigmaScan/Image™ as an "all files" graphic file, and then re-saved as a TIFF file. This procedure was not documented in the SigmaScan/Image Users Manual.

Since the overlay images were inverted (black background, with colored particles and lines), Picture Publisher™ was used to invert the image again to a white background. The overlay files were maintained as 256 gray scale files, since they were later re-imported into SigmmaScan/Image in order to run scanlines across the particles which had earlier been traced. For illustration purposes overlay graphic could be converted to a binary file to translate the overlay colors into black, but the color or gray scale format was necessary to the add gray stipple to represent scanlines such as shown in Figure B4.

B4.4 Scanline Measurements

NIH Image and SigmaScan/Image™ permitted traverses to be made across the images in order to determine the *intensity* (or the gray scale gradient) along the lines. In the biosciences, such intensity measurements may be calibrated to other parameters: regions of different shades in an image may have certain significance. Many of the research images were of the particles previously traced in order to determine individual particle areas and dimensions. Using the intensity measurement function, an efficient way was developed to measure the chord (intersection length) defined by passing a scanline across a particle. NIH Image was not used for intensity measurements, but the Users Manual suggests that the procedure is similar to the one used with SigmaScan/Image™.

One end of the traverse was selected (by clicking the mouse) and the line "drawn" by dragging the cursor across the image to a desired terminus. Another click locked the line in place. SigmaScan/Image™ wrote the gray scale values along the line onto a designated column of the SigmaScan/Image data spreadsheet. To measure another scanline required that another spreadsheet column be designated to receive the data. The method provided considerable detail since a typical 100 mm long scanline yielded some 400 pixel values if a resolution of 100 dpi was used to scan the image. The conversion of scanline pixel values into chord lengths is described in the following section

The track of the scanline was recorded on an overlay as a colored line. Since four different overlay colors were available, it was possible to keep track of a dense array of scanlines. For instance, when investigating the effect of increasing the number of chords (from scanlines) on the chord length distribution, a few widely spaced scanlines, were initially selected and traced in one color on the overlay. Another array, distributed between the first scanlines, was traced in different color, and yet other interspersed arrays added in other colors. The color of the overlay features had no effect on the underlying graphic image or pixel gray scale values.

B4.5 Data Reduction of Graphic Scanline Pixel Values Using SigmaScan/Image Data Transforms

The conversion of pixel gray scale values into chord lengths was performed by three SigmaScan\Image™ *Data Transforms* written for the research. The transforms are what

elsewhere are called *macros*, or short computer programs written in a functional programming language. The SigmaScan\Image™ transform language is very limited, and the code could have been written much faster and more elegantly in BASIC or in the macro language of Microsoft Excel™, which is a form of BASIC.

The principle problem with the SigmaScan\Image™ transform language was that it did not allow the redefinition of a variable within a DO-Loop, which meant that the accumulation of iterations within a register where forbidden. That is to say that instructions such as

COUNT=COUNT+1

were not allowed. The problem was solved by using a register outside of the DO-loop. But as a result, the algorithm was crude, the code clumsy, and processing was relatively slow. A 40 column by 400 row array took about 10 minutes to process (but was still faster than measuring 40 scanlines by hand using a magnifying lens and a scale!). A benefit using SigmaScan\Image™ transforms was that all data collection and processing could be performed without leaving the application. The transform program codes are presented in Section B5.0.

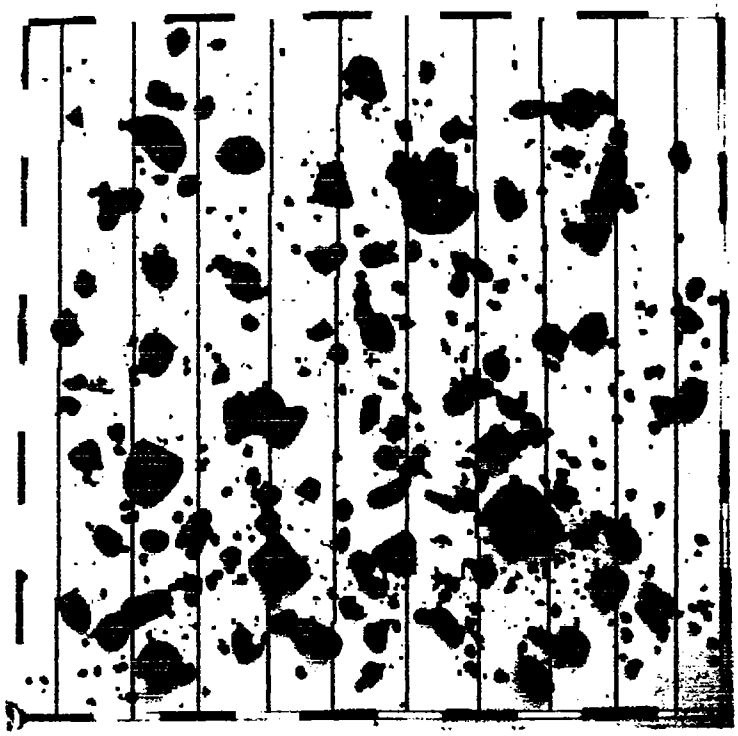

Figure B5 Image with an array of scanlines.

The conversion of scanline pixel values into chord lengths required three steps:

1. The pixels comprising particles or blocks were converted by Transform THRESHOLD.XFM into values of "1" and the matrix into values of "0". This was achieved by comparing each pixel value to a selected threshold gray scale value: values below the threshold were dark shades, normally particle or bimrock block pixels. The threshold value was chosen by sampling a few pixel values at particle and matrix regions of the image and deciding on an absolute minimum particle value. Conventionally, dark particle gray scale values would be mapped to "0" values, (dark gray shades start at 0 and lighten toward white at a value of 256) but the transform mapped them to "1" values since they were added in the next step of data processing. Gray scale values above the threshold were mapped to "0" values and were ultimately discarded. For the linear proportion of particles along the line, a simple addition of "1"s, divided by the total number of pixels in the scanline was sufficient. However, to measure the *individual chords* lengths the next step was necessary.

Scanline 1	Scanline 2	Scanline 3	Scanline 4	Scanline 5	Scanline 6	Scanline 7	Scanline 8	Scanline 9	Scanline10
162	146	127	149	133	150	148	138	130	129
155	107	94	153	132	148	143	141	107	126
154	53	44	152	133	144	141	135	62	124
159	49	36	150	134	148	148	139	52	125
156	56	32	150	136	147	147	130	46	123
157	111	32	151	137	144	147	106	49	123
150	133	33	151	140	139	147	63	40	123
149	147	33	155	141	142	145	51	29	122
153	140	44	153	141	146	147	44	30	127
150	132	37	155	141	147	146	47	29	124
153	126	46	152	139	146	145	46	35	123
153	123	77	157	141	142	141	33	72	124
151	115	127	153	144	126	131	40	90	125
147	64	132	148	145	76	114	75	102	128
153	52	133	149	145	62	126	90	111	126
148	49	135	148	147	52	140	99	113	125
147	47	136	147	150	53	145	112	112	123
148	48	146	149	147	54	145	114	111	124
150	48	151	148	147	56	141	124	106	126
154	42	148	152	135	54	136	133	101	123
159	48	148	151	106	48	129	133	96	124
155	93	154	155	76	47	122	136	85	124
158	103	153	152	96	39	126	135	77	122
159	103	139	152	138	40	126	136	72	125
158	96	149	151	148	56	136	134	80	123
159	88	150	151	152	93	144	139	96	126
159	110	151	148	131	81	148	140	93	125
155	113	150	142	111	90	145	139	63	120
159	119	149	133	117	113	148	138	27	117
159	119	152	79	118	108	149	140	20	103
156	121	151	74	100	118	147	141	31	75

Figure B6 Gray scale pixel values of a portion of the scanline array shown in Figure B5

2. For each scanline, each i-th pixel was compared by Transform CHORD.XFM to the i+1th pixel, and if less, then the i+1th pixel was a "1" and must have been the first pixel

of a chord intersection through a particle. On the other hand, if the i-th pixel was a "1" and the i+1th pixel was a "0", the i-th pixel was the last pixel of a chord. The chord lengths were determined by summing all the serial "1" values in each scanline column and writing the sum to an associated summary column which contained a string of pixel sums representing chords intersected by the scanline and the particles. Special procedures checked for scanlines beginning and ending in chords.

3. A summary table of chord lengths in each scanline was calculated by Transform CONVERT.XFM by applying a spatial calibration factor to the sums of pixels representing each cord (for example, 0.71 pixels per mm). The linear percentage of chords and cumulative linear proportion for each scanline was calculated.

Scanline 1	Scanline 2	Scanline 3	Scanline 4	Scanline 5	Scanline 6	Scanline 7	Scanline 8	Scanline 9	Scanline 10
0	0	0	0	0	0	0	0	0	0
0	0	1	0	0	0	0	0	0	0
0	1	1	0	0	0	0	0	1	0
0	1	1	0	0	0	0	0	1	0
0	1	1	0	0	0	0	0	1	0
0	0	1	0	0	0	0	0	1	0
0	0	1	0	0	0	0	1	1	0
0	0	1	0	0	0	0	1	1	0
0	0	1	0	0	0	0	1	1	0
0	0	1	0	0	0	0	1	1	0
0	0	1	0	0	0	0	1	1	0
0	0	0	0	0	0	0	1	1	0
0	1	0	0	0	1	0	1	0	0
0	1	0	0	0	1	0	1	0	0
0	1	0	0	0	1	0	1	0	0
0	1	0	0	0	1	0	0	0	0
0	1	0	0	0	1	0	0	0	0
0	1	0	0	0	1	0	0	0	0
0	1	0	0	0	1	0	0	0	0
0	1	0	0	0	1	0	0	1	0
0	1	0	0	1	1	0	0	1	0
0	0	0	0	1	1	0	0	1	0
0	0	0	0	0	1	0	0	1	0
0	1	0	0	0	1	0	0	1	0
0	1	0	0	0	1	0	0	1	0
0	0	0	0	0	1	0	0	1	0
0	0	0	0	0	1	0	0	1	0
0	0	0	0	0	0	0	0	1	0
0	0	0	1	0	0	0	0	1	0
0	0	0	1	1	0	0	0	1	1

Figure B7 Array shown in Figure B6, converted to binary values. Pixels representing blocks converted to a value of "1".

B4.6 Example Showing Use Scanlines and Data Transforms

The procedures used to generate chord length data are described and illustrated. Figure B5 shows an image (one of the series of Gravel Tests setups) with superimposed scanlines. The image was enhanced to permit illustration; as a consequence, it has a binary appearance. The original is a 256 gray scale image.

The gray scale pixel values from the SigmaScan™ traverses (scanlines) over a portion of the image is shown as Figure B6. Only a small part of the data from the scanlines are shown, since the complete array contains almost 400 rows. The "Scanline Number" labels were written to the data spreadsheet during the data collection procedure and were preserved by the Transforms. Once processed by Transform THRESHOLD.XFM, the same array was converted binarily. A threshold value of 100 was used: gray scale values below 100 represent particle pixels and were converted to binary value "1". The converted array is shown as Figure B7

Following the THRESHLD.XFM procedure, the data were processed by Transform CHORD.XFM. All solitary and contiguous pixels with a value of "1" were identified and summed. The total number of pixels in each string of ones was directly related to the length of the chord resulting from the intersection of the scanline and the particle. Each sum represented one chord formed by the intersection of a particle and a scanline. Particles that were not completed at the tops or the bottom of the scanline were counted and treated as whole particles. The sums representing the lengths of the particles (in pixels) were written to a summary table as shown in Figure B8.

Scanline 1	Scanline 2	Scanline 3	Scanline 4	Scanline 5	Scanline 6	Scanline 7	Scanline 8	Scanline 9	Scanline 10
17	3	11	11	2	1	1	10	11	1
10	9	9	11	3	15	13	5	53	1
1	2	1	2	26	39	1	4	2	17
	13	3	3	15	12	18	3	7	4
	6	3	26	1	7	32	22	8	30
	8	27	19	1	11	15	10	1	28
	37	19	2	2	3	1	55	2	2
	4	4	7	12	1	7	3	51	3
	24	10	3	5	1	20		5	2
	4		18	5	18	5		1	1
	7		1	2	24	1		2	5
	1		1	12	3	8		2	
			2	14	1	1		1	
			11	10		1		1	
			1	12				1	
								4	

Figure B8 Summary of data written by Transform CHORD.XFM. The numbers represent the lengths of discrete particle chords in terms of the number of pixels representing the intersection.

The final step in the data processing was to convert the pixel-related data into dimensions and spatially-related data. For the data of Figure B8, this was achieved by running Transform CONVERT.XFM. A spatial calibration (in this case 7.16 pixels per cm) was input, as were the number of scanlines. The result is shown as Figure B9, which is a summary of individual chord lengths for scanline intersections with particles, and a summary of the total of chords, individual linear proportions (length of chord intersections divided by the length of the scanline) for each scanline; and a cumulative linear proportion for each scanline. The final cumulative linear proportion was taken as the estimate of the block areal proportion (sum of the areas of individual particles divided by the total area of the image containing the particles). The data was exported into Microsoft Excel™, or other spreadsheet software, for further analyses and plotting.

	Scanline 1	Scanline 2	Scanline 3	Scanline 4	Scanline 5	Scanline 6	Scanline 7	Scanline 8	Scanline 9	Scanline 10
	2.37	0.42	1.54	1.54	0.28	0.14	0.14	1.4	1.54	0.14
	1.4	1.26	1.26	1.54	0.42	2.09	1.82	0.7	7.4	0.14
	0.14	0.28	0.14	0.28	3.63	5.45	0.14	0.56	0.28	2.37
		1.82	0.42	0.42	2.09	1.68	2.51	0.42	0.98	0.56
		0.84	0.42	3.63	0.14	0.98	4.47	3.07	1.12	4.19
		1.12	3.77	2.65	0.14	1.54	2.09	1.4	0.14	3.91
		5.17	2.65	0.28	0.28	0.42	0.14	7.68	0.28	0.28
		0.56	0.56	0.98	1.68	0.14	0.98	0.42	7.12	0.42
		3.35	1.4	0.42	0.7	0.14	2.79		0.7	0.28
		0.56		2.51	0.7	2.51	0.7		0.14	0.14
		0.98		0.14	0.28	3.35	0.14		0.28	0.7
7.16		0 14		0.14	1.68	0.42	1.12		0.28	
pixels per				0.28	1.96	0.14	0.14		0.14	
cm				1.54	1.4		0.14		0.14	
				0.14	1.68				0.14	
									0.56	
total pixels	355	362	354	357	355	357	355	357	355	360
Length scanline	49.58	50.56	49.44	49.86	49.58	49.86	49.58	49.86	49.58	50.28
= chord pixels	28	118	87	118	122	136	124	112	152	94
= chords	3	12	9	15	15	13	14	8	16	11
Length chords	3.91	16.48	12.15	16.48	17.04	18.99	17.32	15.64	21.23	13.13
% chords	7.89	32.6	24.58	33.05	34.37	38.1	34.93	31.37	42.82	26.11
Cum. Length scanline:	49.58	100.14	149.58	199.44	249.02	298.88	348.46	398.32	447.91	498.18
Cum. Length chords	3.91	20.39	32.54	49.02	66.06	85.06	102.37	118.02	139.25	152.37
Cum. chord %	7.89	20.36	21.76	24.58	26.53	28.46	29.38	29.63	31.09	30.59

Figure B9 Final output from Transform CONVERT.XFM: chord lengths and cumulative chord percent (particle linear proportion). Data presented here as a Microsoft Excel™ spreadsheet.

B5 SCANLINE DATA TRANSFORMS: PROGRAM CODES

B5.1 Introduction

The code reproduced in this Appendix will only run with the Image Analysis software SigmaScan/Image™. There are three programs: THRESHLD.XFM converts 256 gray-scale pixel values to binary ("1" and "0"). CHORD.XFM identifies pixels within blocks "1" values and sums them, and calculates the linear proportion of blocks and the lengths of individual block intercepts for each scanline. CONVERT.XFM converts all pixel-based distances produced from CHORD. FM into real dimensions. The SigmaScan/Image ™ transform language is limited, hence an inefficient algorithm was created for Transform CHORD.XFM, which is the main engine for the scanline data conversion process. The code is garnished with comments (preceded by a semi-colon), and should be easily followed by anyone with some programming experience. The purpose of each of the Transforms has been presented in Section B4 but should be evident from the comments. It should be noted that the only reason that the CONVERT.XFM transform was written separately is that SigmaScan/Image™ would not allow any more code in the CHORD.XFM Transform.

B5.2 Program Code for THRESHLD.XFM

;**THRESHLD.XFM** converts 256 gray scale pixle values to binary values

```
                    ;identifies pixels <= , > given threshold
                ;pixels below threshold = particle pixels
                ;pixels above threshold = matrix pixels

;----------------------------INPUT DATA ----------------------------------
threshold=100                   ; INPUT DATA  pixel threshold blocks/matrix

numcols=10                      ; INPUT DATA  number of scanlines
; ------------------------------------------------------------------------------

 for i=1 to numcols do
  endcol=count(col(i))                  ; number of pixels in ith column
      for j=2 to endcol do              ; starts on 2nd row, first data point; to end column,
                                              ;1st row is the scanline label

        cell(i,j)=if(cell(i,j)<=threshold,1,0)   ; discrim blocks from matrix and writes a 0 or a 1
                                              ;into the cell
      end for
end for

                        ; End data transform THRESHOLD.XFM
```

B5.3 Program Code for CHORD.XFM

;**CHORD.XFM** converts binary image data into particle chord intercept data

```
---------- INPUT DATA : ----------
numcol=10          ; number of scanline columns
numpix=357         ; number of pixels in one dimension of image (from image information)
lengthpix= 50      ; length of the calib dimension (from image information)

calibration=numpix/lengthpix     ; computed number of pixels per unit length

units="cm"         ; length units
rowstart=15        ; arbitrary start row for summary data, below chord data
;-------------------------------------------------------------------------------

datacol=numcol+2                 ; establish starting column for summary data

for i=1 to numcol do             ; determine how many scanline data strings and their length
 endcol=count(col(i))+1          ;establish bottom of data column
 cell(datacol+i,1)=cell(i,1)     ; copy Scanline column headings to result cols
 cell(i,1)=0                     ; dummy pixel for (j-1) of loop below; write into label cell

 for j=2 to endcol do            ; find top of a particle chord, the first "1" in a string
  if (cell(i,j)>cell(i,j-1)) then
   top=j
   place=count(col(datacol+i))+1     ;finds location of last result written to the summary col.
  end if

 if (cell(i,j)=cell(i,j-1)) and (cell(i,j)>0 and j=endcol) then   ; bottom of chord, first "0"
                                                                  ;after a "1"
   bottom=j
   intercept=bottom-top+1                ;for when scanline ends in a particle chord
   put intercept into cell(datacol+i,place+1)
  end if

if (cell(i,j) < cell(i,j-1)) then        ;bottom of chord when not at end scanline
   lineend=j-1
   chordend=lineend-top+1
   put chordend into cell(datacol+i,place+1)
  end if
end for                          ; end of jth row but process the following before continue next col
```

```
   cell(i,1)=cell(datacol+i,1)          ; puts Scanline label back above the source data array

 ; calculate  some statistics below results

   length=(endcol-1)/calibration
   sumpix=total(col(datacol+i))
   chordlength=sumpix/calibration
   percent=sumpix/(endcol-1)*100
   numparts=count(col(datacol+i))

     ; put summary stats

   cell(datacol+i,rowstart)=endcol-1          ; total number pixels in scanline
   cell(datacol+i, rowstart+1)=length         ; length of scanline in units of measure
   cell(datacol+i,rowstart+2)=sumpix          ;number of pixels in chords
   cell(datacol+i,rowstart+3)=numparts        ; number of chords
   cell(datacol+i,rowstart+4)=chordlength     ; total length of chords in scanline
   cell(datacol+i,rowstart+5)=percent         ; % chord on pixel basis
end for

        ;LABELS

   cell(datacol,rowstart-1)=units
    cell(datacol,rowstart-2)="pixels per"
    cell(datacol,rowstart-3)=calibration

    cell(datacol,rowstart)="total pixels"
    cell(datacol,rowstart+1)="Lscanline"
     cell(datacol,rowstart+2)="# chord pixels"
     cell(datacol,rowstart+3)="# chords"
     cell(datacol,rowstart+4)="Lchords"
     cell(datacol,rowstart+5)= "% chords"


          ;END TRANSFORM ;    Use CONVERT.XFM for conversion to particle sizes
                             ;    by dimension and cumulative  % particle proportion.
```

B5.4 Program Code for CONVERT. XFM

```
;CONVERT.XFM      changes summary data of chords in terms of pixels into chords of
;                   units of length. requires that CHORD.XFM has been run beforehand

;---------- INPUT ---------- (same variabales as CHORD.XFM)

numcol=10
calibration=0.716
units="cm"
rowstart=15
;-------------------------------------------------------------------------------

datacol=numcol+2  ;set up relative co-ordinates for the summary block prepared under CHORD.XFM


for k=1 to numcol do              ;Convert the pixel-related data in the summary to chord lengths
  endcol=count(col(datacol+k,2,rowstart-1))
    ; (the 2 is second row, and rowstart-1 confines the count to the chord pixel results only (otherwise the
        statistics would be counted in as well.)

for m=2 to endcol+1 do:      purpose is to establish how many rows of data in this particular column
    chord=(cell(datacol+k,m))/calibration
    cell(datacol+k,m)=chord
  end for
end for

cell(datacol+1,rowstart+6)=cell(datacol+1,rowstart+1) ;CUMULATIVE PERCENT routine
        ;(Above line initialize cells for the i=1 iteration below (this line is  the Cum Length Scanlines)

cell(datacol+1,rowstart+7)=cell(datacol+1,rowstart+4)   ; ditto; this is Cum Length Chords
cell(datacol+1,rowstart+9)=cell(datacol+1,rowstart+5)   ; this is cumul. %

for i=2 to numcol do

    cell(datacol+i,rowstart+6)= cell(datacol+i-1,rowstart+6) +
cell(datacol+i,rowstart+1)                                  ; Cum Length Scanlines
   cell(datacol+i,rowstart+7)= cell(datacol+i-1,rowstart+7) +
cell(datacol+i,rowstart+4)                                  ; Cum Length of chords
  cell(datacol+i,rowstart+9)=(cell(datacol+i,rowstart+7)/cell(datacol+i,rowstart+6))*100
                                  ; last line above is cumulative percent of chords
```

end for

; labels added below to those placed by CHORD.XFM

cell(datacol,rowstart+6)="Cum Lscan" ;Cumulative length of scanlines
cell(datacol,rowstart+7)="Cum Lchord" ;Cumulative length of chords
cell(datacol,rowstart+9)="Cum chord %" ; Cumul. percent of chords:
;putting on rowstart+9 leaves blank line above the data on this row

; End Transform CONVERT.XFM

APPENDIX C

Data and Plots from Image Analysis of Gravel Tests

C 1.0 Introduction

The plots and data displayed in this Appendix are summaries of work performed using image analysis on images of gravels spread on a 50 cm square white board. The tests model two-dimensional arrays of blocks. The particle distributions were not deliberately designed to be fractal, but some plots did show self-similar distributions, as shown by the example on page C-22. The areal proportion of the particles ranged from 5 percent to 50 percent. The areas and characteristic dimension of each particle was measured by the NIH Image image analysis software. Block areal proportions were calculated by summing all particle areas and dividing the total by the total area of the tracing. Consult Appendix B for more details on the image analysis techniques used in the research.

Later in the research the gravel test images were again used to understand the relationships between low block areal proportion and the chord length distributions obtained from scanline measurements. For that work, the image analysis program SigmaScan/Image™ was used to generate gray scale intensity values along scanlines across the gravel test images. It is these data that are presented in this Appendix. Conversion to chord lengths was executed by the short computer programs described and presented in Appendix B.

The data are condensed as much as possible. Some conventions, defined in the main test, are repeated here:

CLD is the one-dimensional chord length distribution as measured from scanline intercepts across blocks.
2DBSD is two-dimensional block size distribution generated from the population of $\mathbf{d_{mod}}$s (maximum observed dimensions) measured by the image analysis program, SigmaScan/Image™ . The program defined the major axis of a particles as the distance between the two furthest points on a particle. This is the same as d_{mod} .
3DBSD is the block size distribution used to fabricate the specimens. The distribution was constructed by Lindquist (1994b), and was assumed to be the same for all specimens since that was one of Lindquist's fixed variables. The block proportions change, but not the relative numerical frequency of the different-sized blocks.
WPSD is the weight-based particle size distribution of a population of blocks, and for the gravel tests, measured by mechanical sieve analyses.

The data and plots are presented in the following Figures. They are organized by areal proportion. Only selected data are a shown as a sample of work. Within each group, different configurations of scanlines were tried:

1. Fixed Interval- Fixed Length **(FI-FL)** . The interval is the "horizontal" distance (in "x" direction), usually about 50 mm . The length can be thought of as "depth", usually 500 mm. (both dimensions are true scale)
2. Fixed Interval - Random Length. **(FI-RL)** Random numbers were generated by a pocket calculator, and were used to decide how "deep" a scanline was going to be. The random number, a number between 0.0 and 1.0, was multiplied by the 50 cm (dimension of the square whiteboard) to find the randomized length for that scanline.
3. Random Interval -Fixed Length **(RL-FL)** This was basically the same as FI-RL except the interval between scanlines was randomized.

The data sheets show a photographic record of the image and scanlines, and a plot of the cumulative percent chords against cumulative percent scanline for two series of scanlines. The procedure is described in Section 2.8.3. The cumulative block linear proportions shown in the plots are estimates of the block areal proportions. Also shown on the data sheets are a comparative plot of the WPSD, CLD and 2DBSD of the particles shown in the image and sampled by the scanlines. These distributions are labeled respectively as **Sieve, Chords, NIH Image** (because NIH Image was used to measure the maximum dimensions of the particles).

Some Images show dense arrays of scanlines. These are the end-results of a series of scanlines added incrementally to an image in order to assess what difference the addition of more data made to the CLDs for the particles of that image, and if the 2DBSD was any better estimated. The number of scanlines at the end of each phase of the experiment was 5, 10, 20 and 40 scanlines. Plots are shown of the CLD behavior and summary tables of the change in cumulative linear block linear proportion, as the number of scanlines, and consequently, the number of chords, increased.

C 2.0 Gravel Test Images - Data and Plots

A sample of the gravel test images and data are presented without comment in the following pages C-3 through C-22

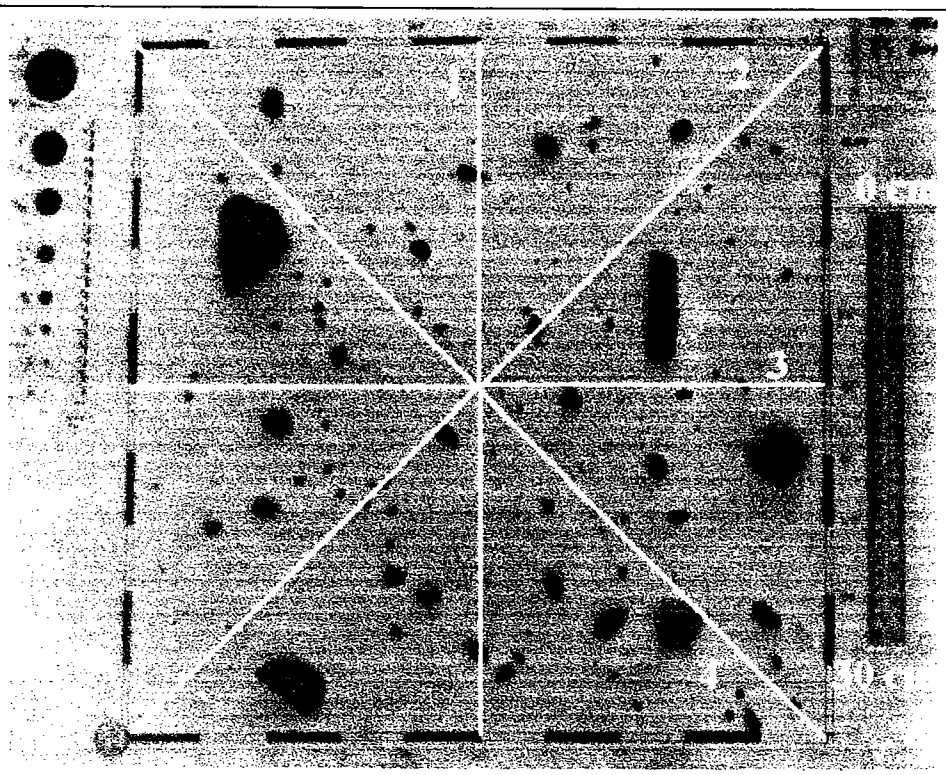

Nominal 5% particle area: scanline data to estimate areal proportion particles

scanline	scanline length (mm)	cumul. scanline (mm)	cum % scanline	chords length (mm)	cumul. chords (mm)	% chords	cum% chords
1.00	500.00	500.00	20.77	1.63	1.63	0.33	0.33
2.00	707.00	1207.00	50.15	8.58	10.21	1.21	0.85
3.00	500.00	1707.00	70.92	0.54	10.75	0.11	0.63
4.00	700.00	2407.00	100.00	6.24	17.00	0.89	0.71

total 2407

conclusion: severe under-estimate

No attempt at PSD using scanline chords...

NOTE: Observe how neatly the scanlines avoid the particles.....

Figure C1 Gravel Test 5.3 percent: Fixed Length-Fixed Interval-DIAGONALS

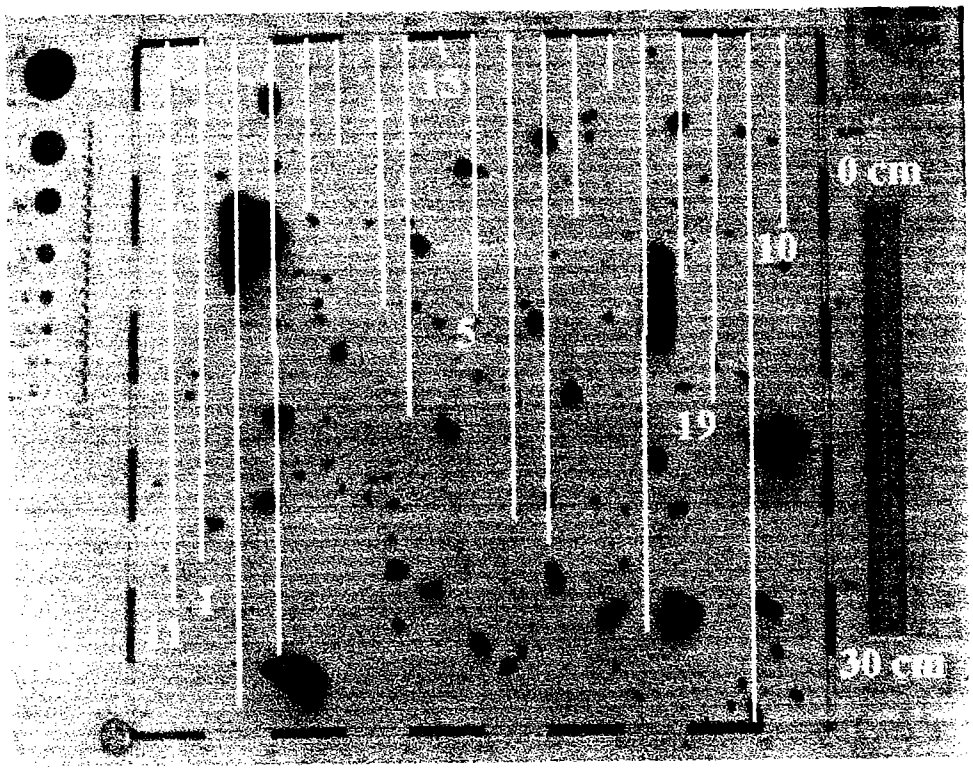

Figure C2 Gravel Test 5.3 percent: Fixed Interval-Random Length

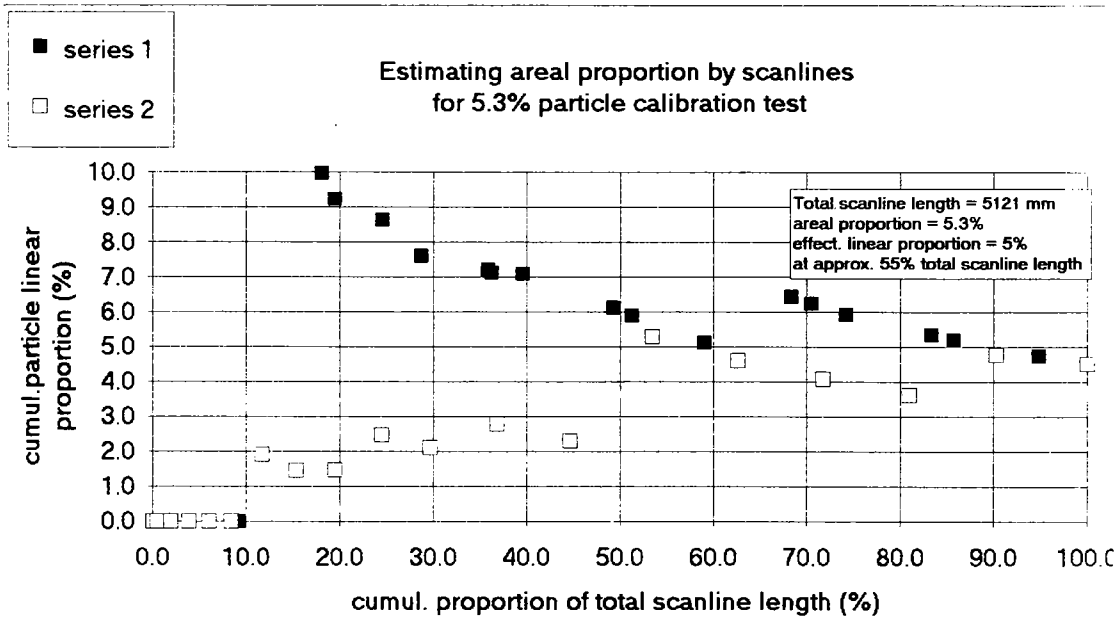

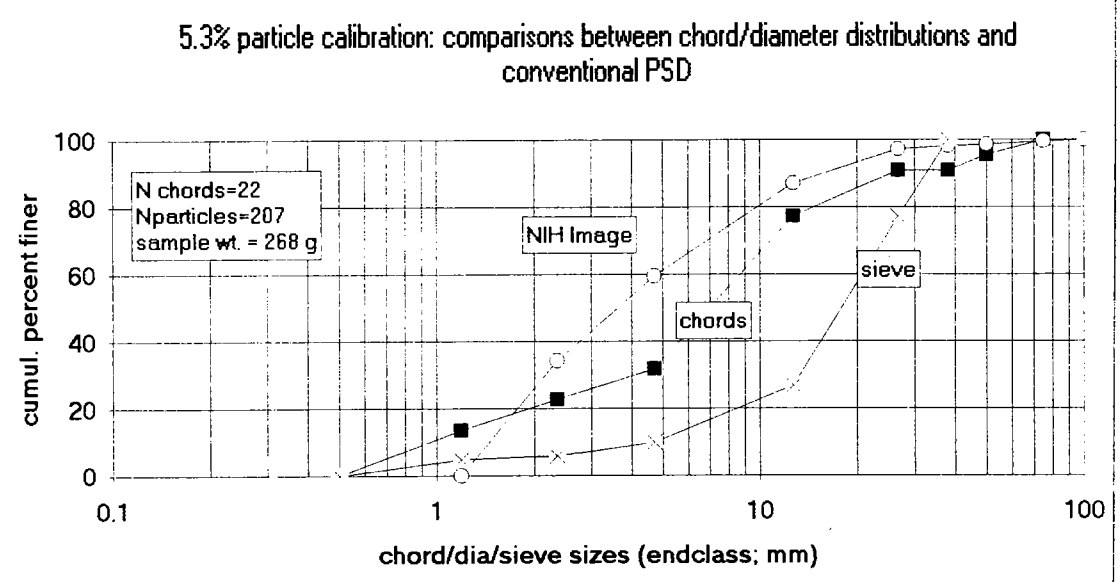

Figure C3 Gravel Test 5.3 percent: Fixed Interval-Random Length **PLOTS**

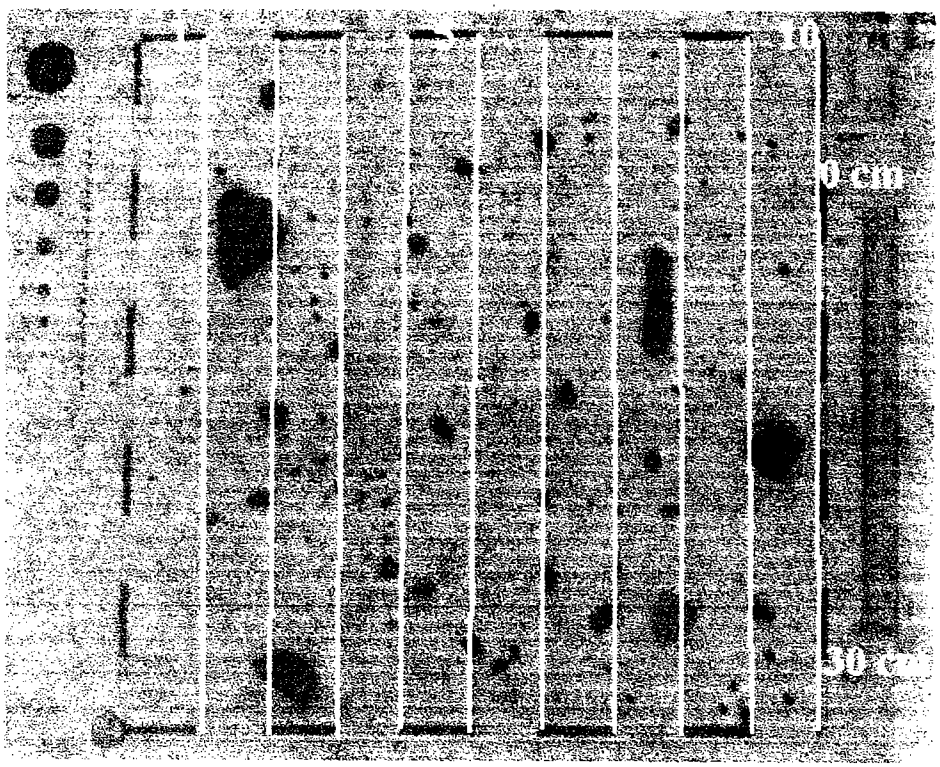

Figure C4 Gravel Test 5.3 percent: Fixed Interval- Fixed Length **IMAGE**

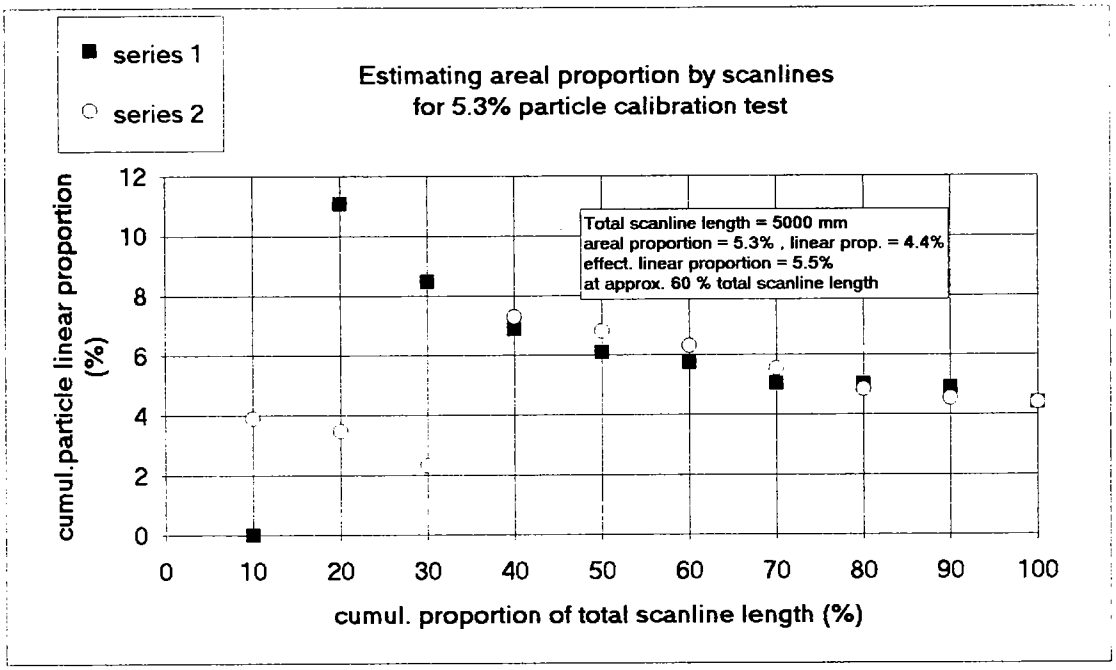

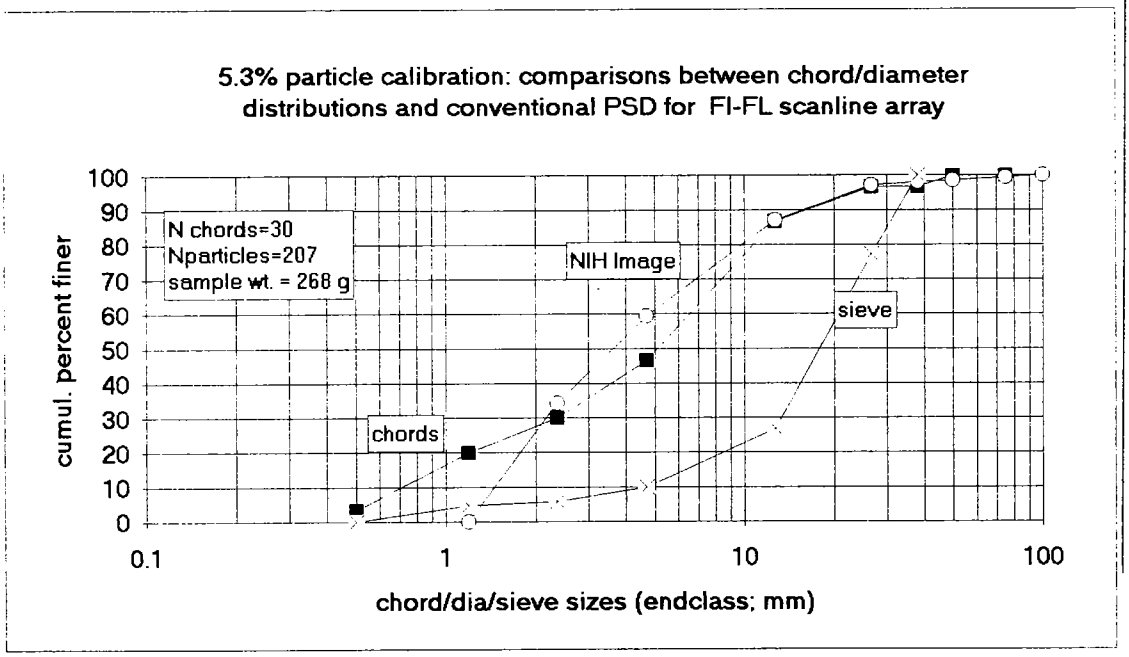

Figure C5 Gravel Test 5.3 percent: Fixed Interval- Fixed Length **PLOTS**

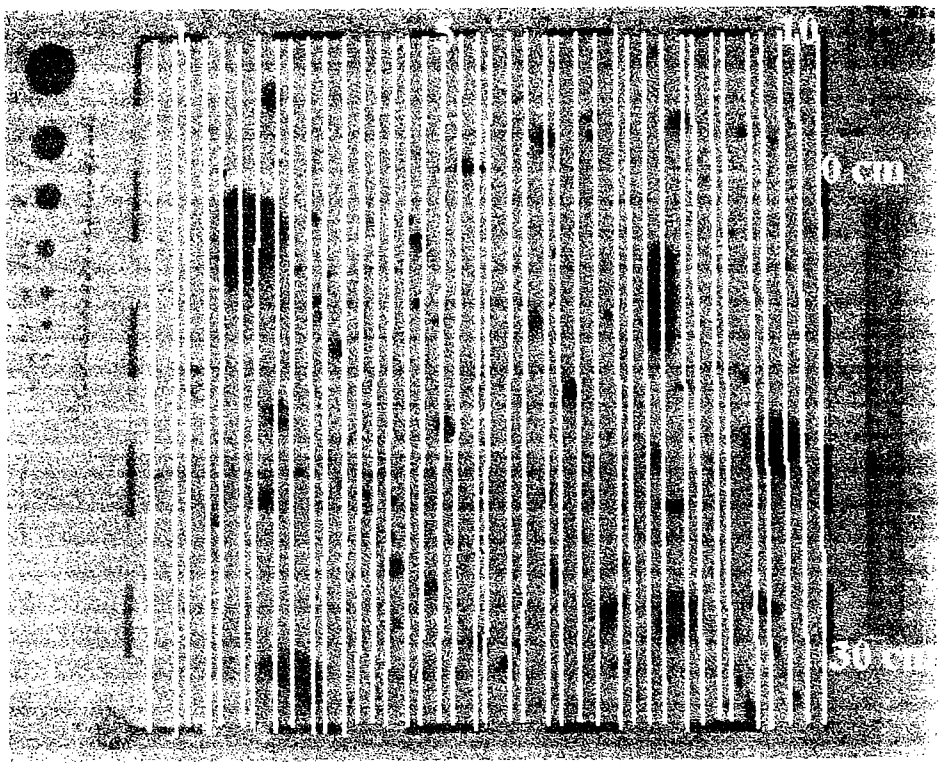

Figure C6 Gravel Test 5.3 percent: Fixed Interval-Fixed Length **IMAGE** INVESTIGATION OF OPTIMUM NUMBER OF SCANLINES

5% particle image
INVESTIGATING THE EFFECT OF INCREASING THE NUMBER OF SCANLINES and CHORDS
SUMMARY of DATA (dimensions in mm)

Number of chords	Cumul% Scanline	Cum. Lin% chords	Number scanlines	Length scanlines (mm)	Length chords (mm)	avg chord length (mm)	std dev chord (mm)	min chord	max chord
20	12.5	8.7	5	2498	258.3	12.92	10.11	1.39	43.06
37	25	8	10	4993	498.7	10.81	9.94	1.39	43.06
56	50	7.1	20	9982	712.5	12.72	15.05	1.39	73.61
81	75	6.6	30	14450	95.8	12.29	15.41	0.00	73.61
107	100	6.6	40	19934	1275	12.40	15.89	0.00	79.17

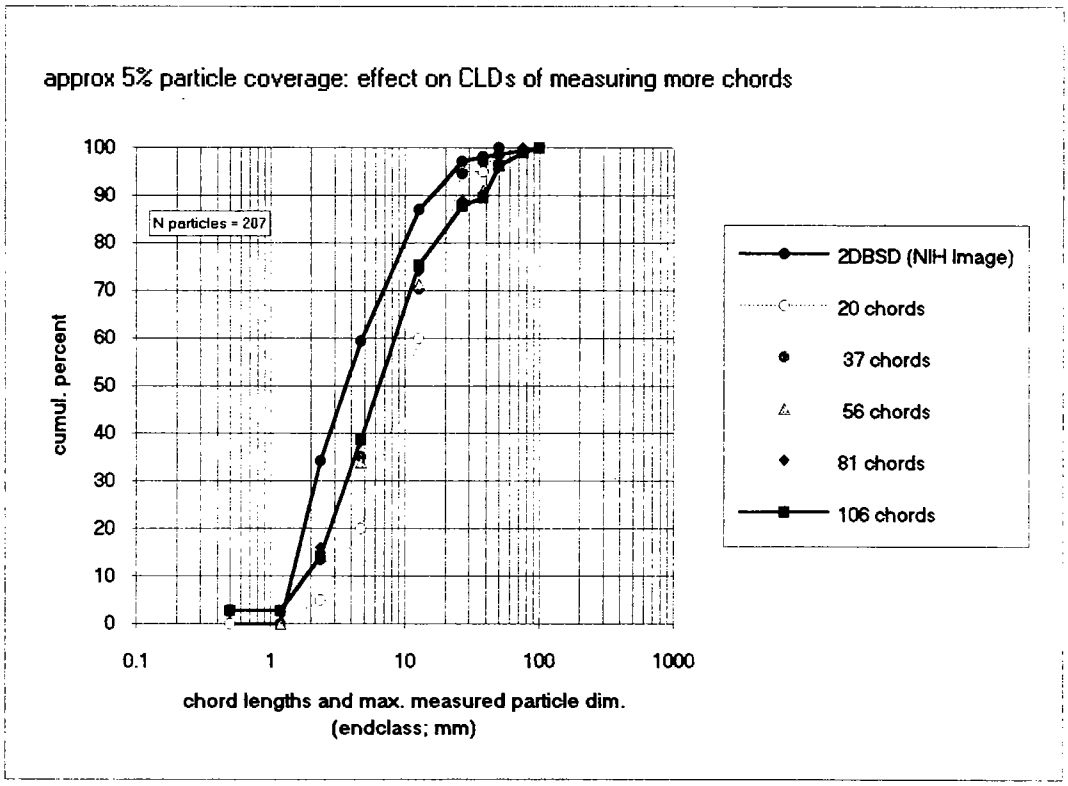

Figure C7 Gravel Test 5.3 percent: Fixed Interval-Fixed Length **DATA/PLOT** INVESTIGATION OF OPTIMUM NUMBER OF SCANLINES

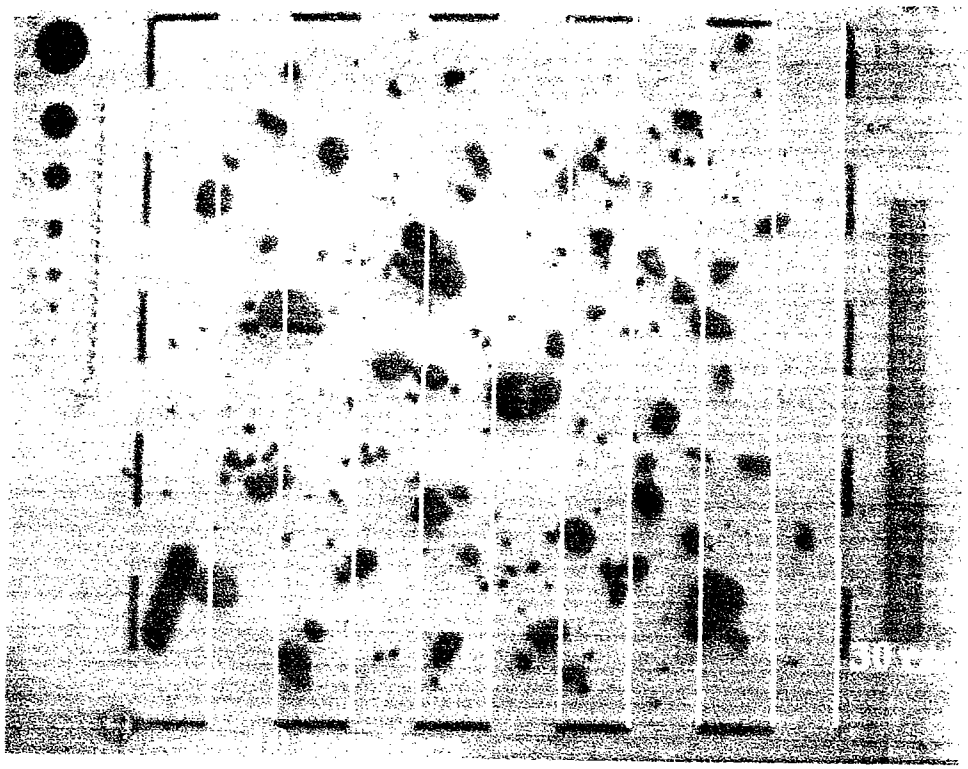

Figure C8 Gravel Test 12 percent: Fixed Interval-Fixed Length **IMAGE**

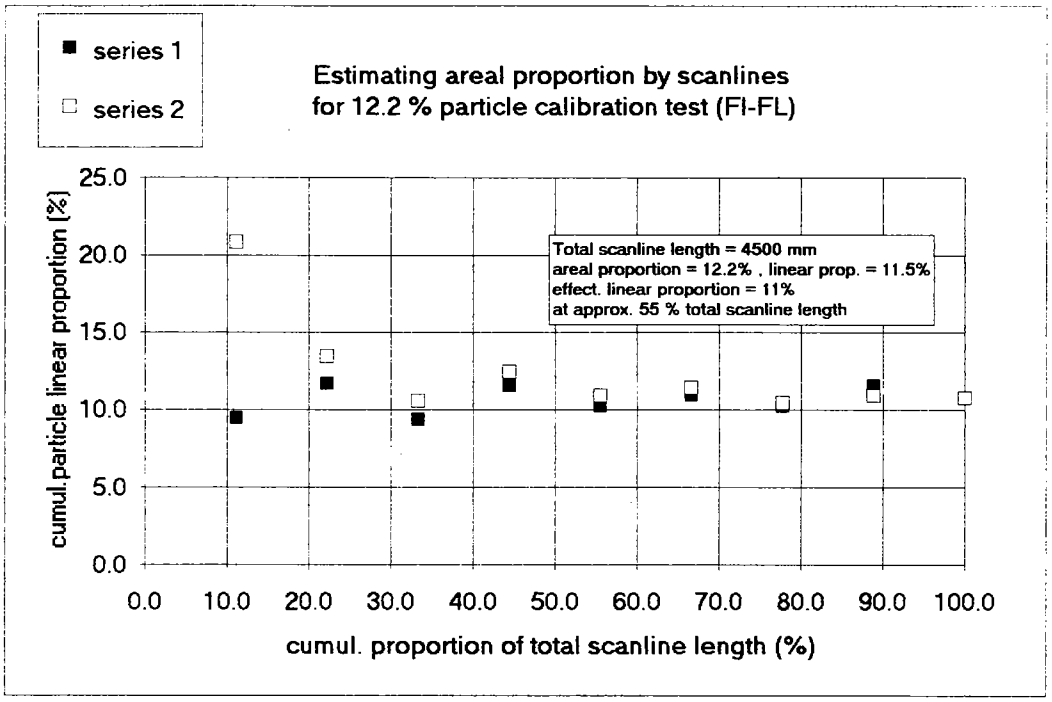

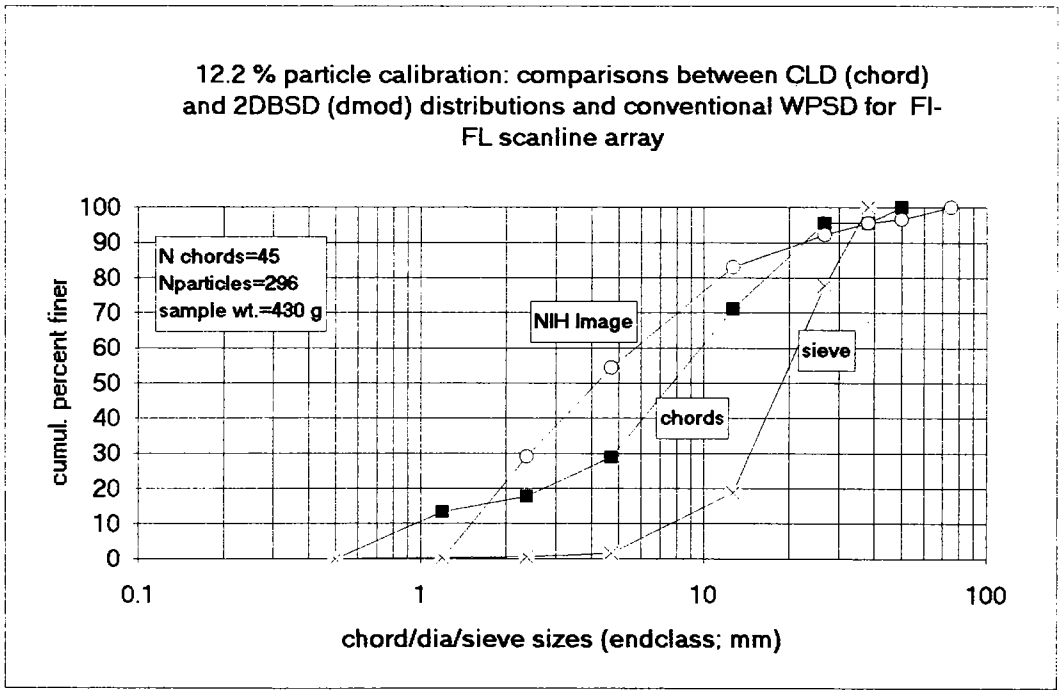

Figure C9 Gravel Test 12 percent: Fixed Interval-Fixed Length **PLOTS**

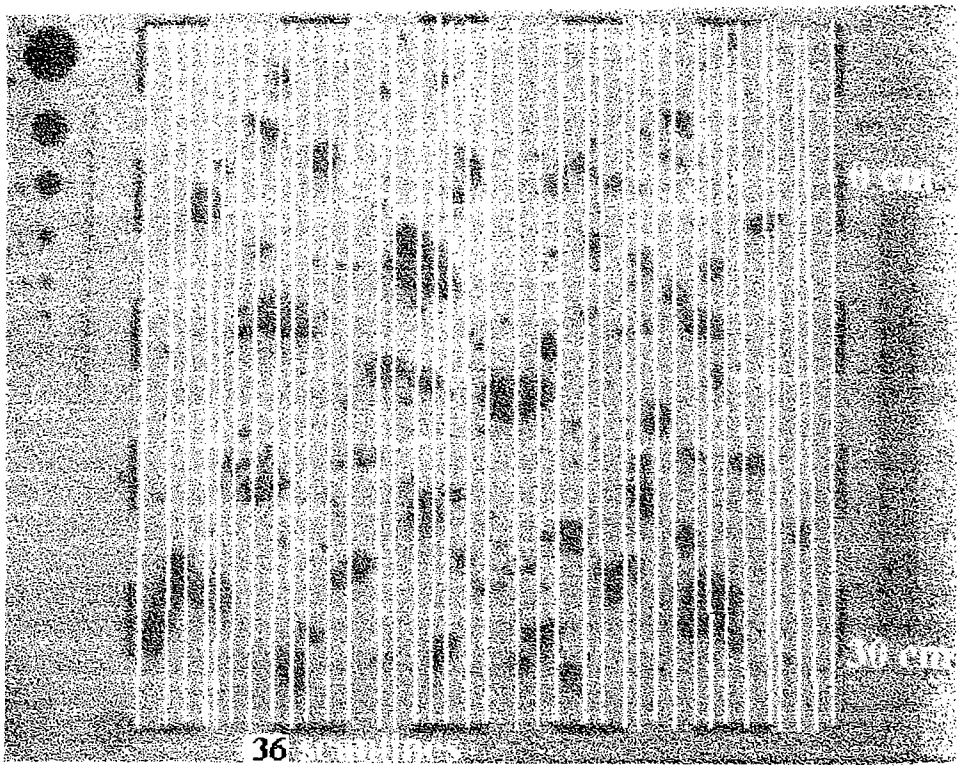

Figure C10 Gravel Test 12 percent: Fixed Interval-Fixed Length **IMAGE INVESTIGATION of OPTIMUM NUMBER OF SCANLINES**

12% particle image:
INVESTIGATING THE EFFECT OF INCREASING THE NUMBER OF SCANLINES and CHORDS
SUMMARY OF DATA: (dimensions in mm)

Number of chords	No. Scanlines	Length Scanlines	Length chords	linear % chords	avg chord	std dev	min	max
117	36	17961	1320.7	7.35	11.3	10.5	1.4	57.1
81	23	11500	986.8	8.58	11.1	10.9	1.4	57.1
45	9	4500	484.7	11.4	10.8	10.6	0.5	45.2
26	6	3000	282.62	9.4	10.9	10.9	1.4	24.5

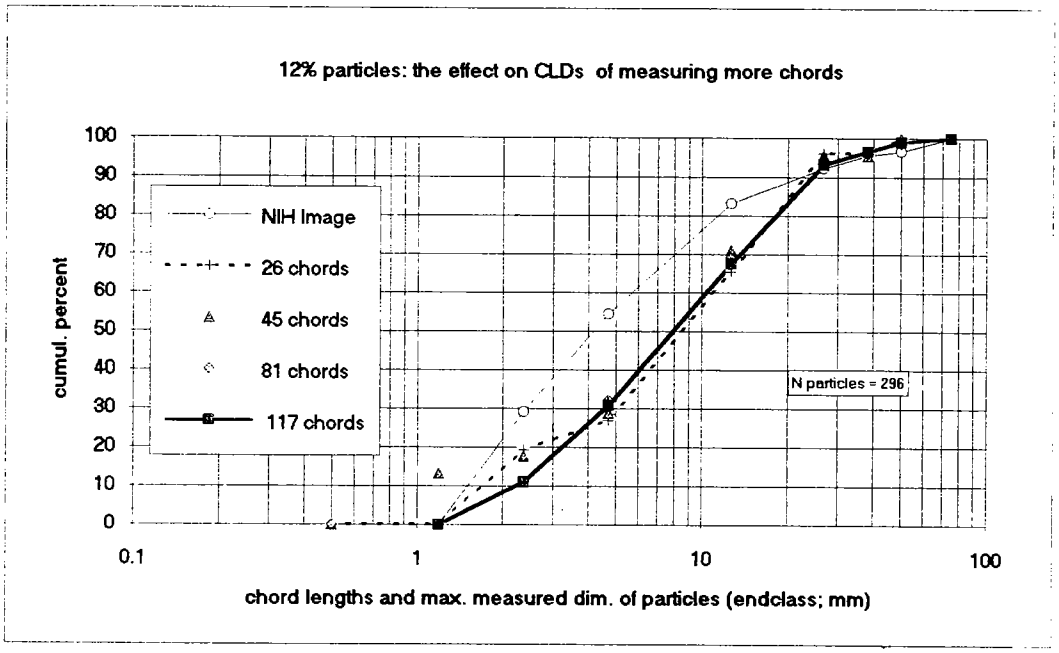

Figure C11 Gravel Test 12 percent: Fixed Interval-Fixed Length **DATA/PLOT INVESTIGATION of OPTIMUM NUMBER OF SCANLINES**

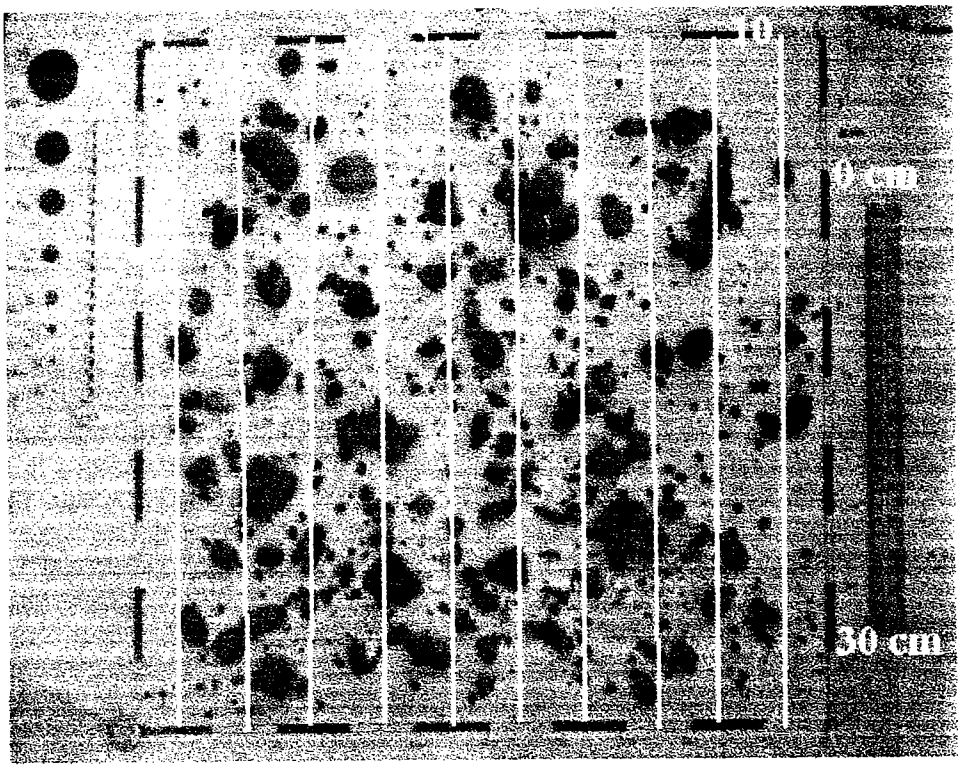

Figure C12 Gravel Test: 24 percent: Fixed Interval-Fixed Length **IMAGE**

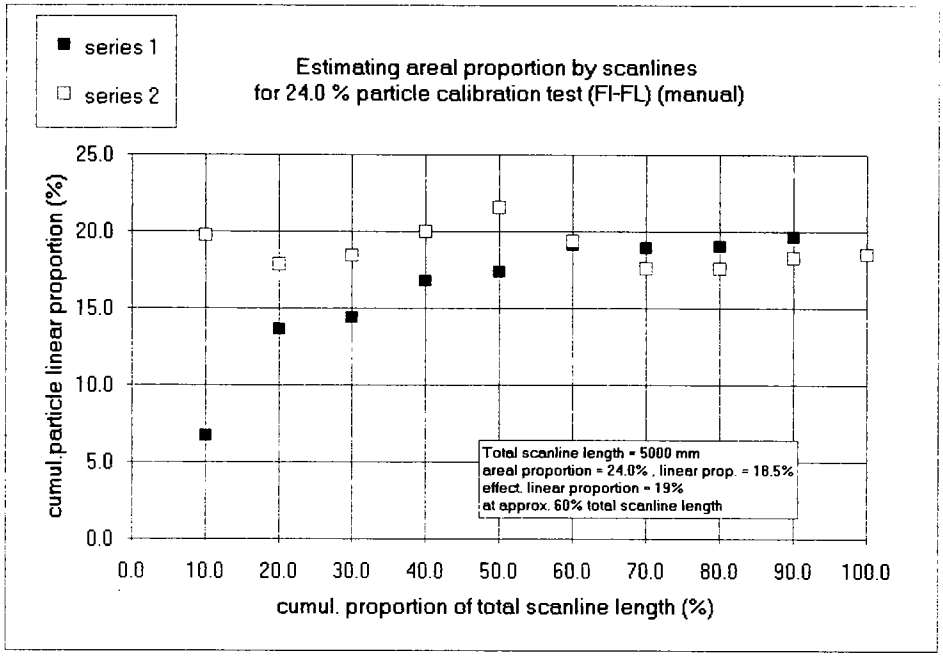

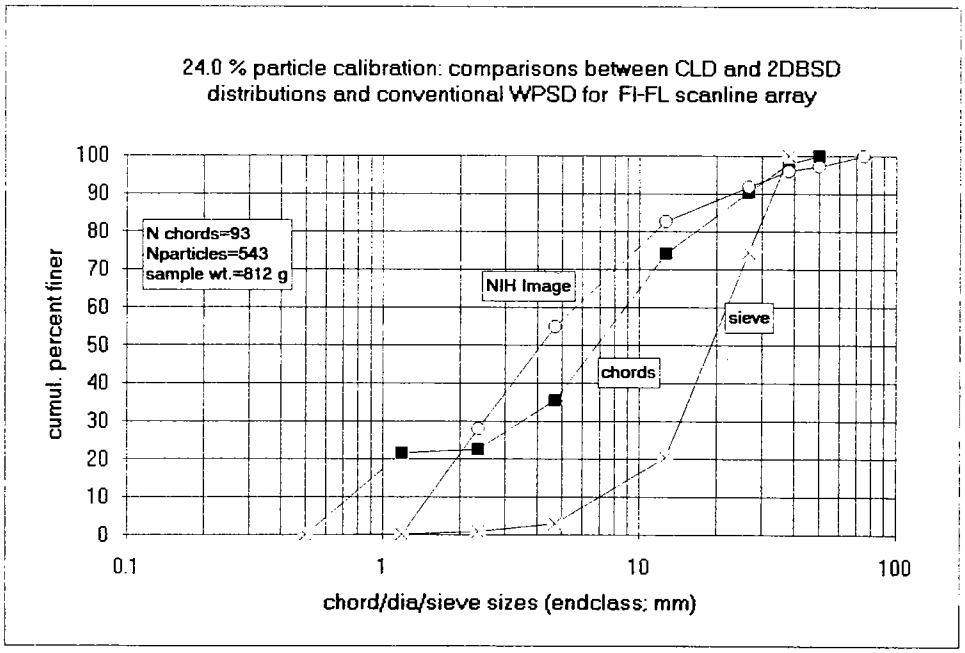

Figure C13 Gravel Test: 24 percent: Fixed Interval-Fixed Length **PLOTS**

NOTE: THERE IS NO FIGURE C 14

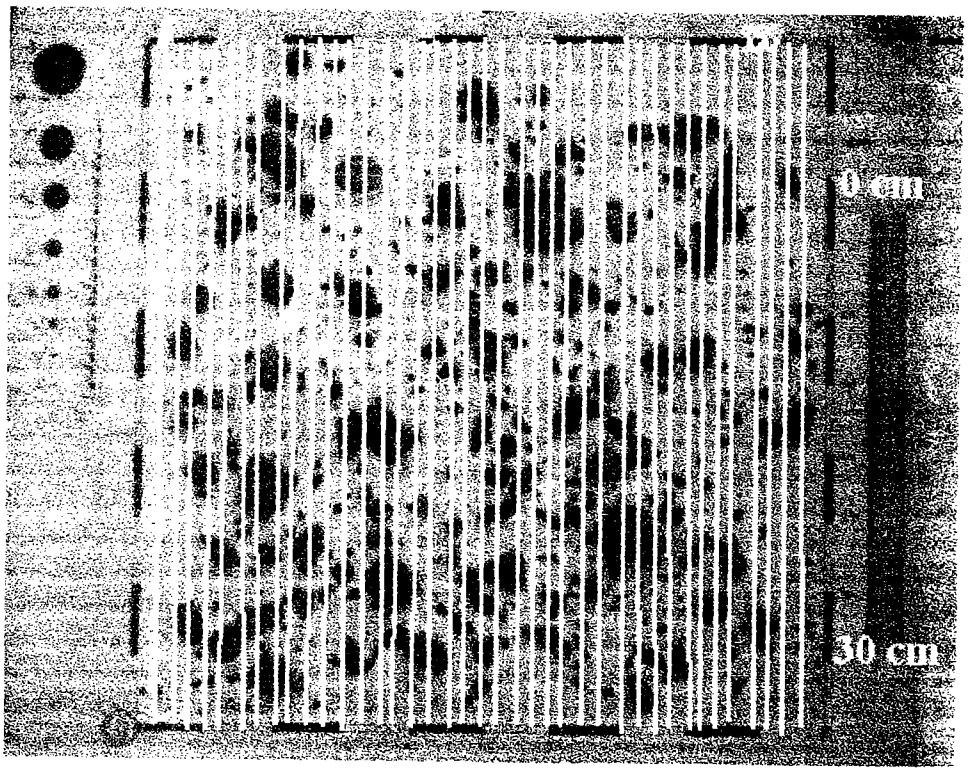

Figure C15 Gravel Test: 24 percent: Fixed Interval-Fixed Length **IMAGE INVESTIGATION of OPTIMUM NUMBER of SCANLINES**

24% particle image
INVESTIGATION of the EFFECT of INCREASING the NUMBER of SCANLINES and CHORDS
SUMMARY of DATA (dimensions in mm)

Number of chords	cumul % scanline	cum. linear% chords	number scanlines	length scanlines	length chords	avg length chords	std. dev. chords	min chord	max chord
51	12.54	24	5	2497	599.4	11.75	11.68	1.4	50.42
88	25.1	21.9	10	4492	969.2	12.41	11.65	1.4	50.42
180	50	22.3	20	9962	2275.9	12.55	11.03	1.4	60.22
261	75	22.2	30	14934	3308.1	12.61	10.83	1.4	60.22
340	100	21.3	40	19909	4238.1	12.45	10.80	1.4	60.22

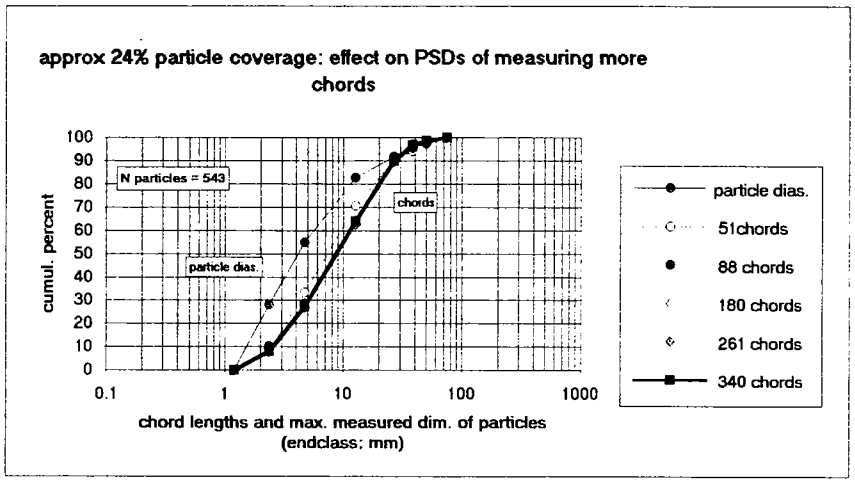

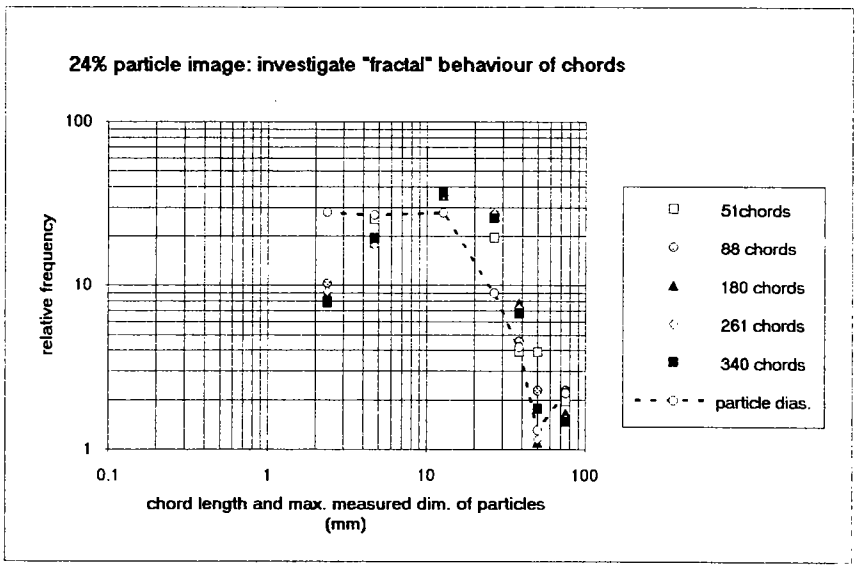

Figure C16 Gravel Test: 24 percent: Fixed Interval-Fixed Length **DATA/PLOTS INVESTIGATION of OPTIMUM NUMBER of SCANLINES**

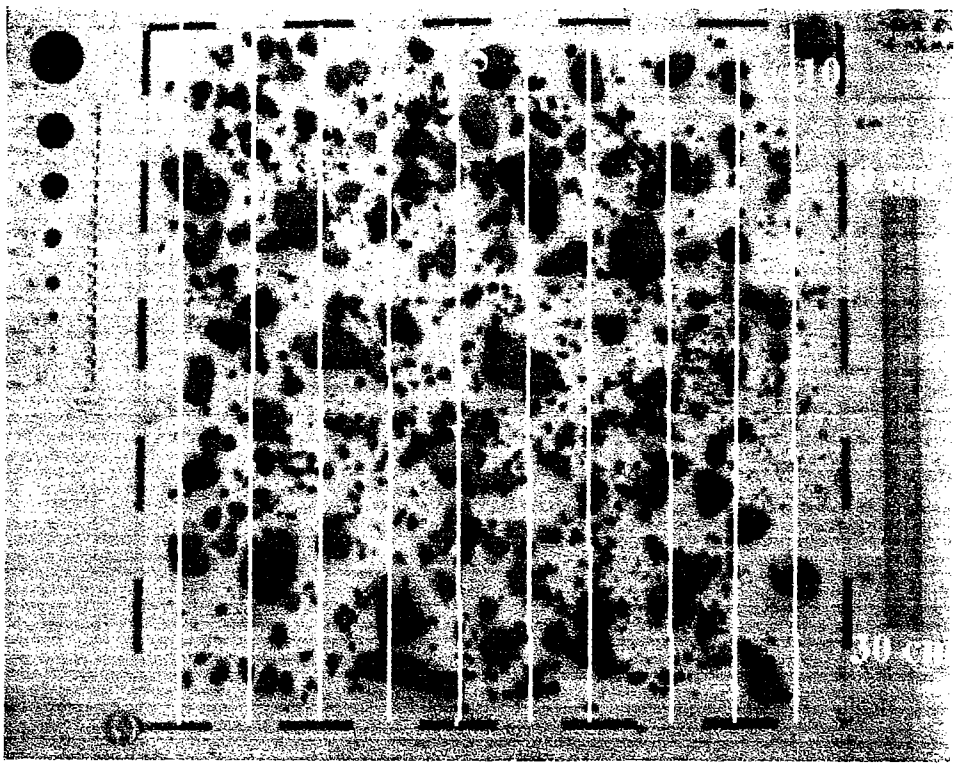

Figure C17 Gravel Test: 37 percent: Fixed Interval-Fixed Length **IMAGE**

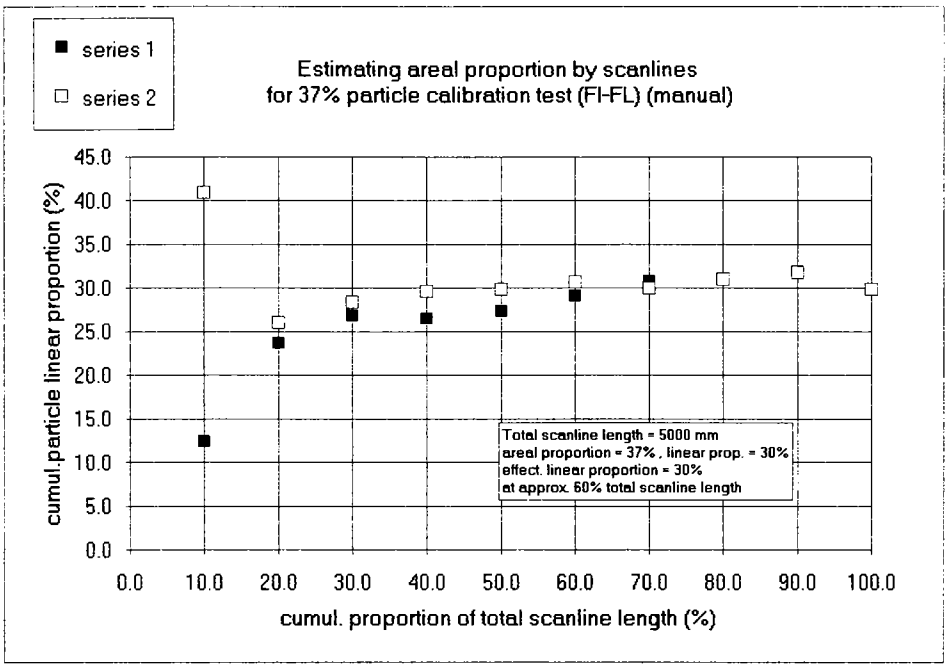

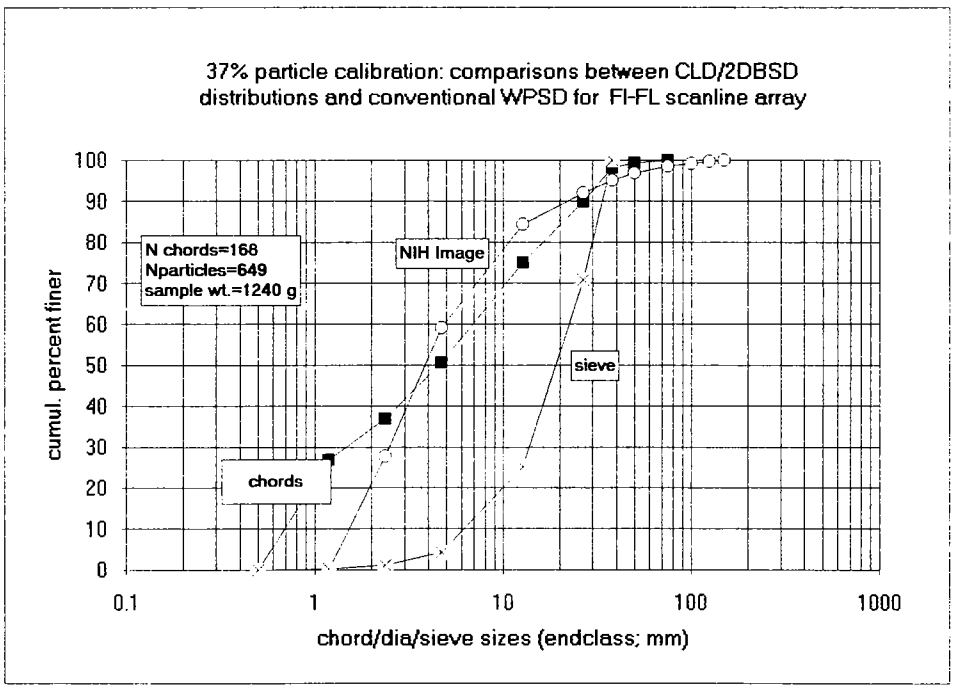

Figure C18 Gravel Test: 37 percent: Fixed Interval-Fixed Length **DATA/PLOTS**

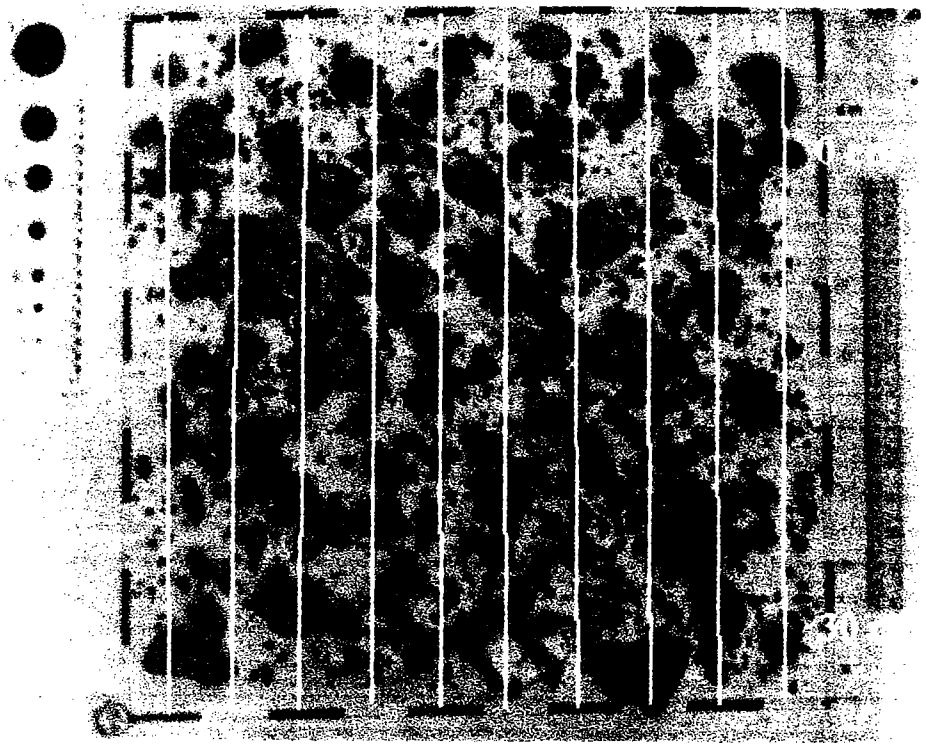

Figure C19 Gravel Test: approx 50 percent: Fixed Interval-Fixed Length **IMAGE**

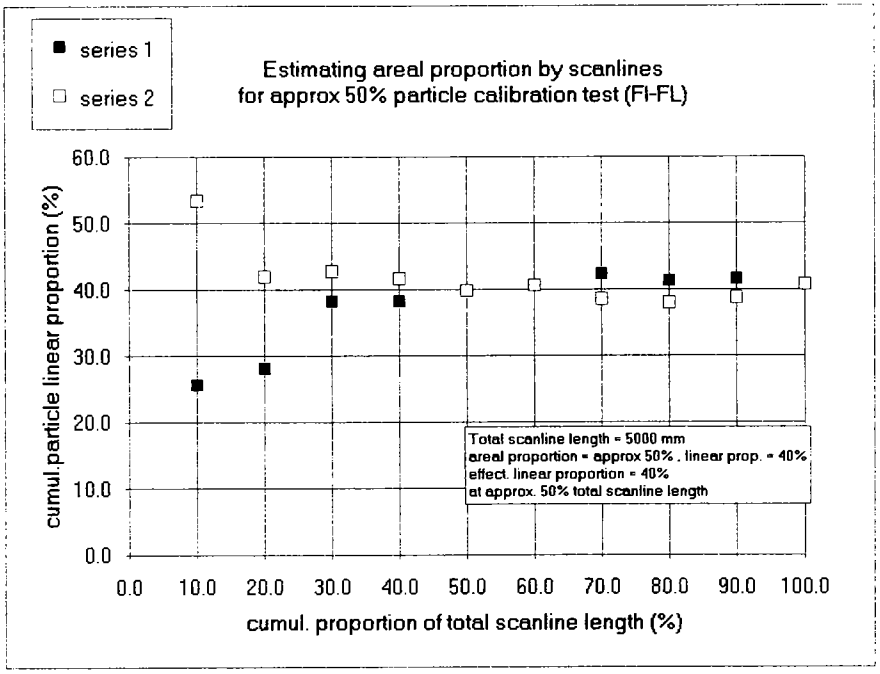

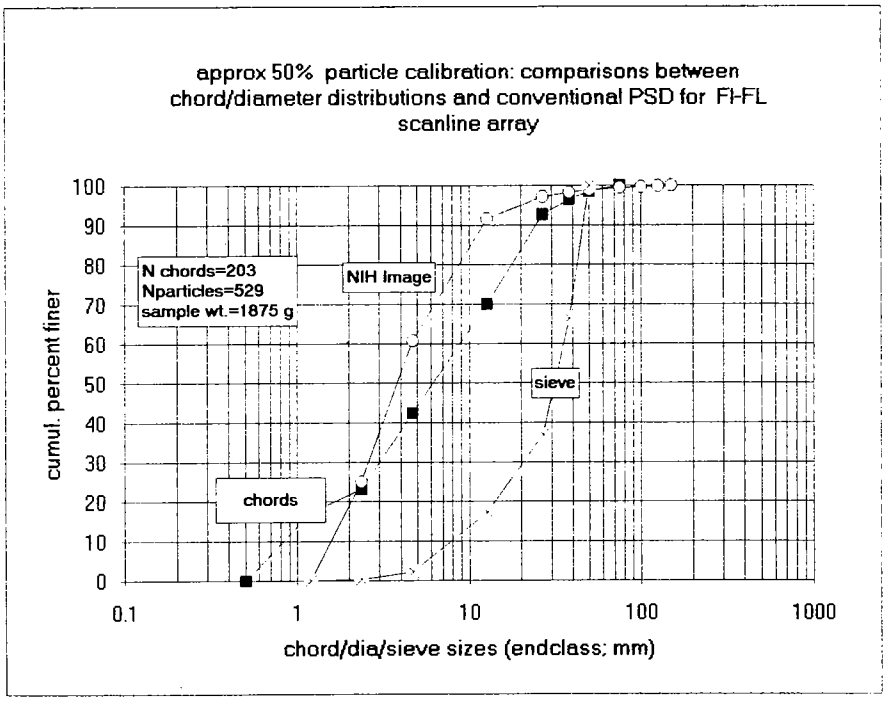

Figure C20 Gravel Test: approx 50 percent: Fixed Interval-Fixed Length
DATA/PLOTS

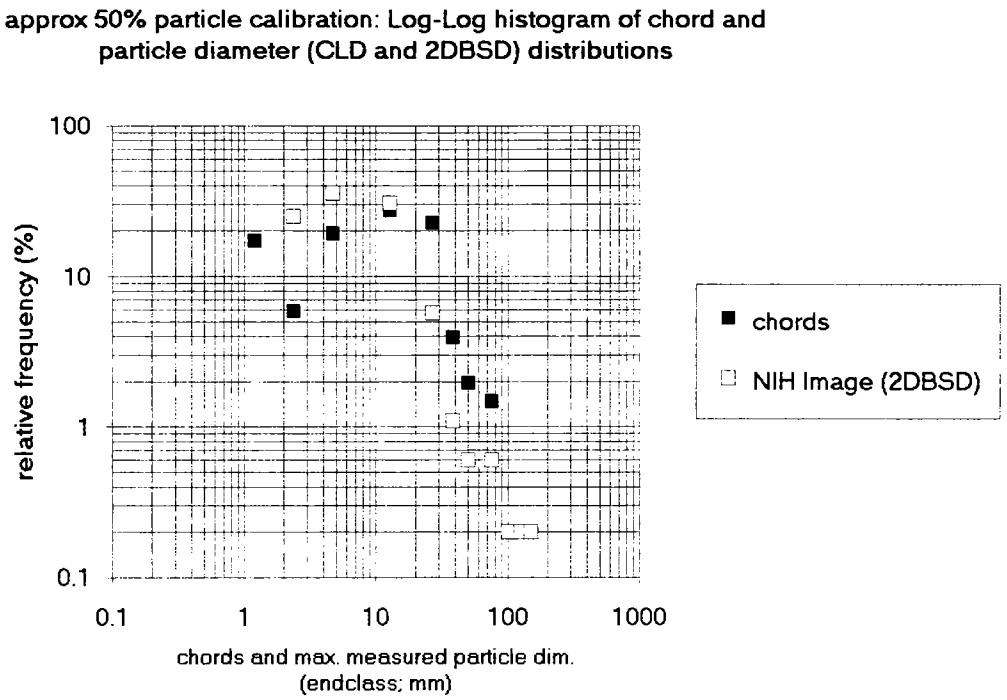

Figure C21 Gravel Test: approx 50 percent: Fixed Interval-Fixed Length **LOG-HISTOGRAM PLOT**

APPENDIX D

Data and Plots From Image Analysis of Triaxial Specimen Tracings

D1.0 Introduction

The plots and data displayed in this Appendix are summaries of work performed using image analysis on images of the 14 unrolled tracings of the surfaces of triaxial specimens, and through 6 cross-sections. The 150 mm diameter, 300 mm high specimens were fabricated by Lindquist (1994b),and the block volumetric proportions of the specimens are as declared by him. SigmaScan/Image™ was used to measure the areas and major axes of all particles exposed on the specimen surfaces, and to generate gray scale intensity values along scanlines. Conversion to chord lengths was executed by the computer programs presented in Appendix B. Areal proportions were calculated by summing all particle areas and dividing the total by the total area of the tracing. Details of the image analysis operations are presented in Appendix B.

The data are condensed as much as possible. Some conventions are repeated :
Block orientations are measured from vertical, and are 0, 30, 60 and 90 degrees
Block proportions: LOW is about 30 percent block volumetric proportion
MEDIUM is about 50 percent block volumetric proportion
HIGH is about 70 percent block volumetric proportion
CLD is the one-dimensional chord length distribution as measured from scanline intercepts across blocks.
2DBSD is two-dimensional block size distribution generated from the population of $\mathbf{d_{mod}s}$ (maximum observed dimensions) measured by SigmaScan/Image™ . The program defines the major axis of a particles as the distance between the two furthest points on a particle. The plots show the theoretical 2DBSD for the blocks, with fractal dimension **D** = 1.0, hinged at d_{max} , which was assumed to be the same for 2DBSD and 3DBSD.
3DBSD is the block size distribution used to fabricate the specimens, as declared by Lindquist (1994b), and was assumed to be the same for all specimens since that was one of Lindquist's fixed variables. The fractal dimension **D**=2.0. The block proportions change, but not the relative numerical frequency of the different-sized blocks.

D2.0 Triaxial Specimen Tracings - Data and Plots

The data and plots are presented in the next 20 Figures, one specimen for each page. These are followed by 7 compilation summaries sheets each showing: a) a semilog style of BSD; b) arithmetic relative frequency histogram; c)log-histogram for 4 sheets (0, 30, 60 90 degrees) showing data for each specimen but sorted by mix; and 3 sheets ((LOW, MEDIUM and HIGH mixes) for the same data sorted by block orientation.

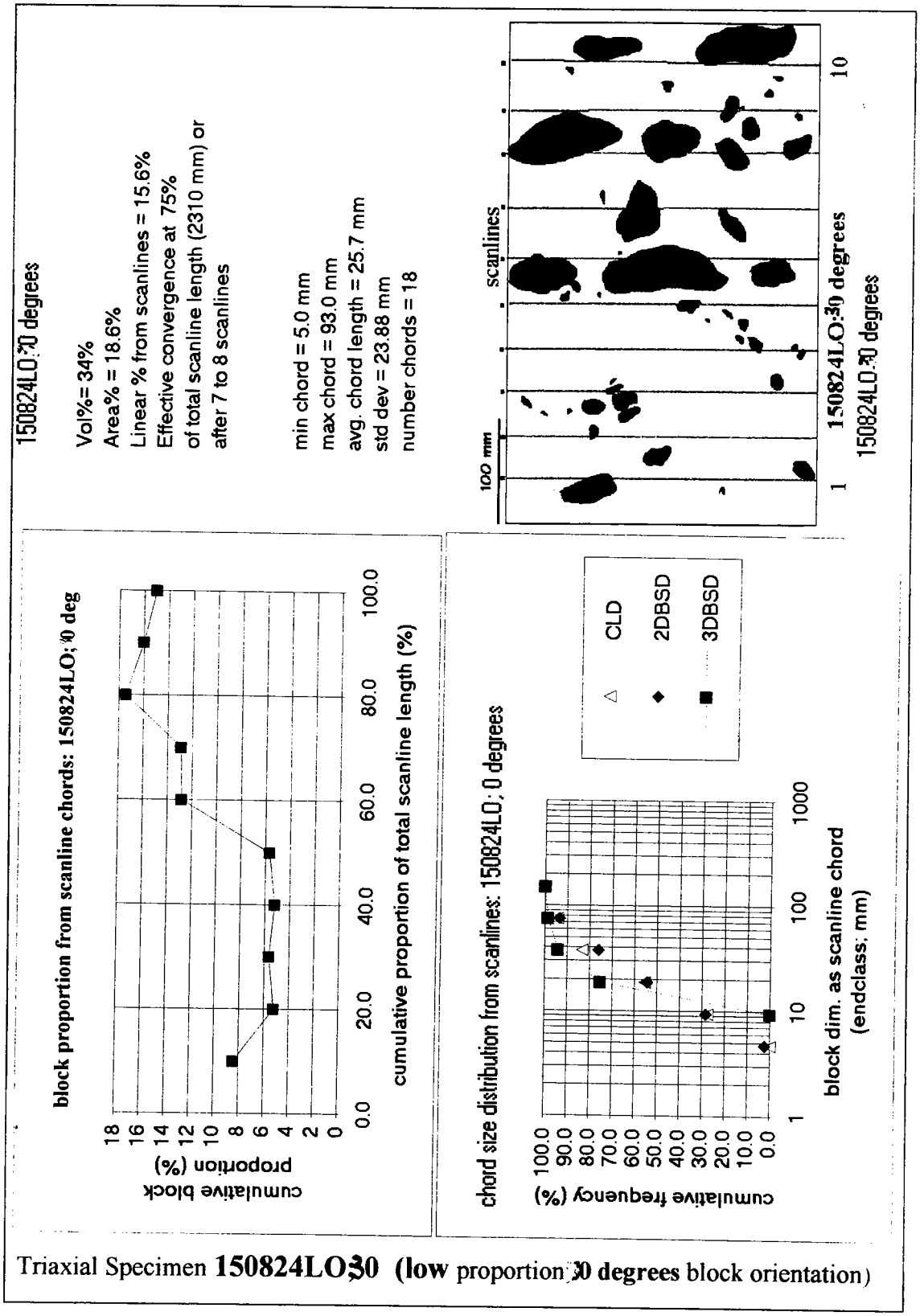

Triaxial Specimen **150824LO30 (low** proportion **30 degrees** block orientation)

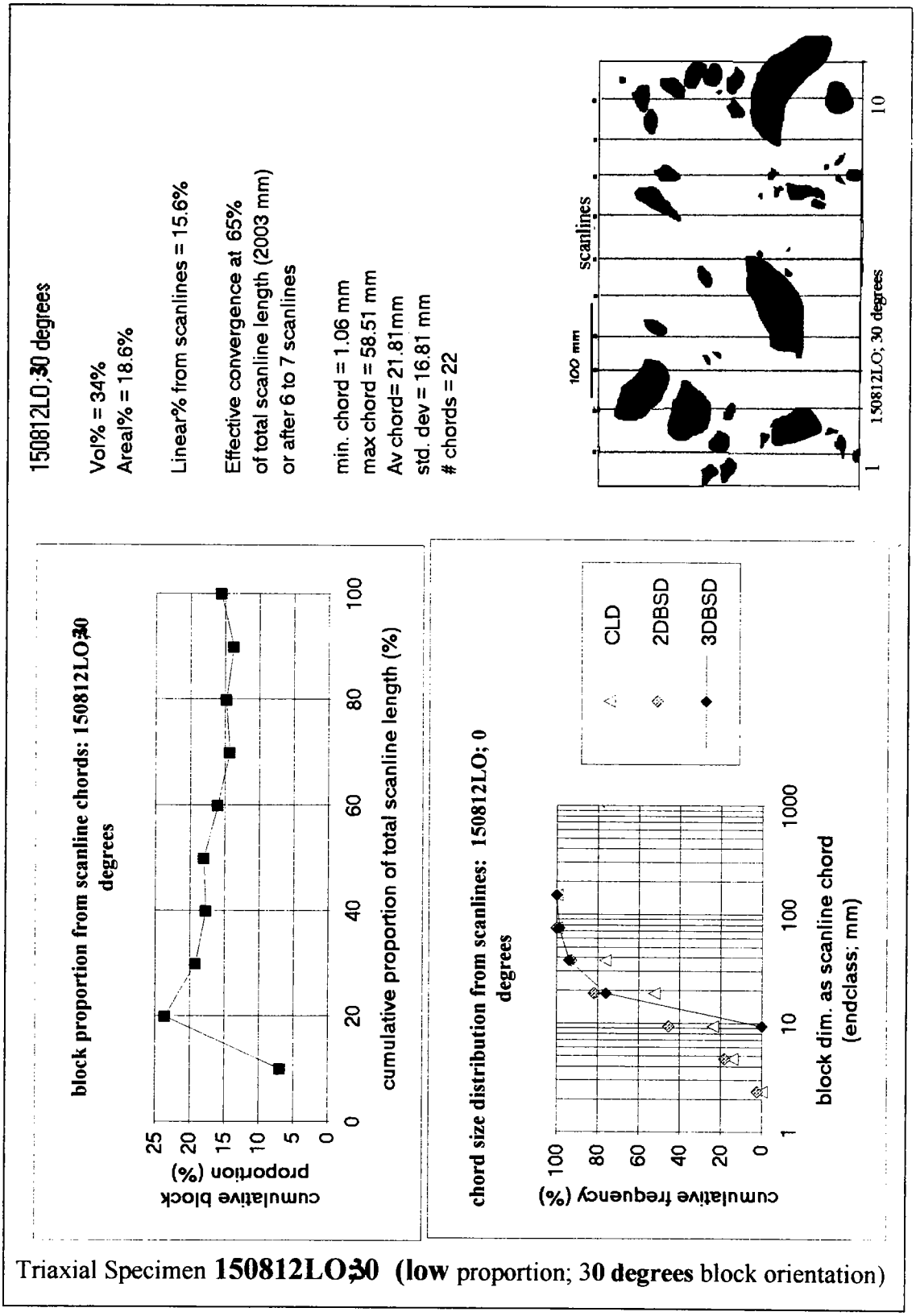

Triaxial Specimen **150812LO;30** (**low** proportion; 30 **degrees** block orientation)

150812LO; 30 degrees CROSS-SECTION
X-S Area= 36.7%; Circum. Area= 18.6%; Vol%= 34%

	maj axis (mm)	area (mm^2)
max	124.9	4167.8
min	9.1	41.1
mean	41.5	883.0
stddev	37.1	1311.9
std err	8.5	301.0
95% conf	17.9	632.3
99% conf	24.5	866.4
count	19	19
total		16777.9

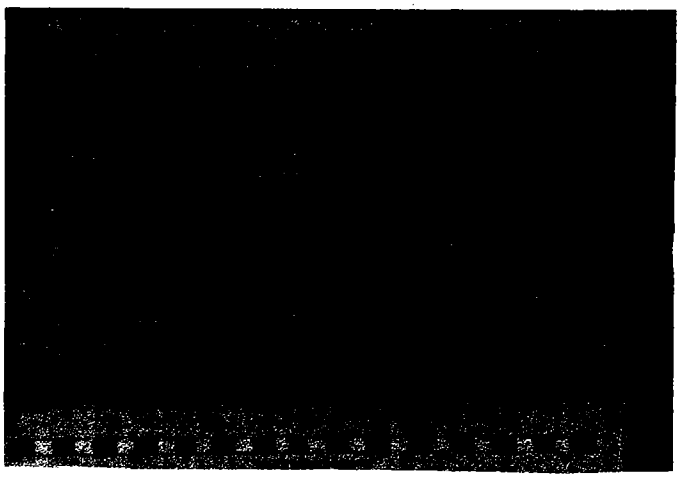

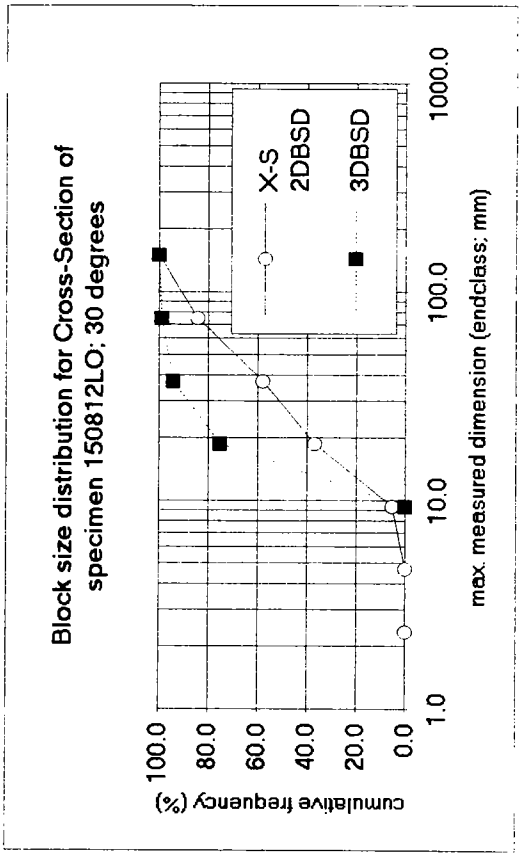

Triaxial Specimen **150812LO; 0 (low** proportion; 30 **degrees** block orientation)
CROSS-SECTION BLOCK AREAL PROPORTION

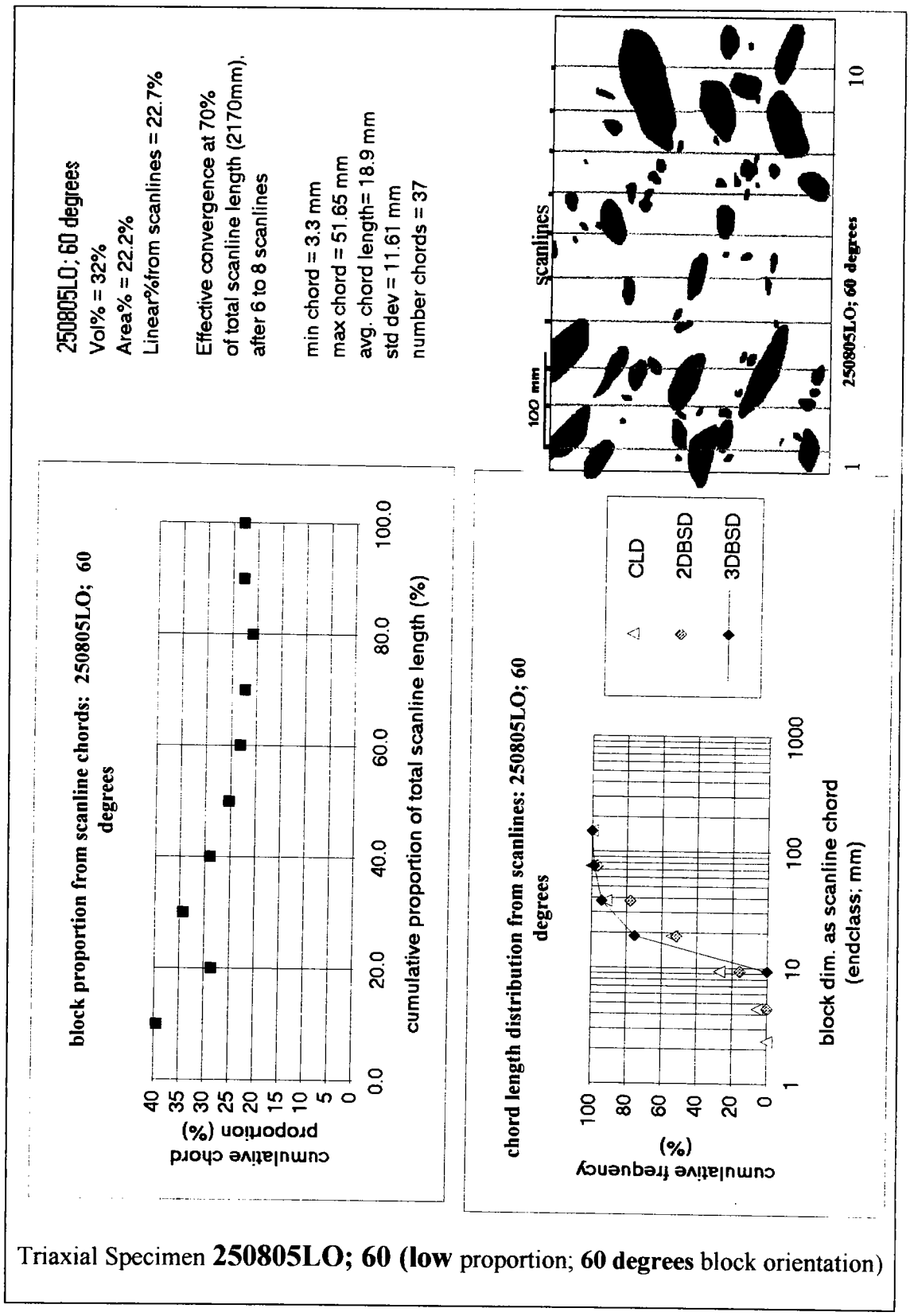

Triaxial Specimen **250805LO; 60 (low** proportion; **60 degrees** block orientation)

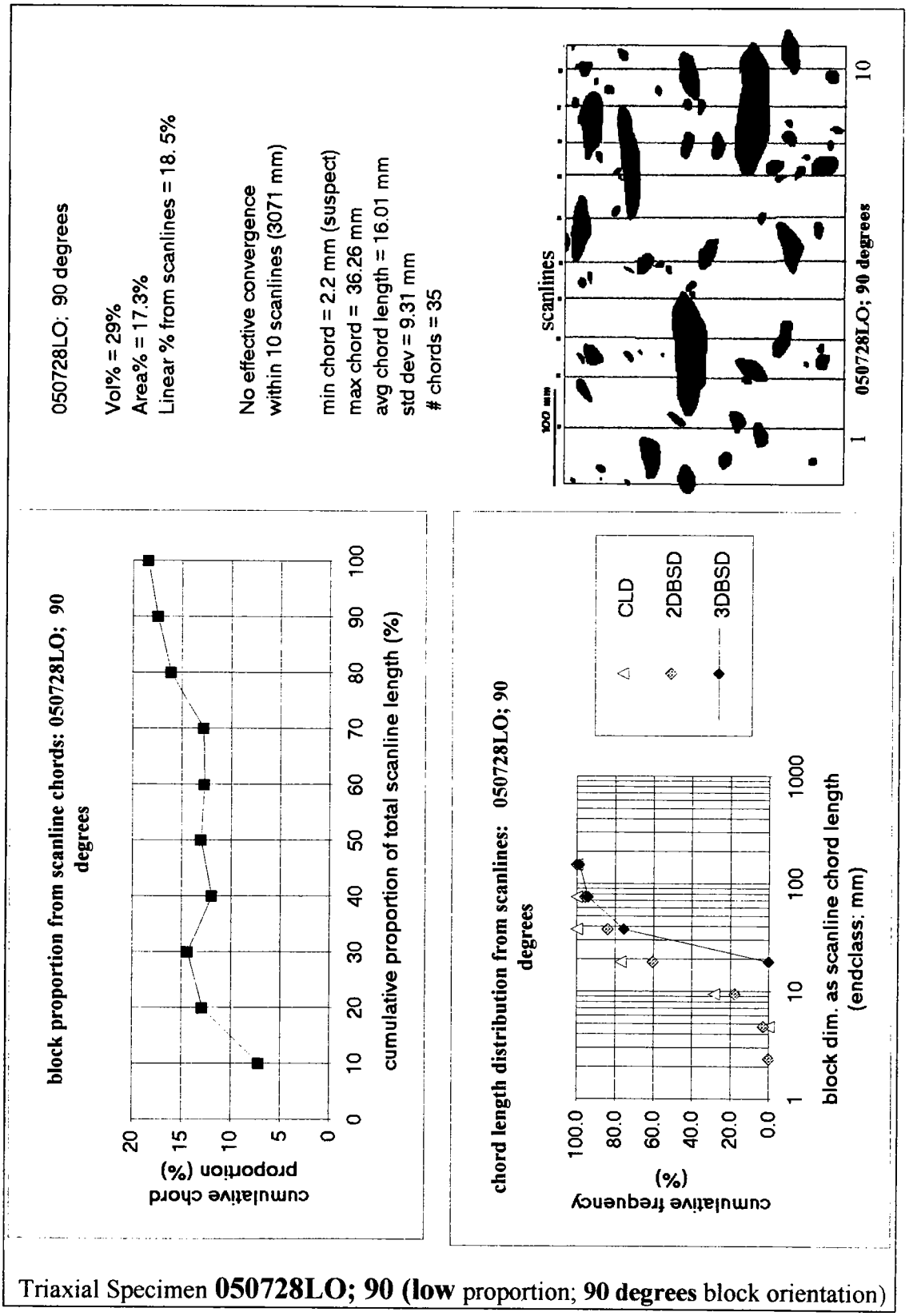

Triaxial Specimen **050728LO; 90 (low** proportion; **90 degrees** block orientation)

050728LO; 90 degrees CROSS SECTION SUMMARY
X-S Area= 29.7%; Circum. Area= 17.3%; Vol%= 29.0%

	maj axis (mm)	area (mm^2)
min	3.0	6.3
max	108.9	3216.2
mean	27.4	424.5
std dev	27.4	742.7
std err	4.9	131.3
95% conf	9.9	267.8
99% conf	13.3	360.3
count	32	32
total		13583.7

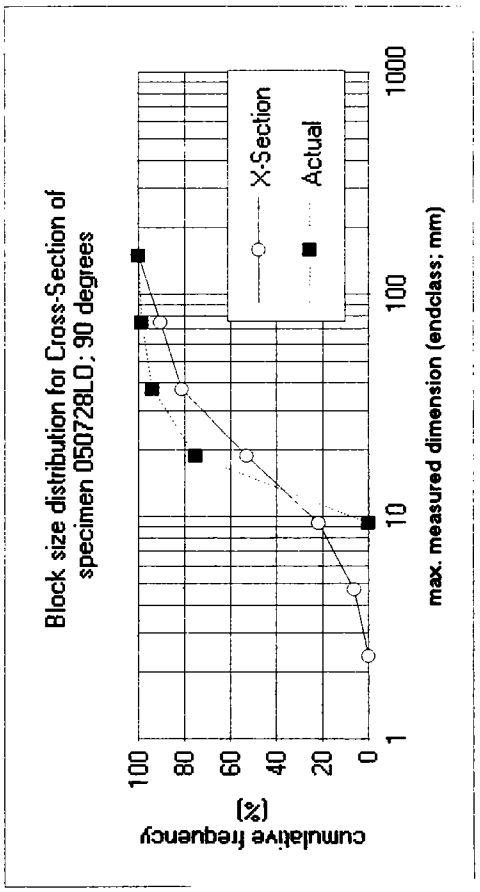

Triaxial Specimen **050728LO; 90 (low** proportion; **90 degrees** block orientation)
CROSS-SECTION BLOCK AREAL PROPORTION

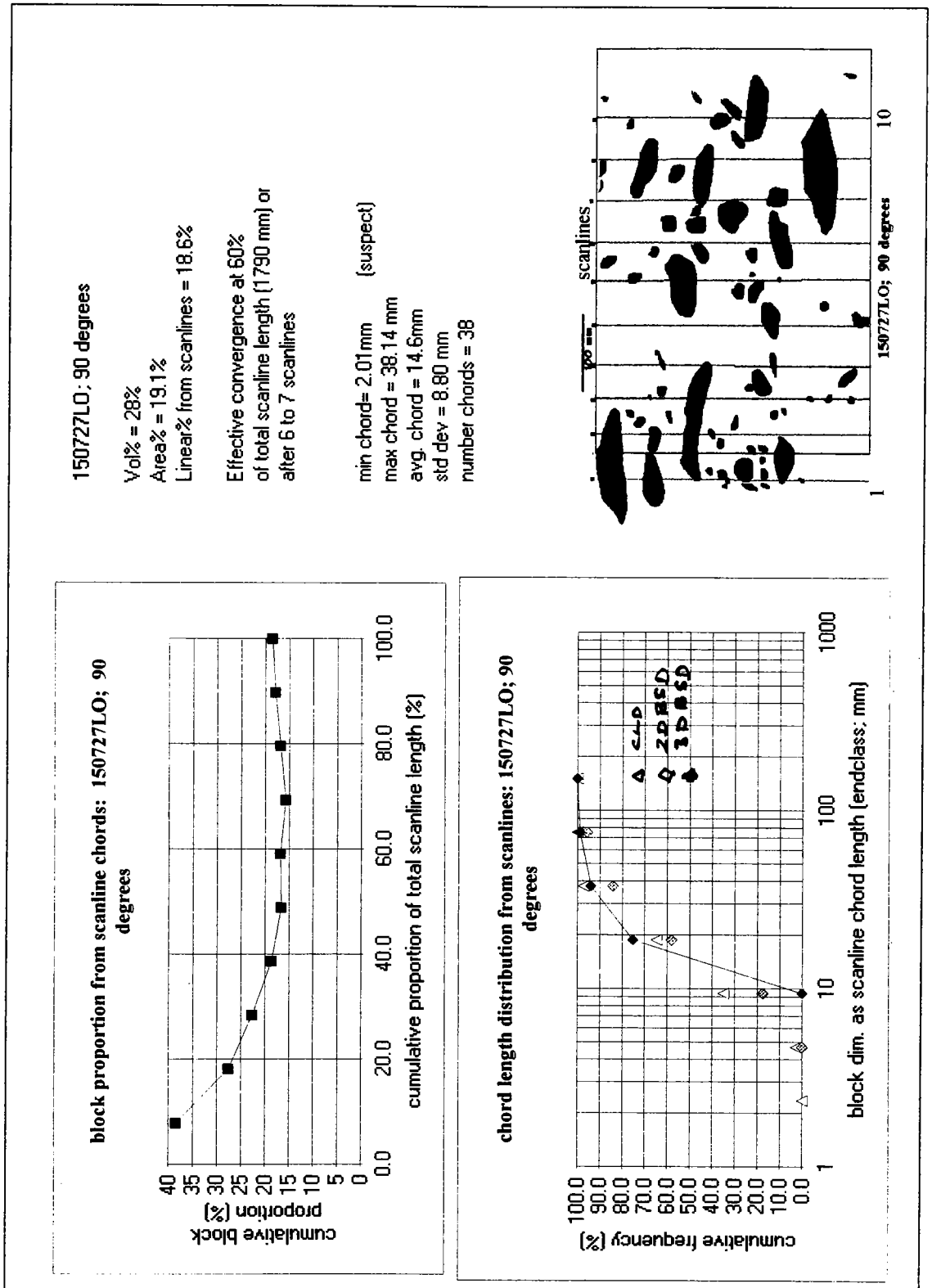

Triaxial Specimen **050727LO; 90 (low** proportion; **90 degrees** block orientation)

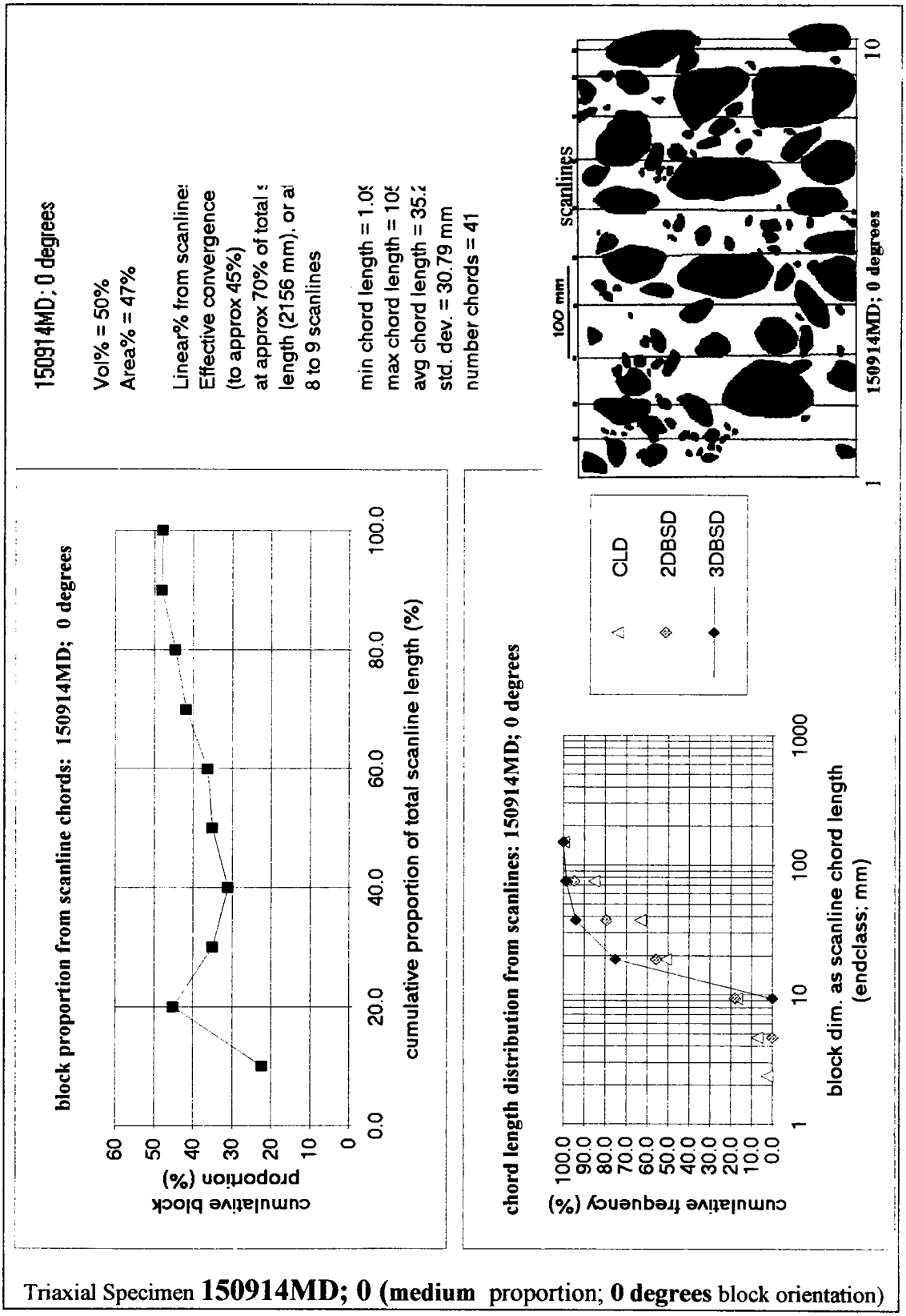

Triaxial Specimen **150914MD; 0 (medium** proportion; **0 degrees** block orientation)

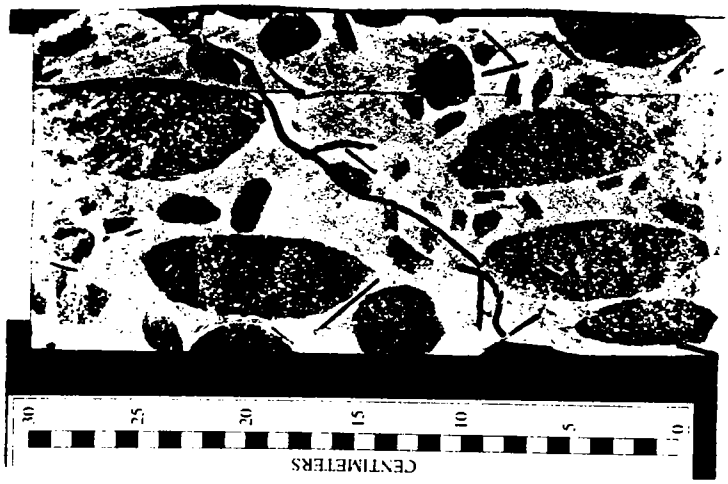

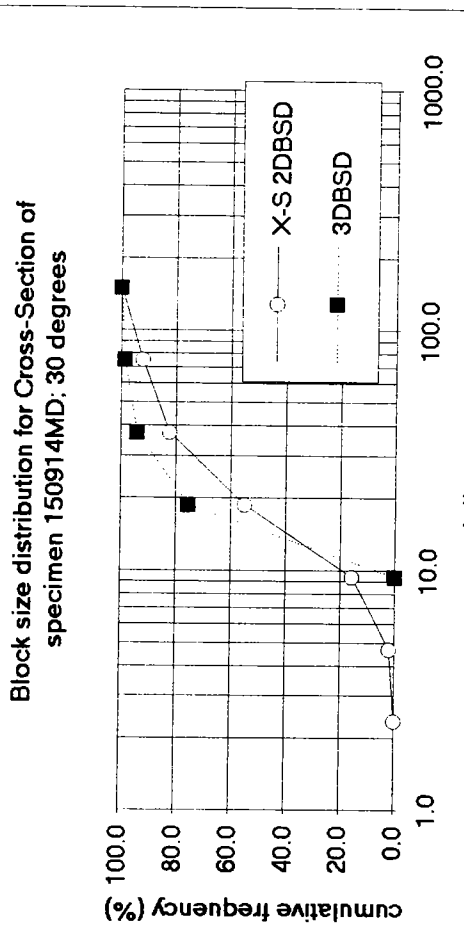

CROSS-SECTION Summary
150914MD; 0 degrees
X-S Area%= 50.7%; Vol%= 50%
Circumference Area%= 47%;

	maj axis (mm)	area (mm^2)
min	4.7	9.7
max	104.3	3774.5
mean	27.2	454.4
std dev	25.5	855.0
std err	3.6	119.7
95% conf	7.2	240.5
99% conf	9.5	320.6
count	51	51
total		23176.2

Triaxial Specimen **150914MD; 0 (medium** proportion; **0 degrees** block orientation)
CROSS-SECTION BLOCK AREAL PROPORTION

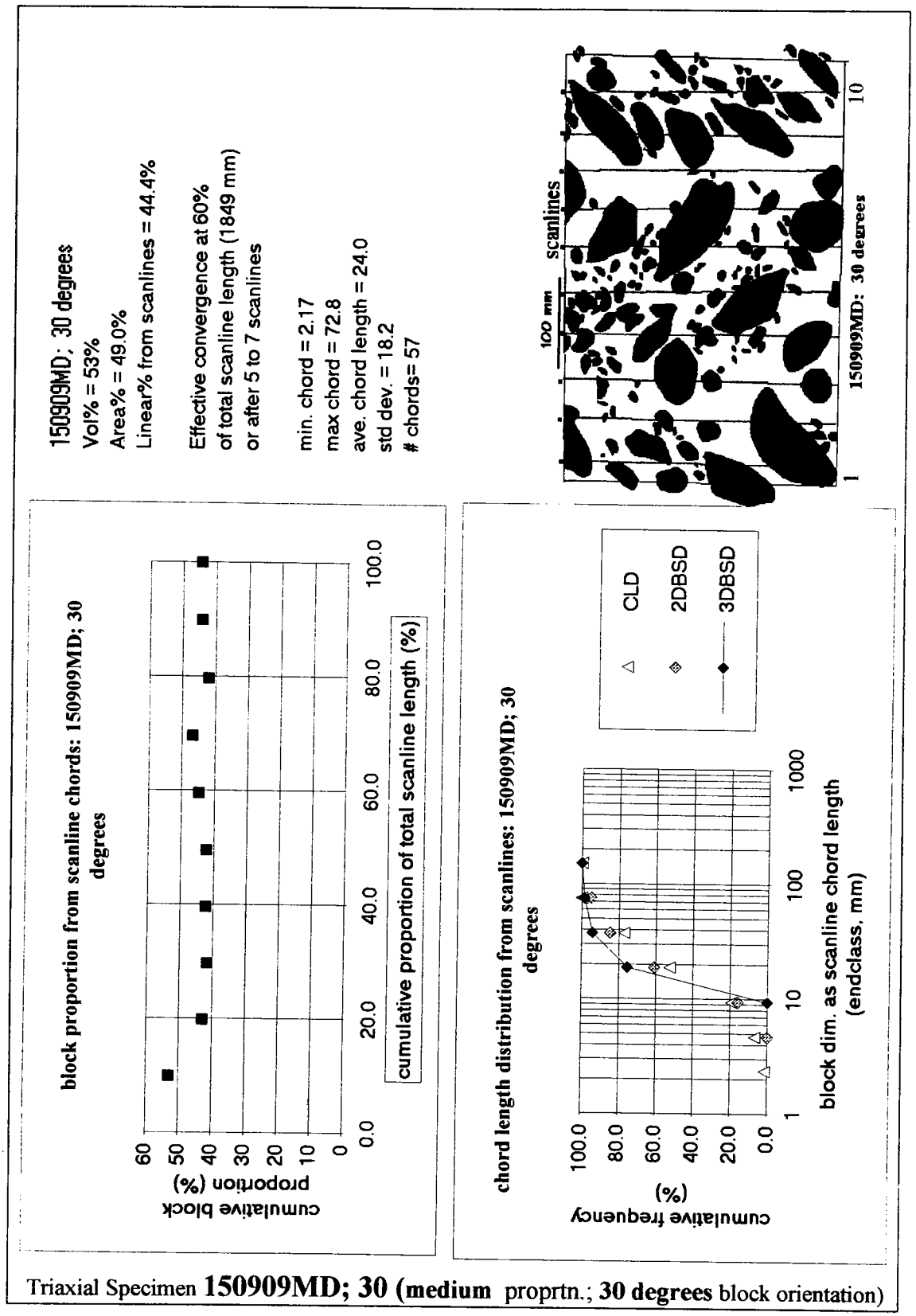

Triaxial Specimen **150909MD; 30 (medium** proprtn.; **30 degrees** block orientation)

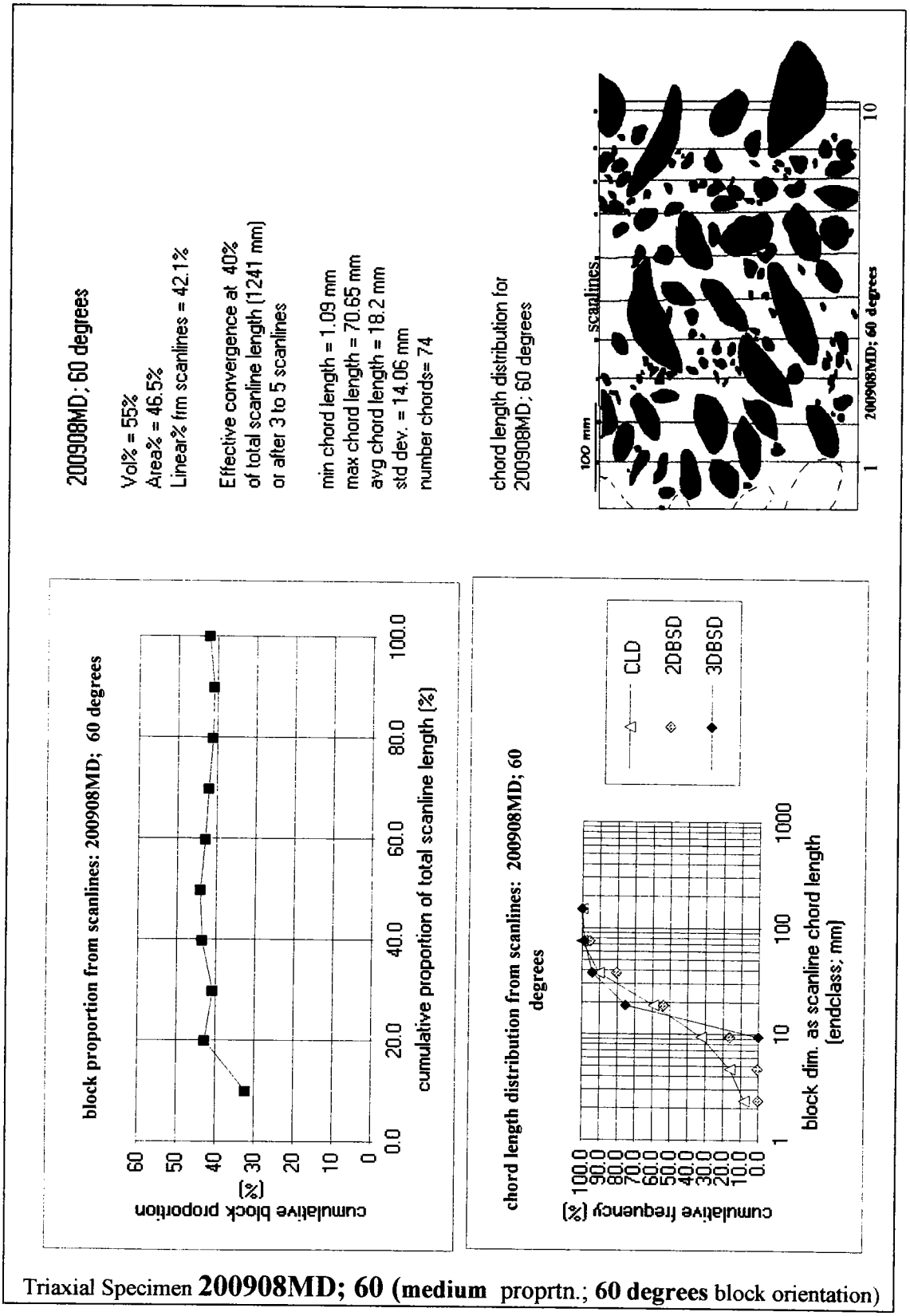

Triaxial Specimen **200908MD; 60 (medium** proprtn.; **60 degrees** block orientation)

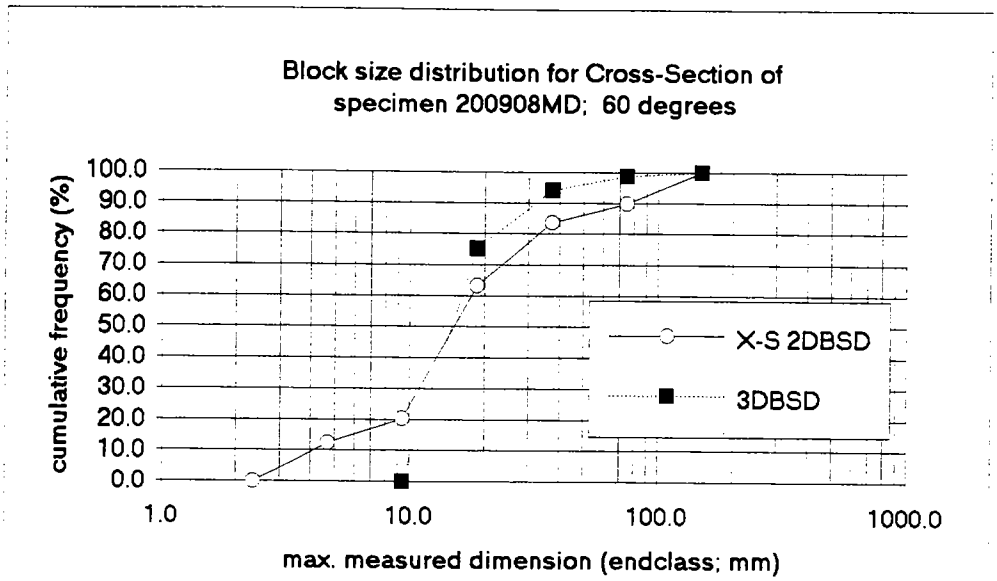

CROSS-SECTION Summary
200980MD; 60 degrees
X-S. Area%= 44.7%; Vol%=55%
Circumference Area%= 46.5%

	maj. axis (mm)	area (mm^2)
min	2.8	6.3
max	110.4	3378.6
mean	25.9	417.4
Std dev	29.5	810.0
std err	4.2	115.7
95% conf	8.5	232.7
99% conf	11.3	310.4
count	49	49
total		20451.1

Triaxial Specimen **200908MD; 60 (medium** proprtn.; **60 degrees** block orientation)
CROSS-SECTION BLOCK AREAL PROPORTION

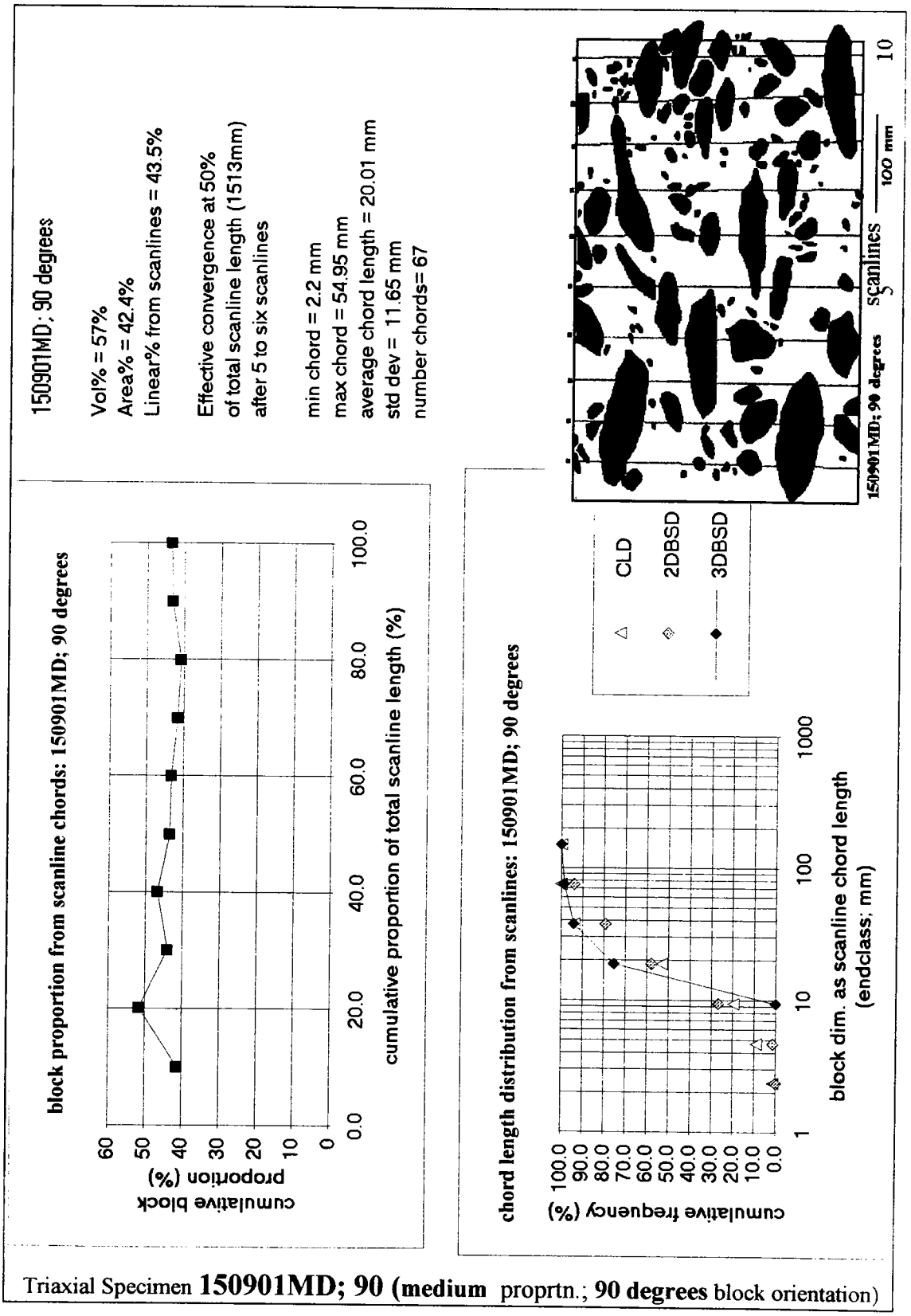

Triaxial Specimen **150901MD; 90 (medium** proprtn.; **90 degrees** block orientation)

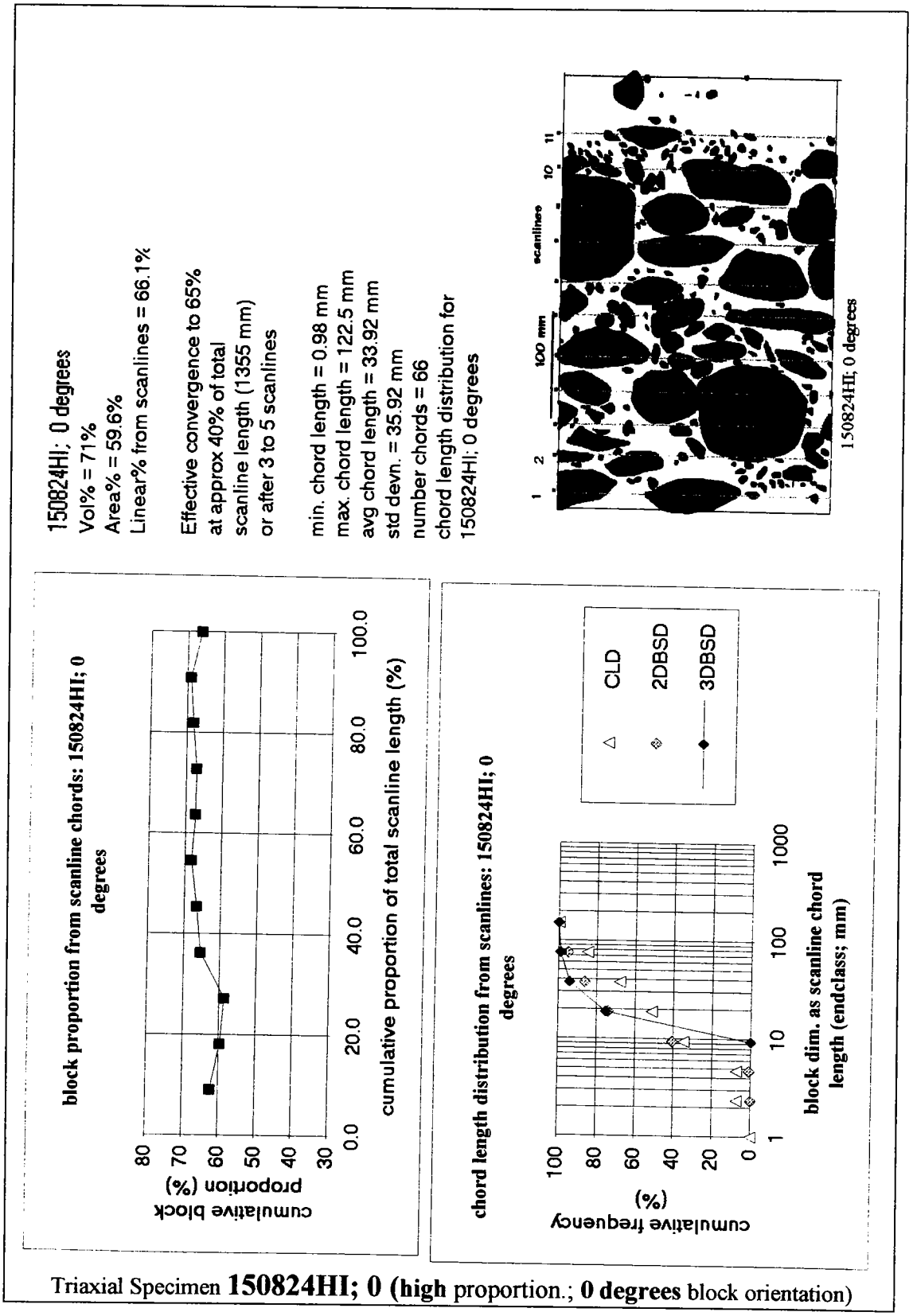

Triaxial Specimen **150824HI; 0 (high** proportion.; **0 degrees** block orientation)

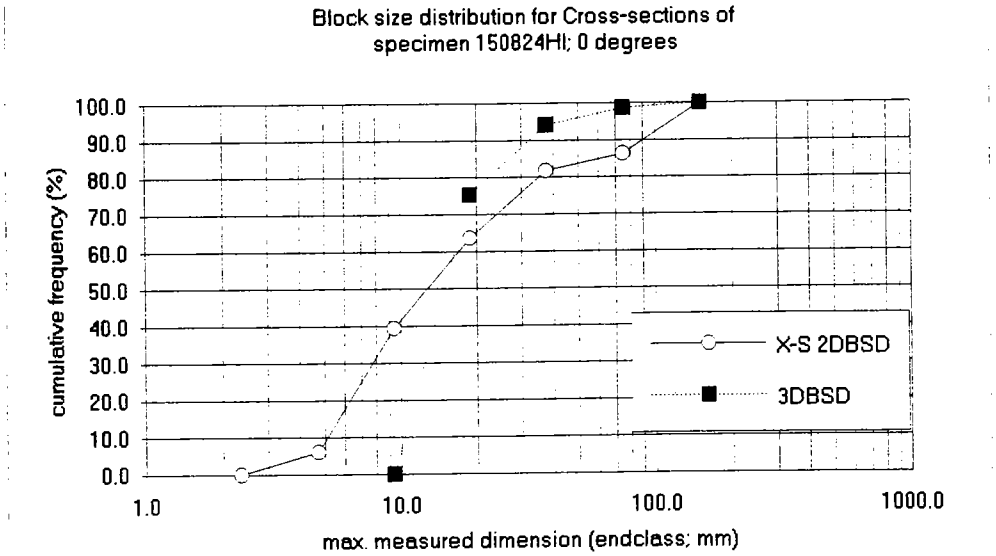

CROSS-SECTION Summary
150824HI; 0 degrees
X-Section Area%= 69.1%; V ol% = 71%
; circumference Area%= 66.1;

	maj. axis (mm)	area (mm^2)
min	2.4	4.9
max	118.8	3715.5
mean	27.3	479.2
std dev	32.9	953.1
std err	4.1	117.3
95% conf	8.1	234.3
99% conf	10.8	311.3
count	66	66
total		31627.2

Triaxial Specimen **150824HI; 0 (high** proportion.; **0 degrees** block orientation)
CROSS-SECTION BLOCK AREAL PROPORTION

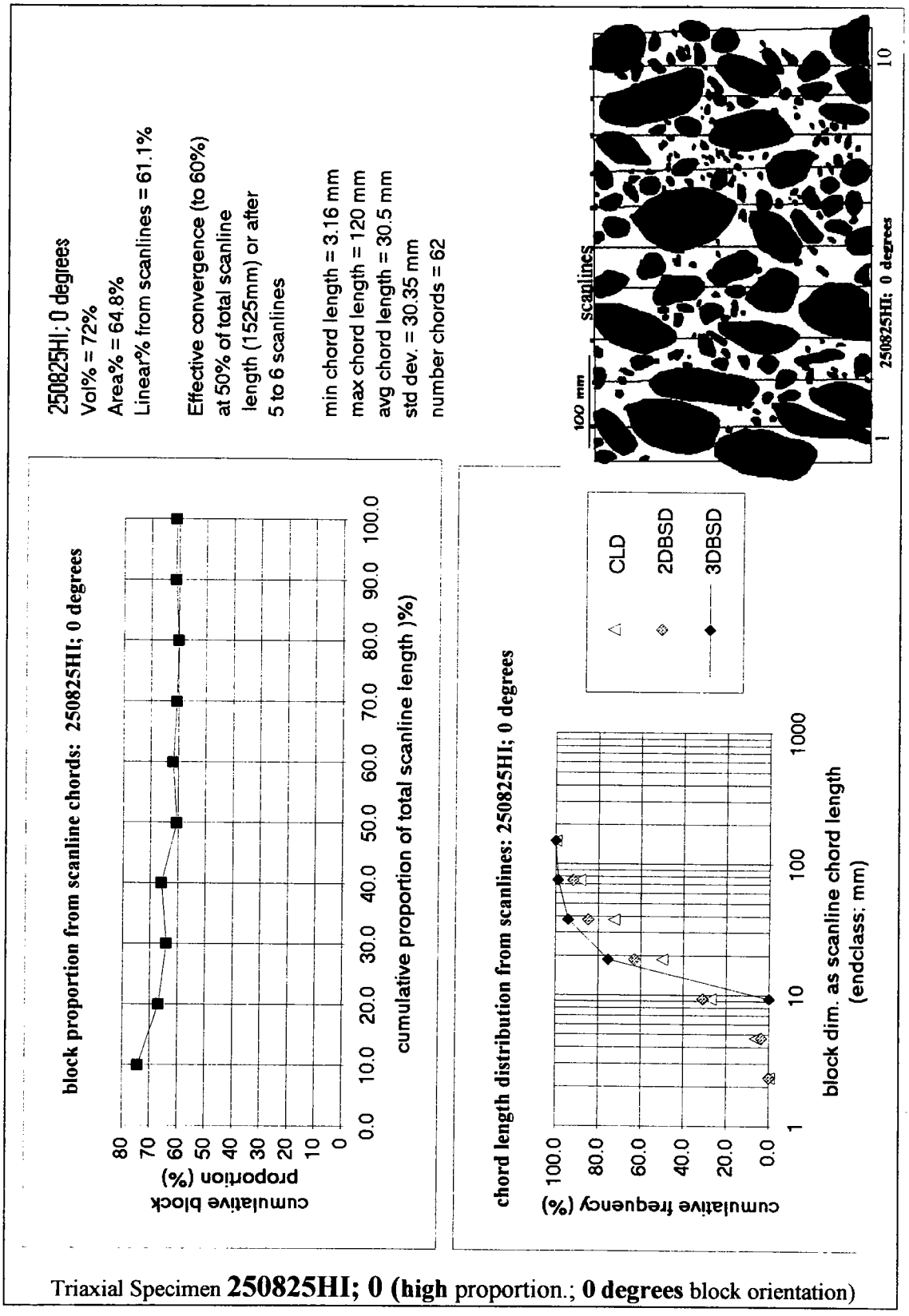

Triaxial Specimen **250825HI; 0 (high** proportion.; **0 degrees** block orientation)

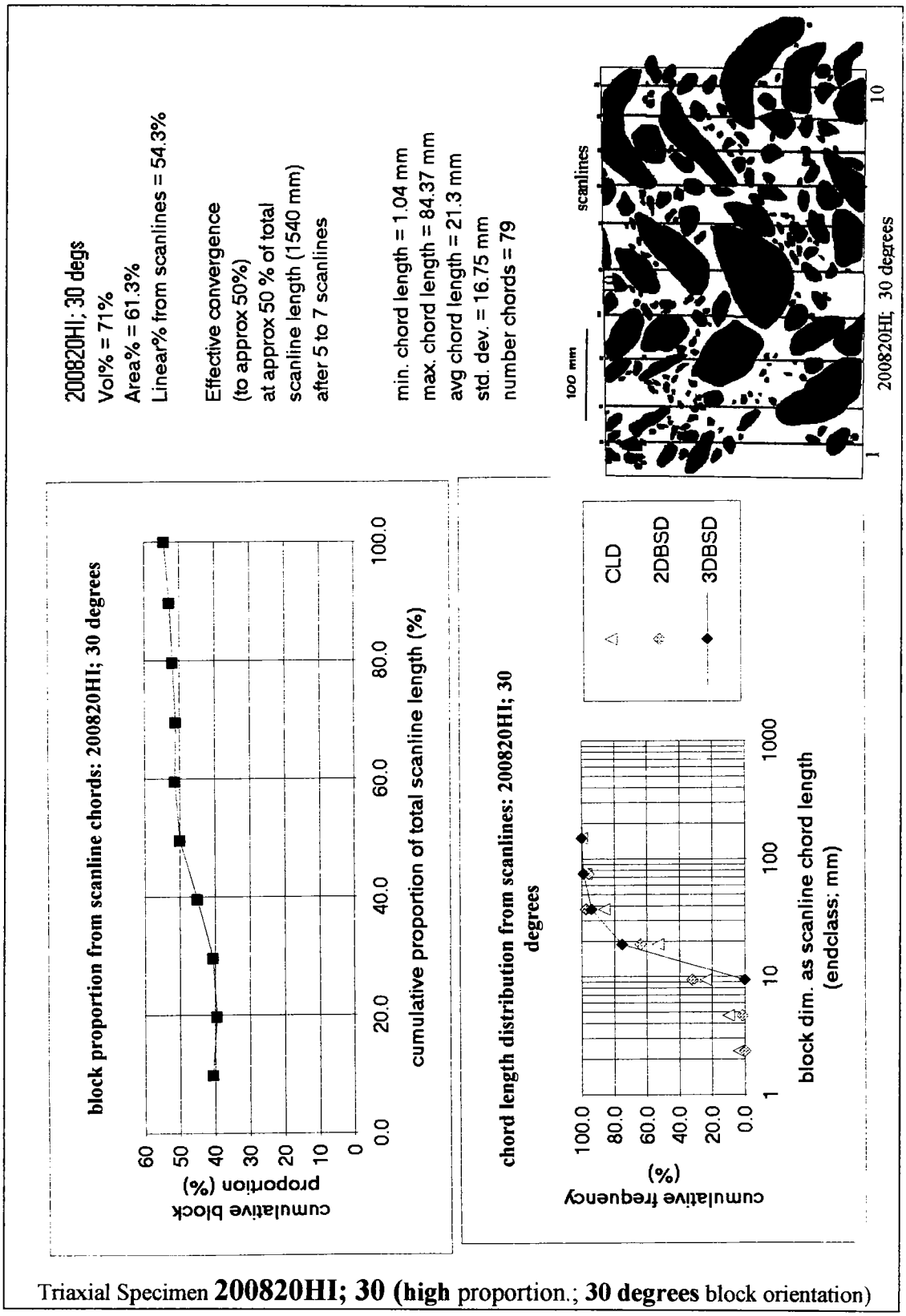

Triaxial Specimen **200820HI; 30 (high** proportion.; **30 degrees** block orientation)

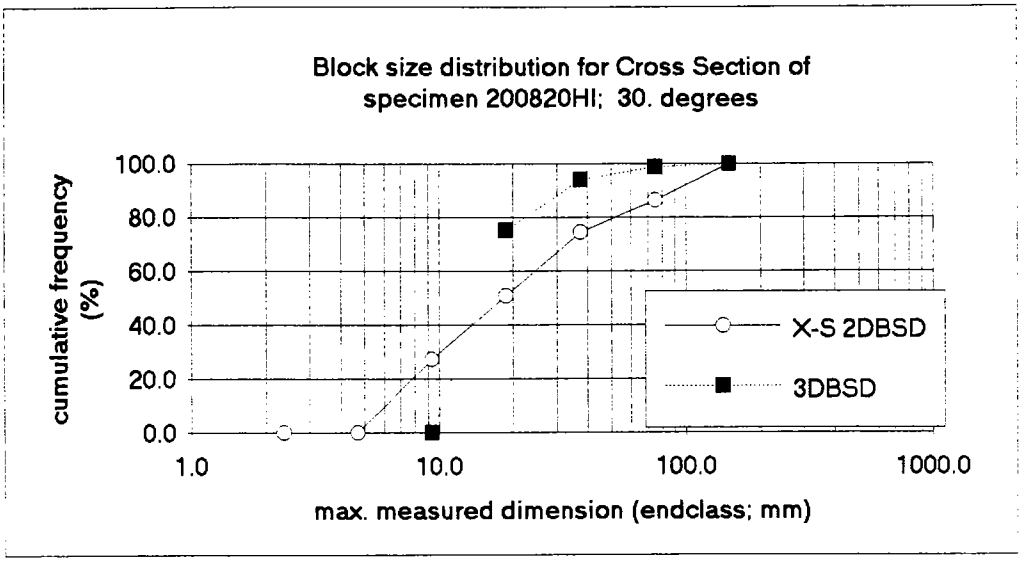

CROSS-SECTION Summary
200820HI; 30 degrees
X-Section Area% =72.3%; Vol%= 74%
Circum Area%= 54.3%

	maj. axis (mm)	area (mm^2)
min	5.2	12.6
max	126.6	4491.5
mean	32.2	648.5
std dev	34.7	1150.0
std err	4.9	161.0
95% conf	9.8	323.4
99% conf	13.0	431.2
count	51	51
total		33075.4

Triaxial Specimen **200820HI; 30 (high** proportion.; **30 degrees** block orientation)
CROSS-SECTION BLOCK AREAL PROPORTION

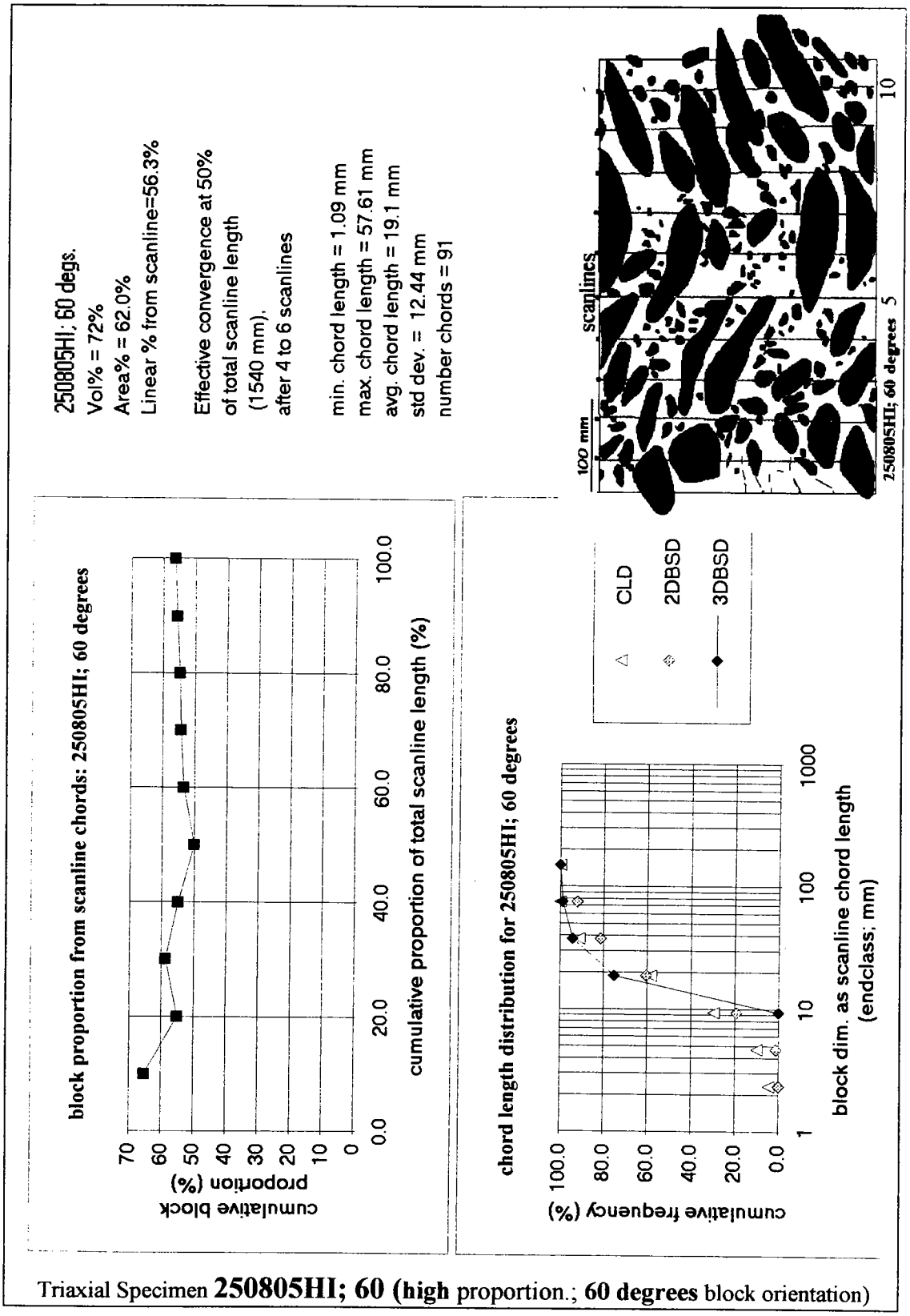

Triaxial Specimen **250805HI; 60 (high** proportion.; **60 degrees** block orientation)

200803HI; 90 degs

Vol% = 71%
Area % = 60.7%
Linear% from scanlines = 57.6%
Effective convergence
(to approx. 55%) at 40% of total
scanline length (1220 mm) , or
after 4 to 5 scanlines

min chord length = 0.98 mm
max. chord length = 40.0 mm
avg. chord length = 17.2 mm
std. dev. = 10.92 mm
number chords = 101

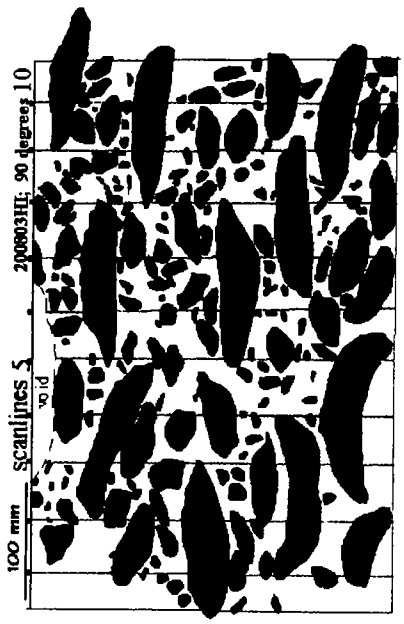

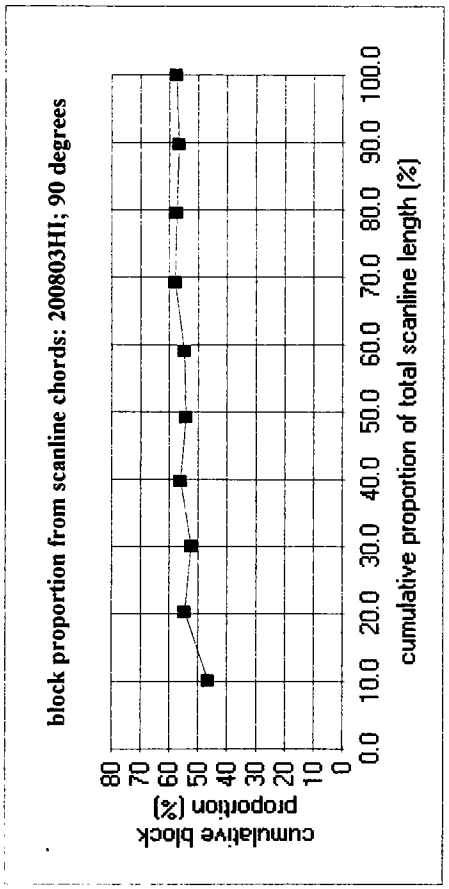

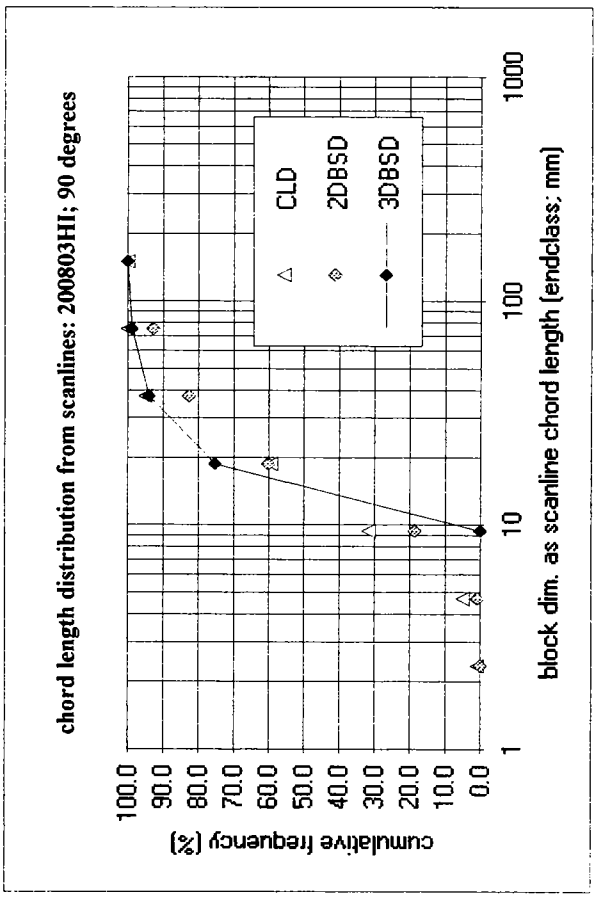

Triaxial Specimen **200803HI; 90 (high** proportion.; **90 degrees** block orientation)

Scanline measurements:
chord length distribution for 0 degree block orientations

LO = low
MD= medium
HI = high

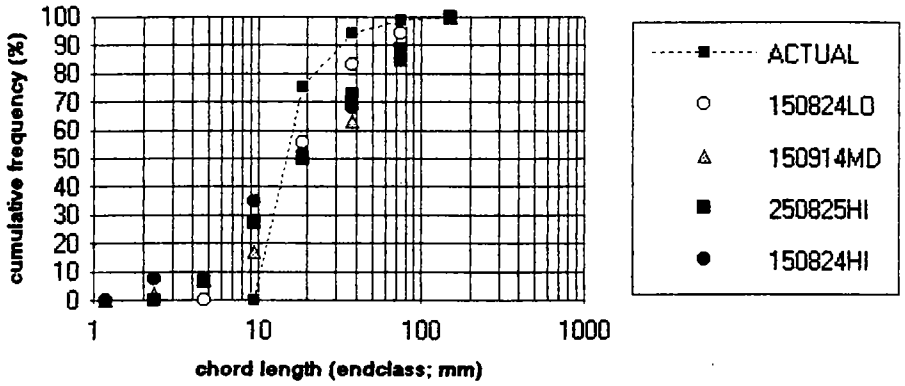

Scanline measurements:
relative frequency of chord lengths for 0 degree orientation

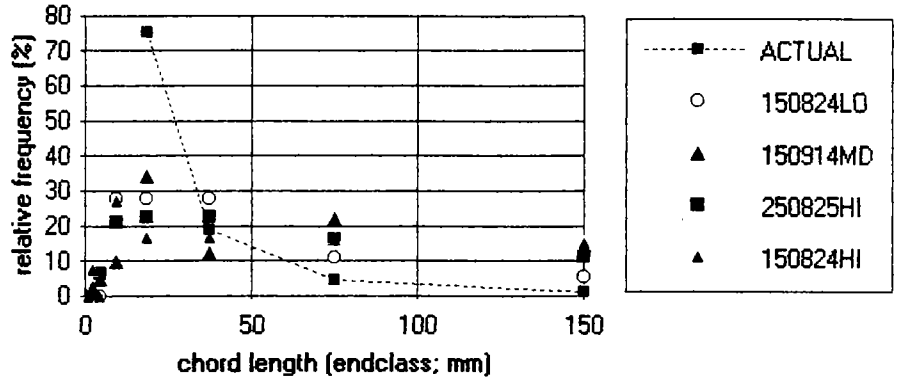

Scanline measurements: log-log plot of
relative frequency of chord lengths for 0 degree orientation

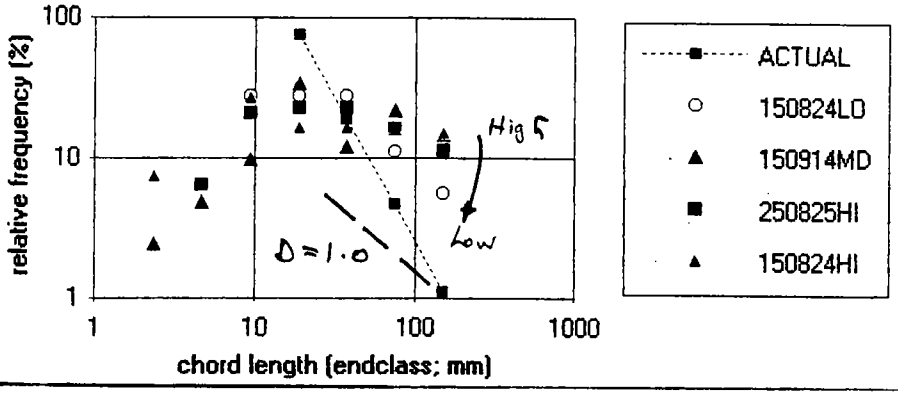

"ACTUAL" is 3DBSD for which D = 2.0

Scanline Data for Triaxial Specimens; **sorted by Block Proportion:**

0 degrees orientation

Scanline measurements:
chord length distribution for 30 degree orientation

LO = low block propn.
MD = medium
HI = high

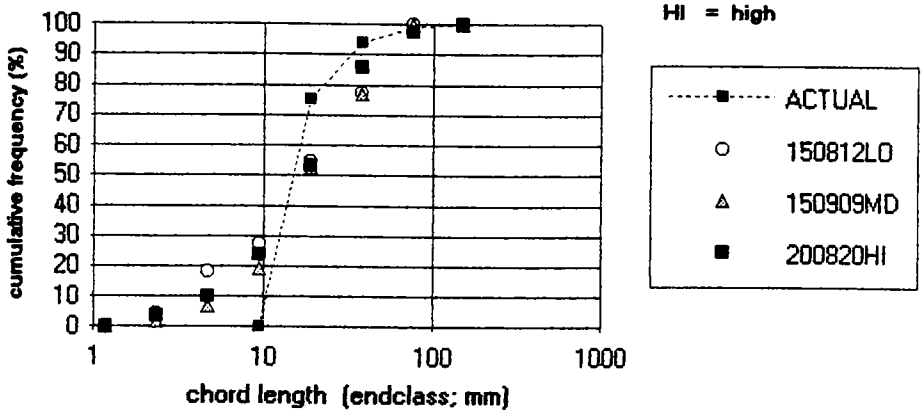

Scanline measurements:
relative frequency of chord lengths for 30 degrees orientation

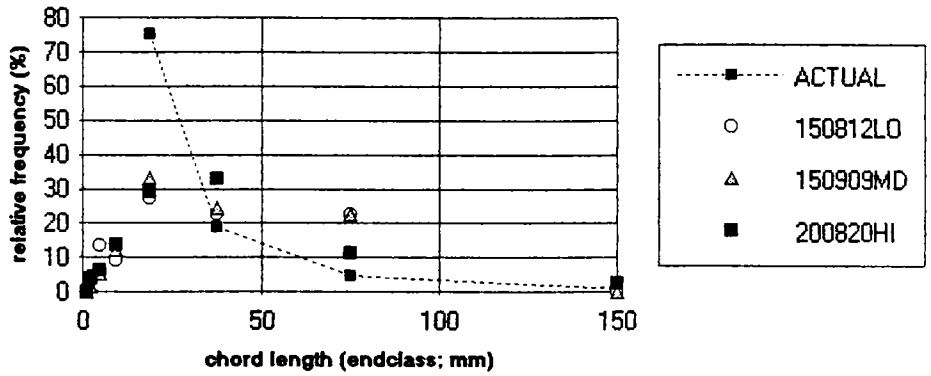

Scanline measurements: log-log plot of
relative frequency of chord lengths for 30 degrees orientation

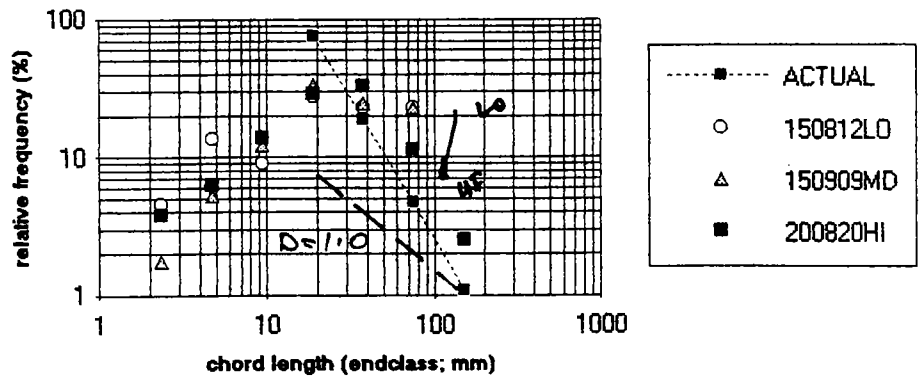

"ACTUAL" is 3DBSD for which D = 2.0

Scanline Data for Triaxial Specimens; **sorted by Block Proportion:**

30 degrees orientation

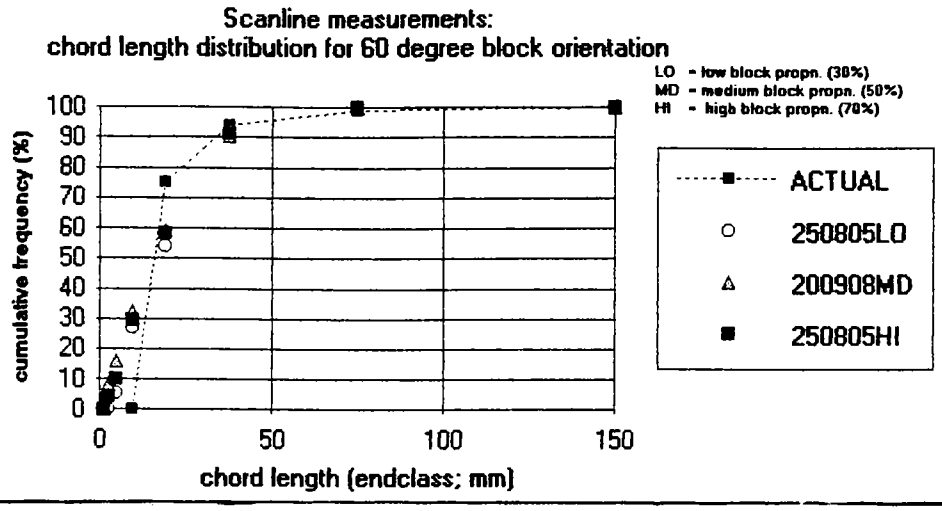

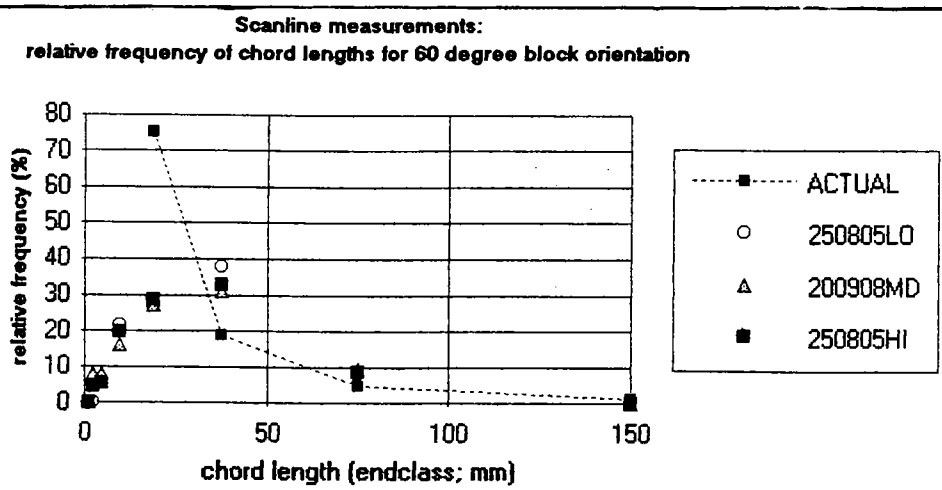

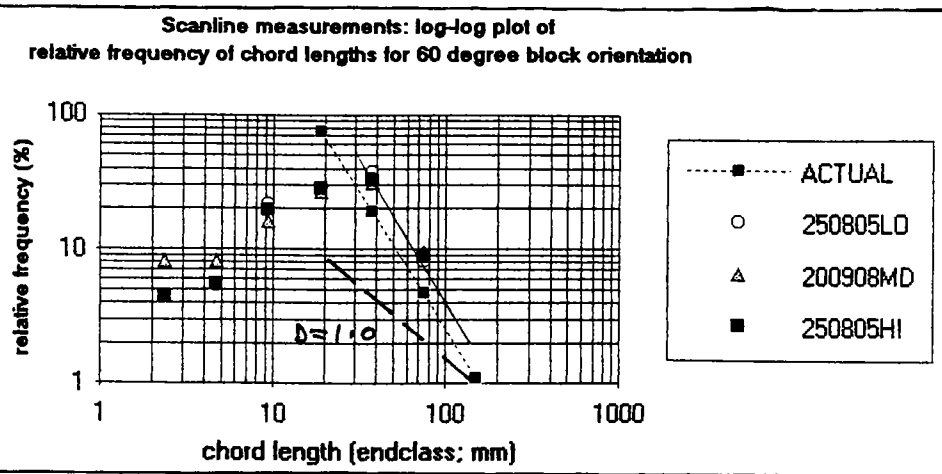

"ACTUAL" is 3DBSD for which D = 2.0

Scanline Data for Triaxial Specimens; **sorted by Block Proportion:**

60 degrees orientation

Scanline measurements:
chord length distribution for 90 degree block orientation

LO = low block propn. (30%)
MD = medium block propn. (5(
HI = high block propn. (~~15~~ 100%

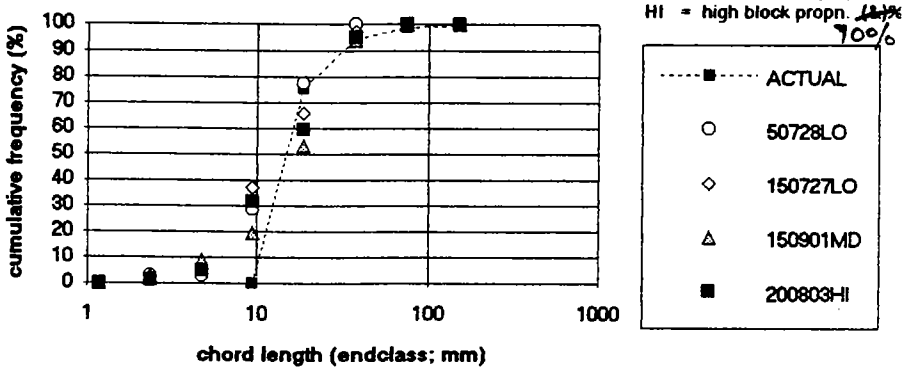

Scanline measurements:
relative frequency of chord lengths for 90 degree orientations

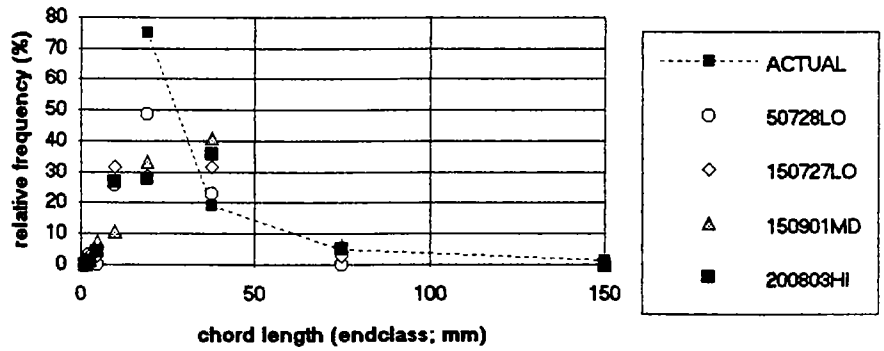

Scanline measurements: log-log plot of
relative frequency of chord lengths for 90 degree orientations

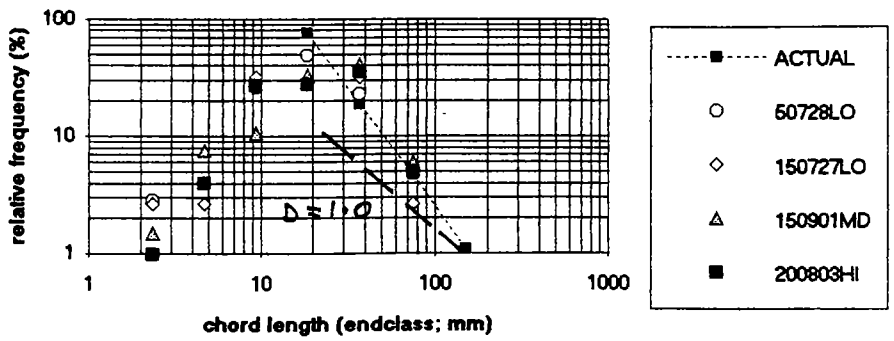

"ACTUAL" is 3DBSD for which D = 2.

Scanline Data for Triaxial Specimens; **sorted by Block Proportion:**

90 degrees orientation

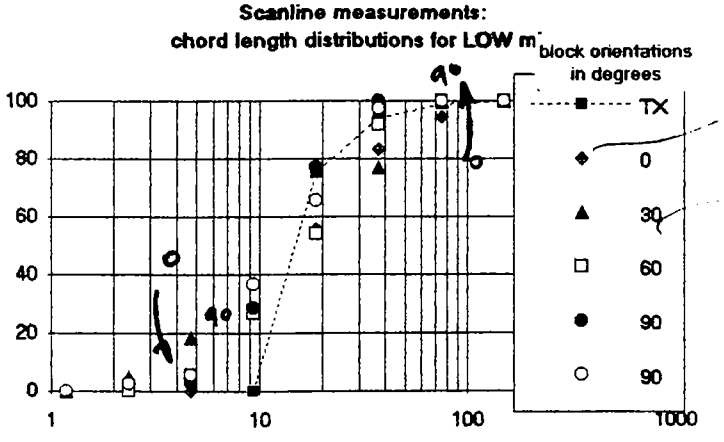

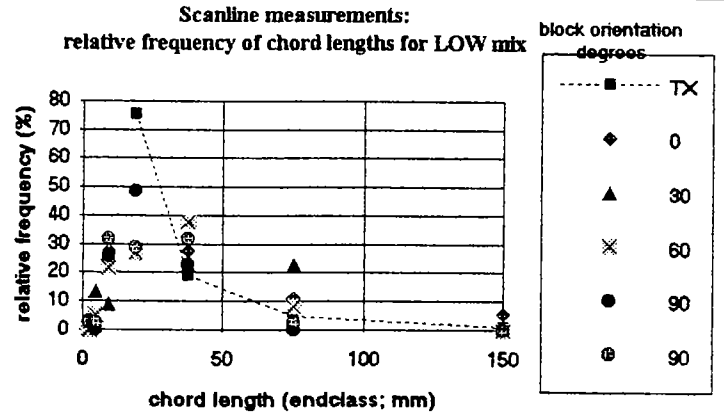

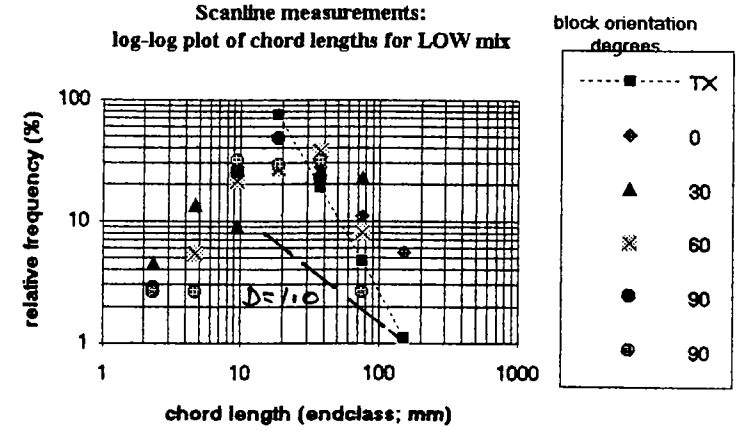

"TX" and "ACTUAL" are 3DBSD for which D=2.0

Scanline Data for Triaxial Specimens; **sorted by Block Orientation:**

LOW BLOCK VOLUMETRIC PROPORTION MIXTURE

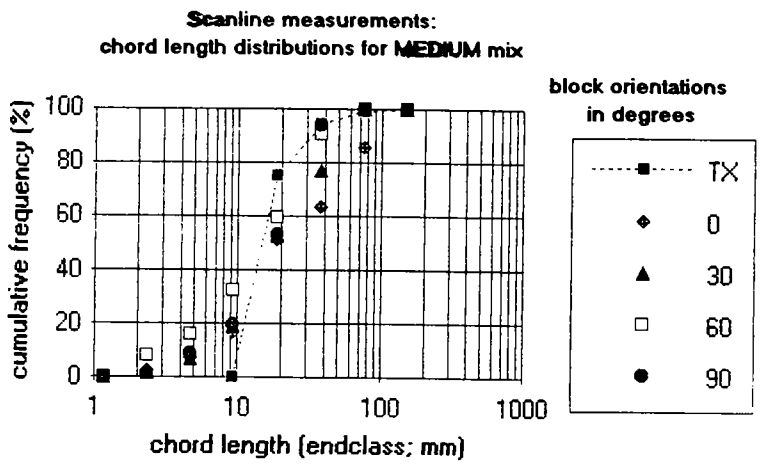

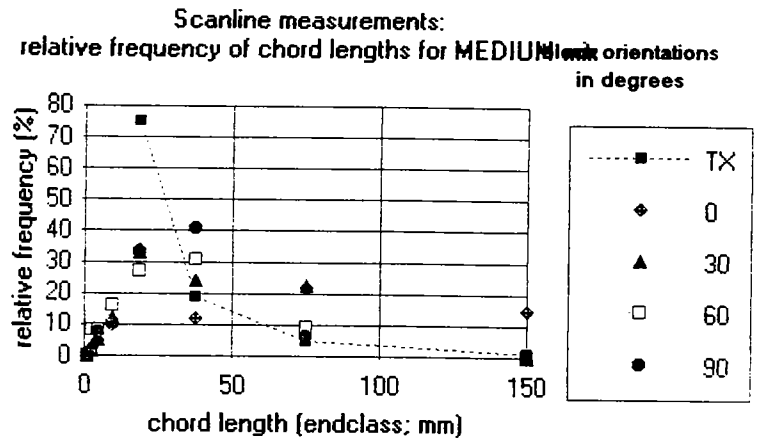

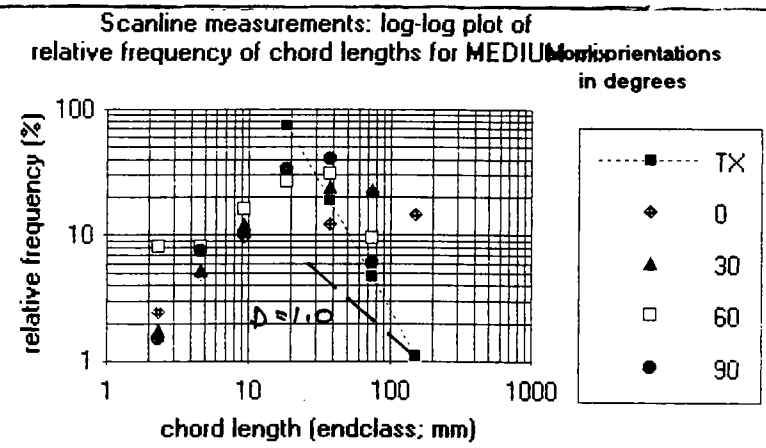

"TX" and "ACTUAL" are 3DBSD for which D=2.0

Scanline Data for Triaxial Specimens; **sorted by Block Orientation:**

MEDIUM BLOCK VOLUMETRIC PROPORTION MIXTURE

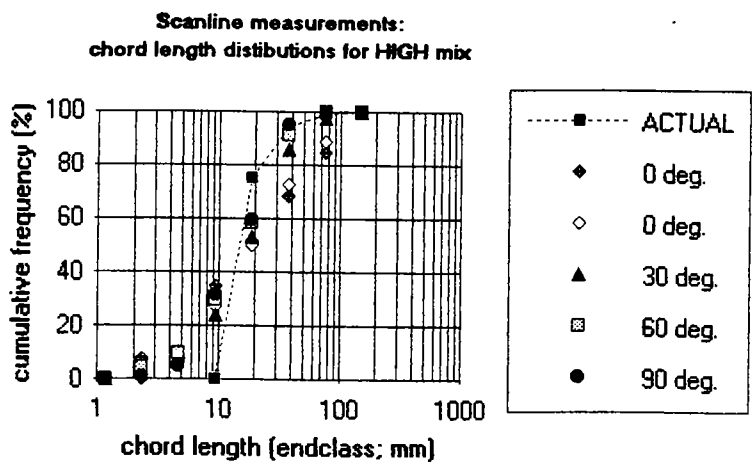

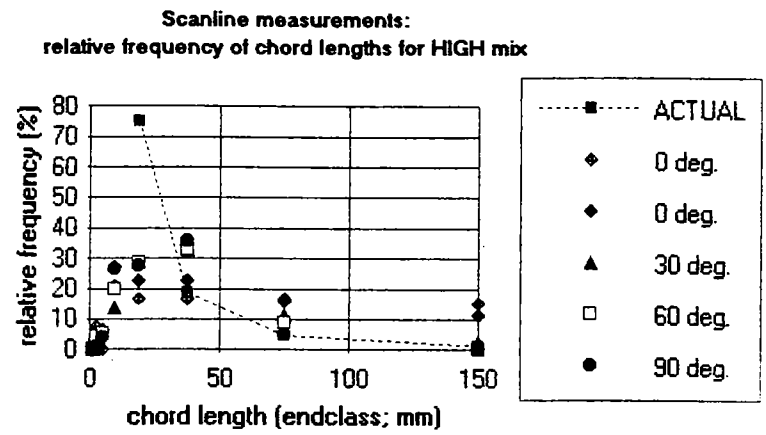

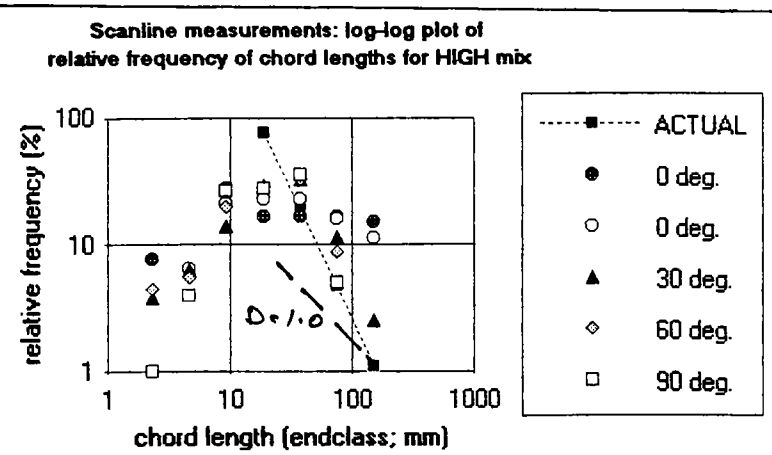

"TX" and "ACTUAL" are 3DBSD for which D=2.0

Scanline Data for Triaxial Specimens; **sorted by Block Orientation:**

HIGH BLOCK VOLUMETRIC PROPORTION MIXTURE

APPENDIX E

FRANCISCAN AREA STUDIES: METHODS OF WORK, DATA and PLOTS

E1.0 INTRODUCTION

This Appendix contains methods of work, data and plots related to the work performed with the maps of Savina (1982); Peterson (1979); Reid (1978) and Seiders (1982) and Erikson, 1994). The maps were studied for two reasons:

1. To measure the block size distributions of Franciscan melange at sub-divisions scales (1 to 2 km^2), in order to bridge the difference in scales between the images used to study the scale-independence of a Franciscan melange at Caspar Headlands, Mendocino (Section 2.7: to 20 m^2) and that using of the geological map of the County of Marin (Figure 2.8: 1000 km^2).

2. To measure block proportion and hillslope data in order to verify if there is a relationship between these two variables. The results of the work was presented in Section 4.6.6).

Most of the Franciscan measurements were made from the detailed (1:4800 and 1:6000) geology maps prepared by Savina (1982), Peterson (1979) and Reid (1978). The study areas for these theses were in Marin County and were originally conducted to provide Dr. Steve Ellen of the USGS, Menlo Park, with ground-truth information to assist in the interpretation of air photos used to map part of Marin (Ellen and others, 1977; Ellen and Wentworth, in press). Colored originals of the maps were generously loaned to me by Dr. Ellen. The map by Erikson (1994) of the metamorphic geology near Cazadero, Sonoma County, was studied to determine if the block size distribution of metamorphic rocks in the Franciscan was self-similar. The results of that study were presented in Section 3.7. The map by Seiders (1982), was selected because it covered a part of the Franciscan south of San Francisco, (San Luis Obispo County); all other studies being for areas north of the city. The locations of the studies are shown on Figure E1.

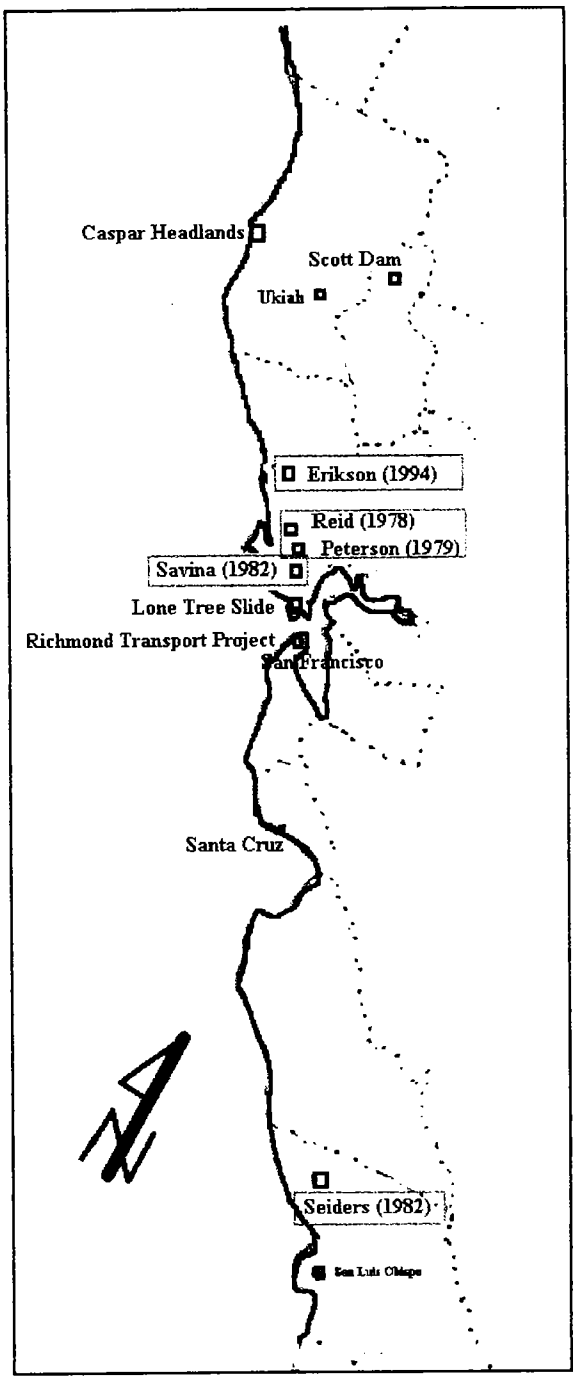

Figure E1 Location of Franciscan Study Areas (boxed captions)

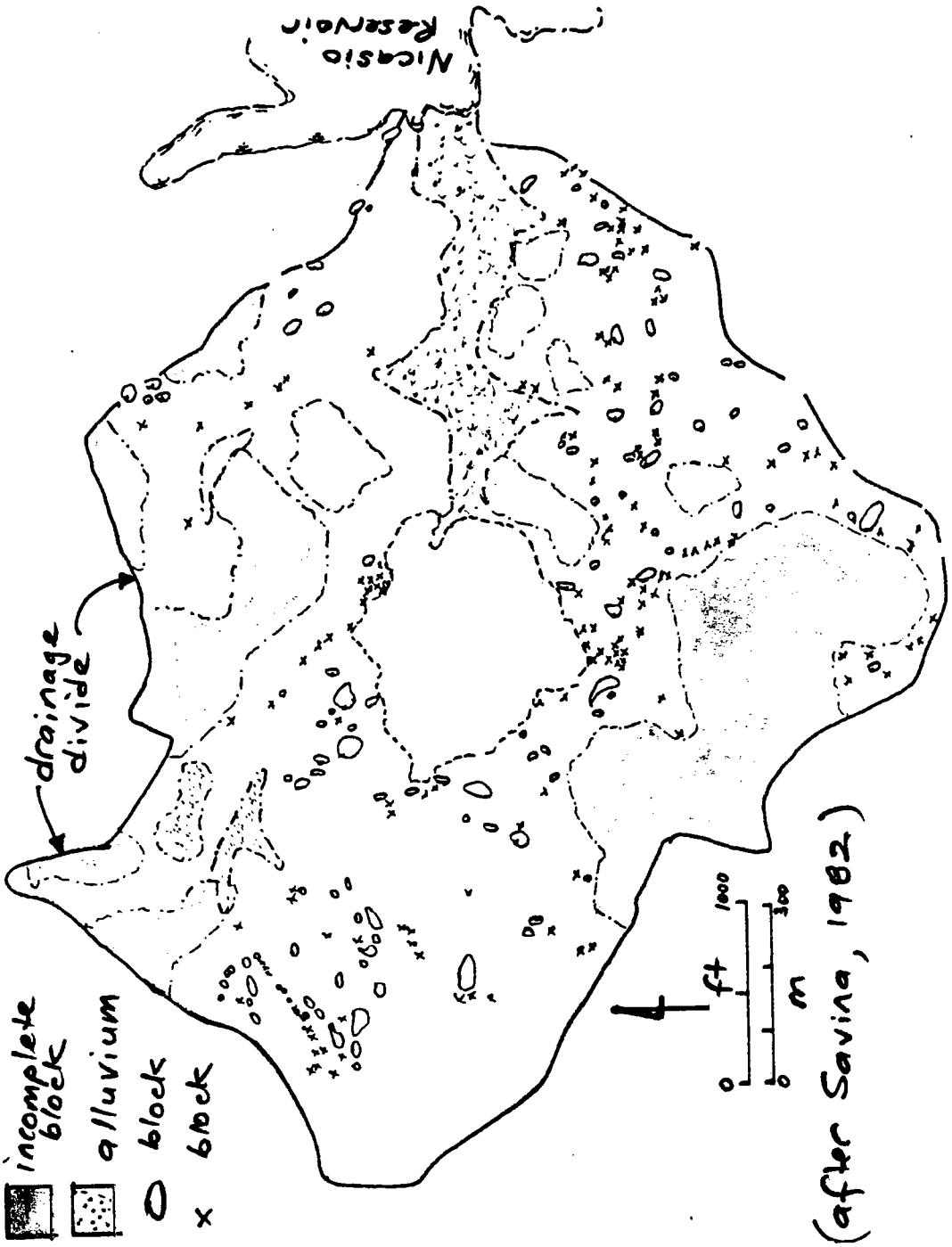

Figure E2 Bedrock geology at Nicasio Reservoir area, Marin County (after Savina, 1982)

E2.0 METHODS OF WORK FOR FRANCISCAN AREA STUDIES: WITH PARTICULAR REFERENCE TO THE MAPS OF SAVINA (1982)

The methods of work for the Franciscan Area Studies are demonstrated using Figures based on the work of Mary Savina (1982). Briefer descriptions follow this section to describe the work performed using the maps of the other geologists. Most of the results of the work have been incorporated into Section 2.7 and 4. 6.6.

Mary Savina performed her investigation on the northeast shores of the Nicasio Reservoir, close to Black Mountain, a piece of oceanic plate/volcanic assemblage (Wright, 1984). The study area (Figure E2) was approximately 1.5 km^2. Savina's original maps separately show bedrock geology, surface geology, slope contours and landslides. The 1965 BATS (Bay Area Transportation Studies air photos (1:4800) at the UC Berkeley Map Library, were used to try to discriminate smaller blocks. This was a difficult chore given the awkward size (1 m square) and the diapositive medium of the photos, which require a light table for useful work..

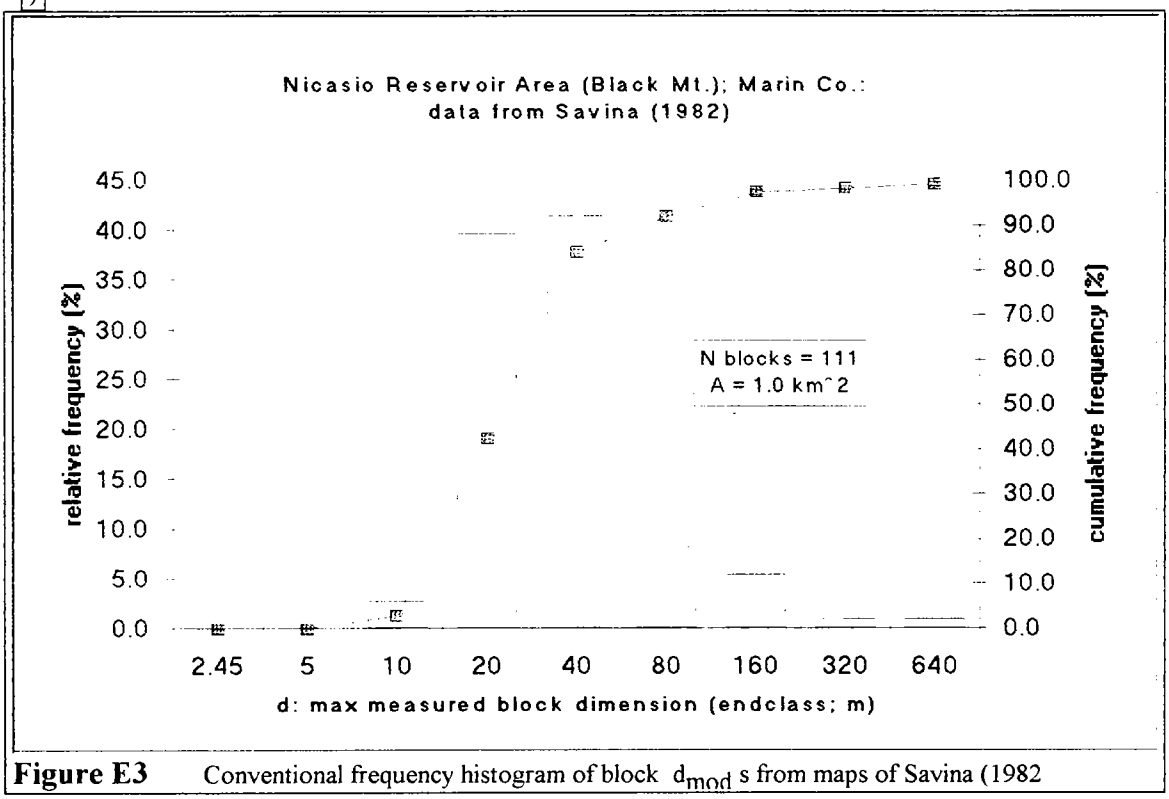

Figure E3 Conventional frequency histogram of block d_{mod} s from maps of Savina (1982

The bedrock geology map was traced onto transparent acetate sheets, which were reduced several times to produce Figure E2. Savina's area is bounded by drainage divides, and contains partial blocks (those not contained entirely within the area) composed of graywacke. There are also patches of alluvium. The areas of the partial blocks and alluvium were subtracted from the total area to give an effective measurement area of 1.06 km^2, with $\sqrt{A}$ equal to 1.0 km. Over 110 individual blocks were measured with the

help of an magnifying lens and a transparent scale. Several additional blocks were shown as "X" by Savina as being too small to map (those less than about 5 m d_{mod}). These were included in the lithological tally but not in the d_{mod} measurements. The data were entered into a spreadsheet for analysis, and a conventional histogram plot was made of the block size data., as shown in Figure E3. A log-histogram plot was also constructed, in which the size classes were chosen using the $d_{peak} = 0.04\sqrt{A}$ criterion discussed in Section 2.4.3. Since $\sqrt{A}$ = 1.0 km, d_{peak} = 40 m. Size classes were doubled-up and halved down around this node. The data are presented in as Figure E4 and were incorporated into the summary plot of the Franciscan melange of shown as Figure 2. 8.

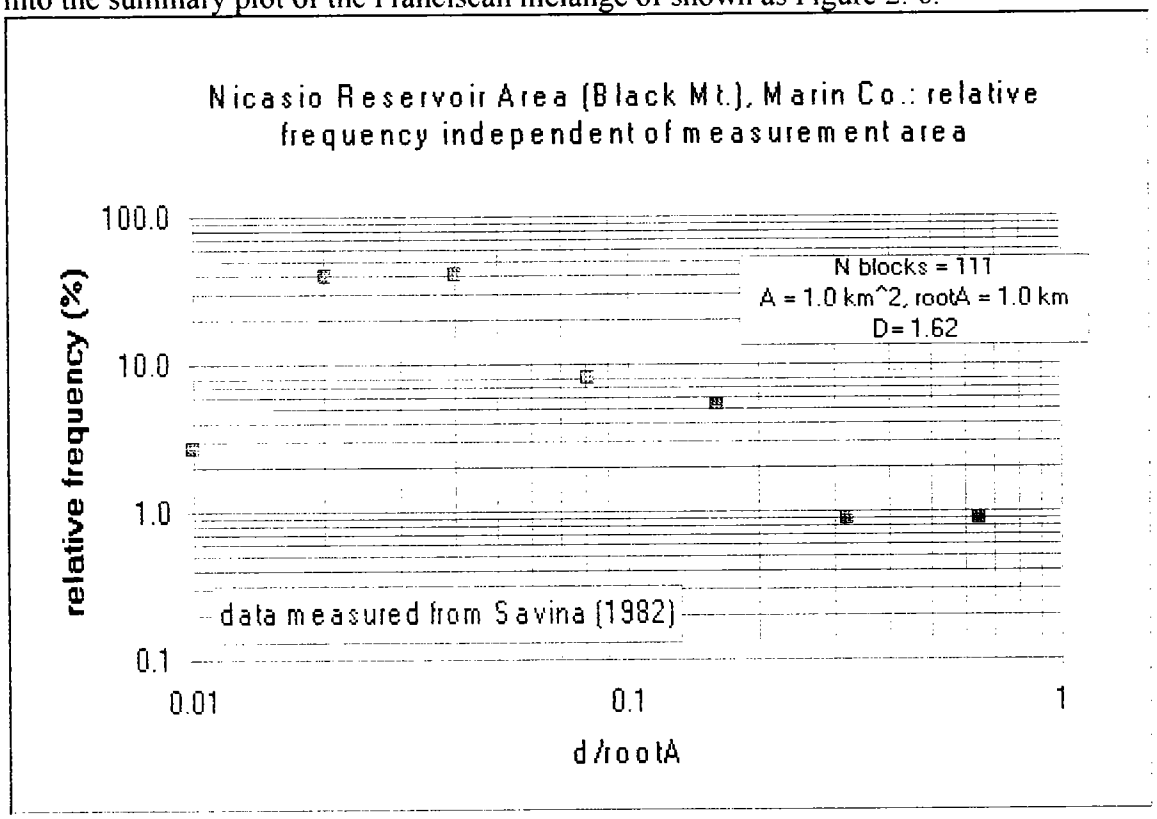

Figure E4 Log-histogram of blocks measured from maps of Savina (1982)

An additional sort of the data was performed to investigate the 2DBSD of the blocks when sorted by lithology. Since it was clear that the area was within the Nicasio Reservoir Sub-terrane (Blake and others, 1984; Wright, 1984), it was of interest to see if the 2DBSD for blocks other than graywacke would be self-similar. Figures E5 suggests that volcanic blocks may not be. The plot in Figure E6 shows that graywacke blocks have an approximate self-similar size distribution, although the descent limb is only approximately self-similar..

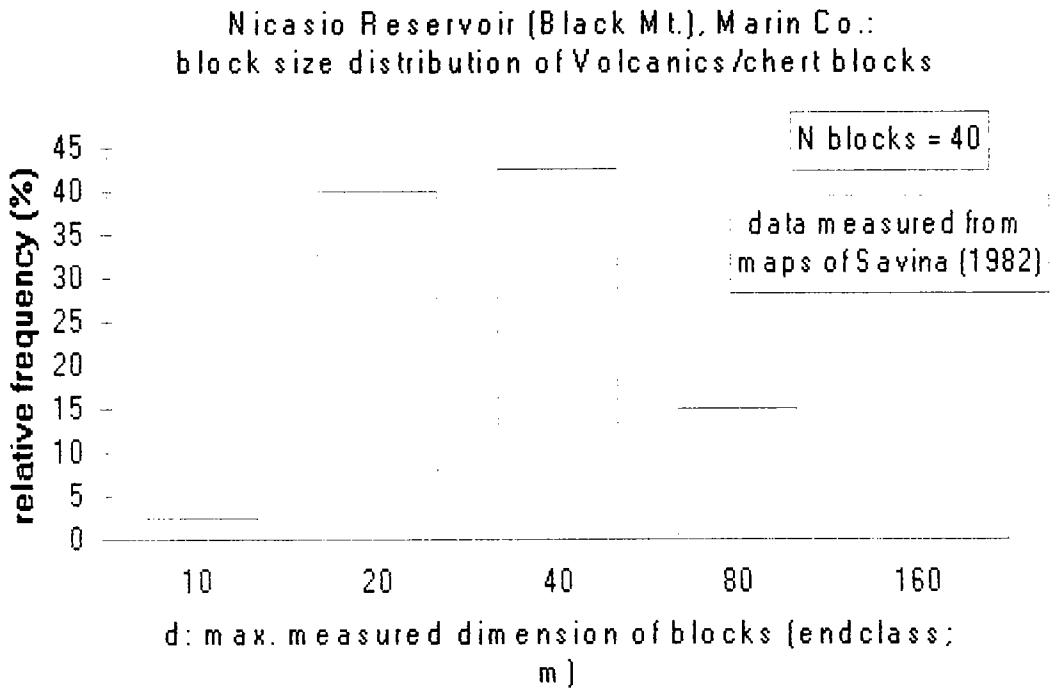

Figure E5 Conventional frequency histogram of volcanic/ chert blocks, measured from the maps of Savina (1982)

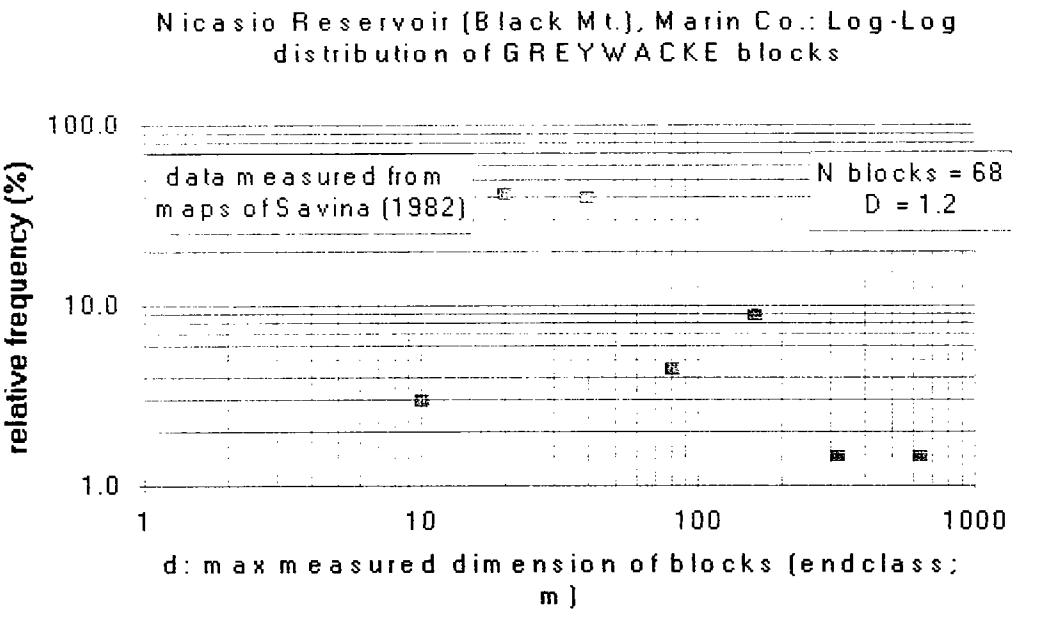

Figure E6 Log-histogram of sizes of graywacke blocks, measured from maps of Savina (1982)

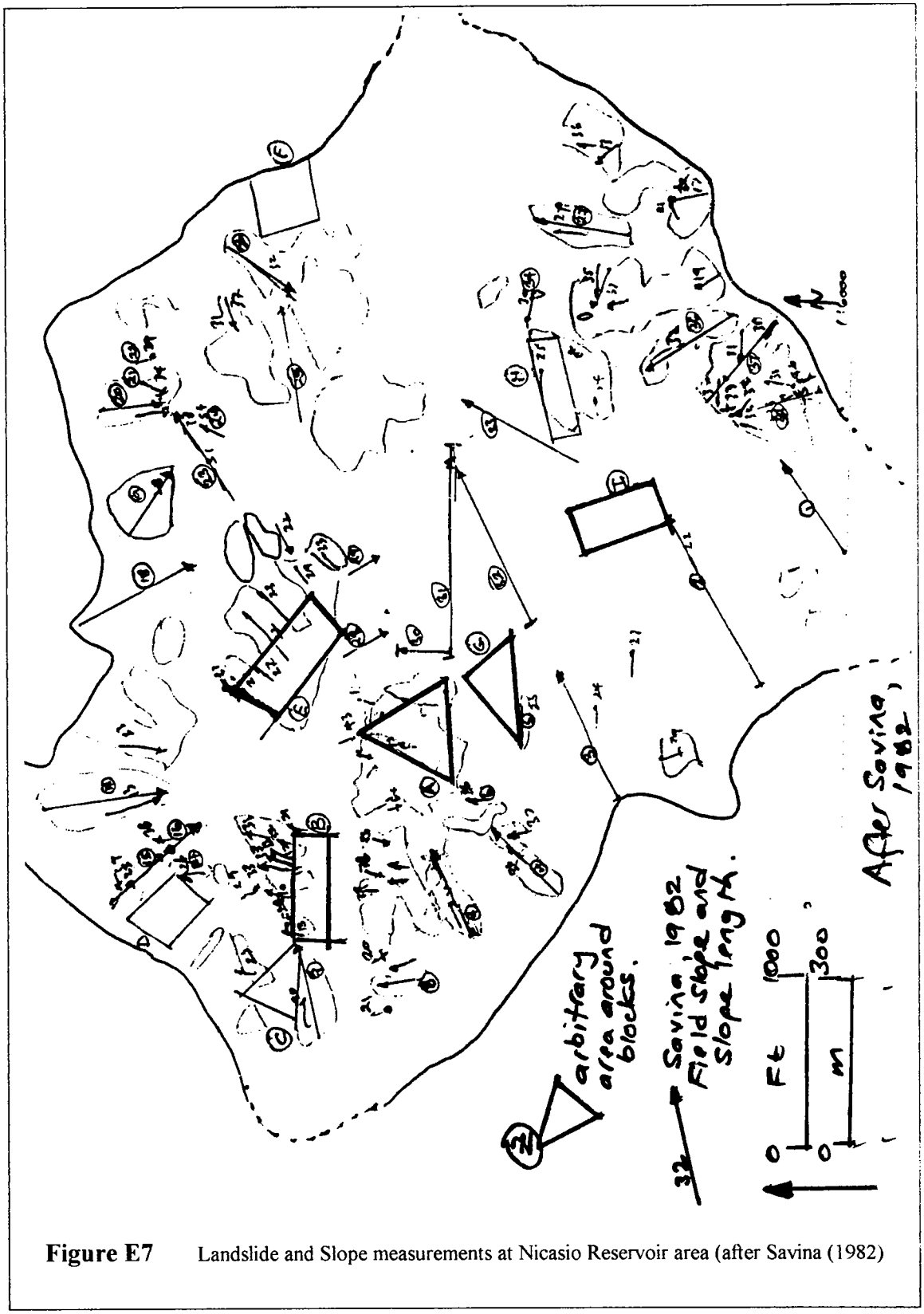

Figure E7 Landslide and Slope measurements at Nicasio Reservoir area (after Savina (1982)

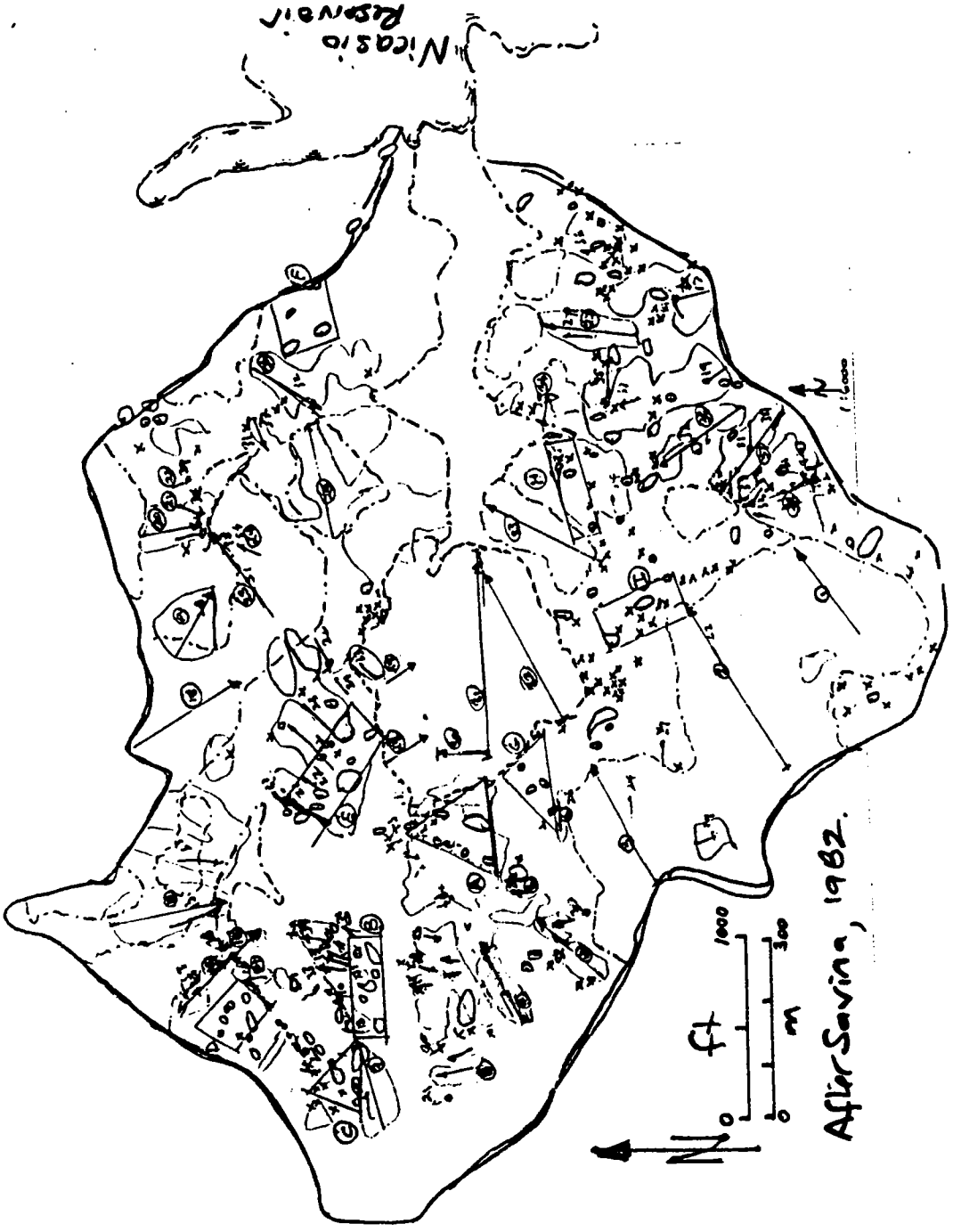

Figure E8 Shows the overlay of two maps: one showing landslides with areas defined for measurements of block areal proportion/hill slope angle; together with Savina's slope measurements; and the other being the bedrock geology showing blocks. Note the small areas (Lettered) bounding groups of blocks.

Acetate tracings were made of the landslides and 38 slope measurements that Savina (1982) had mapped (Figure E7). The slope measurements were hand-leveled traverses. The longest of these slope traverses was about 300 m (horizontal component) and the shortest 8 m (Figure E7). The transparent acetate was placed over the original geology map and efforts made to find:

1. areas of blocks that were not a part of a landslide:
2. areas of blocks entirely within landslide
3. slope measurements entirely within failed material,
4. slope measurements entirely within block material

Figure E8 gives some sense of the difficulty of sorting out the block groupings from the landslides; but also shows that most landslides flow around blocks.

Boundaries were drawn around groups of blocks, the area of enclosure measured, and the rectangular area of the individual blocks calculated by measuring the major and minor axes of the blocks. The areal proportion of blocks in each group was the sum of all the block areas divided by the area of enclosure. Nine groups were measured with areas to 11,700 m^2. The average slope of the groupings were calculated as the arctan of the ratio of maximum relief divided by the longest downslope direction. These measurements resulted in estimates of block proportion and hillside slope for the groups..

The block areal proportions were augmented with the 38 slope measurements made by Savina (1982). These were assigned either 100 percent linear block proportion or 0 percent for "pure" melange. For the slope lines traversing blocks, the linear block proportion of the lines were measured. All data were entered in a spreadsheet. The summary tables of lithology and areal/linear proportion vs. hillside slope are presented Table E1 Figure E9 summarizes the data, which were also included in the compilation of Figure 4.17.

The most serious problem with these procedures is that of working with someone else's data, and being unable to verify the field conditions (because of lack of time). Also, the determination of the correct area around blocks was arbitrary since it was easy to boost the areal proportion by diminishing the size of the bounding area around blocks. Further work should be performed using the block linear proportion, since the scanline for this may be combined conveniently with line used to determine the gradient. Field work should also be performed, augmented by air photos and measurements using a parallax bar, or more formal photogrammetry.

Table E1 Summary of Block Proportions and Hillslope Data from Savina (1982)

Nicasio Reservoir (Black Mt.), Marin Co.

data measured from Savina (1982)

PLOT OF B LOCK AREAL and LINEAR PROPORTIONS and HILLSIDE SLOPES

Initially for the "pure" melange "matrix" and the pure blocks
estimated from existing slope data in Savina (1982), and measured
from her maps.
Secondly, for various block proportions, areas selected from Savina (1982)
Biggest problems are the accuracy of the slope data. Where possible,
calculated slopes checked against Savina's slope measurements.

These data are a mix of linear data and area data.

Line/Area	Hor Dist (m)	Vert Dist (m)	gradient (%)	slope degrees	Lithology	Stability	Block%	slope degrees
4	144	26	33	18.3	melange	failed	0	18.3
5	48		23	13	melange	failed	0	13
6	30		26	14.6	melange	failed	0	14.6
7	132	25.9	31	17.2	melange	failed	0	17.2
8	36	9.2	23	13	melange	failed	0	13
9	144	19.8	18	10.2	melange	failed	0	10.2
10	48		20	11.3	melange	failed	0	11.3
11	42		33	18.3	melange	failed	0	18.3
12	33		32	17.7	melange	failed	0	17.7
13	36		20	11.3	melange	failed	0	11.3
14	30		26	14.6	melange	failed	0	14.6
15	102	10.6	23	13	melange	failed	0	13
16	66	6	9	5.1	melange	failed	0	5.1
17	186	24.5	13	7.4	melange	failed	0	7.4
19	132	38.1	28	15.6	melange	failed	0	15.6
20	96	30.5	33	18.3	melange	failed	0	18.3
21	36		34	18.8	melange	failed	0	18.8
27	150	38	24	13.5	melange	failed	0	13.5
35	60		19	10.8	melange	failed	0	10.8
36	168	49	30	16.7	melange	failed	0	16.7
37	168	42.6	32	17.7	melange	failed	0	17.7
38	126	49	38	20.8	melange	failed	0	20.8
22	30		39	21.3	melange	stable	0	21.3
34	48		35	19.3	melange	stable	0	19.3
1	180	58	32.2	17.9	gy	stable	100	17.9
2	306	60	32	17	gy	stable	100	17
3	222	38.1	30	17	gy	stable	100	17
18	210	19.8	9	5.1	gy	stable	100	5.1
23	168	57.3	50	26.6	gy	stable	100	26.6

24	36		54	28.4	gy	stable	100	28.4
25	180	47.2	26	14.6	gy	stable	100	14.6
26	126	32	32	17.7	gy	stable	100	17.7
28	78	39.6	50	26.6	gy	stable	100	26.6
29	48	36.6	75	36.9	gy	stable	100	36.9
30	84	35.1	42	22.8	gy	stable	100	22.8
31	330	111	34	18.8	gy	stable	100	18.8
32	264	86.9	33	18.3	gy	stable	100	18.3
33	210	60.9	29	16.2	gy	stable	100	16.2

Estimating the block proportion in small areas (5300-11700 m^2)

Area Label	area m^2	gradient (%)	degrees degrees	lithology	stability	block %	degrees degrees
A	8712	23	13	bim	failed	14.4	13
B	7776	20	11.3	bim	stable	15.2	11.3
C	5292	19.8	11.2	bim	stable	30.2	11.2
D	7776	16.9	9.7	bim	stable	13.9	9.7
E	11700	20	11.3	bim	failed	27.6	11.3
F	8100	13.9	7	bim	stable	19.4	7
G	6084	24.4	13.7	bim	stable	5.5	13.7
H	7020	30	16.7	bim	stable	5.7	16.7
I	10368	32.3	17.9	bim	stable	14.8	17.9

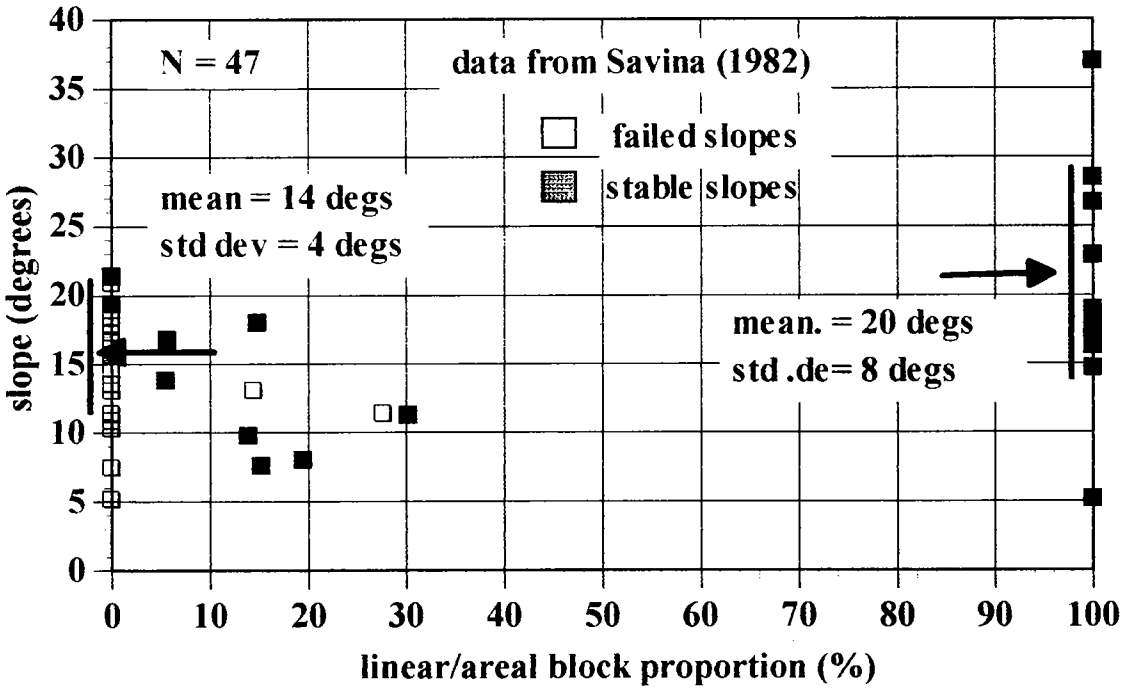

Figure E9 Plot of block linear and areal proportions; and hillslopes; measured from maps of Savina (1982)

E3.0 SUMMARY OF WORK PERFORMED USING THE MAPS OF PETERSON (1979)

A similar approach to the one described for the work with the maps of Savina (1982) was used for the maps of Peterson (1979). However, his work was less detailed than Savina's (hers was for a PhD, his was for an MS). Peterson's study area was in the Three Peaks area of Marin County (Figure E1). The 3.9 km^2 site is a wedge of melange lodged between two hill-sized blocks of graywacke, as shown in Figure E10. Excluding the masses of graywacke and alluvium, the measured area is 1.26 km^2, with $\sqrt{A}$ = 1.12 km. About 124 blocks were measured, using a magnifying lamp and a scale. The blocks were not sorted by lithology. Figure E 11 shows a conventional size frequency histogram. The $0.04\sqrt{A}$ criteria, used to identify a node for defining histogram classes, yielded a d_{peak} of about 55 m. The log-histogram is shown as Figure E12.

Nine areas were defined for the determination of block areal proportion and hill slope, and 19 linear block proportions were measured using the existing slope traverses of Peterson (1979). The data are tabulated as Table E2, and Figure E13 shows the summary plot of block linear and areal proportions related to hillslope angles. The same data were included in the summary plot of Figure 4.17.

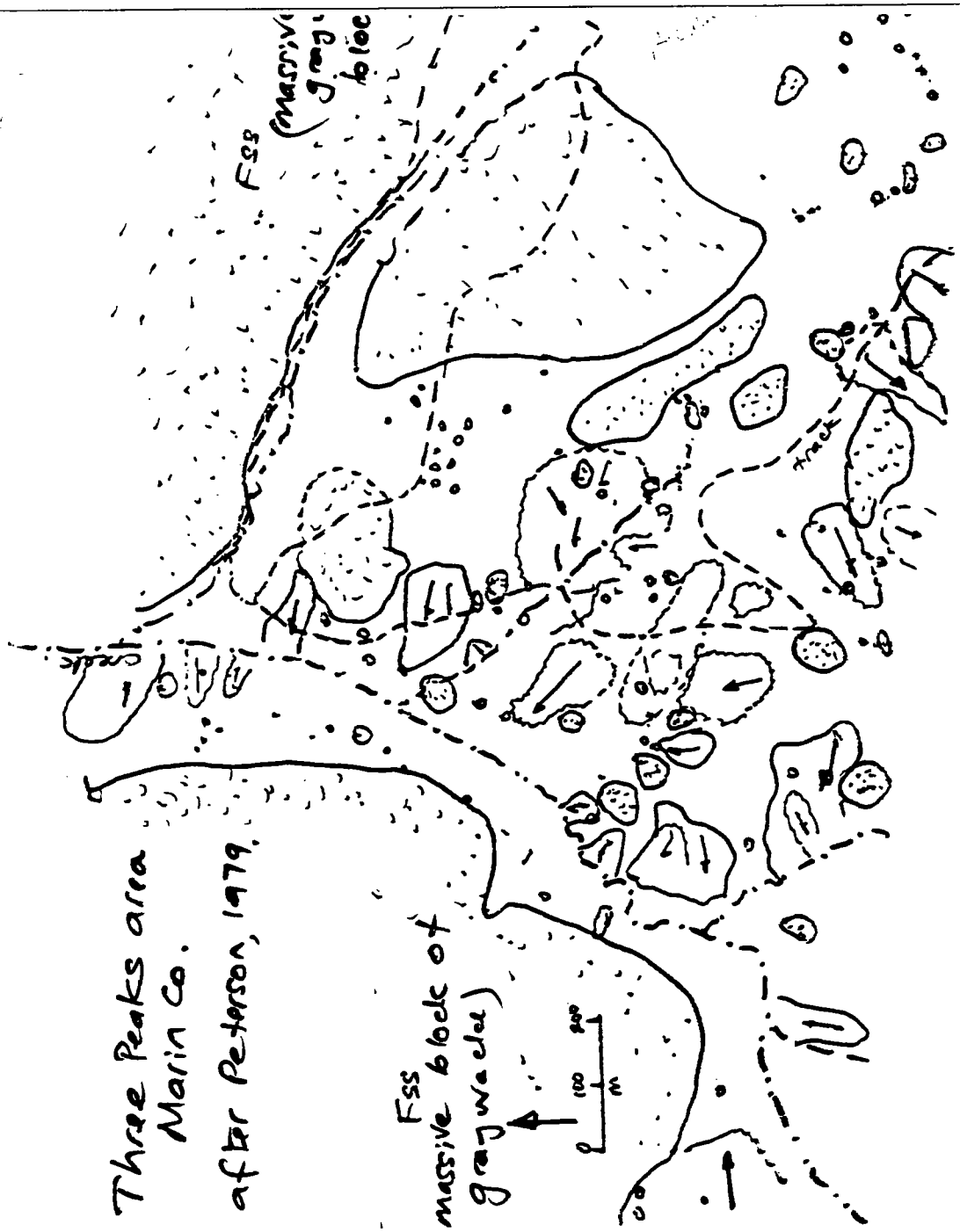

Figure E10 Compilation of bedrock geology and landslides at Three Peaks area (after Peterson, 1979)

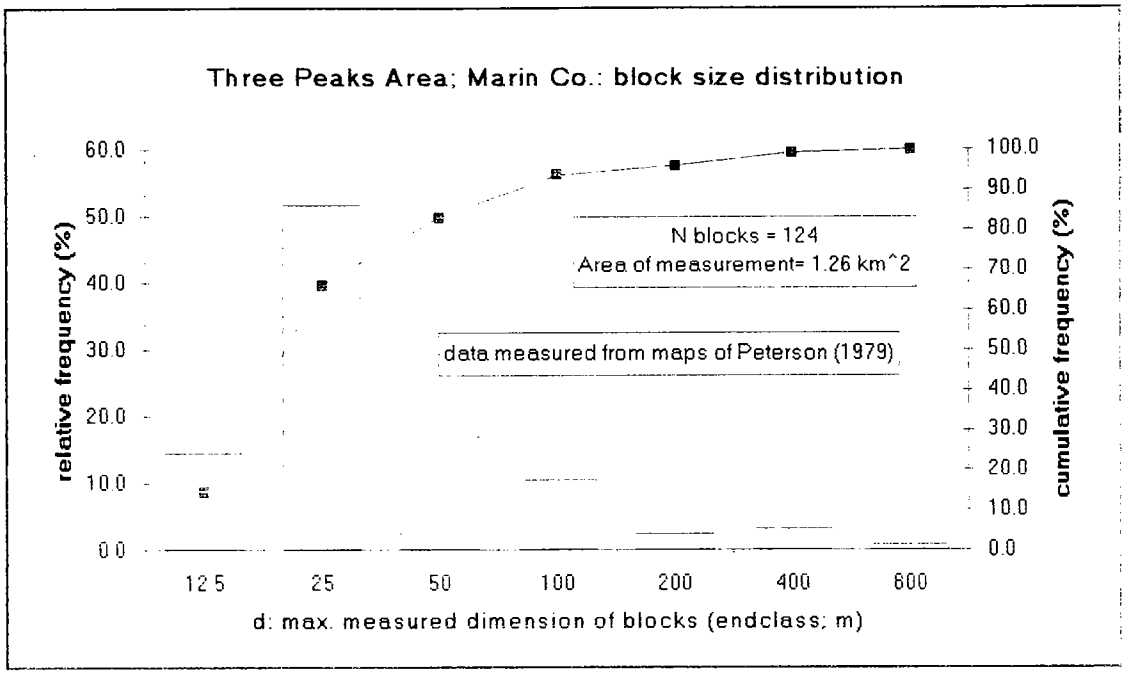

Figure E11 Conventional size frequency histogram of blocks measured from the maps of Peterson (1979)

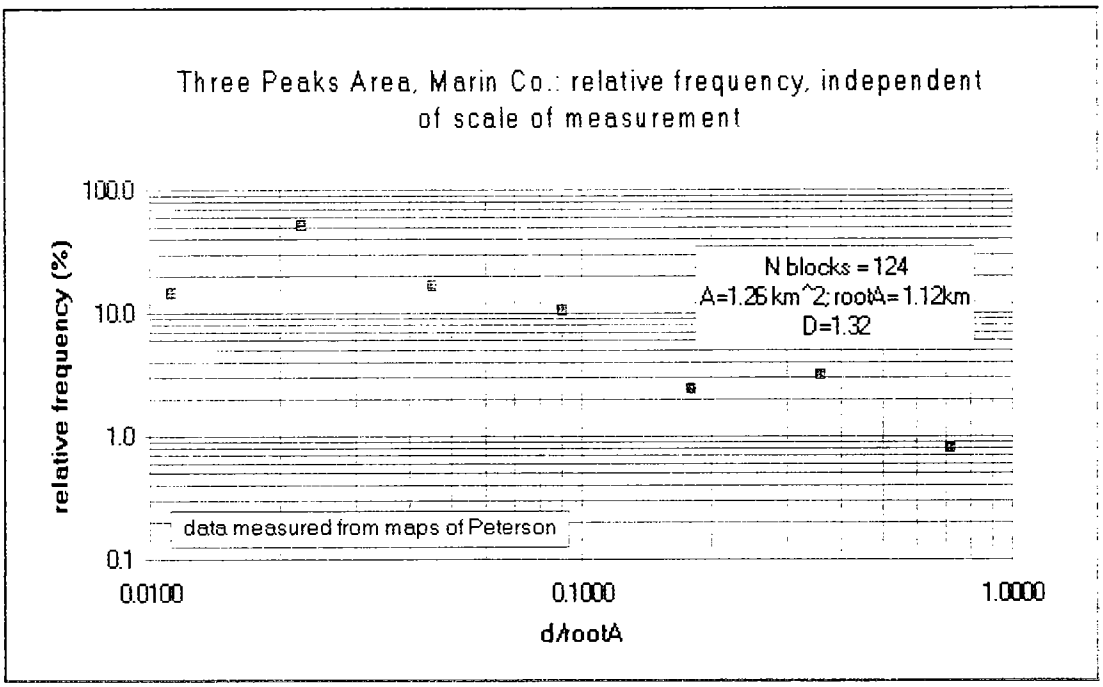

Figure E12 Log-histogram of block sizes measured from the maps of Peterson (1982)

Three Peaks Area, Marin Co. **data measured from maps of Peterson (1979)**

PLOT OF BLOCK LINEA R and AREAL PROPORTIONS vs. HILLSIDE SLOPES

Initially, data shown are for the "pure" block (proportion=100%) data (mostly graywacke)
The "pure" matrix is melange, but of course, the melange is also
studded with blocks. No estimate made of blocks which were not
mapped by Peterson (1979). The BATS photos (1965) show characteristic mottling
that would allow some estimates of near surface blocks.
But, such estimates not made, at least for the data shown here.
The linear block proportions are directly from Peterson's field measurements
of slopes. I judged the lithology from the bedrock maps.

Hor dist (m)	gradient (%)	slope degrees	lithology	stability	Block%
125	24.9	14	melange	failed	0
58	24.9	14	melange	failed	0
38	23.1	13	melange	failed	0
48	15.8	9	melange	failed	0
67	23.1	13	melange	failed	0
29	23.1	13	melange	failed	0
48	23.1	13	melange	failed	0
67	24.9	24.9	melange	failed	0
72	23.1	23.1	melange	failed	0
91	28.7	16	melange	stable	0
106	17.6	10	melange	stable	0
58	24.9	14	melange	stable	0
72	15.8	15.8	melange	stable	0
101	57.7	30	gv	stable	100
38	36.4	36.4	gv	stable	100
62	46.6	46.6	gv	stable	100
53	23.1	23.1	gv	stable	100
77	46.6	46.6	gv	stable	100
62	57.7	57.7	gv	stable	100

Estimating the block proportion in small areas (3120-18800 m^2)

sub-area label	area m^2	gradient (%)	slope degrees	lithology	stability	block %
A	12860	20.8	11.8	bim	stable	11.3
B	18800	24.5	13.8	bim	stable	41
C	12570	16.1	9.1	bim	stable	20.2
D	10370	21.5	12.1	bim	stable	22.7
E1	3720	22.4	12.6	bim	stable	90
E2	3120	26.5	14.8	bim	stable	0
F	15428	17.8	10.1	bim	stable	19.4
G	19180	28.7	16	bim	failed	8.8
H	7800	26.8	15	bim	failed	1.8

Table E2 Summary of Block Proportions and Hillslopes; from of Peterson (1979)

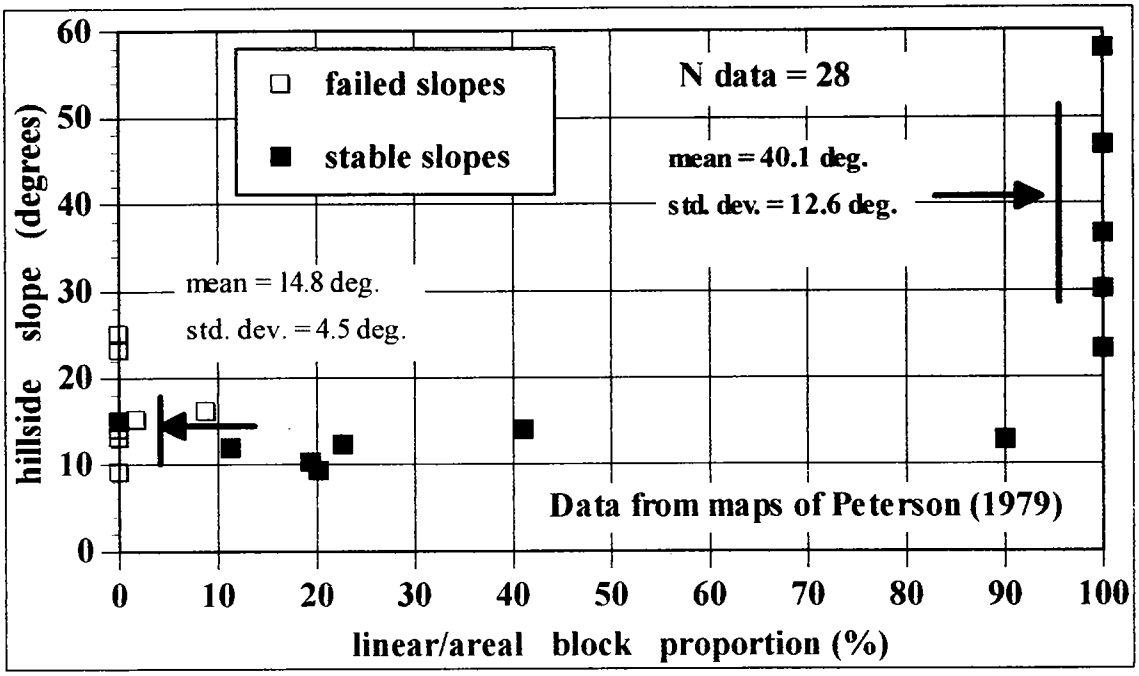

Figure E13 Plot of block linear and areal proportions; and hillslopes; measured from maps of Peterson (1979)

E4.0 DATA AND PLOTS RELATED TO THE MAPS OF REID (1978)

The study area of Reid (1978) at Walker Creek, Marin County (Figure E1) is similar to that of Peterson (1979, being a 2.4 km^2 areas of melange wedged between two hill-sized blocks of graywacke, as shown in Figure E14. Excluding the peripheral massive blocks an alluvium, the measurement area is 1.35 km^2, which yields $\sqrt{A}$ of 1.15 km and the endclass node (d_{peak} = 0.04 $\sqrt{A}$) of about 50 m. Some 94 blocks were measured, but none were sorted by lithology, although lithology was recorded. The block size data are presented as a conventional frequency histogram (Figure E15) and a log-histogram (Figure E16).

Three areas were defined around groups of blocks (not shown on Figure E14), and 35 linear proportions and hill slopes measured. Almost all of the data were for stable ground. The data are summarized in Table E3, and are plotted in Figure E17. The data were also included in Figure 4.17.

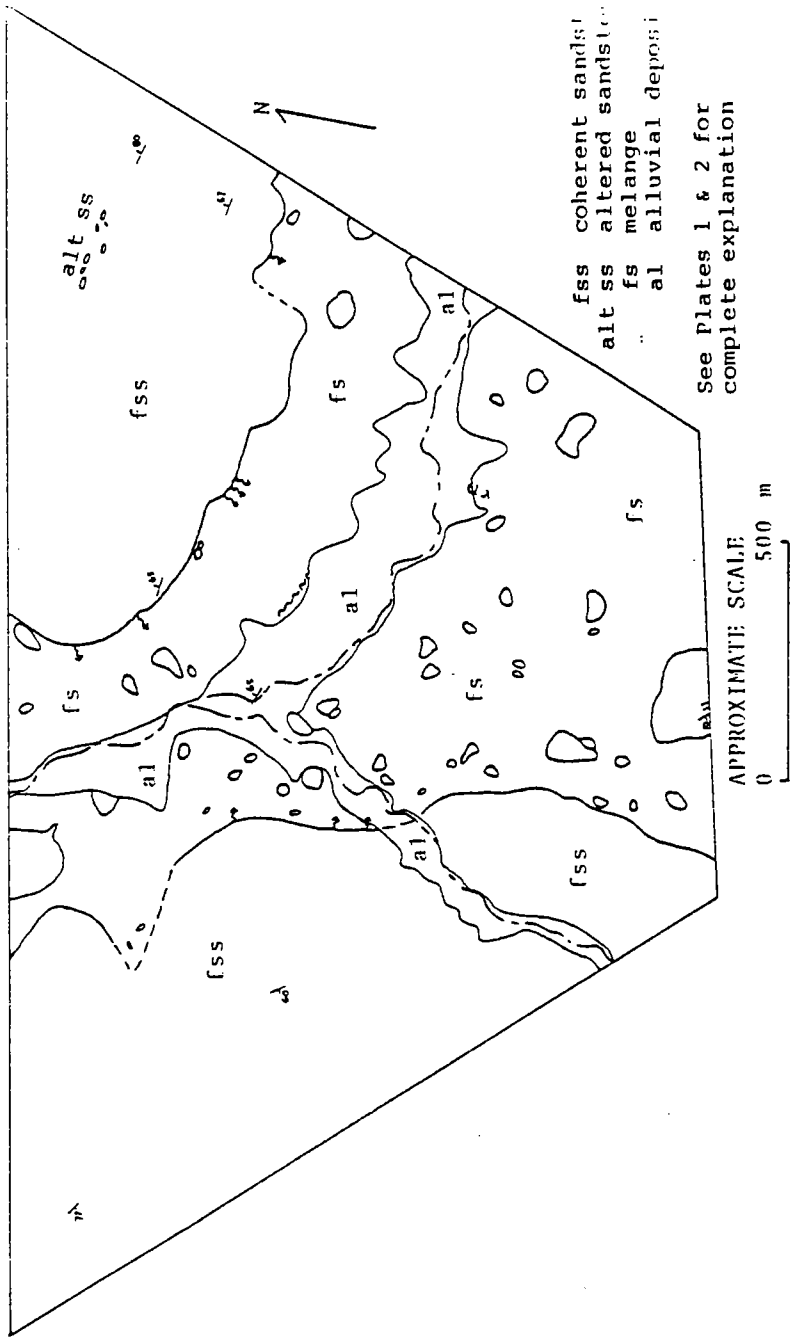

Figure E14 Bedrock geology at Walker Creek area, Marin County; from Reid (1978

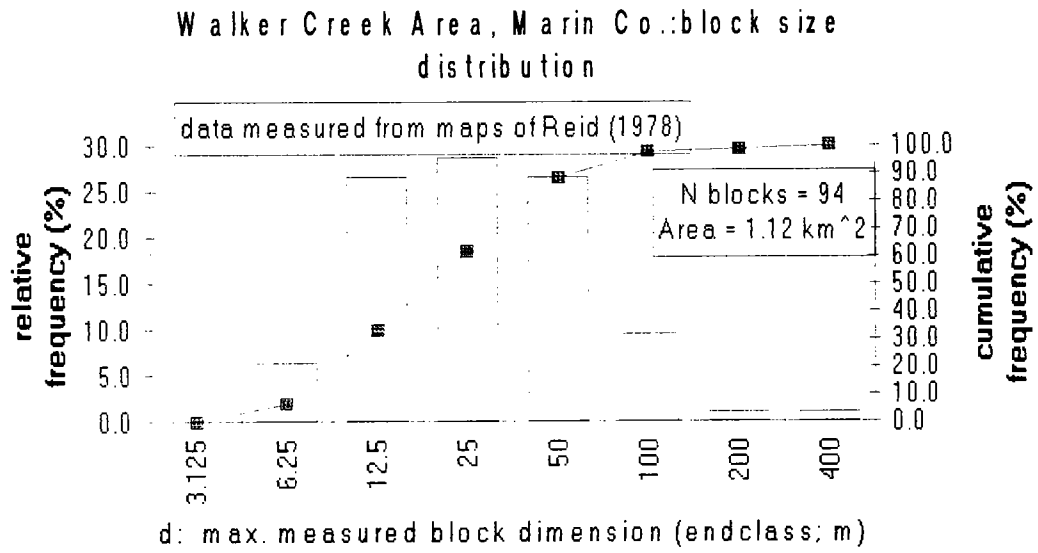

Figure E15 Conventional block size frequency histogram; data measured from the maps of Reid (1978)

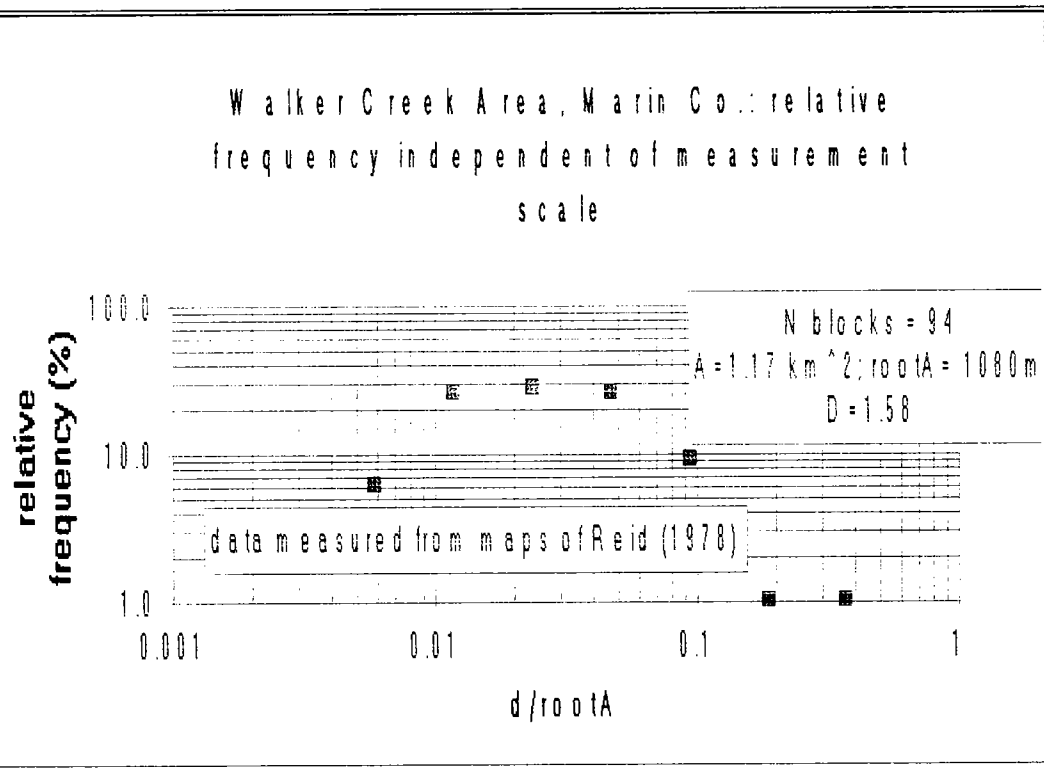

Figure E16 Log-histogram of block sizes measured from the maps of Reid (1978)

TABLE E3 Summary of Block Proportions and Hillslope; Data from of Reid (1978)

Walker Creek, Marin Co. data measured from maps of Reid (1978)
PLOT OF BLOCK LINEA R and AREAL PROPORTIONS vs. HILLSIDE SLOPES
Initially, data shown are for the "pure" block (proportion=100%) data (graywackes)
The "pure" matrix is melange, but of course, the melange is also
studded with blocks. No estimate made of blocks which were not
mapped by Reid (1978). The BATS photos (1965) show characteristic mottling
that would allow some estimates of near surface blocks.
But, such estimated not made, at least for the data shown here.
The linear block proportions here are directly from Reid's field measurements
of slopes. I judged the lithology from the bedrock maps.

Hor dist (m)	gradient (%)	slope degrees	lithology	stability	Block%
77	15.8	9	melange	failed	0
54	23.1	13	melange	failed	0
67	23.1	13	gy	failed	100
58	44.5	24	gy	failed	100
58	26.8	15	melange	stable	0
58	15.8	9	melange	stable	0
58	19.4	11	melange	stable	0
62	8.7	5	melange	stable	0
154	26.8	15	melange	stable	0
67	28.7	16	melange	stable	0
43	28.7	16	melange	stable	0
58	73.7	36	chert	stable	100
38	119	50	chert	stable	100
38	75.3	37	greywacke (gy)	stable	100
48	55.4	29	gy	stable	100
43	75.4	37	gy	stable	100
67	60.1	31	gy	stable	100
58	32.5	18	gy	stable	100
48	46.6	25	gy	stable	100
38	57.7	30	gy	stable	100
38	46.6	25	gy	stable	100
48	55.4	29	gy	stable	100
34	72.7	36	gy	stable	100
62	26.8	15	gy	stable	100
53	57.7	30	greenstone	stable	100
43	46.6	25	gy	stable	100
34	83.9	40	gy	stable	100
34	80.9	39	gy	stable	100
48	46.6	25	gy	stable	100
48	40.4	22	gy	stable	100
53	46.6	25	gy	stable	100
38	55.4	29	gy	stable	100
43	46.6	25	gy	stable	100
58	48.8	26	gy	stable	100
67	46.6	25	gy	stable	100

Estimating the block proportions in small areas

sub_area Label	area m^2	gradient (%)	slope degrees	lithology	stability	block %
A	8653	15.6	8.9	bim	stable	19.7
B	line: 124m	30.1	17	bim	stable	63.8
C	1958	29.8	16.6	bim	stable	26.5

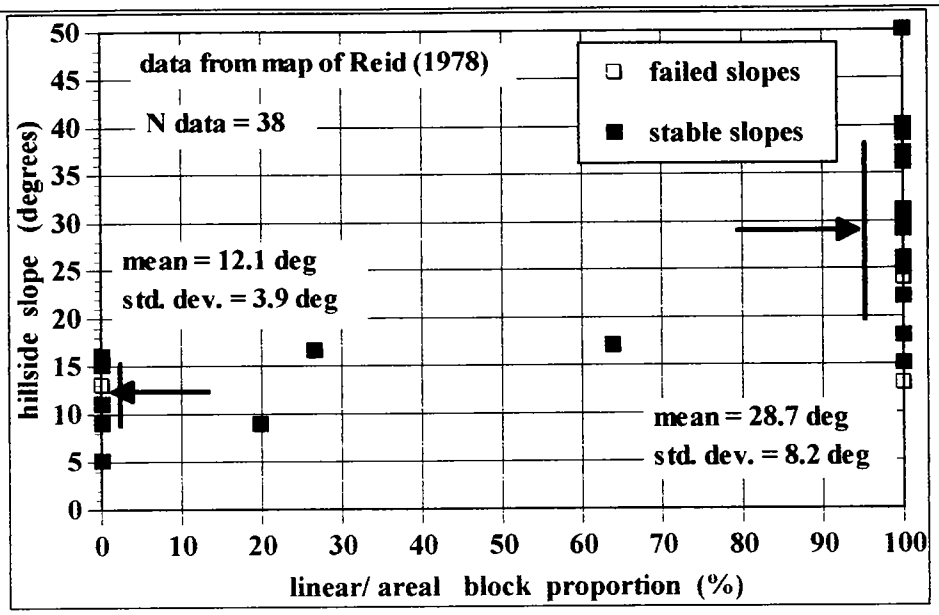

Figure E17 Plot of block linear and areal proportions; and hillslopes; measured from maps of Reid (1978)

E5.0 SUMMARY OF WORK PERFORMED USING THE MAP OF SEIDERS (1982)

The area mapped by Seiders (1982) was in the vicinity of York Mountain, in San Luis Obispo County (Figure E1 and Figure E18). This Franciscan Study Area was the only one south of San Francisco. The area studied was a relatively small part of the coverage, where the Franciscan was relatively intact; elsewhere it was much faulted, and the mapping of blocks was relatively sparse. Most blocks appeared to have been mapped along ridge lines, and probably not all blocks within the area were mapped. The gross area studied (Figure E18) was some 9 km^2, but several large faulted zones and areas of alluvium reduced the measured area to 3.4 km^2. The $\sqrt{A}$ was approximately 1.9 km and $0.04\sqrt{A}$ of was about 90 m., which was rounded to 100 m, and was the node for class expansions for the log-histogram. Figure E19 and Figure E20 show the conventional frequency histogram and the log-histogram. About 180 blocks were measured, but no measurements were made of linear or areal proportion against hillslopes, due to the small scale (1:24,000). The data are presented in Appendix E without comment.

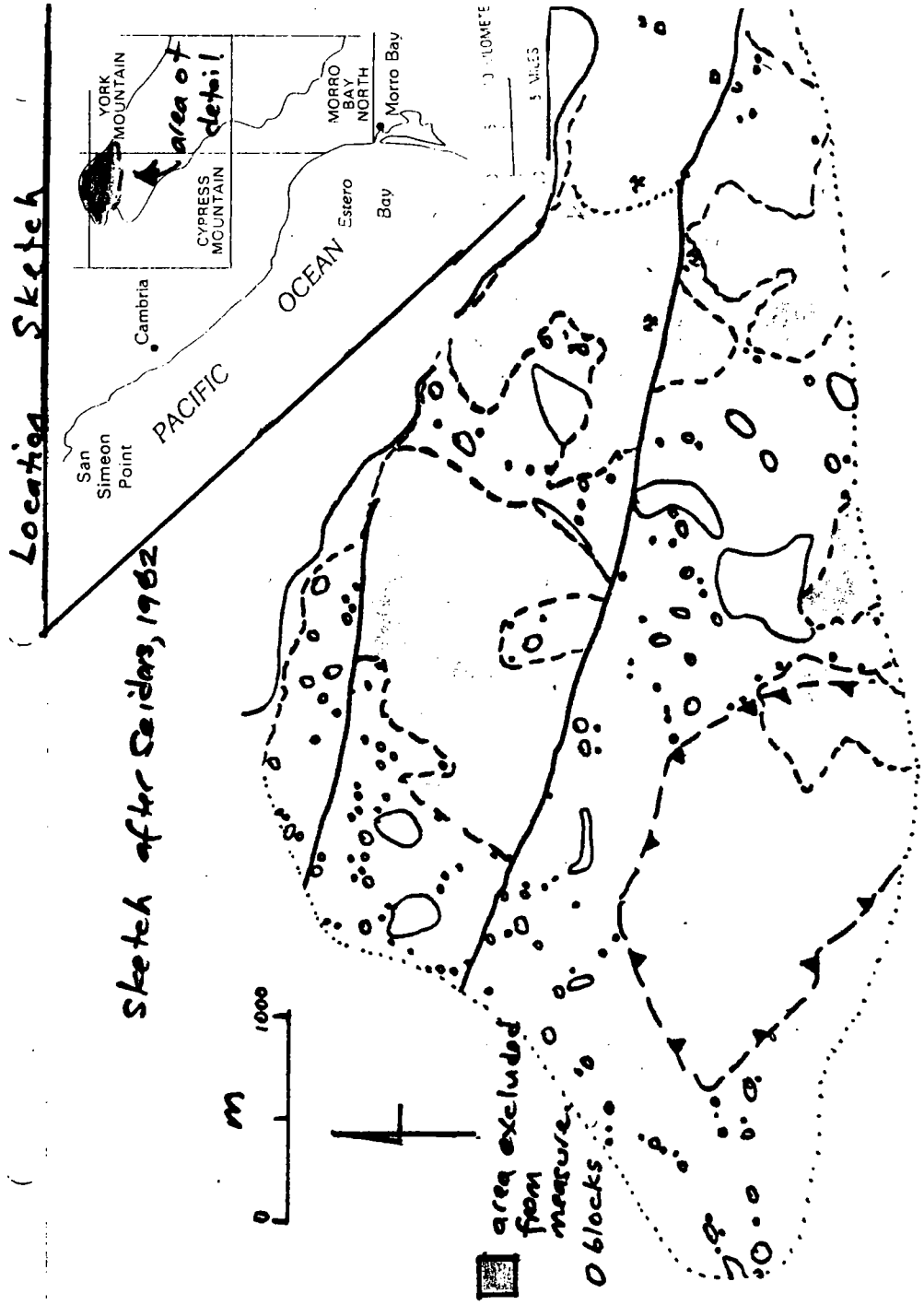

Figure E18 Sketch map of portion of the area mapped by Seiders (1982) in San Luis Obispo County. Shaded areas are faulted blocks and alluvial areas not included in the measurement area.

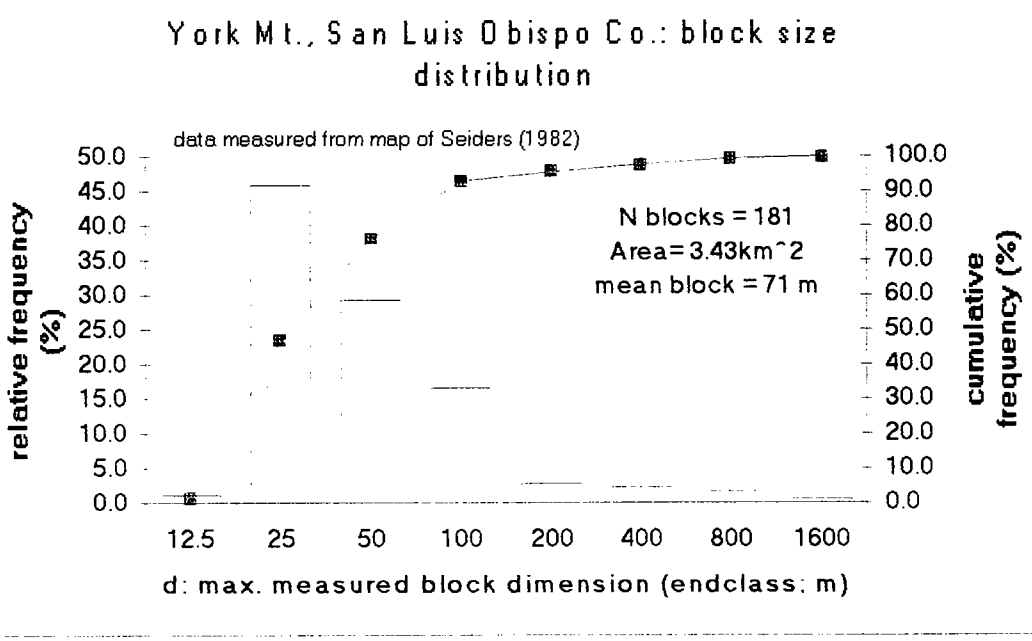

Figure E19 Conventional block size frequency histogram based on measurements from the map of Seiders (1982)

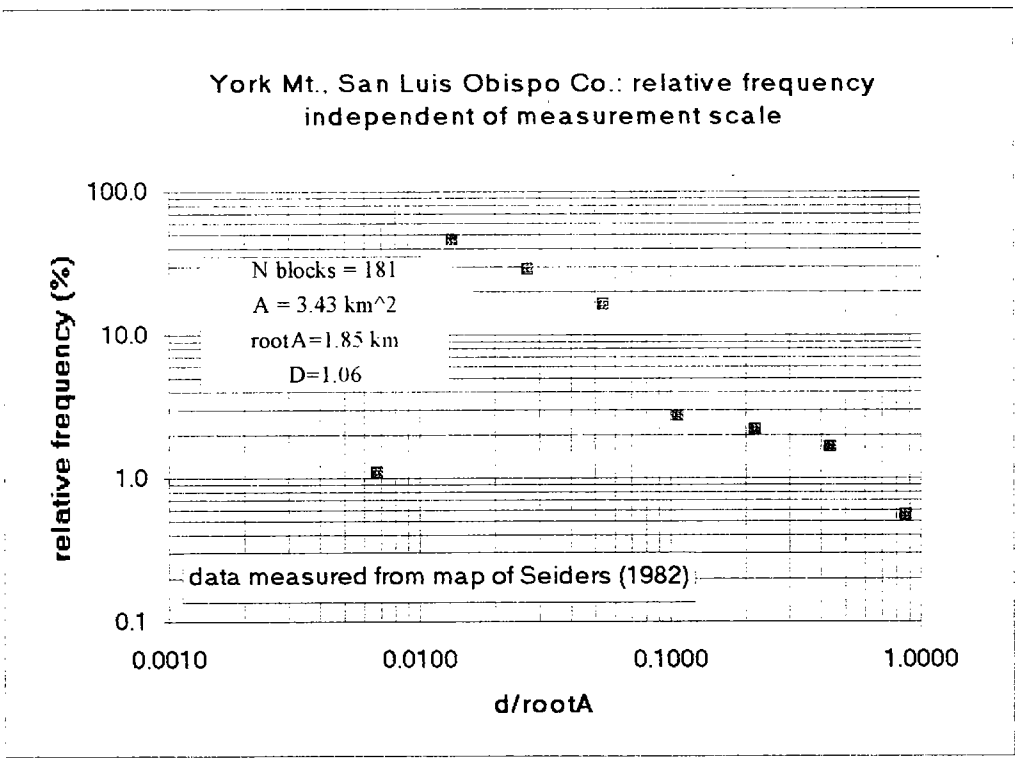

Figure E20 Log-histogram of block sizes measured from the map of Seiders (1982)

E6.0 SUMMARY OF WORK PERFORMED USING THE MAP AND DATA OF ERIKSON, 1994

The results of the work performed using the maps and block size data collected by Erikson (1994) were presented in Section 3.12 (Figure 3.14), in the discussion on block size distribution of some Franciscan melanges; hence no data are presented here. The area is in the locale of Cazadero in Sonoma County (Figure E1; and Figure E21). Erikson (1994) cataloged over 740 blocks in the Cazadero-Ward Creek area, the majority being metamorphic blocks. He estimated the d_{mod} of many of these, and others were measured from his map. In all, some 410 blocks were included in the database. The gross area of the geological map is about 41 km^2, but this was reduced by excluding the Big Oat Creek metabasalt block which is almost 5 km long. Alluvium, Hell Hole conglomerate and partial blocks at the boundary of the area were excluded as well. No attempt was made to sort the data by lithology.

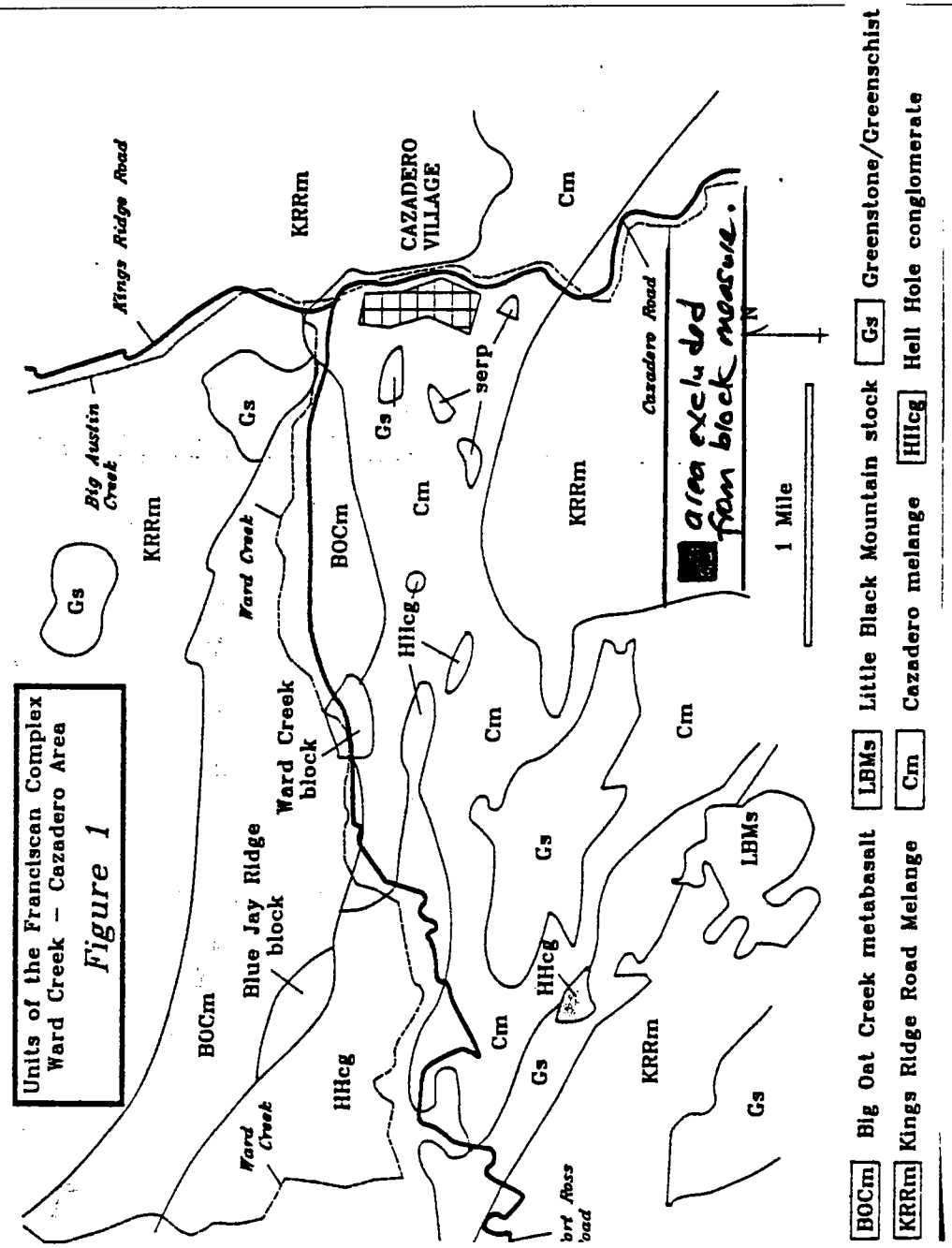

Figure E21 Area mapped by Erikson (1994), in which over 740 metamorphic blocks were cataloged: 440 of these were included as a log-histogram plot to check a self-similarity. Large blocks were excluded (shaded area); after (Erikson, 1992).